

DISSERTATION ZUR ERLANGUNG DES DOKTORGRADES

DER FAKULTÄT FÜR CHEMIE UND PHARMAZIE

DER LUDWIG-MAXIMILIANS-UNIVERSITÄT MÜNCHEN

**SYNTHESIS AND CHARACTERIZATION OF NEW AND  
ADVANCED ENERGETIC MATERIALS BASED ON  
AZOLES AND DIAZINES**



**IVAN GEORGIEV GOSPODINOV**

AUS

DOBRICH, BULGARIEN

2019

## **Erklärung**

Diese Dissertation wurde im Sinne von § 7 der Promotionsordnung vom 28. November 2011 von Herrn Professor Dr. Thomas M. Klapötke betreut.

## **Eidesstattliche Versicherung**

Diese Dissertation wurde eigenständig und ohne unerlaubte Hilfsmittel erarbeitet.

München, den 12. September 2019

---

IVAN GEORGIEV GOSPODINOV

Dissertation eingereicht am:

12. September 2019

1. Gutachter:

Prof. Dr. Thomas M. Klapötke

2. Gutachter:

Prof. Dr. Konstantin Karaghiosoff

Mündliche Prüfung am:

24. Oktober 2019

*This work is dedicated to my beloved father!*

**ГЕОРГИ ГОСПОДИНОВ ГАНЧЕВ**

# Acknowledgement

First of all, I would like to show my gratitude to and thank Prof. Dr. Thomas M. Klapötke for giving me the opportunity to do my Ph.D. thesis under his guidance. I am deeply grateful for the given freedom during my research and allowing me to investigate my own topics and ideas. I would like to thank Prof. Dr. Thomas M. Klapötke for the given opportunities to present my scientific results at many different international conferences during my time in his research group. Prof. Dr. Thomas M. Klapötke is not only a great mentor and scientist but also an incredible leader for which I thank him!

Secondly, I would like to express my gratitude to Prof. Dr. Konstantin Karaghiosoff who I met for the first time in the beginning of my education as a chemist. I would like to thank Prof. Dr. Konstantin Karaghiosoff not only for the endless NMR and crystal structure measurements, but also for the great conversations and all the shared wisdom during the years of my education. Prof. Dr. Konstantin Karaghiosoff is one of the sincerest and heartily professors I have ever met. In addition, I am very grateful to Prof. Dr. Konstantin Karaghiosoff for being the second supervisor of this thesis.

I would also to thank Dr. Jörg Stierstorfer for the provided help by solving all crystal structures, making all calculations for the heats of formation and also for proof reading all of my publications and this thesis. I would like to thank Dr. Jörg Stierstorfer for great discussions regarding chemistry and giving me advices with synthetic work.

I would like to thank also Ms. Irene Scheckenbach, which is the “beating hearth” of Prof. Dr. Thomas M. Klapötke`s group. I am deeply grateful for her help with all bureaucracy, which a Ph.D. student has to face at the university.

I want to express my gratitude to all members of the research groups of Prof. Klapötke and Prof. Karaghiosoff. We had some great conversations during our lunch and coffee breaks. In addition, I cannot forget to mention our “crazy, but funny” talks with Dr. Johann Glück, Dr. Marc Bölter, Cornelia Unger, Teresa Küblböck, Marcel Holler, Dr. Thomas Reith, Anne Friedrichs and Maximilian Wurzenberger. I share some precious and memorable moments with this incredible ladies and gentlemen. I will never forget our trips to Prague. I thank Dr. Johann Glück for organizing all mountain tours, Dr. Marc Bölter for organizing all ski trips and forcing me to buy ski gear and also Marcel Holler for helping me better understand complex energetic formulations and energetic systems. Cornelia Unger, Teresa Küblböck, Anne Friedrichs, Elena Reinhardt and Alicia Dufter must be thanked for being so kind and great toward me.

Marco Reichel is thanked for the great discussions regarding synthetic work and for being a great and friendly colleague.



To my former (Dr. Johann Glück, Dr. Benedikt Stiasny, Dr. Martin Härtel) and current (Marcel Holler, Anne Friedrichs, Maximilian Benz, Stefanie Heimsch, Greta Bikelyte, Marcus Lommel and Michael Gruhne) lab mates I want to thank for the great atmosphere in the laboratory and all great conversations in the early morning.

Stefan Huber is thanked for all sensitivity measurements during the course of this thesis and for proof reading some parts of this work.

Of course, I am very grateful to my bachelor and “F-Praktikum” students Maximilian Benz, Thaddäus Koller, Johannes Singer, Gustav Wulff, Jan Wilhelm Cremers, Daniel Axthammer, Marvin Ertelt and Stefan Wiedemann for their help during all synthetic work.

Last, but not least, I want to show my gratitude to the people who made this work possible: my family. I thank my mother for her support during my whole life and education and for believing in my potential. I want to thank my sister for her support and help during my whole education in Germany. At the end I would like to thank my beloved father, who showed me what it means to be a man, a husband and a father.

*Thank you!*

# Table of Content

<b>1. Introduction.....</b>	<b>1</b>
1.1. Overview .....	1
1.1.1. Definition .....	1
1.1.2. Classification .....	2
1.2. Design of New Secondary Explosives.....	6
1.2.1. Physico-chemical Properties .....	6
1.2.2. Project Origin .....	7
1.3. Objectives .....	11
1.4. References .....	14
<b>2. Summary and Conclusions.....</b>	<b>18</b>
2.1. Chapter 3: 3,4-Bis(4-nitramino-1,2,5-oxadiazol-3-yl)-1,2,5-furoxan (BNAFF).....	20
2.2. Chapters 4 and 5: Energetic Materials Based on the Pyridazine Scaffold .....	21
2.3. Chapter 6: 3,3'-Diamino-4,4'-dinitramino-5,5'-bi-1,2,4-triazole .....	23
2.4. Chapter 7: Polynitrated Derivatives Based on the 4,4'-Bipyrazole Scaffold .....	24
2.5. Chapters 8 and 9: Energetic Derivatives Based on TriNBPz and TNBPz·H <sub>2</sub> O .....	25
2.6. Chapter 10: 1,2,4-Triazol-3-yl-1,3,4-oxadiazole Based Energetic Materials.....	28
2.7. Chapter 11: Toward the Synthesis of 3,5-Diamino-4,6-dinitropyridazine .....	29
2.8. References .....	29
<b>3. Energetic Compounds Based on 3,4-Bis(4-nitramino-1,2,5-oxadiazol-3-yl)-1,2,5-furoxan (BNAFF).....</b>	<b>30</b>
3.1. Introduction .....	31
3.2. Experimental Section.....	32
3.2.1. General procedures.....	32
3.2.2. Synthesis.....	32
3.3. Results and Discussion .....	38
3.3.1. Crystal structures.....	39
3.3.2. NMR Spectroscopy .....	43

3.3.3.	Physicochemical properties .....	44
3.3.4.	Thermal behavior .....	46
3.3.5.	Sensitivities .....	46
3.3.6.	Detonation parameters.....	46
3.4.	Conclusion .....	47
3.5.	Acknowledgement .....	47
3.6.	References .....	47
3.7.	Supporting Information .....	50
3.7.1.	X-ray Diffraction.....	50
3.7.2.	Computations .....	53
3.7.3.	NMR Spectra.....	55
3.7.4.	References .....	56
<b>4.</b>	<b>Energetic Functionalization of the Pyridazine Scaffold: Synthesis and Characterization of 3,5-Diamino-4,6-dinitropyridazine-1-oxide.....</b>	<b>58</b>
4.1.	Introduction .....	59
4.2.	Results and Discussion .....	60
4.2.1.	X-ray diffraction.....	62
4.2.2.	<sup>15</sup> N NMR spectroscopy .....	64
4.2.3.	Physical and detonation properties.....	65
4.3.	Conclusions .....	69
4.4.	Experimental Section.....	69
4.4.1.	General Considerations .....	69
4.5.	Acknowledgements .....	74
4.6.	References .....	74
4.6.	Supporting Information .....	76
4.6.1.	Synthesis and general considerations .....	76
4.6.2.	X-ray diffraction.....	78
4.6.3.	Small-scale shock reactivity test (SSRT).....	82
4.6.4.	Computations .....	82
4.6.5.	Detonation parameters.....	84

4.6.6.	DTA.....	85
4.6.7.	<sup>1</sup> H and <sup>13</sup> C NMR spectra .....	86
4.6.8.	References .....	100
<b>5.</b>	<b>The Pyridazine Scaffold as a Building Block for Energetic Materials: Synthesis, Characterization and Properties.....</b>	<b>102</b>
5.1.	Introduction .....	103
5.2.	Results and Discussion .....	104
5.2.1.	Synthesis.....	104
5.2.2.	Crystal structures.....	106
5.2.3.	<sup>15</sup> N NMR spectroscopy .....	112
5.2.4.	Detonation properties .....	112
5.3.	Conclusions .....	115
5.4.	Experimental Section.....	115
5.5.	Acknowledgements .....	118
5.6.	Supporting Information .....	119
5.6.1.	Synthesis and general considerations .....	119
5.6.2.	X-ray diffraction.....	119
5.6.3.	Computations .....	122
5.6.4.	Detonation parameters.....	124
5.6.5.	Literature .....	124
<b>6.</b>	<b>Metal Salts of 3,3'-Diamino-4,4'-dinitramino-5,5'-bi-1,2,4-triazole in Pyrotechnic Compositions.....</b>	<b>126</b>
6.1.	Introduction .....	126
6.2.	Results and Discussion .....	128
6.2.1.	Syntheses .....	128
6.2.2.	Crystal Structures .....	129
6.2.3.	Thermal and energetic properties .....	133
6.2.4.	Pyrotechnical formulations .....	134
6.3.	Conclusions .....	136
6.4.	Experimental Section.....	136

6.5.	Acknowledgments .....	139
6.6.	References .....	139
6.7.	Supporting Information .....	141
6.7.1.	Crystallographic data.....	141
6.7.2.	References .....	144
<b>7.</b>	<b>Facile and Selective Polynitrations at the 4-Pyrazolyl Dual Backbone: A Straightforward Access to a Series of High-Density Energetic Materials .....</b>	<b>145</b>
7.1.	Introduction .....	146
7.2.	Results and discussion .....	147
7.2.1.	Synthesis.....	147
7.2.2.	Single crystal X-ray diffraction studies.....	149
7.2.3.	Physical and detonation properties.....	152
7.3.	Experimental.....	155
7.3.1.	General Information .....	155
7.3.2.	Crystallography .....	156
7.4.	Conclusions .....	159
7.5.	Conflicts of interest .....	160
7.6.	Acknowledgements .....	160
7.7.	Notes and references.....	160
7.8.	Supporting Information .....	162
7.8.1.	Experimental Procedures.....	162
7.8.2.	X-ray Diffraction.....	163
7.8.3.	Computations .....	183
7.8.4.	Detonation Parameters .....	184
7.8.7.	<sup>1</sup> H and <sup>13</sup> C NMR spectra .....	191
7.8.8.	<sup>15</sup> N NMR spectroscopy .....	196
7.8.9.	References .....	197
<b>8.</b>	<b>On a Midway Between Energetic Molecular Crystals and High-Density Energetic Salts: Crystal Engineering with Hydrogen Bonded Chains of Polynitro Bipyrazoles .....</b>	<b>200</b>
8.1.	Introduction .....	201

8.2.	Results and Discussion .....	204
8.2.1.	Synthesis.....	204
8.2.2.	Single crystal X-ray diffraction studies.....	204
8.2.3.	Toxicity assessment.....	214
8.2.4.	Physical and detonation properties.....	214
8.3.	Conclusions .....	218
8.4.	Experimental.....	218
8.4.1.	Crystallography .....	218
8.5.	Conflicts of interest .....	219
8.6.	Acknowledgements .....	219
8.7.	References .....	219
8.8.	Supporting Information .....	222
8.8.1.	General Information .....	222
8.8.2.	Synthesis.....	223
8.8.3.	Crystallography .....	233
8.8.4.	Computations .....	254
8.8.5.	References .....	255
<b>9.</b>	<b>Energetic Derivatives of 3,3',5,5'-Tetranitro-4,4'-bipyrzole (TNBPz): Synthesis, Characterization and Properties.....</b>	<b>259</b>
9.1.	Introduction .....	259
9.2.	Results and discussion.....	261
9.2.1.	Synthesis.....	261
9.2.2.	Single crystal X-ray diffraction studies.....	262
9.2.3.	<sup>15</sup> N NMR spectroscopy .....	268
9.2.4.	Toxicity assessment.....	269
9.2.5.	Physical and detonation properties.....	270
9.3.	Conclusions .....	274
9.4.	Experimental Part .....	275
9.4.1.	General Information .....	275
9.4.2.	Synthesis.....	275

9.5. Conflicts of interest .....	281
9.6. Acknowledgements .....	281
9.7. References .....	282
9.8. Supporting Information .....	284
9.8.1. Synthesis and general considerations .....	284
9.8.2. X-ray diffraction.....	284
9.8.3. Computations .....	287
9.8.4. References .....	289
<b>10. Combination of Different Azoles – 1,2,4-Triazolyl-1,3,4-Oxadiazoles as Precursor for Energetic Materials .....</b>	<b>291</b>
10.1. Introduction .....	292
10.2. Results and Discussion .....	293
10.2.1. Synthesis.....	293
10.2.2. NMR and Vibrational Spectroscopy .....	295
10.2.3. X-Ray crystallography .....	295
10.2.4. Thermal Analysis, Sensitivities and Physicochemical properties .....	298
10.3. Conclusions .....	300
10.4. References .....	300
10.5. Supplementary Information.....	303
10.5.1. X-ray Diffraction.....	303
10.5.2. Heat of formation calculations .....	305
10.5.3. Experimental Part.....	306
10.5.4. Crystal Structures .....	312
10.5.5. References .....	313
<b>11. Toward the Synthesis of 3,5-Diamino-4,6-dinitropyridazine.....</b>	<b>316</b>
11.1. Introduction .....	316
11.2. Results and Discussion .....	317
11.2.1. Synthesis.....	317
11.2.2. NMR Spectroscopy .....	319
11.2.3. Crystal Structures .....	321

11.2.4. Physico-chemical Properties .....	328
11.3. Conclusions .....	331
11.4. Experimental Part .....	331
11.4.1. General Information .....	331
11.4.2. Synthesis.....	332
11.5. References .....	335
<b>12. Appendix.....</b>	<b>338</b>
1. List of Abbreviations.....	338
2. Curriculum Vitae .....	341



# 1. Introduction

## 1.1. Overview

### 1.1.1. Definition

With progressing advances in modern science, the design and synthesis of novel energetic materials are evolving to develop a new set of high-energy density materials which combine desirable characteristics (*e.g.* excellent performance, vulnerability, insensitivity, stability and environmental safety) with the modern even more challenging application purposes. A more general definition for an energetic material is “a metastable chemical compound or mixture which contains both fuel and oxidizer and can undergo a chemical reaction which results in a rapid release of the stored energy in form of gas and pressure.”<sup>[1-3]</sup> This interpretation of an energetic material is derived from the definition given by the *American Society for Testing and Materials* (“chemical compounds or mixtures that contain both fuel and oxidizer and rapidly react to release energy and gas”).<sup>[4]</sup>

The history and development of energetic materials has been extensively reported in the literature and therefore only a short overview over the most important breakthroughs in this field will be given.<sup>[5]</sup> The accidental discovery of black powder in China (220 BC), a mixture of potassium nitrate, sulfur and charcoal, was most likely the first energetic composition to be ever made.<sup>[6]</sup> It was not until the 19<sup>th</sup> century where with the vastly advancing industrialization, the demand for new more powerful energetic materials was needed. This resulted in the synthesis of numerous new energetic compounds during the course of the next century. Firstly, the syntheses of nitroglycerine (NG),<sup>[7]</sup> mercury fulminate ( $\text{Hg}(\text{CNO})_2$ ),<sup>[8]</sup> nitrocellulose (NC)<sup>[9]</sup> and picric acid<sup>[10]</sup> were reported and used for civil and military applications. These milestones were followed with the development of the next generation of energetic materials 2,4,6-trinitrotoluene (TNT),<sup>[11-16]</sup> *N*-methyl-*N*-2,4,6-tetranitroanilin (Tetryl)<sup>[17]</sup> and pentaerythritetranitrat (PETN, Nitropenta).<sup>[18]</sup> Finally, the next big achievement was the preparation of the still in use high performing explosives 1,3,5-trinitro-1,3,5-triazine (RDX),<sup>[19-22]</sup> 1,3,5,7-tetranitro-1,3,5,7-tetrazocine (HMX),<sup>[23-26]</sup> 6,8,10,12-hexanitro-2,4,6,8,10,12-hexaazaisowurtzitane (CL-20),<sup>[27-29]</sup> 1,2,3,4,5,6,7,8-octanitro-pentacyclo-[4.2.0.0<sup>2,5</sup>.0<sup>3,8</sup>.0<sup>4,7</sup>]octan (ONC)<sup>[30]</sup> and the insensitive and heat resisting explosives 1,3,5-triamino-2,4,6-trinitrobenzene (TATB)<sup>[31-35]</sup> and 1,2-bis(2,4,6-trinitrophenyl)ethylen (HNS).<sup>[36]</sup> Modern trends in research are focused on using nitrogen- and oxygen-rich heterocycles (*e.g.* azoles, pyridines, diazines, triazines and tetrazines) which exhibit high heat of formation and low percentage on C and H atoms.<sup>[37-39]</sup> This class of energetic materials in which a heterocyclic compound is the backbone and is used for energy storage is going to be the main topic in this thesis. **Figure 1** shows few of the above mentioned energetic materials.

## Introduction

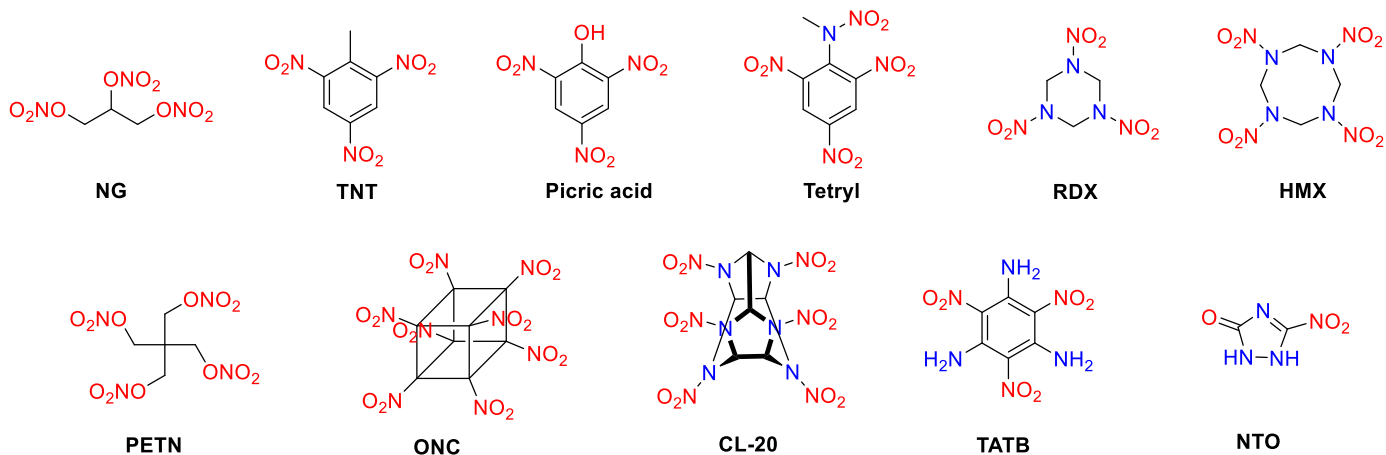


**Figure 1.** Overview of well-known energetic materials, their Lewis structures and the used acronyms for the structures.

### 1.1.2. Classification

A various number of classifications for energetic materials can be found in the literature.<sup>[40]</sup> Depending on the application purpose of the compound, energetic materials can be generally subclassified in three main branches; explosives, propellants and pyrotechnics. Additionally, there are many criteria that have to be considered by the classification of an explosive material and few important ones are:

- according to their chemical nature/ingredient;
  - carbon based
  - based on nitrogen-rich heterocycles
- according to their use, for example military or civil application;
  - general purpose missiles
  - deep oil drilling
- according to their behaviour toward outer stimuli for example mechanical stress or thermal stimuli.<sup>[40]</sup>
  - explosives which are able to undergo a fast DDT when confined or unconfined (primary explosives), secondary and tertiary explosives

Explosives can be divided into primary and secondary explosives, where the former are usually a very sensitive less performing compound, which is used to initiate a more potent and less sensitive secondary

explosive. On the other hand, depending on the application purpose secondary explosives can be further divided into main charge explosives and booster explosives. In comparison to explosives which are generally used for detonation purposes, propellants are compounds which should not detonate. Latter usually deflagrate in a closed chamber with the release of a significant amount of gases, which leads to increase in pressure in the vessel and can provide propulsion and can accelerate an object (*e.g.* missile, projectiles, rockets).<sup>[2,41-43]</sup> Pyrotechnics are usually mixtures which are used for audio or visual effects (gas emission, heat/light generation, explosion, fire, sound generation). **Figure 2** shows the classification for energetic materials.

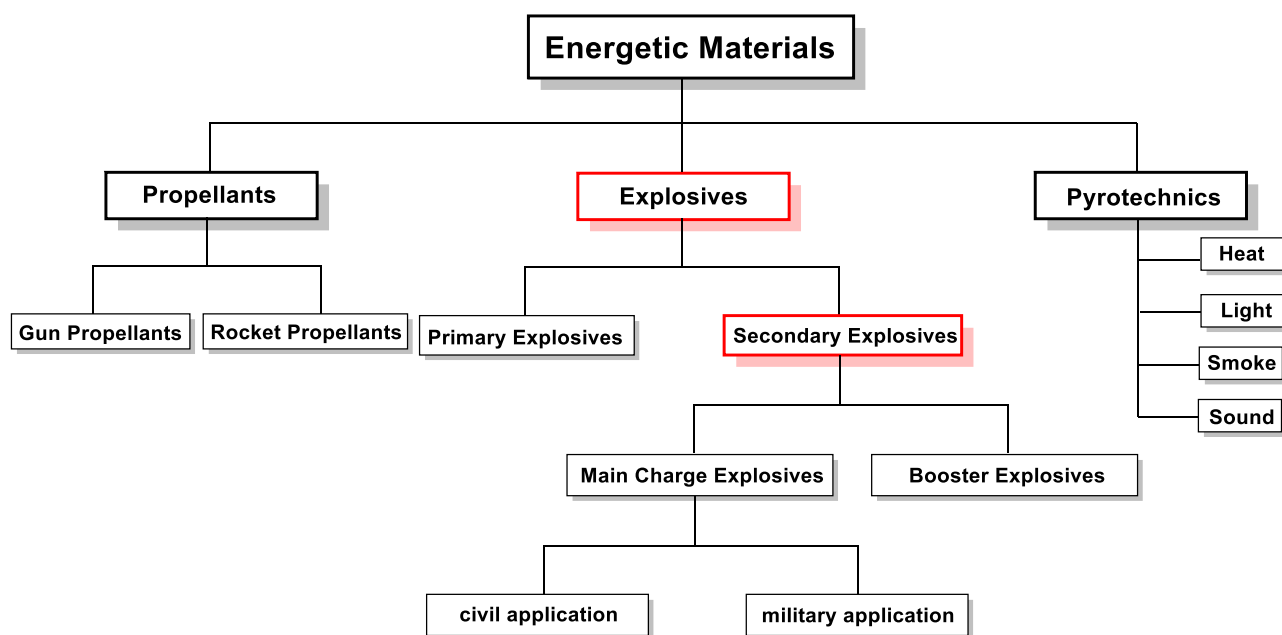


**Figure 2.** Classification of energetic materials into the main branches: Explosives, Propellants and Pyrotechnics. The red marked sections are going to be the main topic of this thesis.

### 1.1.2.1. Primary Explosives

Compounds or mixtures that can be easily initiated by a non-explosive impulse (impact, friction, spark, flame or heat) are assigned to the class of primary explosives. Such explosives exhibit high sensitivity towards destructive stimuli in comparison to secondary explosives and the shock wave generated from the sensitive explosive has the desired efficiency to initiate propellants or main charge explosives. For an primary explosive to be efficient in its application, it should show a fast **deflagration-to-detonation transition** also known in the literature as DDT.<sup>[5,6,40]</sup> The term deflagration is used to describe the propagation of a flame with less than the speed of sound throughout the unreacted material. Typical values for the burn rate of a deflagration are about  $10^2 \text{ m s}^{-1}$ . Under some conditions, a deflagration can evolve to detonation, when the reaction front reaches the speed of sound in the unreacted material and the

## Introduction

generated explosive impulse (shock wave) is used for the initiation of a more insensitive explosive. Typical values for detonation velocity and heat of explosion of primary explosives are in the range of 3500–5000 m s<sup>-1</sup> and 1000–2000 kJ kg<sup>-1</sup>, respectively.<sup>[5]</sup> One of the first ever reported primary explosives are mercury fulminate (Hg(CNO)<sub>2</sub>), lead azide (Pb(N<sub>3</sub>)<sub>2</sub>), silver azide (AgN<sub>3</sub>), cadmium azide (Cd(N<sub>3</sub>)<sub>2</sub>) and lead styphnate (Pb(C<sub>6</sub>H<sub>3</sub>N<sub>3</sub>O<sub>8</sub>)). Nowadays used primary explosives in initiation devices (blasting caps, detonators and etc.) are still heavy metal based explosives (e.g. Pb(N<sub>3</sub>)<sub>2</sub>, AgN<sub>3</sub> and Pb(C<sub>6</sub>H<sub>3</sub>N<sub>3</sub>O<sub>8</sub>)).

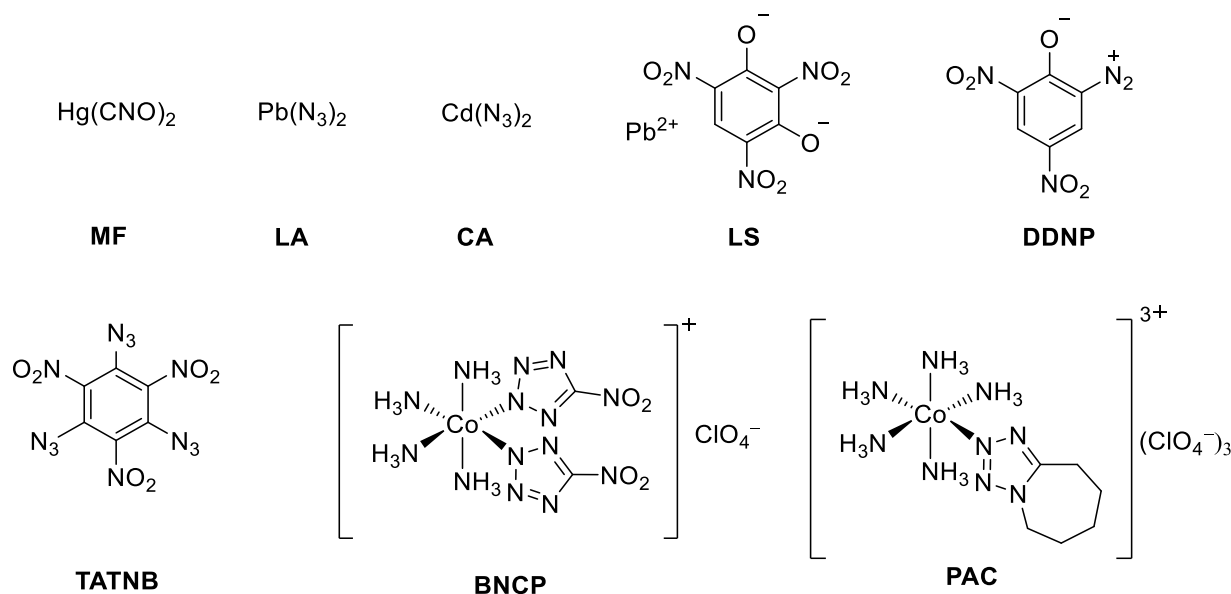


**Figure 3.** Commonly used primary explosives and new generation of primary explosives: mercury fulminate (MF), lead azide (LA), cadmium azide (CA), lead styphnate (LS), 2-diazo-4,6-dinitrophenol (DDNP), 1,3,5-triazido-2,4,6-trinitrobenzol (TATNB), tetrammin-*cis*-bis(5-nitrotetrazolato-*N*<sup>2</sup>)cobalt(III) perchlorate (BNCP) and pentammin(1,5-cyclopentamethylentetrazolato-*N*<sup>3</sup>)cobalt(III) perchlorate (PAC).

The advantages of this heavy metal based primary explosives are low cost of production, good performance, easy ignitability and a small amount of the material is required for the initiation of the booster charge. However, the main disadvantage of the most in use primary explosives is the high toxicity of the heavy metal cations (Pb, Ag or even Cd elements). These metals have a major negative impact on humans and nature.<sup>[44-46]</sup> A study from 1991 on a FBI shooting range showed that employs suffered from a lead poisoning.<sup>[47]</sup> These studies raised the concern on the negative impact of primary explosives, which led to extensive increase on new research in this field. New heavy metal free explosives like DDNP and TATNB have been reported and show promising properties as possible replacements. However, a still remaining problem with this type of organic based primary explosives like DDNP and TATNB is their long-term stability. Prolonged studies show slow decomposition of TATNB and loss of energetic groups.

A new emerging branch that could solve the toxicity problem of primary explosives is the laser ignitable energetic complex systems.<sup>[48-54]</sup> BNCP and PAC are two prominent examples for laser ignitable primary explosives based on Co(III) metal.<sup>[55]</sup> The most important and modern primary explosives are shown in **Fig. 3**.

### 1.1.2.2. Secondary Explosives

As before mentioned secondary explosives are in comparison to primary explosives less sensitive to insensitive to destructive stimuli, cannot be easily initiated, show in general slower DDT and are in general more powerful. General performance data for secondary explosives are in the range of 6500–9000 m s<sup>-1</sup> for the detonation velocity, 5000–6000 kJ kg<sup>-1</sup> for the heat of explosion and the sensitivity values are as followed IS =  $\geq 4$  J, FS =  $\geq 50$  N and ESD =  $\geq 0.1$  J.<sup>[5]</sup> The performance of a high (secondary) explosive depends mainly on the density, oxygen balance (OB) and the heat of formation. The main performance criteria for high explosive depending on this application are detonation energy ( $-A_{EU}$ ), detonation temperature ( $T_{C-J}$ ), detonation pressure ( $p_{C-J}$ ), detonation velocity ( $D_{C-J}$ ) and volume of gas released per kg explosives ( $V$ ).

In addition to the previously reported classification, secondary explosives can be divided into three main branches when it comes to the research purpose of the material: high performance, low sensitivity and low toxicity.<sup>[5]</sup> A common problem in this field is the difficulty to combine all these three parameters in one molecule or mixture. Usually high performing secondary explosives show high sensitivity toward destructive stimuli (impact, friction, electrostatic discharge), which is not desired and can result in accidental initiation. Whereas, less sensitive explosives show lower performance, but more safety and can be easily handled. The problem with insensitive munition is the difficulty to initiate them and therefore more powerful initiators are required. Combining performance with sensitivity in one molecule is the “holy grail” for an EM synthetic chemist. Third and recently arising topic in this field is also the high toxicity of currently used explosives such as RDX, TNT and TATB.<sup>[56,57]</sup> New eco-friendly materials are required, which should show no toxicity and their degradation products should also be not dangerous for humans and nature.

### 1.1.2.3. Propellants

Propellants can be divided into gun propellants and rocket propellants. In comparison to explosives, which detonate and generate a shock wave, propellants combust or deflagrate and are used for their propulsive force. Solid gun propellants can be subclassified into single-, double- and triple-based propellants. In the case of single-based propellants nitrocellulose (NC) is used as the main energetic ingredient.<sup>[5]</sup> The application spectrum of single-based propellants extends from pistols to artillery weapons. Double-based

## Introduction

propellants charges consist of NC and nitroglycerine (blasting oil), which increases the performance. In addition, insensitive plasticizers can be used in different amounts depending on the application purpose. Triple-based propellants consist of NC, NG and nitroguanidine (NQ) or other energetic ingredients. NQ lowers the burning temperature and affects the CO/N<sub>2</sub> ration. This reduces the formation of iron carbide and preserves the barrel wear from erosion.

Rocket propellants can be divided into liquid and solid rocket propellants. Examples for liquid propellants are non-hypergolic mixtures (H<sub>2</sub>/O<sub>2</sub>) and hypergolic mixtures (N<sub>2</sub>O<sub>4</sub> with unsymmetrical dimethylhydrazine or HNO<sub>3</sub> with N<sub>2</sub>H<sub>4</sub>).<sup>[58]</sup> The classical solid rocket propellants are based on ammonium perchlorate (AP) and ammonium nitrate (AN) metal mixtures. The common problem with these mixtures is the toxicity of AP and the needed phase-stabilization of AN. In addition, the perchlorate anion in AP is biomimetic to the iodide in our thyroid which can result to hyperthyroidism.<sup>[59,60]</sup> Besides during the burning process of AP based rockets hydrochloric acid is formed, which leaves white smoke trail.<sup>[61]</sup> A promising replacement for AP is ammonium dinitramide (ADN). ADN has excellent properties e.g. high heat of formation, good oxygen balance, high nitrogen content and moderate sensitivities. These qualities of ADN makes it a good replacement for commonly used solid state propellants.

### 1.1.2.4. Pyrotechnics

In comparison to explosives, pyrotechnics usually do not contain oxidizer and fuel in one molecule. Pyrotechnics can be divided into light, noise, smoke and chemical product generating pyrotechnics.<sup>[62-64]</sup> To the fuel and oxidizer other additives like colorant and binders are added to the pyrotechnic mixture depending on the application purpose. Commonly used oxidizers in pyrotechnic mixtures are potassium perchlorate (KClO<sub>4</sub>, PP) and ammonium perchlorate (NH<sub>4</sub>ClO<sub>4</sub>, AP). As previously mentioned, perchlorate based energetic materials have a negative environmental impact. Both salts show moderate solubility in water and can result to a groundwater contamination.<sup>[61]</sup> Although AP and PP show a negative impact and are not eco-friendly they are still used in current mixtures due to good stability, oxygen balance and low cost of production.

## 1.2. Design of New Secondary Explosives

### 1.2.1. Physico-chemical Properties

As previously mentioned there are few important parameters which have to be considered when designing and synthesizing new secondary explosives. The detonation velocity ( $D$ ), the heat of explosion ( $Q$ ) and the detonation pressure ( $p_{C-J}$ ) are three of the most crucial performance criteria for high explosives. These performance parameters can be influenced by altering the heat of formation (HOF) of the explosive, by

## Introduction

increasing the oxygen balance (OB) and - the most important parameter - by raising the density of the material. Kamlet and Jacobs suggested empirical equations which show the relationship between the detonation velocity and the detonation pressure. According to **Eq. I** and **II** the detonation velocity of an explosive is proportional to the loading density, whereas the detonation pressure is square of the loading density.<sup>[2,5]</sup>

$$p_{C-J} [\text{kbar}] = K\rho_o^2\Phi \quad (\text{Eq. I})$$

$$D [\text{mm } \mu\text{s}^{-1}] = A\Phi^{0.5}(1+B\rho_o) \quad (\text{Eq. II})$$

with  $K = 15.88$ ,  $A = 1.01$ ,  $B = 1.30$ ,  $\rho_o$  = loading density,  $\Phi = N(M)^{0.5}(Q)^{0.5}$  with  $N$  = number of moles of gas released per gram of explosive [mol/g],  $M$  = mass of gas in gram per mole of gas [g/mol],  $Q$  = heat of explosion [cal/g];

In addition, to these physico-chemical properties a good oxygen balance ( $\Omega$ ) is desired for explosives. The oxygen balance is defined as the relative amount of oxygen in deficit or excess in order to achieve a complete oxidation of the C/H/N/O-based explosive to carbon monoxide (or carbon dioxide), water and elemental nitrogen. Equation 3 shows how the  $\Omega$  can be calculated according to  $\text{CO}_2$  or  $\text{CO}$  in percentage (%) for a  $\text{C}_a\text{H}_b\text{N}_c\text{O}_d$  based explosive. The letter  $M$  represents the molecular mass of the explosive.

$$\Omega_{\text{CO}_2} = \frac{[d - (2a) - \frac{b}{2}] \times 1600}{M} \quad \Omega_{\text{CO}} = \frac{[d - a - \frac{b}{2}] \times 1600}{M} \quad (\text{Eq. III})$$

### 1.2.2. Project Origin

Central goal in the design of new energetic materials is the synthesis of monomolecular compounds such as TNT, which contain an oxidizing component and a fuel component. As above mentioned the performance of an explosive generally depends on a high density, good oxygen balance and high heat of formation. All these three parameters can be easily manipulated by selectively choosing the right synthetic backbone and using the right explosophore groups ( $-\text{NO}_2$ ,  $-\text{ONO}_2$ ,  $-\text{NNO}_2$ ,  $-\text{N}_3$ , etc.). Commonly known secondary explosives are based on a carbon backbone (fuel), which is oxidized during the reaction to  $\text{CO}/\text{CO}_2$ . Traditional C/H/N/O based explosives within this class are TNT, RDX, HMX, HNS, TATB, TNAZ, ONC, CL-20 and TEX. The last four mentioned compounds (TNAZ, ONC, CL-20 and TEX) exhibit their excellent properties and performance due to the high ring strain or a high cage strain. The additional energy stored in the small ring or compact cage compound can be released upon decomposition. CL-20 is currently the benchmark molecule for high performing secondary explosive. However, still a major throwback is their complicated and extensive synthesis, which makes scale-up reactions difficult. Although many of the above explosives exhibit good properties, can be easily synthesized or can be used

## Introduction

for special applications, they show a negative ecological impact and are strongly polluting agents. In the case of TNT, RDX, HMX and TATB it has been shown that their degradation products can be toxic and lead to the following diseases jaundice, kidney diseases and methemoglobinemia.<sup>[2,56,65,66]</sup> In addition, this type of aromatic/nitramino based explosives exhibit high toxicity which can range from mutagenic to carcinogenic activity.<sup>[67,68]</sup> Additionally RDX, HMX and CL-20 show reductive decomposition of the nitramino moiety, which forms reactive mutagenic N-nitroso derivatives.<sup>[2]</sup>

For the past few decades the research on high nitrogen containing explosives has received a great deal of interest as possible solution for the high toxicity of already in use materials. Compounds containing high amount of nitrogen (*e.g.* azoles, diazines, triazines, tetrazines and etc.) have a large number of C–N and/or N–N bonds, which results usually in high positive heats of formation. Nitrogen-rich high explosives obtain their good performance from the large heat of formation and not from the oxidation of the carbon backbone. Additionally, these materials show often excellent thermal stability, low sensitivity toward destructive stimuli (impact, friction and spark) and can be easily synthesized. An excellent property of nitrogen-rich based explosives is the high amount of nitrogen in the molecule, which can be released in form of nitrogen gas (N<sub>2</sub>) upon decomposition. The big advantage of nitrogen is that the bond energy for single (N–N 160 kJ/mol), over double (N=N 418 kJ/mol) to triple bonds increases (N≡N 954 kJ/mol), whereas for carbon exactly the opposite is true.<sup>[2,69,70]</sup> During the decompositions this large thermodynamic driving force can be used, thus making nitrogen-rich heterocycles excellent candidates as a core structures for explosives. An interesting class of heterocycles are the azoles, which are five membered heterocycles. Azoles have also usually high densities, allow good oxygen balance, exhibit high thermal stability and upon decomposition release a large amount of gaseous products (N<sub>2</sub>, CO, CO<sub>2</sub>, NO<sub>x</sub>, H<sub>2</sub>O).

The arising challenge in the field of secondary explosives lies in the emerging necessity of improving some desirable characteristics like performance, stability, ignitability and lowering of the toxicity impact. Combining all these molecular properties in one compound has been a great deal of interest. Many synthesized high performing secondary explosives exhibit excellent performance (in terms of detonation velocities and detonation pressure), high densities and high heats of formation. However, a major drawback of the latter are high sensitivities *e.g.* toward impact, flame, friction, electrostatic discharge, low thermal stability and also high toxicity. Whereas highly insensitive and thermally stable secondary explosives show low performance and low ignitability. Finding suitable synthetic ways to design new secondary explosives with excellent performance like HMX and excellent sensitivities like TATB has been of major interest in the HEDM community.



## Introduction

There are different possibilities for a synthetic chemist to try to combine good performance with low sensitivity in a monomolecular based explosive. There are many alternatives that can be used in order to increase or improve the performance of a secondary explosive. The first possibility is to introduce as much explosophoric groups as possible ( $-\text{NO}_2$ ,  $-\text{ONO}_2$ ,  $-\text{NNO}_2$ ,) to the carbon backbone. Prominent examples for this type of explosives are RDX, HMX and PETN. The biggest disadvantage is, however, the high sensitivity of the materials, which is attributed to the unstable moieties in the molecule like the nitramino groups in RDX and HMX. The second strategy that can be used in order to increase the performance of a newly synthesized explosive is to use a small ring system or a cage compound as a building block. These systems not only show high densities, and high heats of formation, but also store an enormous amount of energy in the small ring or cage which can be used upon decomposition. Excellent examples are TNAZ, CL-20 and ONC. The third strategy to increase the performance of explosives is to use nitrogen- and oxygen-rich heterocycles as a building system. As previously mentioned the latter systems exhibit the desired properties for an explosive; high heat of formation, high densities and in addition show good stabilities toward external stimuli. In addition, the combination of different heterocycles in an annulated system results in materials with excellent properties.<sup>[71]</sup>

Increasing the stability of new explosives is the second important necessity when it comes to the design of new materials. In order to achieve these difficult task, scientists have developed many different strategies and reported them in the literature. Agrawal reported four different ways on how to increase the stability of an secondary explosive:<sup>[40]</sup>

- 1) introduction of amino groups
- 2) ionic salt formation.
- 3) introduction of conjugation
- 4) condensation with a triazole ring

There are many examples of reported high explosives, which have been synthesized by using one of the above mentioned strategies. The first approach covers high explosives which contain amino groups, which if used properly can result in stabilization of the intra- and intermolecular structure. This work will extend this strategy by introducing  $\text{NO}_2$  and  $\text{NH}_2$  groups selectively to specific heterocyclic systems. In addition, the conversation of tertiary amines to their  $\text{N}^+-\text{O}^-$  derivative can be investigated. The combination of alternating  $\text{NO}_2/\text{NH}_2$  system (push/pull system) into a nitrogen-rich heterocycle with an  $\text{N}^+-\text{O}^-$  moiety results in high performing, insensitive and thermally resistant secondary explosives.

## Introduction

Excellent examples from the literature are TATB, LLM-116, LLM-119, FOX-7, ANPyO, ANPZ, LLM-105 and TKX-50. Their Lewis structures are shown in **Figure 4**.

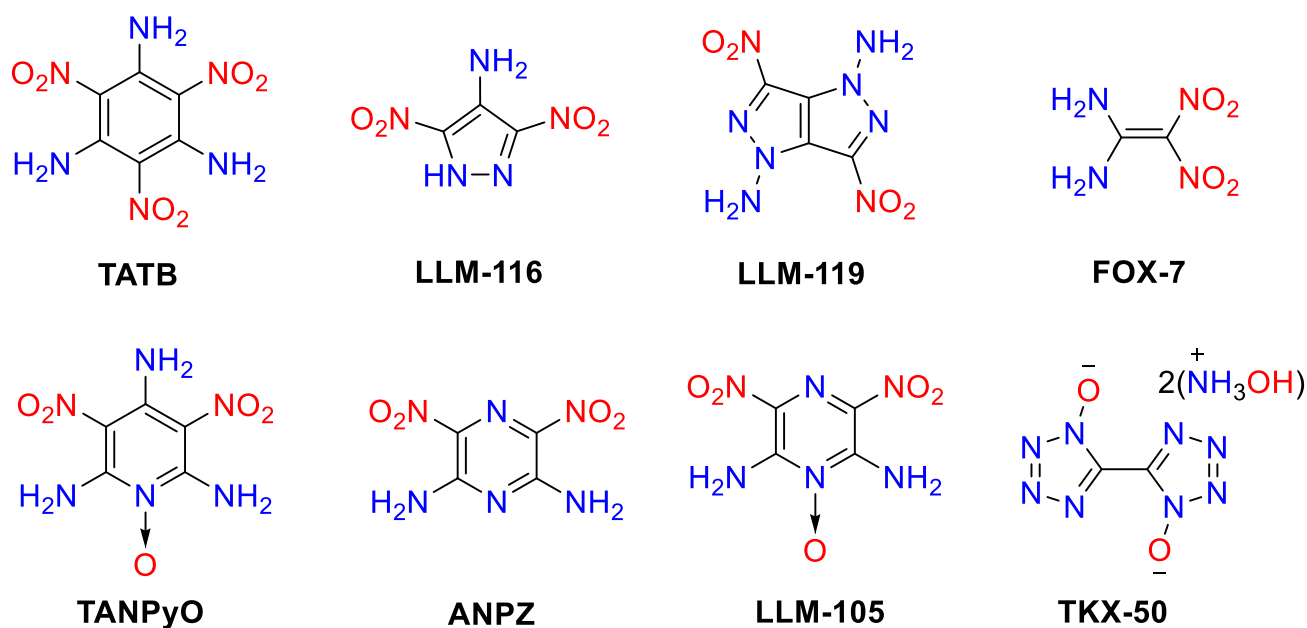


**Figure 4.** Prominent examples for explosives based on benzene and different heterocycles containing push/pull systems and the N<sup>+</sup>–O<sup>–</sup> moiety. 1,3,5-Triamino-2,4,6-trinitrobenzene (TATB), 4-amino-3,5-dinitropyrazole (LLM-116), 1,4-diamino-3,6-dinitropyrazolo[4,3-c]pyrazole (LLM-119), 1,1-diamino-2,2-dinitroethene (FOX-7), 2,4,6-triamino-3,5-dinitropyridine-1-oxide (TANPyO), 2,6-diamino-3,5-dinitropyrazine (ANPZ), 2,6-diamino-3,5-dinitropyrazine-1-oxide (LLM-105) and dihydroxylammonium 5,5'-bistetrazole-1,1'-dioxide (TKX-50).

Energetic salts have received a great amount of attention in the last two decades. These materials often exhibit high heats of formation, low vapor pressure in comparison to the nonionic precursor, good stability toward thermal shock and high densities.<sup>[2,5,72]</sup> The class of five membered aromatic heterocycles (azoles) has been extensively investigated in this regard. Major advances in the chemistry of imidazoles, pyrazoles, triazoles, tetrazoles and pentazoles, have been achieved as possible core for energetic salts.<sup>[73]</sup> Introducing explosophoric groups to these heterocycles can result in good precursors for energetic salts.

1,2-Bis(2,4,6-trinitrophenyl)ethylene (HNS) and 4,6-bis(5-amino-3-nitro-1,2,4-triazolyl)5-nitropyrimidine (DANTNP) are good examples for explosives based on a conjugated system or condensed nitrotriazole explosives. HSN is a thermally insensitive explosive that finds application in the civil sector (deep oil drilling).

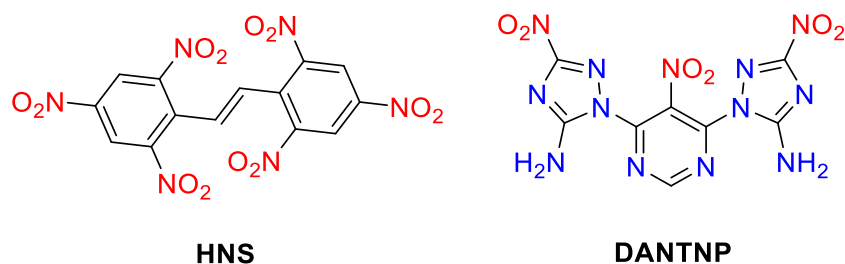


**Figure 5.** Lewis structures of 1,2-bis(2,4,6-trinitrophenyl)ethylene (HNS) and 4,6-bis(5-amino-3-nitro-1,2,4-triazolyl)5-nitropyrimidine (DANTNP).

### 1.3. Objectives

The necessity to combine good performance with excellent stability in one molecule continues to be the highest priority, when it comes to the synthesis and design of new explosives. Desired performance of new secondary explosives should be in the range of commonly known RDX and HMX, or even greater than  $D_{C-J} = > 8500 \text{ m s}^{-1}$ ,  $p_{C-J} = > 340 \text{ kbar}$ , whereas the desired sensitivities should be in the range of LLM-105 and TATB ( $IS = > 20 \text{ J}$ ,  $FS = > 360 \text{ N}$ ). The main purpose of this thesis is to investigate various oxygen- and nitrogen-rich heterocycles as possible precursors for new explosives. As previously explained nitrogen-rich heterocycles exhibit attractive properties like high densities, high positive heats of formation, excellent thermal stabilities and low sensitivity toward destructive stimuli. Thus making heterocycles perfect precursor for high explosives. This work investigates five-membered and six-membered nitrogen- and oxygen-rich heterocycles as possible starting materials for high performing, insensitive secondary explosives. Different heterocycles (such as 1,3,4-oxadiazole, 1,2,5-oxadiazole, 1,2,5-oxadiazole-1-oxide, pyrazole, 1,2,4-triazole) were synthesized and selectively functionalized with explosophoric groups. Additionally, the *N*-functionalization (methylation and amination) and the formation of nitrogen-rich ionic compounds based on the previously mentioned azoles was investigated. **Figure 6** shows the calculated gas phase enthalpies for various five-membered rings. All investigated derivatives in this work are marked with a red arrow.

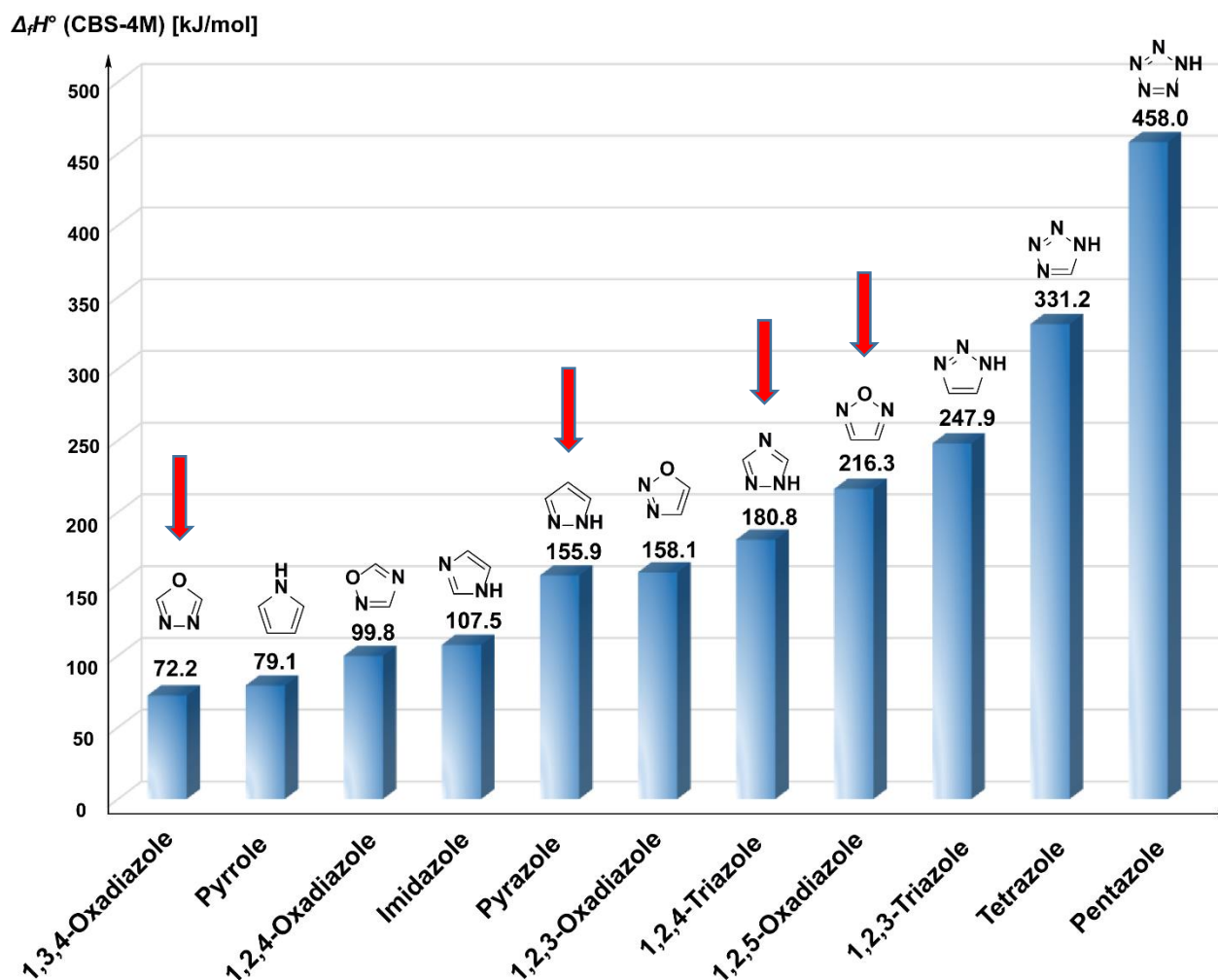


**Figure 6.** Calculated enthalpies of formation for various azole derivatives. Gas phase enthalpies of formation were calculated using the atomized method ( $\Delta_f H^\circ_{(g,M,298)} = H_{(g,M,298)} - \sum H^\circ_{(g,Ai,298)} + \sum \Delta_f H^\circ_{(g,Ai,298)}$ ) using Gaussian09 computed CBS-4M electronic enthalpies.

In addition to the five-membered heterocycles, the relative unexplored 1,2-diazine scaffold (pyridazine) was also synthesized and investigated as possible energetic precursor. The diazines can be deduced from benzene by replacing two of the ring carbon atoms with nitrogen. There are three possible diazine isomers respectively to the position of the nitrogen atoms to each other in the ring system, giving rise to pyridazine, pyrimidine and pyrazine. The pyrazine scaffold is easily accessible and has been already modified by scientists and new pyrazine energetic materials with tailored properties have been already reported (ANPZ and LLM-105). However, the selective modification of the pyridazine scaffold has not been reported and it appears that the electrophilic nitration on this heterocycle is very complex. In this work the selective electrophilic nitration, the selective introduction of alternating push/pull ( $\text{NH}_2/\text{NO}_2$ ) groups and the introduction of the  $\text{N}^+-\text{O}^-$  moiety into the pyridazine heterocycle is investigated. **Figure 7** displays

all studied systems in this work. The different colored arrows represent specific functionalization of the desired scaffold.

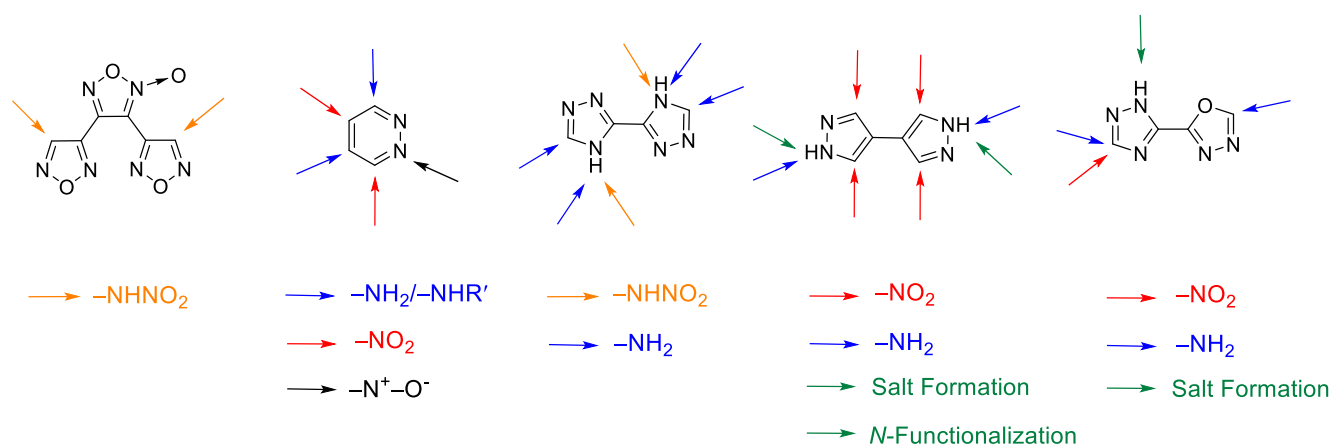


**Figure 7.** Lewis structures of all investigated heterocycles in this thesis. Under every molecule the performed functionalization of the corresponding heterocycle is presented: introduction of a nitramino moiety (orange arrow), introduction of amino groups, secondary and tertiary amines (blue arrow), *N*-oxidation (black arrow), direct electrophilic *C*-nitration (red arrow), formation of ionic derivatives and/or *N*-functionalization (green arrow).

### 1.4. References

- [1] P. C. Schmid, *Dissertation*, Ludwig-Maximilians-Universität München, **2016**, p. 6.
- [2] H. Gao, J. M. Shreeve, *Chem. Rev.* **2011**, *111*, 7377–7436.
- [3] D. Piercey, *Dissertation*, Ludwig-Maximilians-Universität München, **2013**, p. 4.
- [4] [www.astm.org](http://www.astm.org) (accessed 10.06.2019)
- [5] T. M. Klapötke, *Chemistry of High-Energy Materials*, 4th Ed., De Gruyter, Berlin, **2017**.
- [6] J. Akhavan, *The Chemistry of Explosives*, 2nd ed., RSC Paperbacks, Cambridge, United Kingdom, **2004**.
- [7] [http://www.nobelprize.org/alfred\\_nobel/biographical/patents.html](http://www.nobelprize.org/alfred_nobel/biographical/patents.html) (accessed 21.06.2019).
- [8] W. Beck, J. Evers, M. Göbel, G. Oehlinger, T. M. Klapötke, *Z. Anorg. Allg. Chem.* **2007**, *633*, 1417–1422.
- [9] J. B. Bernadou, *Smokeless Powder, Nitro-Cellulose, and Theory of the Cellulose Molecule*, Triese Publishing, **2017**.
- [10] H. Sprengel, British Patent #901, **1871**.
- [11] J. Wilbrand, *Annalen der Chemie und Pharmacie* **1863**, *128*, 178–179.
- [12] A. V. Samet, V. N. Marshalkin, K. A. Lyssenko, V. V. Semenov, *Russ. Chem. Bull.* **2009**, *58*, 347.
- [13] C. W. An, F. S. Li, X. L. Song, Y. Wang, X. D. Guo, *Propellant, Explos., Pyrotech.* **2009**, *34*, 400.
- [14] J. C. Oxley, J. L. Smith, J. Yue, J. Moran, *Propellants Explos. Pyrotech.* **2009**, *34*, 421.
- [15] C. E. Gregory, *Explosives for North American Engineers*, Vol. 5; Trans Tech Publications: Clausthal-Zellerfeld, Germany, **1984**.
- [16] T. L. Davis, *The Chemistry of Powder and Explosives*, Vol. 2; Wiley: New York, **1943**.
- [17] a) K. K. Andreev, *Explosivstoffe* **1962**, *10*, 203–212. b) K. K. Andreev, *Explosivstoffe* **1962**, *10*, 229–237.
- [18] J. Köhler, R. Meyer, in „*Explosivstoffe*“, 9th Edition, Wiley-VCH, Weinheim, **1998**.
- [19] T. Urbanski, *Chemistry and Technology of Explosives*, Vol. 4, Pergamon, Oxford, U. K., **1984**, p. 202.
- [20] T. Urbanski, *Chemistry and Technology of Explosives*, Vol. 4, Pergamon, Oxford, U. K., **1964**.
- [21] A. S. Kumar, V. B. Rao, R. K. Sinha, A. S. Rao, *Propellants Explos., Pyrotech.* **2010**, *35*, 359.
- [22] J. D. Zhang, X. L. Cheng, F. Zhao, *Propellants Explos., Pyrotech.* **2010**, *35*, 315.
- [23] *Encyclopedia of Chemical Technology*, Vol. 10, Wiley, New York, **1994**.

- [24] M. A. Cook, *The Science of High Explosives*, Reinhold, New York, **1958**.
- [25] Y. Q. Wu, F. L. Huang, *J. Hazard. Mater.* **2010**, 183, 324.
- [26] Y. Bayat, M. Eghdamtalab, V. Zeynali, *J. Energetic Mater.* **2010**, 28, 273.
- [27] J. C. Bottaro, *Chem. Ind. (London)* **1996**, 7, 249.
- [28] H. Singh, *Explosion* **2005**, 15, 120.
- [29] S. V. Sysolyatin, A. A. Lobanova, Yu T. Chernikova, G. V. Sakovich, *Russ. Chem. Rev.* **2005**, 74, 757.
- [30] M. X. Zhang, P. E. Eaton, R. Gilardi, *Angew. Chem. Int. Ed.* **2000**, 39, 401–404.
- [31] C. Le Gallic, R. Belmas, P. Lambert, *Propellants Explos., Pyrotech.* **2004**, 29, 339.
- [32] R. W. Millar, J. Hamid, R. Endsor, P. F. Swinton, J. Cooper, *Propellants Explos., Pyrotech.* **2008**, 33, 66–72.
- [33] W. F. Yu, T. L. Zhang, J. Zuo, Y. G. Huang, G. Li, C. Han, J. S. Li, H. Huang, *J. Hazard. Mater.* **2010**, 173, 249.
- [34] D. M. Hoffman, A. T. Fontes, *Propellants Explos., Pyrotech.* **2010**, 35, 15.
- [35] C. M. Tarver, *J. Phys. Chem. A* **2010**, 114, 2727.
- [36] a) T. Rieckmann, S. Völker, L. Lichtblau, R. Schirra, *Chem. Eng. Sci.* **2001**, 56, 1327–1335; b) J. P. Agrawal, R. N. Surve, V. K. Bapat, *Development of high density, high velocity of detonation and thermally stable explosives. HEMRL Report No. HEMRL/99/6*, **1999**; d) R. Mayer, J. Köhler, A. Homburg, *Explosives*, 5th Edition, Weinheim, Wiley-VCH, **2002**, 177–178.
- [37] G. Steinhauser, T. M. Klapötke, *Angew. Chem. Int. Ed.* **2008**, 47, 3330.
- [38] P. K. Swain, H. Singh, S. P. Tewari, *J. Mol. Liq.* **2010**, 151, 87.
- [39] R. P. Singh, R. D. Verma, D. T. Meshri, J. M. Shreeve, *Angew. Chem. Int. Ed.* **2006**, 45, 3584.
- [40] J. P. Agrawal, *High Energy Materials: Propellants, Explosives and Pyrotechnics*, Wiley-VCH, Weinheim, **2010**
- [41] H.-J. Maag, G. Klingenberg, *Propellants Explos., Pyrotech.* **1996**, 21, 1.
- [42] R. W. Miller, J. Hamid, R. Endsor, P. F. Swinton, J. Cooper, *Propellants Explos., Pyrotech.* **2008**, 33, 66.
- [43] J. Boehnlein-Mauss, H. Kroeber, *Propellants Explos., Pyrotech.* **2009**, 34, 239.
- [44] L. T. Fairhall, W. V. Jenrette, S. W. Jones, E. A. Pritchard, *Public Health Rep.* **1943**, 58, 607
- [45] D. Gidlow, *Occup. Med.* **2015**, 65, 348.
- [46] P. Mühle, *Dissertation*, Ludwig-Maximilians-Universität München, **2010**.
- [47] M. E. Barsan, A. Müller, *Lead Health Hazard Evaluation* **1996**, HETA Report (Nat. Inst. For Occupational Safety and Health, Cincinnati), No. 91-0346-2572.

- [48] a) A. A. Brish, I. A. Galeev, B. N. Zaitsev, E. A. Sbitnev, L. V. Tatarintsev, *Fizika Goreniya i Vzryva* **1966**, 2, 132–133. b) A. A. Brish, I. A. Galeev, B. N. Zaitsev, E. A. Sbitnev, L. V. Tatarintsev, *Fizika Goreniyai Vzryva* **1969**, 5, 475–480.
- [49] E. I. Aleksandrov, A. G. Voznyuk, *Combust. Explos. Shock Waves* **1978**, 14, 480–484.
- [50] E. I. Aleksandrov, A. G. Voznyuk, *Combust. Explos. Shock Waves* **1988**, 24, 730–733.
- [51] E. I. Aleksandrov, V. P. Tsipilev, *Combust. Explos. Shock Waves* **1983**, 19, 505–508.
- [52] E. I. Aleksandrov, V. P. Tsipilev, *Combust. Explos. Shock Waves* **1984**, 20, 690–694.
- [53] M. Joas, T. M. Klapötke, J. Stierstorfer, N. Szimhardt, *Chem. Eur. J.* **2013**, 19, 9995–10003.
- [54] T. M. Klapötke, J. Stierstorfer, A. U. Wallek, *Chem. Mater.* **2008**, 20, 4519–4530.
- [55] a) M. A. Ilyushin, I. V. Tselinskiy, A. V. Smirnov, *Razrabotka komponentov vysokoenergeticheskikh kompozitsii* **2006**, 9, Sankt Peterburg; b) A. Y. Zhilin, M. A. Ilyushin, I. V. Tselinskii, A. S. Brykov, *Russ. J. Appl. Chem.* **2001**, 74, 99–102.
- [56] G. R. Lotufo, W. Blackburn, S. J. Marlborough, J. W. Fleeger, *Ecotox. Environ. Safe* **2010**, 73, 1720.
- [57] J. A. Steevens, B. Duke, G. R. Lotufo, T. S. Bridges, *Environ. Toxicol. Chem.* **2002**, 21, 1720.
- [58] C. Pflüger, *Dissertation*, Ludwig-Maximilians-Universität München, **2016**, p. 5.
- [59] a) B. Sellers, K. Weeks, W. R. Alsop, *Perchlorate Environmental Problems and Solutions*, CRC, Boca Raton, FL (USA), **2007**; b) J. Dumont, *SERDP Project ER-1236*, **2008**.
- [60] a) E. D. McLanahan, J. L. Campbell, D. C. Ferguson, B. Harmon, J. M. Hedge, K. M. Crofton, D. R. Mattie, L. Braverman, D. A. Keys, M. Mumtaz, J. W. Fisher, *Toxicol. Sci.* **2007**, 97, 308–317; b) R. E. Tarone, L. Lipworth, J. K. McLaughlin, *Occup. Environ. Med.* **2010**, 52, 653; c) A. K. Mandal, G. M. Kunjir, J. Singh, S. S. Adhav, S. K. Singh, R. K. Pandey, B. Bhattacharya, M. L. Kantam, *Cent. Eur. J. Energ. Mater.* **2014**, 11, 83–97.
- [61] H. Bircher, *Chimia* **2004**, 58, 355–362.
- [62] G. Steinhauser, T. M. Klapötke, *Angew. Chem. Int. Ed.* **2008**, 47, 3330.
- [63] S. M. Danali, R. S. Palaiah, K. C. Raha, *Def. Sci. J.* **2010**, 60, 152.
- [64] A. Ozretic, *Can. Chem. News* **2010**, 62, 12.
- [65] B. Lachence, P. Y. Robidoux, J. Hawari, G. Ampleman, *Mutat. Res., Genet. Toxicol. Environ. Mutagen.* **1999**, 444, 25.



- [66] P. D. Howe, S. Dobson, H. M. Malcolm, T. T. Griffiths, *Proc. Int. Pyrotech. Sem.* **2008**, 35, 9.
- [67] O. Drzazga, T. Gorontzy, A. Schmidt, K. H. Blotevogel, *Arch. Environ. Contam. Toxicol.* **1995**, 28, 229.
- [68] W. H. Griest, A. J. Steart, R. L. Tyndall, J. E. Caton, C. H. Ho, K. S. Ironside, W. M. Caldwell, E. Tan, *Environ. Toxicol. Chem.* **1993**, 12, 1105.
- [69] M. B. Talawar, R. Sibavalan, T. Mukundan, H. Muthurajan, A. K. Sikder, B. R. Dandhe, A. S. Rao, *J. Hazard. Mater.* **2009**, 161, 589.
- [70] L. E. Fried, M. R. Manaa, P. F. Pagoria, R. L. Simpson, *Annu. Rev. Mater. Res.* **2001**, 31, 291–321.
- [71] T. M. Klapötke, P. C. Schmid, S. Schnell, J. Stierstorfer, *Chem. Eur. J.* **2015**, 21, 9219–9228.
- [72] P. K. Swain, H. Singh, S. P. Tewari, *J. Mol. Liq.* **2010**, 151, 87.
- [73] a) Y. I. Kuznetsov, L. P. Kazansky, *Russ. Chem. Rev.* **2008**, 77, 219; b) L. M. T. Frijia, A. Ismael, M. L. S. Cristiano, *Molecules* **2010**, 15, 3757. c) A. Moulin, M. Bibian, A.-L. Blayo, S. El Habnoui, J. Martinez, J.-A. Fehrentz, *Chem. Rev.* **2010**, 110, 1809.

## 2. Summary and Conclusions

During the course of this work, extensive research was undertaken to investigate oxygen- and nitrogen-rich heterocycles as possible precursors for energetic materials. During this time, a great number of new and novel energetic materials were synthesized and their energetic properties were extensively studied. The main goal of this thesis was to investigate different synthetic approaches toward new high performing but insensitive secondary explosives. For this purpose, target-oriented functionalization of five different heterocycles (pyrazole, 1,3,4-oxadiazole, 1,2,5-oxadiazole, 1,2,4-triazole and pyridazine) is reported. These results are all presented in Chapters 3–11, whereas Chapters 3–8 have been published in peer-reviewed scientific journals, Chapter 9 will be submitted to a scientific journal and Chapters 10 and 11 consist of unpublished results. Every Chapter consists of completed research topic with introduction, results and discussion, conclusion, experimental section and supporting information. A short overview and summary will be given for every single chapter.

Chapter 3 investigates the synthesis of various energetic salts based on the unstable molecule 3,4-bis(4-nitramino-1,2,5-oxadiazol-3-yl)-1,2,5-furoxan (BNAFF). BNAFF was synthesized by direct nitration of 3,4-bis(4-amino-1,2,5-oxadiazol-3-yl)-1,2,5-furoxan (BAFF) in 100% nitric acid. The nitramino derivative BNAFF as a free acid is not stable and has to be directly converted to the potassium salt  $K_2BNAFF$  after the nitration. By using  $K_2BNAFF$  a number of different energetic derivatives were synthesized and investigated.

Chapters 4 and 5 discuss novel energetic materials based on the unexploited 1,2-diazine scaffold. The desired introduction of a  $N^+-O^-$  moiety and an alternating push/pull ( $NH_2/NO_2$ ) system into the pyridazine heterocycle was successfully reported. The accompanying problems with the electron-deficient heterocycle are discussed and the solution for a successful electrophilic nitration on the pyridazine scaffold is presented.

In Chapter 6 the synthesis and characterization of new alkali and alkaline salts with the 3,3'-diamino-4,4'-dinitramino-5,5'-bitriazolate anion ( $ANAT^{2-}$ ) is reported. In addition, the  $SrANAT$  salt was investigated in different formulations as possible colorant for red-light-producing signal flares.

The chemistry of different polynitrated derivatives based on the 4,4'-bipyrazole backbone is presented in Chapters 7, 8 and 9. A great number of electrophilic nitration reactions on the 4,4'-bipyrazole are discussed and presented in Chapter 7. Additionally, all experimentally and theoretically determined properties of the synthesized polynitro derivatives have been displayed. Chapters 8 and 9 study further functionalization of 3,3',5-trinitro-4,4'-bipyrazole (TriNBPz) and 3,3',5,5'-tetranitro-4,4'-bipyrazole

## Summary and Conclusions

monohydrate (TNBPz·H<sub>2</sub>O). Neutralization reactions with TriNBPz and TNBPz·H<sub>2</sub>O and further *N*-functionalization of TNBPz·H<sub>2</sub>O are reported.

Chapter 10 combines the heterocycles 1,2,4-triazole and 1,3,4-oxadiazole in one molecule. The synthesized 2-amino-5-(5-amino-1*H*-1,2,4-triazol-3-yl)-1,3,4-oxadiazole and 2-amino-5-(5-nitro-1*H*-1,2,4-triazol-3-yl)-1,3,4-oxadiazole were synthesized and the properties of these energetic materials are reported.

A new possible approach toward the synthesis of 3,5-diamino-4,6-dinitropyridazine was investigated in Chapter 11.

In addition, four compounds from all chapters were selected and their performance on the small scale was evaluated. The small scale shock reactivity test (SSRT) was used in order to investigate the shock reactivity (explosiveness) of the four selected materials. The set-up and preparation of the samples for the SSRT are shown in details in the corresponding chapters. The selected compounds 3,5-diamino-4,6-dinitropyridazine-1-oxide (**7**), 3,3',5,5'-trinitro-4,4'-bipyrazole (**13**), 3,3',5,5'-trinitro-4,4'-bipyrazole (**14**) and 1,1'-diamino-3,3',5,5'-trinitro-4,4'-bipyrazole (**20**) are shown in **Figure 1** and were compared to the commercially used RDX, HNS, PYX and TKX-55.

**Table 1.** SSRT results for compounds **7**, **13**, **14** and **20** compared to RDX, HNS, PYX, TKX-55.

Compound	<b>7</b>	<b>13</b>	<b>14</b>	<b>20</b>	RDX <sup>[1]</sup>	HNS	PYX	TKX-55
$m_E$ [mg] <sup>[a]</sup>	496	500	491	472	504	469	474	496
$m$ [mg] <sup>[b]</sup>	694	640	811	786	858	672	637	641

[a] Mass of the explosive:  $m_E = V_s \rho$  0.95; [b] Mass of SiO<sub>2</sub>.

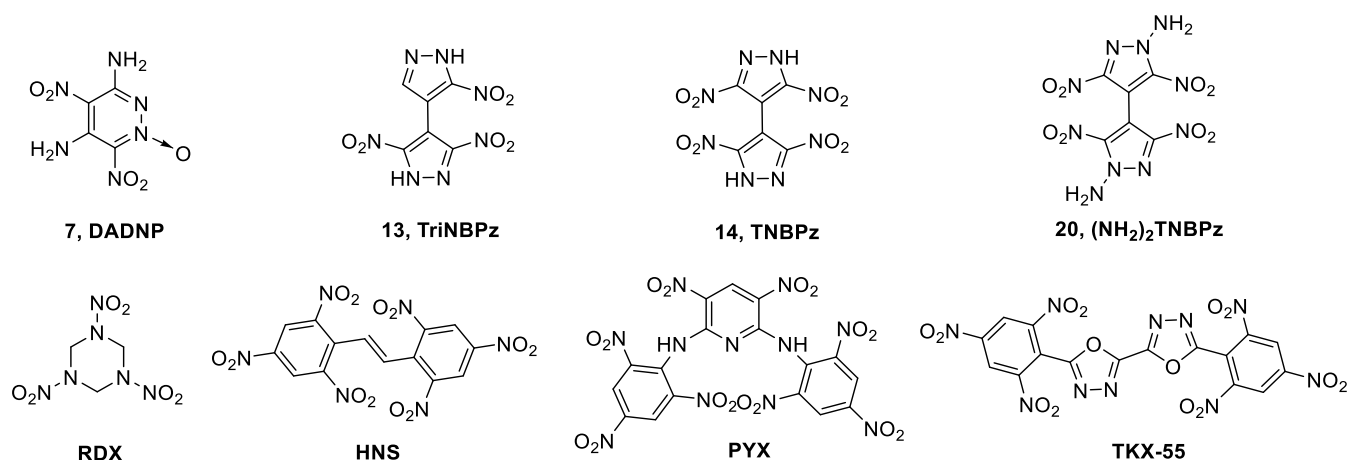


**Figure 1.** Lewis structures of all investigated materials with the small scale shock reactivity test compared to RDX, HNS, PYX and TKX-55.

## Summary and Conclusions

The obtained results are listed in **Table 1**. The obtained values are compared to the high performing RDX and to the heat resisting explosives HNS, PYX, TKX-55. The results for compound **13** (640 mg) are in the range of PYX (637 mg) and TKX-55 (641 mg). DADNP (**9**, 694 mg) and (NH<sub>2</sub>)<sub>2</sub>TNBPz (**20**, 786 mg), consisting of alternating push/pull system, exceed the performance of HNS (672 mg), PYX (637 mg) and TKX-55 (641 mg), however they do not outperform RDX (858 mg). The performance of TNBPz (**14**, 811 mg) in the small scale is slightly lower but in the range of RDX (858 mg).

### 2.1. Chapter 3: 3,4-Bis(4-nitramino-1,2,5-oxadiazol-3-yl)-1,2,5-furoxan (BNAFF)

The nitration of 3,4-bis(4-amino-1,2,5-oxadiazol-3-yl)-1,2,5-furoxan (BAFF) to the desired nitramino derivative is reported. 3,4-Bis(4-nitramino-1,2,5-oxadiazol-3-yl)-1,2,5-furoxan (BNAFF) is unstable at room temperature for a long time and has to be directly converted after the nitration to the potassium salt K<sub>2</sub>BNAFF. Using the latter, the free acid can be generated *in situ* and different nitrogen-rich salts can be synthesized. The nitroamino moiety in the 3,4-bis(1,2,5-oxadiazol-3-yl)-1,2,5-furoxan backbone can be directly stabilized via acid-base reactions.

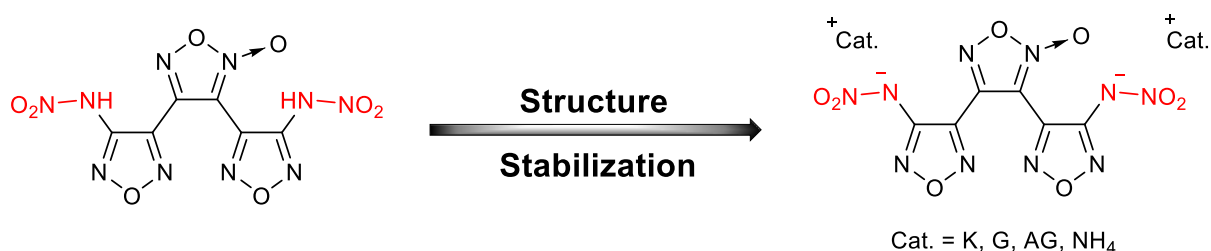
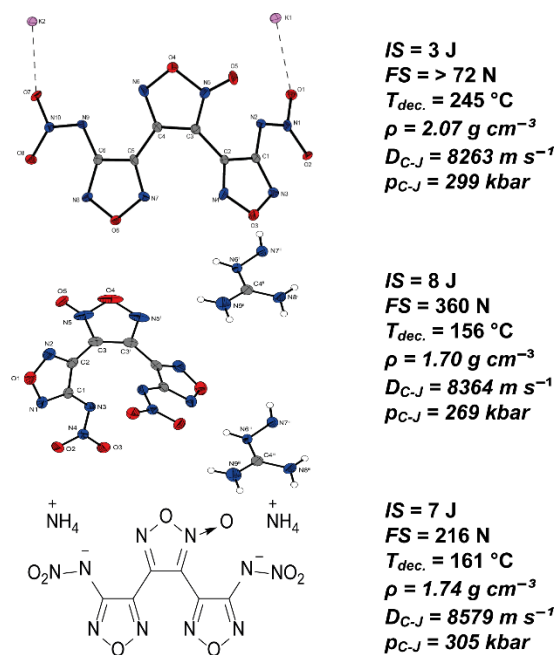


**Figure 2.** Structure stabilization of the nitramino moiety in 3,4-bis(1,2,5-oxadiazol-3-yl)-1,2,5-furoxan through salt formation.

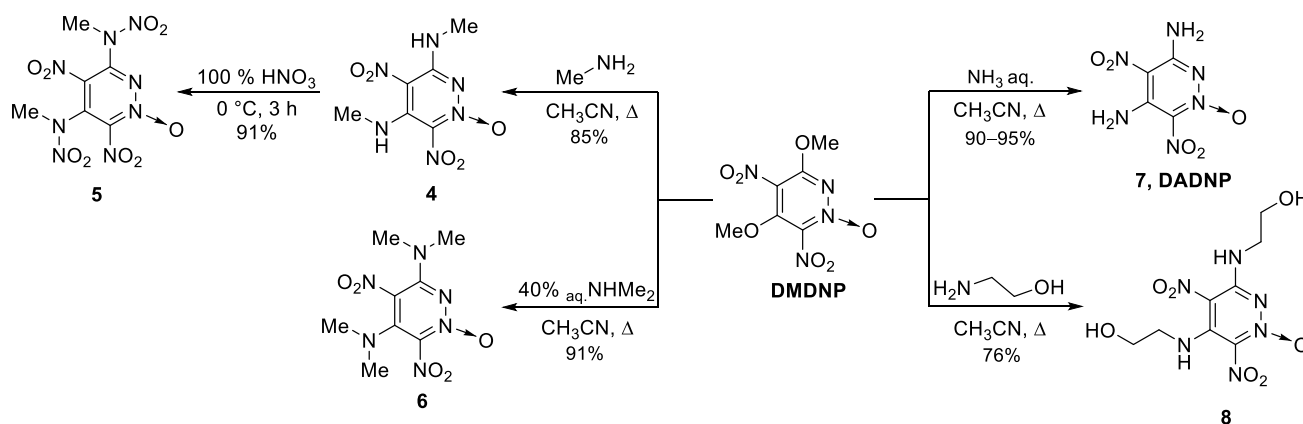


Nitrogen-rich based salts of BNAFF are superior in detonation parameters over the potassium salt. In addition, the aminoguanidinium (**2**,  $IS = 8 \text{ J}$ ,  $FS = 360 \text{ N}$ ) and ammonium (**3**,  $IS = 7 \text{ J}$ ,  $FS = 216 \text{ N}$ ) salts show lower sensitivity toward outer stimuli (impact and friction). In regards to the thermal stability the  $K_2$ BNAFF (**1**) ionic derivative exhibits the highest thermal stability with  $245 \text{ }^{\circ}\text{C}$ , while the nitrogen-rich compounds decompose below  $200 \text{ }^{\circ}\text{C}$ .

**Figure 3.** Molecular units of  $K_2$ BNAFF (**1**, top),  $(AG)_2$ BNAFF (**2**, middle) and Lewis structure of  $(NH_4)_2$ BNAFF (**3**, bottom), respectively and their energetic properties.

## 2.2. Chapters 4 and 5: Energetic Materials Based on the Pyridazine Scaffold

Five new energetic pyridazine derivatives were synthesized and completely characterized by using 3,5-dimethoxy-4,6-dinitropyridazine-1-oxide (DMDNP, **Scheme 1**) as starting material. The difficulty in this topic was the challenging nitration of the electron-poor pyridazine system. This problem was resolved by introducing electron-donating groups ( $-OMe$ ) into the pyridazine scaffold followed by the insertion of a  $N^+-O^-$  moiety, which eventually allowed electrophilic nitration with 20% oleum and 100% nitric acid.



**Scheme 1.** Overview of all synthesized pyridazine derivatives.

## Summary and Conclusions

The most promising compound in this study is 3,5-diamino-4,6-dinitropyridazine-1-oxide (**Figure 5**). DADNP is an excellent example for a high explosive based on a heterocycle functionalized with push/pull ( $\text{NH}_2/\text{NO}_2$ ) systems and *N*-oxidized tertiary amine ( $\text{N}^+-\text{O}^-$ ) moiety. With good sensitivity values ( $IS = 18 \text{ J}$ ,  $FS = 360 \text{ N}$ ) and good thermal stability ( $215^\circ$ ) DADNP is the first pyridazine based secondary explosive to be synthesized. Compound **5** is an excellent example for the increase of sensitivity and performance in comparison to the precursor **4**, when the nitroamino moiety is introduced to the parent molecule.

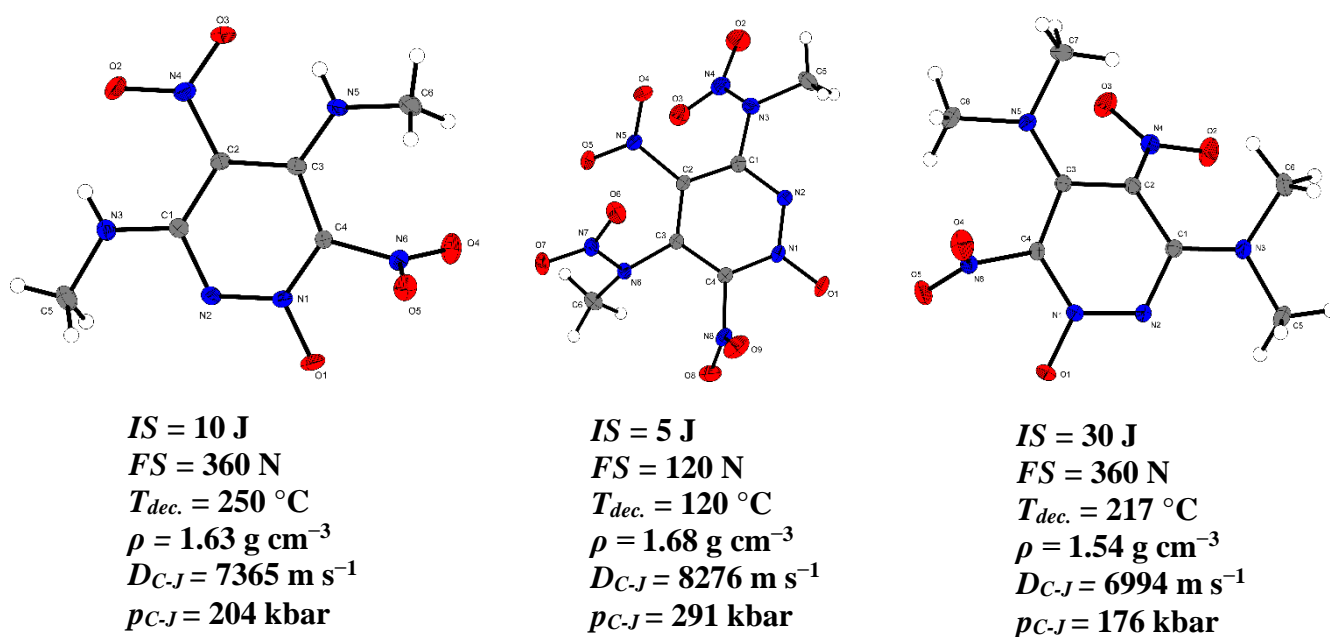


**Figure 4.** Molecular units of 3,5-bis(methylamino)-4,6-dinitropyridazine-1-oxide (**4**, left), 3,5-bis(methylnitramino)-4,6-dinitropyridazine-1-oxide (**5**, middle), 3,5-bis(dimethylamino)-4,6-dinitropyridazine-1-oxide (**6**, right) and their energetic properties.

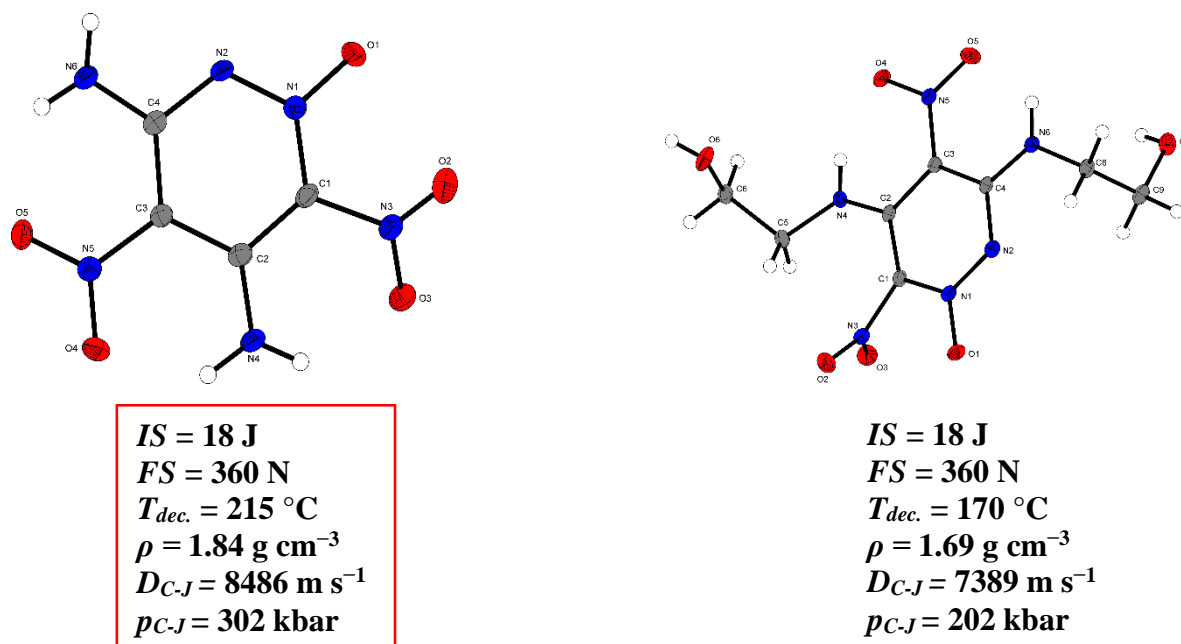


**Figure 5.** Molecular units of 3,5-diamino-4,6-dinitropyridazine-1-oxide (**7**, DADNP, left), 3,5-bis((2-(hydroxyethyl)amino)-4,6-dinitropyridazine-1-oxide (**8**, right) and their energetic properties.

### 2.3. Chapter 6: 3,3'-Diamino-4,4'-dinitramino-5,5'-bi-1,2,4-triazole

In this chapter several alkali and alkaline energetic salts with the 3,3'-diamino-4,4'-dinitramino-5,5'-bitriazolate anion (ANAT<sup>2-</sup>) were synthesized and extensively characterized. The results are focused on the strontium salt and its possible application as an eco friendly colorant for red-light-producing signal flares. Different formulations with the SrANAT (**9**) salt were investigated and it was shown that a strong dominant wavelength can be obtained (620±20 nm). However, all SrANAT based formulations lack on spectral purities (< 76%) and further investigations have to be made.

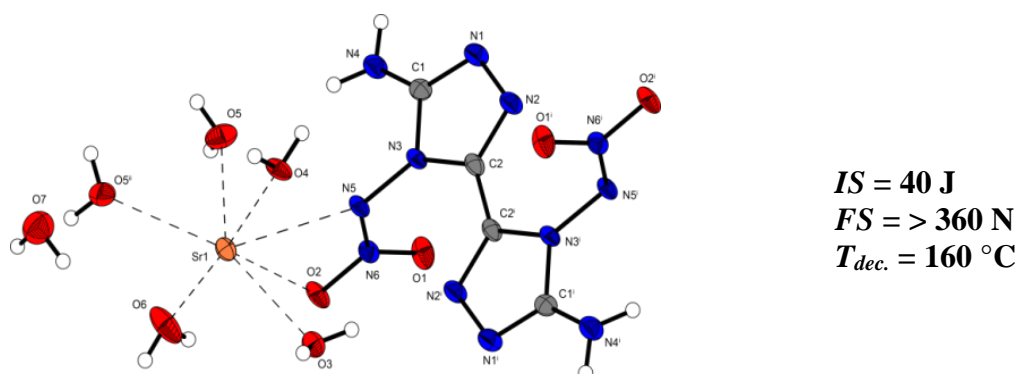


**Figure 6.** Molecular unit of strontium 3,3'-diamino-4,4'-dinitramino-5,5'-bitriazolate hexahydrate (**9**) and its sensitivity values.

## 2.4. Chapter 7: Polynitrated Derivatives Based on the 4,4'-Bipyrazole Scaffold

In the present study different nitration reactions have been investigated on the 4,4'-bipyrazole scaffold. This resulted in the formation of five different derivatives containing one, two, three and four NO<sub>2</sub> groups, respectively. All nitro derivatives were obtained in good to excellent yields and their physico-chemical properties are shown in **Figure 8**. Compounds **12**·H<sub>2</sub>O and **14**·H<sub>2</sub>O were obtained as monohydrates. Both samples can be dried at elevated temperatures (180 °C) to yield the solvate free compounds. Increasing the number of explosophore groups (NO<sub>2</sub>) in the 4,4'-bipyrazole scaffold results in increase of the performance (**10**:  $D_{C-J} = 6506 \text{ m s}^{-1}$ ,  $p_{C-J} = 144 \text{ kbar}$  → **14**:  $D_{C-J} = 8520 \text{ m s}^{-1}$ ,  $p_{C-J} = 311 \text{ kbar}$ ), however it also increases the sensitivity of the materials toward outer stimuli (**10**: IS = 40 J, FS = > 360 N → **14**: IS = 4.5 J, FS = 192 N). Additionally, compounds **10–14** exhibit excellent thermal stability from 298 °C (**14**) up to 382 °C (**11**), thus making the 4,4'-bipyrazole backbone an interesting building block for heat resisting secondary explosives.

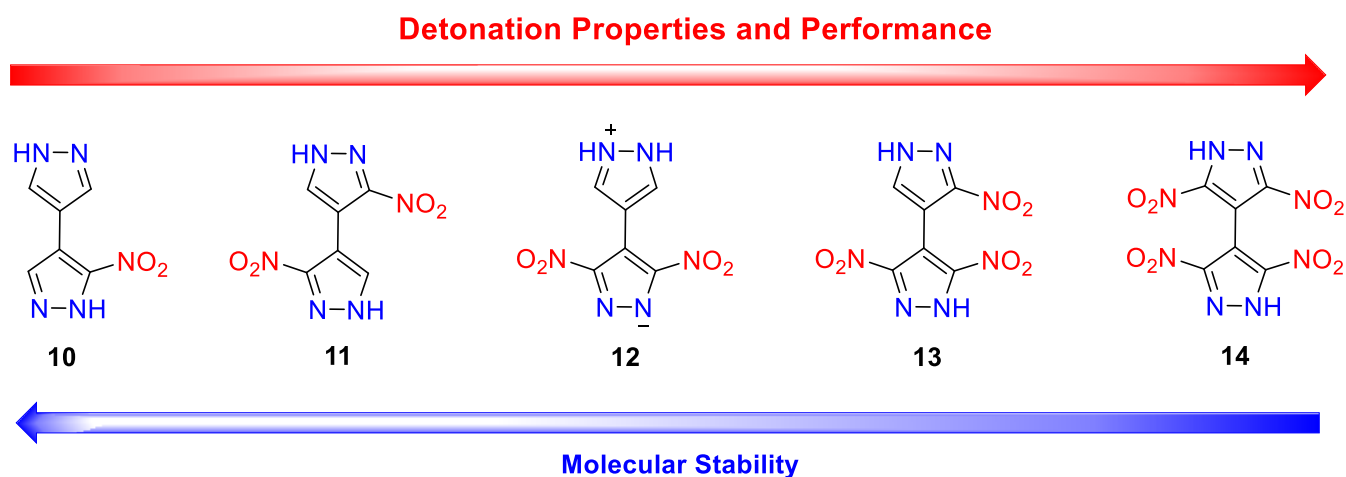


**Figure 7.** Structural relation between molecular stability and detonation properties for compounds **10–14**.



## Summary and Conclusions

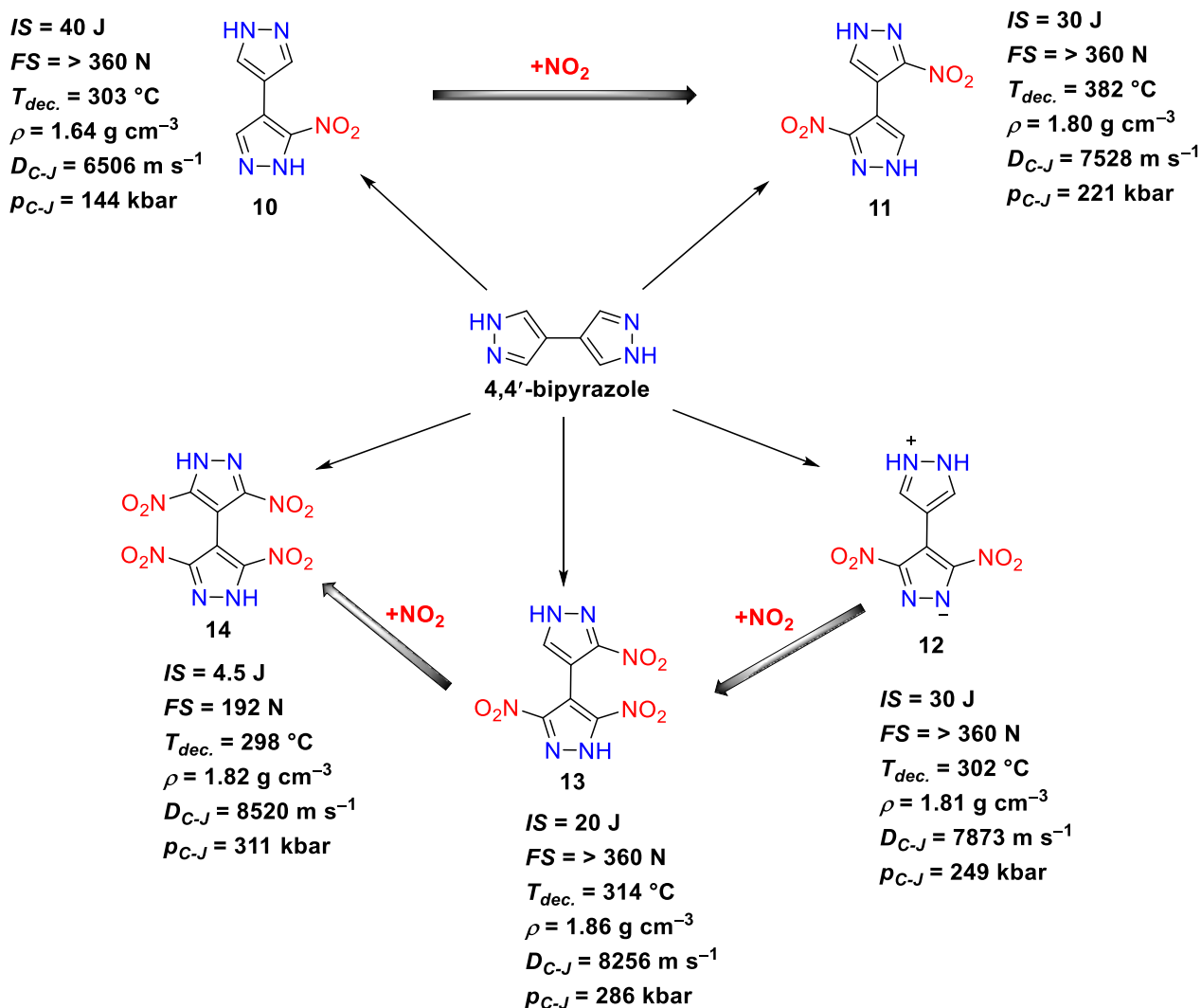


**Figure 8.** Energetic materials based on the 4,4'-bipyrazole scaffold and their physico-chemical properties.

## 2.5. Chapters 8 and 9: Energetic Derivatives Based on TriNBPz and TNBPz·H<sub>2</sub>O

In this study different ionic energetic materials based on 3,3',5-trinitro-4,4'-bipyrazole (TriNBPz) and 3,3',5,5'-tetranitro-4,4'-bipyrazole monohydrate (TNBPz·H<sub>2</sub>O) were synthesized and investigated. In addition, the *N*-functionalization of TNBPz·H<sub>2</sub>O to (Me)<sub>2</sub>TNBPz, K(NH<sub>2</sub>)TNBPz and (NH<sub>2</sub>)<sub>2</sub>TNBPz was reported. Unfortunately the formation of nitrogen-rich salts with TriNBPz resulted in decrease of stability and only one of the synthesized compounds ((NH<sub>3</sub>OH)HTriNBPz) showed better theoretically calculated performance. The hydroxylammonium (**15**) and the hydrazinium (**16**) salts of the TriNBPz<sup>−</sup> anion showed the best performance according to the EXPLO5 code. In addition, the sensitivity values for the ionic compounds (NH<sub>3</sub>OH)HTriNBPz (**15**,  $IS = 10 \text{ J}$ ,  $FS = > 360 \text{ N}$ ) and (N<sub>2</sub>H<sub>5</sub>)HTriNBPz (**16**,  $IS = 15 \text{ J}$ ,  $FS = > 360 \text{ N}$ ) do not show improvement in comparison to the nonionic parent compound TriNBPz ( $IS = 20 \text{ J}$ ,  $FS = > 360 \text{ N}$ ).

## Summary and Conclusions

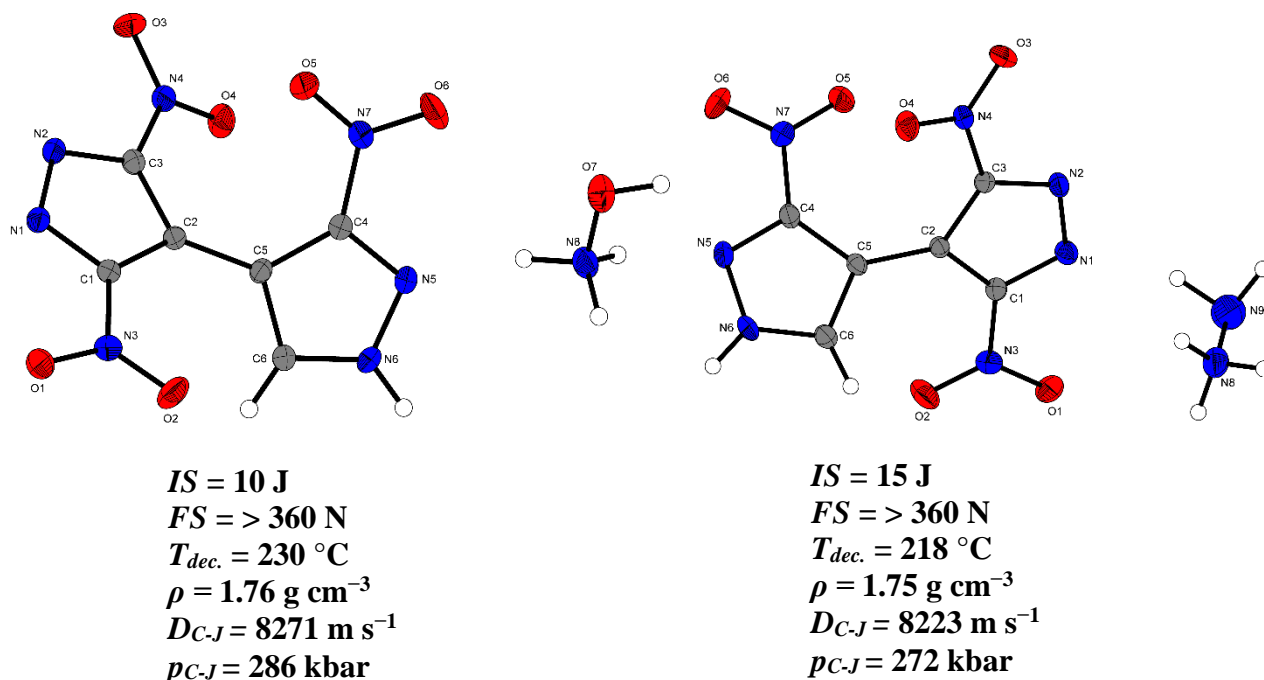


**Figure 9.** Molecular unit of hydroxylammonium 4-(3-nitropyrzazolyl)-3,5-dinitropyrzolate (**15**, left) and hydrazinium 4-(3-nitropyrzazolyl)-3,5-dinitropyrzolate (**16**, right) and their energetic properties.

From all synthesized TNBPz ionic derivatives, compounds  $(\text{NH}_3\text{OH})\text{HTNBPz}$  (**17**),  $(\text{NH}_3\text{OH})_2\text{TNBPz}$  (**18**),  $\text{K}(\text{NH}_2)\text{TNBPz}$  (**19**) and  $(\text{NH}_2)_2\text{TNBPz}$  (**20**) show the most promising properties. The hydroxylammonium salt **17** ( $D_{C-J} = 8673 \text{ m s}^{-1}$ ,  $p_{C-J} = 328 \text{ kbar}$ ) exceeds in performance the nonionic parent molecule TNBPz ( $D_{C-J} = 8520 \text{ m s}^{-1}$ ,  $p_{C-J} = 311 \text{ kbar}$ ). However, at the same time the stability toward outer stimuli of the ionic compound **17** ( $T_{dec.} = 201 \text{ }^{\circ}\text{C}$ ,  $IS = 2 \text{ J}$ ) is decreased in comparison to TNBPz ( $T_{dec.} = 298 \text{ }^{\circ}\text{C}$ ,  $IS = 4.5 \text{ J}$ ). The energetic derivatives  $(\text{NH}_3\text{OH})_2\text{TNBPz}$  (**18**,  $D_{C-J} = 8456 \text{ m s}^{-1}$ ,  $p_{C-J} = 302 \text{ kbar}$ ),  $\text{K}(\text{NH}_2)\text{TNBPz}$  (**19**,  $D_{C-J} = 8517 \text{ m s}^{-1}$ ,  $p_{C-J} = 318 \text{ kbar}$ ) and  $(\text{NH}_2)_2\text{TNBPz}$  (**20**,  $D_{C-J} = 8469 \text{ m s}^{-1}$ ,  $p_{C-J} = 305 \text{ kbar}$ ) exhibit similar performance as the starting material. However, after the *N*-amination of the 4,4'-bipyrazole scaffold in TNBPz the stability of the new formed energetic materials increases toward external stimuli. Sensitivity values of 15 J and 324 N were measured for the diamino compound **20**. The obtained results support furtherly the thesis that alternating push/pull systems ( $\text{NH}_2/\text{NO}_2$ ) in an energetic heterocycle can result in increase of stability in the molecular structure. In addition, the toxicity for three different energetic salts ( $\text{KHTrinBPz}$ ,  $\text{K}_2\text{TNBPz}$ ,  $\text{G}_2\text{TNBPz}$ ) toward aqueous bacteria *Vibrio fischeri* was determined. The investigated polynitro derivatives showed no toxicity.

## Summary and Conclusions

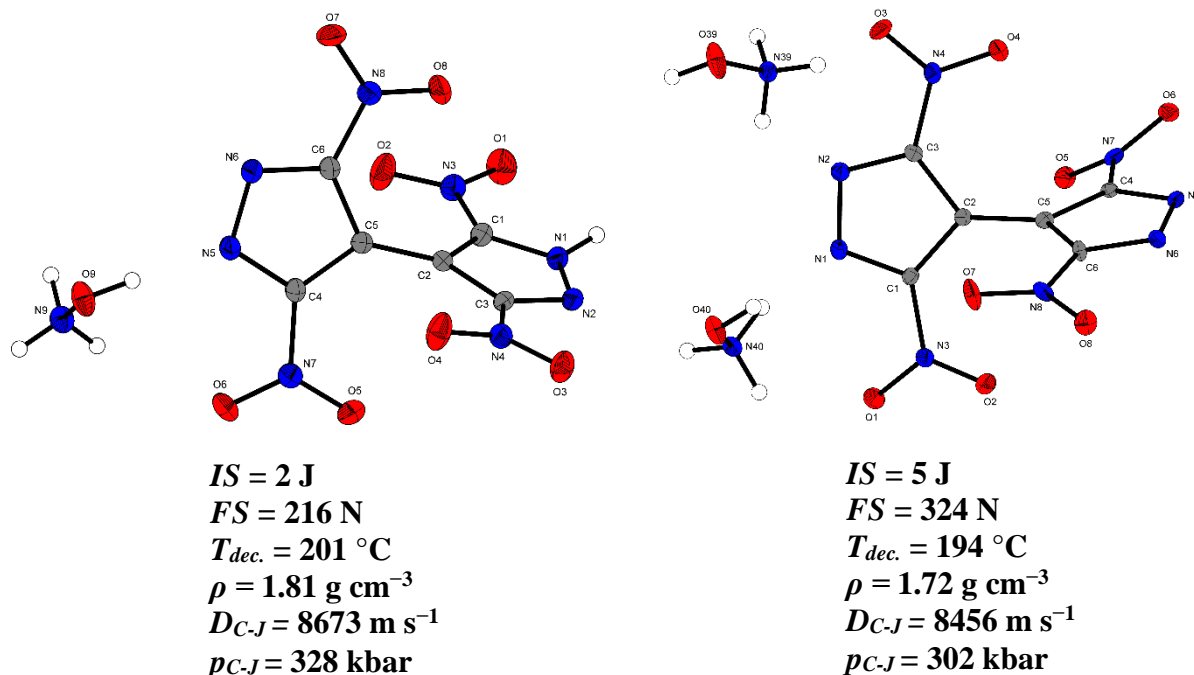


**Figure 9.** Molecular unit of hydroxylammonium 4-(3,5-dinitropyrzoly)-3',5'-dinitropyrzolate (**17**, left) and bis(hydroxylammonium) 3,3',5,5'-tetranitro-4,4'-bipyrazolate (**18**, right) and their energetic properties.

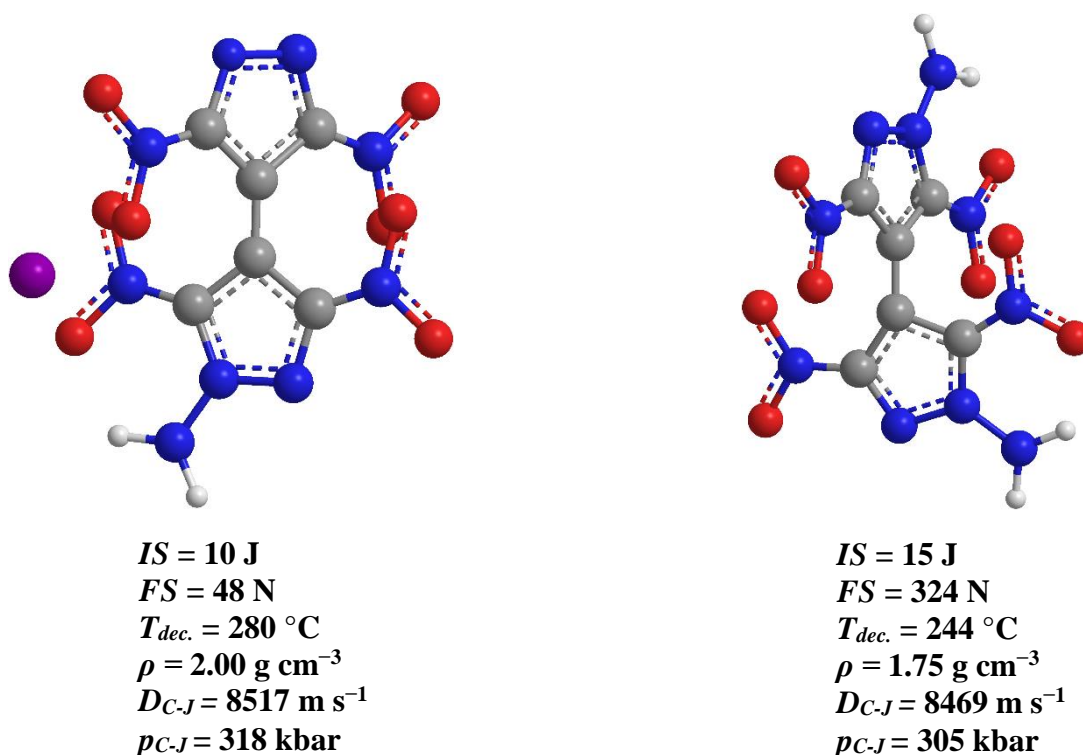


**Figure 10.** Molecular structures of potassium 4-(1-amino-3,5-dinitropyrzoly)-3',5'-dinitropyrzolate (**19**, left) and 1,1'-diamino-3,3',5,5'-tetranitro-4,4'-bipyrazole (**20**, right) and their energetic properties.

## 2.6. Chapter 10: 1,2,4-Triazol-3-yl-1,3,4-oxadiazole Based Energetic Materials

In this study, the synthesis of energetic precursors based on the heterocycles 1,2,4-triazole and 1,3,4-oxadiazole is reported. 2-Amino-5-(5-amino-1*H*-1,2,4-triazol-3-yl)-1,3,4-oxadiazole and 2-amino-5-(5-nitro-1*H*-1,2,4-triazol-3-yl)-1,3,4-oxadiazole were synthesized by using 5-amino-1*H*-1,2,4-triazole-3-carboxylic as the starting material. In addition, four different energetic salts were synthesized with 2-amino-5-(5-nitro-1*H*-1,2,4-triazol-3-yl)-1,3,4-oxadiazole.

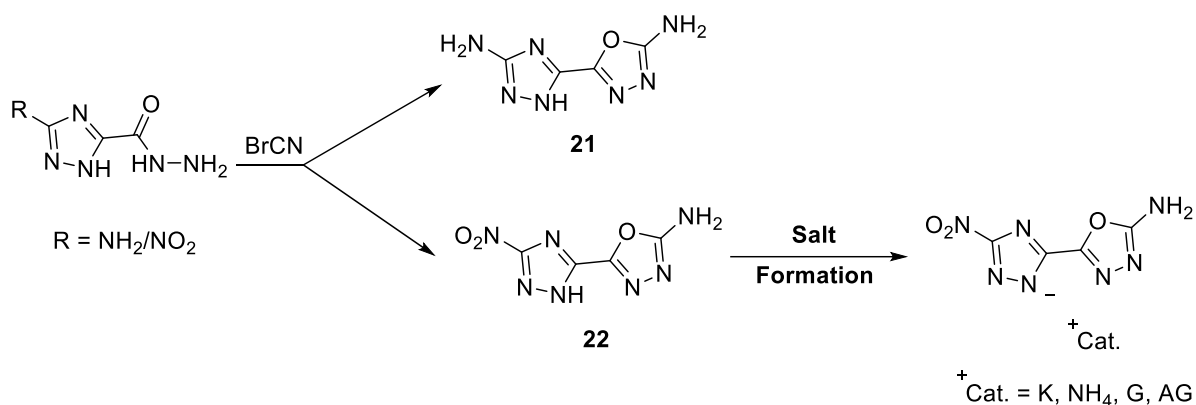


**Figure 11.** Synthesis of 2-amino-5-(5-amino-1*H*-1,2,4-triazol-3-yl)-1,3,4-oxadiazole (**21**) and 2-amino-5-(5-nitro-1*H*-1,2,4-triazol-3-yl)-1,3,4-oxadiazole (**22**).

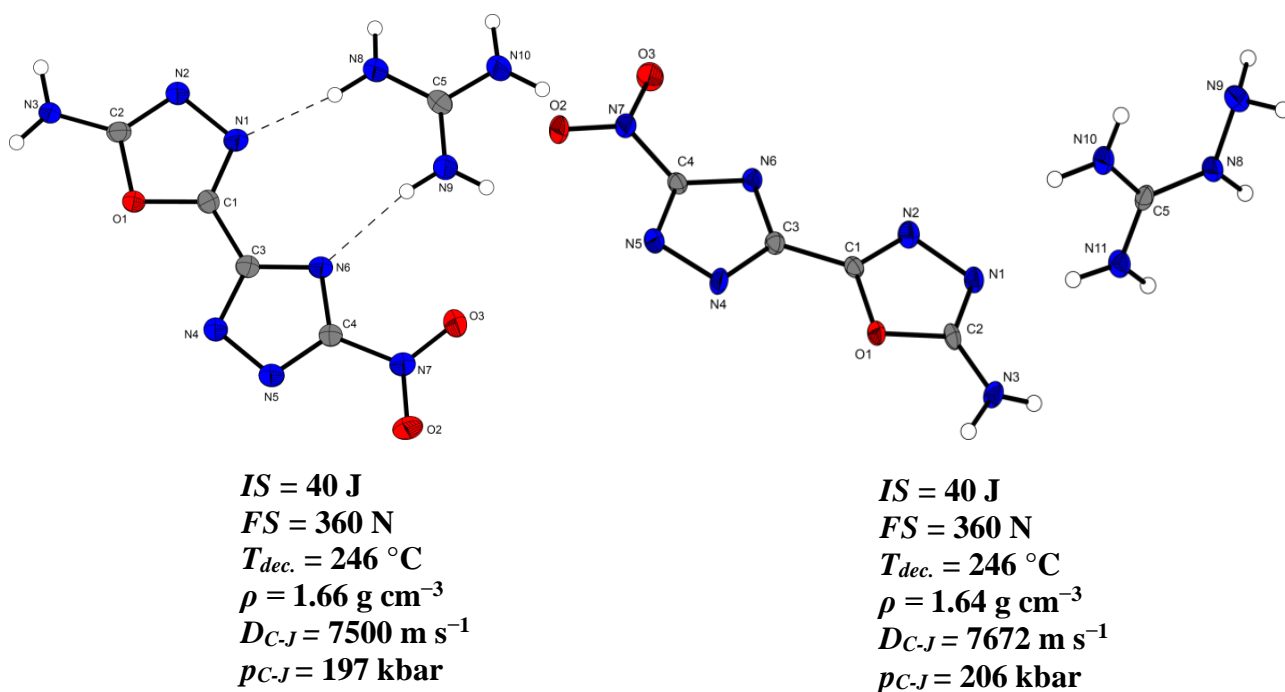


**Figure 12.** Molecular structures of guanidinium 5-(5-amino-1,3,4-oxadiazol-2-yl)-3-nitro-1,2,4-triazolate (**23**, left) and aminoguanidinium 5-(5-amino-1,3,4-oxadiazol-2-yl)-3-nitro-1,2,4-triazolate (**24**, right) and their energetic properties.

## 2.7. Chapter 11: Toward the Synthesis of 3,5-Diamino-4,6-dinitropyridazine

During this work an attempt was made to synthesize 3,5-diamino-4,6-dinitropyridazine. For this purpose, 3,5-diaminopyridazine acetate (**26**) was synthesized from 7-azidotetrazolo[1,5-*b*]pyridazine (**25**) by using the Staudinger reaction. Further nitration of **26** resulted only in the formation of 5-nitramino-3-nitriminopyridazine dihydrate (**27·2H<sub>2</sub>O**) and 3,5-diamino-4-nitropyridazine (**28**). Further functionalization of both compounds to the desired 3,5-diamino-4,6-dinitropyridazine was not successful.

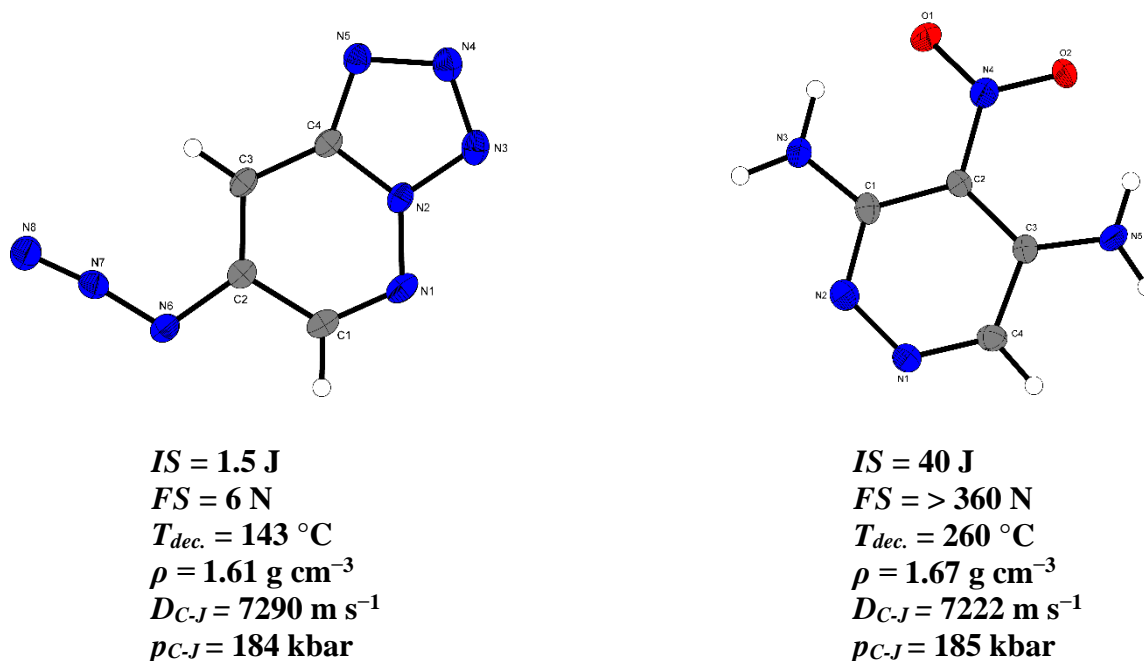


**Figure 13.** Molecular units of 7-azidotetrazolo[1,5-*b*]pyridazine (left, **25**) and 3,5-diamino-4-nitropyridazine (right, **28**).

## 2.8. References

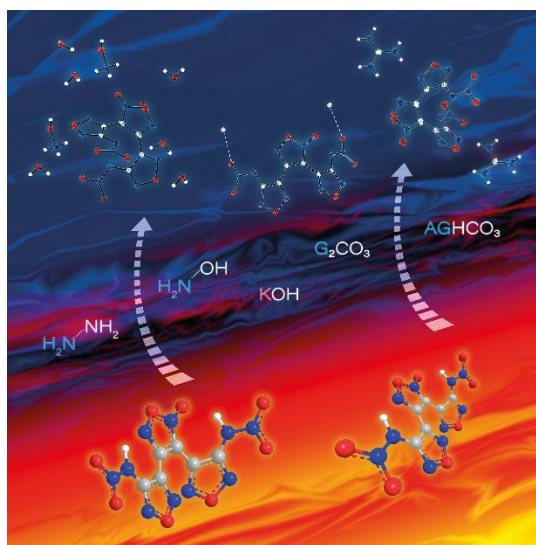
- [1] A. Preimesser, *Dissertation*, Ludwig-Maximilians-Universität München, **2015**, p. 156.

### 3. Energetic Compounds Based on 3,4-Bis(4-nitramino-1,2,5-oxadiazol-3-yl)-1,2,5-furoxan (BNAFF)

Ivan Gospodinov, Tobias Hermann, Thomas M. Klapötke and Jörg Stierstorfer

Published in *Propellants Explos. Pyrotech.* **2018**, 43, 355–363.

DOI: doi.org/10.1002/prop.201700289



**Abstract:** 3,4-Bis(4-amino-1,2,5-oxadiazol-3-yl)-1,2,5-furoxan (BAFF, **1**) was nitrated in 100% HNO<sub>3</sub> at –10 °C and then reacted with KOH to give the corresponding energetic dipotassium salt of 3,4-bis(4-nitramino-1,2,5-oxadiazol-3-yl)-1,2,5-furoxan (**2**, K<sub>2</sub>BNAFF). The neutral nitramino-furoxan compound (**3**, H<sub>2</sub>BNAFF) is unstable at room temperature and can be obtained from K<sub>2</sub>BNAFF with 2 M HCl and ether as H<sub>2</sub>BNAFF•0.5Et<sub>2</sub>O. Several nitrogen-rich salts (*e.g.* ammonium, guanidinium, aminoguanidinium, hydrazinium and hydroxylammonium) were prepared from K<sub>2</sub>BNAFF. The potassium, guanidinium, aminoguanidinium, hydroxylammonium and silver salts of BNAFF were characterized by low-temperature X-ray diffraction. In addition, all compounds were analyzed by vibrational spectroscopy (IR and Raman), multinuclear (<sup>1</sup>H, <sup>13</sup>C, <sup>14</sup>N) NMR spectroscopy, differential thermal analysis (DTA) and elemental analysis. The heats of formation for the anhydrous compounds were calculated using the atomization method based on CBS-4M enthalpies. Several detonation parameters were predicted by using the EXPLO5 code (V6.03). In addition, the sensitivities of all BNAFF salts toward friction, impact and electrostatic discharge were determined.

### 3.1. Introduction

“High energy density materials” (HEDMs) have not only found use for military purposes but also for civilian applications e.g. mining and pyrotechnics.<sup>[1]</sup> In the last century there have been a large number of publications that describe the chemistry, synthesis and properties of new explosive materials.<sup>[2]</sup> Higher performance has always been a main requirement in the development of explosives. Hence explosives are required for even more demanding applications (deep oil drilling or missiles for space missions); new advances in the technology of energetic materials have to be made.<sup>[3]</sup> In addition, newly designed explosives should meet the future environmental requirements, exhibit lower sensitivities toward external stimuli (such as impact, friction and electrostatic discharge) and show high performance.<sup>[4–8]</sup>

Five membered heterocycles containing nitrogen and oxygen have shown promising application as building blocks for energetic materials.<sup>[9–11]</sup> Derivatives of nitro/nitramino substituted furazanes (1,2,5-oxadiazole) and furoxanes (1,2,5-oxadiazole-2-oxide) have been of particular interest in the development of new HEDMs since they usually possess good oxygen balance, high heat of formation and high density.<sup>[12–15]</sup> Some well-known explosives based on furazanes and furoxanes are shown in **Figure 1**.

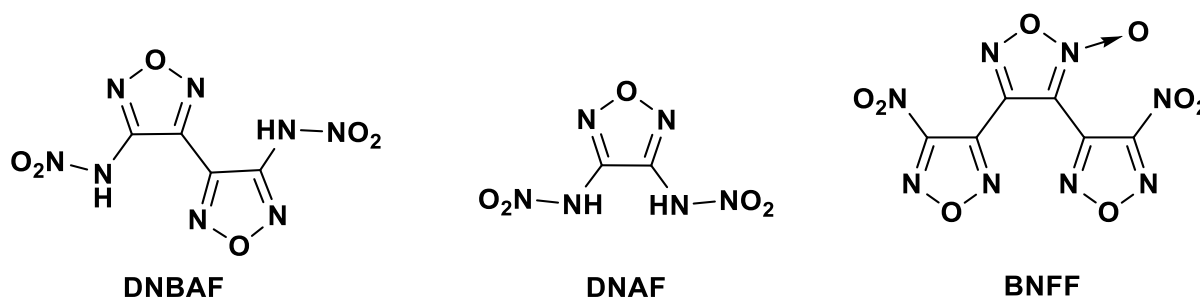


**Figure 1.** Literature known explosives based on furoxanes and furazanes: DNBAF (4,4'-dinitramino-3,3'-bifurazan),<sup>[12]</sup> DNAF (3,4-dinitraminofurazan)<sup>[16]</sup> and BNFF (3,4-bis(4-nitro-1,2,5-oxadiazol-3-yl)-1,2,5-furoxan).<sup>[17]</sup>

Recently, the combination of both, the furazan and furoxan rings with nitro or nitramino groups in the molecule has proven to be a good strategy for the synthesis of new high-nitrogen containing explosives.<sup>[17]</sup> A good example of a new high-density energetic material with good thermal stability and performance based on the furazan and furoxan rings is 3,4-bis(4-nitro-1,2,5-oxadiazol-3-yl)-1,2,5-furoxan (BNFF, also known as DNTF). BNFF can be synthesized by oxidizing 3,4-bis(4-amino-1,2,5-oxadiazol-3-yl)-1,2,5-furoxan (BAFF) with 50% hydrogen peroxide and trifluoroacetic acid.<sup>[18]</sup> BNFF has a crystal density of 1.93 g cm<sup>-3</sup> with a heat of formation of 657 kJ mol<sup>-1</sup> and its energetic performance is 168% better than trinitrotoluene (TNT). It melts at 108–110 °C and decomposes at 292 °C, which makes the compound of special interest as a possible TNT replacement.<sup>[17,19]</sup> All these physico-chemical properties make BNFF a

**Energetic Compounds Based on 3,4-Bis(4-nitramino-1,2,5-oxadiazol-3-yl)-  
1,2,5-furoxan (BNAFF)**

promising candidate to use not only as a melt-castable ingredient in detonators but also as a high performing explosive.<sup>[20,21]</sup> Replacement of the amino groups in BAFF with nitro groups to form BNFF improves the detonation parameters of the energetic material. Surprisingly, the nitration of 3,4-bis(4-amino-1,2,5-oxadiazol-3-yl)-1,2,5-furoxan (BAFF) has not been reported and the nitramino compound is unknown. In this contribution the nitration of BAFF to the nitramino compound (H<sub>2</sub>BNAFF) is described as well as the formation and characterization of some nitrogen-rich salts.

## **3.2. Experimental Section**

### **3.2.1. General procedures**

<sup>1</sup>H, <sup>13</sup>C, <sup>14</sup>N and <sup>15</sup>N NMR spectra were recorded on *JEOL 270* and *BRUKER AMX 400* instruments. The samples were measured at room temperature in standard NMR tubes (Ø 5 mm). Chemical shifts are reported as  $\delta$  values in ppm relative to the residual solvent peaks of *d*<sub>6</sub>-DMSO ( $\delta_{\text{H}}$ : 2.50,  $\delta_{\text{C}}$ : 39.5). Solvent residual signals and chemical shifts for NMR solvents were referenced against tetramethylsilane (TMS,  $\delta$  = 0 ppm) and nitromethane. Unless stated otherwise, coupling constants were reported in hertz (Hz) and for the characterization of the observed signal multiplicities the following abbreviations were used: s (singlet), d (doublet), t (triplet), q (quartet), quint (quintet), sept (septet), m (multiplet) and br (broad). Low resolution mass spectra were recorded on a *JEOL JMS-700 MStation* mass spectrometer (FAB+/-). Infrared spectra (IR) were recorded from 4500 cm<sup>-1</sup> to 650 cm<sup>-1</sup> on a PERKIN ELMER Spectrum BX-59343 instrument with a *SMITHS DETECTION DuraSamplIR II Diamond ATR* sensor. The absorption bands are reported in wavenumbers (cm<sup>-1</sup>). Raman spectra were recorded using a Bruker MultiRAM FT-Raman instrument fitted with a liquid-nitrogen cooled germanium detector and a Nd:YAG laser ( $\lambda$  = 1064 nm). Elemental analysis was carried on a *Elementar Vario el* by pyrolysis of the sample and subsequent analysis of the formed gases. Decomposition temperatures were measured *via* differential thermal analysis (DTA) with an OZM Research DTA 552-Ex instrument at a heating rate of 5 °C min<sup>-1</sup> and in a range of room temperature to 400 °C. Melting points were determined in capillaries with a Büchi Melting Point B-540 instrument and are uncorrected. All sensitivities toward impact (IS) and friction (FS) were determined according to BAM (German: Bundesanstalt für Materialforschung und Prüfung) standards using a BAM drop hammer and a BAM friction apparatus. All energetic compounds were tested for sensitivity towards electrical discharge using an Electric Spark Tester ESD 2010 EN from OZM.

### **3.2.2. Synthesis**

**CAUTION!** All investigated compounds are potentially explosive materials, although no hazards were observed during preparation and handling these compounds. Nevertheless, safety precautions (such as



**Energetic Compounds Based on 3,4-Bis(4-nitramino-1,2,5-oxadiazol-3-yl)-  
1,2,5-furoxan (BNAFF)**

wearing leather coat, face shield, Kevlar sleeves, Kevlar gloves, earthed equipment and ear plugs) should be drawn.

**3,4-Bis(4-amino-1,2,5-oxadiazol-3-yl)-1,2,5-furoxan (BAFF)**

BAFF was synthesized according to the known literature.<sup>[17,18,20]</sup>

**Dipotassium 3,4-bis(4-nitramino-1,2,5-oxadiazol-3-yl)-1,2,5-furoxan K<sub>2</sub>BNAFF (2)**

100% HNO<sub>3</sub> (9.0 mL) was placed in a round bottom flask and 3,4-bis(4-amino-1,2,5-oxadiazol-3-yl)-1,2,5-furoxane (BAFF, 4.0 g, 15.9 mmol) was added in small portions at -10 °C. The reaction was stirred for 1.5 h at the same temperature and then for 1.5 h at -5 °C. The reaction mixture was poured into ice and stirred at room temperature for 2 h. The solution was basified with potassium hydroxide to pH 11. The formed solid material was filtered, washed with small amount of cold water and dried on air to give K<sub>2</sub>BNAFF (6.0 g, 90 %).

DTA (5 °C min<sup>-1</sup>): 245 °C (dec.); BAM: drop hammer: 3 J (100–500 μm); friction tester: >72 N (100–500 μm); ESD: 0.19 J (100–500 μm); IR (ATR),  $\tilde{\nu}$  (cm<sup>-1</sup>) = 2323 (vw), 1630 (s), 1587 (m), 1518 (m), 1492 (w), 1453 (m), 1436 (m), 1397 (s), 1336 (s), 1290 (ws), 1159 (m), 1049 (w), 990 (m), 963 (m), 928 (m), 910 (m), 872 (w), 864 (w), 829 (w), 813 (s), 796 (s), 777 (s), 754 (m), 741 (m), 713 (m), 696 (w), 602 (vw). Raman (1064 nm, 200 mW, 25 °C):  $\tilde{\nu}$  (cm<sup>-1</sup>) = 1633 (11), 1590 (82), 1519 (59), 1492 (38), 1455 (50), 1437 (100), 1413 (13), 1404 (11), 1385 (29), 1214 (12), 1063 (24), 1049 (30), 1013 (61), 816 (19), 519 (22), 503 (17), 326 (17), 239 (12), 196 (24), 131 (93), 90 (52), 78 (26). <sup>13</sup>C NMR (*d*<sub>6</sub>-DMSO, 101 MHz, ppm)  $\delta$  = 158.6, 157.8, 146.6, 140.4, 137.4, 106.8. <sup>14</sup>N NMR (*d*<sub>6</sub>-DMSO, 29 MHz, ppm)  $\delta$  = -14. <sup>15</sup>N NMR (*d*<sub>6</sub>-DMSO, 41 MHz, ppm)  $\delta$  = 34.1, 31.8, 5.8, 5.5, -6.7, -13.3, -13.8, -24.3, -151.7, -152.8. Elem. Anal. (C<sub>6</sub>K<sub>2</sub>N<sub>10</sub>O<sub>8</sub>, 418.32 g mol<sup>-1</sup>) calcd.: C 17.23, N 33.48, H 0.00 %. Found: C 17.50, N 33.36, H 0.00 %. *m/z* (FAB<sup>+</sup>): 39 (cation) *m/z* (FAB<sup>-</sup>): 341 (anion + H<sup>+</sup>);

**3,4-Bis(4-nitramino-1,2,5-oxadiazol-3-yl)-1,2,5-furoxan H<sub>2</sub>BNAFF (3) • 0.5 Et<sub>2</sub>O**

K<sub>2</sub>BNAFF (277 mg, 0.65 mmol) was dissolved in 2 M hydrochloric acid (5 mL) at 50 °C. The water phase was extracted with Et<sub>2</sub>O (4 x 50 mL) and after drying over MgSO<sub>4</sub> the solvent was removed under reduced pressure. 3,4-Bis(4-nitramino-1,2,5-oxadiazol-3-yl)-1,2,5-furoxan (**3**) was obtained with 0.5 Et<sub>2</sub>O solvent as an oily liquid (247 mg, 100 %).

DTA (5 °C min<sup>-1</sup>): 72 °C (dec.); IR (ATR),  $\tilde{\nu}$  (cm<sup>-1</sup>) = 2981 (w), 2883 (br), 2733 (br), 2002 (vw), 1612 (s), 1552 (m), 1536 (m), 1467 (m), 1449 (m), 1385 (w), 1298 (vs), 1212 (w), 1184 (vw), 1153 (m), 1094

**Energetic Compounds Based on 3,4-Bis(4-nitramino-1,2,5-oxadiazol-3-yl)-  
1,2,5-furoxan (BNAFF)**

(m), 1067 (m), 990 (s), 968 (m), 905 (m), 863 (w), 811 (s), 760 (m), 679 (w), 610 (vw), 488 (vw), 462 (vw).  $^1\text{H}$  NMR ( $d_6$ -DMSO, 400 MHz, ppm)  $\delta$  = 12.87 (s, 2H,  $-\text{NHNO}_2$ ), 3.34 (q, 4H,  $-\text{CH}_2\text{CH}_3$ ), 1.04 (t, 6H,  $-\text{CH}_2\text{CH}_3$ ).  $^{13}\text{C}$  NMR ( $d_6$ -DMSO, 101 MHz, ppm)  $\delta$  = 154.1, 152.8, 145.6, 141.1, 137.1, 106.2, 65.2, 15.4.  $^{14}\text{N}$  NMR ( $d_6$ -DMSO, 29 MHz, ppm)  $\delta$  = -26.  $^{15}\text{N}$  NMR ( $d_6$ -DMSO, 41 MHz, ppm)  $\delta$  = 38.7, 37.5, 14.4, 10.9, -5.6, -22.9, -28.3, -29.1, -183.6, -190.4.

**Bis(guanidinium) 3,4-bis(4-nitramino-1,2,5-oxadiazol-3-yl)-1,2,5-furoxan G<sub>2</sub>BNAFF (4)**

K<sub>2</sub>BNAFF (2.00 g, 4.80 mmol) was dissolved in 2 M hydrochloric acid (16 mL) at 50 °C. The water phase was extracted with Et<sub>2</sub>O (4 x 60 mL) and after drying over MgSO<sub>4</sub> the solvent was removed under reduced pressure. The residue was suspended in H<sub>2</sub>O (8 mL) and guanidinium carbonate (0.85 g, 4.70 mmol) was added in small portions. The reaction mixture was heated until all solid material was dissolved. After cooling to room temperature the separated solid material was filtered, washed with water and dried on air to give **4** (1.76 g, 80 %).

DTA (5 °C min<sup>-1</sup>): 189 °C (dec.); BAM: drop hammer: 15 J (100–500 μm); friction tester: 360 N (100–500 μm); ESD: 0.75 J (100–500 μm); IR (ATR),  $\tilde{\nu}$  (cm<sup>-1</sup>) = 3499 (m), 3447 (s), 3322 (m), 3269 (m), 3187 (m), 1651 (s), 1584 (m), 1517 (m), 1491 (w), 1455 (m), 1433 (w), 1396 (s), 1338 (m), 1290 (vs), 1157 (m), 1014 (w), 985 (m), 958 (m), 927 (m), 919 (m), 919 (m), 874 (w), 820 (m), 799 (s), 775 (m), 738 (w), 703 (w), 687 (w), 609 (w). Raman (1064 nm, 200 mW, 25 °C):  $\tilde{\nu}$  (cm<sup>-1</sup>) = 1627 (10), 1585 (100), 1520 (42), 1490 (29), 1456 (47), 1430 (64), 1404 (11), 1385 (16), 1207 (14), 1045 (25), 1016 (86), 821 (12), 516 (20), 493 (10), 462 (10), 338 (12), 312 (10), 254 (10), 243 (10), 170 (20), 96 (89), 71 (36).  $^1\text{H}$  NMR ( $d_6$ -DMSO, 400 MHz, ppm)  $\delta$  = 6.90 (s, 6H, )  $^{13}\text{C}$  NMR ( $d_6$ -DMSO, 101 MHz, ppm)  $\delta$  = 158.6, 157.9, 157.8, 146.6, 140.5, 137.3, 106.8.  $^{14}\text{N}$  NMR ( $d_6$ -DMSO, 29 MHz, ppm)  $\delta$  = -14. Elem. Anal. (C<sub>8</sub>H<sub>12</sub>N<sub>16</sub>O<sub>8</sub>, 460.29 g mol<sup>-1</sup>) calcd.: C 20.88, H 2.63, N 48.69 %. Found: C 20.28, H 2.74, N 48.93 %.  $m/z$  (FAB<sup>+</sup>): 60 (cation);  $m/z$  (FAB<sup>-</sup>): 341 (anion + H<sup>+</sup>);

**Bis(aminoguanidinium) 3,4-bis(4-nitramino-1,2,5-oxadiazol-3-yl)-1,2,5-furoxan AG<sub>2</sub>BNAFF (5)**

K<sub>2</sub>BNAFF (1.50 g, 3.60 mmol) was dissolved in 2 M hydrochloric acid (12 mL) at 50 °C. The water phase was extracted with Et<sub>2</sub>O (4 x 60 mL) and after drying over MgSO<sub>4</sub> the solvent was removed under reduced pressure. The residue was suspended in H<sub>2</sub>O (10 mL) and aminoguanidinium carbonate (0.98 g, 7.20 mmol) was added in small portions. The reaction mixture was heated until all solid was dissolved. After cooling to room temperature the separated solid material was filtered, washed with water and dried on air to give **5** (1.50 g, 85 %).

**Energetic Compounds Based on 3,4-Bis(4-nitramino-1,2,5-oxadiazol-3-yl)-  
1,2,5-furoxan (BNAFF)**

DTA (5 °C min<sup>-1</sup>): 128 (m.p.), 156 °C (dec.); BAM: drop hammer: 8 J (100–500 µm); friction tester: 360 N (100–500 µm); ESD: 1.00 J (100–500 µm); IR (ATR),  $\tilde{\nu}$  (cm<sup>-1</sup>) = 3426 (m), 3347 (m), 3188 (br), 1651 (s), 1607 (m), 1578 (s), 1519 (m), 1494 (m), 1449 (w), 1410 (w), 1389 (m), 1335 (m), 1298 (vs), 1208 (m), 1091 (m), 1012 (w), 989 (m), 961 (s), 929 (m), 835 (m), 819 (m), 804 (m), 769 (m), 736 (w), 696 (vw). Raman (1064 nm, 200 mW, 25 °C):  $\tilde{\nu}$  (cm<sup>-1</sup>) = 1610 (38), 1583 (29), 1561 (24), 1521 (32), 1496 (100), 1448 (45), 1411 (69), 1365 (15), 1215 (10), 1163 (14), 1072 (13), 1041 (40), 1014 (95), 993 (18), 971 (32), 818 (14), 523 (10), 499 (18), 487 (18), 340 (22), 250 (28), 200 (10), 121 (80), 72 (78). <sup>1</sup>H NMR (*d*<sub>6</sub>-DMSO, 400 MHz, ppm)  $\delta$  = 7.00 (br, 4H), 4.67 (s, 2H). <sup>13</sup>C NMR (*d*<sub>6</sub>-DMSO, 101 MHz, ppm)  $\delta$  = 158.8, 158.6, 157.9, 146.6, 140.5, 137.4, 106.8. <sup>14</sup>N NMR (*d*<sub>6</sub>-DMSO, 29 MHz, ppm)  $\delta$  = -13. Elem. Anal. (C<sub>8</sub>H<sub>14</sub>N<sub>18</sub>O<sub>8</sub>, 490.32 g mol<sup>-1</sup>) calcd.: C 19.60, H 2.88, N 51.42 %. Found: C 20.08, H 2.86, N 51.05 %. *m/z* (FAB<sup>+</sup>): 75 (cation); *m/z* (FAB<sup>-</sup>): 341 (anion + H<sup>+</sup>);

**Bis(ammonium) 3,4-bis(4-nitramino-1,2,5-oxadiazol-3-yl)-1,2,5-furoxan (NH<sub>4</sub>)<sub>2</sub>BNAFF (6)**

K<sub>2</sub>BNAFF (1.67 g, 4.00 mmol) was dissolved in 2 M hydrochloric acid (20 mL) at 50 °C. The water phase was extracted with Et<sub>2</sub>O (4 x 50 mL) and after drying over MgSO<sub>4</sub> the solvent was removed under reduced pressure. The residue was dissolved in methanol (10 mL) and aqueous ammonia (25 %, 0.64 mL) with methanol (3 mL) was added. The solution was stirred for 1 h at room temperature and the solvent was removed under reduced pressure. Compound **6** was obtained as white powder (1.41 g, 94 %).

DTA (5 °C min<sup>-1</sup>): 161 °C (dec.); BAM: drop hammer: 7 J (100–500 µm); friction tester: 216 N (100–500 µm); ESD: 0.70 J (100–500 µm); IR (ATR),  $\tilde{\nu}$  (cm<sup>-1</sup>) = 3194 (br), 1624 (m), 1580 (m), 1519 (m), 1492 (w), 1402 (s), 1283 (vs), 1157 (m), 1047 (vw), 1007 (m), 989 (m), 962 (m), 927 (m), 911 (m), 875 (w), 865 (w), 832 (w), 814 (s), 795 (s), 772 (s), 753 (m), 741 (m), 712 (m), 694 (w). Raman (1064 nm, 200 mW, 25 °C):  $\tilde{\nu}$  (cm<sup>-1</sup>) = 1627 (11), 1590 (100), 1520 (57), 1494 (42), 1455 (45), 1439 (37), 1427 (37), 1401 (25), 1213 (14), 1064 (31), 1048 (28), 1011 (79), 817 (20), 518 (26), 501 (19), 330 (17), 185 (26), 126 (68). <sup>1</sup>H NMR (*d*<sub>6</sub>-DMSO, 400 MHz, ppm)  $\delta$  = 7.10 (s, 4H, NH<sub>4</sub><sup>+</sup>). <sup>13</sup>C NMR (*d*<sub>6</sub>-DMSO, 101 MHz, ppm)  $\delta$  = 158.6, 157.8, 146.6, 140.5, 137.4, 106.8. <sup>14</sup>N NMR (*d*<sub>6</sub>-DMSO, 29 MHz, ppm)  $\delta$  = -13. Elem. Anal. (C<sub>6</sub>H<sub>8</sub>N<sub>12</sub>O<sub>8</sub>, 376.21 g mol<sup>-1</sup>) calcd.: C 19.16, H 2.14, N 44.68 %. Found: C 19.36, H 2.12, N 44.48 %. *m/z* (FAB<sup>+</sup>): 18 (cation); *m/z* (FAB<sup>-</sup>): 341 (anion + H<sup>+</sup>);

**Bis(hydrazinium) 3,4-bis(4-nitramino-1,2,5-oxadiazol-3-yl)-1,2,5-furoxan (N<sub>2</sub>H<sub>5</sub>)<sub>2</sub>BNAFF (7)**

K<sub>2</sub>BNAFF (1.67 g, 4.00 mmol) was dissolved in 2 M hydrochloric acid (20 mL) at 50 °C. The water phase was extracted with Et<sub>2</sub>O (4 x 60 mL) and after drying over MgSO<sub>4</sub> the solvent was removed under reduced pressure. The residue was dissolved in methanol (10 mL) and hydrazinium hydroxide (0.40 mL) was

**Energetic Compounds Based on 3,4-Bis(4-nitramino-1,2,5-oxadiazol-3-yl)-  
1,2,5-furoxan (BNAFF)**

added dropwise. The solution was stirred at room temperature for 1 h. The solvent was removed in vacuo and the yellowish solid was dried on air to give **7** (1.52 g, 93 %).

DTA (5 °C min<sup>-1</sup>): 170 °C (dec.); BAM: drop hammer: 8 J (100–500 µm); friction tester: 216 N (100–500 µm); ESD: 0.50 J (100–500 µm); IR (ATR),  $\tilde{\nu}$  (cm<sup>-1</sup>) = 3352 (m), 3186 (m), 3042 (br), 2639 (br), 2048 (vw), 1644 (m), 1608 (m), 1582 (m), 15163 (m), 1492 (m), 1449 (m), 1435 (w), 1401 (m), 1357 (m), 1288 (vs), 1155 (m), 1089 (s), 1009 (w), 992 (m), 962 (s), 925 (m), 873 (w), 821 (m), 795 (s), 770 (s), 755 (m), 738 (m), 708 (w), 697 (m). Raman (1064 nm, 200 mW, 25 °C):  $\tilde{\nu}$  (cm<sup>-1</sup>) = 1591 (28), 1579 (42), 1569 (24), 1561 (23), 1518 (71), 1491 (27), 1450 (43), 1437 (93), 1402 (12), 1374 (11), 1336 (10), 1209 (18), 1060 (33), 1045 (16), 1011 (100), 969 (11), 821 (23), 596 (10), 515 (19), 480 (10), 408 (11), 287 (12), 243 (22), 85 (99). <sup>1</sup>H NMR (*d*<sub>6</sub>-DMSO, 400 MHz, ppm)  $\delta$  = 6.24 (s, 5H, N<sub>2</sub>H<sub>5</sub><sup>+</sup>). <sup>13</sup>C NMR (*d*<sub>6</sub>-DMSO, 101 MHz, ppm)  $\delta$  = 158.6, 157.9, 146.6, 140.5, 137.4, 106.8. <sup>14</sup>N NMR (*d*<sub>6</sub>-DMSO, 29 MHz, ppm)  $\delta$  = -13. Elem. Anal. (C<sub>6</sub>H<sub>10</sub>N<sub>14</sub>O<sub>8</sub>, 406.24 g mol<sup>-1</sup>) calcd.: C 17.74, H 2.48, N 48.27 %. Found: C 18.20, H 2.78, N 47.70 %. *m/z* (FAB<sup>+</sup>): 33 (cation); *m/z* (FAB<sup>-</sup>): 341 (anion + H<sup>+</sup>);

**Bis(hydroxylammonium) 3,4-bis(4-nitramino-1,2,5-oxadiazol-3-yl)-1,2,5-furoxan hexahydrate  
(NH<sub>3</sub>OH)<sub>2</sub>BNAFF (**8**) • 6 H<sub>2</sub>O**

K<sub>2</sub>BNAFF (1.50 g, 3.60 mmol) was dissolved in 2 M hydrochloric acid (16 mL) at 50 °C. The water phase was extracted with Et<sub>2</sub>O (4 x 60 mL) and after drying over MgSO<sub>4</sub> the solvent was removed under reduced pressure. The residue was suspended in H<sub>2</sub>O (8 mL) and hydroxylamine solution (50 wt % in H<sub>2</sub>O, 0.45 mL) was added dropwise. The reaction was cooled down to 0 °C and the separated crystalline powder was filtered and dried on air to give compound **8** as a hexahydrate (1.16 g, 63 %).

DTA (5 °C min<sup>-1</sup>): 134 °C (dec.); BAM: drop hammer: 25 J (100–500 µm); friction tester: 360 N (100–500 µm); ESD: 1.00 J (100–500 µm); IR (ATR),  $\tilde{\nu}$  (cm<sup>-1</sup>) = 3577 (m), 3252 (br), 3014 (br), 2743 (s), 1634 (s), 1611 (m), 1527 (s), 1503 (s), 1463 (m), 1421 (w), 1402 (m), 1333 (vs), 1305 (vs), 1224 (m), 1168 (m), 1075 (vw), 1041 (vw), 1007 (m), 989 (m), 962 (m), 916 (vw), 878 (vw), 827 (w), 800 (m), 768 (m), 696 (w). Raman (1064 nm, 200 mW, 25 °C):  $\tilde{\nu}$  (cm<sup>-1</sup>) = 1630 (36), 1612 (36), 1597 (24), 1583 (39), 1527 (28), 1502 (100), 1464 (55), 1440 (16), 1420 (54), 1404 (23), 1169 (14), 1076 (13), 1042 (36), 1014 (78), 990 (23), 880 (12), 825 (10), 599 (12), 517 (10), 498 (18), 492 (20), 448 (11), 346 (22), 119 (15), 160 (32), 121 (91), 93 (91). <sup>1</sup>H NMR (*d*<sub>6</sub>-DMSO, 400 MHz, ppm)  $\delta$  = 10.02 (s, H, NH<sub>3</sub>OH<sup>+</sup>) <sup>13</sup>C NMR (*d*<sub>6</sub>-DMSO, 101 MHz, ppm)  $\delta$  = 158.7, 157.9, 146.6, 140.5, 137.5, 106.9. <sup>14</sup>N NMR (*d*<sub>6</sub>-DMSO, 29 MHz, ppm)  $\delta$  = -14. Elem. Anal. (C<sub>6</sub>H<sub>20</sub>N<sub>12</sub>O<sub>16</sub>, 516.29 g mol<sup>-1</sup>) calcd.: C 13.96, H 3.90, N 32.56 %. Found: C 14.64, H 3.86, N 32.61 %. *m/z* (FAB<sup>+</sup>): 34 (cation); *m/z* (FAB<sup>-</sup>): 341 (anion + H<sup>+</sup>);

**Energetic Compounds Based on 3,4-Bis(4-nitramino-1,2,5-oxadiazol-3-yl)-  
1,2,5-furoxan (BNAFF)**

**Bis(3,6,7-triamino-[1,2,4]triazolo[4,3-*b*][1,2,4]triazolium) 3,4-bis(4-nitramino-1,2,5-oxadiazol-3-yl)-1,2,5-furoxan trihydrate (TATOT)<sub>2</sub>BNAFF (9) • 3 H<sub>2</sub>O**

K<sub>2</sub>BNAFF (428 mg, 1.02 mmol) was dissolved in 2 M hydrochloric acid (5 mL) at 50 °C. The water phase was extracted with Et<sub>2</sub>O (4 x 30 mL) and after drying over MgSO<sub>4</sub> the solvent was removed under reduced pressure. The residue was dissolved in MeOH/H<sub>2</sub>O (5:5 mL) and TATOT (316 mg, 2.05 mmol) was added. The reaction mixture was heated until the solid material was dissolved. The reaction mixture was stirred for an additional 1 h and then cooled down to room temperature. The separated solid was filtered and dried on air to yield **9** as trihydrate (482 mg, 68 %).

DTA (5 °C min<sup>-1</sup>): 190 °C (dec.); BAM: drop hammer: 40 J (100–500 μm); friction tester: 360 N (100–500 μm); ESD: 0.70 J (100–500 μm); IR (ATR),  $\tilde{\nu}$  (cm<sup>-1</sup>) = 3643 (vw), 3457 (w), 3303 (m), 3124 (br), 1691 (m), 1652 (s), 1513 (m), 1425 (m), 1395 (m), 1288 (vs), 1164 (w), 1042 (m), 1014 (w), 959 (m), 933 (m), 881 (w), 848 (w), 823 (m), 772 (m), 753 (w), 724 (w), 708 (m), 684 (m), 619 (w). Raman (1064 nm, 200 mW, 25 °C):  $\tilde{\nu}$  (cm<sup>-1</sup>) = 1591 (35), 1584 (37), 1515 (41), 1456 (18), 1433 (56), 1263 (20), 1042 (17), 1016 (40), 852 (24), 620 (12), 602 (15), 400 (14), 236 (11), 108 (100), 85 (80). <sup>1</sup>H NMR (*d*<sub>6</sub>-DMSO, 400 MHz, ppm)  $\delta$  = 8.12 (2, 2H, NH<sub>2</sub>), 7.20 (2, 2H, NH<sub>2</sub>), 5.76 (2, 2H, NH<sub>2</sub>). <sup>13</sup>C NMR (*d*<sub>6</sub>-DMSO, 101 MHz, ppm)  $\delta$  = 160.1, 158.7, 157.9, 147.4, 146.6, 141.1, 140.4, 137.3, 106.8. <sup>14</sup>N NMR (*d*<sub>6</sub>-DMSO, 29 MHz, ppm)  $\delta$  = -13. Elem. Anal. (C<sub>12</sub>H<sub>20</sub>N<sub>26</sub>O<sub>11</sub>, 704.46 g mol<sup>-1</sup>) calcd.: C 20.46, H 2.86, N 51.70 %. Found: C 20.80, H 2.81, N 51.36 %. *m/z* (FAB<sup>+</sup>): 155 (cation); *m/z* (FAB<sup>-</sup>): 341 (anion + H<sup>+</sup>);

**Disilver 3,4-bis(4-nitramino-1,2,5-oxadiazol-3-yl)-1,2,5-furoxan dihydrate (Ag)<sub>2</sub>BNAFF• 2 H<sub>2</sub>O (10)**

K<sub>2</sub>BNAFF (420 mg, 1.00 mmol) was dissolved in 2 M hydrochloric acid (5 mL) at 50 °C. The water phase was extracted with Et<sub>2</sub>O (4 x 30 mL) and after drying over MgSO<sub>4</sub> the solvent was removed under reduced pressure. The residue was dissolved in MeOH/H<sub>2</sub>O (6:3 mL) and AgNO<sub>3</sub> (340 mg, 2.00 mmol) was added. The reaction mixture was stirred for 30 min at room temperature. The solid material was then filtered and dried on air to give **10** as a dihydrate (395 mg, 67 %) as white solid.

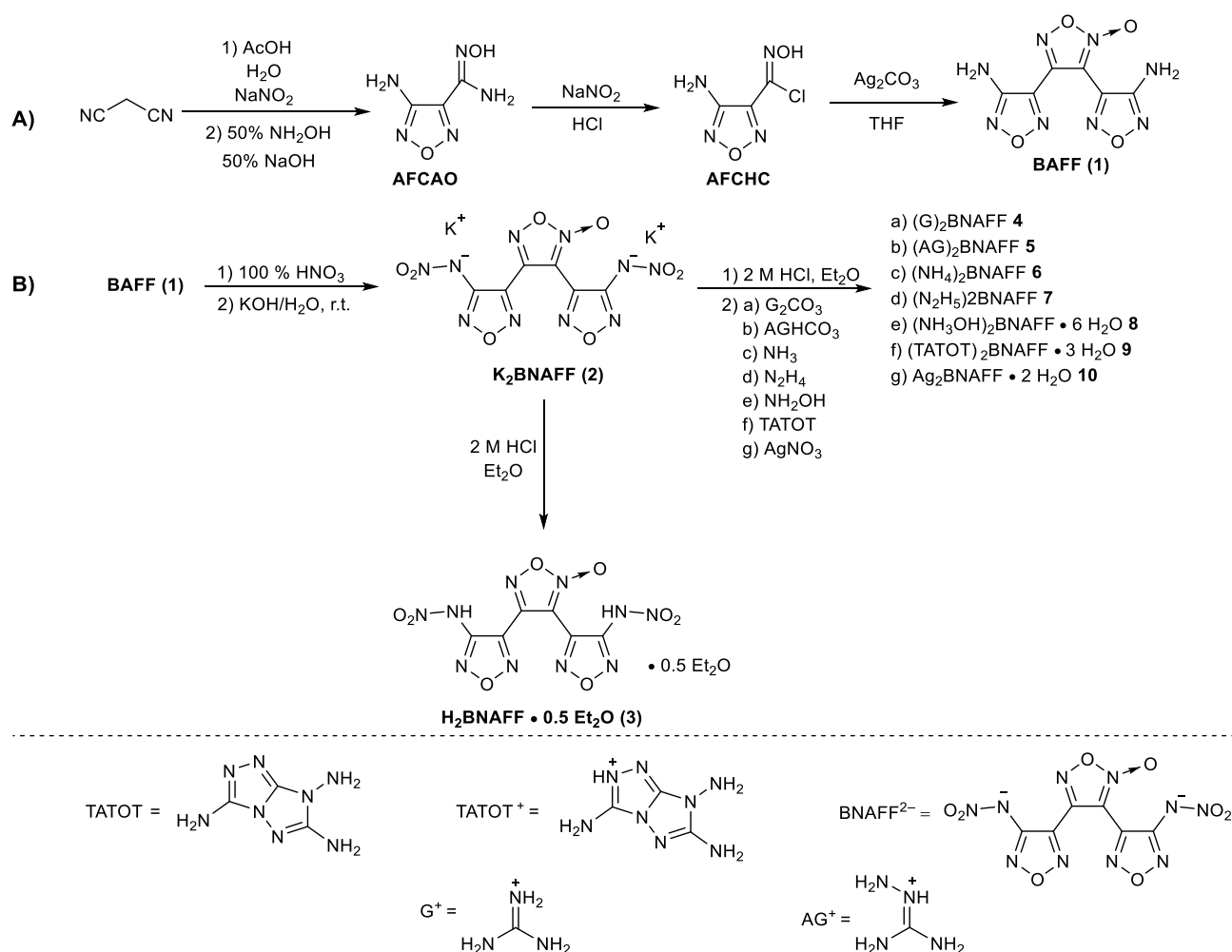
DTA (5 °C min<sup>-1</sup>): 82 °C (dec.); BAM: drop hammer: 1 J (100–500 μm); friction tester: 60 N (100–500 μm); ESD: 50 mJ (100–500 μm); IR (ATR),  $\tilde{\nu}$  (cm<sup>-1</sup>) = 3562 (br), 3242 (br), 1636 (m), 1595 (w), 1563 (m), 1516 (m), 1501 (m), 1432 (s), 1364 (m), 1324 (s), 1290 (vs), 1170 (m), 1072 (w), 1009 (m), 995 (s), 974 (m), 941 (m), 911 (w), 871 (m), 817 (s), 768 (m), 748 (w), 693 (m), 598 (vw), 582 (vw), 521 (w). Raman (1064 nm, 200 mW, 25 °C):  $\tilde{\nu}$  (cm<sup>-1</sup>) = 1646 (15), 1599 (65), 1576 (22), 1531 (70), 1506 (37), 1439 (56), 1372 (20), 1171 (11), 1067 (65), 1014 (32), 926 (12), 815 (16), 773 (11), 762 (15), 753 (25),

## Energetic Compounds Based on 3,4-Bis(4-nitramino-1,2,5-oxadiazol-3-yl)- 1,2,5-furoxan (BNAFF)

598 (15), 552 (11), 505 (44), 460 (17), 434 (11), 321 (20), 308 (15), 248 (19), 98 (100).  $^{13}\text{C}$  NMR ( $d_6$ -DMSO, 101 MHz, ppm)  $\delta$  = 157.9, 156.9, 145.9, 140.1, 137.1, 106.6.  $^{14}\text{N}$  NMR ( $d_6$ -DMSO, 29 MHz, ppm)  $\delta$  = -15. Elem. Anal. ( $\text{C}_6\text{H}_4\text{Ag}_2\text{N}_{10}\text{O}_{10}$ , 591.89 g mol $^{-1}$ ) calcd.: C 12.18, H 0.68, N 23.66 %. Found: C 12.11, H 0.51, N 23.69 %.

### 3.3. Results and Discussion

The synthesis of the starting material BAFF has been performed as reported previously in the literature. Initially 4-amino-1,2,5-oxadiazole-3-carboxamidoxime (AFCAO) was synthesized by reacting commercially available malononitrile with aqueous nitrous acid and then with 50% aqueous hydroxylamine. AFCAO was treated with sodium nitrite in aqueous HCl to give 4-amino-1,2,5-oxadiazole-3-carbohydroximoyl chloride (AFCHC) which is then reacted with  $\text{Ag}_2\text{CO}_3$  in THF to give BAFF.<sup>[17,20,22]</sup> The synthesis and nitration of BAFF are displayed in **Scheme 1**.



**Scheme 1.** A) Literature known synthesis of 3,4-bis(4-amino-1,2,5-oxadiazol-3-yl)-1,2,5-furoxan (**1**, BAFF); B) Nitration of compound **1** and synthesis of new nitrogen-rich salts with BNAFF (**3**).

## Energetic Compounds Based on 3,4-Bis(4-nitramino-1,2,5-oxadiazol-3-yl)-1,2,5-furoxan (BNAFF)

The amino groups of 3,4-bis(4-amino-1,2,5-oxadiazol-3-yl)-1,2,5-furoxan are nitrated with 100%  $\text{HNO}_3$  at  $-10\text{ }^\circ\text{C}$  and the formed, unstable dinitramino derivative ( $\text{H}_2\text{BNAFF}$ ) is converted with potassium hydroxide to the dipotassium salt (**2**,  $\text{K}_2\text{BNAFF}$ ) in a good yield (90 %). The neutral compound **3** can be isolated by dissolving  $\text{K}_2\text{BNAFF}$  (**2**) in 2 M hydrochloric acid and then extracting with diethyl ether giving an oily liquid.  $\text{H}_2\text{BNAFF}$  is only stable at room temperature only with 0.5 equivalents ether as a solvate ( $\text{BNAFF}$  (**3**)  $\cdot$  0.5  $\text{Et}_2\text{O}$ ).

However,  $\text{H}_2\text{BNAFF}$  is unstable at room temperature without  $\text{Et}_2\text{O}$  and decomposes with the release of nitrous gases. Using other solvents as extraction medium resulted in decomposition of the neutral compound. Using  $\text{K}_2\text{BNAFF}$  (**2**) as the starting material nitrogen-rich salts of BNAFF can be synthesized. For this purpose, compound **2** is dissolved in a small amount of 2 M  $\text{HCl}$  and the *in situ* generated neutral compound (**3**) is reacted with the desired base giving compounds **4–10** (Scheme 1).

### 3.3.1. Crystal structures

During this work the crystal structures of compounds **2**, **4**, **5**, **8** and **10** were determined by low-temperature X-ray diffraction. Compounds **2**, **4** and **5** crystallize anhydrously whereas compound **8** crystallizes with six molecules of water. The crystal structure of **10** was determined of single crystals from conc. ammonia solution containing two molecules  $\text{NH}_3$ . Selected data and parameters for the low-temperature X-ray data collection and refinements are given in the Supporting Information. A distortion of the N-oxide moiety in the furoxan ring of the  $\text{BNAFF}^{2-}$  anion can be observed in the obtained crystal structures for compounds **4**, **5**, **8** and **10**.

Dipotassium 3,4-bis(4-nitramino-1,2,5-oxadiazol-3-yl)-1,2,5-furoxane (**2**) crystallizes from water, without inclusion of solvent molecules, in the triclinic space group  $P\bar{1}$  with two molecules per unit cell and a cell volume of  $651.80 \cdot 10^6 \text{ pm}^3$ . The density of **2** at a temperature of 103 K is  $2.132 \text{ g cm}^{-3}$ . Figure 2 illustrates the molecular unit of the potassium salt (**2**). The torsion angle of  $\text{C1-C2-C3-N5}$  and  $\text{N6-C4-C5-C6}$  in  $\text{BNAFF}^{2-}$  anion are  $-63.0(5)$  and  $18.1(6)^\circ$  respectively, showing that both furazan rings are not coplanar to the furoxan ring.

**Energetic Compounds Based on 3,4-Bis(4-nitramino-1,2,5-oxadiazol-3-yl)-  
1,2,5-furoxan (BNAFF)**

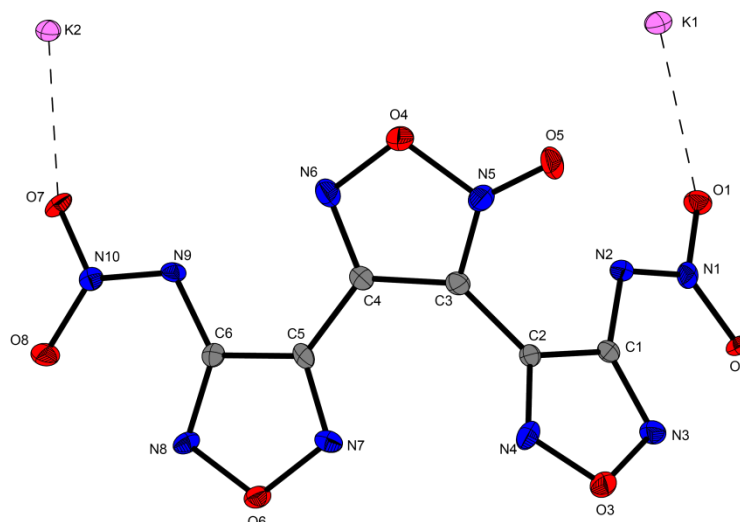


**Figure 2.** Molecular unit of **2**, showing the atom-labeling scheme and bond lengths (pm) with standard deviations. Thermal ellipsoids represent the 50 % probability level and hydrogen atoms are shown as small spheres of arbitrary radius.

Bis(guanidinium) 3,4-bis(4-nitramino-1,2,5-oxadiazol-3-yl)-1,2,5-furoxan (**4**) crystallizes in the monoclinic space group  $P2/c$  with a cell volume of  $1761.43 \cdot 10^6 \text{ pm}^3$  and four molecules per unit cell. The density at a temperature of 123 K is  $1.736 \text{ g cm}^{-3}$ . The furoxan and furazan rings in the  $\text{BNAFF}^{2-}$  anion have a planar structure ( $\text{O4-N6-C4-C3}$   $0.5^\circ$ ,  $\text{N2-O1-N1-C1}$   $-0.3^\circ$  and  $\text{O6-N7-C5-C6}$   $0.2^\circ$ ). However, both furazan rings in the anion are not coplanar to the furoxan ring as indicated by the torsion angle of  $\text{C2-C3-C4-C5}$   $-14.6^\circ$ . Both nitramino groups in  $\text{BNAFF}^{2-}$  are slightly tilted against the furazan rings as shown by the torsion angles of  $\text{N10-N9-C6-N8}$   $6.4^\circ$  and  $\text{N4-N3-C1-N1}$   $-5.4^\circ$ . The bond distances of the furoxan ring ( $\text{C3-C4}$   $1.418 \text{ \AA}$  and  $\text{N5-C3}$   $132.0 \text{ pm}$ ), furazan rings ( $\text{C1-C2}$   $143.6 \text{ pm}$  and  $\text{N8-C6}$   $131.1 \text{ pm}$ ) and the nitramino moiety ( $\text{N3-N4}$   $131.5 \text{ pm}$ ,  $\text{N9-N10}$   $132.2 \text{ pm}$ ,  $\text{O2-N4}$   $125.5 \text{ pm}$  and  $\text{O7-N10}$   $125.7 \text{ pm}$ ) are in accordance with similar nitramino oxadiazoles reported in the literature.<sup>[23]</sup>



**Energetic Compounds Based on 3,4-Bis(4-nitramino-1,2,5-oxadiazol-3-yl)-  
1,2,5-furoxan (BNAFF)**

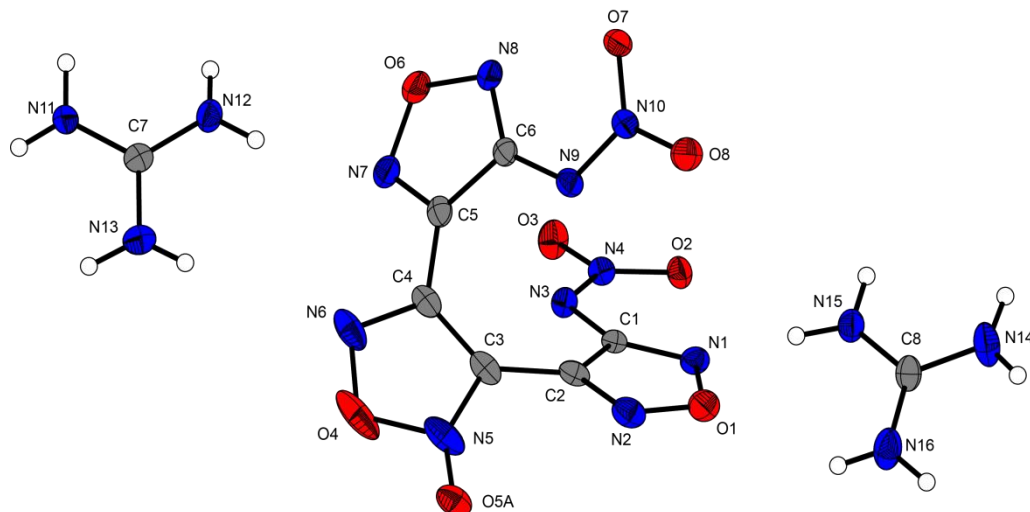


**Figure 3.** Representation of the molecular unit of **4**, showing the atom-labeling scheme. Thermal ellipsoids represent the 50 % probability level and hydrogen atoms are shown as small spheres of arbitrary radius. Selected bond distances (pm) and angles [°]: C3–C4 141.8(4), N5–C3 132.0(3), C1–C2 143.6(3), N8–C6 131.1(3), N3–N4 131.5(3), N9–N10 132.2(3), O7–N10 125.7(2), O4–N6–C4–C3 0.5(3), N2–O1–N1–C1 –0.3(2), O6–N7–C5–C6 0.2(2), C2–C3–C4–C5 –14.6(6), N10–N9–C6–N8 6.4(4), N4–N3–C1–N1 –5.4(4).

Bis(aminoguanidinium) 3,4-bis(4-nitramino-1,2,5-oxadiazol-3-yl)-1,2,5-furoxan (**5**) crystallizes from water, without inclusion of solvent molecules, in the monoclinic space group *P2<sub>1</sub>/c* with four molecules per unit cell and a cell volume of  $1863.35 \cdot 10^6 \text{ pm}^3$ . The density of **5** at a temperature of 123 K is  $1.748 \text{ g cm}^{-3}$ . Figure 4 illustrates the molecular unit of **5**. The torsion angle of C1–C2–C3–C3<sup>i</sup> in BNAFF<sup>2-</sup> anion is  $-39.6^\circ$ , showing that both furazan rings are not coplanar to the furoxan ring. The connecting C–C bond of the oxadiazoles (C2–C3) with a length of 145.9 pm is significantly shorter than a C–C single bond (154.0 pm). The nitramino moiety is slightly twisted from the furazan plane with torsion angle of  $-177.45^\circ$  (C1–N3–N4–O3). The bond distances of the furoxan ring (O4–N5 139.8 pm and N5–C3 131.8 pm), furazan rings (O1–N2 136.5 pm and C1–C2 143.5 pm) and the nitramino moiety (N3–N4 131.42 pm, N3–C1 137.9 pm, O3–N4 126.68 pm) are in accordance with similar nitramino oxadiazoles reported in the literature.<sup>[23]</sup>

Energetic Compounds Based on 3,4-Bis(4-nitramino-1,2,5-oxadiazol-3-yl)-  
1,2,5-furoxan (BNAFF)

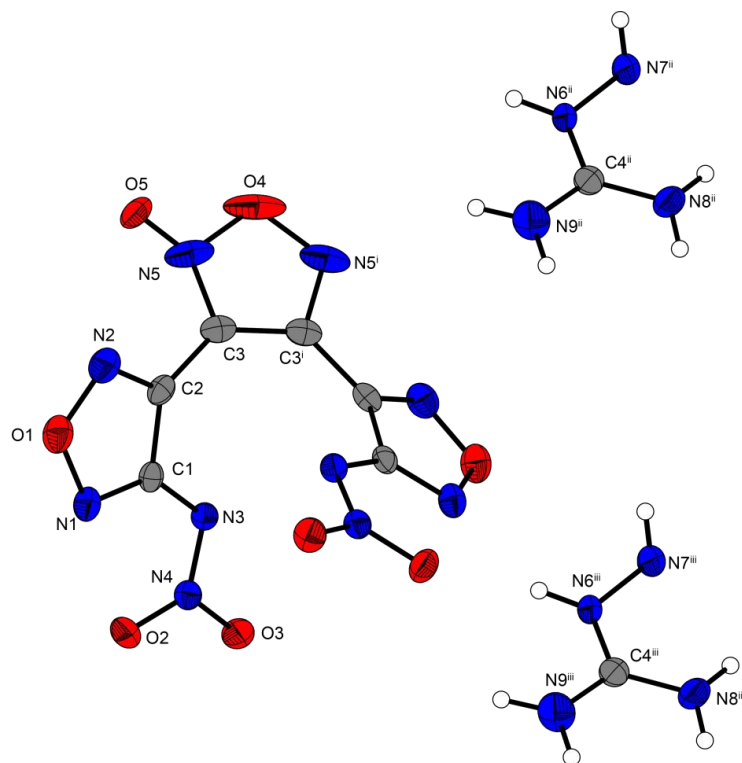


**Figure 4.** Molecular unit of **5**, showing the atom-labeling scheme and bond lengths (pm) with standard deviations. Thermal ellipsoids represent the 50 % probability level and hydrogen atoms are shown as small spheres of arbitrary radius. Symmetry codes: (i)  $x, y, z$ , (ii)  $1-x, y, 0.5-z$ , (iii)  $1-x, 0.5+y, 1-z$ . Selected bond distances (pm) and angles [ $^{\circ}$ ]: C2–C3 145.9(2), O4–N5 139.8(2), N5–C3 131.8(2), O1–N2 136.5(2), C1–C2 143.5(2), C1–C2–C3–C3<sup>i</sup> –39.6(3), C1–N3–N4–O3 –177.45(13).

Disilver 3,4-bis(4-nitramino-1,2,5-oxadiazol-3-yl)-1,2,5-furoxan (**10**) is crystallized from hot water with conc. ammonia solution, with inclusion of two molecules ammonia, in the triclinic space group  $P\bar{1}$  with two molecules per unit cell and a cell volume of  $784.58(12) \cdot 10^6 \text{ pm}^3$ . The density of **10** at a temperature of 173 K is  $2.497 \text{ g cm}^{-3}$ . **Figure 5** illustrates the molecular unit of  $\text{Ag}_2\text{BNAFF} \cdot 2\text{NH}_3$ .

**Energetic Compounds Based on 3,4-Bis(4-nitramino-1,2,5-oxadiazol-3-yl)-  
1,2,5-furoxan (BNAFF)**

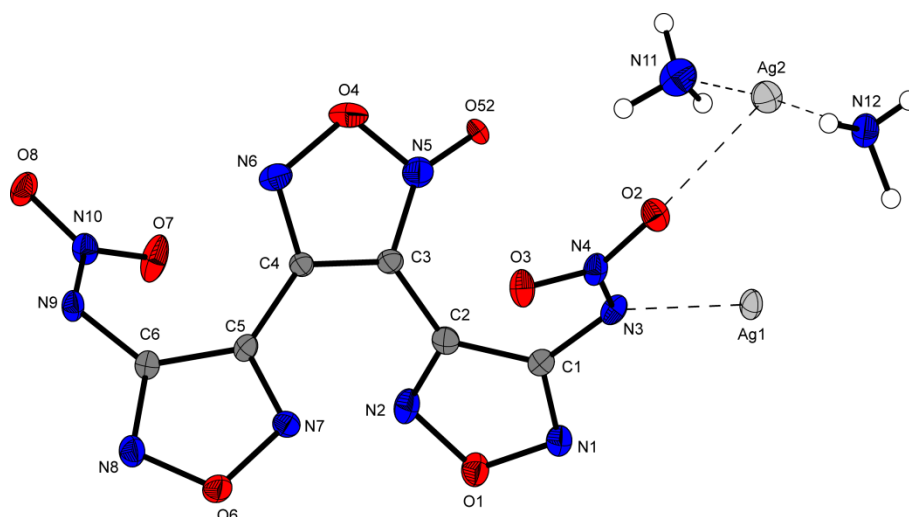


**Figure 5.** Molecular unit of **10**, showing the atom-labeling scheme and bond lengths (pm) with standard deviations. Thermal ellipsoids represent the 50 % probability level and hydrogen atoms are shown as small spheres of arbitrary radius.

### 3.3.2. NMR Spectroscopy

All synthesized compounds were characterized with multinuclear NMR ( $^1\text{H}$ ,  $^{13}\text{C}$  and  $^{14}\text{N}$ ) spectroscopy. In addition,  $^{15}\text{N}$  NMR spectra of **2** and **3**•0.5Et<sub>2</sub>O were recorded. Compound **3**•0.5Et<sub>2</sub>O shows three different resonances in the  $^1\text{H}$  NMR spectrum; one at 12.87 ppm for the acidic protons of the nitramine groups ( $-\text{NHNO}_2$ ) and two at 3.34 ( $-\text{OCH}_2\text{CH}_3$ ) and 1.04 ( $-\text{OCH}_2\text{CH}_3$ ) ppm for the ether solvate ( $^1\text{H}$ ,  $^{13}\text{C}$  and  $^{14}\text{N}$  NMR spectra of compound **3**•0.5Et<sub>2</sub>O are displayed in the Supporting Information). All six observed resonances in  $^{13}\text{C}$  spectrum of the neutral nitramine compound **3**•0.5Et<sub>2</sub>O are high-field shifted in comparison to all observed resonances in the  $^{13}\text{C}$  spectra of all energetic salts with the BNAFF<sup>2-</sup> anion. The  $^{14}\text{N}$  resonances for the nitro groups in compound **3** are detected at –26 ppm and the nitro groups of the energetic salts are observed in the range of –13 to –15 ppm. The values for all  $^1\text{H}$ ,  $^{13}\text{C}$  and  $^{14}\text{N}$  resonances of compounds **2** and **3**•0.5Et<sub>2</sub>O are listed in **Table 1**.

**Table 1.**  $^1\text{H}$ ,  $^{13}\text{C}$  and  $^{14}\text{N}$  NMR shifts of compounds **2** and **3**•0.5Et<sub>2</sub>O.

Compound	$^1\text{H}$ NMR $\delta$ [ppm]	$^{13}\text{C}$ NMR $\delta$ [ppm]	$^{14}\text{N}$ NMR $\delta$ [ppm]
<b>2</b>	–	158.6, 157.8, 146.6, 140.4, 137.4, 106.8.	–14
<b>3</b>	12.87, 3.34, 1.04	154.1, 152.8, 145.6, 141.1, 137.1, 106.2, 65.2, 15.4	–26

**Energetic Compounds Based on 3,4-Bis(4-nitramino-1,2,5-oxadiazol-3-yl)-  
1,2,5-furoxan (BNAFF)**

**Figure 6** shows the comparison between both recorded  $^{15}\text{N}$  NMR spectra for compounds **2** and **3**. In the spectrum of the neutral nitramine compound **3** the nitro groups are found at  $-28.3$  and  $-29.0$  ppm and the NH groups at  $-183.9$  and  $-190.4$  ppm (no coupling to hydrogen due to exchange with the solvent  $d_6$ -DMSO). Upon formation of the potassium salt (deprotonation) all resonances in  $^{15}\text{N}$  NMR show strong low-field shift as observed in the case of the nitro (to  $-13.3$  and  $-13.8$  ppm) and NH groups ( $-151.7$  and  $-152.8$  ppm).

**$^{15}\text{N}$  NMR (41 MHz,  $d_6$ -DMSO)**

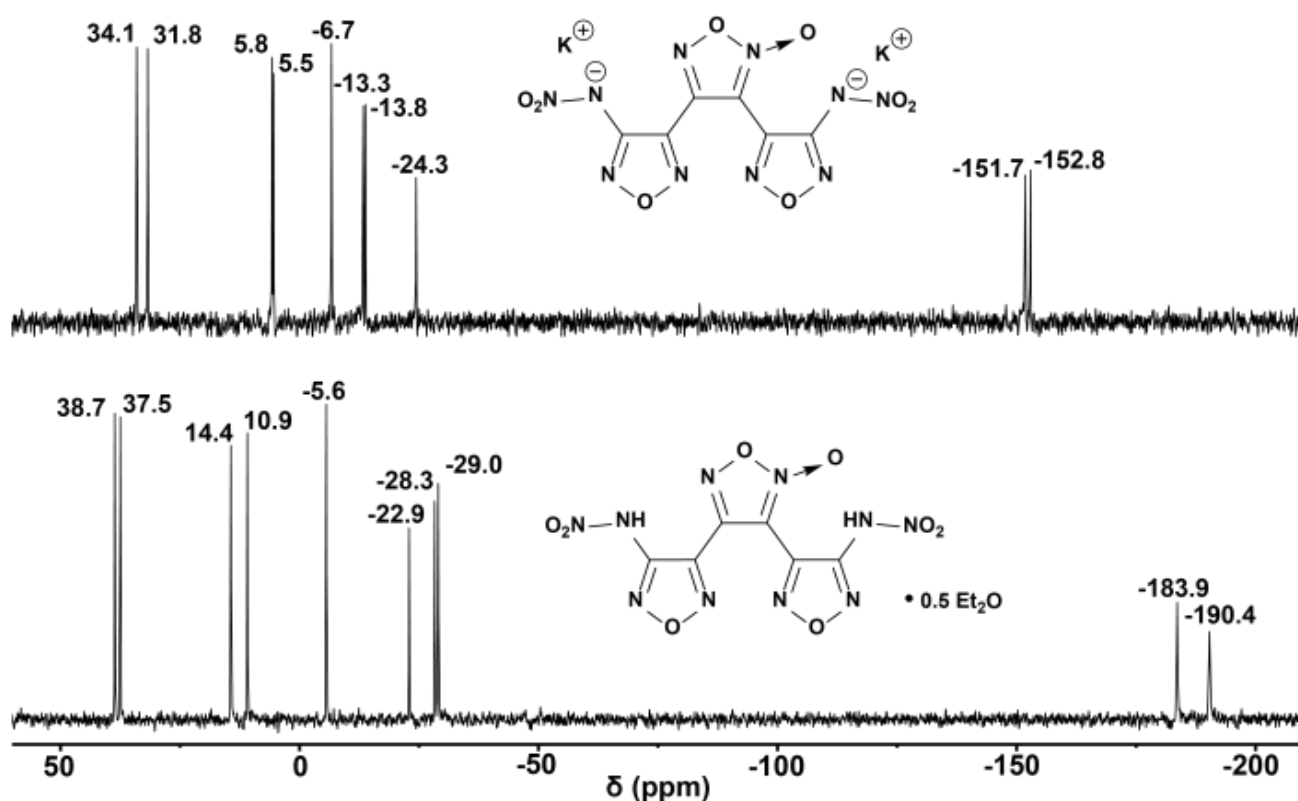


**Figure 6.** Recorded  $^{15}\text{N}$  NMR spectra of K<sub>2</sub>BNAFF (**2**) and BNAFF (**3**) • 0.5 Et<sub>2</sub>O in  $d_6$ -DMSO.

### 3.3.3. Physicochemical properties

Since all synthesized compounds can be considered as energetic materials, their energetic behaviors were investigated. However, only the physicochemical properties of compounds **2**, **4**, **5**, **6** and **7** are discussed because they were obtained as anhydrous compounds. All theoretical calculated and experimentally determined values for compounds **2**, **4**–**7** compared to the high explosive RDX are listed in **Table 2**.

**Energetic Compounds Based on 3,4-Bis(4-nitramino-1,2,5-oxadiazol-3-yl)-  
1,2,5-furoxan (BNAFF)**

**Table 2.** Physico-chemical properties of **2**, **4–7** in comparison to RDX.

	<b>2</b>	<b>4</b>	<b>5</b>	<b>6</b>	<b>7</b>	<b>RDX</b>
Formula	C <sub>6</sub> K <sub>2</sub> N <sub>10</sub> O <sub>8</sub>	C <sub>8</sub> H <sub>12</sub> N <sub>16</sub> O <sub>8</sub>	C <sub>8</sub> H <sub>14</sub> N <sub>18</sub> O <sub>8</sub>	C <sub>6</sub> H <sub>8</sub> N <sub>12</sub> O <sub>8</sub>	C <sub>6</sub> H <sub>10</sub> N <sub>14</sub> O <sub>8</sub>	C <sub>3</sub> H <sub>6</sub> N <sub>6</sub> O <sub>6</sub>
<i>IS</i> <sup>[a]</sup> [J]	3	15	8	7	8	7.5
<i>FS</i> <sup>[b]</sup> [N]	> 72	360	360	216	216	120
<i>ESD</i> <sup>[c]</sup> [J]	0.19	0.75	1.00	0.70	0.50	0.2
<i>Q</i> <sup>[d]</sup> [%]	−19.12	−48.66	−48.95	−34.02	−35.45	−21.6
<i>T<sub>m</sub></i> <sup>[e]</sup> [°C]	–	–	128	–	–	–
<i>T<sub>dec</sub></i> <sup>[f]</sup> [°C]	245	189	156	161	170	210
<i>ρ</i> <sup>[g]</sup> [g cm <sup>−3</sup> ]	2.07	1.692	1.703	1.735(pyc)	1.535(pyc)	1.806 <sup>[24]</sup>
<i>ΔH<sub>f</sub></i> <sup>[h]</sup> [kJ kg <sup>−1</sup> ]	689	1275	1650	1635	2239	387
<b>EXPLO5</b> <b>6.03</b> <sup>[25]</sup>						
<i>−Δ<sub>E</sub>U</i> <sup>[i]</sup> [kJ kg <sup>−1</sup> ]	5483	4721	4981	5701	5953	5798
<i>T<sub>C-J</sub></i> <sup>[j]</sup> [K]	3772	3318	3389	3922	4169	3831
<i>p<sub>C-J</sub></i> <sup>[k]</sup> [kbar]	299	253	269	305	257	354
<i>V<sub>det.</sub></i> <sup>[l]</sup> [m s <sup>−1</sup> ]	8263	8099	8364	8579	8105	8834
<i>V<sub>0</sub></i> <sup>[m]</sup> [dm <sup>3</sup> kg <sup>−1</sup> ]	470	796	819	779	846	792

[a] Impact sensitivity (BAM drophammer, method 1 of 6); [b] friction sensitivity (BAM drophammer, method 1 of 6); [c] electrostatic discharge device (OZM research); [d] oxygen balance; [e] melting point (DTA,  $\beta = 5^{\circ}\text{C}\cdot\text{min}^{-1}$ ); [f] temperature of decomposition (DTA,  $\beta = 5^{\circ}\text{C}\cdot\text{min}^{-1}$ ); [g] density at 298 K; [h] standard molar enthalpy of formation; [i] detonation energy; [j] detonation temperature; [k] detonation pressure; [l] detonation velocity; [m] volume of detonation gases at standard temperature and pressure conditions.

### 3.3.4. Thermal behavior

The thermal behavior of compounds **2**, **4–10** was investigated with an OZM Research DTA 552-Ex instrument at a heating rate of 5 °C min<sup>-1</sup>. Critical temperatures are given as the onset temperature. The neutral compound **3** decomposes simultaneously as soon as the ether solvate is removed from the molecule. The neutral nitramine (**3**) exhibits only one sharp exothermal signal at 72 °C in the DTA plot. Additional data can be found in the Supporting Information. From all synthesized salts of BNAFF, compound **2** has the highest decomposition point at 245 °C. All formed nitrogen-rich salts with the BNAFF<sup>2-</sup> anion decompose in the range of 150–200 °C, whereas the guanidinium salt (**4**) has the highest decomposition temperature of 189 °C.

### 3.3.5. Sensitivities

In addition, the sensitivities for all compounds toward friction, impact and electrostatic discharge were explored using the BAM standards.<sup>[26,27]</sup> The silver (**10**, IS = 1 J, FS = 60 N and ESD = 50 mJ) and potassium salts (**2**, IS = 3 J, FS = > 72 N and ESD = 0.19 J) are the most sensitive compounds from all synthesized energetic materials formed with the BNAFF<sup>2-</sup> anion. From all nitrogen-rich compounds the ammonium salt (**6**) is the most sensitive compound (IS = 7 J and FS = 216 N) toward friction and impact. The impact and friction sensitivities for the others range from 7 J to 15 J and from 216 N to 360 N.

### 3.3.6. Detonation parameters

The detonation parameters for compounds **2**, **4**, **5**, **6** and **7** were calculated using the EXPLO5\_V6.03 computer code.<sup>[25]</sup> The EXPLO5 detonation parameters of compounds **2**, **4–7** were calculated by using the room-temperature density values obtained from the X-ray structures (compounds **2**, **4** and **5**) as described in reference<sup>[28]</sup> or by using pycnometrical measured densities of compounds **6** and **7**. The densities range from 1.535 g cm<sup>-3</sup> (**7**, pyc) to 2.07 g cm<sup>-3</sup> (**2**). All compounds reported in **Table 2** exhibit a highly positive heat of formation from 689 kJ kg<sup>-1</sup> (**2**) to 2239 kJ kg<sup>-1</sup> (**7**), which exceed the value for the heat of formation of RDX (387 kJ kg<sup>-1</sup>). Compounds **2**, **4–7** show good calculated detonation parameters with detonation velocities ( $V_{det.}$ ) between 8000–8600 m s<sup>-1</sup> and detonation pressure ( $p_{C-J}$ ) 250–310 kbar. Compound **6** shows the highest calculated detonation velocity (8579 m s<sup>-1</sup>) and detonation pressure (305 kbar), whereas the guanidinium salt (**4**) exhibits the lowest values ( $V_{det.}$  = 8099 m s<sup>-1</sup> and  $p_{C-J}$  = 253 kbar).

### 3.4. Conclusion

In summary, 3,4-bis(4-nitramino-1,2,5-oxadiazol-3-yl)-1,2,5-furoxan (**3**) was synthesized for the first time by nitration of 3,4-bis(4-amino-1,2,5-oxadiazol-3-yl)-1,2,5-furoxan (**1**) with 100% nitric acid. Compound **3** is only stable at room temperature with 0.5 equivalents ether as a solvate. The stability of the BNAFF<sup>2-</sup> anion can be tamed by forming alkali metal salts or by reacting it with nitrogen-rich bases. Starting from the potassium salt (**2**, K<sub>2</sub>BNAFF), different metal and nitrogen-rich salts with the BNAFF<sup>2-</sup> anion were synthesized and characterized using multinuclear NMR spectroscopy, vibrational spectroscopy (IR and Raman), X-ray single-crystal diffraction, DTA, BAM sensitivity methods and elemental analysis. In addition, the heats of formation and detonation properties of all anhydrous energetic compounds were calculated. Salt formation leads to the stabilization of the BNAFF<sup>2-</sup> anion and increase of the thermal stability up to 245 °C. High detonation velocities (8000–8600 m s<sup>-1</sup>) were calculated for the anhydrous compounds **2**, **4–7**.

### 3.5. Acknowledgement

Financial support of this work by the Ludwig-Maximilian University of Munich (LMU), the Office of Naval Research (ONR) under grant no. ONR.N00014-16-1-2062, and the Bundeswehr–Wehrtechnische Dienststelle für Waffen und Munition (WTD 91) under grant no. E/E91S/FC015/CF049 is gratefully acknowledged. We thank Dr. Burkhard Krumm for NMR measurements and Stefan Huber for his help with the sensitivity testing.

**Keywords:** Furoxanes • Furazanes • Energetic materials • Nitramines • Structure Elucidation

### 3.6. References

- [1] a) P. Yin, J. M. Shreeve, From *N*-Nitro to *N*-Nitroamino: Preparation of High-Performance Energetic Materials by Introducing Nitrogen-Containing Ions, *Angew. Chem. Int. Ed.* **2015**, *54*, 1–6. b) D. Fischer, J. L. Gottfried, T. M. Klapötke, K. Karaghiosoff, J. Stierstorfer and T. G. Witkowski, Synthesis and Investigation of Advanced Energetic Materials Based on Bispyrazolylmethanes, *Angew. Chem., Int. Ed.*, **2016**, *55*, 16132–16135.
- [2] J. P. Agrawal, Recent trends in high-energy materials, *Prog. Energy Combust. Sci.* **1998**, *24*, 1–30.
- [3] T. M. Klapötke, *Chemistry of High-Energy Materials*, 3rd Edition, Walter de Gruyter GmbH & Co KG, Berlin, **2015**.
- [4] J. J. Sabatini, K. D. Oyler, Recent Advances in the Synthesis of High Explosive Materials, *Crystals* **2016**, *6*, 5–22.

**Energetic Compounds Based on 3,4-Bis(4-nitramino-1,2,5-oxadiazol-3-yl)-  
1,2,5-furoxan (BNAFF)**

- [5] R. J. Spear, W. S. Wilson, Recent Approaches to the Synthesis of High Explosives and Energetic Materials: A Review, *J. Energ. Mater.* **1984**, 2, 61–149.
- [6] B. T. Federoff, H. A. Aaronson, E. F. Reese, O. E. Sheffield, G. D. Clift, *Encyclopedia of Explosives and Related Items*; Picatinny Arsenal: Dover, USA, **1960**.
- [7] J. P. Agrawal, R. Hodgson, *Organic Chemistry of Explosives*, 2nd Edition, John Wiley & Sons: Chichester, England, **2007**.
- [8] P. F. Pagoria, G. S. Lee, A. R. Mitchell, R. D. Schmidt, A Review of Energetic Materials Synthesis, *Thermochim. Acta* **2002**, 384, 187–204.
- [9] a) A. B. Sheremetev, E. A. Ivanova, N. P. Spiridonova, S. F. Melnikova, I. V. Tselinsky, K. Y. Suponitsky, M. Y. Antipin, Desilylative, Desilylative Nitration of C,N-Disilylated 3-Amino-4-methylfuran, *J. Heterocycl. Chem.* **2007**, 42, 1237–1242. b) Z. Feng-qi, C. Pei, H. Rong-zu, L. Yang, Z. Zhi-zhong, Z. Yan-shui, Y. Xu-wu, G. Yin, G. Sheng-li, S. Qi-zhen, Thermochemical properties and non-isothermal decomposition reaction kinetics of 3,4-dinitrofurazanfuroxan (DNTF), *J. Hazard. Mater.* **2004**, 113, 67–71
- [10] A. I. Stepanov, D. V. Dashko, A. A. Astrat`ev, 1,2-Di(4-R-furazan-3-yl)glyoximes: Synthesis by the reduction of 3,4-bis(4-R-furazan-3-yl)furoxans and study of the reactivity of these compounds, *Chem. Heterocycl. Comp.* **2013**, 49, 776–790.
- [11] D. E. Chavez, D. A. Parrish, P. Leonard, The Synthesis and Characterization of a New Furazan Heterocyclic System, *Synlett* **2012**, 23, 2126–2128.
- [12] D. Fischer, T. M. Klapötke, M. Reymann, J. Stierstorfer, Dense Energetic Nitraminofurazanes, *Chem. Eur. J.* **2014**, 20, 6401–6411.
- [13] a) Y. Tang, C. He, L. A. Mitchell, D. A. Parrish, J. M. Shreeve, Potassium 4,4'-Bis(dinitromethyl)-3,3'-azofurazanate: A Highly Energetic 3D Metal-Organic Framework as a Promising Primary Explosive, *Angew. Chem.* **2016**, 128, 1–4. b) X. Wang, K. Xu, Q. Sun, B. Wang, C. Zhou, F. Zhao, The Insensitive Energetic Material Trifurazanooxacycloheptatriene (TFO): Synthesis and Detonation Properties, *Propellants Explos. Pyrotech.* **2015**, 40, 9–12.
- [14] D. E. Chavez, *Energetic Heterocyclic N-Oxides. In: Larionov O. (eds) Heterocyclic N-Oxides. Topics in Heterocyclic Chemistry*, 53, Springer, **2017**, 1–27.
- [15] P. W. Leonard, C. J. Pollard, D. E. Chavez, B. M. Rice, D. A. Parrish, 3,6-Bis(4-nitro-1,2,5-oxadiazol-3-yl)-1,4,2,5-dioxadiazene (BNDD): A Powerful Sensitive Explosive, *Synlett* **2011**, 14, 2097–2099.
- [16] Y. Tang, J. Zhang, L. A. Mitchell, D. A. Parrish, J. M. Shreeve, Taming of 3,4-Di(nitramino)furan, *J. Am. Chem. Soc.* **2015**, 123, 15984–15987.



**Energetic Compounds Based on 3,4-Bis(4-nitramino-1,2,5-oxadiazol-3-yl)-  
1,2,5-furoxan (BNAFF)**

- [17] R. Tsyshevsky, P. Pagoria, M. Zhang, A. Racoveanu, A. DeHope, D. Parrish, M. Kuklja, Searching for Low-Sensitivity Cast-Melt High-Energy-Density Materials: Synthesis, Characterization, and Decomposition Kinetics of 3,4-Bis(4-nitro-1,2,5-oxadiazol-3-yl)-1,2,5-oxadiazole-2-oxide, *J. Phys. Chem. C* **2015**, *119*, 3509–3521.
- [18] S. Loebbecke, H. Schuppler, W. Schweikert, Thermal Properties of Different Substituted Energetic Furoxans. *Proceedings of the 33rd International Annual Conference of ICT (Energetic Materials)*, Karlsruhe, Germany, June 25–28, **2002**.
- [19] F.-Q. Zhao, P. Chen, R.-Z. Hu, Y. Luo, Z.-Z. Zhang, Y.-S. Zhou, X.-W. Yang, Y. Gao, S.-L. Gao, Q.-Z. Shi, Thermochemical properties and non-isothermal decomposition reaction kinetics of 3,4-dinitro-furazanfuroxan (DNTF), *J. Hazard. Mater.* **2004**, *113*, 67–71.
- [20] R. Tsyshevsky, P. Pagoria, M. Zhang, A. Racoveanu, D. A. Parrish, A. S. Smirnov, M. M. Kuklja, Comprehensive End-to-End Design of Novel High Energy Density Materials: I. Synthesis and Characterization of Oxadiazole Based Heterocycles, *J. Phys. Chem. C* **2017**, *121*, 23853–23864.
- [21] a) W. Zheng, J.-N. Wang, Review on 3,4-Bisnitrofurazanfuroxan (DNTF), *Chin. J. Energ. Mater.* **2006**, *14*, 463–466. b) C.-H. Lim, T.-K. Kim, K.-H. Kim, K.-H. Chung, J.-S. Kim, Synthesis and Characterization of Bisnitrofurazanofuroxan, *Bull. Korean Chem. Soc.* **2010**, *31*, 1400–1402. c) A. A. Kotomin, A. S. Kozlov, S. A. Dushenok, Detonability of High-Energy-Density Heterocyclic Compounds, *Russ. J. Phys. Chem. B* **2007**, *1*, 573–575.
- [22] I. V. Tselinski, S. F. Mel'nikova, T. V. Romanova, N. P. Spiridonova, E. A. Dundukova, Dimerization of Nitrile Oxides of the 1,2,5-Oxadiazole Series, *Russ. J. Org. Chem.* **2001**, *37*, 1335–1356.
- [23] T. M. Klapötke, P. Schmid, J. Stierstorfer, Crystal Structures of Furazanes, *Crystals* **2015**, *5*, 518–432.
- [24] C. S. Choi, E. Prince, The crystal structure of cyclotrimethylene-trinitramine, *Acta Crystallographica Section B* **1972**, *28*, 2857–2862.
- [25] M. Sućeska, EXPLO5 Version 6.03 User's Guide. Zagreb, Croatia: OZM; 2015.
- [26] Reichel & Partner GmbH, <http://www.reichelt-partner.de>.
- [27] *Test Methods According to the UN Recommendations on the Transport of Dangerous Goods, Manual of Test and Criteria, Fourth Revised Edition, United Nations Publication, New York and Geneva, 2003, ISBN 92-1-139087-7, Sales No. E.03.VIII. 2; 13.4.2 Test 3a (ii) BAM Fallhammer.*
- [28] J. S. Murray, P. Politzer, Impact sensitivity and crystal lattice compressibility/free space. *J. Mol. Model* **2014**, *20*, 2223–2227.

## 3.7. Supporting Information

### 3.7.1. X-ray Diffraction

The low-temperature single-crystal X-ray diffraction measurements were performed on an Oxford XCalibur3 diffractometer equipped with a Spellman generator (voltage 50 kV, current 40 mA) and a KappaCCD detector operating with MoK $\alpha$  radiation ( $\lambda = 0.7107 \text{ \AA}$ ). Data collection was performed using the CRYSLIS CCD software.<sup>[S1]</sup> The data reduction was carried out using the CRYSLIS RED software.<sup>[S2]</sup> The solution of the structure was performed by direct methods (SIR97)<sup>[S3]</sup> and refined by full-matrix least-squares on F<sup>2</sup> (SHELXL)<sup>[S4]</sup> implemented in the WINGX software package<sup>[S5]</sup> and finally checked with the PLATON software.<sup>[S6]</sup> All DIAMOND2 plots are shown with thermal ellipsoids at the 50% probability level and hydrogen atoms are shown as small spheres of arbitrary radius.

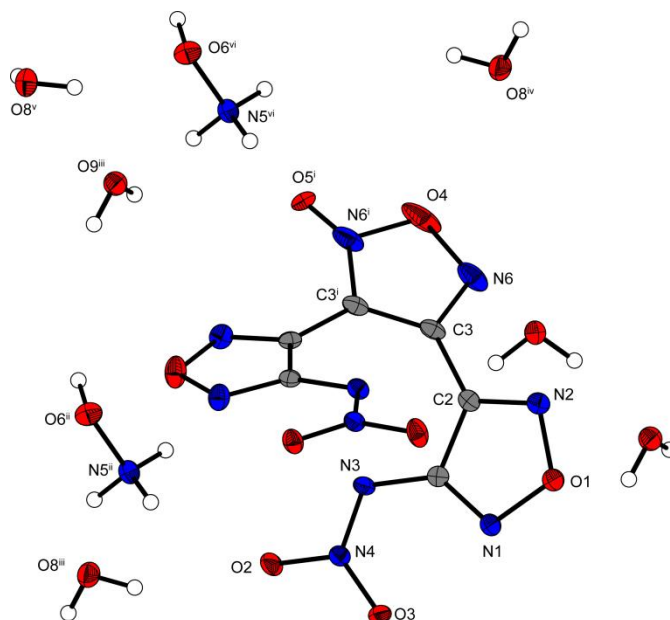


**Figure 1.** Representation of the molecular unit of **8**, showing the atom-labeling scheme. Thermal ellipsoids represent the 50 % probability level and hydrogen atoms are shown as small spheres of arbitrary radius. Symmetry code: (i) 1-x, y, 0.5-z; (ii) 1-x, 1-y, 1-z; (iii) -0.5+x, -0.5+y, z; (iv) 1.5-x, 1.5-y, 1-z; (v) -0.5+x, 1.5-y, 0.5+z; (vi) 1-x, 2-y, 1-z;

Bis(hydroxylammonium) 3,4-bis(4-nitramino-1,2,5-oxadiazol-3-yl)-1,2,5-furoxan (**8**) hexahydrate crystallizes with inclusion of six molecules of crystal water per molecular unit in the monoclinic space group *C2/c*. The measured density at 123 K of  $1.665 \text{ g cm}^{-3}$  is rather low due to the six molecules water in the crystal structure.

**Energetic Compounds Based on 3,4-Bis(4-nitramino-1,2,5-oxadiazol-3-yl)-  
1,2,5-furoxan (BNAFF)**

**Table S1.** Crystallographic details of compounds **2**, **4** and **5**.

Compound	<b>2</b>	<b>4</b>	<b>5</b>
Formula	C <sub>6</sub> K <sub>2</sub> N <sub>10</sub> O <sub>8</sub>	C <sub>8</sub> H <sub>12</sub> N <sub>16</sub> O <sub>8</sub>	C <sub>8</sub> H <sub>14</sub> N <sub>18</sub> O <sub>8</sub>
Form. Mass [g mol <sup>-1</sup> ]	418.36	460.29	490.32
Crystal system	triclinic	monoclinic	orthorhombic
Space Group	<i>P</i> -1 (No. 2)	<i>P</i> 2/ <i>c</i> (No. 13)	<i>C</i> 2/ <i>c</i> (No. 15)
Color / Habit	colorless block	colorless block	colorless block
Size [mm]	0.01 x 0.03 x 0.04	0.26 × 0.18 × 0.12	0.20 × 0.15 × 0.10
<i>a</i> [pm]	453.13(3)	1787.44(5)	1561.13(10)
<i>b</i> [pm]	693.55(5)	775.80(2)	826.35(4)
<i>c</i> [pm]	2156.75(16)	1356.32(4)	1480.72(8)
$\alpha$ [°]	91.561(3)	90	90
$\beta$ [°]	91.303(3)	110.523(3)	102.714(7)
$\gamma$ [°]	105.748(3)	90	90
<i>V</i> [pm <sup>3</sup> ]	651.80(8) · 10 <sup>6</sup>	1761.43(9) · 10 <sup>6</sup>	1863.35(19) · 10 <sup>6</sup>
<i>Z</i>	2	4	4
$\rho_{\text{calc.}}$ [g cm <sup>-3</sup> ]	2.132	1.736	1.748
$\mu$ [mm <sup>-1</sup> ]	0.805	0.153	0.153
<i>F</i> (000)	416	944	1008
$\lambda_{\text{MoK}\alpha}$ [pm]	71.073	71.073	71.073
<i>T</i> [K]	103	123(2)	123(2)
$\vartheta$ min-max [°]	3.2, 26.3	4.1, 26.5	4.6, 30.5
Dataset <i>h</i> ; <i>k</i> ; <i>l</i>	−5:5; −8:8; 0:26	−22:22; −9:9; −17:17	−19:19; −10:9; −18:18
Reflect. coll.	2272	26218	7036
Independ. refl.	2272	3626	1928
<i>R</i> <sub>int</sub>	0.079	0.029	0.028
Reflection obs.	2272	3150	1591
No. parameters	236	347	187
<i>R</i> <sub>1</sub> (obs)	0.0295	0.0484	0.0378
w <i>R</i> <sub>2</sub> (all data)	0.0716	0.0996	0.0872
<i>S</i>	1.20	1.22	1.08

**Energetic Compounds Based on 3,4-Bis(4-nitramino-1,2,5-oxadiazol-3-yl)-  
1,2,5-furoxan (BNAFF)**

Resd. Dens. [e pm <sup>-3</sup> ]	−0.33, 0.29 · 10 <sup>−6</sup>		−0.35, 0.26 · 10 <sup>−6</sup>		−0.32, 0.20 · 10 <sup>−6</sup>	
Device type	Oxford	Xcalibur3	Oxford	Xcalibur3	Oxford	Xcalibur3
	CCD		CCD		CCD	
Solution	SIR-92		SIR-92		SIR-92	
Refinement	SHELXL-97		SHELXL-97		SHELXL-97	
Absorpt. corr.	multi-scan		multi-scan		multi-scan	
CCDC	1589059		1589062		1589063	

**Table S2.** Crystallographic details of compounds **8** and **10**.

Compound	<b>8</b> · 6 H <sub>2</sub> O	<b>10</b> · 2 NH <sub>3</sub>
Formula	C <sub>6</sub> H <sub>20</sub> N <sub>12</sub> O <sub>16</sub>	C <sub>8</sub> H <sub>6</sub> Ag <sub>2</sub> N <sub>12</sub> O <sub>8</sub>
Form. Mass [g mol <sup>−1</sup> ]	516.34	589.97
Crystal system	monoclinic	triclinic
Space Group	<i>C</i> 2/ <i>c</i> (No. 15)	<i>P</i> −1 (No. 2)
Color / Habit	colorless block	colorless block
Size [mm]	0.25 × 0.15 × 0.10	0.02 x 0.08 x 0.17
<i>a</i> [pm]	2118.44(12)	706.07(6)
<i>b</i> [pm]	751.25(3)	1046.69(8)
<i>c</i> [pm]	1333.39(7)	1191.19(9)
α [°]	90	64.293(8)
β [°]	103.849(6)	81.963(7)
γ [°]	90	88.871(7)
<i>V</i> [pm <sup>3</sup> ]	2060.37(19) · 10 <sup>6</sup>	784.58(12) · 10 <sup>6</sup>
<i>Z</i>	4	2
ρ <sub>calc.</sub> [g cm <sup>−3</sup> ]	1.665	2.497
μ [mm <sup>−1</sup> ]	0.162	2.572
<i>F</i> (000)	1072	568
λ <sub>MoKα</sub> [pm]	71.073	71.073
<i>T</i> [K]	123(2)	173(2)
θ min-max [°]	4.4, 27.0	4.3, 26.0
Dataset h; k; l	−21:26; −9:9; −17:15	−8:8 ; −12:12; −14:12

**Energetic Compounds Based on 3,4-Bis(4-nitramino-1,2,5-oxadiazol-3-yl)-  
1,2,5-furoxan (BNAFF)**

Reflect. coll.	8343	5774
Independ. refl.	2247	3073
$R_{\text{int}}$	0.030	0.031
Reflection obs.	1898	2403
No. parameters	199	287
$R_1$ (obs)	0.0356	0.0322
$wR_2$ (all data)	0.0772	0.0710
$S$	1.08	1.01
Resd. Dens. [ $e \text{ pm}^{-3}$ ]	$-0.38, 0.33 \cdot 10^{-6}$	$-0.67, 0.90 \cdot 10^{-6}$
Device type	Oxford Xcalibur3 CCD	Oxford Xcalibur3 CCD
Solution	SIR-92	SIR-92
Refinement	SHELXL-97	SHELXL-97
Absorpt. corr.	multi-scan	multi-scan
CCDC	1589061	1589060

### 3.7.2. Computations

Quantum chemical calculations were carried out using the Gaussian G09 program package.<sup>[S7]</sup> The enthalpies (H) and free energies (G) were calculated using the complete basis set (CBS) method of Petersson and co-workers in order to obtain very accurate energies. The CBS models use the known asymptotic convergence of pair natural orbital expressions to extrapolate from calculations using a finite basis set to the estimated CBS limit. CBS-4 begins with an HF/3-21G(d) geometry optimization; the zero-point energy is computed at the same level. It then uses a large basis set SCF calculation as a base energy, and an MP2/6-31+G calculation with a CBS extrapolation to correct the energy through second order. An MP4(SDQ)/6-31+ (d,p) calculation is used to approximate higher order contributions. In this study, we applied the modified CBS.

Heats of formation of ionic compounds were calculated using the atomization method (equation 1) using room temperature CBS-4M enthalpies summarized in **Table S3**.<sup>[S8,S9]</sup>

$$\Delta_f H^\circ_{(\text{g, M, 298})} = H_{(\text{Molecule, 298})} - \sum H^\circ_{(\text{Atoms, 298})} + \sum \Delta_f H^\circ_{(\text{Atoms, 298})} \quad (1)$$

**Table S3.** CBS-4M electronic enthalpies for atoms C, H, N and O and their literature values for atomic  $\Delta_f H^\circ_{298} / \text{kJ mol}^{-1}$

$-H^{298} / \text{a.u.}$	NIST <sup>[S10]</sup>
--------------------------	-----------------------

**Energetic Compounds Based on 3,4-Bis(4-nitramino-1,2,5-oxadiazol-3-yl)-  
1,2,5-furoxan (BNAFF)**

H	0.500991	218.2
C	37.786156	717.2
N	54.522462	473.1
O	74.991202	249.5

In the case of the ionic compounds, the lattice energy ( $U_L$ ) and lattice enthalpy ( $\Delta H_L$ ) were calculated from the corresponding X-ray molecular volumes according to the equations provided by *Jenkins* and *Glasser*.<sup>[S11]</sup> With the calculated lattice enthalpy the gas-phase enthalpy of formation was converted into the solid state (standard conditions) enthalpy of formation. These molar standard enthalpies of formation ( $\Delta H_m$ ) were used to calculate the molar solid state energies of formation ( $\Delta U_m$ ) according to equation 2.

$$\Delta U_m = \Delta H_m - \Delta n RT \quad (2)$$

( $\Delta n$  being the change of moles of gaseous components)

The calculation results are summarized in **Tables S4** and **S5**.

**Table S4.** CBS-4M results and calculated gas-phase enthalpies.

Ion	M [g mol <sup>-1</sup> ] [a]	$-H^{298}$ [b] / a.u.	$\Delta_f H^\circ(g,M)$ / kJ mol <sup>-1</sup> [c]
<b>BNAFF<sup>2-</sup></b>	340.1	1375.855059	563.9
<b>K<sup>+</sup></b>	39.1	599.03597	487.7
<b>G<sup>+</sup></b>	60.1	205.453192	571.2
<b>AG<sup>+</sup></b>	75.1	260.701802	671.6
<b>NH<sub>4</sub><sup>+</sup></b>	18.1	56.796608	635.8
<b>N<sub>2</sub>H<sub>5</sub><sup>+</sup></b>	66.1	112.030523	774.5

[a] Molecular weight; [b] CBS-4M electronic enthalpy; [c] gas phase enthalpy of formation;

**Table S5.** Calculation results.

Compound	$\Delta_f H^\circ(g,M)$ / kJ mol <sup>-1</sup> [a]	$V_M$ / nm <sup>3</sup> [b]	$\Delta U_L$ kJ mol <sup>-1</sup> [c]	$\Delta H_L$ kJ mol <sup>-1</sup> [d]	$\Delta_f H^\circ(s)$ kJ mol <sup>-1</sup> [e]	$\Delta n$ [f]	$\Delta_f U(s)$ kJ kg <sup>-1</sup> [g]
<b>2</b>	1539.3	0,3479348	1243.8	1251.2	288.1	9	742.4
<b>4</b>	1707.7	0.4641811	1113.4	1120.9	586.8	18	1371.8

**Energetic Compounds Based on 3,4-Bis(4-nitramino-1,2,5-oxadiazol-3-yl)-  
1,2,5-furoxan (BNAFF)**

<b>5</b>	1907.1	0.4894795	1090.8	1098.2	808.9	20	1750.9
<b>6</b>	1835.6	0.3714202	1213.1	1220.6	614.9	14	1726.9
<b>7</b>	2112.2	0.3861776	1195.2	1202.6	909.6	16	2336.7

<sup>[a]</sup> gas phase enthalpy of formation; <sup>[b]</sup> molecular volumes taken from X-ray structures and corrected to room temperature; <sup>[c]</sup> lattice energy (calculated using Jenkins and Glasser equations); <sup>[d]</sup> lattice enthalpy (calculated using Jenkins and Glasser equations); <sup>[e]</sup> standard solid state enthalpy of formation; <sup>[f]</sup> change of moles of gaseous components when formed; <sup>[g]</sup> solid state energy of formation.

### 3.7.3. NMR Spectra

<sup>1</sup>H, <sup>13</sup>C and <sup>14</sup>N NMR Data for H<sub>2</sub>BNAFF • 0.5 Et<sub>2</sub>O

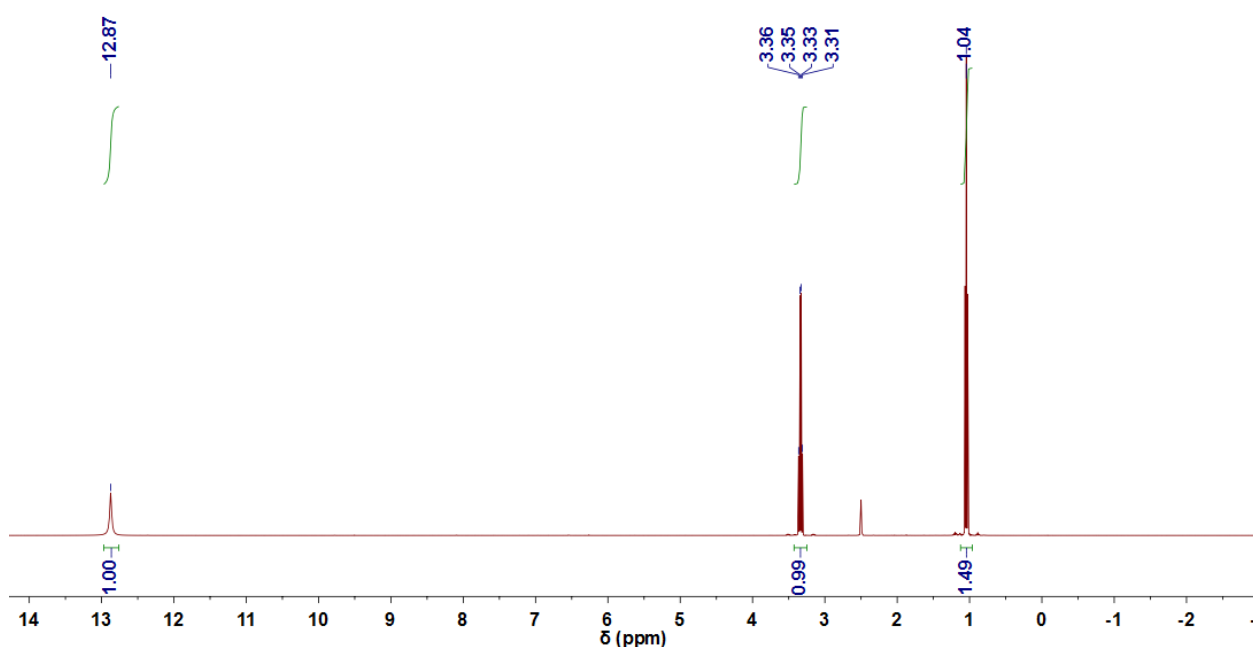


**Figure 2.** Recorded <sup>1</sup>H NMR spectrum of H<sub>2</sub>BNAFF • 0.5 Et<sub>2</sub>O (**3**) in *d*<sub>6</sub>-DMSO.

**Energetic Compounds Based on 3,4-Bis(4-nitramino-1,2,5-oxadiazol-3-yl)-  
1,2,5-furoxan (BNAFF)**

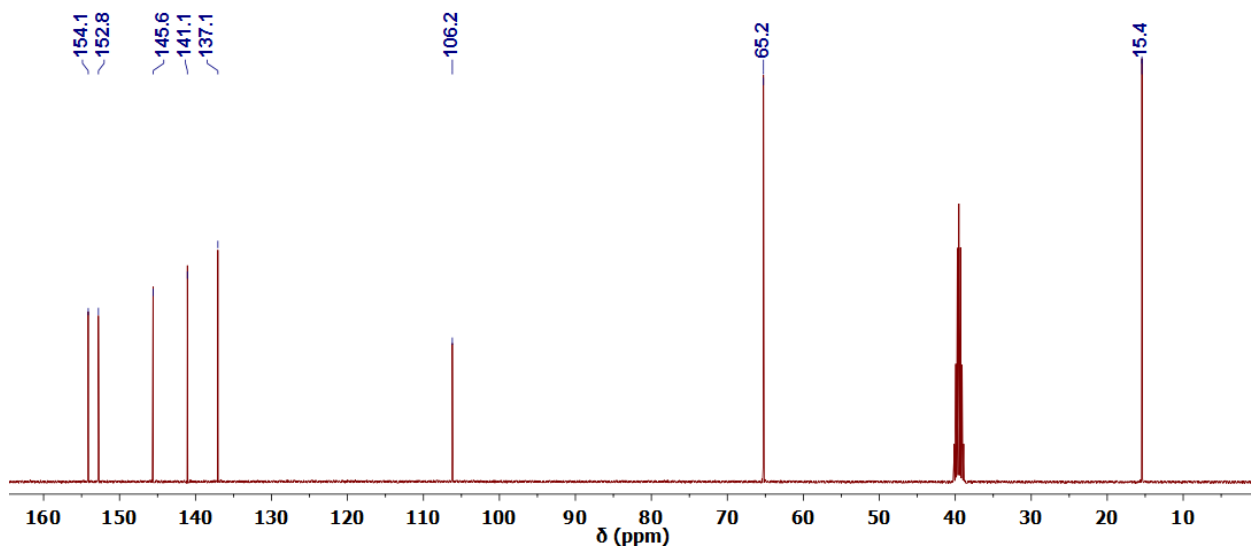


**Figure 3.** Recorded  $^{13}\text{C}$  NMR spectrum of  $\text{H}_2\text{BNAFF} \cdot 0.5 \text{Et}_2\text{O}$  (**3**) in  $d_6$ -DMSO.

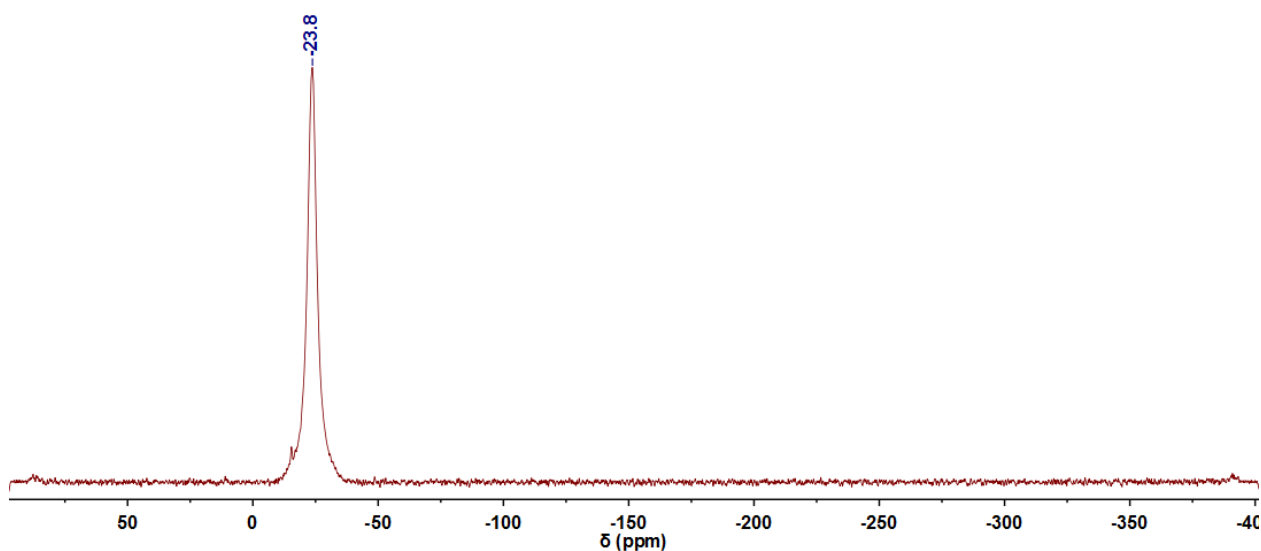


**Figure 4.** Recorded  $^{14}\text{N}$  NMR spectrum of  $\text{H}_2\text{BNAFF} \cdot 0.5 \text{Et}_2\text{O}$  (**3**) in  $d_6$ -DMSO.

### 3.7.4. References

- [S1] CrysAlisPro, Oxford Diffraction Ltd. version 171.33.41, **2009**.
- [S2] CrysAlis RED, Version 1.171.35.11 (release 16-05-2011 CrysAlis 171.Net), Oxford Diffraction Ltd., Abingdon, Oxford (U.K.), **2011**.
- [S3] A. Altomare, M. C. Burla, M. Camalli, G. L. Cascarano, C. Giacovazzo, A. Guagliardi, A. G. G. Moliterni, G. Polidori and R. Spagna, SIR97: A New Tool for Crystal Structure Determination and Refinement, *J. Appl. Crystallogr.*, **1999**, 32, 115–119.



**Energetic Compounds Based on 3,4-Bis(4-nitramino-1,2,5-oxadiazol-3-yl)-  
1,2,5-furoxan (BNAFF)**

- [S4] G. M. Sheldrick, A Short History of SHELX, *Acta Crystallogr., Sect. A: Found. Crystallogr.*, **2008**, *64*, 112–122.
- [S5] L. J. Farrugia, WinGX Suite for Small-Molecule Single-Crystal Crystallography, *J. Appl. Crystallogr.*, **1999**, *32*, 837–838.
- [S6] A. L. Spek, *PLATON*, **1999**, A Multipurpose Crystallographic Tool, Utrecht University, The Diffraction Ltd.
- [S7] M. J. Frisch, G. W. Trucks, H. B. Schlegel, G. E. Scuseria, M. A. Robb, J. R. Cheeseman, G. Scalmani, V. Barone, B. Mennucci, G. A. Petersson, H. Nakatsuji, M. Caricato, X. Li, H.P. Hratchian, A. F. Izmaylov, J. Bloino, G. Zheng, J. L. Sonnenberg, M. Hada, M. Ehara, K. Toyota, R. Fukuda, J. Hasegawa, M. Ishida, T. Nakajima, Y. Honda, O. Kitao, H. Nakai, T. Vreven, J. A. Montgomery, Jr., J. E. Peralta, F. Ogliaro, M. Bearpark, J. J. Heyd, E. Brothers, K. N. Kudin, V. N. Staroverov, R. Kobayashi, J. Normand, K. Raghavachari, A. Rendell, J. C. Burant, S. S. Iyengar, J. Tomasi, M. Cossi, N. Rega, J. M. Millam, M. Klene, J. E. Knox, J. B. Cross, V. Bakken, C. Adamo, J. Jaramillo, R. Gomperts, R. E. Stratmann, O. Yazyev, A. J. Austin, R. Cammi, C. Pomelli, J. W. Ochterski, R. L. Martin, K. Morokuma, V. G. Zakrzewski, G. A. Voth, P. Salvador, J. J. Dannenberg, S. Dapprich, A. D. Daniels, O. Farkas, J.B. Foresman, J. V. Ortiz, J. Cioslowski, D. J. Fox, Gaussian 09 A.02, Gaussian, Inc., Wallingford, CT, USA, **2009**.
- [S8] (a) J. W. Ochterski, G. A. Petersson, and J. A. Montgomery Jr., A complete basis set model chemistry. V. Extensions of six or more heavy atoms, *J. Chem. Phys.* **1996**, *104*, 2598–2619; (b) J. A. Montgomery Jr., M. J. Frisch, J. W. Ochterski G. A. Petersson, A complete basis set model chemistry. VII. Use of the minimum population localization method, *J. Chem. Phys.* **2000**, *112*, 6532–6542.
- [S9] (a) L. A. Curtiss, K. Raghavachari, P. C. Redfern, J. A. Pople, Assessment of Gaussian-2 and density functional theories for the computation of enthalpies of formation, *J. Chem. Phys.* **1997**, *106*, 1063–1079; (b) E. F. C. Byrd, B. M. Rice, Improved Prediction of Heats of Formation of Energetic Materials Using Quantum Mechanical Calculations, *J. Phys. Chem. A* **2006**, *110*, 1005–1013; (c) B. M. Rice, S. V. Pai, J. Hare, Predicting heats of formation of energetic materials using quantum mechanical calculations, *Comb. Flame* **1999**, *118*, 445–458.
- [S10] P. J. Lindstrom, W. G. Mallard (Editors), NIST Standard Reference Database Number 69, <http://webbook.nist.gov/chemistry/> (accessed November **2017**).
- [S11] (a) H. D. B. Jenkins, H. K. Roobottom, J. Passmore, L. Glasser, Relationships among Ionic Lattice Energies, Molecular (Formula Unit) Volumes, and Thermochemical Radii, *Inorg. Chem.* **1999**, *38*, 3609–3620. (b) H. D. B. Jenkins, D. Tudela, L. Glasser, Lattice Potential Energy Estimation for Ionic Salts from Density Measurements, *Inorg. Chem.* **2002**, *41*, 2364–2367.

## 4. Energetic Functionalization of the Pyridazine Scaffold: Synthesis and Characterization of 3,5-Diamino-4,6-dinitropyridazine-1-oxide

Ivan Gospodinov, Thomas M. Klapötke and Jörg Stierstorfer

Published in *Eur. J. Org. Chem.* **2018**, 1004–1010.

DOI: 10.1002/ejoc.201800068



**Abstract:** The synthesis of 3,5-diamino-4,6-dinitropyridazine-1-oxide (**8**) is reported. It is prepared in a six step synthetic procedure starting from the acyclic compounds and shows good properties (detonation velocity  $D_{\text{C-J}} = 8486 \text{ m} \cdot \text{s}^{-1}$ , detonation pressure  $p_{\text{C-J}} = 302 \text{ kbar}$  and sensitivity toward mechanical stimuli). Compound **8** and its precursor (**7**, 3,5-dimethoxy-4,6-dinitropyridazine-1-oxide) were characterized by means of multinuclear ( $^1\text{H}$ ,  $^{13}\text{C}$ ,  $^{14}\text{N}$ ,  $^{15}\text{N}$ ) NMR spectroscopy, mass spectrometry, vibrational spectroscopy (IR and Raman), elemental analysis and DTA measurements. Compounds **4**, **5**, **6**, **7**, **8** and **9** were also characterized by low-temperature single-crystal X-ray diffraction. The heats of formation for **7** and **8** were calculated using the atomization method based on CBS-4M enthalpies. With the experimentally determined (X-ray) densities and the calculated standard molar enthalpies of formation, several detonation parameters such as the detonation pressure, energy and velocity were predicted by using the EXPLO5 code (V6.03). The sensitivities of 3,5-dimethoxy-4,6-dinitropyridazine-1-oxide (**7**) and 3,5-diamino-4,6-dinitropyridazine-1-oxide (**8**) toward impact, friction and electrical discharge were tested according to BAM standards. In addition, the shock reactivity of **8** was measured by applying the small-scale shock reactivity test, showing similar values to HNS, PYX and TKX-55.

## 4.1. Introduction

Due to increasing safety regulations the research on new energetic materials based on nitrogen-rich heterocycles has attracted considerable interest in the past decades, not only for military application but also for industrial.<sup>[1]</sup> The arising challenge on combining good detonation performance and sensitivity for the synthesis of new high-energy density materials has come into focus.<sup>[2]</sup> There are different strategies reported in the literature for achieving this goal; introduction of conjugation into the system, formation of nitrogen-rich salts or introduction of an alternating C–NH<sub>2</sub>/C–NO<sub>2</sub> into the system, which leads to the formation of intra- and intermolecular hydrogen bonds.<sup>[3]</sup> A well-known example for a heat resisting and insensitive explosive is 2,4,6-triamino-1,3,5-trinitrobenzene (TATB) consisting of alternating amino and nitro groups on the benzene scaffold.<sup>[4]</sup> In recent years, the synthesis of new energetic materials based on nitrogen-rich heterocycles has received great interest.<sup>[5]</sup> Some synthesized and well known heterocyclic, energetic materials based on pyridines (TANPyO)<sup>[6]</sup> and 1,4-diazines (ANPZ and LLM-105)<sup>[7,8]</sup> are shown in Figure 1. LLM-105 and TANPyO exhibit good thermal stability and sensitivity combined with good detonation performance. The introduction of the N-oxide moiety to the energetic backbone has been proven to increase not only the performance of the energetic material, but also its oxygen balance and improves the crystal packing, leading to higher density of the material.<sup>[9]</sup> For example, 2,6-diamino-3,5-dinitropyridazine-1-oxide (LLM-105,  $\rho = 1.92 \text{ g}\cdot\text{cm}^{-3}$  and  $D = 8516 \text{ m}\cdot\text{s}^{-1}$ ) shows higher energetic performance compared to its precursor 2,6-diamino-3,5-dinitropyridazine (ANPZ,  $\rho = 1.84 \text{ g}\cdot\text{cm}^{-3}$  and  $D = 7892 \text{ m}\cdot\text{s}^{-1}$ ).<sup>[5,10]</sup>

## Energetic Functionalization of the Pyridazine Scaffold: Synthesis and Characterization of 3,5-Diamino-4,6-dinitropyridazine-1-oxide

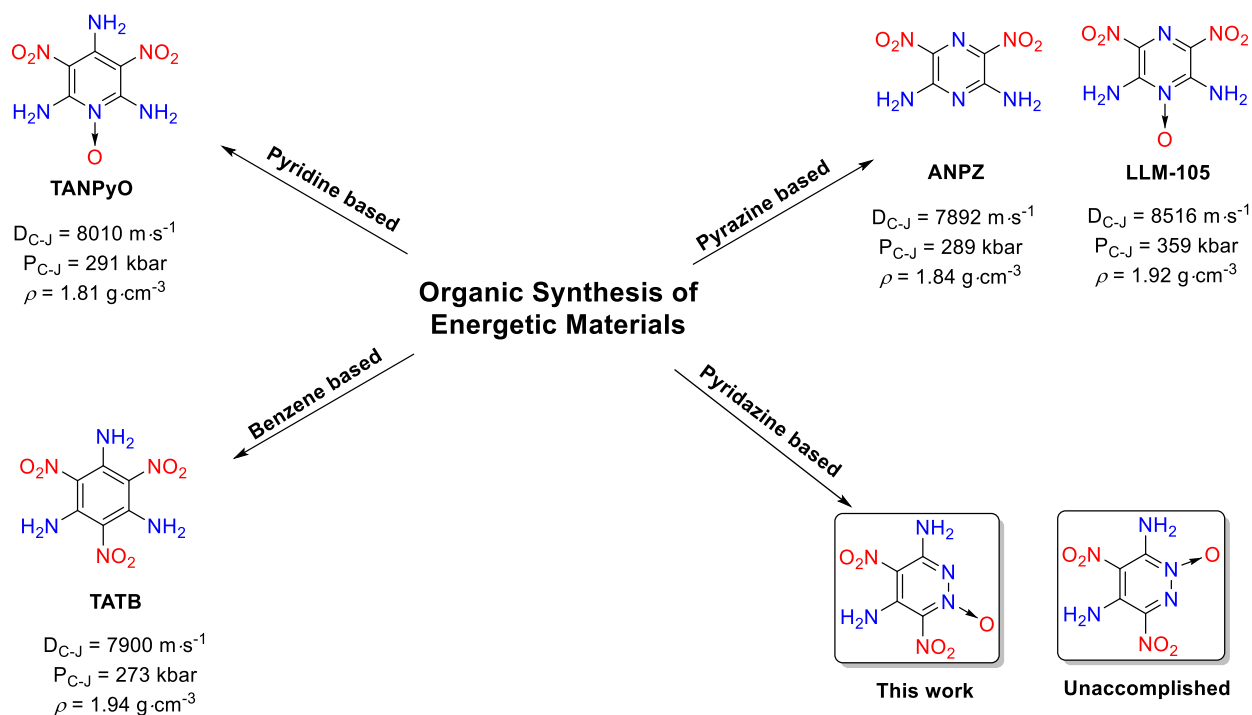


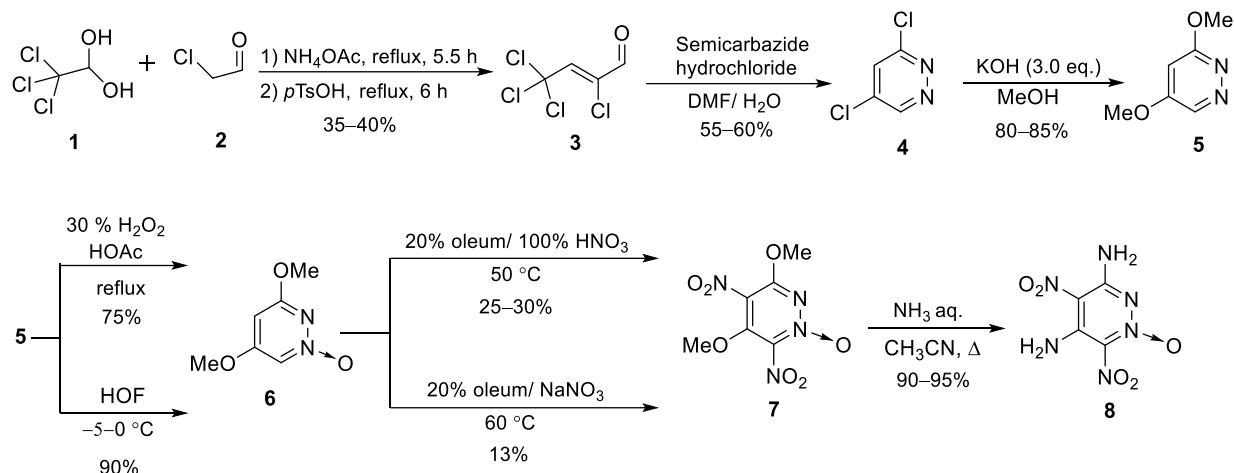
**Figure 1.** Energetic compounds TATB, TANPyO, ANPZ, LLM-105 and the investigated pyridazine derivatives.

Although 1,4-diazines have been well investigated in the literature as energetic materials, 1,3- and 1,2-diazines are relatively unexploited systems. This can be explained by the fact that electrophiles directly attack the ring N-atoms in the pyridazine/pyrimidine system resulting for instance in protonation, alkylation or N-oxidation, thus hindering nitration attempts.<sup>[11]</sup> In addition, the nitro group is an excellent leaving group and can be easily substituted even by weak nucleophiles.<sup>[12]</sup> However, recently reported literature shows that 1,2-diazine (pyridazine) derivatives and their N-oxides can be synthesized and may be interesting new building blocks for the synthesis of new energetic materials.<sup>[13]</sup> The idea of this work was to synthesize 3,5-diamino-4,6-dinitropyridazine-1-oxide and 4,6-diamino-3,5-dinitropyridazine-1-oxide (**Figure 1**); two structural isomers to LLM-105 which are based on the pyridazine scaffold. Due to the additional N–N bond both pyridazine derivatives should exhibit even higher heat of formation compared to LLM-105.

## 4.2. Results and Discussion

Herein, we report the selective functionalization of the pyridazine scaffold (**Scheme 1**).

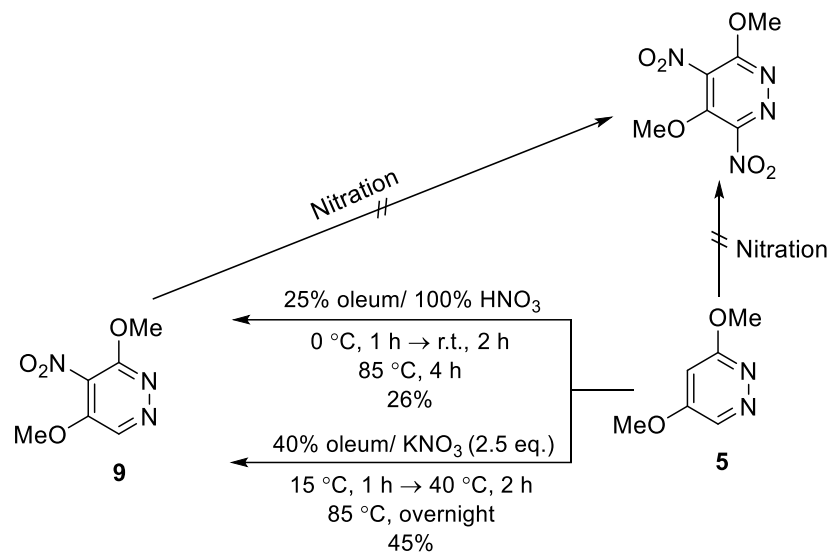
## Energetic Functionalization of the Pyridazine Scaffold: Synthesis and Characterization of 3,5-Diamino-4,6-dinitropyridazine-1-oxide



**Scheme 1.** Synthesis of 3,5-dimethoxy-4,6-dinitropyridazine-1-oxide (**7**) and 3,5-diamino-4,6-dinitropyridazine-1-oxide (**8**).

The target molecules 3,5-dimethoxy-4,6-dinitropyridazine-1-oxide (**7**) and 3,5-diamino-4,6-dinitropyridazine-1-oxide (**8**) were synthesized by using 3,5-dichloropyridazine (**4**) as the starting material. Initially, compound **4** was synthesized according to the literature.<sup>[14]</sup> Treatment of chloral hydrate (**1**) with chloroacetaldehyde (**2**) in the presence of ammonium acetate and *p*-toluenesulfonic acid monohydrate on the DEAN-STARK apparatus gave (Z)-2,4,4,4-tetrachlorobut-2-enal (**3**). The cyclization of compound **3** with semicarbazide hydrochloride yielded 3,5-dichloropyridazine (**4**). Subsequently, compound **4** was converted into 3,5-dimethoxypyridazine-1-oxide (**6**)<sup>[15]</sup> by first reacting it with potassium hydroxide in methanol, which gave 3,5-dimethoxypyridazine (**5**),<sup>[16]</sup> followed by oxidation of the pyridazine nitrogen with 30% hydrogen peroxide in glacial acetic acid. The introduction of the N-oxide was also accomplished by using HOF increasing the yield of the reaction up to 90%.<sup>[17]</sup> The insertion of the N-oxide and the introduction of electron-donating functional groups (–OMe) into the pyridazine scaffold allowed the nitration with 20% oleum and 100% nitric acid of compound **6** to the desired product 3,5-dimethoxy-4,6-dinitropyridazine-1-oxide (**7**). Nitration of **6** was also possible with a mixture of 20% oleum and sodium nitrate at elevated temperature. The second nitro group in compound **7** was able to be introduced only when the N-oxide was present in the parent molecule. Finally, 3,5-diamino-4,6-dinitropyridazine-1-oxide (**8**) was synthesized by reacting compound **7** with concentrated ammonia solution in acetonitrile.

## Energetic Functionalization of the Pyridazine Scaffold: Synthesis and Characterization of 3,5-Diamino-4,6-dinitropyridazine-1-oxide



**Scheme 2.** Nitration reactions with 3,5-dimethoxy-4-nitropyridazine (**9**).

The first step in the synthesis of 4,6-diamino-3,5-dinitro-pyridazine-1-oxide was the nitration of 3,5-dimethoxy-4-nitropyridazine (**9**). As shown in **Scheme 2** the nitration of compound **9** gave only 3,5-dimethoxy-4,6-dinitropyridazine (**10**) and not the desired product 3,5-dimethoxy-4,6-dinitropyridazine-1-oxide. Further nitration of compound **10** was not successful and yielded either the starting material or decomposition products. The crystal structure of compound **9** is reported in the Supporting Information. As it seems without the N→O moiety the introduction of the second nitro group into the pyridazine system cannot be achieved. Different strategies toward the synthesis of 4,6-diamino-3,5-dinitropyridazine-1-oxide are currently under investigation.

### 4.2.1. X-ray diffraction

Suitable crystals of **7** and **8** for X-ray diffraction analysis were obtained by slow evaporation from a solution of **7** in dichloromethane and a solution of **8** in water, respectively. In addition, the crystal structures of compounds **4–6** are shown in the Supporting Information. CCDC-1590457 (**4**), CCDC-1590458 (**5**), CCDC-1590459 (**6** • 3 H<sub>2</sub>O), CCDC-1590461 (**7**), CCDC-1590460 (**8**) and CCDC-1816507 (**9**) contain the supplementary crystallographic data for this paper. These data can be obtained free of charge from The Cambridge Crystallographic Data Centre via [www.ccdc.cam.ac.uk/data\\_request/cif](http://www.ccdc.cam.ac.uk/data_request/cif). Compound **7** crystallizes in the orthorhombic space group *Pbcn* and has a calculated density of 1.637 g·cm<sup>-3</sup> at 123 K (**Figure 2**). The bond angles and bond lengths in the pyridazine ring are between typical C–N/N–N single and C=N/N=N double bonds

## Energetic Functionalization of the Pyridazine Scaffold: Synthesis and Characterization of 3,5-Diamino-4,6-dinitropyridazine-1-oxide

due to the aromaticity. Among them, the bond lengths of N2–C1 and N1–N2 are 1.329(3) and 1.347(3) Å, respectively. The N–O bond length in the N→O moiety is 1.268(2) Å.

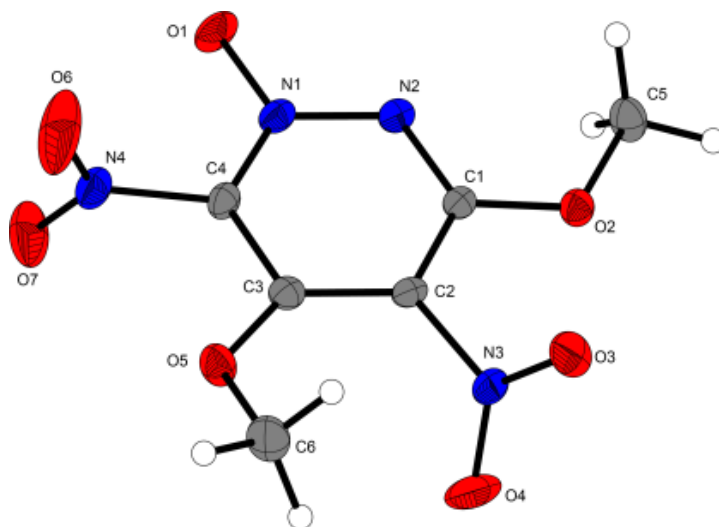


**Figure 2.** Molecular structure of compound **7** in the solid state. Ellipsoids correspond to 50 % probability levels. Selected bond distances [Å] and angles [°]: O1–N1 1.268(2), N1–N2 1.347(3), N1–C4 1.341(3), C3–C4 1.401(3), N4–C4 1.468(3), O2–C1 1.323(2), N2–N1–C4 121.75(17), N3–C2–C1 117.48(18), C5–O2–C1–N2 –2.6(3), O1–N1–N2–C1 178.22(17), O3–N3–C2–C3 –120.9(2), C6–O5–C3–C4 –160.6(2);

Compound **8** crystallizes in the monoclinic space group  $P2_1/c$  and has a calculated density of  $1.888 \text{ g}\cdot\text{cm}^{-3}$  at 123 K (**Figure 3**). Compared to compound **7** (N1–O1 1.268(2) Å) the N–O bond length in the N→O moiety of **8** does not show any significant difference (N1–O1 1.2681(19) Å). Compound **8** is almost planar in the crystal structure with a small aberration for the nitro group next to the N→O with torsion angle of  $36.5(2)^\circ$  and  $-144.95(17)^\circ$  for O2–N3–C1–N1 and O3–N3–C1–N1, respectively. Both amino groups and the second nitro group are in the same plane as the pyridazine ring. The C–C (C1–C2 1.422(2) Å) lengths in compound **8** are in the range of those reported for LLM-105 (C–C 1.417 Å); however, the C–N (N1–C2 1.357(2) Å) bond lengths for compound **8** are slightly shorter than those reported for LLM-105 (C–N 1.374 Å). In addition, the N–O bond length (1.3172 Å) in the N→O moiety for LLM-105 is longer than the determined value (N1–O1 1.2681(19) Å) for compound **8**.<sup>[20b]</sup>

## Energetic Functionalization of the Pyridazine Scaffold: Synthesis and Characterization of 3,5-Diamino-4,6-dinitropyridazine-1-oxide

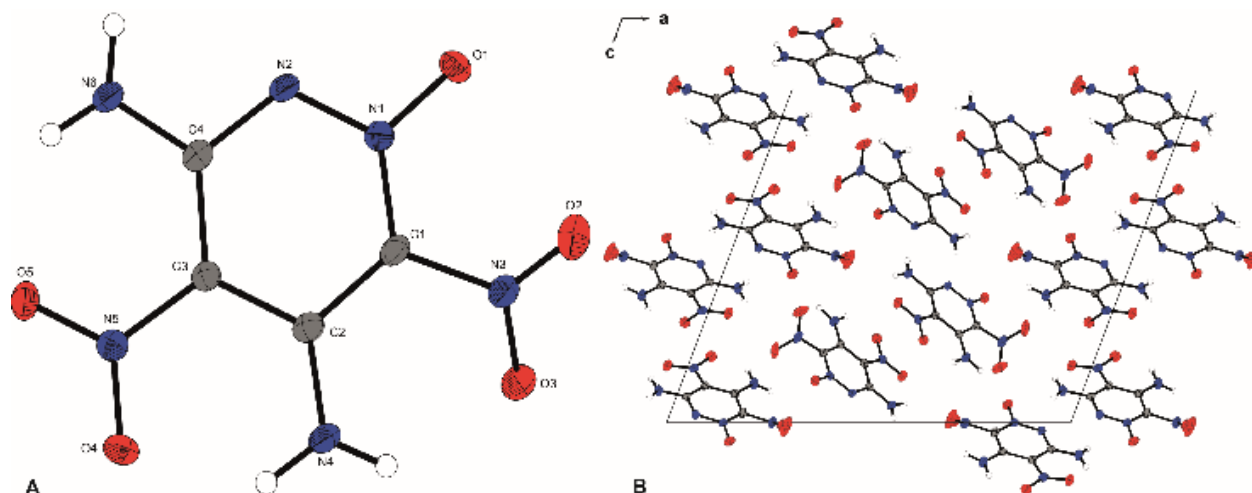


**Figure 3.** A) Molecular structure of compound **8** in the solid state. Ellipsoids correspond to 50 % probability levels. Selected bond distances [ $\text{\AA}$ ] and angles [ $^\circ$ ]: O1–N1 1.2681(19), N1–N2 1.323(2), N1–C1 1.357(2), C1–C2 1.422(2), N6–C4 1.322(2), O3–N3 1.229(2), O1–N1–N2 114.67(15), N1–N2–C4 118.94(15), O2–N3–C1 119.99(15), O1–N1–C1–N3 4.9(2), O2–N3–C1–N1 36.5(2), O5–N5–C3–C2  $-168.62(15)$ , N4–C2–C3–N5  $-5.5(2)$ ; B) View of the unit cell of compound **8** along the b-axis.

### 4.2.2. $^{15}\text{N}$ NMR spectroscopy

All synthesized compounds were characterized by vibrational spectroscopy (IR and Raman), mass spectrometry, multinuclear NMR ( $^1\text{H}$ ,  $^{13}\text{C}$  and  $^{14}\text{N}$ ) spectroscopy and elemental analysis. In addition,  $^{15}\text{N}$  and  $^{15}\text{N}\{^1\text{H}\}$  NMR spectra of compound **8** were recorded (**Figure 4**).  $^{15}\text{N}$  NMR spectrum of **8** exhibits only five signals; both nitro groups are observed at  $-15.6$  and  $-26.0$  ppm, the N-oxide has a resonance at  $-69.5$  ppm and the pyridazine nitrogen at  $-100.3$  ppm. Only one amino group can be observed at  $-286.7$  ppm ( $^1J_{\text{NH}} = 92.9$  Hz) in the proton coupled  $^{15}\text{N}$  NMR spectrum of **8**. All six resonances for the nitrogen atoms can be observed in the proton decoupled  $^{15}\text{N}$  NMR spectrum of **8**. Both nitro groups ( $-15.6$  and  $-26.0$  ppm) and the pyridazine nitrogen atoms ( $-69.5$  and  $-100.3$  ppm) exhibit the same chemical shift as listed before. Both amino groups can be observed as singlets at  $-286.7$  and  $-292.9$  ppm.



## Energetic Functionalization of the Pyridazine Scaffold: Synthesis and Characterization of 3,5-Diamino-4,6-dinitropyridazine-1-oxide

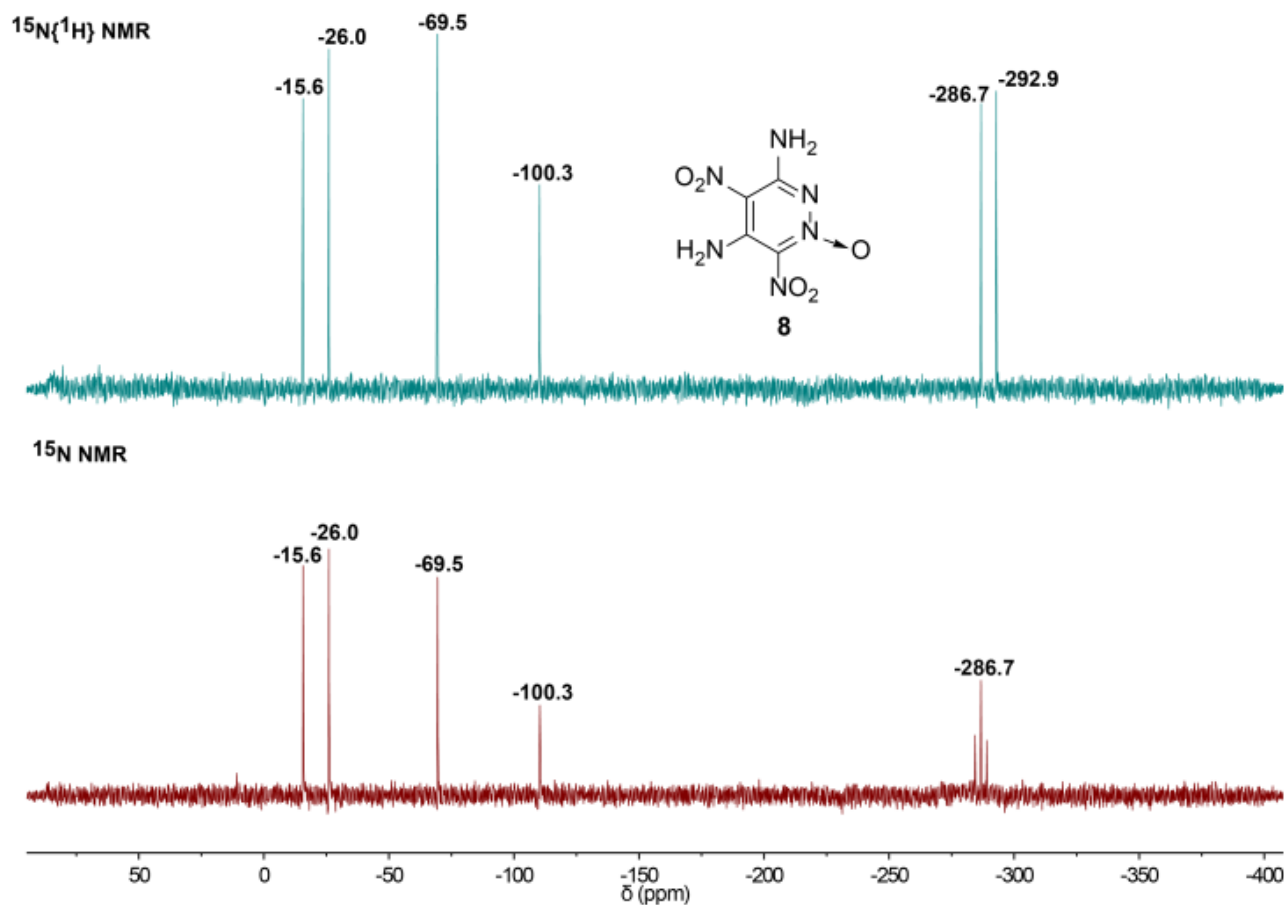


**Figure 4.**  $^{15}\text{N}\{^1\text{H}\}$  and  $^{15}\text{N}$  NMR spectra of compound **8**.

### 4.2.3. Physical and detonation properties

Since compounds **7** and **8** can be classified as energetic materials, their energetic behavior was investigated. All theoretically calculated and experimentally determined values for **7** and **8** compared to the insensitive explosive LLM-105 are listed in Table 1. The thermal behavior for both compounds was investigated with an OZM Research DTA 552-Ex instrument at a heating rate of  $5\text{ }^{\circ}\text{C min}^{-1}$ . Compound **7** decomposes at  $151\text{ }^{\circ}\text{C}$ , while 3,6-diamino-4,6-dinitropyridazine-1-oxide (**8**) decomposes first at  $215\text{ }^{\circ}\text{C}$ . The increased stability of compound **8** compared to the precursor, compound **7**, can be explained by the intra- and intermolecular hydrogen bonds in the structure of **8**. This observation of change in the thermal behavior from compound **7** to compound **8** verifies that the introduction of alternating C-NH<sub>2</sub>/C-NO<sub>2</sub> functionalities into the pyridazine system not only improves the energetic properties of the material, but also increases the thermal stability. The difference in the thermal stability of **8** ( $215\text{ }^{\circ}\text{C}$ ) compared to LLM-105 ( $342\text{ }^{\circ}\text{C}$ ) is

## Energetic Functionalization of the Pyridazine Scaffold: Synthesis and Characterization of 3,5-Diamino-4,6-dinitropyridazine-1-oxide

significant. This can be explained with the weakening of the N–N bond in the pyridazine with the introduction of the N-oxide and its position next to the NO<sub>2</sub> group.

In addition, the sensitivities for both compounds were determined according to the BAM standards and the detonation parameters were calculated using the EXPLO5\_V6.03 computer code.<sup>[18]</sup> The EXPLO5 detonation parameters of **7** and **8** were calculated by using the room-temperature density values obtained from the X-ray structures as described in reference.<sup>[19]</sup> The density at room temperature for compound **7** is 1.591 g·cm<sup>−3</sup> and for **8** is 1.837 g·cm<sup>−3</sup>. The determined experimental sensitivities toward friction and impact for **7** (IS = 20 J and FS = 360 N) and **8** (IS = 18 J and FS = 360 N) are in the range for those of the insensitive explosive LLM-105 (IS = 20 J and FS = 360 N). The synthesized compounds **7** (0.65 J) and **8** (0.75 J) are even less sensitive than LLM-105 (0.60 J) toward electrostatic discharge. The calculated physico-chemical properties of compound **8** compared to those of LLM-105 are quite surprising (Table 1). Although the room temperature density of 3,5-diamino-4,6-dinitropyridazine-1-oxide (**8**,  $\rho = 1.837 \text{ g}\cdot\text{cm}^{-3}$ ) is lower than those of LLM-105 ( $\rho = 1.919 \text{ g}\cdot\text{cm}^{-3}$ ),<sup>[20]</sup> the calculated detonation parameters for **8** are similar to those of LLM-105. The detonation pressure ( $p_{C-J} = 302 \text{ kbar}$ ) and detonation velocity ( $D_{C-J} = 8486 \text{ m}\cdot\text{s}^{-1}$ ) of **8** are in the range of those for LLM-105 ( $p_{C-J} = 317 \text{ kbar}$  and  $D_{C-J} = 8639 \text{ m}\cdot\text{s}^{-1}$ ). However, the values of **8** for the detonation energy (4913 kJ·kg<sup>−1</sup>) and for the detonation temperature (3470 K) exceed those values for LLM-105 (4506 kJ·kg<sup>−1</sup> and 3202 K).

**Table 1.** Physico-chemical properties of compounds **7** and **8** in comparison to LLM-105.

	<b>7</b>	<b>8</b>	<b>LLM-105</b>
Formula	C <sub>6</sub> H <sub>6</sub> N <sub>4</sub> O <sub>7</sub>	C <sub>4</sub> H <sub>4</sub> N <sub>6</sub> O <sub>5</sub>	C <sub>4</sub> H <sub>4</sub> N <sub>6</sub> O <sub>5</sub>
IS <sup>[a]</sup> [J]	20	18	20*
FS <sup>[b]</sup> [N]	360	360	360*
ESD <sup>[c]</sup> [J]	0.65	0.75	0.60*
Q <sup>[d]</sup> [%]	−52	−37	−37
T <sub>m</sub> <sup>[e]</sup> [°C]	—	—	—
T <sub>dec</sub> <sup>[f]</sup> [°C]	151	215	342 <sup>[20a]</sup>
$\rho$ <sup>[g]</sup> [g·cm <sup>−3</sup> ]	1.59	1.84	1.92 <sup>[20b]</sup>
$\Delta_f H^{\circ[h]}$ [kJ·kg <sup>−1</sup> ]	−465	511	51

**Energetic Functionalization of the Pyridazine Scaffold: Synthesis and Characterization of 3,5-Diamino-4,6-dinitropyridazine-1-oxide**

$\Delta_f H^{o[h]}$ [kJ·mol <sup>-1</sup> ]	-114	110	11
<b>EXPLO5 6.03</b>			
$-\Delta_E U^{o[i]}$ [kJ·kg <sup>-1</sup> ]	4767	4913	4506
$T_{C-J}^{[j]}$ [K]	3442	3470	3202
$p_{C-J}^{[k]}$ [kbar]	208	302	317
$D_{C-J}^{[l]}$ [m·s <sup>-1</sup> ]	7227	8486	8639
$V^{[m]}$ [L <sup>3</sup> ·kg <sup>-1</sup> ]	722	720	706

[a] Impact sensitivity (BAM drophammer, method 1 of 6); [b] friction sensitivity (BAM drophammer, method 1 of 6); [c] electrostatic discharge device (OZM research); [d] oxygen balance with respect to CO<sub>2</sub>; [e] melting point (DTA,  $\beta = 5^\circ\text{C}\cdot\text{min}^{-1}$ ); [f] temperature of decomposition (DTA,  $\beta = 5^\circ\text{C}\cdot\text{min}^{-1}$ ); [g] density at 298 K; [h] standard molar enthalpy of formation; [i] detonation energy; [j] detonation temperature; [k] detonation pressure; [l] detonation velocity; [m] volume of detonation gases at standard temperature and pressure conditions. \*experimentally determined values for LLM-105 (grain size 100–500  $\mu\text{m}$ ).

The evaluation of the explosive performance of compound **8** on a small scale was investigated with the small-scale shock reactivity test (SSRT). With this test the shock reactivity (explosiveness) of the investigated explosive is measured below the critical diameter, without requiring a transition to detonation.<sup>[21]</sup> The set-up for the small-scale shock reactivity test (SSRT) has been prepared as previously reported in the literature (**Figure 5**).<sup>[22]</sup> Compound **8** was pressed at a consolidation dead load of 3 t with a dwell time of 5 s into a perforated steel block. Initiation of the tested explosive was performed by using a commercially available detonator.

## Energetic Functionalization of the Pyridazine Scaffold: Synthesis and Characterization of 3,5-Diamino-4,6-dinitropyridazine-1-oxide

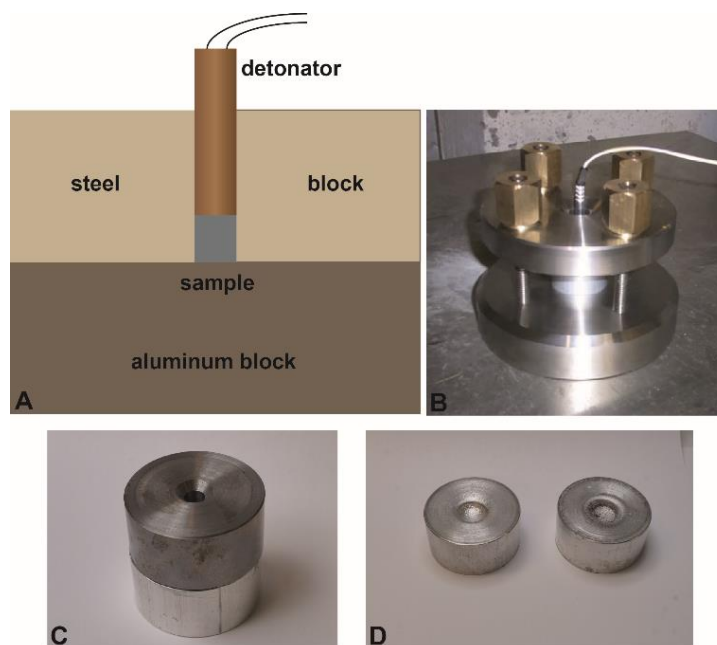


**Figure 5.** SSRT results: A) schematical illustration; B) photograph of the setup; C) aluminum block and steel block filled with compound **8**; D) dented aluminum block after initiation of the explosive with a commercial detonator.

The results of the SSRT are displayed in **Figure 5** (D). The dent sizes were measured by filling them with finely powdered  $\text{SiO}_2$  and measuring the resulting weight. The result of **8** is compared with the corresponding values for HNS, PYX and TKX-55 (Table 2).<sup>[22]</sup> The measured dent volume for compound **8** (694 mg) compared to HNS (672 mg), PYX (637 mg) and TKX-55 (641 mg) shows that the performance of **8** on a small scale is slightly higher than the known heat resistant explosives.

**Table 2.** The SSRT for compound **8** compared to HNS, PYX and TKX-55.

SSRT for <b>8</b> compared to HNS, PYX and TKX-55				
	HNS	PYX	TKX-55	<b>8</b>
$m_E$ [mg] <sup>[a]</sup>	469	474	496	496
$m$ [mg] <sup>[b]</sup>	672	637	641	694

[a] Mass of the explosive:  $m_E = V_s \rho$  0.95; [b] Mass of  $\text{SiO}_2$ .

### 4.3. Conclusions

In summary, we report the synthesis of new selectively functionalized pyridazine derivative consisting of alternating amino/nitro groups and N-oxide moiety. Compounds **7** and **8** were synthesized by starting from the acyclic compounds chloral hydrate and chloroacetaldehyde. The introduction of the N-oxide was achieved by reacting 3,5-dimethoxypyridazine (**5**) either with a mixture of glacial acetic acid and 30% H<sub>2</sub>O<sub>2</sub> or by reacting **5** with HOF solution. Nitration of 3,5-dimethoxypyridazine-1-oxide (**6**) to 3,5-dimethoxy-4,6-dinitropyridazine-1-oxide (**7**) was achieved with 20% oleum and 100% nitric acid. The key step in the synthesis was the introduction of electron-donating groups (–OMe) and the N-oxide moiety into the pyridazine scaffold allowing successful nitration. Amination of **7** with concentrated ammonia solution yielded 3,5-diamino-4,6-dinitropyridazine-1-oxide (**8**). Compound **8** shows good detonation properties similar to LLM-105 and also low sensitivities (IS = 18 J; FS = 360 N and ES = 0.75 J). In addition, the small-scale shock reactivity test (SSRT) with compound **8** was performed and compared to other energetic materials (HNS, PYX, TKX-55). Further functionalization of the pyridazine scaffold is currently under investigation in our laboratories.

### 4.4. Experimental Section

#### 4.4.1. General Considerations

<sup>1</sup>H, <sup>13</sup>C, <sup>14</sup>N and <sup>15</sup>N NMR spectra were recorded on JEOL 270 and BRUKER AMX 400 instruments. The samples were measured at room temperature in standard NMR tubes (Ø 5 mm). Chemical shifts are reported as  $\delta$  values in ppm relative to the residual solvent peaks of CDCl<sub>3</sub> ( $\delta$ H: 7.26,  $\delta$ C: 77.1), d<sub>6</sub>-Acetone ( $\delta$ H: 2.05,  $\delta$ C: 29.8 and 206.3) and d<sub>6</sub>-DMSO ( $\delta$ H: 2.50,  $\delta$ C: 39.5). Solvent residual signals and chemical shifts for NMR solvents were referenced against tetramethylsilane (TMS,  $\delta$  = 0 ppm) and nitromethane. Unless stated otherwise, coupling constants were reported in hertz (Hz) and for the characterization of the observed signal multiplicities the following abbreviations were used: s (singlet), d (doublet), t (triplet), q (quartet), quint (quintet), sept (septet), m (multiplet) and br (broad). Low resolution mass spectra were recorded on a JEOL JMS-700 MStation mass spectrometer (EI<sup>+</sup>/DEI<sup>+</sup>). Infrared spectra (IR) were recorded from 4500 cm<sup>–1</sup> to 650 cm<sup>–1</sup> on a PERKIN ELMER Spectrum BX-59343 instrument with SMITHS

## Energetic Functionalization of the Pyridazine Scaffold: Synthesis and Characterization of 3,5-Diamino-4,6-dinitropyridazine-1-oxide

DETECTION DuraSamplIR II Diamond ATR sensor. The absorption bands are reported in wavenumbers ( $\text{cm}^{-1}$ ). Elemental analysis was carried out by the department's internal micro analytical laboratory on a Elementar Vario el by pyrolysis of the sample and subsequent analysis of the formed gases. Decomposition temperatures were measured via differential thermal analysis (DTA) with an OZM Research DTA 552-Ex instrument at a heating rate of  $5\text{ }^{\circ}\text{C min}^{-1}$  and in a range of room temperature to  $400\text{ }^{\circ}\text{C}$ . Melting points were determined in capillaries with a Büchi Melting Point B-540 instrument and are uncorrected. All sensitivities toward impact (IS) and friction (FS) were determined according to BAM (German: Bundesanstalt für Materialforschung und Prüfung) standards using a BAM drop hammer and a BAM friction apparatus.<sup>[23]</sup> Compounds **7** and **8** were tested for sensitivity towards electrical discharge using an Electric Spark Tester ESD 2010 EN.

### 3,5-Dimethoxypyridazine (**5**)

3,5-Dichloropyridazine (16.26 g, 109.15 mmol) was dissolved in MeOH (400 mL) and potassium hydroxide (20.82 g, 371.1 mmol, 3.36 eq.) was added. The resulting reaction mixture was stirred at room temperature for 3 days. The suspension was filtrated and the solvent was removed under reduced pressure. The solid material was dissolved in a mixture of DCM (350 mL)/  $\text{H}_2\text{O}$  (150 mL) and the water phase was extracted again with DCM ( $2 \times 150\text{ mL}$ ). The combined organic layers were dried over  $\text{MgSO}_4$  and the solvent was evaporated *in vacuo* to yield compound **5** (12.40, 88.49 mmol, 81 %) as a yellowish solid.

m.p.  $73\text{ }^{\circ}\text{C}$ ; IR (ATR),  $\tilde{\nu}$  ( $\text{cm}^{-1}$ ) = 3322 (br), 3056 (w), 3020 (vw), 2962 (w), 1595 (vs), 1554 (vw), 1468 (s), 1447 (s), 1419 (vw), 1387 (vs), 1345 (vs), 1297 (w), 1247 (vw), 1218 (vs), 1191 (s), 1170 (vs), 1092 (m), 1043 (s), 1016 (vs), 986 (m), 926 (m), 898 (m), 876 (s), 861 (vw), 750 (m), 659 (m). Raman (1064 nm, 200 mW,  $25\text{ }^{\circ}\text{C}$ ):  $\tilde{\nu}$  ( $\text{cm}^{-1}$ ) = 3088 (20), 3046 (28), 3022 (53), 2993 (17), 2965 (35), 2945 (23), 2584 (17), 2826 (10), 1602 (9), 1468 (10), 1445 (13), 1418 (11), 1348 (31), 1245 (33), 1190 (13), 1179 (9), 1093 (11), 1046 (11), 1016 (22), 992 (17), 750 (39), 459 (21), 250 (9), 220 (13), 73 (100).  $^1\text{H}$  NMR ( $d_6$ -DMSO, 400 MHz, ppm)  $\delta$  = 8.63 (d,  $^4J$  = 2.50 Hz, 1H), 6.69 (d,  $^4J$  = 2.50 Hz, 1H), 3.99 (s, 3H), 3.86 (s, 3H).  $^{13}\text{C}$  NMR ( $d_6$ -DMSO, 101 MHz, ppm)  $\delta$  = 165.9, 159.7, 141.1, 96.9, 55.8, 54.5. Elem. Anal. ( $\text{C}_6\text{H}_8\text{N}_2\text{O}_2$ ,  $140.14\text{ g mol}^{-1}$ ) calcd.: C 51.42, H 5.75, N 19.99 %. Found: C 51.46, H 5.79, N 19.85 %.  $m/z$  ( $\text{DEI}^+$ ): 140 (100)  $[\text{M}]^+$ , 139 (92), 69 (55), 68 (84);

## Energetic Functionalization of the Pyridazine Scaffold: Synthesis and Characterization of 3,5-Diamino-4,6-dinitropyridazine-1-oxide

### 3,5-Dimethoxypyridazine-1-oxide (**6**)

#### Procedure 1:

To a solution of 3,5-dimethoxypyridazine (6.00 g, 42.8 mmol) in acetic acid (60 mL) was added 30% H<sub>2</sub>O<sub>2</sub> (8 mL) and the reaction mixture was stirred at 75 °C. After 2.5 h 30% H<sub>2</sub>O<sub>2</sub> (8 mL) was added to the reaction dropwise and stirring was continued for another 2.5 h at 75 °C. After cooling down, the reaction mixture was diluted with H<sub>2</sub>O (250 mL) and basified with Na<sub>2</sub>CO<sub>3</sub>. The water phase was extracted with DCM (3 × 250 mL) and the combined organic layers were washed with H<sub>2</sub>O (250 mL). After drying over MgSO<sub>4</sub> the solvent was removed *in vacuo* and compound **6** (4.94 g, 75 %) was obtained as white solid.

#### Procedure 2:

3,5-Dimethoxypyridazine (0.51 g, 3.27 mmol) was dissolved in DCM (15 mL) and the reaction was cooled to −5–0 °C. To the solution was slowly added freshly prepared HOF in acetonitrile solution (0.26 M, 63 mL, 5.0 eq.) and the reaction mixture was stirred for 1 h at 0 °C and overnight at room temperature. The excess of acid was quenched with saturated sodium carbonate solution and the reaction was extracted with DCM (5 × 150 mL). The combined organic layers were dried over MgSO<sub>4</sub> and the solvent was removed *in vacuo*. Compound **6** was obtained as a white solid in a good yield (0.46 g, 90%).

m.p. 131 °C; IR (ATR),  $\tilde{\nu}$  (cm<sup>−1</sup>) = 3114 (w), 3059 (w), 2948 (w), 1567 (s), 1457 (m), 1379 (s), 1212 (vs), 1175 (s), 1080 (m), 1043 (m), 965 (w), 927 (m), 855 (m), 825 (s). Raman (1064 nm, 200 mW, 25 °C):  $\tilde{\nu}$  (cm<sup>−1</sup>) = 3115 (15), 3061 (16), 3025 (43), 2991 (15), 2943 (22), 2840 (14), 1572 (35), 1475 (11), 1447 (9), 1430 (15), 1232 (35), 1221 (30), 1200 (15), 1176 (18), 1054 (12), 1003 (11), 970 (25), 624 (52), 397 (19), 258 (15), 203 (14), 117 (100). <sup>1</sup>H NMR (*d*<sub>6</sub>-DMSO, 400 MHz, ppm)  $\delta$  = 7.98 (d, <sup>4</sup>*J* = 1.65 Hz, 1H), 6.55 (d, <sup>4</sup>*J* = 1.65 Hz, 1H), 3.88 (s, 3H), 3.86 (s, 3H). <sup>13</sup>C NMR (*d*<sub>6</sub>-DMSO, 101 MHz, ppm)  $\delta$  = 165.6, 165.2, 118.8, 90.9, 56.9 55.0. Elem. Anal. (C<sub>6</sub>H<sub>8</sub>N<sub>2</sub>O<sub>3</sub>, 156.14 g mol<sup>−1</sup>) calcd.: C 46.15, H 5.16, N 17.94 %. Found: C 46.17, H 5.11, N 17.86 %. *m/z* (DEI<sup>+</sup>): 156 (100) [M]<sup>+</sup>, 85 (29), 69 (21), 68 (16);

## Energetic Functionalization of the Pyridazine Scaffold: Synthesis and Characterization of 3,5-Diamino-4,6-dinitropyridazine-1-oxide

### 3,5-Dimethoxy-4,6-dinitropyridazine-1-oxide (7)

#### Procedure 1:

3,5-Dimethoxypyridazine-1-oxide (3.00 g, 19.2 mmol) was dissolved in 20% oleum (20 mL) at 5 °C and sodium nitrate (8.50 g, 100 mmol) was added in small portions by maintaining the temperature of the solution below 5 °C. The reaction mixture was stirred for 1 h and then brought to room temperature slowly. Subsequently, the reaction was stirred overnight at 60 °C and afterwards quenched on crushed ice. The resulting suspension was stirred until all ice dissolved and the resulting precipitate was filtered. The crude product was dissolved in conc. H<sub>2</sub>SO<sub>4</sub> (13 mL), stirred at 60 °C for 3 h, then quenched on ice and the resulting precipitate was filtered. The product was washed with ice-water until the filtrate was acid free and dried on air (0.62 g, 13%).

#### Procedure 2:

3,5-Dimethoxypyridazine-1-oxide (6.70 g, 42.9 mmol) was dissolved in 20-25% oleum (35 mL) at 10 °C and 100% HNO<sub>3</sub> (26 mL) was added dropwise by maintaining the temperature of the solution below 8 °C. After the addition was complete the reaction mixture was first stirred for 1.5 h at 0 °C, then for 2 h at room temperature and finally for 20 h at 45-50 °C. After cooling down the reaction was poured onto crushed ice. The resulting suspension was stirred for 2 h and then the yellowish precipitate was filtered off, washed with water until the filtrate was acid free and dried on air. The crude product was dissolved in conc. H<sub>2</sub>SO<sub>4</sub> (35 mL) and stirred at 60 °C for 2 h. The reaction mixture was quenched on crushed ice. The resulting precipitate was filtrated, washed with ice-water until the filtrate was acid free and dried on air (2.94 g, 28 %).

DTA (5 °C min<sup>-1</sup>): 151 °C (dec.); BAM: drop hammer: 20 J (100–500 μm); friction tester: 360 N (100–500 μm); ESD: 0.65 J (100–500 μm); IR (ATR),  $\tilde{\nu}$  (cm<sup>-1</sup>) = 3000 (w), 2962 (m), 2906 (w), 2890 (w), 1563 (s), 1541 (s), 1504 (m), 1443 (m), 1416 (m), 1379 (s), 1343 (s), 1285 (s), 1252 (m), 1214 (s), 1136 (m), 1082 (m), 1016 (m), 985 (m), 942 (w), 828 (m), 784 (m), 760 (w), 711 (vs), 648 (m), 614 (w). Raman (1064 nm, 200 mW, 25 °C):  $\tilde{\nu}$  (cm<sup>-1</sup>) = 3052 (10), 2963 (22), 1564 (32), 1528 (9), 1452 (12), 1419 (27), 1379 (22), 1346 (41), 1253 (40), 830 (21), 642 (10), 616 (9), 403 (8), 333 (12), 313 (24), 230 (15), 186 (17), 158 (23), 96 (100). <sup>1</sup>H NMR (*d*<sub>6</sub>-DMSO, 400 MHz, ppm)  $\delta$  = 3.98 (s, 3H), 3.87 (s, 3H). <sup>13</sup>C NMR (*d*<sub>6</sub>-DMSO, 101 MHz, ppm)  $\delta$  = 156.8, 155.6, 144.4, 124.1, 62.1, 55.5. <sup>14</sup>N NMR (*d*<sub>6</sub>-DMSO, 29 MHz, ppm)  $\delta$  = -18, -82. Elem. Anal. (C<sub>6</sub>H<sub>6</sub>N<sub>4</sub>O<sub>7</sub>,



## Energetic Functionalization of the Pyridazine Scaffold: Synthesis and Characterization of 3,5-Diamino-4,6-dinitropyridazine-1-oxide

246.14 g mol<sup>-1</sup>) calcd.: C 29.28, H 2.46, N 22.76 %. Found: C 29.25, H 2.69, N 22.78 %. *m/z* (DEI<sup>+</sup>): 246 (100) [M]<sup>+</sup>, 216 (24), 140 (39), 83 (10);

### 3,5-Diamino-4,6-dinitropyridazine-1-oxide (8)

3,5-Dimethoxy-4,6-dinitropyridazine-1-oxide (1.40 g, 6.69 mmol) was dissolved in acetonitrile (50 mL) and an aqueous 25% NH<sub>3</sub> solution (5.0 mL) was added dropwise at room temperature. The solution was then refluxed for 24 h. After cooling down the solvent was removed *in vacuo* and the residue was dissolved in acetone. After removing the solvent under reduced pressure the product was obtained as yellow solid (1.20 g, 90 %).

DTA (5 °C min<sup>-1</sup>): 215 °C (dec.); BAM: drop hammer: 18 J (100–500 μm); friction tester: 360 N (100–500 μm); ESD: 0.75 J (100–500 μm); IR (ATR),  $\tilde{\nu}$  (cm<sup>-1</sup>) = 3419 (w), 3280 (m), 1600 (s), 1573 (s), 1513 (vs), 1381 (m), 1271 (s), 1219 (s), 1181 (vs), 1078 (s), 1034 (s), 891 (w), 834 (m), 775 (w), 754 (w), 726 (w), 699 (m), 659 (w), 638 (w), 559 (s). Raman (1064 nm, 200 mW, 25 °C):  $\tilde{\nu}$  (cm<sup>-1</sup>) = 3287 (7), 1514 (52), 1456 (23), 1395 (16), 1311 (67), 1284 (73), 1200 (15), 1133 (8), 1042 (9), 896 (10), 836 (29), 667 (23), 633 (8), 582 (29), 417 (7), 204 (10), 122 (100), 107 (100). <sup>1</sup>H NMR (*d*<sub>6</sub>-DMSO, 400 MHz, ppm)  $\delta$  = 8.75 (br, 2H), 8.64 (br, 2H). <sup>13</sup>C NMR (*d*<sub>6</sub>-DMSO, 101 MHz, ppm)  $\delta$  = 154.3, 142.2, 133.9, 110.9. <sup>14</sup>N NMR (*d*<sub>6</sub>-DMSO, 29 MHz, ppm)  $\delta$  = -15, -26, -70. <sup>15</sup>N NMR (*d*<sub>6</sub>-DMSO, 41 MHz, ppm)  $\delta$  = -15.6, -26.0, -69.5, -110.3, -286.7 (t, *J*<sub>NH</sub> = 92.9 Hz, 2N). <sup>15</sup>N{H} NMR (*d*<sub>6</sub>-DMSO, 41 MHz, ppm)  $\delta$  = -15.6, -26.0, -69.5, -110.3, -286.8, -292.9. Elem. Anal. (C<sub>4</sub>H<sub>4</sub>N<sub>6</sub>O<sub>5</sub>, 216.11 g mol<sup>-1</sup>) calcd.: C 22.23, H 1.87, N 38.89 %. Found: C 22.60, H 1.97, N 38.61 %. *m/z* (DEI<sup>+</sup>): 216 (94) [M]<sup>+</sup>, 200 (47), 186 (28), 110 (36);

### 3,5-Dimethoxy-4-nitropyridazine (9)

Procedure 1:

3,5-Dimethoxypyridazine (1.60 g, 11.4 mmol, 1.0 eq.) was dissolved in 25% oleum (7 mL) and 100% HNO<sub>3</sub> (1.30 mL) was added dropwise at 0–10 °C. The reaction mixture was stirred for 1 h at 0 °C and then at room temperature for 2 h. Subsequently, the reaction was stirred for 4 h at 80–85 °C and afterwards quenched on crushed ice. The resulting precipitate was filtered and washed with ice-water until the filtrate was acid free to yield 3,5-dimethoxy-4-nitropyridazine (554 mg, 26%) as a pale-yellow solid.

## Energetic Functionalization of the Pyridazine Scaffold: Synthesis and Characterization of 3,5-Diamino-4,6-dinitropyridazine-1-oxide

### Procedure 2:

3,5-Dimethoxypyridazine (1.80 g, 12.8 mmol, 1.0 eq.) was dissolved in 40% oleum (9 mL) and KNO<sub>3</sub> (1.29 g, 12.8 mmol, 1.0 eq.) was added at 15–20 °C. The reaction mixture was slowly heated to 40 °C and KNO<sub>3</sub> (1.95 g, 19.2 mmol, 1.5 eq.) was added. The reaction was stirred at 80 °C overnight. The reaction mixture was poured on ice and the precipitate was filtrated, washed with ice water and dried on air to yield compound **9** (1.07 g, 5.76 mmol, 45%) as a pale-yellow solid.

IR (ATR),  $\tilde{\nu}$  (cm<sup>-1</sup>) = 3091 (vw), 3047 (vw), 3012 (vw), 2960 (vw), 2863 (vw), 1608 (s), 1531 (s), 1490 (m), 1454 (m), 1429 (w), 1362 (vs), 1336 (m), 1241 (s), 1178 (w), 1135 (vs), 1058 (m), 997 (m), 910 (m), 882 (m), 865 (s), 776 (w), 754 (m), 650 (m), 617 (w), 579 (m), 507 (vw). <sup>1</sup>H NMR (*d*<sub>6</sub>-DMSO, 400 MHz, ppm)  $\delta$  = 9.38 (s, 1H), 4.15 (s, 3H), 4.15 (s, 3H). <sup>13</sup>C NMR (*d*<sub>6</sub>-DMSO, 101 MHz, ppm)  $\delta$  = 154.9, 149.0, 139.5, 125.7, 58.8, 56.2. <sup>14</sup>N NMR (*d*<sub>6</sub>-DMSO, 29 MHz, ppm)  $\delta$  = -20. Elem. Anal. (C<sub>6</sub>H<sub>7</sub>N<sub>3</sub>O<sub>4</sub>, 185.14 g mol<sup>-1</sup>) calcd.: C 38.93, H 3.81, N 22.70 %. Found: C 38.73, H 3.74, N 22.78 %. *m/z* (DEI<sup>+</sup>): 185 (62) [M<sup>+</sup>], 96 (100), 53 (24).

## 4.5. Acknowledgements

Financial support of this work by the Ludwig-Maximilian University of Munich (LMU), the Office of Naval Research (ONR) under grant no. ONR.N00014-16-1-2062, and the Bundeswehr-Wehrtechnische Dienststelle für Waffen und Munition (WTD 91) under grant no. E/E91S/FC015/CF049 is gratefully acknowledged. We thank Dr. Burkhard Krumm for NMR measurements and Stefan Huber for his help with the sensitivity testing.

**Keywords:** Energetic heterocycles • 1,2-Diazine • Insensitive explosive • High explosive • Nitration of 1,2-diazines;

## 4.6. References

- [1] a) J. P. Agrawal, R. D. Hodgson, *Organic Chemistry of Explosives*, Wiley, New York, **2007**.  
b) T. M. Klapötke, *Chemistry of High-Energy Materials*, 4th ed., De Gruyter, Berlin, **2017**. c)  
M. H. Keshavarz, T. M. Klapötke, *Energetic Compounds: Methods for Prediction of Their Performance*, De Gruyter, Berlin, **2017**. d) M. H. Keshavarz, T. M. Klapötke, *The Properties*

**Energetic Functionalization of the Pyridazine Scaffold: Synthesis and Characterization of  
3,5-Diamino-4,6-dinitropyridazine-1-oxide**

*of Energetic Materials: Sensitivity, Physical and Thermodynamic Properties*, De Gruyter, Berlin, **2017**.

- [2] a) D. Fischer, J. L. Gottfried, T. M. Klapötke, K. Karaghiosoff, J. Stierstorfer, T. G. Witkowski, *Angew. Chem. Int. Ed.* **2016**, *55*, 16132–16135.; *Angew. Chem.* **2016**, *128*, 16366–16369. b) T. M. Klapötke, *Chemistry of High-Energy Materials*, 3rd ed., Walter de Gruyter, Berlin, **2015**. c) Y. Tang, J. Zhang, L. A. Mitchell, D. A. Parrish, J. M. Shreeve, *J. Am. Chem. Soc.* **2015**, *137*, 15984–15987. d) D. E. Chavez, *Topics in Heterocyclic Chemistry*, Springer, Berlin, Heidelberg, **2017**, 1–27. e) H. Gao, J. M. Shreeve, *Chem. Rev.* **2011**, *111*, 7377–7436.
- [3] J. P. Agrawal, *Prog. Energy Combust. Sci.* **1998**, *24*, 1–30.
- [4] J. R. Kolb, H. F. Rizzo, *Propell. Explos.* **1979**, *4*, 10–16.
- [5] a) P. F. Pagoria, G. S. Lee, A. R. Mitchell, R. D. Schmidt, *Thermochimica Acta* **2002**, *384*, 187–204. b) T. M. Klapötke, R. D. Chapman, *Struct. Bond.* **2016**, *172*, 49–64.
- [6] a) R. A. Hollins, L. H. Merwin, R. A. Nissan, W. S. Wilson, R. Gilardi, *J. Heterocycl. Chem.* **1996**, *33*, 895. b) R. A. Hollins, L. H. Merwin, R. A. Nissan, W. S. Wilson, R. Gilardi, *Material Research Society Symposium Proceedings* **1996**, *418*, Pittsburgh, PA.
- [7] D. S. Donald, U.S. Patent No.3, 808, 209 (30 April **1974**).
- [8] P. F. Pagoria, A. R. Mitchell, R. D. Schmidt, R. L. Simpson, F. Garcia, J. Forbes, J. Cutting, R. Lee, R. Swansiger, D. M. Hoffman, *Presented at the Insensitive Munitions and Energetic Materials Technology Symposium*, San, Diego, CA, **1998**.
- [9] a) A. Albini, S. Pietra, *Heterocyclic-N-Oxides*, CRC Press, Boca Raton, FL, **1991**. b) A. M. Churakov, V. A. Tartakovsky, *Chem. Rev.* **2004**, *104*, 2601–2616.
- [10] a) H. Wei, H. Gao, J. M. Shreeve, *Chem. Eur. J.* **2014**, *20*, 16943–16952. b) C. Zhang, Y. Shu, X. Zhao, H. Dong, X. Wang, *J. Mol. Struct.: THEOCHEM* **2005**, *728*, 129–134.
- [11] T. Eicher, S. Hauptmann, *The Chemistry of Heterocycles*, 2nd ed., Wiley-VCH, Weinheim, **2003**.
- [12] a) M. Yanai, T. Kinoshita, S. Takeda, *Chem. Pharm. Bull.* **1971**, *19*, 2181–2183. b) H. Igeta, T. Tsuchiya, M. Nakajima, T. Sekiya, Y. Kumaki, T. Nakai, T. Nojima, *Chem. Pharm. Bull.* **1969**, *17*, 756–762. c) H. Igeta, *Chem. Pharm. Bull.* **1960**, *8*, 550–552.
- [13] Y. Tang, C. He, G. H. Imler, D. A. Parrish, J. M. Shreeve, *Chem. Eur. J.* **2017**, *23*, 1–5.
- [14] a) W. Deinhammer, M. Wick, Patent DE 19772706701, **1977**. b) G. Lu, F. Liu, X. Sun, F. Qi, Y. Gao, Patent CN 102838548, **2012**.
- [15] T. Itai, S. Natsumi, *Chem. Pharm. Bull.* **1964**, *12*, 228–235.

## Energetic Functionalization of the Pyridazine Scaffold: Synthesis and Characterization of 3,5-Diamino-4,6-dinitropyridazine-1-oxide

- [16] R. D. Bryant, F.-A. Kunng, M. S. South, *J. Heterocycl. Chem.* **1995**, 32, 1473–1476.
- [17] S. Rozen, A. Shaffer, *Org. Lett.* **2017**, 19, 4707–4709.
- [18] M. Sućeska, *EXPLO5 Version 6.03 User's Guide*, Zagreb, Croatia: OZM; **2015**.
- [19] J. S. Murray, P. Politzer, *J. Mol. Model* **2014**, 20, 2223–2227.
- [20] a) P. F. Pagoria, A. R. Mitchell, R. D. Schmidt, R. L. Simpson, F. Garcia, J. W. Forbes, R. W. Swansiger, D. M. Hoffman, *Synthesis, Scale-up and Characterization of 2,6-Diamino-3,5-dinitropyridazine-1-oxide (LLM-105)*, Report UCRL-JC-130518, Lawrence Livermore National Laboratory, Livermore, CA, **1998**. b) Gilardi, R. J. Butcher, *Acta Cryst. Section E* **2001**, 57, o657–o658.
- [21] a) H. W. Sandusky, R. H. Granholm, D. G. Bohl, IHTR 2701, Naval Surface Warfare Center, Indian Head Division, MD, USA, August 12, **2005**; b) J. E. Felts, H. W. Sandusky, R. H. Granholm, *AIP Conf. Proc.* **2009**, 1195, 233–236.
- [22] T. M. Klapötke, T. G. Witkowski, *ChemPlusChem* **2016**, 81, 357–360.
- [23] a) Reichel & Partner GmbH, <http://www.reichelt-partner.de>; b) Test methods according to the UN Recommendations on the Transport of Dangerous Goods, Manual of Test and Criteria, 4th edn., United Nations Publication, New York and Geneva, **2003**, ISBN 92–1-139087 7, Sales No. E.03.VIII.2; 13.4.2 Test 3 a (ii) BAM Fallhammer.

## 4.6. Supporting Information

### 4.6.1. Synthesis and general considerations

#### General procedure for the preparation of HOF:

A 10% F<sub>2</sub> mixture (mixed with 90% N<sub>2</sub>) was bubbled through a mixture of acetonitrile (120 mL) and water (12 mL) at –15 °C in a dry-ice bath for 2–3 h. The oxidizing power of the HOF solution was monitored by reacting aliquots (1 mL) with an acid aqueous 0.1 M KI solution (5 mL). The formed iodine was titrated with 0.1 M thiosulfate solution. Concentrations of the oxidizing agent were in the range of 0.20 M to 0.30 M.

Compounds **3** and **4** were synthesized according the known literature.<sup>[S1]</sup>

## Energetic Functionalization of the Pyridazine Scaffold: Synthesis and Characterization of 3,5-Diamino-4,6-dinitropyridazine-1-oxide

### (Z)-2,4,4,4-Tetrachlorobut-2-enal (**3**)

Chloral hydrate (**1**, 164.5 g, 1.00 mol) and ammonium acetate (4.94 g, 0.064 mol) were dissolved in toluene (225 mL) and heated to reflux on a water separator. Chloroacetaldehyde (**2**, 102.5 g, 0.65 mol) was added dropwise within 1 h, while the reaction mixture was stirred vigorously. The solution was refluxed for 3 h on the water separator. Then *p*-toluenesulfonic acid monohydrate (10.84 g, 0.057 mol) was added to the reaction and refluxing was further continued for 5 h. The resulting suspension was allowed to cool down to room temperature, was filtered off and the filtrate was concentrated under reduced pressure. The residue was subjected to vacuum distillation (1.1 mbar, 83–85 °C) to give compound **3** (44.0 g, 32 %) as yellowish oily liquid. The product was used for further reactions without any purification.

**IR (ATR)**,  $\tilde{\nu}$  (cm<sup>-1</sup>) = 3048 (vw), 2849 (vw), 1703 (vs), 1614 (m), 1389 (w), 1302 (vw), 1349 (w), 1201 (vw), 1141 (s), 1120 (vw), 1090 (vw), 1055 (vs), 988 (vw), 923 (vw), 841 (vs), 811 (vs), 724 (vs), 663 (vs). **<sup>1</sup>H NMR** (*d*<sub>6</sub>-Acetone, 400 MHz, ppm)  $\delta$  = 9.58 (s, 1H), 8.01 (s, 1H). **<sup>13</sup>C NMR** (*d*<sub>6</sub>-Acetone, 101 MHz, ppm)  $\delta$  = 186.0, 149.2, 138.1, 90.0.

### 3,5-Dichloropyridazine (**4**)

(Z)-2,4,4,4-Tetrachlorobut-2-enal (**3**, 22.0 g, 106 mmol) was dissolved in DMF (100 mL) and the resulting solution was cooled down to 15 °C. Semicarbazide hydrochloride (14.17 g, 127 mmol, 1.2 eq.) was dissolved in a mixture of H<sub>2</sub>O (45 mL)/ DMF (16 mL) at room temperature. The resulting semicarbazide hydrochloride solution was then added dropwise to the (Z)-2,4,4,4-tetrachlorobut-2-enal solution by maintaining the reaction temperature between 15–20 °C. After the addition was completed the reaction temperature was kept in the same range for 1 h. The reaction mixture was stirred for 2 days at room temperature giving a dark brown solution. The solution was given in H<sub>2</sub>O (600 mL) and stirred at room temperature for 30 min. The brown suspension was extracted with Et<sub>2</sub>O (3 × 500 mL). The organic phase was first washed with H<sub>2</sub>O (4 × 200 mL) and then with brine (4 × 200 mL). The combined organic layers were dried over MgSO<sub>4</sub>, filtered and the solvent was removed *in vacuo*. Recrystallizing the crude product from *n*-hexane yielded compound **4** (8.63 g, 55 %) as yellowish solid. Single crystals were obtained from *n*-hexane as yellow plates.

## Energetic Functionalization of the Pyridazine Scaffold: Synthesis and Characterization of 3,5-Diamino-4,6-dinitropyridazine-1-oxide

m.p. 61 °C; IR (ATR),  $\tilde{\nu}$  (cm<sup>-1</sup>) = 3102 (vw), 3013 (s), 2924 (w), 1545 (vs), 1389 (w), 1350 (vs), 1200 (m), 1171 (vs), 1171 (vs), 1101 (vs), 1058 (vs), 993 (s), 938 (m), 895 (s), 849 (m), 816 (vs), 726 (m), 693 (w). Raman (1064 nm, 200 mW, 25 °C):  $\tilde{\nu}$  (cm<sup>-1</sup>) = 3078 (12), 3056 (11), 3017 (47), 1548 (16), 1519 (14), 1390 (15), 1204 (15), 1175 (52), 1062 (19), 998 (80), 695 (46), 452 (21), 402 (55), 372 (21), 220 (30), 206 (54), 178 (54), 120 (100), 95 (44). <sup>1</sup>H NMR (CDCl<sub>3</sub>, 400 MHz, ppm)  $\delta$  = 9.12 (d, <sup>4</sup>*J* = 2.10 Hz, 1H), 7.60 (d, <sup>4</sup>*J* = 2.10 Hz, 1H). <sup>13</sup>C NMR (CDCl<sub>3</sub>, 101 MHz, ppm)  $\delta$  = 156.7, 150.6, 139.4, 127.7. <sup>1</sup>H NMR (*d*<sub>6</sub>-DMSO, 400 MHz, ppm)  $\delta$  = 9.44 (d, <sup>4</sup>*J* = 2.10 Hz, 1H), 8.35 (d, <sup>4</sup>*J* = 2.10 Hz, 1H). <sup>13</sup>C NMR (*d*<sub>6</sub>-DMSO, 101 MHz, ppm)  $\delta$  = 155.9, 151.1, 139.0, 128.2. Elem. Anal. (C<sub>4</sub>H<sub>2</sub>Cl<sub>2</sub>N<sub>2</sub>, 148.97 g mol<sup>-1</sup>) calcd.: C 32.25, H 1.35, N 18.80 %. Found: C 32.29, H 1.61, N 19.07 %.

### 4.6.2. X-ray diffraction

The low-temperature single-crystal X-ray diffraction measurements were performed on an Oxford XCalibur3 diffractometer equipped with a Spellman generator (voltage 50 kV, current 40 mA) and a KappaCCD detector operating with MoK $\alpha$  radiation ( $\lambda$  = 0.7107 Å). Data collection was performed using the CRYSLIS CCD software.<sup>[S2]</sup> The data reduction was carried out using the CRYSLIS RED software.<sup>[S3]</sup> The solution of the structure was performed by direct methods (SIR97)<sup>[S4]</sup> and refined by full-matrix least-squares on F<sup>2</sup> (SHELXL)<sup>[S5]</sup> implemented in the WINGX software package<sup>[S6]</sup> and finally checked with the PLATON software.<sup>[S7]</sup> All DIAMOND2 plots are shown with thermal ellipsoids at the 50% probability level and hydrogen atoms are shown as small spheres of arbitrary radius.

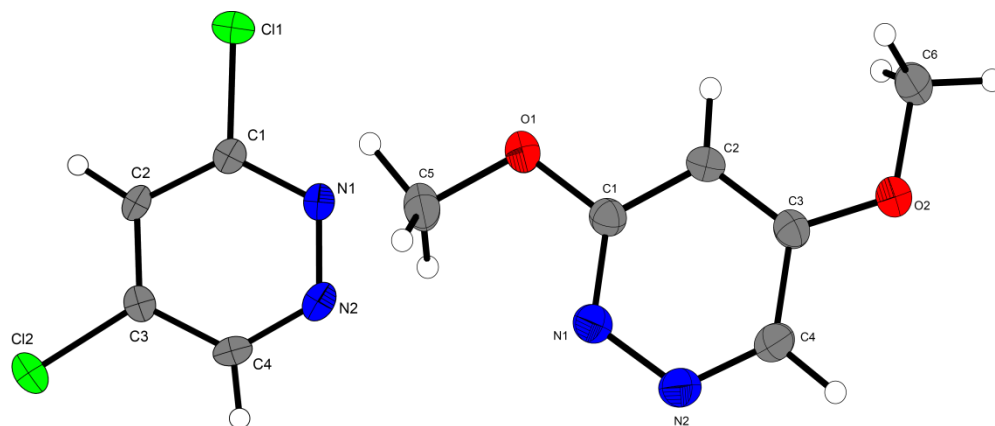


**Figure S1.** Molecular structures of 3,5-dichloropyridazine (**4**, left) and 3,5-dimethoxypyridazine (**5**, right) in the solid state. Ellipsoids correspond to 50 % probability levels.

## Energetic Functionalization of the Pyridazine Scaffold: Synthesis and Characterization of 3,5-Diamino-4,6-dinitropyridazine-1-oxide

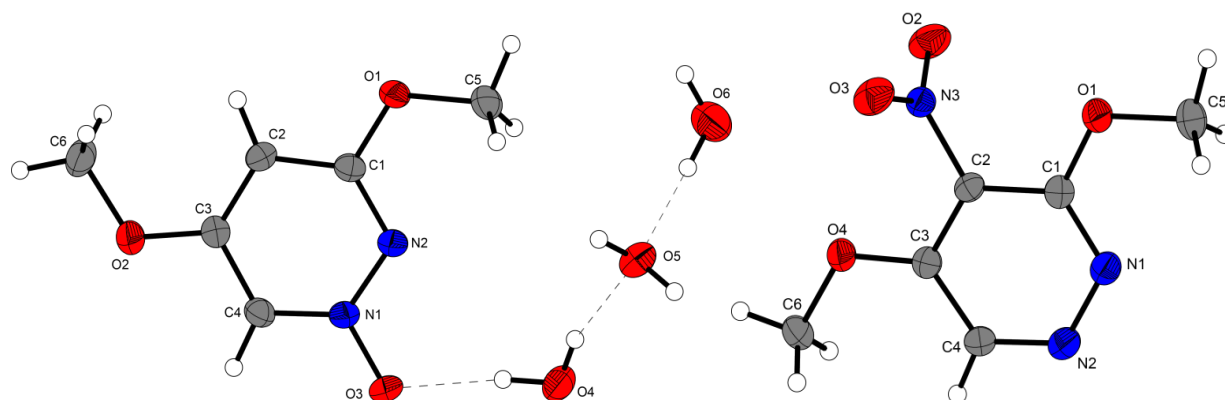


**Figure S2.** Molecular structures of 3,5-dimethoxypyridazine-1-oxide trihydrate (**6** • 3 H<sub>2</sub>O, left) and 3,5-dimethoxy-4-nitropyridazine (**9**, right) in the solid state. Ellipsoids correspond to 50 % probability levels.

**Table S1.** Crystallographic details of compounds **4**, **5** and **6** • 3 H<sub>2</sub>O.

Compound	<b>4</b>	<b>5</b>	<b>6</b> • 3 H <sub>2</sub> O
Formula	C <sub>4</sub> H <sub>2</sub> Cl <sub>2</sub> N <sub>2</sub>	C <sub>6</sub> H <sub>8</sub> N <sub>2</sub> O <sub>2</sub>	C <sub>6</sub> H <sub>14</sub> N <sub>2</sub> O <sub>6</sub>
Form. Mass [g/mol]	148.98	140.14	210.19
Crystal system	monoclinic	monoclinic	monoclinic
Space Group	<i>P</i> 2 <sub>1</sub> / <i>m</i> (No. 11)	<i>P</i> 2 <sub>1</sub> / <i>c</i> (No. 14)	<i>P</i> 2 <sub>1</sub> / <i>c</i> (No. 14)
Color / Habit	yellow plate	colorless plate	colorless plate
Size [mm]	0.09 × 0.15 × 0.23	0.03 × 0.27 × 0.31	0.05 × 0.15 × 0.35
<i>a</i> [Å]	6.0629(9)	3.9195(3)	4.4956(2)
<i>b</i> [Å]	6.3152(11)	10.7140(7)	24.0168(10)
<i>c</i> [Å]	7.9343(11)	15.9858(10)	9.3979(4)
$\alpha$ [°]	90	90	90
$\beta$ [°]	110.955(17)	93.025(7)	90.284(4)
$\gamma$ [°]	90	90	90
<i>V</i> [Å <sup>3</sup> ]	283.70(8)	670.37(8)	1014.68(8)
<i>Z</i>	2	4	4
$\rho_{\text{calc.}}$ [g cm <sup>-3</sup> ]	1.744	1.389	1.376

**Energetic Functionalization of the Pyridazine Scaffold: Synthesis and Characterization of  
3,5-Diamino-4,6-dinitropyridazine-1-oxide**

$\mu$ [mm <sup>-1</sup> ]	1.017	0.106	0.123
<i>F</i> (000)	148	296	448
$\lambda_{\text{MoK}\alpha}$ [Å]	0.71073	0.71073	0.71073
T [K]	173	173	123
$\theta$ min-max [°]	4.2, 26.0	4.3, 26.5	4.3, 26.0
Dataset h; k; l	−7:7; −7:6; −9:7	−4:4; −13:13; −20:19	−5:5; −29:27; −9:11
Reflect. coll.	1035	4223	7295
Independ. refl.	613	1376	1988
<i>R</i> <sub>int</sub>	0.025	0.045	0.022
Reflection obs.	474	877	1649
No. parameters	55	123	166
<i>R</i> <sub>1</sub> (obs)	0.0387	0.0498	0.0365
<i>wR</i> <sub>2</sub> (all data)	0.0849	0.1129	0.0949
<i>S</i>	1.07	1.06	1.05
Resd. Dens. [e Å <sup>-3</sup> ]	−0.34, 0.32	−0.19, 0.23	−0.19, 0.21
Device type	Oxford Xcalibur3 CCD	Oxford Xcalibur3 CCD	Oxford Xcalibur3 CCD
Solution	SIR-92	SIR-92	SIR-92
Refinement	SHELXL-97	SHELXL-97	SHELXL-97
Absorpt. corr.	multi-scan	multi-scan	multi-scan
CCDC	1590457	1590458	1590459

**Table S2.** Crystallographic details of compounds **7**, **8** and **9**.

Compound	<b>7</b>	<b>8</b>	<b>9</b>
Formula	C <sub>6</sub> H <sub>6</sub> N <sub>4</sub> O <sub>7</sub>	C <sub>4</sub> H <sub>4</sub> N <sub>6</sub> O <sub>5</sub>	C <sub>6</sub> H <sub>7</sub> N <sub>3</sub> O <sub>4</sub>



**Energetic Functionalization of the Pyridazine Scaffold: Synthesis and Characterization of  
3,5-Diamino-4,6-dinitropyridazine-1-oxide**

Form.	Mass	246.15	216.13	185.15
[g/mol]				
Crystal system		orthorombic	monoclinic	monoclinic
Space Group		<i>Pbcn</i> (No.60)	<i>P2<sub>1</sub>/c</i> (No. 14)	<i>C2/c</i> (No. 15)
Color / Habit		colorless plate	orange block	colorless plate
Size [mm]		0.05 x 0.30 x 0.40	0.10 x 0.15 x 0.20	0.09 x 0.36 x 0.48
<i>a</i> [Å]		8.0548(5)	18.6988(7)	17.1783(12)
<i>b</i> [Å]		8.6809(4)	5.2697(2)	7.6006(3)
<i>c</i> [Å]		28.5759(19)	16.4946(6)	14.4345(16)
$\alpha$ [°]		90	90	90
$\beta$ [°]		90	110.647(6)	122.085(11)
$\gamma$ [°]		90	90	90
<i>V</i> [Å <sup>3</sup> ]		1998.1(2)	1520.94(11)	1596.8(3)
<i>Z</i>		8	8	8
$\rho_{\text{calc.}}$ [g cm <sup>-3</sup> ]		1.637	1.888	1.540
$\mu$ [mm <sup>-1</sup> ]		0.152	0.173	0.131
<i>F</i> (000)		1008	880	768
$\lambda_{\text{MoK}\alpha}$ [Å]		0.71073	0.71073	0.71073
<i>T</i> [K]		123	123	173
$\vartheta$ min-max [°]		4.3, 26.5	4.1, 26.5	4.5, 26.0
Dataset h; k; l		−10:9; −5:10; −35:35	−23:23; −6:6; −20:18	−21:21; −9:9; −17:17
Reflect. coll.		15731	12156	11183
Independ. refl.		2054	3150	1570
<i>R</i> <sub>int</sub>		0.060	0.028	0.023
Reflection obs.		1570	2641	1377
No. parameters		178	303	146
<i>R</i> <sub>1</sub> (obs)		0.0490	0.0359	0.0325
w <i>R</i> <sub>2</sub> (all data)		0.1182	0.0942	0.0861
<i>S</i>		1.04	1.02	1.07
Resd.	Dens.	−0.25, 0.25	−0.40, 0.41	−0.17, 0.21
[e Å <sup>-3</sup> ]				

## Energetic Functionalization of the Pyridazine Scaffold: Synthesis and Characterization of 3,5-Diamino-4,6-dinitropyridazine-1-oxide

Device type	Oxford Xcalibur3	Oxford Xcalibur3	Oxford Xcalibur3
	CCD	CCD	CCD
Solution	SIR-92	SIR-92	SIR-92
Refinement	SHELXL-97	SHELXL-97	SHELXL-97
Absorpt. corr.	multi-scan	multi-scan	multi-scan
CCDC	1590461	1590460	1816507

---

### 4.6.3. Small-scale shock reactivity test (SSRT)

To evaluate the shock reactivity (explosiveness) of **8** a small-scale shock reactivity test (SSRT) was performed. The SSRT measures the shock reactivity of potentially energetic materials, often below critical diameter, without requiring a transition to detonation. The amount *ms* of compound **8** was calculated using the following formula:  $ms = V_s \cdot \rho \cdot 0.95$ , (where:  $V_s = 284 \text{ mm}^3$ ). Compound **8** was pressed at a consolidation dead load of 3 t with a dwell time of 5 s into a perforated steel block. Neither attenuator (between detonator and sample) nor air gap (between sample and aluminum block) were applied. Initiation of the tested explosive was performed using a commercially available detonator (Orica-DYNADET C2-0ms). The dent sizes were measured by filling them with powdered SiO<sub>2</sub> and measuring the resulting weight.

### 4.6.4. Computations

All calculations were carried out using the Gaussian G09W (revision A.02) program package.<sup>[S8]</sup> The enthalpies (H), were calculated using the complete basis set (CBS) method of Petersson and coworkers. The CBS models use the known asymptotic convergence of pair natural orbital expressions to extrapolate from calculations using a finite basis set to the estimated complete basis set limit. CBS-4 begins with a HF/3-21G(d) structure optimization and the zero point energy computation. Subsequently, applying a larger basis set a base energy is computed. A MP2/6-31+G calculation with a CBS extrapolation gives the perturbation-theory corrected energy (takes the electron correlation into account). A MP4(SDQ)/6-31+(d,p) calculation is used to correlate higher order contributions. In this study we applied the modified CBS-4M method (M referring to the use of minimal population localization) which is a re-parameterized version of the original CBS-4 method and also includes some additional empirical corrections.<sup>[S9]</sup> The gas-phase enthalpies

## Energetic Functionalization of the Pyridazine Scaffold: Synthesis and Characterization of 3,5-Diamino-4,6-dinitropyridazine-1-oxide

( $\Delta_f H^\circ_{(g, M, 298)}$ ) of the species were computed according to the atomization energy method (equation 1).<sup>[S10]</sup>

$$\Delta_f H^\circ_{(g, M, 298)} = H_{(g, M, 298)} - \sum H^\circ_{(g, A_i, 298)} + \sum \Delta_f H^\circ_{(g, A_i, 298)} \quad (1)$$

$\Delta_f H^\circ_{(g, A_i, 298)}$  for the corresponding atoms ( $A_i$ ) were determined experimentally and are reported in the literature while  $H^\circ_{(g, A_i, 298)}$  were calculated theoretically (Table S3).<sup>[S11]</sup>

**Table S3.** CBS-4M electronic enthalpies for atoms C, H, N and O and their literature values for atomic  $\Delta_f H^\circ_{298}$  / kJ mol<sup>-1</sup>

Atom	$-H^{298}$ / a.u.	$\Delta_f H^\circ_{(g, A_i, 298)}$ [kcal mol <sup>-1</sup> ]
H	0.500991	52.103
C	37.786156	171.29
N	54.522462	112.97
O	74.991202	59.56

Standard molar enthalpies of formation were calculated using and the standard molar enthalpies of  $\Delta_f H^\circ_{(g, M, 298)}$  sublimation (estimated using Trouton's rule, equation 2).<sup>[S12]</sup>

$$\Delta_f H^\circ_M = \Delta_f H^\circ_{(g, M, 298)} - \Delta_{sub} H^\circ_M = \Delta_f H^\circ_{(g, M, 298K)} - 188 \cdot T \left[ \frac{J}{mol} \right] \quad (2)$$

Where [K] is either the melting point or the decomposition temperature (if no melting occurs prior to decomposition).

The calculation results are summarized in **Tables S4**.

**Table S4.** Calculation results.

Compound	$-H^{298}$ a.u.	<sup>[a]</sup> $\Delta_f H^\circ_{(g, M)}$ kJ mol <sup>-1</sup> <sup>[b]</sup>	$\Delta_f H^\circ(s)$ kJ mol <sup>-1</sup> <sup>[c]</sup>	$\Delta_f U(s)$ kJ kg <sup>-1</sup> <sup>[d]</sup>
<b>7</b>	976.28483	-34.6	-114.4	-379.1
<b>8</b>	858.141084	202.2	110.5	597.2

## Energetic Functionalization of the Pyridazine Scaffold: Synthesis and Characterization of 3,5-Diamino-4,6-dinitropyridazine-1-oxide

<b>LLM-105</b>	858.170557	126.7	11.0	137.0
----------------	------------	-------	------	-------

<sup>[a]</sup> CBS-4M electronic enthalpy; <sup>[b]</sup> gas phase enthalpy of formation; <sup>[c]</sup> standard solid state enthalpy of formation; <sup>[d]</sup> solid state energy of formation.

### 4.6.5. Detonation parameters

The Chapman-Jouguet (C-J) characteristics, (*i.e.* heat of detonation,  $\Delta EU^\bullet$ ; detonation temperature,  $T_{C-J}$ ; detonation pressure,  $P_{C-J}$ ; detonation velocity  $D_{C-J}$ ) based on the calculated  $\Delta_f H^\circ_M$  values, and the theoretical maximum densities were computed using the EXPLO5 V6.03 thermochemical computer code.<sup>[S13]</sup> Calculations for explosives assume ideal behavior. The estimation of detonation parameters is based on the chemical equilibrium steady-state model of detonation. The Becker-Kistiakowsky-Wilson equation of state (BKW EOS) with the following sets of constants:  $\alpha = 0.5$ ,  $\beta = 0.38$ ,  $\kappa = 9.4$ , and  $\Theta = 4120$  for gaseous detonation products and the Murnaghan equation of state for condensed products (compressible solids and liquids) were applied. The calculation of the equilibrium composition of the detonation products uses modified White, Johnson and Dantzig's free energy minimization technique. The specific energies of explosives ( $f$ ) were calculated according to the ideal gas equation of state assuming isochoric conditions (equation 3).

$$f = p_e \cdot V = n \cdot R \cdot T_c \left[ \frac{JkJ}{molkg} \right] \quad (3)$$

Where  $p_e$  is the maximum pressure through the explosion,  $V$  is the volume of detonation gases ( $m^3 \cdot kg^{-1}$ ),  $n$  is the number of moles of gas formed by the explosion per kilogram of explosive (*Volume of Explosive Gases*),  $R$  is the ideal gas constant and  $T_c$  is the absolute temperature of the explosion.<sup>[S13,S14]</sup>

## Energetic Functionalization of the Pyridazine Scaffold: Synthesis and Characterization of 3,5-Diamino-4,6-dinitropyridazine-1-oxide

### 4.6.6. DTA

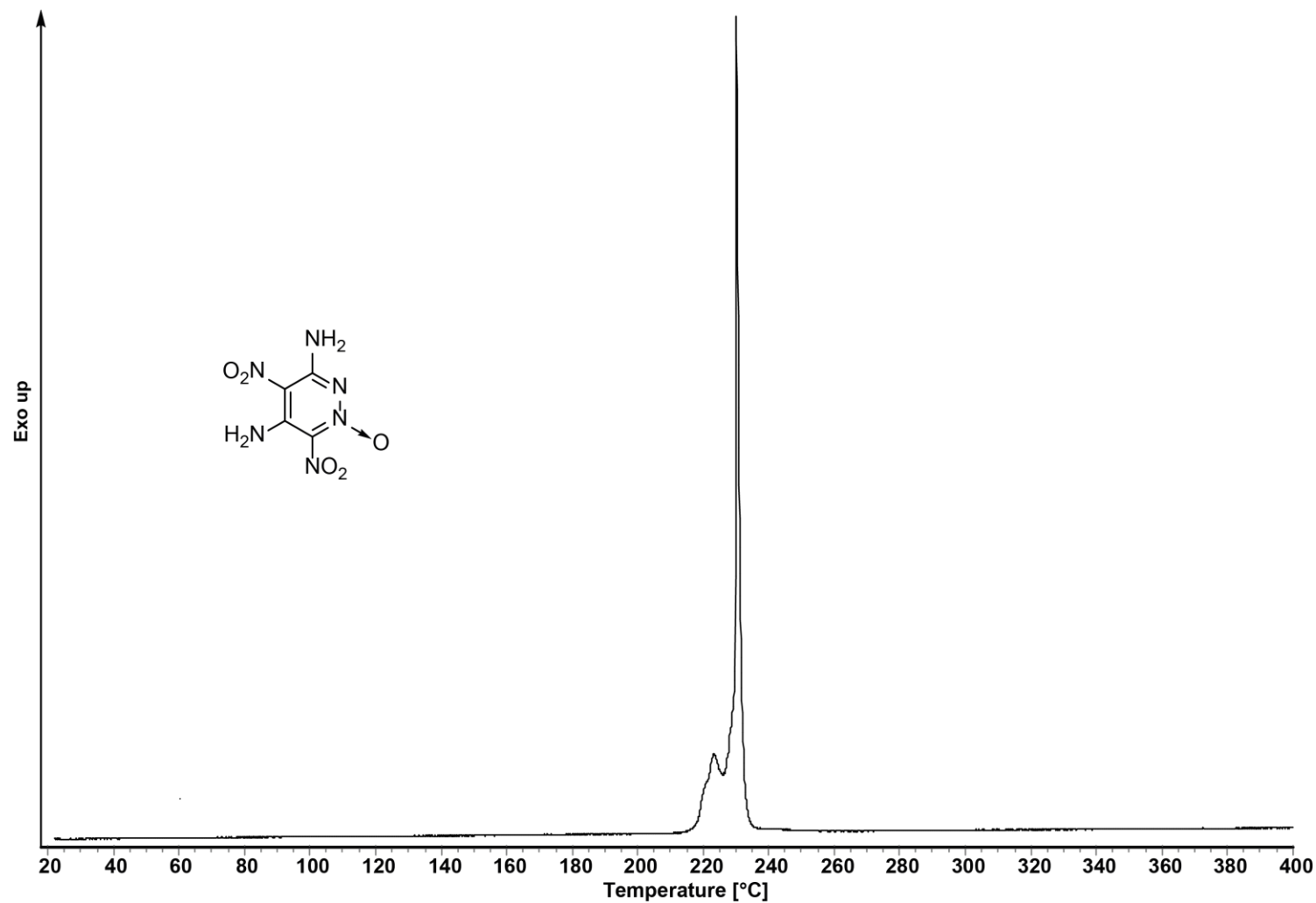
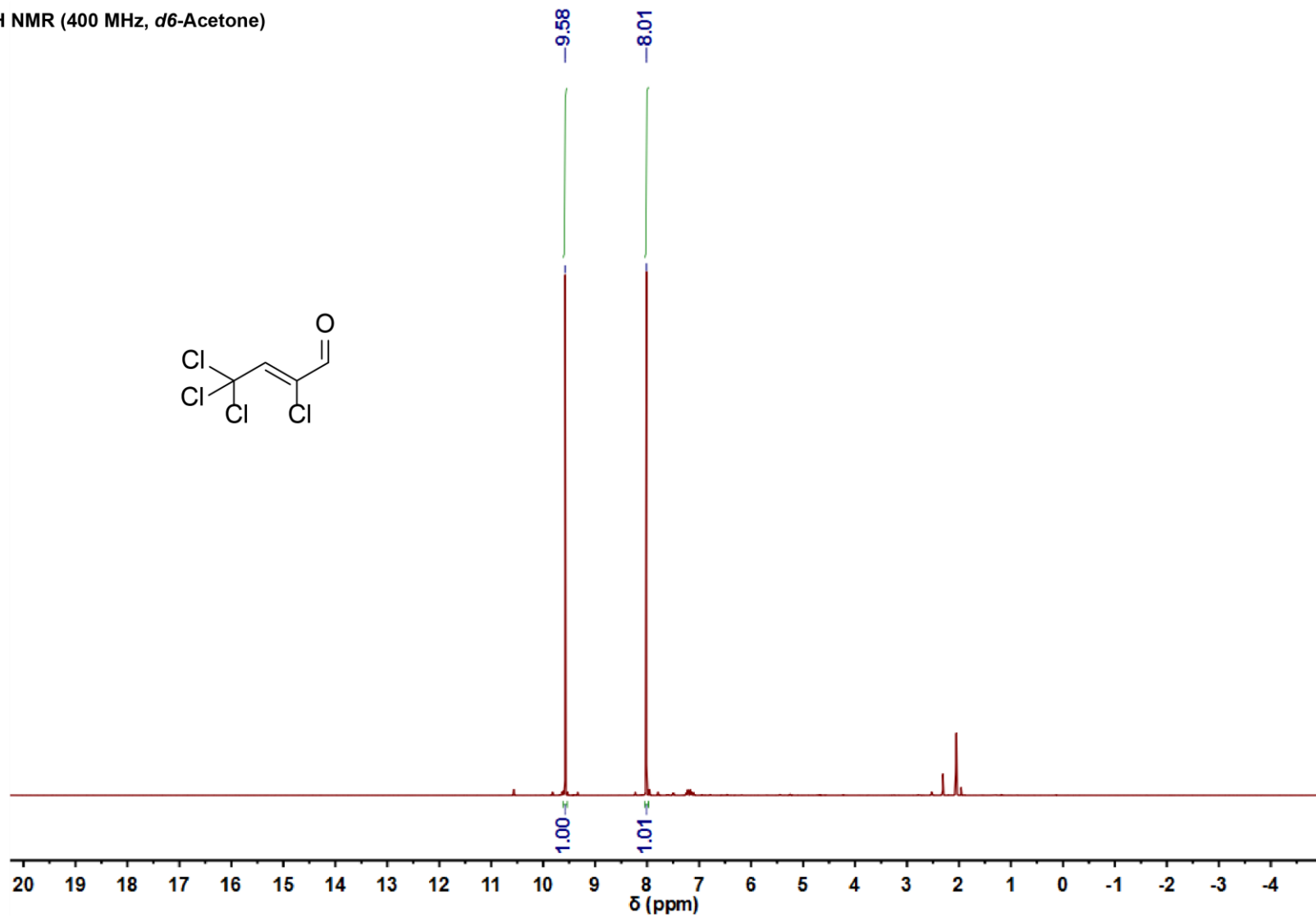


**Figure S3.** DTA plot of 3,5-diamino-4,6-dinitropyridazine-1-oxide (**8**).

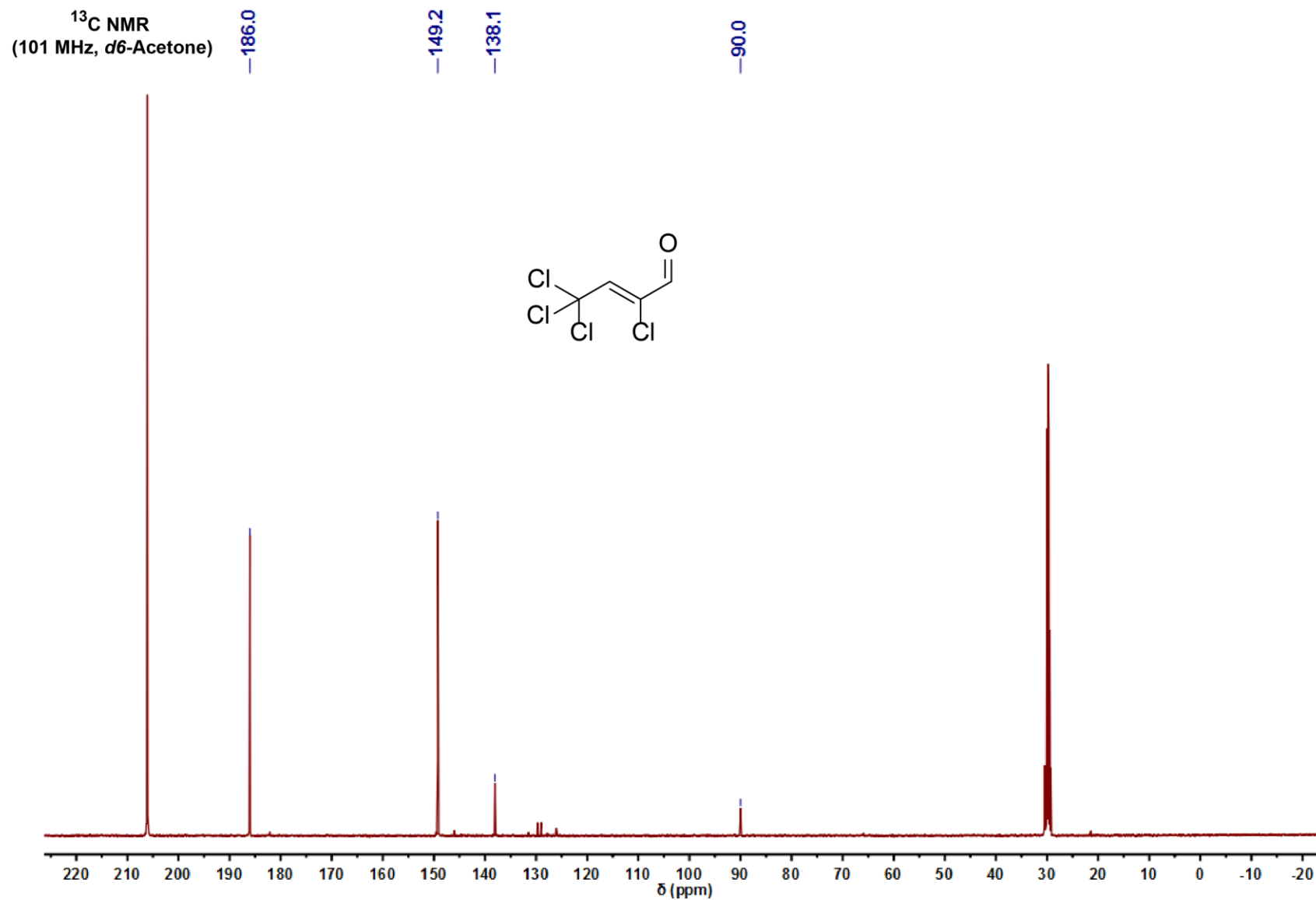
## Energetic Functionalization of the Pyridazine Scaffold: Synthesis and Characterization of 3,5-Diamino-4,6-dinitropyridazine-1-oxide

### 4.6.7. $^1\text{H}$ and $^{13}\text{C}$ NMR spectra

$^1\text{H}$  NMR (400 MHz,  $d_6$ -Acetone)

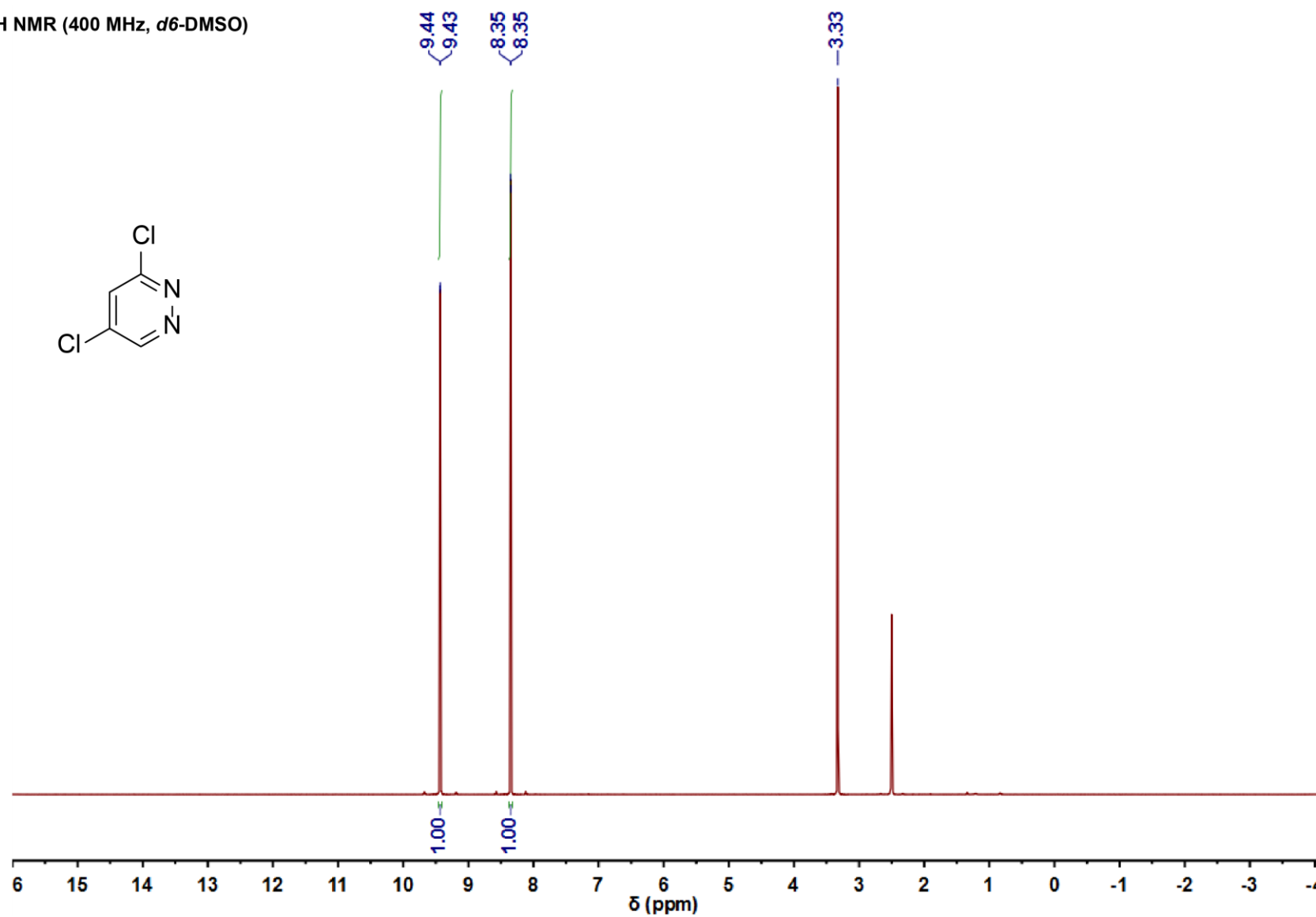


# Energetic Functionalization of the Pyridazine Scaffold: Synthesis and Characterization of 3,5-Diamino-4,6-dinitropyridazine-1-oxide



# Energetic Functionalization of the Pyridazine Scaffold: Synthesis and Characterization of 3,5-Diamino-4,6-dinitropyridazine-1-oxide

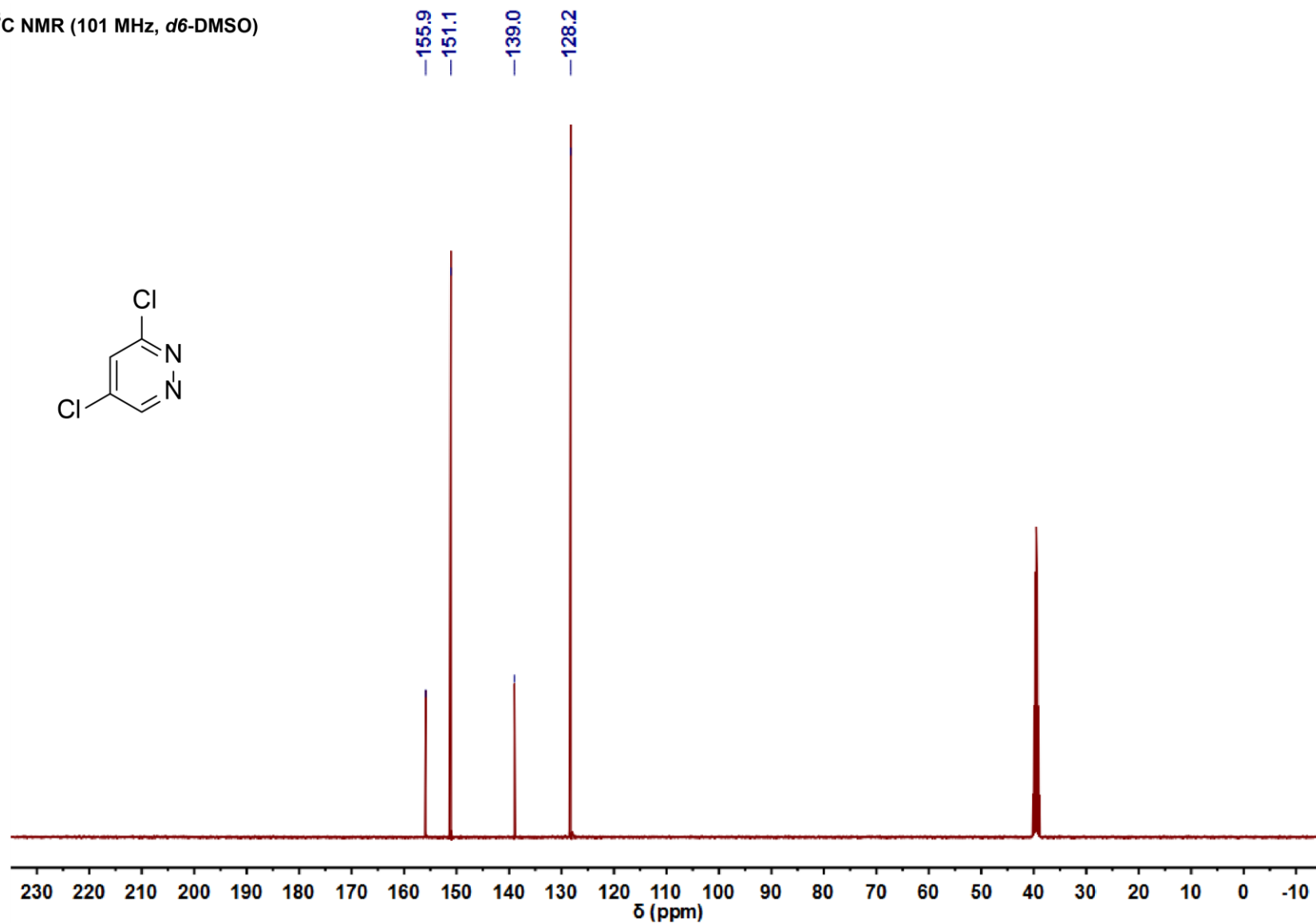
$^1\text{H}$  NMR (400 MHz,  $d_6$ -DMSO)





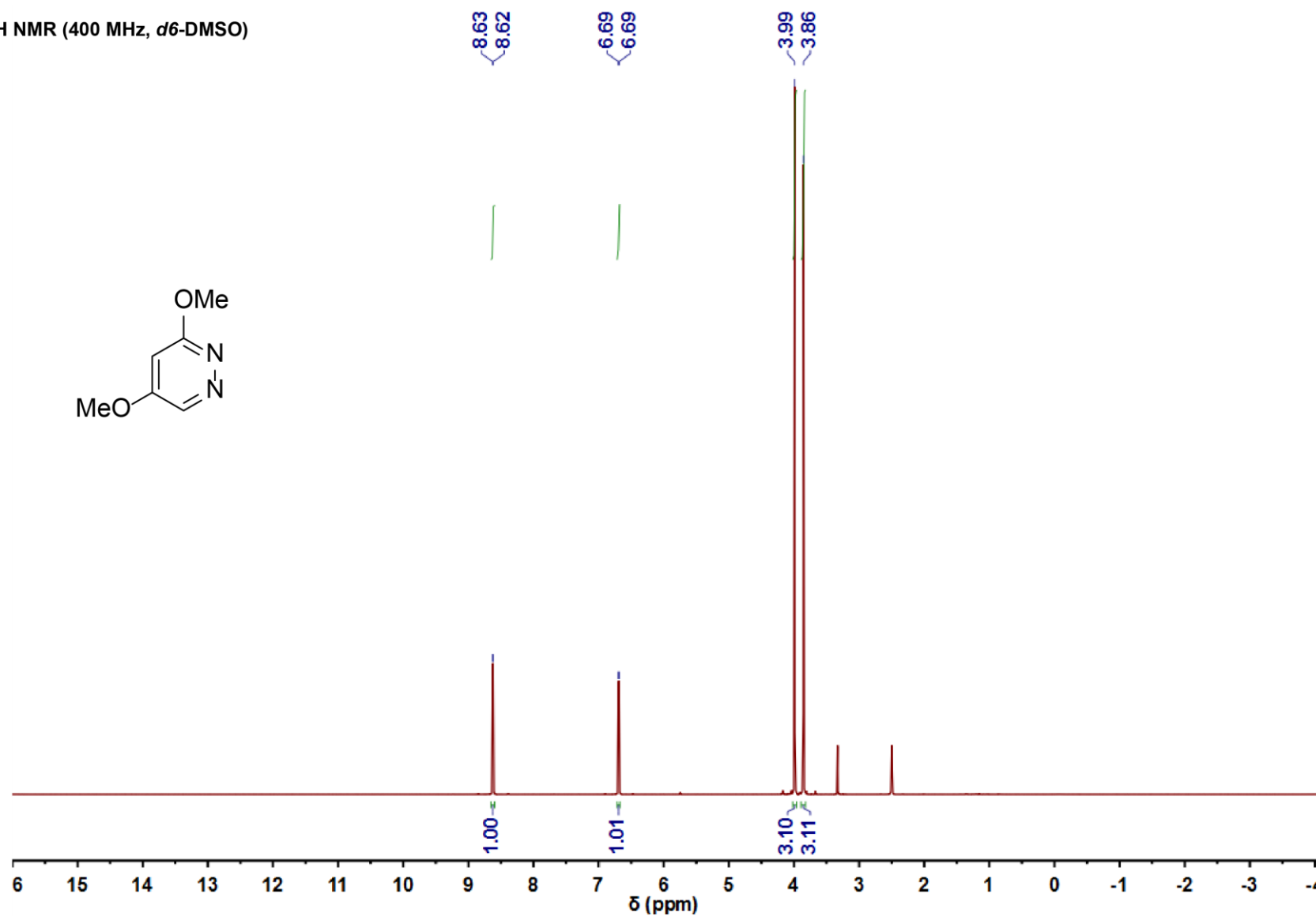
# Energetic Functionalization of the Pyridazine Scaffold: Synthesis and Characteriaztion of 3,5-Diamino-4,6-dinitropyridazine-1-oxide

$^{13}\text{C}$  NMR (101 MHz,  $d_6$ -DMSO)



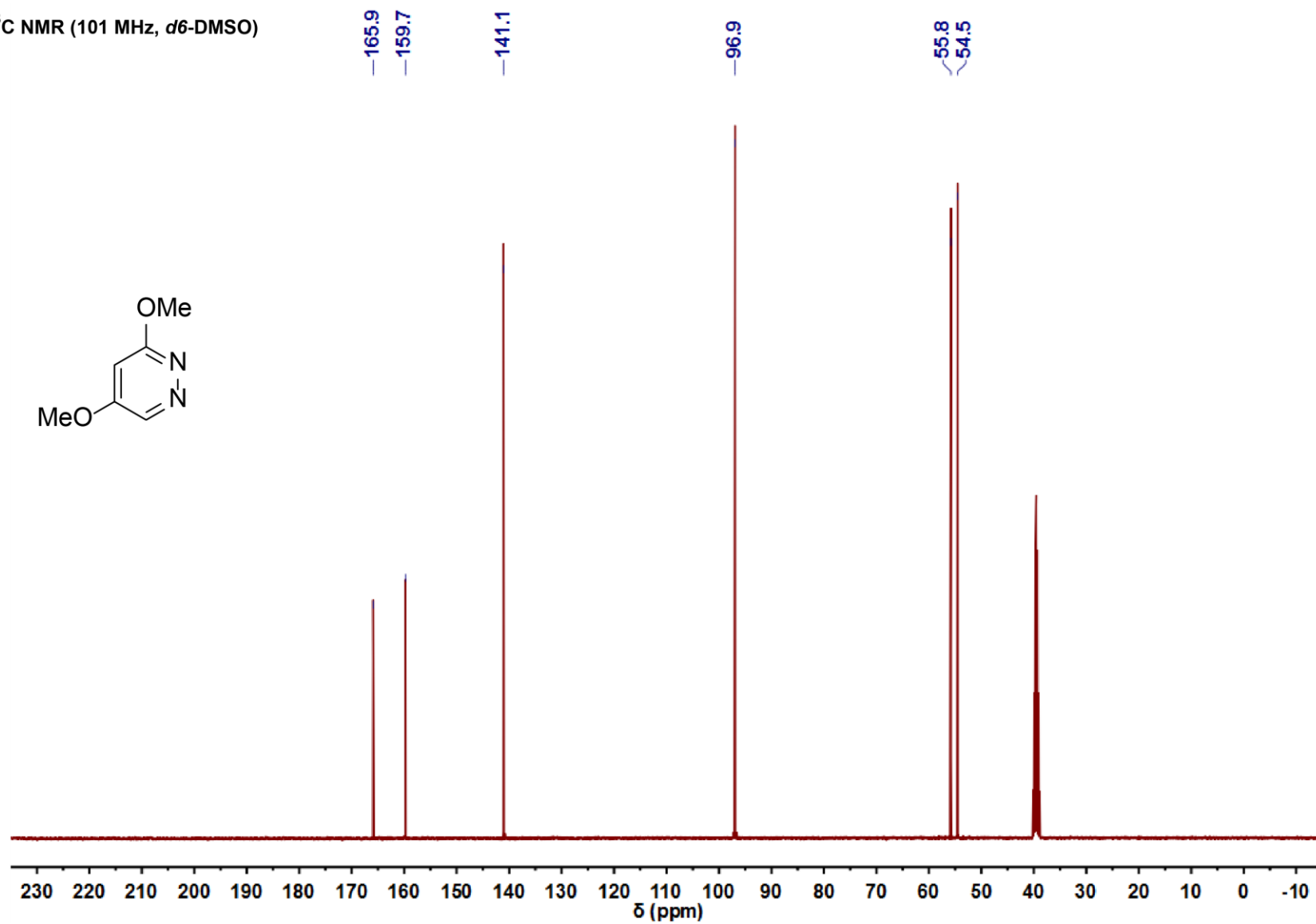
# Energetic Functionalization of the Pyridazine Scaffold: Synthesis and Characterization of 3,5-Diamino-4,6-dinitropyridazine-1-oxide

$^1\text{H}$  NMR (400 MHz,  $d_6$ -DMSO)



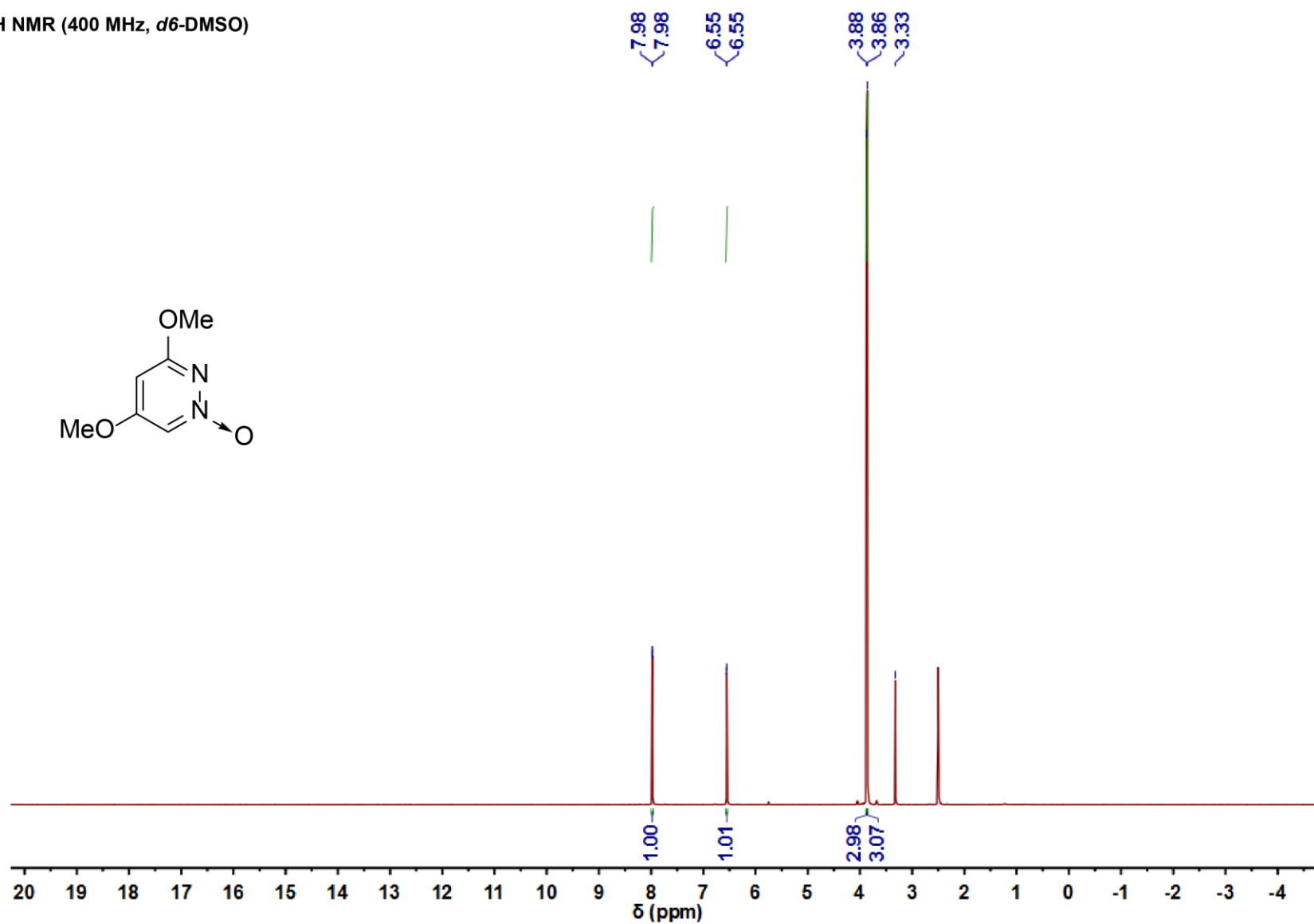
## Energetic Functionalization of the Pyridazine Scaffold: Synthesis and Characterization of 3,5-Diamino-4,6-dinitropyridazine-1-oxide

$^{13}\text{C}$  NMR (101 MHz,  $d_6$ -DMSO)



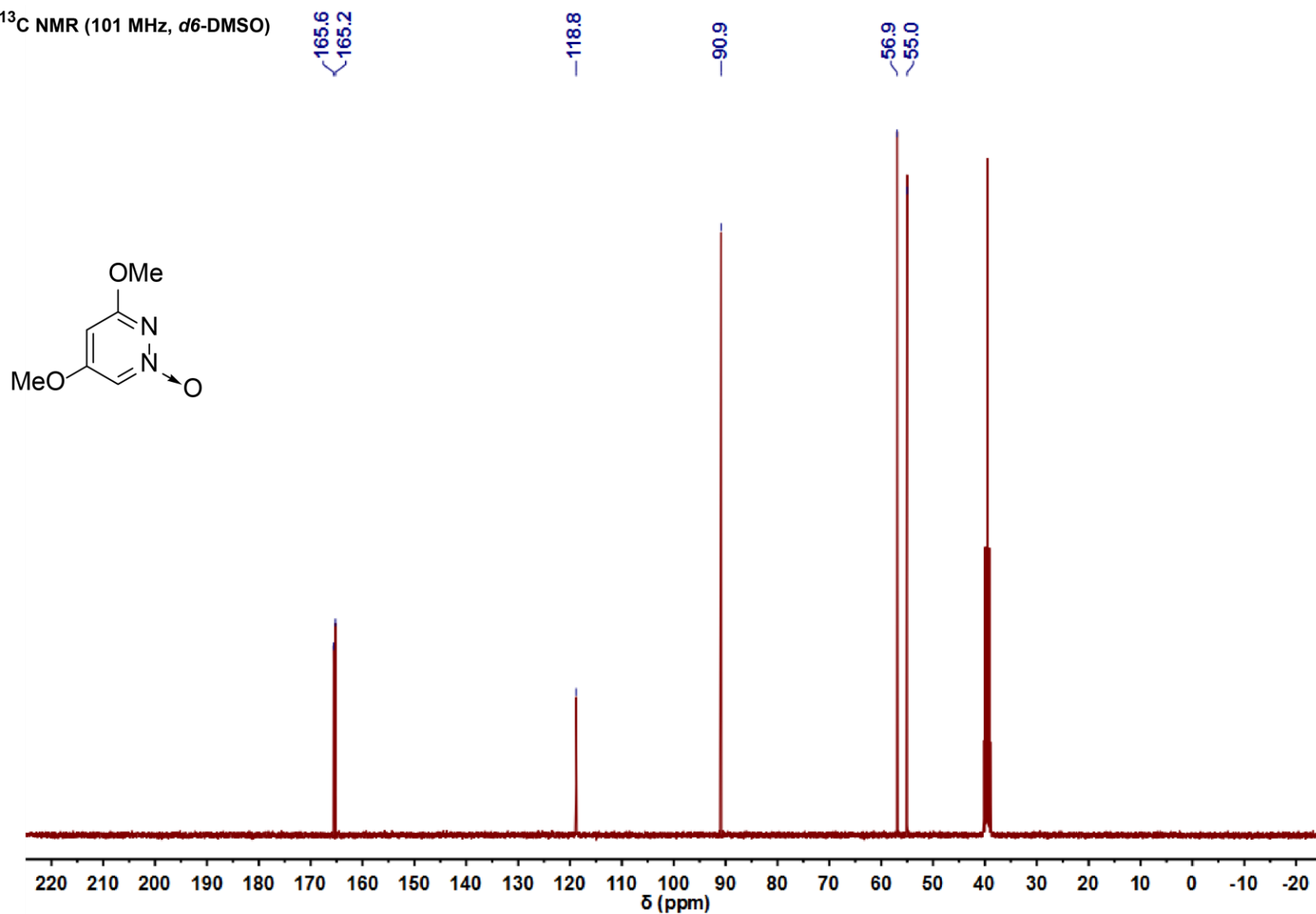
# Energetic Functionalization of the Pyridazine Scaffold: Synthesis and Characterization of 3,5-Diamino-4,6-dinitropyridazine-1-oxide

$^1\text{H}$  NMR (400 MHz,  $d_6$ -DMSO)



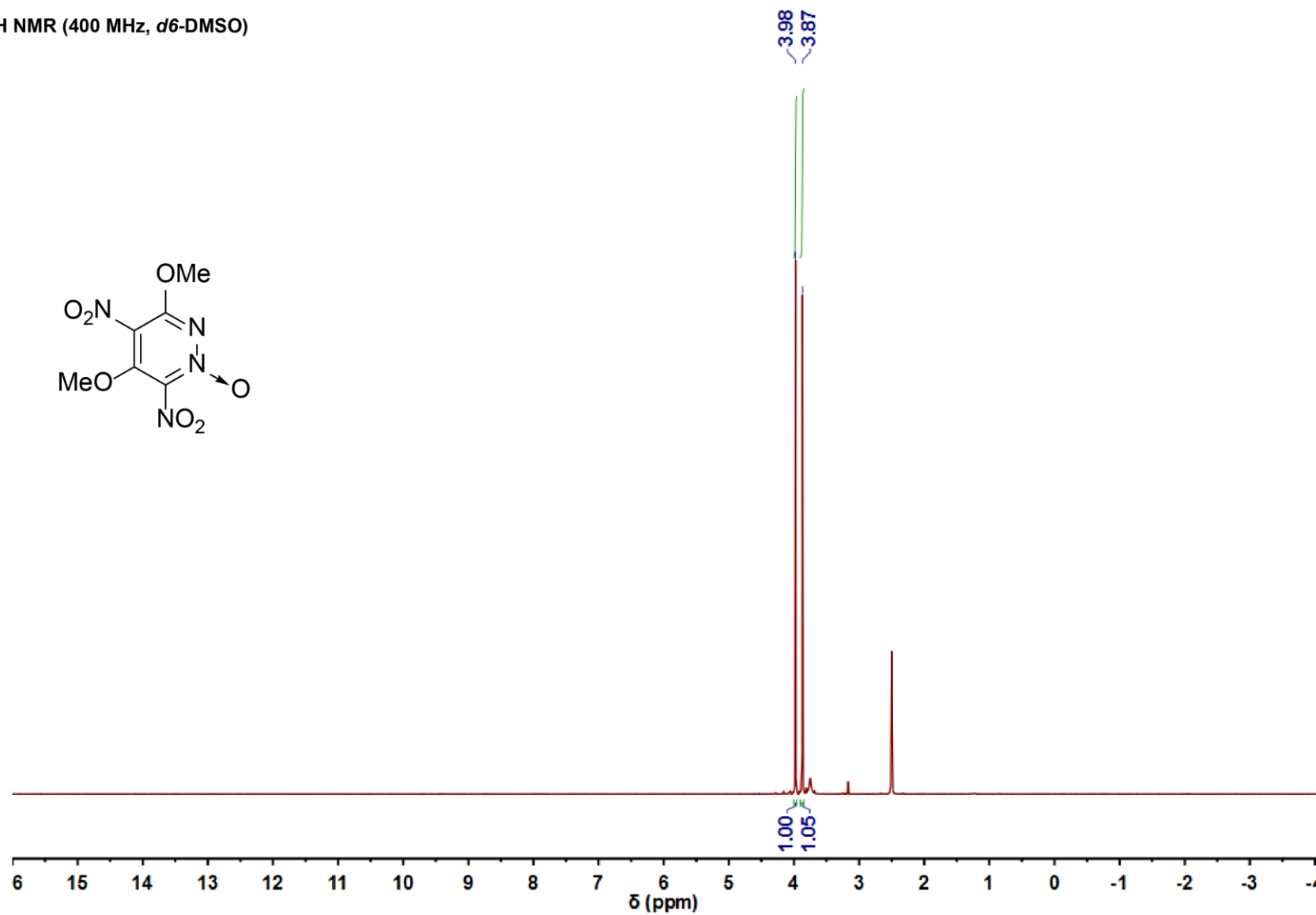
# Energetic Functionalization of the Pyridazine Scaffold: Synthesis and Characterization of 3,5-Diamino-4,6-dinitropyridazine-1-oxide

$^{13}\text{C}$  NMR (101 MHz,  $d_6$ -DMSO)



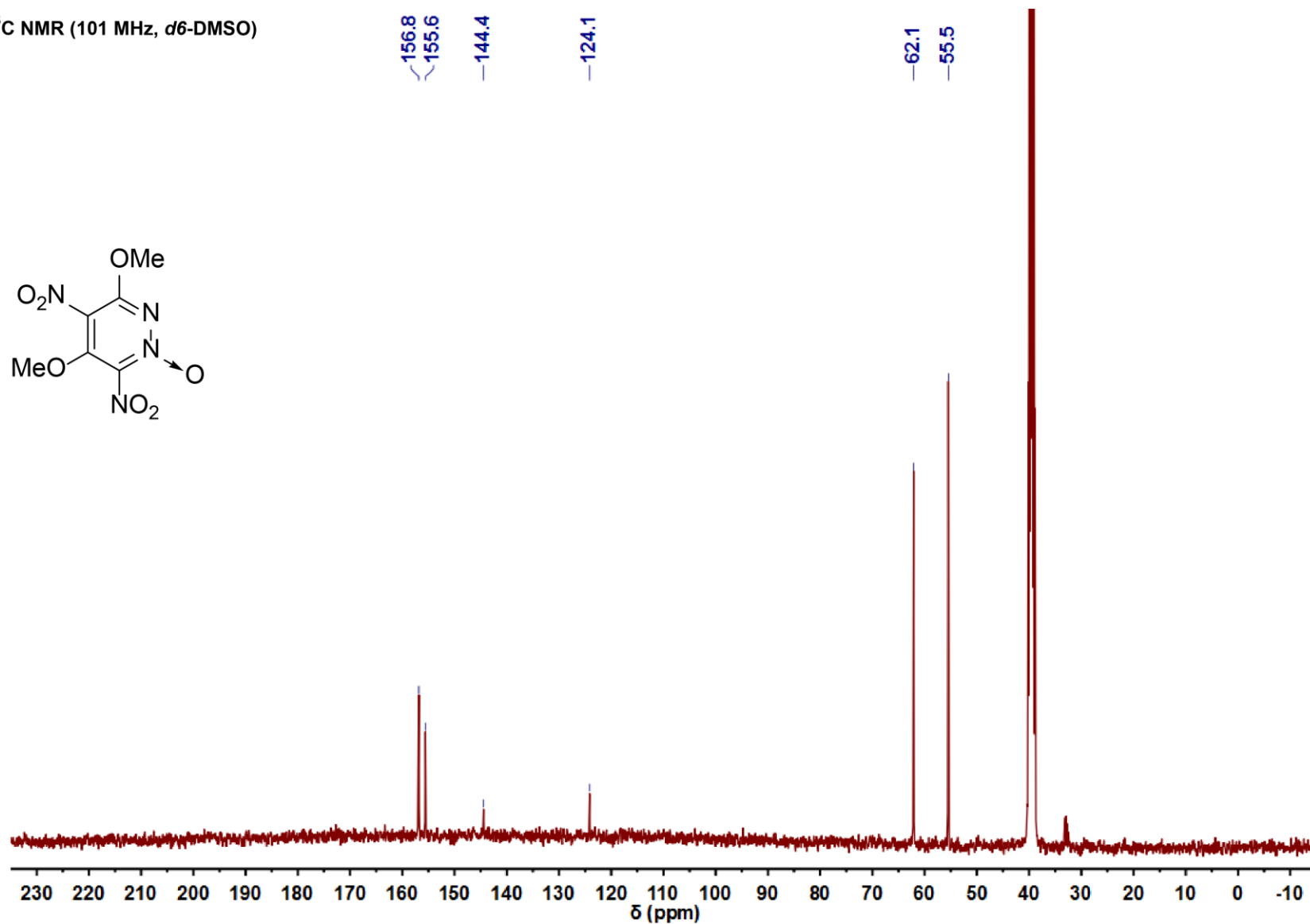
# Energetic Functionalization of the Pyridazine Scaffold: Synthesis and Characterization of 3,5-Diamino-4,6-dinitropyridazine-1-oxide

$^1\text{H}$  NMR (400 MHz,  $d_6$ -DMSO)



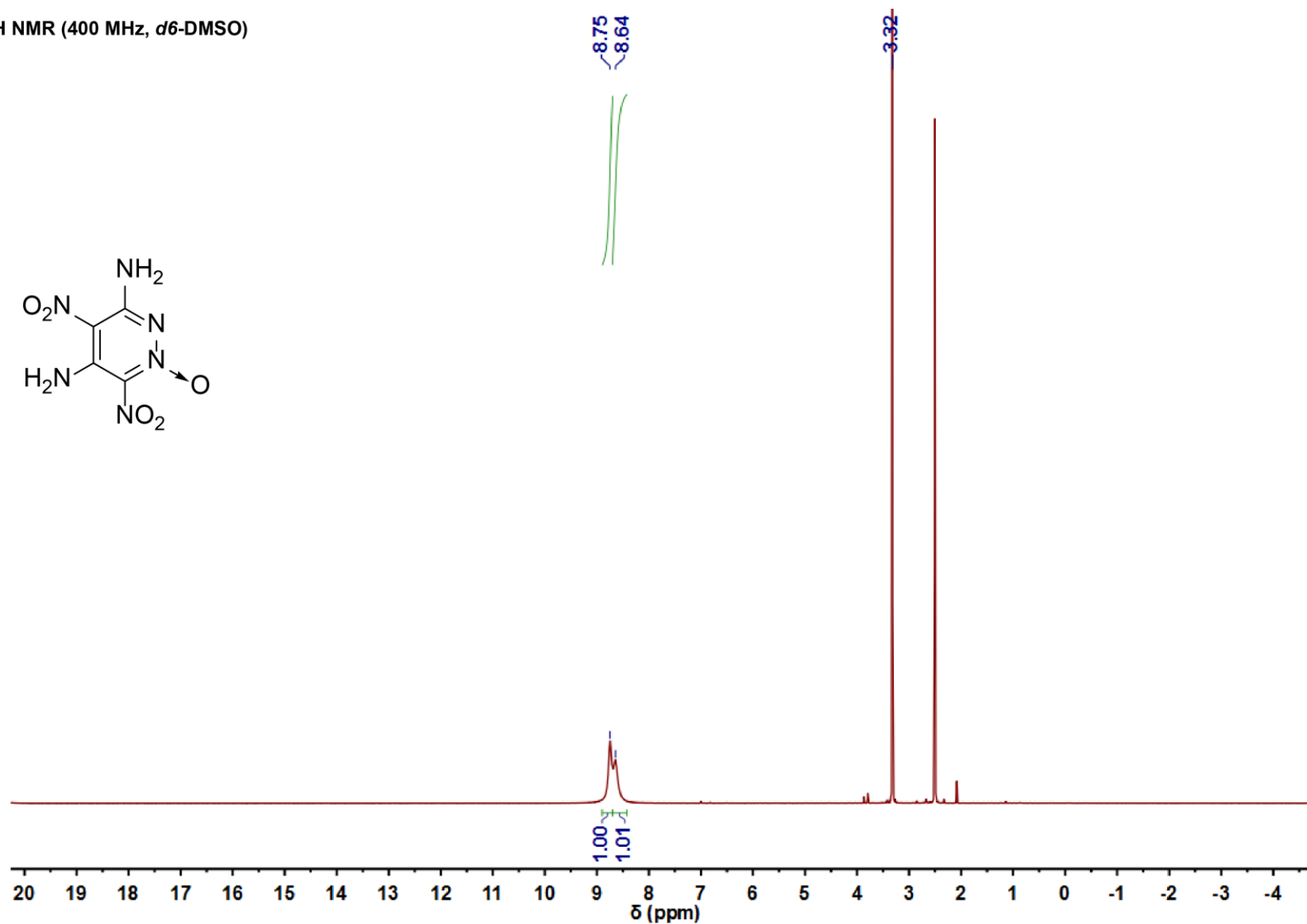
# Energetic Functionalization of the Pyridazine Scaffold: Synthesis and Characterization of 3,5-Diamino-4,6-dinitropyridazine-1-oxide

$^{13}\text{C}$  NMR (101 MHz,  $d_6$ -DMSO)



# Energetic Functionalization of the Pyridazine Scaffold: Synthesis and Characterization of 3,5-Diamino-4,6-dinitropyridazine-1-oxide

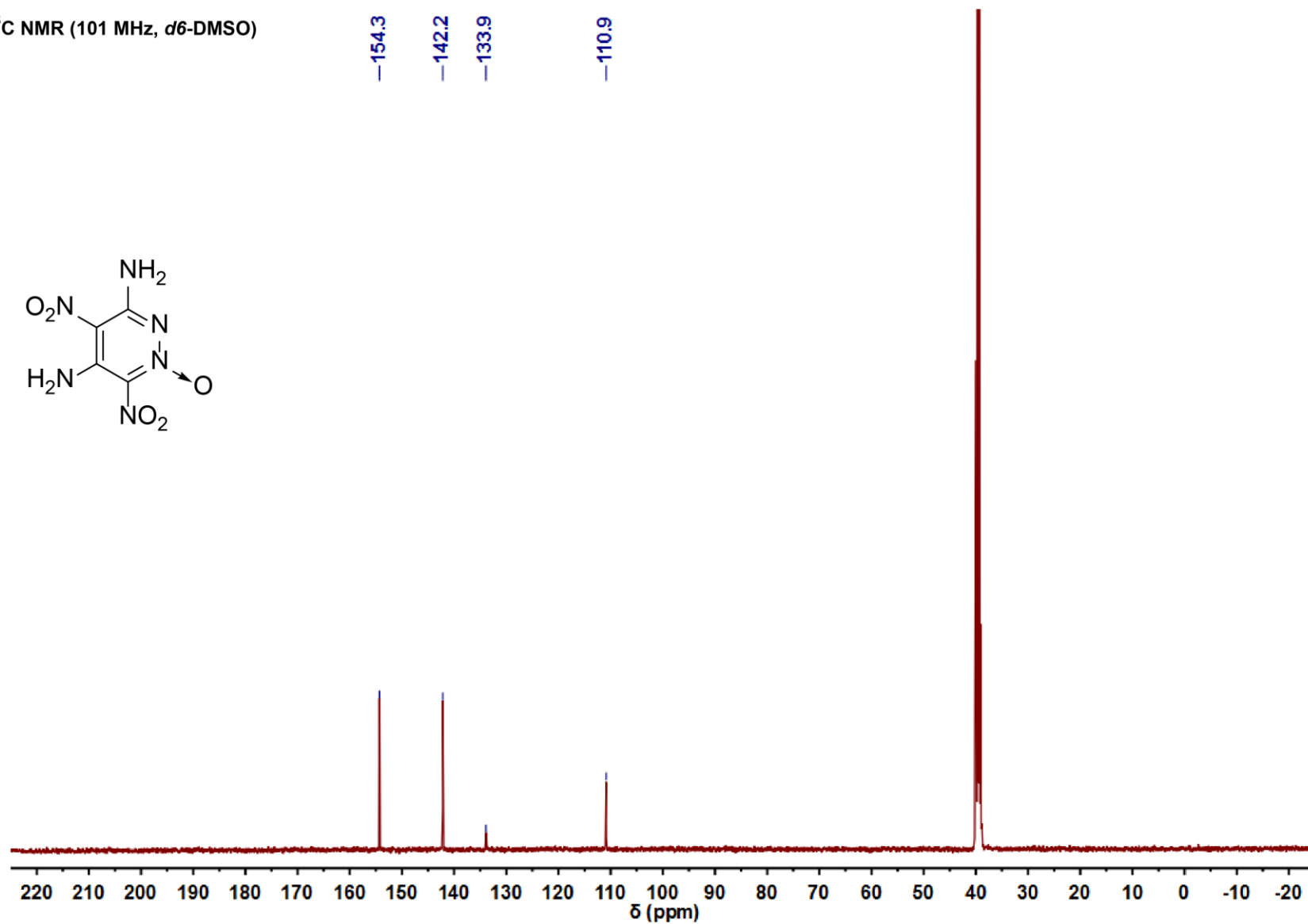
$^1\text{H}$  NMR (400 MHz,  $d_6$ -DMSO)





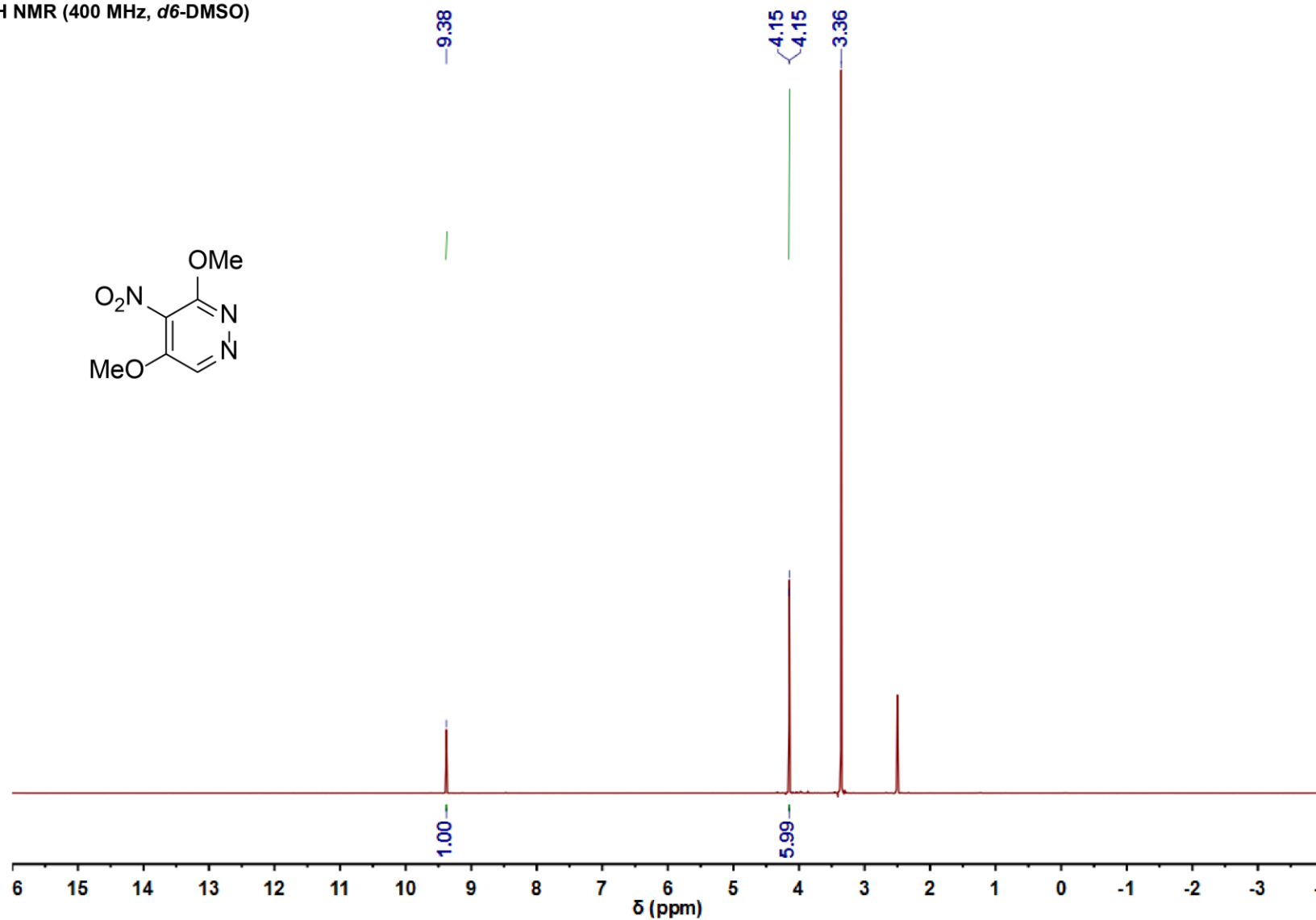
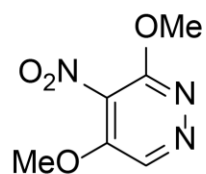
## Energetic Functionalization of the Pyridazine Scaffold: Synthesis and Characterization of 3,5-Diamino-4,6-dinitropyridazine-1-oxide

$^{13}\text{C}$  NMR (101 MHz,  $d_6$ -DMSO)



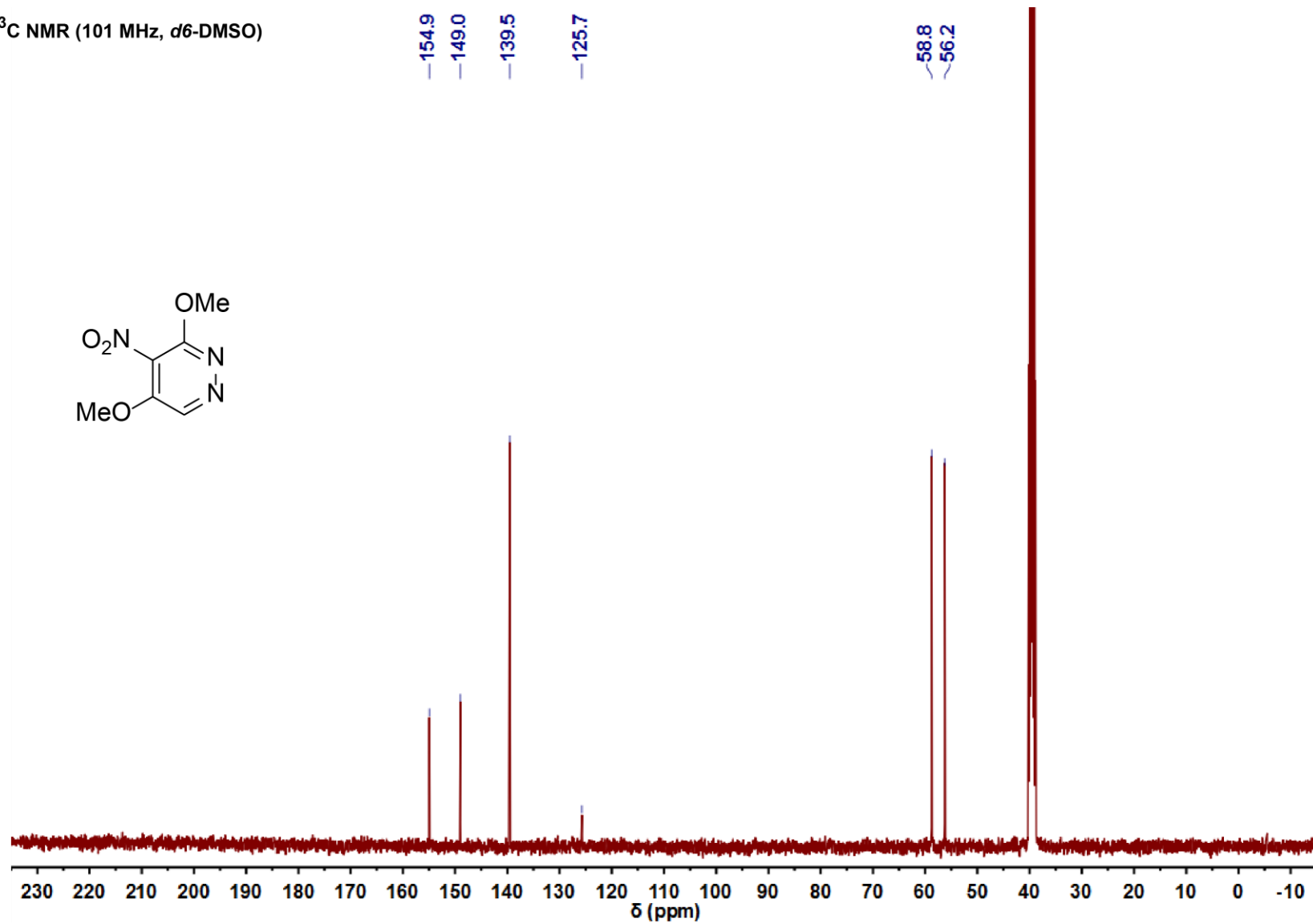
# Energetic Functionalization of the Pyridazine Scaffold: Synthesis and Characterization of 3,5-Diamino-4,6-dinitropyridazine-1-oxide

$^1\text{H}$  NMR (400 MHz,  $d_6$ -DMSO)



## Energetic Functionalization of the Pyridazine Scaffold: Synthesis and Characterization of 3,5-Diamino-4,6-dinitropyridazine-1-oxide

$^{13}\text{C}$  NMR (101 MHz, *d*<sub>6</sub>-DMSO)



#### 4.6.8. References

- [S1] a) W. Deinhammer, M. Wick, Patent DE 19772706701, **1977**. b) G. Lu, F. Liu, X. Sun, F. Qi, Y. Gao, Patent CN 102838548, **2012**.
- [S2] CrysAlisPro, *Oxford Diffraction Ltd. version 171.33.41*, **2009**.
- [S3] CrysAlis RED, *Version 1.171.35.11 (release 16-05-2011 CrysAlis 171.Net)*, Oxford Diffraction Ltd., Abingdon, Oxford (U.K.), **2011**.
- [S4] A. Altomare, M. C. Burla, M. Camalli, G. L. Cascarano, C. Giacovazzo, A. Guagliardi, A. G. G. Moliterni, G. Polidori and R. Spagna, SIR97: A New Tool for Crystal Structure Determination and Refinement, *J. Appl. Crystallogr.*, **1999**, 32, 115–119.
- [S5] G. M. Sheldrick, A Short History of SHELX, *Acta Crystallogr., Sect. A: Found. Crystallogr.*, **2008**, 64, 112–122.
- [S6] L. J. Farrugia, WinGX Suite for Small-Molecule Single-Crystal Crystallography, *J. Appl. Crystallogr.*, **1999**, 32, 837–838.
- [S7] A. L. Spek, *PLATON*, **1999**, A Multipurpose Crystallographic Tool, Utrecht University, The Diffraction Ltd.
- [S8] M. J. Frisch, G. W. Trucks, B. Schlegel, G. E. Scuseria, M. A. Robb, J. R. Cheeseman, G. Scalmani, V. Barone, B. Mennucci, G. A. Petersson, H. Nakatsuji, M. Caricato, X. Li, H.P. Hratchian, A. F. Izmaylov, J. Bloino, G. Zheng, J. L. Sonnenberg, M. Hada, M. Ehara, K. Toyota, R. Fukuda, J. Hasegawa, M. Ishida, T. Nakajima, Y. Honda, O. Kitao, H. Nakai, T. Vreven, J. A. Montgomery, Jr., J. E. Peralta, F. Ogliaro, M. Bearpark, J. J. Heyd, E. Brothers, K. N. Kudin, V. N. Staroverov, R. Kobayashi, J. Normand, K. Raghavachari, A. Rendell, J. C. Burant, S. S. Iyengar, J. Tomasi, M. Cossi, N. Rega, J. M. Millam, M. Klene, J. E. Knox, J. B. Cross, V. Bakken, C. Adamo, J. Jaramillo, R. Gomperts, R. E. Stratmann, O. Yazyev, A. J. Austin, R. Cammi, C. Pomelli, J. W. Ochterski, R. L. Martin, K. Morokuma, V. G. Zakrzewski, G. A. Voth, P. Salvador, J. J. Dannenberg, S. Dapprich, A. D. Daniels, O. Farkas, J.B. Foresman, J. V. Ortiz, J. Cioslowski, D. J. Fox, Gaussian 09 A.02, Gaussian, Inc., Wallingford, CT, USA, **2009**.
- [S9] (a) J. W. Ochterski, G. A. Petersson, and J. A. Montgomery Jr., *J. Chem. Phys.* **1996**, 104, 2598–2619; (b) J. A. Montgomery Jr., M. J. Frisch, J. W. Ochterski, G. A. Petersson, , *J. Chem. Phys.* **2000**, 112, 6532–6542.
- [S10] (a) L. A. Curtiss, K. Raghavachari, P. C. Redfern, J. A. Pople, *J. Chem. Phys.* **1997**, 106, 1063–1079; (b) E. F. C. Byrd, B. M. Rice, *J. Phys. Chem. A* **2006**, 110, 1005–1013; (c) B. M. Rice, S. V. Pai, *Comb. Flame* **1999**, 118, 445–458.
- [S11] P. J. Linstrom, W. G. Mallard, *National Institute of Standards and Technology*, Gaithersburg MD, 20899.

## Energetic Functionalization of the Pyridazine Scaffold: Synthesis and Characterization of 3,5-Diamino-4,6-dinitropyridazine-1-oxide

[S12] a) F. Trouton, *Philos. Mag. (1876-1900)* **1884**, 18, 54-57; b) M. S. Westwell, M. S. Searle, D. J. Wales, D. H. Williams, *J. Am. Chem. Soc.* **1995**, 117, 5013-5015.

[S13] M. Sućeska, *EXPLO5 Version 6.03 User's Guide*, Zagreb, Croatia: OZM; **2015**.

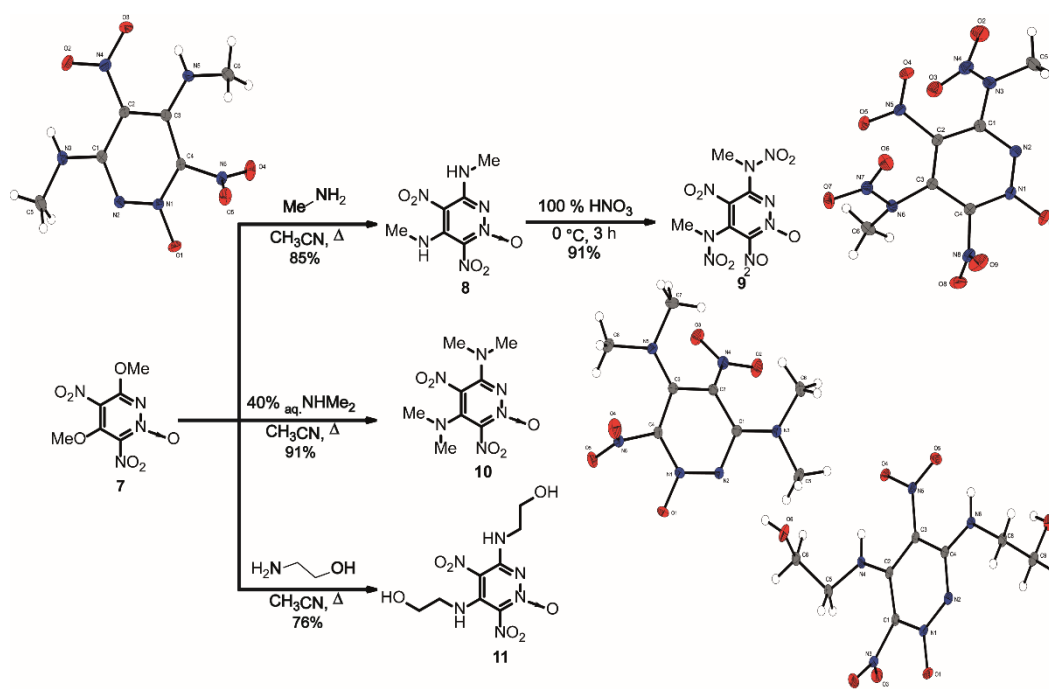
[S14] a) R. Meyer, J. Köhler, A. Homburg, *Explosives*, 6th edn., Wiley, Weinheim, **2007**, p. 291-292; b) T. M. Klapötke, *Chemistry of High-Energy Materials*, Walter de Gruyter, Berlin, **2015**;

## 5. The Pyridazine Scaffold as a Building Block for Energetic Materials: Synthesis, Characterization and Properties

Ivan Gospodinov, Johannes Singer, Thomas M. Klapötke and Jörg Stierstorfer

Published in *Z. Anorg. Allg. Chem.* **2019**, 645, 1–9.

DOI: 10.1002/zaac.201900146



**Abstract:** In the present studies, the synthesis of new energetic materials based on the pyridazine scaffold and their characterization is the main subject. For this purpose, literature known 3,5-dimethoxy-4,6-dinitropyridazine-1-oxide (**7**) was synthesized in the first instance. The persubstituted pyridazine precursor laid the groundwork for further preparative modification. The targeted functionalization through the regioselective introduction of various smaller amine nucleophiles such as methylamine or 2-aminoethanol gave several new energetic materials. Among them are 3,5-bis(methylamino)-4,6-dinitropyridazine-1-oxide (**8**), 3,5-bis(methylnitramino)-4,6-dinitropyridazine-1-oxide (**9**), 3,5-bis(dimethylamino)-4,6-dinitropyridazine-1-oxide (**10**) and 3,5-bis((2-hydroxyethyl)amino)-4,6-dinitropyridazine-1-oxide (**11**). With the aim of increasing the detonation performance, compound **8** was additionally nitrated and 3,5-bis(methylnitramino)-4,6-dinitropyridazine-1-oxide (**9**) was obtained. These new energetic materials were characterized and identified by multi-nuclear NMR ( $^1\text{H}$ ,  $^{13}\text{C}$ ,  $^{14}\text{N}$ ,  $^{15}\text{N}$ ) and IR spectroscopy, elemental analysis and mass spectrometry. In addition, their sensitivities

towards impact, friction and electrostatic discharge were thoroughly examined. Furthermore, obtained single-crystals of the substances were characterized by low-temperature single-crystal X-ray diffraction.

## **5.1. Introduction**

During the last decades, extensive work and efforts have been made to discover highly efficient and performing new energetic materials with high thermal stability and good sensitivities toward accidental stimuli.<sup>[1]</sup> In addition, the production of new environmental benign energetic materials is desired process, due to the fact that mostly of the nowadays synthesized HEDM (RDX, TATB and TNT) are either carcinogenic or toxic.<sup>[2]</sup> For this purpose scientists worldwide have been developing modern approaches for the synthesis of new energetic materials. An emerging approach is the use of polyfunctionalized nitrogen-rich heterocycles as a building block for new materials. In several instances, azole and diazine based energetic materials have been found to have promising physico-chemical properties *e.g.* 3,4,5-trinitropyrazole,<sup>[3]</sup> bis(4-amino-3,5-dinitropyrazolyl)-methane<sup>[4]</sup> and 2,6-diamino-3,5-dinitropyrazine-1-oxide (LLM-105).<sup>[5]</sup> It appears that the combination of nitrogen-rich heterocycles with an alternating C–NH<sub>2</sub>/ C–NO<sub>2</sub> and N<sup>+</sup>–O<sup>−</sup> moiety results in the formation of thermally stable, insensitive materials with good detonation parameters. The introduction of an N<sup>+</sup>–O<sup>−</sup> moiety to the energetic materials results in an increase of the density,<sup>[6]</sup> improves the oxygen balance<sup>[7]</sup>, increases the stability in the molecular structure<sup>[8]</sup> and in addition improves the detonation properties.<sup>[9]</sup> Good examples for this class of *N*-oxidized energetic materials are dihydroxylammonium 5,5'-bistetrazole-1,1'-diolate (TKX-50) and 2,6-diamino-3,5-dinitropyrazine-1-oxide (LLM-105). In comparison to its O-free analogue, dihydroxylammonium 5,5'-bistetrazolate, the density of TKX-50 increases from 1.74 to 1.88 g cm<sup>−3</sup>, and its calculated detonation velocity increases from 8854 m s<sup>−1</sup> to 9698 m s<sup>−1</sup>.<sup>[10,11]</sup> The same effect is observed with LLM-105 ( $\rho = 1.92 \text{ g cm}^{-3}$ ,  $D_{C-J} = 8516 \text{ m s}^{-1}$ ) and its precursor 2,6-diamino-3,5-dinitropyrazine (ANPZ,  $\rho = 1.84 \text{ g cm}^{-3}$ ,  $D_{C-J} = 7892 \text{ m s}^{-1}$ ).<sup>[7,12]</sup>

## The Pyridazine Scaffold as a Building Block for Energetic Materials: Synthesis, Characterization and Properties

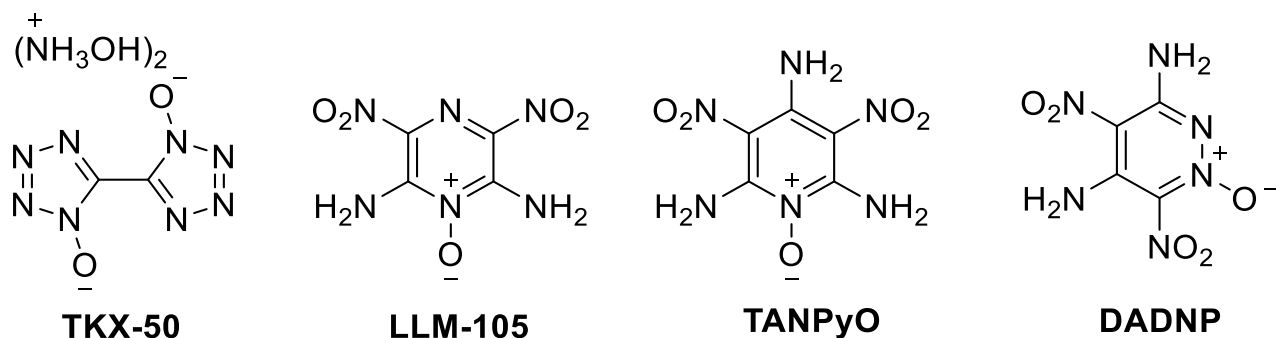


**Figure 1.** Literature known *N*-oxidized energetic materials.

Recently, in our research group we managed to functionalize the 1,2-diazine scaffold by synthesizing 3,5-diamino-4,6-dinitropyridazine-1-oxide and its precursor 3,5-dimethoxy-4,6-dinitropyridazine-1-oxide.<sup>[13]</sup> For this purpose, a selective functionalization of the pyridazine scaffold was carried out by introducing explosophore NO<sub>2</sub> groups and selectively introducing an N<sup>+</sup>–O<sup>–</sup> moiety. In this present work we reacted 3,5-dimethoxy-4,6-dinitropyridazine-1-oxide (**7**) with different amines and investigated the physico-chemical properties of the newly synthesized derivatives **8–11**. The detonation properties and the sensitivities of the energetic pyridazines can be adjusted depending on the used amine for the reaction.

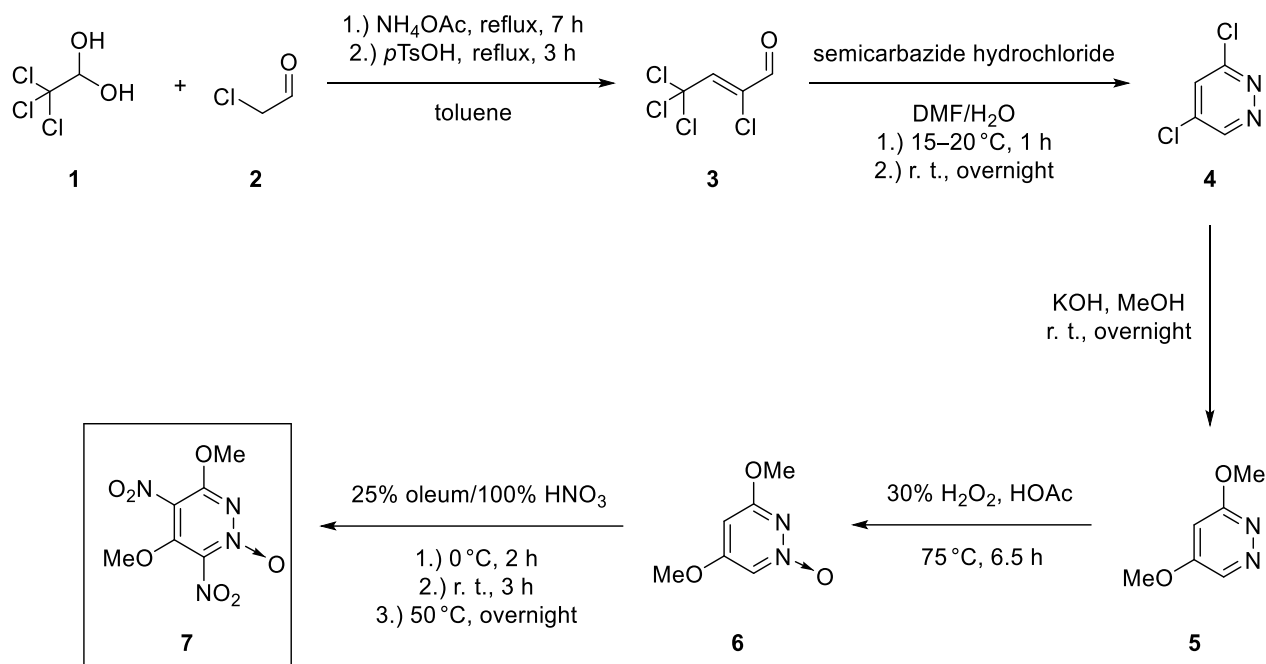
## 5.2. Results and Discussion

### 5.2.1. Synthesis

Herein, we report the synthesis of new pyridazine based energetic materials. The target molecules 3,5-bis(methylamino)-4,6-dinitropyridazine-1-oxide (**8**), 3,5-bis(methylnitramino)-4,6-dinitropyridazine-1-oxide (**9**), 3,5-bis(dimethylamino)-4,6-dinitropyridazine-1-oxide (**10**) and 3,5-bis((2-hydroxyethyl)amino)-4,6-dinitropyridazine-1-oxide (**11**) were synthesized by using 3,5-dimethoxy-4,6-dinitropyridazine-1-oxide (**7**) as starting material. Compound **7** was prepared according the literature known five step procedure and will not be discussed in this work.<sup>[13]</sup> The exact synthetic path for **7** is shown in **Scheme 1**.



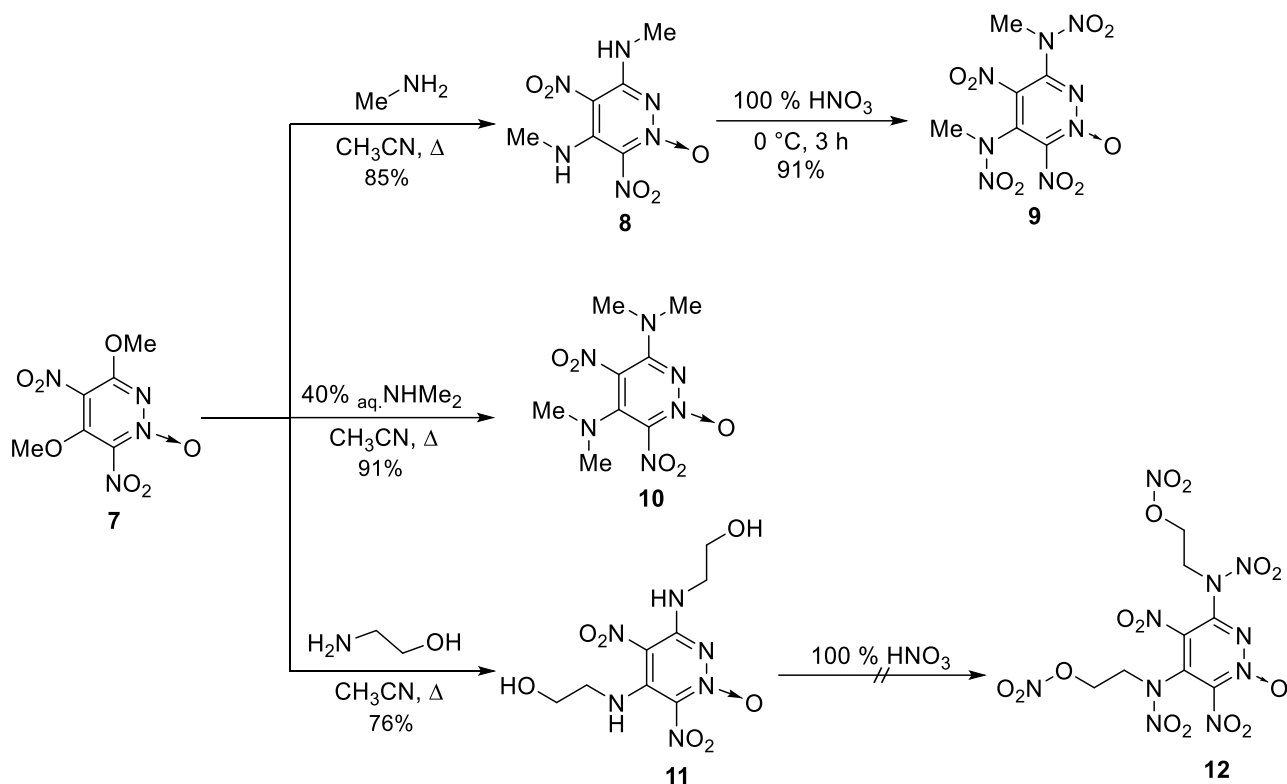
## The Pyridazine Scaffold as a Building Block for Energetic Materials: Synthesis, Characterization and Properties



**Scheme 1.** Literature known synthesis for 3,5-dimethoxy-4,6-dinitropyridazine-1-oxide.

Compound **7** was used as the starting material for further functionalization of the pyridazine scaffold. Further nucleophilic substitution of the methoxy groups allows regioselective functionalization of compound **7**. As appropriate nucleophiles various smaller amines *e.g.* methylamine, dimethylamine and 2-aminoethanol were reacted with compound **7**. Compounds **8–11** were obtained in good yields 76–91 %. To enhance the performance of the newly synthesized pyridazine based energetic materials compounds **8** and **11** were further nitrated. Nitration of compound **8** resulted in the formation of 3,5-bis(methylnitramino)-4,6-dinitropyridazine-1-oxide (**9**) in 91 % yield. Nitration of compound **11** resulted in decomposition of the starting material and the polynitrated compounds **12** was not obtained. All obtained energetic materials were thoroughly characterized and further examined regarding their sensitivities toward mechanical and electrostatic stimuli. All reactions are displayed in **Scheme 2**.

## The Pyridazine Scaffold as a Building Block for Energetic Materials: Synthesis, Characterization and Properties



**Scheme 2.** Synthesis of new energetic pyridazine derivatives by functionalizing the 3,5-dimethoxy-4,6-dinitropyridazine-1-oxide scaffold (**7**).

### 5.2.2. Crystal structures

During this work the crystal structures of all four synthesized compounds (**8–11**) were obtained. Selected data and parameters from the low-temperature X-ray data collection are given in the Supporting Information (Tables S1 and S2). Single-crystals of compound **8** were obtained by evaporating a solution of **8** in acetone and water. Compound **8** crystallizes in the orthorhombic space group  $Pbca$  (no. 61) with eight formula units per cell and has a cell volume of  $1941.40(7) \text{ \AA}^3$ . The cell constants are  $a = 9.7734(2) \text{ \AA}$ ,  $b = 13.5583(3) \text{ \AA}$  and  $c = 14.6509(3) \text{ \AA}$ . The calculated density at  $143(2) \text{ K}$  is  $1.67 \text{ g cm}^{-3}$ . Looking at the determined bond lengths  $1.3276(18) \text{ \AA}$  (N1–N2),  $1.3506(19) \text{ \AA}$  (C4–N1),  $1.352(2) \text{ \AA}$  (N2–C1),  $1.432(2) \text{ \AA}$  (C1–C2),  $1.433(2) \text{ \AA}$  (C2–C3) and  $1.412(2) \text{ \AA}$  (C3–C4), the existing aromaticity inside the ring structure can be comprehended (**Figure 2**). They are all between the typical values for single and double bonds concerning these involved elements.<sup>[14,15,16]</sup> The interatomic distances of N3–C1 ( $1.329 \text{ \AA}$ ) and N5–C3 ( $1.332(2) \text{ \AA}$ ) also display a participation of these bonds in aromatic resonance. The bond in the  $\text{N}^+-\text{O}^-$  moiety is  $1.2635(17) \text{ \AA}$  and herewith slightly shorter than that of its precursor 3,5-dimethoxy-4,6-dinitropyridazine-1-oxide (**7**) with  $1.268(2) \text{ \AA}$ .<sup>[13]</sup> The slight deformation of the planar ring structure can be recognized by the observed divergent dihedral angles  $4.5(2)^\circ$  (N1–N2–C1–C2) and  $-6.6(2)^\circ$  (N2–C1–C2–C3). The C4-connected nitro group is twisted against the ring plane

## The Pyridazine Scaffold as a Building Block for Energetic Materials: Synthesis, Characterization and Properties

according to the O5–N6–C4–N1 torsions angle of  $-74.69(18)^\circ$ . Its significant rotation can be understood by both the high spatial demand of the voluminous methylamine neighbor, which even shows only a moderate displacement regarding the ring plane, and especially the high electrostatic repulsion between the vicinal-located  $N^+-O^-$  moiety and the nitro-oxygens. As a result of its noticeable turn, the C4–N6 bond length of  $1.4637(19)$  Å is elongated compared that of the other intramolecular nitro group with  $1.4157(19)$  Å.

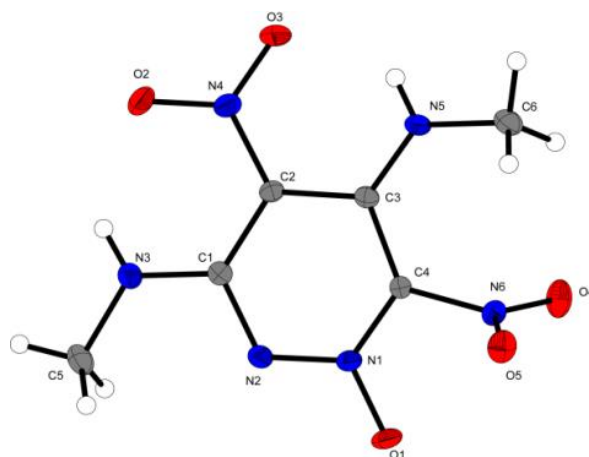


**Figure 2.** Molecular unit of compound **8** in the crystalline state. Ellipsoids correspond to 50% probability levels. Hydrogen radii are arbitrary. Selected bond lengths reported in [Å] and angles reported in [°]: N1–N2 1.3276(18), C4–N1 1.3506(19), N2–C1 1.352(2), C1–C2 1.432(2), C2–C3 1.433(2), C3–C4 1.412(2), O1–N1 1.2635(17), N3–C1 1.329(2), N5–C3 1.332(2), N4–C2 1.4157(19), O2–N4 1.2401(19), N6–C4 1.4637(19), O4–N6 1.2229(18), N2–N1–C4 123.90(13), N1–C4–N6 111.94(13), O1–N1–N2–C1  $-177.94(14)$  N1–N2–C1–C2 4.5(2), N2–C1–C2–C3  $-6.6(2)$ , C2–C3–C4–N1 2.7(2), C5–N3–C1–N2  $-2.6(2)$ , C6–N5–C3–C4  $-9.1(3)$ , O2–N4–C2–C1 12.6(2), N5–C3–C4–N6  $-0.2(2)$ , O5–N6–C4–N1  $-74.69(18)$ .

Single-crystals for **9** were obtained by evaporating a solution of compound **9** in a mixture of acetone and water. Compound **9** crystallizes in the orthorhombic space group  $P 2_1 2_1 2_1$  (*no. 16*) with four formula units per cell and has a cell volume of  $1287.01(10)$  Å<sup>3</sup>. The cell constants are  $a = 6.6245(3)$  Å,  $b = 10.1031(5)$  Å and  $c = 19.2297(8)$  Å. The calculated density at 143(2) K is  $1.73$  g cm<sup>-3</sup>, which is higher than the density of its precursor **8** with  $1.67$  g cm<sup>-3</sup>.

## The Pyridazine Scaffold as a Building Block for Energetic Materials: Synthesis, Characterization and Properties

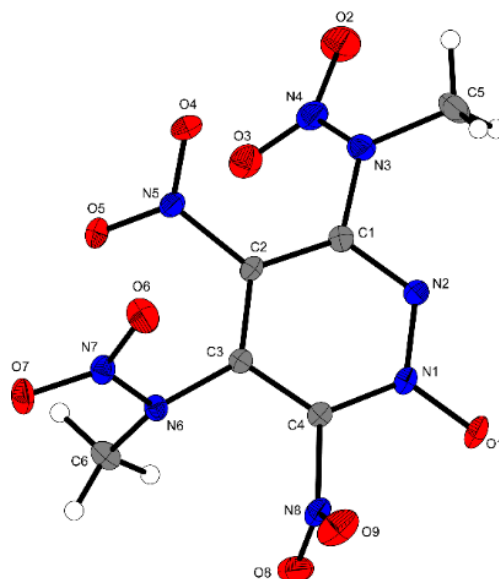


**Figure 3.** Molecular unit of compound **9** in the crystalline state. Ellipsoids correspond to 50% probability levels. Hydrogen radii are arbitrary. Selected bond lengths reported in [Å] and angles reported in [°]: N1–N2 1.335(2), C4–N1 1.358(2), N2–C1 1.325(2), C1–C2 1.399(3), C2–C3 1.384(3), C4–C3 1.372(2), O1–N1 1.2561(17), N3–C1 1.403(2), N3–N4 1.408(3), N4–O2 1.215(2), N3–C5 1.462(3), N5–C2 1.465(2), O4–N5 1.221(2), N6–C3 1.417(2), N6–N7 1.385(2), C4–N8 1.459(2), O1–N1–N2 118.26(15), N2–C1–N3 112.77(16), N2–C1–C2 124.01(18), N4–N3–C5 116.68(18), N1–N2–C1–C2 –0.1(3), N2–C1–C2–C3 –2.7(3), C1–C2–C3–C4 3.4(2), C5–N3–C1–N2 –26.0(2), C5–N3–N4–O2 –17.0(3), N3–C1–C2–N5 –5.4(3), O4–N5–C2–C1 –40.3(2), N5–C2–C3–N6 9.4(3), N7–N6–C3–C2 –58.0(2), C3–N6–N7–O6 –17.2(2), N8–C4–N1–O1 1.9(2), C3–C4–N8–O8 81.8(2).

The N–O distance 1.2561(17) Å in the N<sup>+</sup>–O<sup>–</sup> moiety is distinctly shortened compared to those values found in precursor **8** (1.2635(17) Å) and related 3,5-diamino-4,6-dinitropyridazine-1-oxide (1.2681(19) Å).<sup>[13]</sup> These differences in length can be understood by comparing the mesomeric impacts of the different amino substituents to the aromatic system in each compound. With increasing the degree of substitution regarding the amino substituents their +M character is diminished. In consequence, the less electron density inside the aromatic ring causes the observed bond contractions. In molecule **9** this effect attains an extra dimension due to the nitration of the respective amino substituents because of the strong electron-withdrawing nitro groups. In contrast, the N–N distances in the pyridazine ring structure show an opposing trend. The N–N bond lengths in DADNP with 1.323(2) Å and compound **8** 1.3276(18) Å are shorter than that found in pyridazine **9** with 1.335(2) Å (N1–N2).<sup>[13]</sup> All remaining N–C and C–C bonds in the ring are with slightly divergence to each other in the aromatic range.<sup>[14,15,16]</sup> The ring-internal dihedral angles such as C1–C2–C3–C4 with 3.4(2)° and N2–C1–C2–C3 with –2.7(3)° show only slight aberration. This reflects the high planarity of the aromatic backbone. The nitro groups

## The Pyridazine Scaffold as a Building Block for Energetic Materials: Synthesis, Characterization and Properties

connected to the backbone exhibit different amounts of rotation against the ring plane according to the torsions angles O4–N5–C2–C1 with  $-40.3(2)^\circ$  and C3–C4–N8–O8 with even  $81.8(2)^\circ$ . The eminently twist of latter substituent, which is surprisingly near to  $90^\circ$ , restricts the  $p_z$ -orbital of the N8-nitrogen to participate in aromaticity because of the slim  $\pi$ -overlap. In further consequence, the considerable elongation of the interatomic distance between N8 and C4 results. In its precursor **8** the bond length of the analogous nitro group is  $1.4157(19)$  Å with a twist of  $-74.69(18)^\circ$ . In comparison, this bond in pyridazine derivative **9** is  $1.459(2)$  Å and thus slightly elongated. The dihedral angles for the tertiary amino substituents are  $-58.0(2)^\circ$  (N7–N6–C3–C2) and  $-26.0(2)^\circ$  (C5–N3–C1–N2). The distances of the N3–N4 and N5–N6 bonds in the nitramine moieties are  $1.408(3)$  Å and  $1.385(2)$  Å, respectively. The bond angle  $123.21(17)^\circ$  included from C2–C1–N3 is somewhat widened, while the adjacent N2–C1–N3 bond angle with  $112.77(16)^\circ$  is noticeably compressed (**Figure 3**).

Single-crystals from compound **10** were obtained by evaporating a solution of **10** in acetone and water. Compound **10** crystallizes in the monoclinic space group  $P 2_1/c$  (*no. 14*) with four formula units per cell and has a cell volume of  $1144.00(8)$  Å<sup>3</sup>. The cell constants are  $a = 9.7162(4)$  Å,  $b = 13.6057(5)$  Å and  $c = 8.7037(4)$  Å with  $\beta = 96.137(4)^\circ$ . The calculated density at  $143(2)$  K is  $1.58$  g cm<sup>-3</sup>.

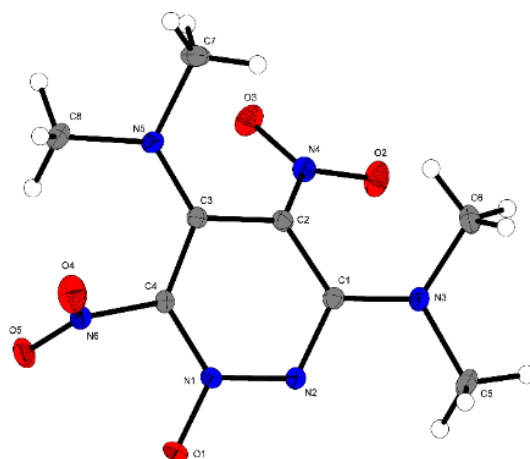


**Figure 4.** Molecular unit of compound **10** in the crystalline state. Ellipsoids correspond to 50% probability levels. Hydrogen radii are arbitrary. Selected bond lengths reported in [Å] and angles reported in [°]: N1–N2  $1.3289(17)$ , N1–C4  $1.3645(18)$ , N2–C1  $1.3553(18)$ , C1–C2  $1.4408(19)$ , C2–C3  $1.432(2)$ , C3–C4  $1.4057(19)$ , O1–N1  $1.2577(15)$ , N3–C1  $1.3238(19)$ , N3–C5  $1.4717(19)$ , N4–C2  $1.4234(18)$ , O2–N4  $1.2403(17)$ , O4–N6  $1.2215(17)$ , N5–C7  $1.4611(19)$ , N1–N2–C1  $116.76(12)$ , C4–C3–C2  $113.49(12)$ , O1–N1–N2  $117.12(11)$ , C1–N3–C5  $120.74(13)$ , C6–N3–C5  $115.07(13)$ , C7–N5–C8  $113.46(12)$ , N1–N2–C1–C2  $-14.7(2)$ , N2–C1–C2–C3, C1–C2–C3–C4  $-19.07(19)$ , N2–C1–C2–C3  $28.2(2)$ , N1–N2–C1–N3  $166.97(13)$ , C5–N3–C1–N2  $5.0(2)$ , N3–C1–C2–N4  $50.1(2)$ , O2–N4–C2–C1  $-17.9(2)$ , C7–N5–C3–C2  $-21.6(2)$ , N5–C3–C4–N6  $-2.5(2)$ , O4–N6–C4–C3  $-71.22(19)$ .

## The Pyridazine Scaffold as a Building Block for Energetic Materials: Synthesis, Characterization and Properties

Compared to 3,5-diamino-4,6-dinitropyridazine-1-oxide (**DADNP**) with  $1.89 \text{ g cm}^{-3}$  and related 3,5-bis(methylamino)-4,6-dinitropyridazine-1-oxide (**8**) with  $1.67 \text{ g cm}^{-3}$  its crystal-structure is clearly less dense.<sup>[13]</sup> The N–N bond length in the pyridazine ring is  $1.3289(17) \text{ \AA}$  (**Figure 4**). The ring-internal N–C bonds are  $1.3645(18) \text{ \AA}$  and  $1.3553(18) \text{ \AA}$  and the remaining C–C distances are  $1.426 \text{ \AA}$  on average. These length values are all in the aromatic range and show no significant difference to the bonds inside the pyridazine ring of **8**.<sup>[13,14,15,16]</sup> Indeed, despite the existing aromaticity the expected flat pyridazine ring is drastically deformed. The C1–C2–C3–C4 and N2–C1–C2–C3 torsions angles aberrate from the ring plane with  $-19.07(19)^\circ$  and even  $28.2(2)^\circ$ , respectively. Compared to the dihedral angles C1–C2–C3–C4 with  $2.8(2)^\circ$  and N2–C1–C2–C3  $-6.6(2)^\circ$ , the aberration of planarity found for related **8** is eminently smaller. Also, the ring-internal bond angles diverge from the regular angle of  $120^\circ$  for  $sp^2$ -hybridized bond centers. Among them is the C4–C3–C2 bond angle with the divergence of  $6.5^\circ$ . The bond length between the nitrogen and oxygen inside the  $\text{N}^+\text{--O}^-$  function is  $1.2577(15) \text{ \AA}$  (N1–O1). In comparison, this N–O distance is markedly shorter than those found in precursor **7** ( $1.268(2) \text{ \AA}$ ), 3,5-diamino-4,6-dinitropyridazine-1-oxide ( $1.2681(19) \text{ \AA}$ , **DADNP**) and even 3,5-bis(methylamino)-4,6-dinitropyridazine-1-oxide (**8**,  $1.2635(17) \text{ \AA}$ ).<sup>[13]</sup> Besides, the N–C bonds connecting the spatially demanding dimethylamino substituents to the molecular backbone of **10** have no significant difference. Against this, the amount of rotation noticeably differs. The dimethylamino substituent connected to the C1-carbon shows only a slight turn against the ring plane, whereas the other one in between of both nitro groups is significantly more rotated against the plane according to the C7–N5–C3–C2 torsions angle of  $-21.6(2)^\circ$ . The medium length of the four bonds between the methyl groups and the tertiary substituted amino groups is  $1.463 \text{ \AA}$ , which is in the typical range for N–C single bonds.<sup>[14]</sup> Despite the relatively high spatial demand of dimethylamino substituents, the nitro group in between is slightly rotated against the molecule plane (O2–N4–C2–C1  $-17.9(2)^\circ$ ). In contrast, the torsions angle of O4–N6–C4–C3 with  $-71.22(19)^\circ$  displays the very high aberration of the other nitro group. In spite of the higher spatial need concerning the vicinal tertiary amino substituent, the amount of rotation for this substituent is even lower than that found in compound **8** ( $-74.69(18)^\circ$ ).

Single crystals of **11** were obtained by evaporating a solution of compound **11** in acetone. Compound **11** crystallizes in the monoclinic space group  $P 2_1/c$  (*no. 14*) with four formula units per cell and has a cell volume of  $1165.20(11) \text{ \AA}^3$ . The cell constants are  $a = 6.6388(4) \text{ \AA}$ ,  $b = 22.0275(12) \text{ \AA}$  and  $c = 8.0977(4) \text{ \AA}$  with  $\beta = 100.271(5)^\circ$ . The calculated density at  $416(2) \text{ K}$  is  $1.73 \text{ g cm}^{-3}$ .

## The Pyridazine Scaffold as a Building Block for Energetic Materials: Synthesis, Characterization and Properties

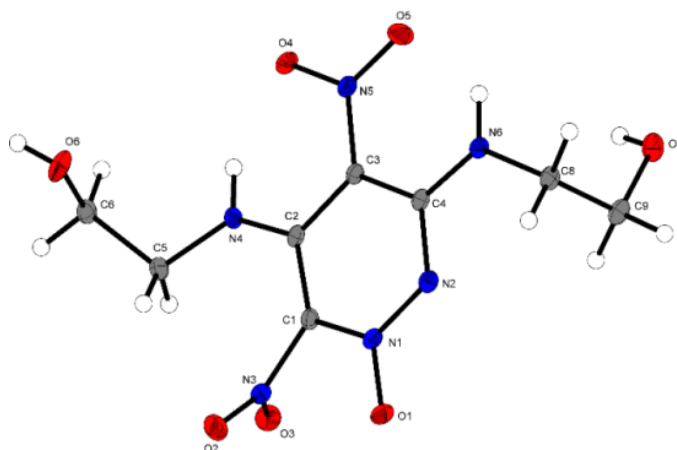


**Figure 5.** Molecular unit of compound **11** in the crystalline state. Ellipsoids correspond to 50% probability levels. Hydrogen radii are arbitrary. Selected bond lengths / [Å] and angles / [°]: N1–N2 1.328(2), N1–C1 1.353(2), N2–C4 1.358(2), C1–C2 1.411(2), C2–C3 1.428(2), C3–C4 1.433(2), O1–N1 1.2603(17), N6–C4 1.329(2), N6–C8 1.462(2), C8–C9 1.513(3), C9–O7 1.422(2), N5–C3 1.420(2), O4–N5 1.2423(18), N2–N1–C1 122.74(14), C2–C3–C4 119.07(15), N2–C4–C3 122.14(15), C4–N6–C8 122.87(15), N6–C8–C9 111.10(15), O7–C9–C8 112.11(16), C2–N4–C5 129.24(15), O6–C6–C5 109.28(15), C1–N1–N2–C4 1.7(2), N1–N2–C4–C3 –0.6(2), C1–C2–C3–C4 –0.1(2), O1–N1–N2–C4 179.54(14), N2–N1–C1–N3 174.94(14), O2–N3–C1–N1 70.1(2), N1–C1–C2–N4 –179.50(16), C5–N4–C2–C1 14.6(3), C2–N4–C5–C6 150.46(18), N4–C2–C3–N5 3.6(3), O4–N5–C3–C2 2.5(2), N1–N2–C4–N6 179.21(15), C8–N6–C4–N2 6.5(2), C4–N6–C8–C9 82.1(2).

The N–N, N–C and C–C distances inside the pyridazine ring are all in the range for typical single and double bond lengths concerning these elements (**Figure 5**).<sup>[13,14,15,16]</sup> Among them, the N1–N2 distance is 1.328(2) Å and the N2–C4 distance is 1.358(2) Å. Also, the internal bond angles such as N2–N1–C1 of 122.74(14)°, C2–C3–C4 of 119.07(15)° and N2–C4–C3 of 122.14(15)° are all near to the characteristic 120° for  $sp^2$  hybridized bond centers. All of these bond lengths and angles indicate the existing aromaticity.<sup>[14]</sup> The N–O bond lengths in the  $N^+-O^-$  moiety is 1.2603(17) Å, which is somewhat shorter than that found in precursor **7** (1.268(2) Å) and related compound **8** (1.2635(17) Å).<sup>[13]</sup> The interatomic distances between the nitrogen atoms of the (2-(hydroxyl)ethyl)amino substituents and the pyridazine backbone also show an aromatic participation. All torsions angles between the ring-internal atoms show only slight deformation ( $|\theta_{out\ of\ plane}| \leq 2.1(3)^\circ$ ) and is lower than that in precursor **7** ( $|\theta_{out\ of\ plane}| \leq 6.6^\circ$ ) and even **10** ( $|\theta_{out\ of\ plane}| \leq 28.2(2)^\circ$ ). The nitro group next to the *N*-oxide shows the significant twist of 70.1(2)° (O2–N3–C1–N1). This amount of rotation is in the range of those found for the analogous substituents in **8** (–74.69(18)°) and **10** (–71.22(19)°).

### 5.2.3. $^{15}\text{N}$ NMR spectroscopy

In addition,  $^{15}\text{N}$  NMR spectra of compounds **8** and **11** were recorded (**Figure 6**). Compound **8** exhibits six resonances in the  $^{15}\text{N}$  spectrum; both  $\text{NO}_2$  groups are observed at  $-17.1$  and  $-22.2$  ppm, the pyridazine nitrogen atoms at  $-69.8$  ( $\text{N}^+-\text{O}^-$ ) and  $-113.2$  ppm. Both methylamine nitrogen atoms show a low intensity and can be observed at  $-317.9$  and  $-323.1$  ppm as singlet.

$^{15}\text{N}$  NMR (41 MHz,  $d_6$ -DMSO)

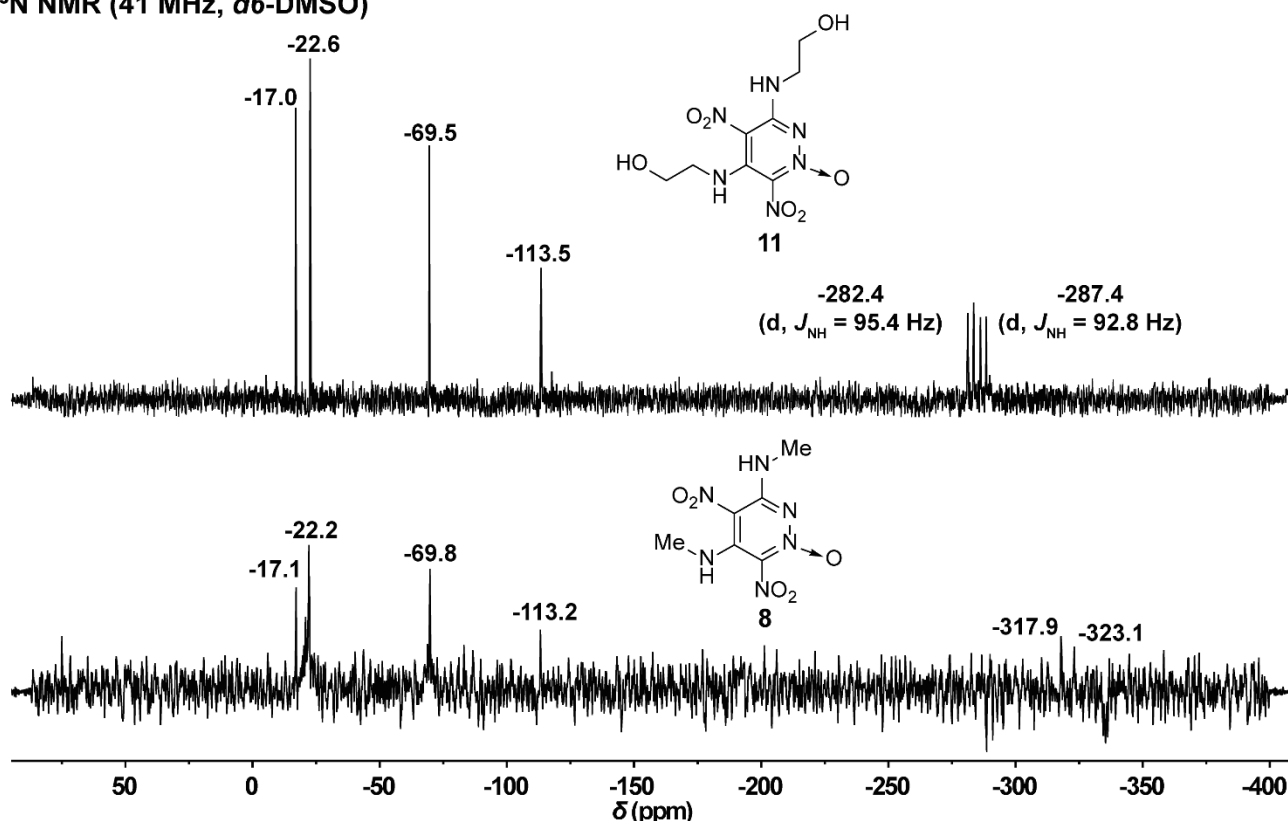


**Figure 6.**  $^{15}\text{N}$  NMR spectra of compounds **8** and **11**.

Six resonances can be observed in the  $^{15}\text{N}$  spectrum of compound **11**. The nitro groups appear at  $-17.0$  and  $-22.6$  ppm and the pyridazine nitrogen atoms exhibit similar shift as compound **8**  $-69.5$  ( $\text{N}$ -oxide) and  $113.5$  ppm. Both duplets at  $-282.4$  ( $J_{\text{NH}} = 95.4$  Hz) and  $-287.4$  ( $J_{\text{NH}} = 92.8$  Hz) ppm can be assigned to both NH atoms.

### 5.2.4. Detonation properties

Compounds **8–11** can be classified as energetic materials, therefore their energetic properties were investigated. All theoretically and experimentally determined values for all four compounds are reported in **Table 1**. In addition, the thermal behavior was investigated with an OZM Research DTA 552-Ex instrument with a heating rate of  $5\text{ }^{\circ}\text{C min}^{-1}$ . All compounds show sharp decomposition in the DTA plots and decompose without melting prior. Compound **8** decomposes at  $250\text{ }^{\circ}\text{C}$ , whereas the nitrated



## The Pyridazine Scaffold as a Building Block for Energetic Materials: Synthesis, Characterization and Properties

derivative **9** shows sharp decomposition at 120 °C. The reason for the drastic change in the thermal behavior from compound **8** to **9** can be explained with the formation of the thermally sensitive  $\text{--NHNO}_2$  moiety in 3,5-bis(methylnitramino)-4,6-dinitropyridazine-1-oxide (**9**). DTA plots of compounds **8**, **9** and **11** are shown in **Figure 7**. Compounds **10** and **11** decompose at 217 and 170 °C, respectively.

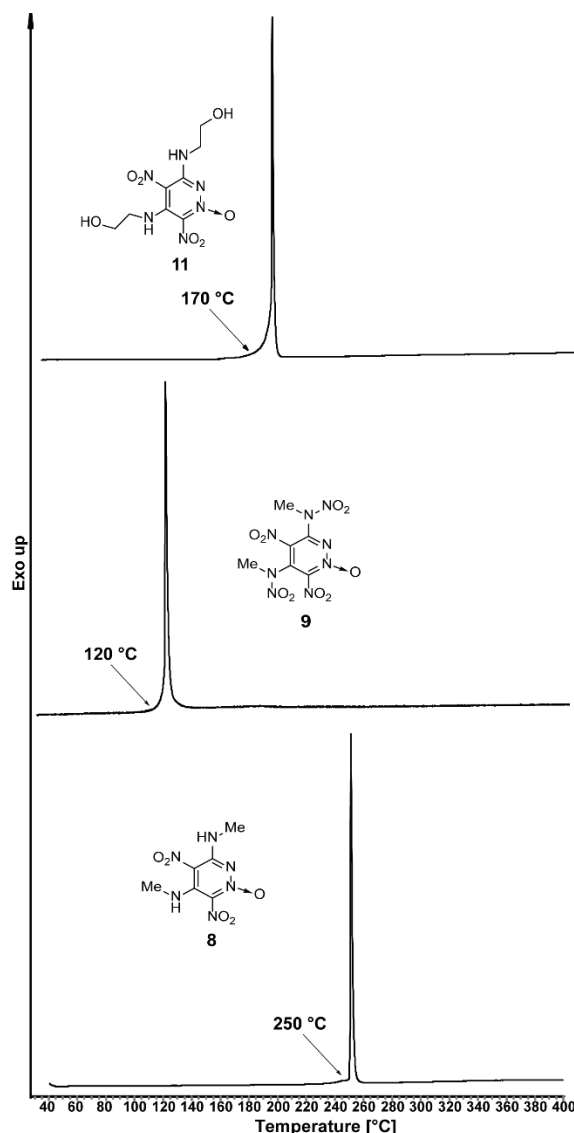


**Figure 7.** DTA plots of compounds **8**, **9** and **11**.

Further, the sensitivities of all compounds were determined toward external stimuli (friction and impact) by using the BAM standards and the theoretical detonation properties were calculated by using the EXPLO5\_V6.03 computer code.<sup>[17]</sup> For all computer calculations with the EXPLO5 code the room temperature densities of all compounds were calculated by using the obtained X-ray structures as reported in the literature.<sup>[18]</sup>

The highest room temperature density was measured for compound **11** with  $1.69 \text{ g cm}^{-3}$  and the lowest was determined for **10** with  $1.54 \text{ g cm}^{-3}$ . The sensitivity values of all four compounds toward impact,

## The Pyridazine Scaffold as a Building Block for Energetic Materials: Synthesis, Characterization and Properties

friction and electrostatic discharge were determined. Compounds **8**, **10** and **11** exhibit impact sensitivity of 10, 30 and 18 J, respectively. The determined friction sensitivity for all three compounds is 360 N. Compound **9** is the most sensitive compound with values of IS = 5 J, FS = 120 N and ESD = 0.033 J. Compound **9** contains the nitramino moiety ( $-\text{NHNO}_2$ ), which leads to lower thermal stability of the molecule and lower sensitivity toward external stimuli. This is supported with the obtained physico-chemical properties for the pyridazine derivative **9**. According to the EXPLO5 calculations compound **9** shows the best performance with detonation pressure and detonation velocity of 29.1 kbar and  $8276 \text{ m}\cdot\text{s}^{-1}$ , respectively. Compounds **8** and **11** have similar properties with  $p_{\text{C-J}}=20.4 \text{ kbar}$  and  $D_{\text{C-J}}=7365 \text{ m}\cdot\text{s}^{-1}$  for **8** and  $p_{\text{C-J}}=20.2 \text{ kbar}$  and  $D_{\text{C-J}}=7389 \text{ m}\cdot\text{s}^{-1}$  for **11**. The calculated detonation properties for **9** in comparison to its precursor **8** and compound **11** can be explained again with the introduced nitramino groups, which result in a good performance but decreases the stability of the molecule.

**Table 1.** Physico-chemical properties of compounds **8–11**.

	<b>8</b>	<b>9</b>	<b>10</b>	<b>11</b>
$IS^{[a]}$ [J]	10	5	30	18
$FS^{[b]}$ [N]	360	120	360	360
$ESD^{[c]}$ [J]	0.203	0.033	0.37	0.25
$\Omega^{[d]}$ [%]	−72	−29	−100	−79
$T_m^{[e]}$ [°C]	—	—	—	—
$T_{dec}^{[f]}$ [°C]	250	120	217	170
$\rho^{[g]}$ [ $\text{g}\cdot\text{cm}^{-3}$ ]	1.63	1.68	1.54	1.69
$\Delta_f H^{o[h]}$ [ $\text{kJ}\cdot\text{kg}^{-1}$ ]	420.6	892.7	574.6	824.4
$\Delta_f H^{o[h]}$ [ $\text{kJ}\cdot\text{mol}^{-1}$ ]	102.7	298.3	156.4	−250.8
EXPLO5 6.03				
$-\Delta_E U^{o[i]}$ [ $\text{kJ}\cdot\text{kg}^{-1}$ ]	4403	5844	4267	3828
$T_{C-J}^{[j]}$ [K]	3036	4164	2790	2632
$p_{C-J}^{[k]}$ [kbar]	204	291	176	202
$D_{C-J}^{[l]}$ [ $\text{m}\cdot\text{s}^{-1}$ ]	7365	8276	6994	7389
$V^{[m]}$ [ $\text{L}^3\cdot\text{kg}^{-1}$ ]	756	753	767	757

[a] Impact sensitivity (BAM drophammer, method 1 of 6); [b] friction sensitivity (BAM drophammer, method 1 of 6); [c] electrostatic discharge device (OZM research); [d] oxygen balance with respect to  $\text{CO}_2$ ; [e] melting point (DTA,  $\beta = 5^\circ\text{C}\cdot\text{min}^{-1}$ ); [f] temperature of decomposition (DTA,  $\beta = 5^\circ\text{C}\cdot\text{min}^{-1}$ ); [g] density at 298 K; [h] standard molar enthalpy of formation; [i] detonation energy; [j] detonation temperature;

[k] detonation pressure; [l] detonation velocity; [m] volume of detonation gases at standard temperature and pressure conditions.

### 5.3. Conclusions

In conclusion, we report the synthesis of four new *N*-oxidized pyridazine based energetic materials (**8–11**). For this purpose, 3,5-dimethoxy-4,6-dinitropyridazine-1-oxide (**7**) was reacted with methylamine, dimethylamine and 2-aminoethanol to result in the formation of 3,5-bis(methylamino)-4,6-dinitropyridazine-1-oxide (**8**), 3,5-bis(methylnitramino)-4,6-dinitropyridazine-1-oxide (**10**) and 3,5-bis((2-hydroxyethyl)amino)-4,6-dinitropyridazine-1-oxide (**11**). Further, the acidity of the protons in the –NHMe moiety of compound **8** was used and **8** was nitrated in 100% nitric acid to give 3,5-bis(methylnitramino)-4,6-dinitropyridazine-1-oxide (**9**) in excellent yields. The synthesized energetic pyridazine derivatives (**8–11**) were characterized extensively using multinuclear NMR spectroscopy, vibrational spectroscopy, DTA, elemental analysis and BAM sensitivity methods. In addition, the crystal structures of all four compounds were obtained and extensively discussed. The experimentally and theoretically determined energetic properties were well investigated. Compounds **8** (IS = 10 J; FS = 360 N), **10** (IS = 30 J; FS = 360 N) and **11** (IS = 18 J; FS = 360 N) exhibit similar properties toward impact and friction, whereas compound **9** with the nitramino moiety exhibits higher sensitivity toward external stimuli (IS = 5 J; FS = 120 N).

### 5.4. Experimental Section

**CAUTION!** All investigated compounds are potentially explosive materials, although no hazards were observed during preparation and handling these compounds. Nevertheless, safety precautions such as (wearing leather coat, face shield, Kevlar sleeves, Kevlar gloves, earthed equipment and ear plugs) should be drawn.

<sup>1</sup>H, <sup>13</sup>C, <sup>14</sup>N and <sup>15</sup>N NMR spectra were recorded on *JEOL 270* and *BRUKER AMX 400* instruments. The samples were measured at room temperature in standard NMR tubes (Ø 5 mm). Chemical shifts are reported as  $\delta$  values in ppm relative to the residual solvent peaks of *d*<sub>6</sub>-DMSO ( $\delta_{\text{H}}$ : 2.50,  $\delta_{\text{C}}$ : 39.5). Solvent residual signals and chemical shifts for NMR solvents were referenced against tetramethylsilane (TMS,  $\delta$  = 0 ppm) and nitromethane. Unless stated otherwise, coupling constants were reported in hertz (Hz) and for the characterization of the observed signal multiplicities the following abbreviations were used: s (singlet), d (doublet), t (triplet), q (quartet), quint (quintet), sept (septet), m (multiplet) and br (broad). Infrared spectra (IR) were recorded from 4500 cm<sup>–1</sup> to 650 cm<sup>–1</sup> on a PERKIN ELMER

## The Pyridazine Scaffold as a Building Block for Energetic Materials: Synthesis, Characterization and Properties

Spectrum BX-59343 instrument with a *SMITHS DETECTION DuraSamplIR II Diamond ATR* sensor. The absorption bands are reported in wavenumbers ( $\text{cm}^{-1}$ ). Elemental analysis was carried on a *Elementar Vario el* by pyrolysis of the sample and subsequent analysis of the formed gases. Decomposition temperatures were measured *via* differential thermal analysis (DTA) with an OZM Research DTA 552-Ex instrument at a heating rate of  $5\text{ }^{\circ}\text{C min}^{-1}$  and in a range of room temperature to  $400\text{ }^{\circ}\text{C}$ . All sensitivities toward impact (IS) and friction (FS) were determined according to BAM (German: Bundesanstalt für Materialforschung und Prüfung) standards using a BAM drop hammer and a BAM friction apparatus.[19] All energetic compounds were tested for sensitivity towards electrical discharge using an Electric Spark Tester ESD 2010 EN from OZM.

### 3,5-Bis(methylamino)-4,6-dinitropyridazine-1-oxide (8)

3,5-Dimethoxy-4,6-dinitropyridazine-1-oxide (**7**, 1.00 g, 4.06 mmol, 1.0 eq.) was dissolved in acetonitrile (50 ml) and an aqueous methylamine solution (40%, 2.5 mL, 29 mmol, 7.1 eq.) was added dropwise. The reaction mixture was stirred at room temperature overnight. The solvent was removed *in vacuo*. The residue was suspended in a small amount of water, filtered and washed with ice-water. Drying on air yielded compound **8** as yellow solid (841 mg, 3.44 mmol, 85%).

BAM: drop hammer: 10 J (100–500  $\mu\text{m}$ ); friction tester: 360 N (100–500  $\mu\text{m}$ ); ESD: 203 mJ (100–500  $\mu\text{m}$ ). IR (ATR),  $\tilde{\nu}$  ( $\text{cm}^{-1}$ ) = 3351 (m), 3236 (m), 2955 (vw), 1573 (s), 1537 (s), 1403 (s), 1327 (s), 1244 (s), 1189 (s), 1135 (s), 1037 (s), 986 (m), 799 (m), 768 (s), 715 (s), 649 (s), 625 (s), 510 (m).  $^1\text{H}$  NMR ( $d_6$ -DMSO, 400 MHz, [ppm]):  $\delta$  = 9.71 (s, 1H), 9.27 (d,  $^3J$  = 4.8 Hz, 1H), 2.95 (d,  $^3J$  = 4.9 Hz, 3H), 2.86 (s, 3H).  $^{13}\text{C}$  NMR ( $d_6$ -DMSO, 101 MHz, [ppm]):  $\delta$  = 152.2, 142.5, 133.9, 112.1, 30.0, 29.1.  $^{14}\text{N}$  NMR ( $d_6$ -DMSO, 29 MHz, [ppm]):  $\delta$  = –24, –71.  $^{15}\text{N}$  NMR ( $d_6$ -DMSO, 41 MHz, [ppm]):  $\delta$  = –17.1, –22.2, –69.7, –113.0, –288.7, –291.1. Elem. Anal. ( $\text{C}_6\text{H}_8\text{N}_6\text{O}_5$ ,  $244.06\text{ g}\cdot\text{mol}^{-1}$ ): Calc.: C 29.56, H 3.30, N 34.42%. Found: C 29.56, H 3.20, N 34.42%.

### 3,5-Bis(methylnitramino)-4,6-dinitropyridazine-1-oxide (9)

3,5-Bis(methylamino)-4,6-dinitropyridazine-1-oxide (**8**, 500 mg, 2.05 mmol, 1.0 eq.) was added in small portions to 100%  $\text{HNO}_3$  (3.33 mL) at  $0\text{ }^{\circ}\text{C}$  and stirred for 3.5 h. After pouring onto crushed ice and stirring until the ice had melted, the resulting suspension was filtered and washed with ice-water until the filtrate was acid free. Drying on air gave compound **9** as yellow solid (625 mg, 1.87 mmol, 91%).

## The Pyridazine Scaffold as a Building Block for Energetic Materials: Synthesis, Characterization and Properties

BAM: drop hammer: 5 J (100–500  $\mu\text{m}$ ); friction tester: 120 N (100–500  $\mu\text{m}$ ); ESD: 33 mJ (100–500  $\mu\text{m}$ ). IR (ATR),  $\tilde{\nu}$  ( $\text{cm}^{-1}$ ) = 1573 (s), 1557 (s), 1453 (w), 1426 (w), 1386 (vw), 1336 (m), 1301 (m), 1260 (vs), 1150 (vw), 1094 (w), 1064 (w), 999 (m), 911 (w), 799 (m).  $^1\text{H}$  NMR ( $\text{CDCl}_3$ , 400 MHz, [ppm]):  $\delta$  = 3.94 (s, 3H), 3.74 (s, 3H).  $^{13}\text{C}$  NMR ( $\text{CDCl}_3$ , 101 MHz, [ppm]):  $\delta$  = 162.6, 148.0, 132.9, 121.8, 41.7, 39.4.  $^{14}\text{N}$  NMR ( $\text{CDCl}_3$ , 29 MHz, [ppm]):  $\delta$  = –30, –38, –40, –42, –71. Elem. Anal. ( $\text{C}_6\text{H}_6\text{N}_8\text{O}_9$ , 334.14  $\text{g}\cdot\text{mol}^{-1}$ ): Calc.: C 21.57, H 1.81, N 33.53%. Found: C 21.83, H 1.98, N 33.29%.

### 3,5-Bis(dimethylamino)-4,6-dinitropyridazine-1-oxide (10)

3,5-Dimethoxy-4,6-dinitropyridazine-1-oxide (**7**, 500 mg, 2.03 mmol, 1.0 eq.) was dissolved in acetonitrile (25 mL) and an aqueous dimethylamine solution (40%, 0.600 mL, 4.74 mmol, 2.3 eq.) was added dropwise. The reaction was stirred at room temperature overnight. The resulting suspension was filtered and the solvent was removed under reduced pressure. The residue was resuspended in water, filtered and washed with ice-water. After drying on air compound **10** was obtained as orange solid (503 mg, 1.85 mmol, 91%).

BAM: drop hammer: 30 J (100–500  $\mu\text{m}$ ); friction tester: 360 N (100–500  $\mu\text{m}$ ); ESD: 0.37 mJ; IR (ATR),  $\tilde{\nu}$  ( $\text{cm}^{-1}$ ) = 1573 (s), 1521 (m), 1484 (m), 1464 (w), 1431 (w), 1378 (m), 1334 (w), 1250 (vs), 1210 (s), 1184 (s), 1135 (m), 1072 (s), 933 (vw), 906 (vw), 841 (w), 823 (w), 798 (w), 760 (m).  $^1\text{H}$  NMR ( $d_6$ -DMSO, 400 MHz, [ppm]):  $\delta$  = 3.15 (s, 6H), 3.07 (s, 6H).  $^{13}\text{C}$  NMR ( $d_6$ -DMSO, 101 MHz, [ppm]):  $\delta$  = 155.1, 145.5, 137.7, 111.6, 43.8, 41.1.  $^{14}\text{N}$  NMR ( $d_6$ -DMSO, 29 MHz, [ppm]):  $\delta$  = –20, –69. Elem. Anal. ( $\text{C}_8\text{H}_{12}\text{N}_6\text{O}_5$ , 272.22  $\text{g}\cdot\text{mol}^{-1}$ ): Calc.: C 35.30, H 4.44, N 30.87%. Found: C 34.78, H 3.99, N 30.24%.  $m/z$  ( $\text{DEI}^+$ ): 272(100) [ $\text{M}$ ] $^+$ .

### 3,5-Bis((2-hydroxyethyl)amino)-4,6-dinitropyridazine-1-oxide (11)

3,5-Dimethoxy-4,6-dinitropyridazine-1-oxide (**7**, 632 mg, 2.57 mmol, 1.0 eq.) was dissolved in acetonitrile (30 mL) and 2-aminoethanol (0.330 mL, 5.39 mmol, 2.1 eq.) was added dropwise. The solution was stirred at room temperature overnight. The solvent was removed *in vacuo*. Subsequently, the residue was suspended in a small amount of water, filtered and thoroughly washed with ice-water. Drying on air yielded compound **11** as yellow solid (709 mg, 2.33 mmol, 91%).

BAM: drop hammer: 15 J (100–500  $\mu\text{m}$ ); friction tester: 360 N (100–500  $\mu\text{m}$ ); ESD: 250 mJ (100–500  $\mu\text{m}$ ). IR (ATR),  $\tilde{\nu}$  ( $\text{cm}^{-1}$ ) = 3411 (w), 3327 (m), 3209 (w), 2950 (vw), 2887 (vw), 1593 (m), 1525 (s), 1427 (m), 1411 (m), 1337 (s), 1281 (m), 1236 (s), 1180 (s), 1123 (m), 1047 (s), 943 (w), 866 (m), 767 (s), 715 (s), 632 (s), 517 (m).  $^1\text{H}$  NMR ( $d_6$ -DMSO, 400 MHz, [ppm]):  $\delta$  = 9.90 (t,  $^3J$  = 4.8 Hz, 1H),

## The Pyridazine Scaffold as a Building Block for Energetic Materials: Synthesis, Characterization and Properties

9.35 (t,  $^3J = 5.3$  Hz, 1H), 5.25 (t,  $^3J = 5.0$  Hz, 1H), 4.96 (t,  $^3J = 5.2$  Hz, 1H), 3.63–3.56 (m, 4H), 3.53 (q,  $^3J = 5.3$  Hz, 2H), 3.15 (q,  $^3J = 5.0$  Hz, 2H).  $^{13}\text{C}$  NMR ( $d_6$ -DMSO, 101 MHz, [ppm]):  $\delta = 152.1, 142.2, 133.9, 112.2, 58.5, 58.4, 45.4, 44.1$ .  $^{14}\text{N}$  NMR ( $d_6$ -DMSO, 29 MHz, [ppm]):  $\delta = -23, -71$ .  $^{15}\text{N}$  NMR ( $d_6$ -DMSO, 41 MHz, [ppm]):  $\delta = -17.0, -22.6, -69.5, -113.5, -282.4, -287.4$ . Elem. Anal. ( $\text{C}_8\text{H}_{12}\text{N}_6\text{O}_7$ ,  $304.22 \text{ g}\cdot\text{mol}^{-1}$ ): Calc.: C 31.59, H 3.98, N 27.63%. Found: C 31.58, H 3.87, N 27.43%.  $m/z$  (DEI $^+$ ): 305(100)  $[\text{M}+\text{H}]^+$ .

## 5.5. Acknowledgements

Financial support of this work by the Ludwig-Maximilian University of Munich (LMU) and the Office of Naval Research (ONR) under grant no. ONR.N00014-16-1-2062 is gratefully acknowledged. We thank Stefan Huber for his help with the sensitivity testing.

**Keywords:** Nitrogen-rich heterocycle • Energetic pyridazines • Crystal structure elucidation • Thermal behaviour • Energetic properties

## References

- [1] a) T. M. Klapötke, *Chemistry of High-Energy Materials*, 4th ed., De Gruyter, Berlin, **2017**. b) M. H. Keshavarz, T. M. Klapötke, *Energetic Compounds: Methods for Prediction of Their Performance*, De Gruyter, Berlin, **2017**. c) M. H. Keshavarz, T. M. Klapötke, *The Properties of Energetic Materials: Sensitivity, Physical and Thermodynamic Properties*, De Gruyter, Berlin, **2017**.
- [2] a) T. Brinck, *Green Energetic Materials*, John Wiley and Sons, **2014**; b) G. I. Sunahara, G. Lotufo, R. G. Kuperman, J. Hawari, *Ecotoxology of Explosives*, 1<sup>st</sup> Ed., CRC Press, **2009**; c) G. R. Lotufo, W: Blackburn, S. J. Marlborough, J. W: Fleeger, *Ecotoxicology and Environmental Safety* **2010**, 73, 1720–1727.
- [3] a) H. Hervé, C. Roussel, H. Graindorge, *Angew. Chem. Int. Ed.* **2010**, 49, 3177; b) P. Yin, J. M. Shreeve, *Adv. Heterocycl. Chem.* **2017**, 121, 89; c) P. Yin, J. Zhang, C. He, D: A. Parrish, J. M. Shreeve, *J. Mater. Chem. A* **2014**, 2, 3200.
- [4] D. Fischer, J. L. Gottfried, T. M. Klapötke, K. Karaghisoff, J. Stierstorfer, T. G. Witkowski, *Angew. Chem. Int. Ed.* **2016**, 55, 16132–16135.
- [5] a) D. S. Donald, U.S. Patent No.3, 808, 209 (30 April **1974**); b) P. F. Pagoria, A. R. Mitchell, R. D. Schmidt, R. L. Simpson, F. Garcia, J. Forbes, J. Cutting, R. Lee, R. Swansiger, D. M. Hoffman, *Presented at the Insensitive Munitions and Energetic Materials Technology Symposium*, San, Diego, CA, **1998**.

## The Pyridazine Scaffold as a Building Block for Energetic Materials: Synthesis, Characterization and Properties

- [6] a) A. Albini, S. Pietra, *Heterocyclic-N-Oxides*, CRC Press, Boca Raton, FL, **1991**. b) A. M. Churakov, V. A. Tartakovsky, *Chem. Rev.* **2004**, *104*, 2601–2616.
- [7] P. F. Pagoria, G. S. Lee, A. R. Mitchell, R. D. Schmidt, *Thermochim. Acta* **2002**, *384*, 187–204.
- [8] J. Yuan, X. Long, C. Zhang, *J. Phys. Chem. A* **2016**, *120*, 9446–9457.
- [9] M. J. Kamlet, S. J. Jacobs, *J. Chem. Phys.* **1968**, *48*, 23–35.
- [10] N. Fischer, D. Fischer, T. M. Klapötke, D. G. Piercey, J. Stierstorfer, *J. Mater. Chem.* **2012**, *22*, 20418–20422.
- [11] N. Fischer, D. Izsák, T. M. Klapötke, S. Rappengck, J. Stierstorfer, *Chem. Eur. J.* **2012**, *18*, 4051–4062.
- [12] a) H. Wei, H. Gao, J. M. Shreeve, *Chem. Eur. J.* **2014**, *20*, 16943–16952. b) C. Zhang, Y. Shu, X. Zhao, H. Dong, X. Wang, *J. Mol. Struct.: THEOCHEM* **2005**, *728*, 129–134.
- [13] I. Gospodinov, T. M. Klapötke, J. Stierstorfer, *Eur. J. Org. Chem.* **2018**, 1004–1010.
- [14] T. L. Cottrell, *The Strengths of Chemical Bonds*, Butterworths Scientific Publications, London, **1958**.
- [15] F.-Z. Hu, M. Zhang, H.-B. Song, X.-M. Zou, H.-Z. Yang, *Acta Cryst.* **2005**, *E61*, o2486–o2488.
- [16] A. F. Holleman, E. Wiberg, N. Wiberg, *Lehrbuch der Anorganischen Chemie*, 102. Auflage, de Gruyter, **2007**.
- [17] M. Sućeska, *EXPLO5 Version 6.03 User's Guide*, Zagreb, Croatia: OZM; **2015**.
- [18] J. S. Murray, P. Politzer, *J. Mol. Model* **2014**, *20*, 2223–2227.
- [19] a) Reichel & Partner GmbH, <http://www.reichelt-partner.de>; b) Test methods according to the UN Recommendations on the Transport of Dangerous Goods, Manual of Test and Criteria, 4th edn., United Nations Publication, New York and Geneva, **2003**, ISBN 92–1-139087 7, Sales No. E.03.VIII.2; 13.4.2 Test 3 a (ii) BAM Fallhammer.

## 5.6. Supporting Information

### 5.6.1. Synthesis and general considerations

3,5-Dimethoxy-4,6-dinitropyridazine-1-oxide (**7**) was prepared according the known literature.<sup>[S1]</sup>

### 5.6.2. X-ray diffraction

The low-temperature single-crystal X-ray diffraction measurements were performed on an Oxford XCalibur3 diffractometer equipped with a Spellman generator (voltage 50 kV, current 40 mA) and a KappaCCD detector operating with MoK $\alpha$  radiation ( $\lambda = 0.7107 \text{ \AA}$ ). Data collection was performed

## The Pyridazine Scaffold as a Building Block for Energetic Materials: Synthesis, Characterization and Properties

using the CRYSLIS CCD software.<sup>[S2]</sup> The data reduction was carried out using the CRYSLIS RED software.<sup>[S3]</sup> The solution of the structure was performed by direct methods (SIR97)<sup>[S4]</sup> and refined by full-matrix least-squares on F2 (SHELXL)<sup>[S5]</sup> implemented in the WINGX software package<sup>[S6]</sup> and finally checked with the PLATON software.<sup>[S7]</sup> All DIAMOND2 plots are shown with thermal ellipsoids at the 50% probability level and hydrogen atoms are shown as small spheres of arbitrary radius.

**Table S1.** Crystallographic details for compounds **8** and **9**.

Compound	8	9
Formula	C <sub>6</sub> H <sub>8</sub> N <sub>6</sub> O <sub>5</sub>	C <sub>6</sub> H <sub>6</sub> N <sub>8</sub> O <sub>9</sub>
Molar mass / [g mol <sup>-1</sup> ]	244.18	334.19
Crystal system	orthorhombic	orthorhombic
Space group	<i>P bca</i> (no. 61)	<i>P 2 2 2</i> (no. 16)
Color / Habit	yellow block	yellow platelet
Size / [mm]	0.15 × 0.28 × 0.35	0.20 × 0.15 × 0.10
Lattice constants / [Å]	<i>a</i> = 9.7734(2) <i>b</i> = 13.5583(3) <i>c</i> = 14.6509(3)	<i>a</i> = 6.6245(3) <i>b</i> = 10.1031(5) <i>c</i> = 19.2297(8)
Lattice angle / [°]	<i>a</i> = 90 <i>β</i> = 90 <i>γ</i> = 90	<i>a</i> = 90 <i>β</i> = 90 <i>γ</i> = 90
Cell volume / [Å <sup>3</sup> ]	1941.40(7)	1287.01(10)
Formula per unit cell	8	4
Calc. density / [g cm <sup>-3</sup> ]	1.67	1.73
Abs. coefficient / [mm <sup>-1</sup> ]	0.146	0.162
<i>F</i> (000)	1008	680
Wavelength (λ <sub>MoKα</sub> ) / [Å]	0.71073	0.71073
Meas. temperature / [K]	143(2)	143(2)
Diff. range min-max / [°]	4.170 ≤ <i>θ</i> ≤ 26.500	4.2360 ≤ <i>θ</i> ≤ 27.4010
Index range	-12 ≤ <i>h</i> ≤ 12 -17 ≤ <i>k</i> ≤ 17 -18 ≤ <i>l</i> ≤ 18	-7 ≤ <i>h</i> ≤ 7 -12 ≤ <i>k</i> ≤ 12 -23 ≤ <i>l</i> ≤ 20
Parameters/restraints	186/0	210/1
Total no. of reflections	27841	9368
Independent reflections	8839 ( <i>R</i> <sub>int</sub> = 0.0308)	2337 ( <i>R</i> <sub>int</sub> = 0.0404)



## The Pyridazine Scaffold as a Building Block for Energetic Materials: Synthesis, Characterization and Properties

Obs. reflection $I > 2\sigma(I)$	2003	2073
Goodness of fit (GooF)	1.075	1.019
$R$ indices for $I > 2\sigma(I)$ (all data)	$R_1 = 0.0374$ (0.0425)	$R_1 = 0.0379$ (0.0299)
Res. dens. max/min / [ $\text{e } \text{\AA}^{-3}$ ]	$wR_2 = 0.0997$ (0.0964)	$wR_2 = 0.0666$ (0.0628)
Device type	0.315/−0.220	0.145/−0.145
Solution	Oxford Xcalibur3 CCD	Oxford Xcalibur3 CCD
Refinement	SIR-92	SIR-92 SHELXL-97
Absorption correction	SHELXL-2013	multi-scan
	multi-scan	1917211
CCDC	1917212	

**Table S2.** Crystallographic details for compounds **10** and **11**.

Compound	10	11
Formula	$\text{C}_8\text{H}_{12}\text{N}_6\text{O}_5$	$\text{C}_8\text{H}_{12}\text{N}_6\text{O}_7$
Molar mass / [ $\text{g mol}^{-1}$ ]	272.24	304.24
Crystal system	monoclinic	monoclinic
Space group	$P 2_1/c$ ( <i>no. 14</i> )	$P 2_1/c$ ( <i>no. 14</i> )
Color / Habit	orange platelet	yellow plate
Size / [mm]	$0.50 \times 0.50 \times 0.05$	$0.50 \times 0.25 \times 0.05$
Lattice constants / [ $\text{\AA}$ ]	$a = 9.7162(4)$ $b = 13.6057(5)$ $c = 8.7037(4)$	$a = 6.6388(4)$ $b = 22.0275(12)$ $c = 8.0977(4)$
Lattice angle / [ $^\circ$ ]	$a = 90$ $\beta = 96.137(4)$ $\gamma = 90$	$a = 90$ $\beta = 100.271(5)$ $\gamma = 90$
Cell volume / [ $\text{\AA}^3$ ]	1144.00(8)	1165.20(11)
Formula per unit cell	4	4
Calc. density. / [ $\text{g cm}^{-3}$ ]	1.58	1.73
Abs. coefficient / [ $\text{mm}^{-1}$ ]	0.133	0.153
$F(000)$	568	632
Wavelength ( $\lambda_{\text{MoK}\alpha}$ ) / [ $\text{\AA}$ ]	0.71073	0.71073
Meas. temperature / [K]	143(2)	416(2)
Diff. range min-max / [ $^\circ$ ]	$4.219 \leq \theta \leq 25.999$	$4.176 \leq \theta \leq 32.357$

## The Pyridazine Scaffold as a Building Block for Energetic Materials: Synthesis, Characterization and Properties

Index range	$-11 \leq h \leq 9$	$-5 \leq h \leq 9$
	$-15 \leq k \leq 16$	$-32 \leq k \leq 32$
	$-10 \leq l \leq 10$	$-12 \leq l \leq 11$
Parameters/restraints	176/0	238 / 0
Total no. of reflections	8565	12846
Independent reflections	2236 ( $R_{int} = 0.0270$ )	3852 ( $R_{int} = 0.0624$ )
Obs. reflection $I > 2\sigma(I)$	1802	2329
Goodness of fit (GooF)	1.054	1.016
$R$ indices for $I > 2\sigma(I)$ (all data)	$R_1 = 0.0474$ (0.0351)	$R_1 = 0.1061$ (0.0529)
Res. dens. max/min / [ $e \text{ \AA}^{-3}$ ]	$wR_2 = 0.0956$ (0.0887)	$wR_2 = 0.1207$ (0.0991)
Device type	0.219/−0.220	0.391 /−0.309
Solution	Oxford Xcalibur3 CCD	Oxford Xcalibur3 CCD
Refinement	SIR-92	SIR-92
Absorption correction	SHELXL-2013	SHELXL-2013
CCDC	multi-scan	multi-scan
	1917213	1917211

### 5.6.3. Computations

All calculations were carried out using the Gaussian G09W (revision A.02) program package.<sup>[S8]</sup> The enthalpies (H), were calculated using the complete basis set (CBS) method of Petersson and coworkers. The CBS models use the known asymptotic convergence of pair natural orbital expressions to extrapolate from calculations using a finite basis set to the estimated complete basis set limit. CBS-4 begins with a HF/3-21G(d) structure optimization and the zero-point energy computation. Subsequently, applying a larger basis set a base energy is computed. A MP2/6-31+G calculation with a CBS extrapolation gives the perturbation-theory corrected energy (takes the electron correlation into account). A MP4(SDQ)/6-31+(d,p) calculation is used to correlate higher order contributions. In this study we applied the modified CBS-4M method (M referring to the use of minimal population localization) which is a re-parameterized version of the original CBS-4 method and also includes some additional empirical corrections.<sup>[S9]</sup> The gas-phase enthalpies ( $\Delta_f H^\circ_{(g, M, 298)}$ ) of the species were computed according to the atomization energy method (equation 1).<sup>[S10]</sup>

$$\Delta_f H^\circ_{(g, M, 298)} = H_{(g, M, 298)} - \sum H^\circ_{(g, Ai, 298)} + \sum \Delta_f H^\circ_{(g, Ai, 298)} \quad (1)$$

## The Pyridazine Scaffold as a Building Block for Energetic Materials: Synthesis, Characterization and Properties

$\Delta_f H^\circ(g, A_i, 298)$  for the corresponding atoms ( $A_i$ ) were determined experimentally and are reported in the literature while  $H^\circ(g, A_i, 298)$  were calculated theoretically (**Table S3**).<sup>[S11]</sup>

**Table S3.** CBS-4M electronic enthalpies for atoms C, H, N and O and their literature values for atomic  $\Delta_f H^\circ_{298} / \text{kJ mol}^{-1}$

Atom	$-H^{298} / \text{a.u.}$	$\Delta_f H^\circ(g, A_i, 298) [\text{kcal mol}^{-1}]$
H	0.500991	52.103
C	37.786156	171.29
N	54.522462	112.97
O	74.991202	59.56

Standard molar enthalpies of formation were calculated using and the standard molar enthalpies of  $\Delta_f H^\circ_{(g, M, 298)}$  sublimation (estimated using Trouton's rule, equation 2).<sup>[S12]</sup>

$$\Delta_f H^\circ_M = \Delta_f H^\circ_{(g, M, 298)} - \Delta_{sub} H^\circ_M = \Delta_f H^\circ_{(g, M, 298K)} - 188 \cdot T \left[ \frac{J}{mol} \right] \quad (2)$$

Where [K] is either the melting point or the decomposition temperature (if no melting occurs prior to decomposition).

The calculation results are summarized in **Tables S4**.

**Table S4.** Calculation results.

Compound	$-H^{298} [a] \text{ a.u.}$	$\Delta_f H^\circ(g, M) \text{ kJ mol}^{-1} [b]$	$\Delta_f H^\circ(s) \text{ kJ mol}^{-1} [c]$	$\Delta_f U(s) \text{ kJ kg}^{-1} [d]$
<b>8</b>	936.595874	201.1	102.3	517.1
<b>9</b>	1345.112057	372.3	298.3	978.1
<b>10</b>	1015.032129	248.5	156.4	679.2
<b>11</b>	1165.3628	-167.5	-250.8	-722.5

[a] CBS-4M electronic enthalpy; [b] gas phase enthalpy of formation; [c] standard solid state enthalpy of formation; [d] solid state energy of formation.

### 5.6.4. Detonation parameters

The Chapman-Jouguet (C-J) characteristics, (i.e. heat of detonation,  $\Delta E_{\text{U}}^{\circ}$ ; detonation temperature,  $T_{\text{C-J}}$ ; detonation pressure,  $P_{\text{C-J}}$ ; detonation velocity  $D_{\text{C-J}}$ ) based on the calculated  $\Delta_f H^{\circ}_{\text{M}}$  values, and the theoretical maximum densities were computed using the EXPLO5 V6.03 thermochemical computer code.<sup>[S13]</sup> Calculations for explosives assume ideal behavior. The estimation of detonation parameters is based on the chemical equilibrium steady-state model of detonation. The Becker-Kistiakowsky-Wilson equation of state (BKW EOS) with the following sets of constants:  $\alpha = 0.5$ ,  $\beta = 0.38$ ,  $\kappa = 9.4$ , and  $\Theta = 4120$  for gaseous detonation products and the Murnaghan equation of state for condensed products (compressible solids and liquids) were applied. The calculation of the equilibrium composition of the detonation products uses modified White, Johnson and Dantzig's free energy minimization technique. The specific energies of explosives ( $f$ ) were calculated according to the ideal gas equation of state assuming isochoric conditions (equation 3).

$$f = p_e \cdot V = n \cdot R \cdot T_c \left[ \frac{\text{JkJ}}{\text{molkg}} \right] \quad (3)$$

Where  $p_e$  is the maximum pressure through the explosion,  $V$  is the volume of detonation gases ( $\text{m}^3 \cdot \text{kg}^{-1}$ ),  $n$  is the number of moles of gas formed by the explosion per kilogram of explosive (Volume of Explosive Gases),  $R$  is the ideal gas constant and  $T_c$  is the absolute temperature of the explosion.<sup>[S13,S14]</sup>

### 5.6.5. Literature

- [S1] I. Gospodinov, T. M. Klapötke, J. Stierstorfer, *Eur. J. Org. Chem.* **2018**, 1004–1010.
- [S2] CrysAlisPro, *Oxford Diffraction Ltd. version 171.33.41*, **2009**.
- [S3] *CrysAlis RED, Version 1.171.35.11 (release 16-05-2011 CrysAlis 171.Net)*, Oxford Diffraction Ltd., Abingdon, Oxford (U.K.), **2011**.
- [S4] A. Altomare, M. C. Burla, M. Camalli, G. L. Cascarano, C. Giacovazzo, A. Guagliardi, A. G. G. Moliterni, G. Polidori and R. Spagna, SIR97: A New Tool for Crystal Structure Determination and Refinement, *J. Appl. Crystallogr.*, **1999**, 32, 115–119.
- [S5] G. M. Sheldrick, A Short History of SHELX, *Acta Crystallogr., Sect. A: Found. Crystallogr.*, **2008**, 64, 112–122.
- [S6] L. J. Farrugia, WinGX Suite for Small-Molecule Single-Crystal Crystallography, *J. Appl. Crystallogr.*, **1999**, 32, 837–838.
- [S7] A. L. Spek, *PLATON*, **1999**, A Multipurpose Crystallographic Tool, Utrecht University, The Diffraction Ltd.

## The Pyridazine Scaffold as a Building Block for Energetic Materials: Synthesis, Characterization and Properties

- [S8] M. J. Frisch, G. W. Trucks, B. Schlegel, G. E. Scuseria, M. A. Robb, J. R. Cheeseman, G. Scalmani, V. Barone, B. Mennucci, G. A. Petersson, H. Nakatsuji, M. Caricato, X. Li, H.P. Hratchian, A. F. Izmaylov, J. Bloino, G. Zheng, J. L. Sonnenberg, M. Hada, M. Ehara, K. Toyota, R. Fukuda, J. Hasegawa, M. Ishida, T. Nakajima, Y. Honda, O. Kitao, H. Nakai, T. Vreven, J. A. Montgomery, Jr., J. E. Peralta, F. Ogliaro, M. Bearpark, J. J. Heyd, E. Brothers, K. N. Kudin, V. N. Staroverov, R. Kobayashi, J. Normand, K. Raghavachari, A. Rendell, J. C. Burant, S. S. Iyengar, J. Tomasi, M. Cossi, N. Rega, J. M. Millam, M. Klene, J. E. Knox, J. B. Cross, V. Bakken, C. Adamo, J. Jaramillo, R. Gomperts, R. E. Stratmann, O. Yazyev, A. J. Austin, R. Cammi, C. Pomelli, J. W. Ochterski, R. L. Martin, K. Morokuma, V. G. Zakrzewski, G. A. Voth, P. Salvador, J. J. Dannenberg, S. Dapprich, A. D. Daniels, O. Farkas, J.B. Foresman, J. V. Ortiz, J. Cioslowski, D. J. Fox, Gaussian 09 A.02, Gaussian, Inc., Wallingford, CT, USA, **2009**.
- [S9] (a) J. W. Ochterski, G. A. Petersson, and J. A. Montgomery Jr., *J. Chem. Phys.* **1996**, *104*, 2598–2619; (b) J. A. Montgomery Jr., M. J. Frisch, J. W. Ochterski G. A. Petersson, *J. Chem. Phys.* **2000**, *112*, 6532–6542.
- [S10] (a) L. A. Curtiss, K. Raghavachari, P. C. Redfern, J. A. Pople, *J. Chem. Phys.* **1997**, *106*, 1063–1079; (b) E. F. C. Byrd, B. M. Rice, *J. Phys. Chem. A* **2006**, *110*, 1005–1013; (c) B. M. Rice, S. V. Pai, *Comb. Flame* **1999**, *118*, 445–458.
- [S11] P. J. Linstrom, W. G. Mallard, *National Institute of Standards and Technology*, Gaithersburg MD, 20899.
- [S12] a) F. Trouton, *Philos. Mag. (1876-1900)* **1884**, *18*, 54-57; b) M. S. Westwell, M. S. Searle, D. J. Wales, D. H. Williams, *J. Am. Chem. Soc.* **1995**, *117*, 5013-5015.
- [S13] M. Sućeska, *EXPLO5 Version 6.03 User's Guide*, Zagreb, Croatia: OZM; **2015**.
- [S14] a) R. Meyer, J. Köhler, A. Homburg, *Explosives*, 6th edn., Wiley, Weinheim, **2007**, p. 291-292; b) T. M. Klapötke, *Chemistry of High-Energy Materials*, Walter de Gruyter, Berlin, **2015**;

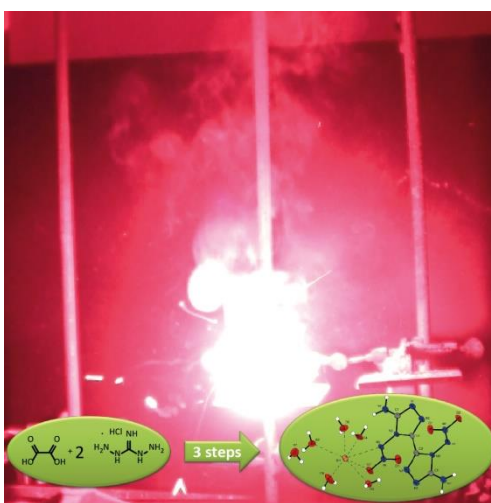
## 6. Metal Salts of 3,3'-Diamino-4,4'-dinitramino-5,5'-bi-1,2,4-triazole in Pyrotechnic Compositions

Johann Glück, Ivan Gospodinov, Thomas M. Klapötke, and Jörg Stierstorfer

Dedicated to Prof. Dr. Thomas Fässler on the occasion of his 60<sup>th</sup> birthday

Published in *Z. Anorg. Allg. Chem.* **2019**, 645, 370–376.

DOI: 10.1002/zaac.201800179



**Abstract:** The synthesis of alkali and alkaline earth salts of 3,3'-diamino-4,4'-dinitramino-5,5'-bi-1,2,4-triazole (H<sub>2</sub>ANAT) is reported. The fast and convenient three steps reaction toward the target compounds does not require any organic solvents. In addition to an intensive characterization of all synthesized metal salts, the focus was on developing chlorine and nitrate-free red-light-generating pyrotechnical formulations. Strontium 3,3'-diamino-4,4'-dinitramino-5,5'-bitriazolate hexahydrate served as colorant and oxidizer in one molecule. The energetic properties of all developed pyrotechnical formulations assure safe handling and manufacturing.

### 6.1. Introduction

In recent years the development of environmental friendly pyrotechnics for both military and civilian application became more and more important.<sup>[1]</sup> This affected all ingredients of a typical light-producing pyrotechnical formulation such as the oxidizer, fuel, colorant, and additives.<sup>[2]</sup> One of the first steps toward this goal is correlated with the commonly used oxidizers ammonium perchlorate (NH<sub>4</sub>ClO<sub>4</sub>) and potassium perchlorate (KClO<sub>4</sub>). Next to their advantageous properties, like a high oxygen balance,

## Metal Salts of 3,3'-Damino-4,4'-dinitramino-5,5'-bi-1,2,4-triazole in Pyrotechnic Compositions

stability, low cost and low hygroscopicity, both were identified as environmental and human health hazards.<sup>[3]</sup> The high solubility makes them a successful groundwater contaminant, which is addressed by American authorities resulting in increasing regulations regarding the permissible concentration in

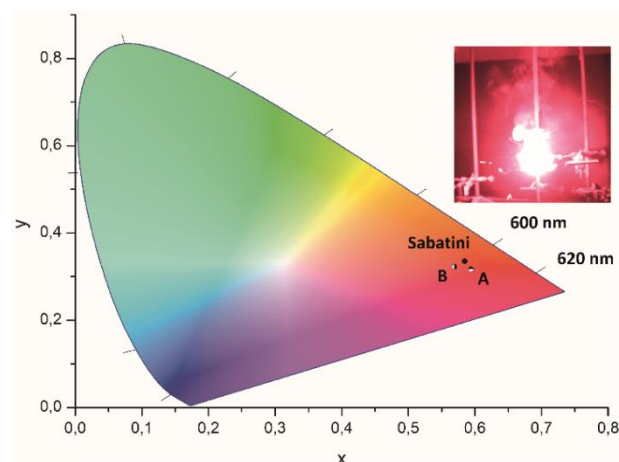


**Figure 1.** CIE 1931 chromaticity diagram of **A**, **B** and the reference formulation by Sabatini.

the water supply.<sup>[3,4]</sup> In the case of red-light-emitting pyrotechnics, additional chlorine sources like PVC are usually combined with strontium salts, typically strontium nitrate (colorant) to produce the metastable red light emitter  $\text{Sr(I)Cl}$ .<sup>[5]</sup> During the combustion of chlorine-containing pyrotechnic formulations, highly carcinogenic polychlorinated biphenyls, polychlorinated dibenzofurans, and polychlorinated dibenzo-*p*-dioxins are formed.<sup>[6]</sup>

In 2015, Sabatini *et al.* reported first about a chlorine-free red light composition based on strontium nitrate, which meets the U.S. Army performance requirements for red light (dominant wavelength (DW) =  $620 \pm 20$  nm; spectral purity (SP)  $\geq 76\%$ ) and at the same time prevents the formation of toxic chlorine-containing compounds (**Figure 1**).<sup>[7]</sup> In addition to the perchlorate issue, a new environmental issue may arise. In November 2016, the European Union sued Germany for excessive nitrate concentrations in the groundwater. According to the new regulations, the groundwater concentration of nitrates between 2012–2014 exceeded the threshold value of 50 mg/L in 28% of the checkpoints. Further 8.5 % were already in between 40–50 mg/L. Such a high value may harm expectant mothers and young children. Even though the candidate to blame is clearly identified as the intensive agriculture, military practice grounds and civilian fireworks are a source of environmental pollution, too.<sup>[5d,8]</sup> A possible solution for “greener” pyrotechnics is the application of high-nitrogen compounds.<sup>[5a,5b, 9]</sup> High-nitrogen energetic salts derive their energy from their high positive heat of formation upon release of non-toxic dinitrogen gas as a main combustion product.<sup>[10]</sup> This is beneficial to achieve brilliant colors and a good color performance.<sup>[11]</sup>

Introducing additional nitro, nitramino or N-oxide moieties to high-nitrogen compounds such as tetrazoles or triazoles may optimize the energetic performance and the oxygen balance of the target

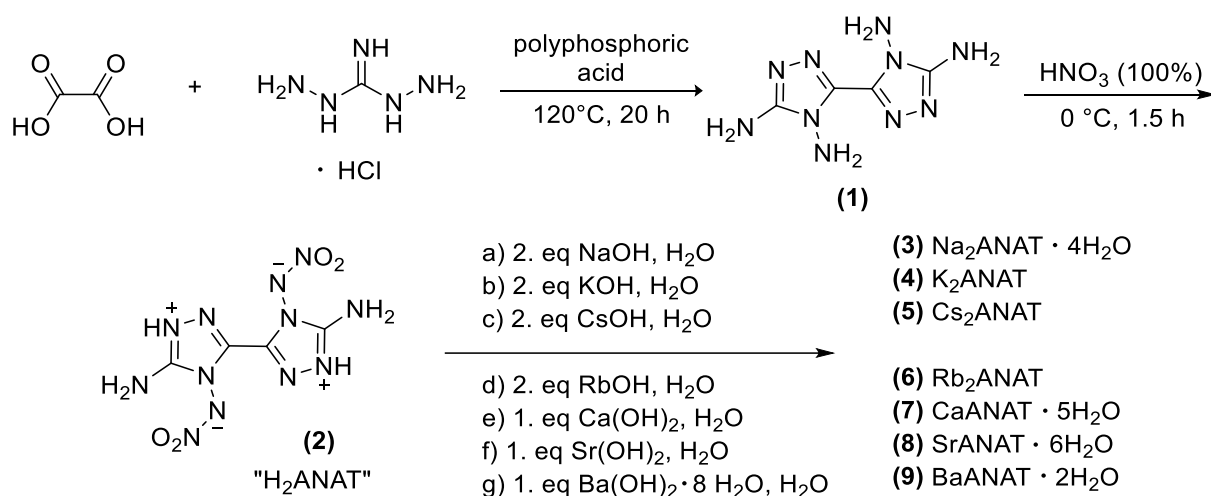
## Metal Salts of 3,3'-Diamino-4,4'-dinitramino-5,5'-bi-1,2,4-triazole in Pyrotechnic Compositions

molecule.<sup>[12]</sup> As a consequence, no further oxidizers like nitrates would be needed. Since future applications of new environmentally friendly compounds in the pyrotechnic sector are often cost forbidden, we focused on the recently reported 3,3'-diamino-4,4'-dinitramino-5,5'-bi-1,2,4-triazole and the corresponding alkali/alkaline earth metal salts thereof.<sup>[13]</sup> The target metal salts can be synthesized in a simple three steps synthesis starting from commercially available compounds. No organic solvents are needed. The new developed chlorine/nitrate free red-light-emitting pyrotechnical formulations based on the newly synthesized strontium salt achieve a dominant wavelength (DW) = 616 nm and a spectral purity (SP) = 75%. The present paper discusses the syntheses of the corresponding metal salts and the results of DW and SP for the developed strontium-containing formulations. In addition, sensitivity measurements have been carried out to secure safe handling.

## 6.2. Results and Discussion

### 6.2.1. Syntheses

The starting material 3,3'-diamino-4,4'-dinitramino-5,5'-bi-1,2,4-triazole (**2**) was synthesized according to a literature procedure by stepwise condensation of 1,3-diamino-guanidine monohydrochloride with oxalic acid and further selective N-amino nitration (**Scheme 1**).<sup>[13a]</sup> The preparation of **2** and its energetic salts **3–9** is displayed in **Scheme 1**. 1,3-Diaminoguanidine hydrochloride and oxalic acid were dissolved in polyphosphoric acid and heated to give 4,4',5,5'-tetraamino-3,3'-bi-1,2,4-triazole (**1**). **1** was slowly added to ice-cooled 100% HNO<sub>3</sub> and stirred at 0 °C for 1.5 h. Afterward the solution was quenched with ice-water and the formed precipitate was filtered off yielding pure **2**. Compound **2** can be used as obtained and does not require further purification such as chromatography, or recrystallization.



**Scheme 1.** Synthetic route toward compounds **1–9**.



## Metal Salts of 3,3'-Diamino-4,4'-dinitramino-5,5'-bi-1,2,4-triazole in Pyrotechnic Compositions

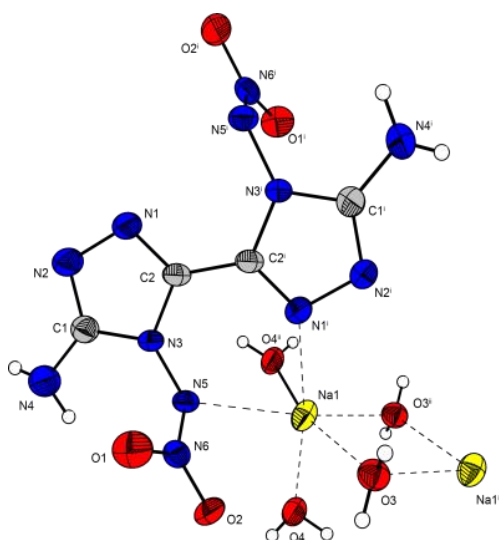
The alkali and alkaline earth salts of **2** were obtained by the reaction of compound **2** with the corresponding metal hydroxides. Therefore **2** was suspended in water and the corresponding base was added. The suspension was heated until a clear solution appeared and then left for crystallization to obtain compounds **3–9**. Compound **9** was obtained as a brown powder. The corresponding lithium salt was reported earlier.<sup>[13b]</sup>

### 6.2.2. Crystal Structures

The crystal structures of compounds **3–8** were determined. The crystal structures were uploaded to the CSD database<sup>[14]</sup> and can be obtained free of charge with the CCDC nos. 1837414 (**3**), 1837411 (**4**), 1837410 (**5**), 1837413 (**6**), 1837409 (**7**), and 1837412 (**8**). In addition, selected data and parameters of the X-ray measurement can be found in the Supporting Information.

The molecular structures of compounds **3–8** are similar to the neutral compound **1**. All bond lengths and angles are similar to the neutral compound. Also, the anion of **3–8** is in plane except for the two nitramino groups. The two nitramino groups are tilted out of the plane by 70–73°. Only compound **5** slightly differ from the neutral compound.

Disodium 3,3'-diamino-4,4'-dinitramino-5,5'-bitriazolate tetrahydrate (**3**) crystallizes from water in the triclinic space group *P*-1 with two molecules per unit cell and a density of 1.716 g cm<sup>-3</sup> at 293 K. The molecular unit of **3** is illustrated in **Figure 2**. The sphere of atom Na1 is characterized by distorted tetrahedral coordination of four atoms (O3i, O3ii, N1, N5i). A dimeric motif is formed by two bridging water molecules O3<sup>ii</sup>/O3 and the atoms Na1/Na1<sup>ii</sup> (**Figure 2**). The dimeric motif is in plane and revealed a distance between the atoms Na1-O3 of approximately 2.45 Å. The observed angles between the atoms Na1-O3<sup>ii</sup>-Na1<sup>ii</sup> and O3<sup>ii</sup>-Na1-O3 are approximately 90°. The coordination distance between the atoms Na1-O3 (2.43 Å) is in good agreement with the literature reported values (2.37 Å).<sup>[15]</sup>





## Metal Salts of 3,3'-Diamino-4,4'-dinitramino-5,5'-bi-1,2,4-triazole in Pyrotechnic Compositions

atoms C1-C3 is in the range of the neutral and the guanidinium compound (1.45 Å). The nitramino moiety is twisted out of plane ( $\text{N3-N5-N6-O1} = 71^\circ$ ).

The cesium atom (Cs1) is coordinated by one oxygen atom (O1). The observed distance between the atoms Cs1-O1 is 3.20 Å and is in good agreement with literature reported values.<sup>[16]</sup>

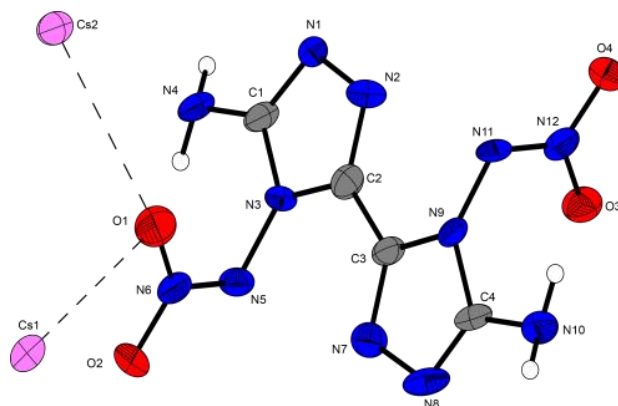


**Figure 4.** Molecular unit of **5** showing the atom-labeling scheme. Ellipsoids represent the 50% probability level. Selected bond length (Å): Cs1-O1 3.292(9), Cs2-O1 3.375(8). Selected torsion angles ( $^\circ$ ): N2-C2-N3-N5 2.275(9), N3-N5-N6 108.521(1).

Dirubidium 3,3'-diamino-4,4'-dinitramino-5,5'-bitriazolate (**6**) crystallizes from water in the monoclinic space group  $P2_1/n$  with two molecules per unit cell and a density of  $2.424 \text{ g cm}^{-3}$  at 173 K. The molecular unit of **6** is illustrated in **Figure 5**. The rubidium atom is distorted coordinated by one oxygen atom of the nitro group. The observed distance between the atoms Rb1-O2 is approximately 2.85 Å.

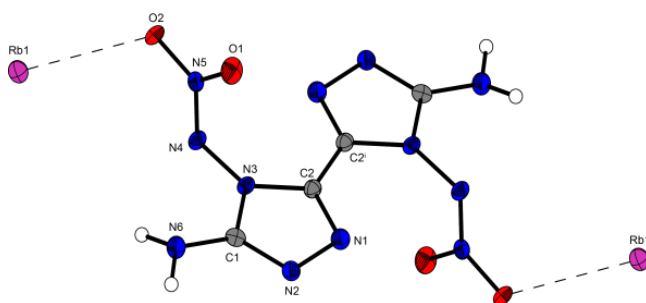


**Figure 5.** Molecular unit of **6** showing the atom-labeling scheme. Ellipsoids represent the 50% probability level. ( $i = 1-x, 1-y, 2-z$ ). Selected bond length (Å): Rb1-O2 2.8519(1).

Calcium 3,3'-diamino-4,4'-dinitramino-5,5'-bitriazolate pentahydrate (**7**) crystallizes from water in the monoclinic space group  $C2/c$  with five molecules per unit cell and a density of  $1.737 \text{ g cm}^{-3}$  at 173 K. The molecular unit of **7** is illustrated in **Figure 6**. The calcium atom (Ca1) is distorted coordinated by four water molecules (O3, O3i, O4, O4i) and two times by one oxygen atom (O2) and one nitrogen atom (N5) of the nitramino group. The observed coordination distance between the atoms Ca1-O3, Ca1-O3i,

## Metal Salts of 3,3'-Diamino-4,4'-dinitramino-5,5'-bi-1,2,4-triazole in Pyrotechnic Compositions

Ca1-O4, Ca1-O4i is approximately 2.37 Å. The distance between the atoms Ca1-O2, Ca1-O2i, and Ca1-N5, Ca1-N5i is 2.48 Å and 2.58 Å respectively. The view of multiple unit cells along the *a* axis indicates a stacking of both the anions and the calcium atoms.

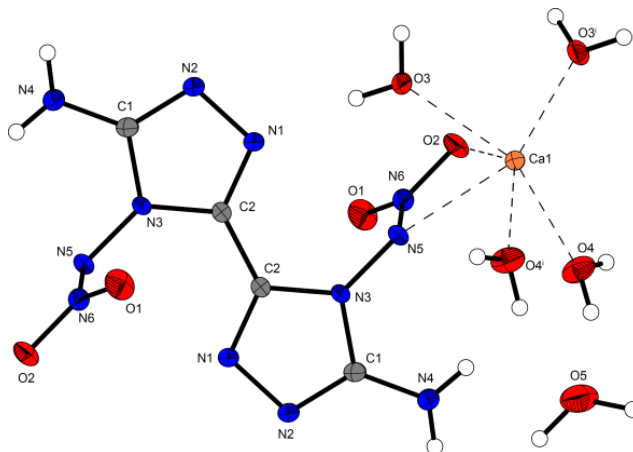


**Figure 6.** Molecular unit of **7** showing the atom-labeling scheme. Ellipsoids represent the 50% probability level. Symmetry codes: (i = 0.5+x, 0.5+y, z). Selected bond length (Å): Ca1-O2 2.4801(14), Ca1-O3 2.3797(14), Ca1-O4 2.3614(1), Ca1-N5 2.5785(1).

Strontium 3,3'-diamino-4,4'-dinitramino-5,5'-bitriazolate hexahydrate (**8**) crystallizes from water in the monoclinic space group  $P2_1/m$  with two molecules per unit cell and a density of 1.908 g cm<sup>-3</sup> at 295 K. The molecular unit of **8** is illustrated in **Figure 7**. The bond lengths between all the atoms in the triazole ring are in the range of the reported guanidinium salt.<sup>[13a]</sup> The observed bond length of the ring nitrogen atoms are between the values for a N-N single bond (1.47 Å) and a N=N double bond (1.25 Å).<sup>[17]</sup> The strontium atom (Sr1) is distorted septahedral coordinated by five water molecules (O2, O3, O6, O5i, O5, O4), as well as by one oxygen atom (O2) and one nitrogen atom (N5) of the nitramino group. The observed distances between the atoms Sr1-O2, Sr-O3, Sr1-O4, Sr1-O5 is in the range of 2.53–2.66 Å. The coordination distance between the atoms Sr1-O2 and Sr1-N5 is 2.77 Å. The view of multiple unit cells along the *a* axis indicates a stacking of both the anions and the strontium atoms. Two strontium atoms are connected to each other via two hydrogen bridges Sr1-O6-H7a (2.76 Å) and O7-H7b-O4 (2.25 Å).

## Metal Salts of 3,3'-Damino-4,4'-dinitramino-5,5'-bi-1,2,4-triazole in Pyrotechnic Compositions

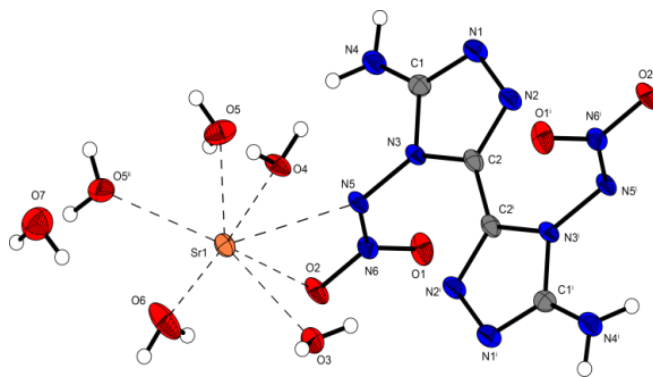


**Figure 7.** Molecular unit of **8** showing the atom-labeling scheme. Ellipsoids represent the 50% probability level. Symmetry codes: (i = 1+x, 0.5-y, z). Selected bond length (Å): Sr1-O2 2.7687(18), Sr1-O3 2.582(3), Sr1-O4 2.531(3), Sr1-O5 2.601(2), Sr1-O6 2.624(3), Sr1-N5 2.765(2).

### 6.2.3. Thermal and energetic properties

The decomposition temperatures  $T_{dec}$  of compounds **2–9** was determined by means of differential thermal analysis (DTA) with a heating rate of 5 °C min<sup>-1</sup>. The decomposition temperatures are given as onset temperatures (**Table 1/Table 2**).

**Table 1.** Thermal and energetic properties of compounds **2–5**.

	<b>2</b> <sup>[13]</sup>	<b>3</b>	<b>4</b>	<b>5</b>
<i>FS</i> [N]	120	360	360	360
<i>IS</i> [J]	9	40	3	8
<i>T<sub>onset</sub></i> [°C]	259	287	250	220

Annotation: BAM standard; FS = friction sensitivity; IS = impact sensitivity;  $T_{onset}$  = decomposition temperature (heating rate of 5 °C min<sup>-1</sup>).

All tested metal salts are completely insensitive toward friction. Compounds **3**, **7**, **8** and **9** contain at least two water molecules per unit cell and are insensitive toward impact. In contrast, the crystal water-free compounds **4**, **5** and **6** are categorized as impact sensitive. Compound **4** is very sensitive toward impact (**Table 1/Table 2**).

**Table 2.** Thermal and energetic properties of compounds **6–9**.

<b>6</b>	<b>7</b>	<b>8</b>	<b>9</b>
----------	----------	----------	----------

**Metal Salts of 3,3'-Damino-4,4'-dinitramino-5,5'-bi-1,2,4-triazole in  
Pyrotechnic Compositions**

<b>FS [N]</b>	360	360	360	360
<b>IS [J]</b>	10	40	40	40
<b>T<sub>onset</sub> [°C]</b>	250	150 <sub>dehdyr.-dec.</sub>	160 <sub>dehdyr.-dec.</sub>	280

Annotation: BAM standard; FS = friction sensitivity; IS = impact sensitivity; T<sub>onset</sub> = decomposition temperature (heating rate of 5 °C min<sup>-1</sup>).

All tested metal salts show high decomposition temperatures in the range from 250 °C to 287 °C. Only compound **7** and **8** showed an earlier dehydration-decomposition transition at 150 °C and 160 °C (Table 1/Table 2).

#### 6.2.4. Pyrotechnical formulations

In this project, we focused on the use of strontium salt **8** as a colorant for red-light-producing signal flares. The obtained formulations were compared to a chlorine-free strontium containing formulation published by Sabatini *et al.* in 2015 which meets the US Army requirement for the spectral purity (SP) and dominant wavelength (DW) (Table 3). A major goal was to achieve comparable good red light applying no chlorine and nitrate compounds in our formulations to meet potential future regulations.

**Table 3.** Reference formulation by Sabatini.<sup>[7]</sup>

<b>Mixture/ wt%</b>	<b>Sr(NO<sub>3</sub>)<sub>2</sub></b>	<b>Mg 50/100 Mesh</b>	<b>5-AT</b>	<b>Epoxy Binder<sup>[a]</sup></b>
<b>Sabatini</b>	48.0	33.0	12.0	7.0

[a] = Epon 813/Versamid 140 (80:20).

The current US Army in-service M158 red star cluster formulation consists of strontium nitrate (48 wt%), Mg (30/50 Mesh, 33 wt%), PVC (15 wt%) and Laminac 4116 /Lupersol (4 wt%). Starting from this formulation, Sabatini *et al.* replaced the Laminac 4116/Lupersol binder system with a simple “drop-in” of Epon 813/Versamid 140 for environmental reasons.<sup>[7]</sup>

**Table 4.** New formulations based on **8**.

<b>Mixture/ wt%</b>	<b>Mg 30/50 Mesh</b>	<b>8</b>	<b>5-AT</b>	<b>Epoxy Binder<sup>[a]</sup></b>	<b>NC<sup>[b]</sup></b>
<b>A</b>	35.3	47.1	11.7	3.9	2.0
<b>B</b>	33.0	50.0	13.0	–	4.0

## Metal Salts of 3,3'-Damino-4,4'-dinitramino-5,5'-bi-1,2,4-triazole in Pyrotechnic Compositions

[a] = Epon 813/Versamid 140 (50:50); [b] = Nitrocellulose solution (4–8%) in ethanol/diethyl ether (2 wt% = 1 mL on 1 g scale).

Compound **8** served as an oxidizer and colorant in one molecule. Mg and 5-AT act as fuel (Table 4). Formulation **A** applied a mixture of two binders (NC and epoxy binder); however, NC may also act as fuel in this formulation. In contrast, only the epoxy binder system was applied in formulation **B**.

**Table 5.** Performance values of tested formulations.

	<i>BT</i> [s]	<i>DW</i> [nm]	<i>SP</i> [%]
<b>US Army requirement</b> <sup>[7]</sup>	–	620±20	≥76
<b>Sabatini</b>	5	607	79
<b>A</b>	8	616	75
<b>B</b>	8	612	71

[a] = Epon 813/Versamid 140 (50:50); [b] = Nitrocellulose solution (4-8%) in ethanol/diethylether (2 wt% = 1 mL on 1 g scale).

Testing the new developed formulations, **A** and **B** on a 1 g scale revealed an increased DW compared to the reference formulation. However, both formulations failed to meet the SP requirement.

**Table 6.** Sensitivities of the tested formulations.

	<i>IS</i> [J]	<i>FS</i> [N]	<i>T<sub>onset</sub></i> [°C]
<b>Sabatini</b>	9	240	231
<b>A</b>	30	360	156
<b>B</b>	30	360	156

Annotation: BAM standard; FS = friction sensitivity; IS = impact sensitivity; *T<sub>onset</sub>* = decomposition temperature (heating rate of 5 °C min<sup>−1</sup>).

The safe handling of formulations **A** and **B** can be guaranteed by low sensitivities compared to Sabatini's formulation (**Table 6**). Applying a binder mixture of NC and an epoxy binder system in **A** resulted in the same sensitivity toward mechanical stimuli as measured for formulation **B**. Formulation **A** and **B** displayed identical decomposition temperatures at 156 °C which is close to the decomposition temperature of the pure compound **8**.

### 6.3. Conclusions

Several alkali and alkaline earth salts of 3,3'-diamino-4,4'-dinitramino-5,5'-bi-1,2,4-triazole (H<sub>2</sub>ANAT) were synthesized and intensively characterized. Crystal structures with the exception of the barium salt were determined and discussed. The herein presented synthesis is free of organic solvents, which helps to reduce solvent and other wastes in flare manufacturing. The energetic and thermal investigations revealed low sensitivities toward mechanical stimuli and high decomposition temperatures of the corresponding metals salts. Future investigations will focus on improving the spectral purities while maintaining the high dominant wavelengths of the developed red-light-emitting pyrotechnical formulations. Since all pyrotechnical formulations are to some extent scale-sensitive, the investigation of the luminous intensity is postponed to full-scale test, which will also show the compatibility with other requirements such as burn time and ignition reliability of the prototype device.

### 6.4. Experimental Section

**CAUTION!** The compounds described in this work are potential explosives, which are sensitive to external stimuli such as impact, friction, heat or electrostatic discharge. While no issues in the handling of these materials were encountered, appropriate precautions and proper protective measures (safety glasses, face shields, leather coat, Kevlar gloves and ear protectors) should be taken when preparing and manipulating these materials.

**General:** All reagents and solvents were purchased from Sigma-Aldrich, Fluka, and Acros Organics. Decomposition temperatures were measured with a OZM Research DTA 552-Ex Differential Thermal Analyzer using heating rates of 5 °C min<sup>-1</sup>. <sup>1</sup>H and <sup>13</sup>C NMR spectra were measured with a JEOL Eclipse 400, JEOL Eclipse 270 or JEOL EX400 instrument at an ambient temperature. All chemical shifts are quoted in ppm relative to TMS (<sup>1</sup>H, <sup>13</sup>C) as external standards. Infrared spectra were measured using a Perkin-Elmer Spectrum One FT-IR spectrometer. Elemental analyses were performed with an Elementar Vario EL or an Elementar Vario EL micro cube. The impact and friction sensitivities were determined using a BAM drophammer and a BAM friction tester. The sensitivities of the compounds were indicated according to the UN Recommendations on the Transport of Dangerous Goods. (+): impact: insensitive >40 J, less sensitive >35 J, sensitive >4 J, very sensitive <4 J; friction: insensitive >360 N, less sensitive=360 N, sensitive <360 N, very sensitive <80 N, extreme sensitive <10 N.<sup>[19]</sup> The values represent the lowest impact energy at which the result “explosion or deflagration” is obtained from at least one out of at least six trials. The controlled burn down of the pyrotechnic formulations was filmed with a digital video camera recorder (SONY, DCR-HC37E). Spectrometric measurements of the



## Metal Salts of 3,3'-Diamino-4,4'-dinitramino-5,5'-bi-1,2,4-triazole in Pyrotechnic Compositions

formulations were performed with a HR2000+ES spectrometer with an ILX511B linear silicon CCD-array detector and included software from Ocean Optics with a detector-sample distance of 1 meter. The dominant wavelength and spectral purity were measured based on the 1931 CIE method using illuminant C as the white reference point. Four samples were measured for each formulation.

**Preparation of pyrotechnic formulations:** The samples were weighed out according to their weight percentages (max. 1 g total) into a mortar. After grinding by hand for 3 min, both the Epon 813 (20 mg/mL) and the Versamid 140 solution (10 mg/mL) in ethyl acetate were added using a syringe. The mixture was blended with a spatula every 10 min until the solvent was evaporated. The solid material was stored over night at 70 °C in the drying oven for curing. Before consolidation, the pyrotechnic material was ground again by hand for 3 min. The formulations were pressed with the aid of a tooling die (inner diameter 12.9 mm) into a cylindrical shape. The formulation powders were pressed at a consolidation dead load of 2 t with a dwell time of 3 s.

**Metal 3,3'-Diamino-4,4'-dinitramino-5,5'-bi-1,2,4-triazole Salts:** The 3,3'-diamino-4,4'-dinitramino-5,5'-bi-1,2,4-triazole (**2**) salts were synthesized by suspending **2** (300 mg, 1.05 mmol) in water. The corresponding metal bases were added in stoichiometric amounts and heated until a clear solution appeared. After cooling to ambient temperatures, the solution was left for crystallization. The obtained solids were recrystallized from a solvent mixture of ethanol/water (1:2).

### Disodium 3,3'-diamino-4,4'-dinitramino-5,5'-bitriazolate tetrahydrate (**3**)

**3** was obtained as a brown powder. Recrystallization leads to yellow crystals. **Yield:** 363 mg (0.902 mmol, 86 %). **<sup>1</sup>H NMR** ([D<sub>6</sub>]DMSO):  $\delta$  = 5.26 (s, 4 H, -NH<sub>2</sub>) ppm. **<sup>13</sup>C NMR** ([D<sub>6</sub>]DMSO):  $\delta$  = 138.1 (2C, CC), 153.4 (2C, -CNO<sub>2</sub>) ppm. C<sub>4</sub>H<sub>4</sub>N<sub>12</sub>O<sub>4</sub>Na<sub>2</sub> · 4H<sub>2</sub>O (402.19): calcd. C 11.95, H 3.01, N 41.79%; found C 12.13, H 2.99, N 41.29%. **IR** (ATR):  $\tilde{\nu}$  = 3455 (m), 3390 (m), 3292 (m), 3225 (m), 1687 (w), 1618 (s), 1558 (m), 1465 (m), 1393 (s), 1286 (s), 1221 (s), 1093 (w), 1031 (m), 972 (m), 887 (m), 738 (w), 707 (w) cm<sup>-1</sup>. **IS** (grain size <100µm): 40 J. **FS** (grain size <100µm): 360 N. **DTA:** 287 °C (onset.).

### Dipotassium 3,3'-diamino-4,4'-dinitramino-5,5'-bitriazolate (**4**)

**4** was obtained as a brown powder. Recrystallization leads yellow crystals. **Yield:** 353 mg (0.973 mmol, 93 %). **<sup>1</sup>H NMR** ([D<sub>6</sub>]D<sub>2</sub>O):  $\delta$  = 9.55 (s, 4 H, -NH<sub>2</sub>) ppm. **<sup>13</sup>C NMR** ([D<sub>6</sub>]DMSO):  $\delta$  = 137.6 (2C, CC), 153.7 (2C, -CNO<sub>2</sub>) ppm. C<sub>4</sub>H<sub>4</sub>N<sub>12</sub>O<sub>4</sub>K<sub>2</sub> (362.35): calcd. C 13.26, H 1.11, N 46.93%; found C 13.36, H 1.47, N 45.36%. **IR** (ATR):  $\tilde{\nu}$  = 3373 (m), 3291 (w), 3218 (w), 3079 (m), 1639 (s), 1561 (m), 1467 (m),

**Metal Salts of 3,3'-Diamino-4,4'-dinitramino-5,5'-bi-1,2,4-triazole in  
Pyrotechnic Compositions**

1426 (w), 1372 (s), 1286 (s), 1101 (m), 1030 (m), 1004 (w), 965 (m), 879 (m), 782 (m), 717 (m), 653 (w)  $\text{cm}^{-1}$ . **IS** (grain size <100 $\mu\text{m}$ ): 3 J. **FS** (grain size <100 $\mu\text{m}$ ): 360 N. **DTA**: 250 °C (onset.).

**Dicesium 3,3'-diamino-4,4'-dinitramino-5,5'-bitriazolate (5)**

**5** was obtained as yellow crystals. **Yield**: 541 mg (0.983 mmol, 94 %).  **$^1\text{H}$  NMR** ([D6]  $\text{D}_2\text{O}$ ):  $\delta$  = 9.57 (s, 4 H,  $-\text{NH}_2$ ) ppm.  **$^{13}\text{C}$  NMR** ([D6] $\text{D}_2\text{O}$ ):  $\delta$  = 137.7 (2C, CC), 154.0 (2C,  $-\text{CNO}_2$ ) ppm.  $\text{C}_4\text{H}_4\text{N}_{12}\text{O}_4\text{Cs}_2$  (549.96): calcd. C 8.74, H 0.73, N 30.56%; found C 8.73, H 0.91, N 29.51%. **IR** (ATR):  $\tilde{\nu}$  = 3343 (w), 3291 (w), 3080 (w), 1636 (m), 1554 (m), 1465 (m), 1367 (s), 1281 (s), 1219 (m), 1119 (w), 1029 (m), 997 (w), 964 (w), 876 (m), 833 (w), 779 (w), 715 (m), 696 (m), 653 (w)  $\text{cm}^{-1}$ . **IS** (grain size <100 $\mu\text{m}$ ): 8 J. **FS** (grain size <100 $\mu\text{m}$ ): 360 N. **DTA**: 220 °C (onset.).

**Dirubidium 3,3'-diamino-4,4'-dinitramino-5,5'-bitriazolate (6)**

**6** was obtained as a brown powder. Recrystallization leads to colorless crystals. **Yield**: 430 mg (0.945 mmol, 90 %).  **$^1\text{H}$  NMR** ([D6] $\text{D}_2\text{O}$ ):  $\delta$  = 9.55 (s, 4 H,  $-\text{NH}_2$ ) ppm.  **$^{13}\text{C}$  NMR** ([D6] $\text{DMSO}$ ):  $\delta$  = 138.37 (2C, CC), 154.6 (2C,  $-\text{CNO}_2$ ) ppm.  $\text{C}_4\text{H}_4\text{N}_{12}\text{O}_4\text{Rb}_2$  (455.09): calcd. C 10.65, H 0.89, N 36.93%; found C 10.94, H 1.28, N 37.40%. **IR** (ATR):  $\tilde{\nu}$  = 3376 (m), 3289 (w), 3215 (s), 3096 (m), 1740 (w), 1635 (s), 1559 (m), 1465 (m), 1374 (s), 1283 (s), 1220 (s), 1105 (m), 1026 (m), 1105 (w), 1026 (m), 964 (m), 877 (m), 782 (w), 717 (w), 650 (w)  $\text{cm}^{-1}$ . **IS** (grain size <100 $\mu\text{m}$ ): 10 J. **FS** (grain size <100 $\mu\text{m}$ ): 360 N. **DTA**: 250 °C (onset.).

**Calcium 3,3'-diamino-4,4'-dinitramino-5,5'-bitriazolate pentahydrate (7)**

**7** was obtained as a brown powder. Recrystallization leads to yellow crystals. **Yield**: 383 g (924 mmol, 88 %).  **$^1\text{H}$  NMR** ([D6] $\text{DMSO}$ ):  $\delta$  = 5.33 (s, 4 H,  $-\text{NH}_2$ ) ppm.  **$^{13}\text{C}$  NMR** ([D6] $\text{DMSO}$ ):  $\delta$  = 138.0 (2C, CC), 153.4 (2C,  $-\text{CNO}_2$ ) ppm.  $\text{C}_4\text{H}_4\text{N}_{12}\text{O}_4\text{Ca} \cdot 5\text{H}_2\text{O}$  (414.31): calcd. C 11.60, H 3.41, N 40.57%; found C 11.93, H 3.42, N 40.39%. **IR** (ATR):  $\tilde{\nu}$  = 3435 (m), 3346 (m), 1739 (w), 1616 (s), 1554 (m), 1470 (m), 1435 (m), 1418 (m), 1283 (s), 1247 (m), 1102 (w), 1035 (w), 1017 (m), 973 (m), 904 (m), 776 (w), 756 (w), 719 (w), 677 (w), 653 (w)  $\text{cm}^{-1}$ . **IS** (grain size <100 $\mu\text{m}$ ): 40 J. **FS** (grain size <100 $\mu\text{m}$ ): 360 N. **DTA**: 150 °C (onset.).

**Strontium 3,3'-diamino-4,4'-dinitramino-5,5'-bitriazolate hexahydrate (8)**

**8** was obtained as an orange powder. Recrystallization leads to colorless crystals. **Yield**: 459 mg (0.957 mmol, 91 %).  **$^1\text{H}$  NMR** ([D6] $\text{DMSO}$ ):  $\delta$  = 6.00 (s, 4 H,  $-\text{NH}_2$ ) ppm.  **$^{13}\text{C}$  NMR** ([D6] $\text{DMSO}$ ):  $\delta$  = 138.1 (2C, CC), 153.0 (2C,  $-\text{CNO}_2$ ) ppm.  $\text{C}_4\text{H}_4\text{N}_{12}\text{O}_4\text{Sr} \cdot 6\text{H}_2\text{O}$  (479.86): calcd. C 10.01, H 3.31, N 35.03%;

## Metal Salts of 3,3'-Damino-4,4'-dinitramino-5,5'-bi-1,2,4-triazole in Pyrotechnic Compositions

found C 9.94, H 3.19, N 34.62%. **IR** (ATR):  $\tilde{\nu}$  = 3549 (m), 3292 (s), 3229 (s), 3176 (s), 17139 (w), 1621 (s), 1566 (s), 1472 (m), 1412 (s), 1299 (s), 1234 (s), 1130 (m), 1050 (m), 1024 (w), 976 (m), 900 (m), 779 (w), 714 8w), 658 (w)  $\text{cm}^{-1}$ . **IS** (grain size <100 $\mu\text{m}$ ): 40 J. **FS** (grain size <100 $\mu\text{m}$ ): 360 N. **DTA**: 250 °C (onset.).

### Barium 3,3'-diamino-4,4'-dinitramino-5,5'-bitriazolate dihydrate (**9**)

**9** already precipitated in boiling water and was obtained as a brown powder. Due to solubility issues, no further NMR analysis or recrystallization was possible since even boiling DMSO (Reflux 170 °C / 2h) failed to dissolve the crude product. **Yield**: 355 mg (0.770 mmol, 73 %).  $\text{C}_4\text{H}_4\text{N}_{12}\text{O}_4\text{Ba} \cdot 2\text{H}_2\text{O}$  (461.54): calcd. C 10.41, H 2.62, N 36.42%; found C 10.55, H 1.92, N 36.22%. **IR** (ATR):  $\tilde{\nu}$  = 3608 (w), 3410 (m), 3316 (m), 3252 (m), 3187 (m), 3000 (m), 2190 (w), 1629 (s), 1566 (s) 1472 (m)1442 (s), 1417 (s), 1291 (s) 1229 (s) 1092 (m) 1034 (m), 966 (m), 898 (s), 772 (m), 721 (w), (667 (w), 637 (w)  $\text{cm}^{-1}$ . **IS** (grain size <100 $\mu\text{m}$ ): 40 J. **FS** (grain size <100 $\mu\text{m}$ ): 360 N. **DTA**: 280 °C (onset.).

## 6.5. Acknowledgments

Financial support of this work by the Ludwig-Maximilian University of Munich (LMU) and the Office of Naval Research (ONR.N00014-16-1-2062) is gratefully acknowledged.

**Keywords:** Pyrotechnics • Chlorine-free • High-nitrogen Compound • Crystal Structure • Red Colorant

## 6.6. References

- [1] a)J. D. Moretti, C. M. Csernica, J. C. Poret, A. P. Shaw, N. E. Carlucci, M. G. Seiz, J. D. Conway, *ACS Sustainable Chem. Eng.* **2017**, 10.1021/acssuschemeng.7b02623; b)J. T. Koenig, A. P. Shaw, J. C. Poret, W. S. Eck, L. J. Groven, *ACS Sustainable Chem. Eng.* **2017**, 10.1021/acssuschemeng.7b02579; c)J. S. Brusnahan, A. P. Shaw, J. D. Moretti, W. S. Eck, *Propellants, Explos., Pyrotech.* **2017**, 42, 62-70; d)J. S. Brusnahan, J. C. Poret, J. D. Moretti, A. P. Shaw, R. K. Sadangi, *ACS Sustainable Chem. Eng.* **2016**, 4, 1827-1833; e); f)J. D. Moretti, J. J. Sabatini, A. P. Shaw, R. Gilbert, *ACS Sustainable Chem. Eng.* **2014**, 2, 1325-1330; g)E. J. Miklaszewski, A. P. Shaw, J. C. Poret, S. F. Son, L. J. Groven, *ACS Sustainable Chem. Eng.* **2014**, 2, 1312-1317.
- [2] a)P. Yin, J. Zhang, C. He, D. A. Parrish, J. n. M. Shreeve, *J. Mater. Chem. A* **2014**, 2, 3200-3208; b)C. K. Wilharm, A. Chin, S. K. Pliskin, *Propellants, Explos., Pyrotech.* **2014**, 39, 173-179; c)J. D. Moretti, J. J. Sabatini, G. Chen, *Angew. Chem. Int. Ed.* **2012**, 51, 6981-6983.

**Metal Salts of 3,3'-Damino-4,4'-dinitramino-5,5'-bi-1,2,4-triazole in  
Pyrotechnic Compositions**

- [3] K. Sellers, K. Weeks, W. R. Alsop, S. R. Clough, M. Hoyt, B. Pugh, *Perchlorate Environmental Problems and Solutions*, Taylor & Francis, Boca Raton, FL (USA), **2007**.
- [4] Health and Ecological Criteria Division, Office of Science and Technology, Office of Water, U.S. Environmental Protection Agency, *Interim Drinking Water Health Advisory for Perchlorate*, U.S. Environmental Protection Agency, Washington, DC, **2008**, EPA 822-R-08-025.
- [5] a)T. M. Klapötke, T. G. Müller, M. Rusan, J. Stierstorfer, *Z. Anorg. Allg. Chem.* **2014**, 640, 1347-1354; b)I. E. Drukenmüller, T. M. Klapötke, Y. Morgenstern, M. Rusan, J. Stierstorfer, *Z. Anorg. Allg. Chem.* **2014**, 640, 2139-2148; c)I. M. Tuukkanen, E. L. Charsley, P. G. Laye, J. J. Rooney, T. T. Griffiths, H. Lemmetyinen, *Propellants, Explos., Pyrotech.* **2006**, 31, 110-115; d)J. J. Sabatini, J. D. Moretti, *Chem. - Eur. J.* **2013**, 19, 12839-12845; e)B. E. Douda, *Theory of Colored Flame Production*, ADA951815, NSWC Crane, Indiana, USA, **1964**; f)J. A. Conkling, C. Mocella, *Chemistry of Pyrotechnics: Basic Principles and Theory*, CRC Press, Boca Raton **2010**.
- [6] W. Christmann, D. Kasiske, K. D. Klöppel, H. Partscht, W. Rotard, *Chemosphere* **1989**, 387-392.
- [7] J. J. Sabatini, E.-C. Koch, J. C. Poret, J. D. Moretti, S. M. Harbol, *Angew. Chem. Int. Ed.* **2015**, 54, 10968-10970.
- [8] G. Steinhauser, T. M. Klapötke, *Angew. Chem., Int. Ed.* **2008**, 47, 3330-3347.
- [9] a)J. Glück, T. M. Klapötke, M. Rusan, J. Stierstorfer, *Chem. - Eur. J.* **2014**, 20, 15947-15960; b)N. Fischer, M. Feller, T. M. Klapötke, M. Kowalewski, S. Scheutzow, J. Stierstorfer, *Propellants, Explos., Pyrotech.* **2014**, 39, 166-172; c)N. Fischer, T. M. Klapötke, S. Marchner, M. Rusan, S. Scheutzow, J. Stierstorfer, *Propellants, Explos., Pyrotech.* **2013**, 38, 448-459; d)N. Fischer, T. M. Klapötke, K. Peters, M. Rusan, J. Stierstorfer, *Z. Anorg. Allg. Chem.* **2011**, 637, 1693-1701; e)T. M. Klapötke, J. Stierstorfer, K. R. Tarantik, I. D. Thoma, *Z. Anorg. Allg. Chem.* **2008**, 634, 2777-2784; f)V. Ernst, T. M. Klapötke, J. Stierstorfer, *Z. Anorg. Allg. Chem.* **2007**, 633, 879-887; g)D. E. Chavez, M. A. Hiskey, D. L. Naud, *J. Pyrotech.* **1999**, 10, 17-36; h)D. E. Chavez, M. A. Hiskey, *J. Pyrotech.* **1998**, 7, 11-14; i)T. M. Klapötke, H. Radies, J. Stierstorfer, K. R. Tarantik, G. Chen, A. Nagori, *Propellants, Explos., Pyrotech.* **2010**, 35, 213-219; j)L. H. Finger, F. G. Schröder, J. Sundermeyer, *Z. Anorg. Allg. Chem.* **2013**, 639, 1140-1152.
- [10] T. M. Klapötke, *Chemistry of High-Energy Materials*, 10.1515/9783110536515, 4th ed., De Gruyter, Berlin, Boston, **2017**.
- [11] J. J. Sabatini, in *Green Energetic Materials* (Ed.: T. Brinck), John Wiley & Sons, Ltd, West Sussex, United Kingdom, **2014**, pp. 63-102.
- [12] P. Yin, Q. Zhang, J. M. Shreeve, *Acc. Chem. Res.* **2016**, 49, 4-16.

## Metal Salts of 3,3'-Damino-4,4'-dinitramino-5,5'-bi-1,2,4-triazole in Pyrotechnic Compositions

- [13] a) T. M. Klapötke, M. Leroux, P. C. Schmid, J. Stierstorfer, *Chem. - Asian J.* **2016**, *11*, 844-851;  
b) J. Glück, T. M. Klapötke, M. Rusan, J. J. Sabatini, J. Stierstorfer, *Angew. Chem., Int. Ed.* **2017**, *56*, 16507.
- [14] Crystallographic data for the structures have been deposited with the Cambridge Crystallographic Data Centre. Copies of the data can be obtained free of charge on application to The Director, CCDC, 12 Union Road, Cambridge CB2 1EZ, UK (Fax: int.code\_(1223)336-033; e-mail for inquiry: fileserv@ccdc.cam.ac.uk; e-mail for deposition: (deposit@ccdc.cam.ac.uk)).
- [15] L. E. Tønnesen, B. F. Pedersen, J. Klaveness, *Acta Chem. Scand.* **1996**, *50*, 603-608.
- [16] J. Mähler, I. Persson, *Inorg. Chem.* **2012**, *51*, 425-438.
- [17] A. Bondi, *J. Phys. Chem.* **1964**, *68*, 441-451.
- [18] J. C. Cackett, *Monograph on pyrotechnic compositions*, (Ed.: Royal Armament Research and Development Establishment), Ministry of Defence (Army), Fort Halstead, Seven Oaks, United Kingdom, **1965**, 53-54.
- [19] United Nations, *Recommendations on the Transport of Dangerous Goods: Manual of Tests and Criteria - Amendment 1 of the 5th Revised Edition*, 5th ed., **2011**, doi:http://dx.doi.org/10.18356/fbc2c205-en.

## 6.7. Supporting Information

### 6.7.1. Crystallographic data

The crystal structures were uploaded to the CSD database<sup>[1]</sup> and can be obtained free of charge with the CCDC nos. 1837414 (**3**), 1837411 (**4**), 1837410 (**5**), 1837413 (**6**), 1837409 (**7**), and 1837412 (**8**).

**Table S1.** Crystallographic data of **3–5**.

Compound	<b>3</b>	<b>4</b>	<b>5</b>
Formula	C <sub>4</sub> H <sub>4</sub> N <sub>12</sub> O <sub>4</sub> Na <sub>2</sub> · 4H <sub>2</sub> O	C <sub>4</sub> H <sub>4</sub> N <sub>12</sub> O <sub>4</sub> K <sub>2</sub>	C <sub>4</sub> H <sub>4</sub> N <sub>12</sub> O <sub>4</sub> Cs <sub>2</sub>
Form. Mass [g/mol]	201.12	181.20	550.01
Crystal system	triclinic	monoclinic	orthorhombic
Space Group	<i>P</i> -1 (No. 2)	<i>P</i> 2 <sub>1</sub> / <i>n</i> (No. 14)	<i>P</i> ca2 <sub>1</sub> (No. 29)
Color / Habit	yellow block	yellow block	yellow needle
Size [mm]	0.10 × 0.20 × 0.25	0.10 × 0.10 × 0.35	0.05 × 0.06 × 0.40

**Metal Salts of 3,3'-Damino-4,4'-dinitramino-5,5'-bi-1,2,4-triazole in  
Pyrotechnic Compositions**

<i>a</i> [Å]	5.7190(7)	8.7758(4)	15.4025(9)
<i>b</i> [Å]	8.0939(10)	4.9394(2)	4.9514(3)
<i>c</i> [Å]	9.4531(10)	14.3239(7)	17.9392(9)
$\alpha$ [°]	111.276(11)	90	90
$\beta$ [°]	103.533(10)	104.426(5)	90
$\gamma$ [°]	94.954(10)	90	90
<i>V</i> [Å <sup>3</sup> ]	389.28(9)	601.32(5)	1368.11(13)
<i>Z</i>	2	4	4
$\rho_{\text{calc.}}$ [g cm <sup>-3</sup> ]	1.716	2.001	2.670
$\mu$ [mm <sup>-1</sup> ]	0.201	0.836	5.372
<i>F</i> (000)	206	364	1016
$\lambda_{\text{MoK}\alpha}$ [Å]	0.71073	0.71073	0.71073
<i>T</i> [K]	293	294	296
$\vartheta$ min-max [°]	4.2, 26.0	4.4, 26.0	4.1, 26.0
Dataset <i>h</i> ; <i>k</i> ; <i>l</i>	-6:7; -7:9; -11:11	-10:10; -6:6; -17:17	-19:13; -6:5; -9:22
Reflect. coll.	2812	8041	3419
Independ. refl.	1516	1178	1820
<i>R</i> <sub>int</sub>	0.024	0.026	0.024
Reflection obs.	1157	1178	1857
No. parameters	142	108	200
<i>R</i> <sub>1</sub> (obs)	0.0394	0.0254	0.0327
<i>wR</i> <sub>2</sub> (all data)	0.1099	0.0683	0.0854
<i>S</i>	1.03	1.06	1.09
Resd. Dens. [e Å <sup>-3</sup> ]	-0.20, 0.41	-0.22, 0.35	-1.24, 1.87
Device type	Oxford Xcalibur3 CCD	Oxford Xcalibur3 CCD	Oxford Xcalibur3 CCD
Solution	SIR-92	SIR-92	SIR-92
Refinement	SHELXL-97	SHELXL-97	SHELXL-97
Absorpt. corr.	multi-scan	multi-scan	multi-scan
CCDC	1837414	1837411	1837410

**Table S2.** Crystallographic data of **6–8**.

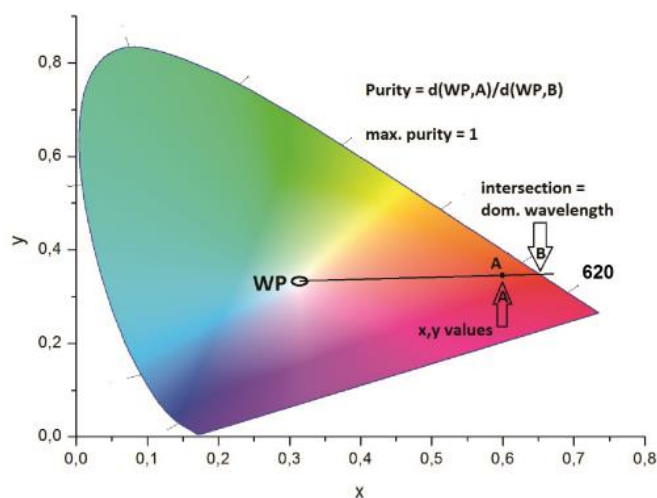
Compound	6	7	8
Formula	C <sub>4</sub> H <sub>4</sub> N <sub>12</sub> O <sub>4</sub> Rb <sub>2</sub>	C <sub>4</sub> H <sub>4</sub> N <sub>12</sub> O <sub>4</sub> Ca · 5H <sub>2</sub> O	C <sub>4</sub> H <sub>4</sub> N <sub>12</sub> O <sub>4</sub> Sr · 6H <sub>2</sub> O
Form. Mass [g/mol]	455.13	414.31	479.91
Crystal system	monoclinic	monoclinic	monoclinic
Space Group	<i>P</i> 2 <sub>1</sub> / <i>n</i> (No. 14)	<i>C</i> 2/ <i>c</i> (No. 15)	<i>P</i> 2 <sub>1</sub> / <i>m</i> (No. 11)
Color / Habit	colorless needle	yellow crystals	colorless block
Size [mm]	0.08 × 0.08 × 0.18	0.4 x 0.4 x 0.4	0.10 × 0.16 × 0.20

**Metal Salts of 3,3'-Damino-4,4'-dinitramino-5,5'-bi-1,2,4-triazole in  
Pyrotechnic Compositions**

<i>a</i> [Å]	8.8652(4)	11.4009(8)	6.3002(5)
<i>b</i> [Å]	5.1322(2)	13.7933(5)	13.4566(9)
<i>c</i> [Å]	14.1922(6)	11.5508(7)	10.1845(7)
$\alpha$ [°]	90	90	90
$\beta$ [°]	105.030(4)	119.273(9)	104.650(8)
$\gamma$ [°]	90	90	90
<i>V</i> [Å <sup>3</sup> ]	623.63(5)	1584.5(2)	835.36(11)
<i>Z</i>	2	4	2
$\rho_{\text{calc.}}$ [g cm <sup>-3</sup> ]	2.424	1.737	1.908
$\mu$ [mm <sup>-1</sup> ]	7.894	0.473	3.308
<i>F</i> (000)	436	856	484
$\lambda_{\text{MoK}\alpha}$ [Å]	0.71073	0.71073	0.71073
<i>T</i> [K]	173	173	295
$\theta$ min-max [°]	4.2, 26.0	4.6, 26.0	4.3, 27.0
Dataset <i>h</i> ; <i>k</i> ; <i>l</i>	-8:10; -6:6; -17:17	-12:14; -16:15 ; -14:14	-7:8; -17:16; -13:5
Reflect. coll.	4270	5873	3577
Independ. refl.	1226	1546	1880
<i>R</i> <sub>int</sub>	0.025	0.021	0.030
Reflection obs.	1226	1366	1880
No. parameters	108	147	164
<i>R</i> <sub>1</sub> (obs)	0.0223	0.0286	0.0315
<i>wR</i> <sub>2</sub> (all data)	0.0557	0.0767	0.0694
<i>S</i>	1.08	1.05	1.04
Resd. Dens. [e Å <sup>-3</sup> ]	-0.89, 0.37	-0.21, 0.43	-0.38, 0.72
Device type	Oxford Xcalibur3 CCD	Oxford Xcalibur3 CCD	Oxford Xcalibur3 CCD
Solution	SIR-92	SIR-92	SIR-92
Refinement	SHELXL-97	SHELXL-97	SHELXL-97
Absorpt. corr.	multi-scan	multi-scan	multi-scan
CCDC	1837413	1837409	1837412

## Metal Salts of 3,3'-Damino-4,4'-dinitramino-5,5'-bi-1,2,4-triazole in Pyrotechnic Compositions

### CIE 1931 chromaticity diagram



An easy way to show or compare the spectral purity and dominant wavelength of various formulations is CIE 1931 chromaticity diagram. The color purity of a visible flare with the chromaticity (x, y) is its difference from the illuminant's white point (WP) relative to the furthest point on the chromaticity diagram with the same hue (dominant wavelength for monochromatic sources). The color purity can be calculated by dividing the distance WP to A ( $x, y$ ) =  $d(\text{WP}, A)$  by the distance WP to B =  $d(\text{WP}, B)$ . B is the point with the maximum purity of 100% for the dominant wavelength of formulation A.<sup>[2]</sup> The higher the spectral purity of A, the more the point moves to the right until it ends up having the coordinates of B.

### 6.7.2. References

- [1] Crystallographic data for the structures have been deposited with the Cambridge Crystallographic Data Centre. Copies of the data can be obtained free of charge on application to The Director, CCDC, 12 Union Road, Cambridge CB2 1EZ, UK (Fax: int. code (1223)336-033; e-mail for inquiry: [fileserv@ccdc.cam.ac.uk](mailto:fileserv@ccdc.cam.ac.uk); e-mail for deposition: [deposit@ccdc.cam.ac.uk](mailto:deposit@ccdc.cam.ac.uk)).
- [2] T. M. Klapötke, *Chemistry of High-Energy Materials*, 4th ed., De Gruyter, Berlin, Boston, **2017**.

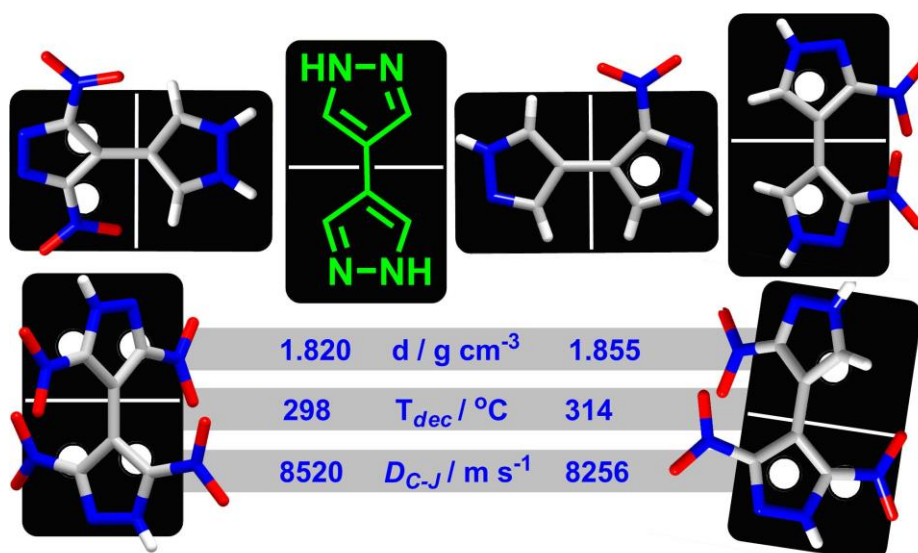


## 7. Facile and Selective Polynitrations at the 4-Pyrazolyl Dual Backbone: A Straightforward Access to a Series of High-Density Energetic Materials

Kostiantyn V. Domasevitch, Ivan Gospodinov, Harald Krautscheid, Thomas M. Klapötke and Jörg Stierstorfer

Published in *New J. Chem.* **2019**, *43*, 1305–1312.

DOI: 10.1039/c8nj05266b



**Abstract:** Nitro-functionalized energetic materials are still needed to meet new safety, performance and chemical accessibility demands. The problem of multiple C-nitrations on N-containing heterocycles was resolved successfully for the 4,4'-bipyrazole scaffold. A progression of gradually functionalized 3-nitro-4,4'-bipyrazole (**2**), 3,3'-dinitro-4,4'-bipyrazole (**3**), 3,5-dinitro-4,4'-bipyrazole (**4**), 3,3',5-trinitro-4,4'-bipyrazole (**5**) and 3,3',5,5'-tetranitro-4,4'-bipyrazole (**6**) was obtained in excellent yields by highly selective direct nitrations of 4,4'-bipyrazole (**1**). All synthesized polynitro derivatives **3–6** exhibit high decomposition temperatures of above 290 °C. The introduction of three (**5**) and four nitro groups (**6**) into the 4,4'-bipyrazole scaffold yields insensitive and thermally stable high explosives with excellent densities and detonation properties.

## Facile and Selective Polynitrations at the 4-Pyrazolyl Dual Backbone: A Straightforward Access to a Series of High-Density Energetic Materials

The anhydrous structures of compounds **2–6** were obtained by low-temperature XRD. In addition, the performance of compounds **5** and **6** was investigated with the small scale shock reactivity test

### 7.1. Introduction

Practical uses of high energy density materials, in particular those based on common explosives nitro groups, imply needs for performance in a combination with thermal stability and insensitivity toward external stimuli.<sup>[1]</sup> Environmental benign energetic materials, either in the view of green decomposition products or safety of production and storage, is also recognized as an important limitation.<sup>[2]</sup> The development of such materials is an ongoing challenge since many of the above issues are inherently hardly compatible and the compounds, which fulfill the sensitivity, stability, and performance requirements are still rare.<sup>[1]</sup> Recent years indicate an enormous interest toward design of such materials, while utilizing polynitrogen heterocycle platforms for accommodation of multiple explosives groups.<sup>[3]</sup> In this respect, the nitro-functionalized pyrazole backbone offers many special and valuable possibilities, with such key inputs as high nitrogen content, good thermal stability, chemical robustness and versatility of structural functions due to original protolytic behavior. The prototypical 3,4,5-trinitropyrazole reveals detonation velocity comparable to RDX and HMX and impact sensitivity value close to TNT,<sup>[4]</sup> while 3,4-dinitropyrazole could be used as a melt-castable explosive, alternatively to TNT.<sup>[5]</sup> Rapid extension of the nitropyrazole family provided further attractive examples of N-functionalized and N,N'-bridged compounds,<sup>[6]</sup> bis-pyrazoles,<sup>[7,8a]</sup> ring-fused systems,<sup>[8]</sup> amino-, nitramino- and other derivatives<sup>[9]</sup> used also for production of energetic ionic nitropyrazolates,<sup>[1a,10]</sup> MOFs,<sup>[11]</sup> molecular co-crystals<sup>[12]</sup> and eutectics.<sup>[13]</sup>

In spite of the satisfactory and promising properties of nitropyrazole materials, their practical impact is still limited in the view of typically insufficient synthetic protocols. All-carbon-nitrated pyrazoles are inaccessible by direct reaction since the initial electrophilic substitution at the 4-position of the ring totally inactivates the substrate.<sup>[14]</sup> Thus the accumulation of multiple nitro-functions at the pyrazole platform claims for a cascade of sequential reactions, such as *N*-nitrations and thermal rearrangements to 3-nitropyrazoles,<sup>[15]</sup> oxidation, diazotization, and direct nitration, which have been involved towards the syntheses of any of the highly substituted species, such as 3,4,5-trinitropyrazole,<sup>[3,4]</sup> 4,4',5,5'-tetranitro-3,3'-bipyrazole,<sup>[7b]</sup> etc. (**Fig. 1**).

## Facile and Selective Polynitrations at the 4-Pyrazolyl Dual Backbone: A Straightforward Access to a Series of High-Density Energetic Materials

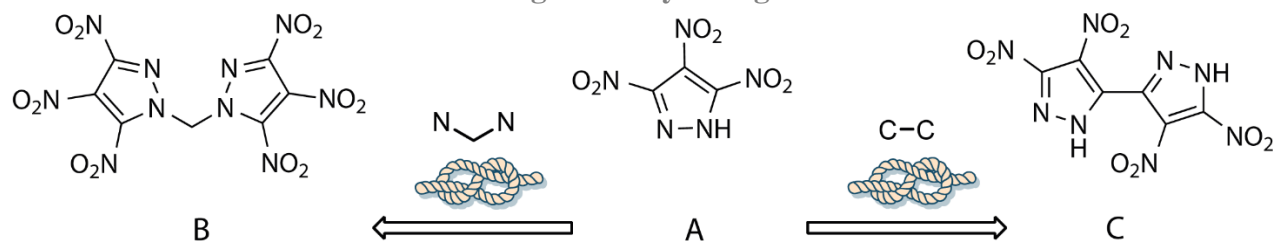


**Figure 1.** Controlling the energetic properties via hypothetical link-up of nitro-pyrazoles based energetic materials: A) 3,4,5-trinitrophenylhydrazine; B) bis(3,4,5-trinitrophenyl) methane; C) 4,4',5,5'-tetranitro-3,3'-bipyrazole.

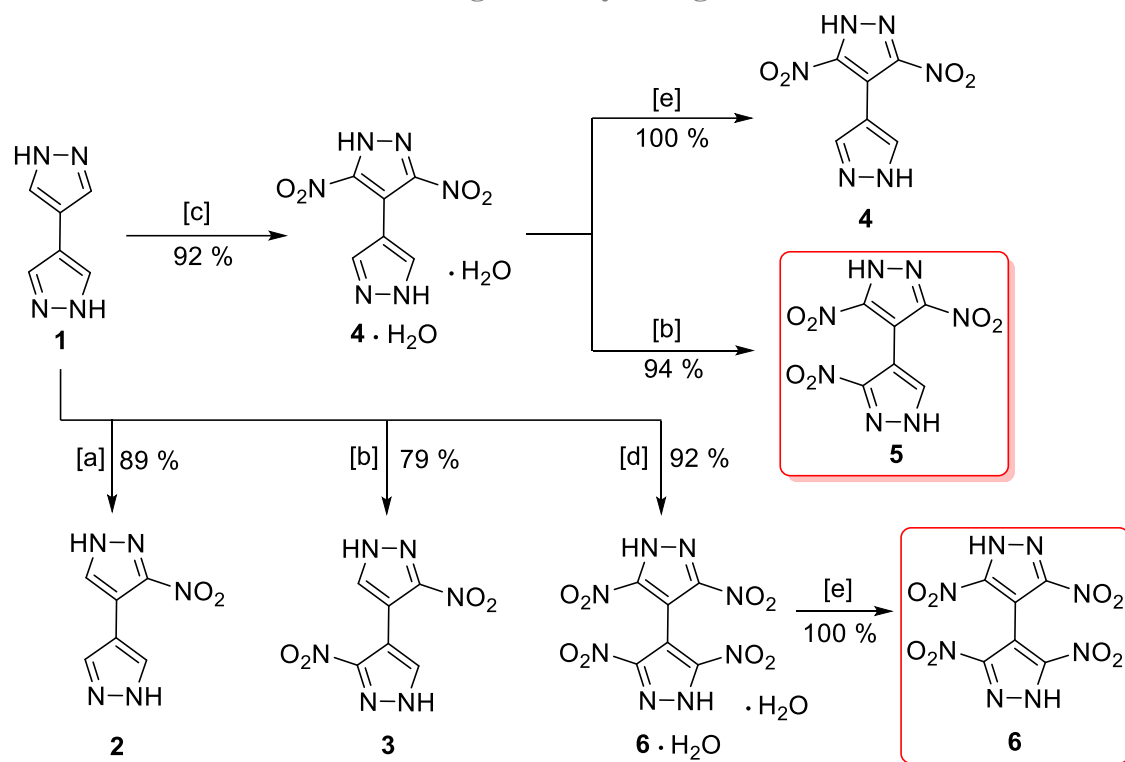
In the present study, we introduce a paradigm resolving these disadvantages, while providing direct access to a series of high-density polynitrophenyl compounds **2–6** by very simple procedures, which do not extend beyond common nitration in mixed acid. Coupling of two phenyl rings, with a mutual interlock of reactive 4,4'-positions, is a key prerequisite for subsequent easy substitution at every of the four C3(5)-positions left. Therefore, the system is especially suited for accumulation of multiple nitro groups and generation of polynitrated species, in particular of exhaustively substituted backbone combining two 3,5-dinitrophenyl groups. Energetic potency of such the dual could be referred to a simple prototype of 3,5-dinitrophenyl, possessing higher heat effect of decomposition than that one for HMX.<sup>[16]</sup>

## 7.2. Results and discussion

### 7.2.1. Synthesis

Reactivity of the 4,4'-bipyrazole (**1**) supports special prospects for gradual nitro-functionalization, while all five nitration products (including two isomeric dinitro derivatives) may be prepared highly selectively and in excellent yields (**Scheme 1**). This reflects versatile behavior of the substrate, which is susceptible either to electrophilic substitutions or unconventional reactions in very dilute HNO<sub>3</sub> media, similar to reactions of phenol.<sup>[17]</sup> The latter case is illustrated by surprisingly ease mononitration of **1** in 1-5% acid, which presumably may

## Facile and Selective Polynitrations at the 4-Pyrazolyl Dual Backbone: A Straightforward Access to a Series of High-Density Energetic Materials



**Scheme 1.** Reaction pathways for selective nitro functionalization of the 4,4'-bipyrazole scaffold. Reagents and conditions: [a] 4% HNO<sub>3</sub>, 95 °C, 6 h; [b] HNO<sub>3</sub>, 82% H<sub>3</sub>PO<sub>4</sub>, 135 °C, 3 h; [c] 2.2 eq. HNO<sub>3</sub>, 91% H<sub>2</sub>SO<sub>4</sub>, 100 °C, 3 h; [d] excess HNO<sub>3</sub>, 91% H<sub>2</sub>SO<sub>4</sub>, 100 °C, 8 h; [e] 170 °C, 48 h.

not be associated with common electrophilic substitution. Under these conditions, pyrazole itself as well as 4-methyl- and 4-(pyridyl-4)-pyrazoles are completely inert giving corresponding nitrates only whereas similar 4,4'-bipyrazolium dinitrate was obtained by heating in concentrated acid.<sup>[18]</sup> With more drastic reaction conditions, such as heating at 140 °C in autoclave, further substitution occurs at the second pyrazole ring yielding symmetric 3,3'-dinitro-4,4'-bipyrazole (**3**). From preparative view, the latter reaction is more convenient in the media of 80% phosphoric acid, as high-boiling inert solvent. The observed selective mononitration of every pyrazole ring is strictly contrary to the behavior of **1** in the respect of typical electrophilic nitration in mixed acid. In this case, two pyrazole rings gradually undergo exhaustive C-nitration with the formation of 3,5-dinitro- (**4**) or 3,3',5,5'-tetranitro-4,4'-bipyrazoles (**6**), depending on the ratio of the reagents. Selective dinitration at the same ring (compound **4**), leaving the second ring unaffected, could be viewed as a chemical paradox, which is highly illustrative for general reactivity and protolytic properties of azoles. In fact, for the intermediate **2**, the nitro group formally activates the carrier ring towards further substitution since nitration of the N-unsubstituted pyrazoles occurs on the conjugate acids<sup>[19]</sup> whereas weakly basic 3-nitropyrazoles undergo substitution as more reactive free bases. The normal deactivating (by over 8 log units) effect of nitro group was observed for 1,4-

## Facile and Selective Polynitrations at the 4-Pyrazolyl Dual Backbone: A Straightforward Access to a Series of High-Density Energetic Materials

dimethylpyrazole nitrating as free base only.<sup>[20]</sup> When combined, the above selective mono- and dinitrations suggest a reliable two-stage reaction sequence toward the only remaining trinitroderivative **5**. In this way, **1** is first converted to intermediate **3** and then to the desired **4** (94%) by successive nitrations in the media of H<sub>2</sub>SO<sub>4</sub> and H<sub>3</sub>PO<sub>4</sub>, respectively. Compound **6**·H<sub>2</sub>O was previously mentioned in the conference proceedings without preparative details.<sup>[21]</sup> Our findings provide much wider versatility of the nitration reactions and the complete synthesis of the nitro derivatives **2–6** is shown in **Scheme 1**.

### 7.2.2. Single crystal X-ray diffraction studies

The solid-state structures of compounds **2–6** and **6**·H<sub>2</sub>O were determined by XRD (Fig. 2). A particular example of **4** suggests that the basic pyrazole and appreciably acidic dinitropyrazole sites ( $pK_a = 3.14$  for 3,5-dinitropyrazole<sup>[22]</sup>) are incompatible within the molecule and the latter exists rather as a peculiar pyrazolium/pyrazolate zwitter-ion.

Impact of progressive nitro substitution on molecular conformation of the bipyrazole core is best detected by gradual growth of the twist angle  $\phi$  across the central C-C bond, as the number of nitro groups increases. Unlike exactly planar 4,4'-bipyrazole itself,<sup>[23]</sup> and nearly planar **2** [ $\phi = 5.63(12)^\circ$ ], two isomeric dinitro compounds essentially lose coplanarity of two pyrazole halves and this effect is even more pronounced for **5** and **6** (**Table 1**).

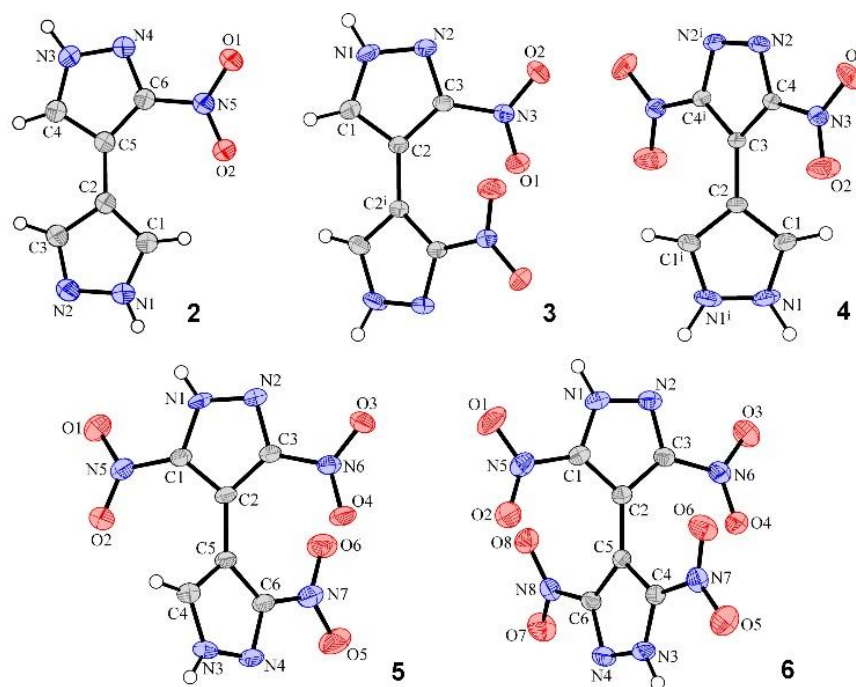


**Figure 2.** Molecular structures of **2–6** with atom labels and the thermal ellipsoids representing the 50% probability level.

# Facile and Selective Polynitrations at the 4-Pyrazolyl Dual Backbone: A Straightforward Access to a Series of High-Density Energetic Materials

**Table 1.** Selected parameters for structures of nitro 4,4'-bipyrazoles **2-6**.

	NO <sub>2</sub> groups	Twist angle/ <sup>o</sup> a)	Density/ g cm <sup>-3</sup>	Packing index	H-bonded connectivity
<b>1</b> <sup>[23]</sup>	0	0	1.424	69.9	Flat layer
<b>2</b>	1	5.63(12)	1.668	74.5	3D framework
<b>3</b>	2	46.48(4)	1.817	76.5	Flat layer
<b>4</b>	2	50.28(5)	1.836	76.6	Flat layer
<b>5</b>	3	58.58(9)	1.880	75.4	Corrugated layer
<b>6</b>	4	71.44(5)	1.847	72.2	Supramolecular tube
<b>6·H<sub>2</sub>O</b>	4	78.99(6)	1.857	73.6	3D framework

<sup>a)</sup> The dihedral angle subtended by mean planes of two rings; for 4,4'-bipyrazole these rings were related by inversion.

However, the actual spread of twist angles for **3-6** is relatively small and the introduction of the third and fourth nitro groups does not provoke significant strains. Moreover, probably counterintuitive conformation of **3** (**Fig. 2**), which maintains short nitro-nitro stack [N...O = 3.019(14) Å], invokes certain attractiveness of intramolecular nitro-nitro interactions, as a special kind of  $\pi$ -hole/lone pair bonding.<sup>[24]</sup>

At the first glance, the twisted conformation of the molecules mitigates against dense molecular packings and thus the density of exhaustively nitrated **6** (1.847 g cm<sup>-3</sup>) is even slightly less than that of **5** (1.880 g cm<sup>-3</sup>). However, a variety of supramolecular interactions in the structures contribute to the high packing indices [72.2-76.6%], at the upper limit of the 65–75% range expected for organic solids.<sup>[25]</sup> Pyrazole  $\pi$ -stacking is relevant only for pack of planar molecules of **2**, with two distinct H-bonded patterns segregating pyrazole or nitropyrazole sites within complicated 3D topology (further details can be found in the Supporting Information). It is worth noting that the conventional NH...N hydrogen bonds to nitropyrazole moiety commonly appear as bifurcated, with a second branch to the adjacent nitro-O acceptor [N...O = 2.8808(16)–3.1849(16) Å, for **2-6**] (**Fig. 3**). Evolution of supramolecular patterns, which coincides with progressive nitro substitution at the molecular frame, reflects increased role of nitro groups for H-bonding and  $\pi$ -hole/lone pair interactions.

Energetics and structural significance of the latter ones are comparable with weak CH...O bonding<sup>[24]</sup> and therefore the layered structures of **3-5** are very similar. In particular, the layers seen in the structure of **3** remain intact even with substitution at the third CH group thus yielding

## Facile and Selective Polynitrations at the 4-Pyrazolyl Dual Backbone: A Straightforward Access to a Series of High-Density Energetic Materials

corrugated layers of **5** with short  $\pi$ -hole/lone pair  $\text{NO}_2/\text{NO}_2$  stacks [ $\text{N}\cdots\text{O} = 2.947(2) \text{ \AA}$ ] instead of the  $\text{CH}\cdots\text{O}$  bonds found in **3** (**Fig. 3**).

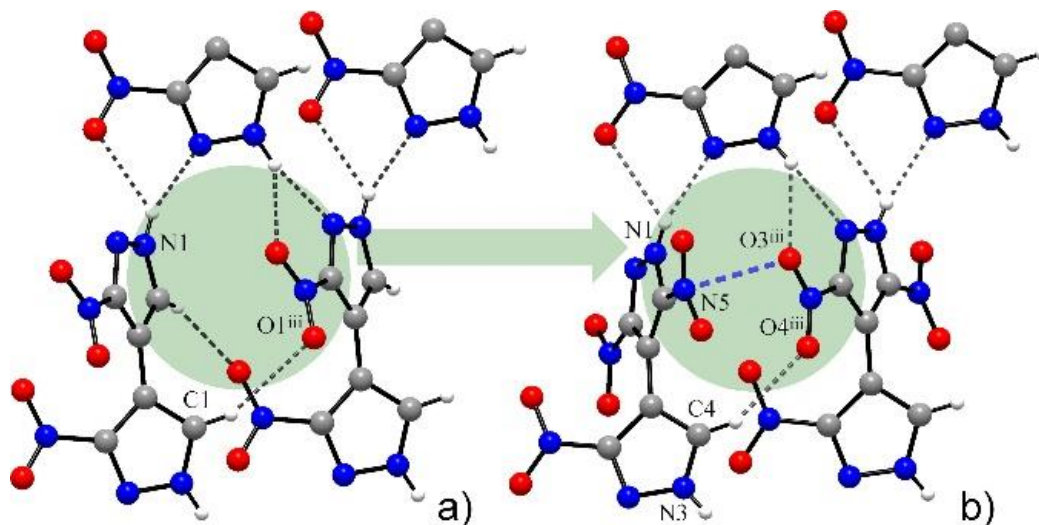


**Figure 3.** Inheritance of supramolecular motifs with increased number of nitro functionalities: the layers of **3** (a) and **5** (b) show comparable significance of  $\text{CH}\cdots\text{O}$  and  $\text{NO}_2/\text{NO}_2$  bonding [ $\text{N5}\cdots\text{O3}^{\text{iii}} = 2.947(2) \text{ \AA}$ ].

Effect of fourth nitro group is rather spectacular (**6**): with a larger twist angle imposed by the molecular frame and loss of interlayer  $\text{CH}\cdots\text{O}$  linkage, the 2D array of H-bonded molecules collapses forming supramolecular tubes, *i.e.* one-periodic 2D structure (**Fig. 4**). The short  $\text{NH}\cdots\text{O}$  bonds [ $2.8457(14) \text{ \AA}$ ], generated in the replace of more common  $\text{NH}\cdots\text{N}$  bonding, maintain tetramers of **6**, while bifurcate  $\text{NH}\cdots\text{O}, \text{N}$  bonds extend the connectivity in one dimension. With a total elimination of competitive  $\text{CH}\cdots\text{O}$  and stacking interactions, the role of nitro groups becomes crucial even beyond the hydrogen bonding: in total twelve short  $\pi$ -hole/lone pair  $\text{N}\cdots\text{O}$  contacts (with a cut-off limit of  $3.25 \text{ \AA}$ ) of  $\text{NO}_2/\text{NO}_2$  and  $\text{NO}_2/\text{pyrazole}$  types [shortest separations are  $2.9115(15)$  and  $2.8015(16) \text{ \AA}$ , respectively] contribute to the dense packing of this energetic material. These interactions approach the shortest reported contact of that type ( $2.80 \text{ \AA}$ ) in the structure of the highly explosive heptanitrocubane<sup>[26]</sup> and they are relevant also for co-crystal **6**·**H<sub>2</sub>O**. Moreover, the water molecule also follows the trend by establishing its own  $\pi$ -hole/lone pair contact [ $\text{N}(\text{nitro})\cdots\text{OH}_2 = 3.058(2) \text{ \AA}$ ], in addition to directional H-bonds and particularly strong  $\text{NH}\cdots\text{O}$  bond [ $\text{N}\cdots\text{O} = 2.6470(16) \text{ \AA}$ ] with pyrazole (for further details on structure of **6**·**H<sub>2</sub>O** see the Supporting Information).



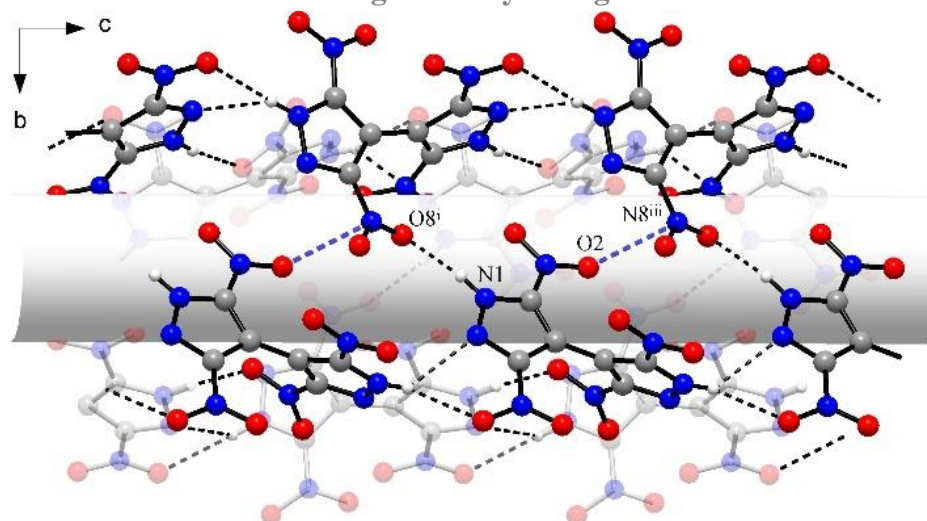


**Figure 4.** Structure of **6**: a supramolecular tube by interplay of hydrogen bonding and  $\pi$ -hole/lone pair interactions of nitro groups [ $\text{N1}\cdots\text{O8}^{\text{i}} = 2.8457(14) \text{ \AA}$ ;  $\text{O2}\cdots\text{N8}^{\text{iii}} = 2.9115(15) \text{ \AA}$ ].

### 7.2.3. Physical and detonation properties

Since all synthesized nitro pyrazoles can be viewed either as important precursors for the synthesis of energetic materials (compounds **2**, **3** and **4**) or can be already classified as energetic materials (compounds **5** and **6**), their energetic behavior was investigated. All theoretically calculated and experimentally determined values for **2–6** compared to the thermally stable explosive HNS are listed in **Table 2**. Compound **6** ( $T_{\text{dec.}} = 298 \text{ }^{\circ}\text{C}$ ) decomposes slightly under  $300 \text{ }^{\circ}\text{C}$ , whereas compounds **2** ( $T_{\text{dec.}} = 303 \text{ }^{\circ}\text{C}$ ), **3** ( $T_{\text{dec.}} = 382 \text{ }^{\circ}\text{C}$ ), **4** ( $T_{\text{dec.}} = 302 \text{ }^{\circ}\text{C}$ ) and **5** ( $T_{\text{dec.}} = 314 \text{ }^{\circ}\text{C}$ ) decompose above  $300 \text{ }^{\circ}\text{C}$ . Although compounds **3** and **4** are structural isomers with only two  $\text{NO}_2$  groups on the 4,4'-bipyrazole exoskeleton the difference in the decomposition temperature is significant. Increasing the number of  $\text{NO}_2$  groups from three to four on the bipyrazole scaffold leads to only small decrease of the decomposition temperature from  $314 \text{ }^{\circ}\text{C}$  to  $298 \text{ }^{\circ}\text{C}$  for compounds **5** and **6**, respectively. All DTA and TGA plots for compounds **5** and **6** are depicted in the Supporting Information. The room temperature density values for compounds **5** and **6** are  $1.855 \text{ g cm}^{-3}$  and  $1.820 \text{ g cm}^{-3}$ , respectively. Experimentally determined sensitivity values toward impact and friction of **5** (IS = 20 J, FS = >360 N) exceed the reported values for PYX (IS = 10 J, FS = 360 N), HNS (IS = 5 J, FS = 240 N) and TKX-55 (IS = 5 J, FS = >360 N). Although the impact sensitivity of compound **6**· $\text{H}_2\text{O}$  (IS = 9 J) is in the range of PYX (IS = 10 J), this value changes drastically for the anhydrous **6** (IS = 4.5 J). **Figure 5** shows the change of the physico-chemical properties for the polynitrated pyrazoles **2–6** with increasing  $\text{NO}_2$  groups in the 4,4'-bipyrazole scaffold.



# Facile and Selective Polynitrations at the 4-Pyrazolyl Dual Backbone: A Straightforward Access to a Series of High-Density Energetic Materials

**Table 2.** Energetic properties and detonation parameters of compounds **2–6** compared to HNS.

Compound	<b>2</b>	<b>3</b>	<b>4</b>	<b>5</b>	<b>6</b>	<b>6·H<sub>2</sub>O</b>	<b>HNS</b>
$IS^{[a]}$ [J]	40	30	30	20	4.5	9	5
$FS^{[b]}$ [N]	>360	>360	>360	>360	192	324	240
$ESD^{[c]}$ [J]	0.74	0.63	0.54	0.50	0.30	0.40	0.80
$\Omega^{[d]}$ [%]	−111.64	−71.38	−71.38	−44.58	−25.46	−24.08	−67.60
$T_m^{[e]}$ [°C]	284	377	284	306	292	292	–
$T_{dec}^{[f]}$ [°C]	303	382	302	314	298	298	318
$\rho^{[g]}$ [g cm <sup>−3</sup> ]	1.635	1.794	1.813	1.855	1.820	1.830	1.74
$\Delta H_f^{o[h]}$ [kJ mol <sup>−1</sup> ]	224.6	203.5	371.7	224.9	227.8	−11.0	78.2
<b>EXPL05 6.03</b>							
$-\Delta_E U^{o[i]}$ [kJ kg <sup>−1</sup> ]	3116.4	4036.4	4742.0	4821	5287	5039	5142
$T_{C-J}^{[j]}$ [K]	2367	3000	3357	3565	4054	3724	3677
$p_{C-J}^{[k]}$ [kbar]	144	221	249	286	311	307	243
$D_{C-J}^{[l]}$ [m s <sup>−1</sup> ]	6506	7528	7873	8256	8520	8451	7612
$V^{[m]}$ [dm <sup>3</sup> kg <sup>−1</sup> ]	481	436	430	417	419	418	602

[a] Impact sensitivity (BAM drophammer, method 1 of 6); [b] friction sensitivity (BAM drophammer, method 1 of 6); [c] electrostatic discharge device (OZM research); [d] oxygen balance; [e] melting point (DTA,  $\beta = 5^\circ\text{C}\cdot\text{min}^{-1}$ ); [f] temperature of decomposition (DTA onset points,  $\beta = 5^\circ\text{C}\cdot\text{min}^{-1}$ ); [g] density at 298 K; [h] standard molar enthalpy of formation; [i] detonation energy; [j] detonation temperature; [k] detonation pressure; [l] detonation velocity; [m] volume of detonation gases at standard temperature and pressure conditions.

For compounds **5** and **6** were estimated positive enthalpies of formation (**5** = 225 kJ mol<sup>−1</sup> and **6** = 228 kJ mol<sup>−1</sup>). Using these values, several detonation parameters for **2–6** were calculated (see the Supporting Information for details). The detonation pressure and velocity for **5** ( $p_{C-J} = 286$  kbar,  $D_{C-J} = 8256$  m s<sup>−1</sup>) and **6** ( $p_{C-J} = 311$  kbar,  $D_{C-J} = 8520$  m s<sup>−1</sup>) surpass the reported values for PYX ( $p_{C-J} = 251$  kbar,  $D_{C-J} = 7757$  m s<sup>−1</sup>), HNS ( $p_{C-J} = 243$  kbar,  $D_{C-J} = 7612$  m s<sup>−1</sup>) and TKX-55 ( $p_{C-J} = 273$  kbar,  $D_{C-J} = 8020$  m s<sup>−1</sup>).<sup>27</sup>

## Facile and Selective Polynitrations at the 4-Pyrazolyl Dual Backbone: A Straightforward Access to a Series of High-Density Energetic Materials

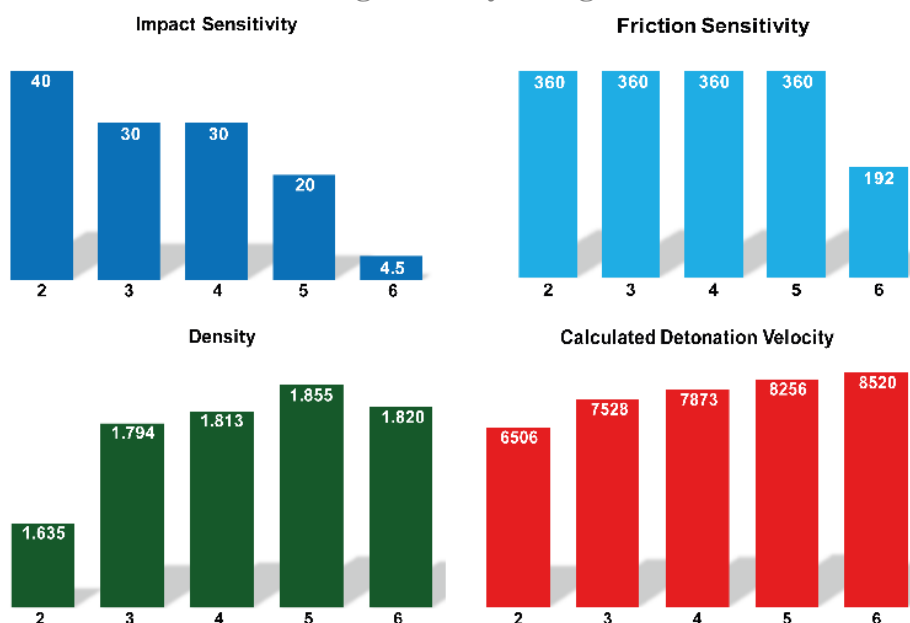


**Figure 5.** Bar charts for compounds **2–6** showing the change of the energetic behavior with increasing NO<sub>2</sub> groups in the 4,4'-bipyrazole scaffold. Impact Sensitivity [J], Friction Sensitivity [N], Density [g cm<sup>-3</sup>] and Calculated Detonation Velocity [m s<sup>-1</sup>].

In addition, the explosive performance of **5** and **6** on a small scale was investigated with the small scale shock reactivity test (SSRT, **Fig. 6**). The dent sizes were measured volumetrically by filling them with finely powdered SiO<sub>2</sub> and measuring the resulting weight.

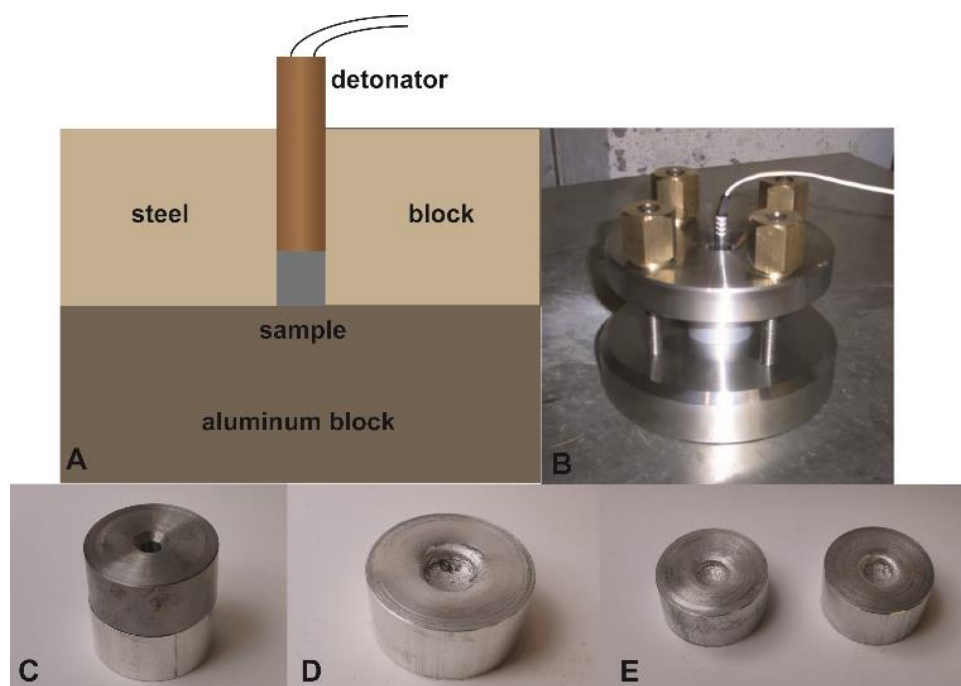


**Figure 6.** SSRT results for **5** and **6**; A) schematical illustration; B) photograph of the setup; C) aluminum block and steel block filled with the desired compound; D) dented aluminum block after initiation of

## Facile and Selective Polynitrations at the 4-Pyrazolyl Dual Backbone: A Straightforward Access to a Series of High-Density Energetic Materials

compound **6** with a commercial detonator; E) dented aluminum blocks after initiation of compound **5** with a commercial detonator.

The obtained results for **5** and **6** are gathered in **Table 3**. The measured dent volume for **5** (640 mg) is in the range for the reported value for TKX-55 (641 mg) and slightly lower than the reported value for HNS (672 mg).<sup>[27]</sup> However, the solvent free **6** (811 mg) outperforms HNS, PYX and TKX-55 in the small scale shock test.

**Table 3.** The SSRT for **5** and **6** compared to HNS, PYX and TKX-55.

	HNS	PYX	TKX-55	<b>5</b>	<b>6</b>
$m_E$ [mg] <sup>[a]</sup>	469	474	496	500	491
$m$ [mg] <sup>[b]</sup>	672	637	641	640	811

[a] Mass of the explosive:  $m_E = V_s \rho$  0.95; [b] Mass of SiO<sub>2</sub>.

## 7.3. Experimental

### 7.3.1. General Information

All reagents and solvents were used as received. The synthesis of 4,4'-bipyrazole **1** was performed by the previously published method.<sup>[23]</sup> Decomposition temperatures were measured *via* differential thermal analysis (DTA) with an OZM Research DTA 552-Ex instrument at a heating rate of 5 °C min<sup>-1</sup> and in a range of room temperature to 400 °C and in addition thermal gravimetric analysis (TGA) of compounds **5**, **6** and **6**·H<sub>2</sub>O was performed. The NMR spectra were recorded with a 400 MHz instrument (<sup>1</sup>H 399.8 MHz, <sup>13</sup>C 100.5 MHz, <sup>14</sup>N 28.9 MHz, and <sup>15</sup>N 40.6 MHz) at ambient temperature. Chemical shifts are quoted in parts per million with respect to TMS (<sup>1</sup>H, <sup>13</sup>C) and nitromethane (<sup>14</sup>N, <sup>15</sup>N). Infrared spectra (IR) were recorded from 4500 cm<sup>-1</sup> to 650 cm<sup>-1</sup> on a Perkin Elmer Spectrum BX-59343 instrument with *Smiths Detection DuraSamplIR II Diamond ATR* sensor. The absorption bands are reported in wavenumbers (cm<sup>-1</sup>). Raman spectra were recorded in glass tubes with Nd:YAG laser excitation up to 300 mW (at 1064 nm) in the range between 200 and 4000 cm<sup>-1</sup>. The intensities are reported as percentages of the most intense peak and are given in parentheses. The sensitivities toward friction and impact of compounds **2-6** were determined according the BAM standards and the detonation parameters were calculated using the EXPLO5-V6.03 computer code.<sup>[28]</sup> All detonation parameters for the polynitro derivatives **2-6** were calculated by using the room-temperature densities obtained from

## Facile and Selective Polynitrations at the 4-Pyrazolyl Dual Backbone: A Straightforward Access to a Series of High-Density Energetic Materials

the X-ray structures as described in the reference.<sup>[29]</sup> Compounds **2–6** and **6·H<sub>2</sub>O** were tested for sensitivity towards electrical discharge using an Electric Spark Tester ESD 2010 EN.

### 7.3.2. Crystallography

Single-crystal X-ray diffraction data were collected with graphite-monochromated Mo K $\alpha$  radiation ( $\lambda = 0.71073 \text{ \AA}$ ) using a Stoe Image Plate Diffraction System ( $\varphi$  oscillation scans). The structures were solved by direct methods and refined by full-matrix least-squares on  $F^2$  using the programs SHELXS-97 and SHELXL-2014/7.<sup>[30]</sup> All hydrogen atoms were located and freely refined with isotropic thermal parameters. Crystallographic data for the reported structures in this contribution have been deposited with the Cambridge Crystallographic Data Centre as supplementary publication numbers (CCDC 1836403-1836408 for **2–6** and **6·H<sub>2</sub>O**). These data can be obtained free of charge from the Cambridge Crystallographic Data Centre via [www.ccdc.cam.ac.uk/data\\_request/cif](http://www.ccdc.cam.ac.uk/data_request/cif).

**3-Nitro-4,4'-bipyrazole (2):** 4,4'-Bipyrazole (**1**, 8.04 g, 60.0 mmol) was added to 4.5% aqueous solution of HNO<sub>3</sub> (820 mL,  $d = 1.023 \text{ g cm}^{-3}$ ; 0.6 mol) and the mixture was stirred at 95 °C for 6 h. The initially formed colorless crystalline deposit of 4,4'-bipyrazolium dinitrate dissolved for the first 30-40 min and during the next 2-3 h the mixture developed yellow color. The solution, while hot, was neutralized with 49.5 g (0.59 mol) of solid NaHCO<sub>3</sub> and then cooled to r.t. Orange crystalline product (9.56 g, 89%) was filtered, washed with 20 mL water and dried on air. Pure material was obtained after recrystallization from hot water (3.5 g per 1 L).

**2:** Bright-orange platelets. DTA (5 °C min<sup>-1</sup>): 256 °C (endo), 284 °C (melt.), 303 °C (exo.); BAM: drop hammer: 40 J (100–500  $\mu\text{m}$ ); friction tester: >360 N (100–500  $\mu\text{m}$ ); ESD: 0.74 J (100–500  $\mu\text{m}$ ). IR (ATR),  $\tilde{\nu} \text{ (cm}^{-1}\text{)} = 3268 \text{ (m)}, 3233 \text{ (s)}, 3124 \text{ (m)}, 2923 \text{ (m)}, 2871 \text{ (m)}, 1698 \text{ (vw)}, 1609 \text{ (m)}, 1540 \text{ (w)}, 1502 \text{ (m)}, 1478 \text{ (w)}, 1406 \text{ (m)}, 1398 \text{ (m)}, 1334 \text{ (s)}, 1320 \text{ (s)}, 1297 \text{ (m)}, 1274 \text{ (m)}, 1241 \text{ (m)}, 1193 \text{ (m)}, 1208 \text{ (m)}, 1162 \text{ (m)}, 1106 \text{ (w)}, 1076 \text{ (m)}, 1034 \text{ (w)}, 960 \text{ (w)}, 943 \text{ (s)}, 877 \text{ (m)}, 851 \text{ (w)}, 829 \text{ (m)}, 796 \text{ (s)}, 762 \text{ (s)}, 649 \text{ (w)}, 640 \text{ (w)}, 614 \text{ (s)}, 504 \text{ (vw)}$ . Raman (1064 nm, 200 mW, 25 °C):  $\tilde{\nu} \text{ (cm}^{-1}\text{)} = 3136 \text{ (4)}, 1614 \text{ (79)}, 1518 \text{ (18)}, 1409 \text{ (53)}, 1371 \text{ (5)}, 1341 \text{ (100)}, 1323 \text{ (3)}, 1301 \text{ (3)}, 1246 \text{ (5)}, 1223 \text{ (3)}, 1211 \text{ (5)}, 1164 \text{ (3)}, 1109 \text{ (3)}, 1085 \text{ (14)}, 929 \text{ (3)}, 831 \text{ (7)}, 506 \text{ (4)}, 400 \text{ (3)}, 222 \text{ (8)}$ . <sup>1</sup>H NMR ( $d_6$ -DMSO, 400 MHz, ppm)  $\delta = 13.98 \text{ (s, 1H)}, 13.00 \text{ (s, 1H)}, 8.26 \text{ (s, 1H)}, 8.09 \text{ (s, 1H)}, 7.85 \text{ (s, 1H)}$ . <sup>13</sup>C NMR ( $d_6$ -DMSO, 101 MHz, ppm)  $\delta = 151.7, 138.6, 130.3, 127.9, 109.9, 109.1$ . <sup>14</sup>N NMR ( $d_6$ -DMSO, 29 MHz, ppm)  $\delta = -18$ . Anal. Calcd for C<sub>6</sub>H<sub>5</sub>N<sub>5</sub>O<sub>2</sub>: C 40.23, H 2.81, N 39.10 %. Found: C 40.21, H 2.75, N 38.80 %.  $m/z$  (DEI<sup>+</sup>): 179.04 (4) [M]<sup>+</sup>, 149.07 (32), 119.05 (31), 106.04 (20).

## Facile and Selective Polynitrations at the 4-Pyrazolyl Dual Backbone: A Straightforward Access to a Series of High-Density Energetic Materials

**3,3'-Dinitro-4,4'-bipyrazole (3).** **Method A:** 4,4'-Bipyrazole (1, 6.70 g, 50.0 mmol) and 35.0 mL (0.5 mol) of 65% nitric acid ( $d = 1.389 \text{ g cm}^{-3}$ ) were added to concentrated phosphoric acid (400 mL, 82%,  $d = 1.646 \text{ g cm}^{-3}$ ) held in 1 L round-bottom flask equipped with short air-cooled reflux condenser. The flask was placed into a pre-heated oil bath and the mixture was stirred at 130–135 °C for 3 h. The mixture containing deposit of the reaction product was transferred onto 1.5 kg of crushed ice, the solid was filtered, washed with two portions of water and dried in air to yield compound 3 (8.85 g, 79%). The product was recrystallized from boiling water (0.4 g per 1 L) or, better, from 20% aqueous dimethylformamide (6.5 g per 1 L). **Method B:** 4,4'-Bipyrazole (1, 26.8 mg, 0.2 mmol),  $\text{Al}(\text{NO}_3)_3 \cdot 9\text{H}_2\text{O}$  (93.8 mg, 0.25 mmol) and 15% HF (6 mL) were placed in a teflon-lined steel autoclave, heated at 140 °C for 24 h and then cooled to r.t. over the period of 48 h. Large pale-yellow crystals of 3 (31.8 mg, 71%) were filtered, thoroughly washed with water and dried in air. The product is identical to the product of nitration by method A.

**3:** light yellow prisms. DTA (5 °C min<sup>-1</sup>): 377 °C (melt.), 382 °C (exo.); BAM: drop hammer: 30 J (100–500 µm); friction tester: >360 N (100–500 µm); ESD: 0.63 J (100–500 µm). IR (ATR),  $\tilde{\nu}$  (cm<sup>-1</sup>) = 3198 (m), 3130 (m), 2960 (m), 1637 (vw), 1541 (w), 1532 (w), 1512 (m), 1482 (m), 1377 (s), 1351 (s), 1307 (m), 1246 (m), 1214 (m), 1140 (w), 1095 (m), 993 (m), 939 (w), 861 (w), 838 (m), 824 (s), 758 (s), 679 (w), 643 (s), 610 (w), 572 (m). Raman (1064 nm, 200 mW, 25 °C):  $\tilde{\nu}$  (cm<sup>-1</sup>) = 1637 (49), 1551 (9), 1537 (13), 1496 (5), 1427 (3), 1398 (100), 1390 (13), 1377 (10), 1356 (26), 1308 (38), 1249 (6), 1209 (16), 1143 (8), 942 (19), 838 (17), 772 (6), 397 (6), 253 (7), 234 (18), 218 (7). <sup>1</sup>H NMR (*d*<sub>6</sub>-DMSO, 400 MHz, ppm)  $\delta$  = 14.13 (s, 2H), 8.20 (s, 2H). <sup>13</sup>C NMR (*d*<sub>6</sub>-DMSO, 101 MHz, ppm)  $\delta$  = 153.0, 132.5, 106.9. <sup>14</sup>N NMR (*d*<sub>6</sub>-DMSO, 29 MHz, ppm)  $\delta$  = -20. Anal. Calcd for C<sub>6</sub>H<sub>4</sub>N<sub>6</sub>O<sub>4</sub>: C 32.15, H 1.80, N 37.50 %. Found: C 32.10, H 1.94, N 37.35 %. *m/z* (DEI<sup>+</sup>): 224.03 (99) [M]<sup>+</sup>, 194.06 (41), 179.05 (47), 119.05 (100).

**3,5-Dinitro-4,4'-bipyrazole (4):** Fuming HNO<sub>3</sub> (5.65 mL, 98%,  $d = 1.501 \text{ g cm}^{-3}$ ) was added to a warm solution of **1** (8.04 g, 60 mmol) in 91% H<sub>2</sub>SO<sub>4</sub> (240 mL,  $d = 1.820 \text{ g cm}^{-3}$ ). The mixture was placed into pre-heated oil bath and the clear solution was stirred at 100 °C (bath temperature) for 3 h. When cold, the mixture was poured into 0.5 kg of crushed ice giving clear pale-yellow solution. This was neutralized to pH = 4–5, with external ice cooling, by slow addition of concentrated ammonia (approximately 670 mL). The voluminous light-yellow precipitate of **4**·H<sub>2</sub>O (13.36 g, 92%) was filtered and thoroughly washed with two 50 mL portions of ice water. Pure compound was obtained by recrystallization from boiling water (5.9 g per 1 L). The anhydrous material was obtained by recrystallization from ethanol.

**4**·H<sub>2</sub>O: Light-yellow platelets. DTA (5 °C min<sup>-1</sup>): 118 °C (H<sub>2</sub>O, endo), 284 °C (melt.), 302 °C (exo.); IR (ATR),  $\tilde{\nu}$  (cm<sup>-1</sup>) = 3578 (m), 3307 (w), 3142 (m), 2416 (m), 1806 (w), 1606 (w), 1523

**Facile and Selective Polynitrations at the 4-Pyrazolyl Dual Backbone: A Straightforward Access to a Series of High-Density Energetic Materials**

(m), 1490 (s), 1401 (s), 1329 (s), 1241 (m), 1155 (m), 1097 (w), 1018 (w), 939 (m), 882 (s), 841 (s), 767 (m), 691 (w), 672 (vw), 619 (m), 560 (m). Raman (1064 nm, 200 mW, 25 °C):  $\tilde{\nu}$  (cm<sup>-1</sup>) = 3142 (6), 1611 (100), 1525 (17), 1495 (23), 1383 (92), 1299 (14), 1245 (14), 1214 (87), 1163 (6), 1112 (17), 941 (43), 822 (28), 761 (8), 674 (7), 404 (4), 384 (2), 374 (8), 335 (5), 283 (6), 264 (9). <sup>1</sup>H NMR (*d*<sub>6</sub>-DMSO, 400 MHz, ppm)  $\delta$  = 7.93 (s, 2H). <sup>13</sup>C NMR (*d*<sub>6</sub>-DMSO, 101 MHz, ppm)  $\delta$  = 148.2, 135.6 107.2, 104.5. <sup>14</sup>N NMR (*d*<sub>6</sub>-DMSO, 29 MHz, ppm)  $\delta$  = -24. Anal. Calcd for C<sub>6</sub>H<sub>4</sub>N<sub>6</sub>O<sub>4</sub>·H<sub>2</sub>O: C 29.76, H 2.50, N 34.71 %. Found: C 29.86, H 2.48, N 34.85 %. *m/z* (DEI<sup>+</sup>): 224.03 (100) [M]<sup>+</sup>, 194.06 (75), 105.03 (54).

**4:** Pale-yellow prisms. DTA (5 °C min<sup>-1</sup>): 284 °C (melt.), 302 °C (exo.); BAM: drop hammer: 30 J (100–500 μm); friction tester: >360 N (100–500 μm); ESD: 0.54 J (100–500 μm). Anal. Calcd for C<sub>6</sub>H<sub>4</sub>N<sub>6</sub>O<sub>4</sub>: C 32.15, H 1.80, N 37.50 %. Found: C 32.03, H 1.90, N 37.49 %.

**3,3',5-Trinitro-4,4'-bipyrazole (5):** Fuming HNO<sub>3</sub> (24.0 mL, 98%, *d* = 1.501 g cm<sup>-3</sup>) was added to a slurry of **4**·H<sub>2</sub>O (6.05 g, 25 mmol) in 82% H<sub>3</sub>PO<sub>4</sub> (270 mL, *d* = 1.646 g cm<sup>-3</sup>). The mixture was placed into pre-heated oil bath and the clear solution formed was stirred at 150°C (bath temperature) for 10 h. Precipitation of the reaction product was observed after first 5-6 h. The mixture was cooled, poured into 0.5 kg of crushed ice and left overnight at 5-10 °C. Pale-yellow deposit (5.64 g) was filtered and twice washed with 30 mL portions of water. Additional portion of the product (0.68 g) was isolated by extraction of the filtrates with EtOAc (3 × 300 mL). The combined yield was 6.32 g (94%). Pure **5** was obtained by crystallization from boiling water (8.0 g per 1 L).

**5:** Pale-yellow prisms. DTA (5 °C min<sup>-1</sup>): 306 °C (melt.), 314 °C (exo.); BAM: drop hammer: 20 J (100–500 μm); friction tester: >360 N (100–500 μm); ESD: 0.50 J (100–500 μm). IR (ATR),  $\tilde{\nu}$  (cm<sup>-1</sup>) = 3329 (m), 3156 (w), 3051 (w), 2801 (w), 1639 (w), 1549 (m), 1512 (m), 1478 (m), 1400 (s), 1334 (vs), 1298 (s), 1260 (m), 1228 (m), 1212 (m), 1167 (m), 1100 (m), 995 (m), 945 (w), 871 (w), 847 (s), 834 (s), 764 (m), 685 (vs), 629 (m), 604 (m), 587 (m), 546 (w), 518 (vw). Raman (1064 nm, 200 mW, 25 °C):  $\tilde{\nu}$  (cm<sup>-1</sup>) = 1640 (31), 1562 (5), 1544 (7), 1426 (11), 1399 (100), 1390 (13), 1340 (11), 1299 (5), 1265 (9), 1227 (6), 1210 (10), 947 (9), 833 (15), 754 (5), 519 (2), 360 (4), 316 (3), 270 (6), 237 (5), 209 (28). <sup>1</sup>H NMR (*d*<sub>6</sub>-DMSO, 400 MHz, ppm)  $\delta$  = 14.27 (br, 1H), 10.34 (br, 1H), 8.31 (s, 1H). <sup>13</sup>C NMR (*d*<sub>6</sub>-DMSO, 101 MHz, ppm)  $\delta$  = 153.2, 149.0, 134.4, 103.5, 102.6. <sup>14</sup>N NMR (*d*<sub>6</sub>-DMSO, 29 MHz, ppm)  $\delta$  = -24. <sup>15</sup>N NMR (*d*<sub>6</sub>-DMSO, 41 MHz, ppm)  $\delta$  = -20.3, -25.8, -82.8, -121.9, -170.5. Anal. Calcd for C<sub>6</sub>H<sub>3</sub>N<sub>6</sub>O<sub>6</sub>: C 26.78, H 1.12, N 36.43 %. Found: C 26.82, H 1.23, N 36.15 %. *m/z* (DEI<sup>+</sup>): 269 (4) [M]<sup>+</sup>, 239 (14), 223 (31), 93 (34), 77 (100).

## Facile and Selective Polynitrations at the 4-Pyrazolyl Dual Backbone: A Straightforward Access to a Series of High-Density Energetic Materials

**3,3',5,5'-Tetranitro-4,4'-bipyrazole (6):** Fuming  $\text{HNO}_3$  (43.7 mL, 98%,  $d = 1.501 \text{ g cm}^{-3}$ ) was added to a warm solution of **1** (8.04 g, 60 mmol) in 91%  $\text{H}_2\text{SO}_4$  (350 mL,  $d = 1.820 \text{ g cm}^{-3}$ ). The mixture was placed into pre-heated oil bath and the clear solution formed was stirred at 98–100 °C (bath temperature) for 8 h. After cooling, the mixture containing colorless solid reaction product was poured into 1.2 kg of crushed ice and left overnight at 5–10 °C. Crystalline deposit of **6**· $\text{H}_2\text{O}$  (18.32 g, 92%) was filtered, washed with 40 mL of ice water and dried. It was purified by crystallization from boiling water (45.0 g per 1 L). The compound crystallizes as monohydrate **6**· $\text{H}_2\text{O}$  from a variety of wet solvents (alcohols, ethylacetate, acetone, 1,4-dioxane *etc.*). Anhydrous material **6** was obtained by crystallization from hot 1,2-dichlorobenzene (3.0 g per 1 L).

**6**· $\text{H}_2\text{O}$ : Colorless prisms. DTA (5 °C  $\text{min}^{-1}$ ): 115 °C ( $\text{H}_2\text{O}$ ), 292 °C (melt.), 298 °C (exo.); BAM: drop hammer: 9 J (100–500  $\mu\text{m}$ ); friction tester: 324 N (100–500  $\mu\text{m}$ ); ESD: 0.40 J (100–500  $\mu\text{m}$ ). IR (ATR),  $\tilde{\nu}$  ( $\text{cm}^{-1}$ ) = 3619 (w), 3520 (w), 3096 (w), 2954 (w), 2352 (w), 1844 (vw), 1574 (m), 1544 (s), 1512 (s), 1488 (s), 1421 (s), 1352 (s), 1329 (s), 1310 (s), 1288 (m), 1215 (m), 1198 (w), 1022 (m), 1004 (m), 951 (w), 839 (vs), 814 (m), 798 (m), 772 (m), 691 (m), 643 (vw), 613 (vw), 589 (vw), 514 (w). Raman (1064 nm, 200 mW, 25 °C):  $\tilde{\nu}$  ( $\text{cm}^{-1}$ ) = 1660 (7), 1565 (5), 1423 (4), 1400 (100), 1370 (4), 1313 (2), 1289 (2), 1226 (9), 1200 (2), 1007 (2), 829 (16), 756 (4), 590 (4), 374 (2), 269 (4).  $^1\text{H}$  NMR ( $d_6$ -DMSO, 400 MHz, ppm)  $\delta$  = 10.07 (s, 2H).  $^{13}\text{C}$  NMR ( $d_6$ -DMSO, 101 MHz, ppm)  $\delta$  = 149.7, 101.0.  $^{14}\text{N}$  NMR ( $d_6$ -DMSO, 29 MHz, ppm)  $\delta$  = −18.  $^{15}\text{N}$  NMR ( $d_6$ -DMSO, 41 MHz, ppm)  $\delta$  = −25.9, −114.8. Anal. Calcd for  $\text{C}_6\text{H}_2\text{N}_8\text{O}_8\cdot\text{H}_2\text{O}$ : C 21.70, H 1.21, N 33.74 %. Found: C 21.89, H 1.46, N 33.57 %.

**6**: Colorless needles. DTA (5 °C  $\text{min}^{-1}$ ): 292 °C (melt.), 298 °C (exo.); BAM: drop hammer: 4.5 J (100–500  $\mu\text{m}$ ); friction tester: 192 N (100–500  $\mu\text{m}$ ); ESD: 0.30 J (100–500  $\mu\text{m}$ ). IR (ATR),  $\tilde{\nu}$  ( $\text{cm}^{-1}$ ) = 3740 (vw), 3208 (m), 2967 (w), 1567 (s), 1519 (vs), 1482 (s), 1416 (s), 1348 (s), 1320 (vs), 1274 (w), 1207 (m), 1018 (w), 994 (m), 842 (vs), 758 (m), 744 (m), 712 (m), 675 (m), 635 (m), 580 (w), 518 (m). Anal. Calcd for  $\text{C}_6\text{H}_2\text{N}_8\text{O}_8$ : C 22.94, H 0.64, N 35.67 %. Found: C 23.04, H 0.85, N 35.66 %.

## 7.4. Conclusions

Our findings are important for a reliable approach towards facile accumulation of nitro functionalities at the pyrazole platform. C-nitrations at the 4,4'-bipyrazole (**1**), were performed under very simple, cost-effective and environmentally benign reaction conditions. The step-wise nitration causes a significant change increasing impact sensitivity and density and therefore

## Facile and Selective Polynitrations at the 4-Pyrazolyl Dual Backbone: A Straightforward Access to a Series of High-Density Energetic Materials

energetic performance. Compounds **2–4** are especially promising intermediates, while exhibiting excellent thermal stability and low sensitivity towards external stimuli. Moreover, compounds **5** and **6** can be already classified as explosive materials showing excellent thermals stability and good sensitivities. Further functionalization of the 4,4'-bipyrazole scaffold is currently under investigation in our laboratories.

### 7.5. Conflicts of interest

There are no conflicts to declare.

### 7.6. Acknowledgements

Financial support of this work by the Ludwig-Maximilian University of Munich (LMU) and the Office of Naval Research (ONR) under grant no. ONR.N00014-16-1-2062 is gratefully acknowledged. We thank Dr. Burkhard Krumm for NMR measurements and Stefan Huber for his help with the sensitivity testing.

### 7.7. Notes and references

- [1] (a) H. Gao and J. M. Shreeve, *Chem. Rev.*, 2011, **111**, 7377; (b) T. M. Klapötke, *Chemistry of High-Energy Materials*, 3rd ed., De Gruyter, Berlin, 2015.
- [2] (a) T. Brinck (Ed.), *Green Energetic Materials*, John Wiley & Sons, 2014. (b) G. I. Sunahara, G. Lotufo, R. G. Kuperman and J. Hawari (Eds.), *Ecotoxicology of Explosives*, CRC Press, 2009.
- [3] (a) P. Yin and J. M. Shreeve, *Adv. Het. Chem.*, 2017, **121**, 89; (b) P. Yin, J. Zhang, C. He, D. A. Parrish, and J. M. Shreeve, *J. Mater. Chem. A*, 2014, **2**, 3200.
- [4] G. Hervé, C. Roussel and H. Graindorge, *Angew. Chem. Int. Ed.*, 2010, **49**, 3177.
- [5] (a) W.-Q. Tang, H. Ren, Q.-J. Jiao and W. Zheng, *Chin. J. Energ. Mat.*, 2017, **25**, 44; (b) S. Du, Y. Wang, L. Chen, W. Shi, F. Ren, Y. Li, J. Wang and D. Cao, *J. Mol. Model.*, 2012, **18**, 2105. (c) P. Ravi, D. M. Badgujar, G. M. Gore, S. P. Tewari and A. K. Sikder, *Propellants Explos. Pyrotech.* 2011, **36**, 393.
- [6] (a) D. Fischer, J. L. Gottfried, T. M. Klapötke, K. Karaghiosoff, J. Stierstorfer and T. G. Witkowski, *Angew. Chem. Int. Ed.*, 2016, **55**, 16132; (b) D. Kumar, G. H. Imler, D. A. Parrish and J. M. Shreeve, *J. Mater. Chem. A*, 2017, **5**, 10437; (c) D. Kumar, G. H. Imler, D. A. Parrish and J. M. Shreeve, *Chem. Eur. J.*, 2017, **23**, 7876; (d) P. Yin, J. Zhang, D. A. Parrish and J. M. Shreeve, *Chem. Eur. J.*, 2014, **20**, 16529.



**Facile and Selective Polynitrations at the 4-Pyrazolyl Dual Backbone: A Straightforward Access to a Series of High-Density Energetic Materials**

- [7] (a) C. Li, L. Liang, K. Wang, C. Bian, J. Zhang and Z. Zhou, *J. Mat. Chem. A*, 2014, **2**, 18097; (b) Y. Tang, C. He, G. H. Imler, D. A. Parrish and J. M. Shreeve, *J. Mat. Chem. A*, 2018, **6**, 5136.
- [8] (a) Y. Tang, D. Kumar and J. M. Shreeve, *J. Am. Chem. Soc.*, 2017, **139**, 13684; (b) P. Yin, J. Zhang, G. H. Imler, D. A. Parrish and J. M. Shreeve, *Angew. Chem. Int. Ed.*, 2017, **56**, 8834; (c) P. Yin, C. He and J. M. Shreeve, *J. Mat. Chem. A*, 2016, **4**, 1514.
- [9] (a) P. Yin, D. A. Parrish and J. M. Shreeve, *J. Am. Chem. Soc.*, 2015, **137**, 4778; (b) Y. Zhang, Y. G. Huang, D. A. Parrish, and J. M. Shreeve, *J. Mater. Chem.*, 2011, **21**, 6891; (c) Y. Zhang, D. A. Parrish and J. M. Shreeve, *Chem. Eur. J.*, 2012, **18**, 987.
- [10] (a) P. Yin, L. A. Mitchell, D. A. Parrish and J. M. Shreeve, *Chem. Asian J.*, 2017, **12**, 378; (b) Y. Zhang, Y. Guo, Y. Joo, D. A. Parrish and J. M. Shreeve, *Chem. Eur. J.*, 2010, **16**, 10778.
- [11] (a) C. Li, M. Zhang, Q. Chen, Y. Li, H. Gao, W. Fu and Z. Zhou, *Chem. Eur. J.*, 2017, **23**, 1490; (b) J. Zhang and J. M. Shreeve, *Dalton Trans.*, 2016, **45**, 2363.
- [12] (a) J. C. Bennion, Z. R. Siddiqi and A. J. Matzger, *Chem. Commun.*, 2017, **53**, 6065; (b) J. Zhang and J. M. Shreeve, *CrystEngComm*, 2016, **18**, 6124.
- [13] S. F. Zhu, S. H. Zhang, R. J. Gou and F. D. Ren, *J. Mol. Model.*, 2018, 24:9.
- [14] L. Larina and V. Lopyrev, *Nitroazoles: synthesis, structure and applications*, Springer, Dordrecht, 2009.
- [15] J. W. A. M. Janssen, H. J. Kolners, G. G. Kruse and C. L. Habraken, *J. Org. Chem.*, 1973, **38**, 1777.
- [16] A. Bragin, A. Pivkina, N. Muravyev, K. Monogarov, O. Gryzlova, T. Shkineva and I. Dalinger, *Physics Procedia* 2015, **72**, 358.
- [17] J. H. Ridd, *Acta Chem. Scand.*, 1998, **52**, 11.
- [18] S. Trofimenko, *J. Org. Chem.*, 1964, **29**, 3046.
- [19] M. W. Austin, J. R. Blackborow, J. H. Ridd and B. V. Smith, *J. Chem. Soc.*, 1965, 1051.
- [20] A. R. Katritzky, H. O. Tarhan and B. Terem, *J. Chem. Soc. Perkin Trans. 2*, 1975, 1632.
- [21] I. L. Dalinger, T. K. Shkinyova, S. A. Shevelev, V. S. Kuz'min, E. A. Arnautove and T. S. Pivina, *Proceedings of the 29th International Annual Conference of ICT*, Karlsruhe, Germany, 1998, 57-1.
- [22] J. W. A. M. Janssen, C. C. Kruse, H. J. Koeners and C. L. Habraken, *J. Heterocycl. Chem.*, 1973, **10**, 1055.
- [23] I. Boldog, E. B. Rusanov, A. N. Chernega, J. Sieler and K. V. Domasevitch, *Angew. Chem. Int. Ed.*, 2001, **40**, 3435.

- [24] (a) A. Bauzá, T. J. Mooibroek and A. Frontera, *Chem. Commun.*, 2015, **51**, 1491; (b) A. Bauzá, A. V. Sharko, G. A. Senchyk, E. B. Rusanov, A. Frontera and K. V. Domasevitch, *CrystEngComm*, 2017, **19**, 1933.
- [25] J. D. Dunitz, *X-ray analysis and the structure of organic solids*, 2nd corrected reprint, 1995, Basel: Verlag Helvetica Chimica Acta, 106.
- [26] M.-X. Zhang, P. E. Eaton and R. Gilardi, *Angew. Chem. Int. Ed.*, 2000, **39**, 401.
- [27] T. M. Klapötke and T. G. Witkowski, *ChemPlusChem*, 2016, **81**, 357.
- [28] M. Sućeska, *EXPLO5 Version 6.03 User's Guide*, Zagreb, Croatia: OZM; 2015.
- [29] J. S. Murray and P. Politzer, *J. Mol. Model.*, 2014, **20**, 2223.
- [30] (a) G. M. Sheldrick, *Acta Crystallogr., Sect. A: Found. Crystallogr.*, 2008, **64**, 112. (b) G. M. Sheldrick, *Acta Crystallogr., Sect. C: Cryst. Struct. Commun.*, 2015, **71**, 3.

## 7.8. Supporting Information

### 7.8.1. Experimental Procedures

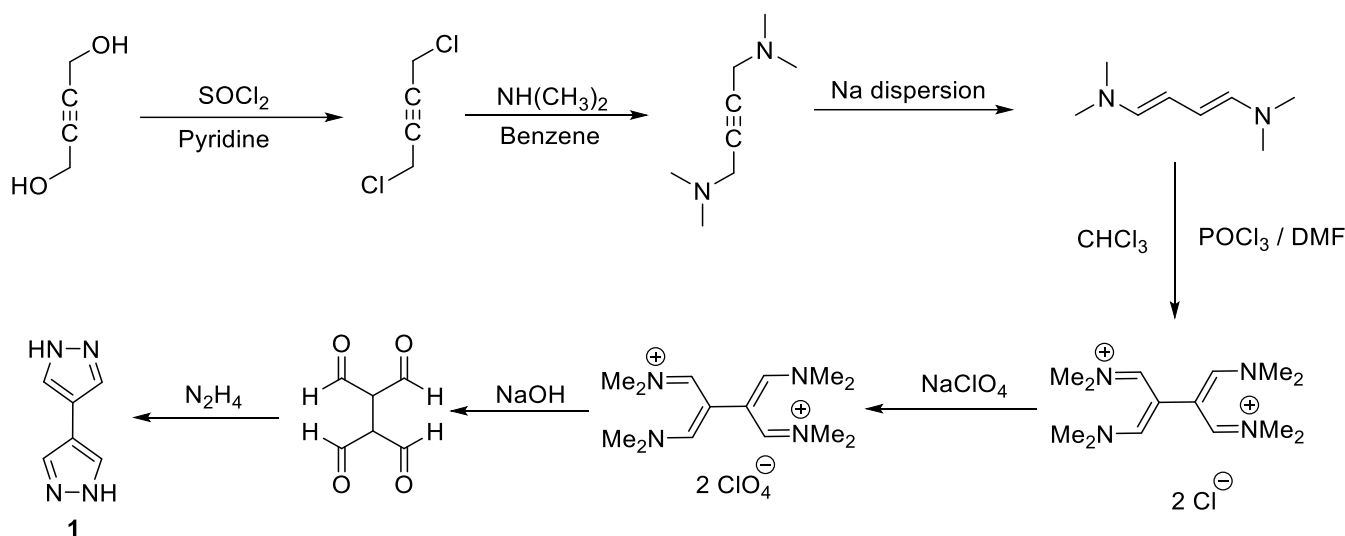
#### 7.8.1.1. General Procedures

$^1\text{H}$  and  $^{13}\text{C}$  NMR spectra were recorded on *JEOL 270* and *BRUKER AMX 400* instruments. The samples were measured at room temperature in standard NMR tubes ( $\varnothing$  5 mm). Chemical shifts are reported as  $\delta$  values in ppm relative to the residual solvent peaks *d*<sub>6</sub>-DMSO ( $\delta_{\text{H}}$ : 2.50,  $\delta_{\text{C}}$ : 39.5). Solvent residual signals and chemical shifts for NMR solvents were referenced against tetramethylsilane (TMS,  $\delta$  = 0 ppm) and nitromethane. Unless stated otherwise, coupling constants were reported in hertz (Hz) and for the characterization of the observed signal multiplicities the following abbreviations were used: s (singlet), d (doublet), t (triplet), q (quartet), quint (quintet), sept (septet), m (multiplet) and br (broad). Low resolution mass spectra were recorded on a *JEOL JMS-700 MStation* mass spectrometer (EI+/DEI+). Infrared spectra (IR) were recorded from 4500  $\text{cm}^{-1}$  to 650  $\text{cm}^{-1}$  on a PERKIN ELMER Spectrum BX-59343 instrument with *SMITHS DETECTION DuraSamplIR II Diamond ATR* sensor. The absorption bands are reported in wavenumbers ( $\text{cm}^{-1}$ ). Elemental analysis was carried out by the department's internal micro analytical laboratory on an *Elementar Vario el* by pyrolysis of the sample and subsequent analysis of the formed gases. All sensitivities toward impact (IS) and friction (FS) were determined according to BAM (German: Bundesanstalt für Materialforschung und Prüfung) standards using a BAM drop hammer and a BAM friction apparatus.<sup>[S1]</sup> Compounds **2–6** and **6**·H<sub>2</sub>O were tested for sensitivity towards electrical discharge using an Electric Spark Tester ESD 2010 EN.

#### 7.8.1.2. Synthesis

## Facile and Selective Polynitrations at the 4-Pyrazolyl Dual Backbone: A Straightforward Access to a Series of High-Density Energetic Materials

The synthesis of **1** was performed by the literature known method<sup>[S2]</sup> starting with readily available and inexpensive industrial product 2-butyne-1,4-diole. This simple (and easily scalable for bulk preparations) procedure was essentially a compilation of literature methods for preparation of 1,4-dichloro-2-butyne, either with  $\text{SOCl}_2$ <sup>[S3]</sup> or  $\text{POCl}_3$ <sup>[S4]</sup> as the reagents; preparation of 1,4-*bis*(dimethylamino)butyne<sup>[S5,6]</sup> and its rearrangement into the conjugated *cis-trans*-butadiene over Na metal dispersion<sup>[S6]</sup> and the subsequent Vilsmeier-Haack-Arnold formylation providing symmetric *bis*-trimethinium salt (isolated and purified as perchlorate salt).<sup>[S7]</sup> The latter was hydrolyzed to *bis*-dialdehyde and then converted into the desired 4,4'-bipyrazole (**1**).



**Scheme S1.** Performed synthesis for 4,4'-bipyrazole (**1**) according the known literature.

### 7.8.2. X-ray Diffraction

The diffraction data were collected with graphite-monochromated Mo  $K\alpha$  radiation ( $\lambda = 0.71073 \text{ \AA}$ ) using a Stoe Image Plate Diffraction System,  $\phi$  oscillation scans (typically,  $\phi 0 \rightarrow 180^\circ$ ;  $\Delta\phi = 0.8\text{-}0.9^\circ$ ; exposure times 7-8 min per frame).<sup>[S8]</sup> For **1** and **5**, the data were collected with IPDS-2T diffractometer. The structures were solved by direct methods and refined by full-matrix least-squares on  $F^2$  using the programs SHELXS-97 and SHELXL-2014/7.<sup>[S9]</sup> All the CH-hydrogen atoms were located and freely refined with isotropic thermal parameters. Table S1 lists main crystallographic data and parameters of crystal structure refinement. Graphical visualization of the structure was made using the program Diamond 2.1e,<sup>[S10]</sup> and the topological analysis was performed using TOPOS 4.0.<sup>[S11]</sup>

The most important molecular geometry parameter, which is sensitive to the progressive nitro substitution at the 4,4'-bipyrazole platform, is dihedral angle (twist angle)  $\phi$  subtended by mean planes of two pyrazole halves. Unsubstituted 4,4'-bipyrazole is exactly planar, while lying across a center of inversion in the crystal,<sup>[S2]</sup> and the molecule of mononitro derivative **2** retains appreciably flat structure

### Facile and Selective Polynitrations at the 4-Pyrazolyl Dual Backbone: A Straightforward Access to a Series of High-Density Energetic Materials

[ $\varphi = 5.63(12)^\circ$ ] as well. With the second nitro group, either in the case of 3,5- or 3,3'-derivatives, the bipyrazole core lose planarity [ $\varphi = 46.48(4)$  and  $50.28(5)^\circ$ , for **2** and **3**, respectively], but similar effect from further substitution (**2**, **3**  $\rightarrow$  **4**  $\rightarrow$  **5**) is much weaker (Table S2). Moreover, the mutual orientation of two pyrazole rings for **4** and **5** does not differ significantly [ $\varphi = 50.28(5)$  vs.  $58.58(9)^\circ$ ] and thus the third and fourth NO<sub>2</sub> groups installed at the molecular frame do not lead to essential steric strains. This situation may be compared with conformations of 4,4'-bipyrazole and its 3,3'-dimethyl- [ $\varphi = 5-30^\circ$ ] and 3,3',5,5'-tetramethyl [ $\varphi = 60-90^\circ$ ] derivatives in many examined salts<sup>[S12]</sup> and coordination compounds.<sup>[S13]</sup>

# Facile and Selective Polynitrations at the 4-Pyrazolyl Dual Backbone: A Straightforward Access to a Series of High-Density Energetic Materials

**Table S1.** Crystal data for compounds **2-6** and **6·H<sub>2</sub>O**.

	<b>2</b>	<b>3</b>	<b>4</b>	<b>5</b>	<b>6</b>	<b>6·H<sub>2</sub>O</b>
Formula	C <sub>6</sub> H <sub>5</sub> N <sub>5</sub> O <sub>2</sub>	C <sub>6</sub> H <sub>4</sub> N <sub>6</sub> O <sub>4</sub>	C <sub>6</sub> H <sub>4</sub> N <sub>6</sub> O <sub>4</sub>	C <sub>6</sub> H <sub>3</sub> N <sub>7</sub> O <sub>6</sub>	C <sub>6</sub> H <sub>2</sub> N <sub>8</sub> O <sub>8</sub>	C <sub>6</sub> H <sub>4</sub> N <sub>8</sub> O <sub>9</sub>
<i>M</i>	179.15	224.15	224.15	269.15	314.16	332.17
<i>T</i> / K	173	213	213	213	203	213
Color and habit	Orange plate	Pale-yellow prism	Pale-yellow plate	Colorless prism	Colorless prism	Colorless block
Size / mm	0.26 × 0.24 × 0.22	0.26 × 0.24 × 0.20	0.27 × 0.25 × 0.22	0.22 × 0.18 × 0.17	0.28 × 0.22 × 0.20	0.27 × 0.24 × 0.23
Crystal system	Tetragonal	Monoclinic	Monoclinic	Monoclinic	Tetragonal	Monoclinic
Space group	<i>P</i> 4 <sub>1</sub> 2 <sub>1</sub> 2 (No. 92)	<i>C</i> 2/ <i>c</i> (No. 15)	<i>C</i> 2/ <i>c</i> (No. 15)	<i>P</i> 2 <sub>1</sub> / <i>c</i> (No. 14)	<i>P</i> 4 <sub>2</sub> / <i>n</i> (No. 86)	<i>Cc</i> (No. 9)
<i>Z</i>	8	4	4	4	8	4
<i>a</i> / Å	5.4831(2)	15.9744(9)	6.1653(7)	8.6064(8)	16.4281(13)	11.1017(9)
<i>b</i> / Å	5.4831(2)	6.5428(8)	15.7789(12)	11.9636(9)	16.4281(13)	13.9227(10)
<i>c</i> / Å	47.463(3)	8.9414(8)	8.7387(10)	10.1200(9)	8.3705(6)	8.2166(8)
<i>α</i> / °	90	90	90	90	90	90
<i>β</i> / °	90	118.739(10)	107.434(10)	114.148(10)	90	110.654(10)
<i>γ</i> / °	90	90	90	90	90	90
<i>V</i> / Å <sup>3</sup>	1426.95(12)	819.41(13)	811.06(14)	950.81(14)	2259.1(3)	1188.38(17)
<i>μ</i> (Mo-Kα)/ mm <sup>-1</sup>	0.132	0.156	0.157	0.170	0.172	0.175
<i>D</i> <sub>calc</sub> / g cm <sup>-3</sup>	1.668	1.817	1.836	1.880	1.847	1.857
2 <i>θ</i> <sub>max</sub> / °	27.95	28.03	27.94	28.01	28.28	27.99
Measd/ Unique reflns	6517 / 1701	3236 / 986	3458 / 959	8130 / 2294	9974 / 2783	5099 / 2319
Completeness/ %	98.8	99.0	98.5	997	992	982
Reflns with <i>I</i> > 2 <i>σ</i> ( <i>I</i> )	1584	829	835	1365	2122	2059
<i>R</i> <sub>int</sub>	0.035	0.023	0.024	0.043	0.041	0.017
Parameters refined	138	81	82	184	207	224
<i>R</i> 1, <i>wR</i> 2 ( <i>I</i> > 2 <i>σ</i> ( <i>I</i> ))	0.032, 0.078	0.037, 0.094	0.034, 0.090	0.038, 0.081	0.034, 0.080	0.021, 0.049
<i>R</i> 1, <i>wR</i> 2 (all data)	0.034, 0.079	0.042, 0.097	0.039, 0.091	0.070, 0.086	0.049, 0.083	0.024, 0.050
Goof on <i>F</i> <sup>2</sup>	1.102	1.045	1.089	0.814	1.001	0.936
Max, min peak/ e Å <sup>-3</sup>	0.16, -0.13	0.29, -0.24	0.34, -0.19	0.22, -0.20	0.23, -0.24	0.15, -0.11
CCDC	1836403	1836404	1836405	1836406	1836407	1836408

## Facile and Selective Polynitrations at the 4-Pyrazolyl Dual Backbone: A Straightforward Access to a Series of High-Density Energetic Materials

Unlike these very individual conformational features, the bond lengths and bond angles are less sensitive to the progressive nitro substitution and the corresponding parameters for 4,4'-bipyrazole,<sup>[S2]</sup> **2-6** and **6·H<sub>2</sub>O** appear to be actually uniform. In particular, the central C-C bond lengths are nearly identical for all the species, when lying within the narrow range of 1.4589(19)-1.467(2) Å (Table S2). These bonds are very similar even in the case of **3** and **4** (existing as pyrazolium/pyrazolate zwitterion) [1.4589(19) and 1.4621(19) Å, respectively]. Very subtle differences in the bond lengths parameters may be detected for the pyrazole N-N bonds, which experience certain shortening as the number of nitro group increased [1.32-1.33 Å for dinitropyrazole rings and 1.34-1.35 Å for unsubstituted pyrazole rings, see **Table S2**].

**Table S2.** Selected geometry parameters for 4,4'-bipyrazole **1**,<sup>[S2]</sup> **2-6** and **6·H<sub>2</sub>O**.

	NO <sub>2</sub> groups	Twist angle/°	d(C-C)/ Å	d(N-N)/ Å for the rings:		
				pyrazole	nitropyrazole	dinitropyrazole
<b>1</b>	0	0	1.464(2)	$1.3462(15) \times 2$	-	-
<b>2</b>	1	5.63(12)	1.462(2)	1.350(2)	1.333(2)	-
<b>3</b>	2	46.48(4)	1.4589(19)	-	$1.3334(15) \times 2$	-
<b>4</b>	2	50.28(5)	1.4621(19)	1.341(2)	-	1.3352(17)
<b>5</b>	3	58.58(9)	1.468(2)	-	1.339(2)	1.323(2)
<b>6</b>	4	71.44(5)	1.4644(15)	-	-	1.3263(16); 1.3321(16)
<b>6·H<sub>2</sub>O</b>	4	78.99(6)	1.467(2)	-	-	1.320(2); 1.322(2)

### 7.8.2.1. Crystal structure of 3-nitro-4,4'-bipyrazole (**2**)

The compound crystallizes in a chiral group *P4<sub>1</sub>2<sub>1</sub>2* (enantiomorphous to *P4<sub>3</sub>2<sub>1</sub>2*) (with relatively long period *c* of the unit cell of 47.463(3) Å) and it adopts complicated 3D supramolecular structure, dominated by conventional hydrogen bonding of pyrazole NH donors. These interactions reveal some kind of segregation: two sites of the molecules establish two distinct supramolecular patterns incorporating either pyrazole or nitropyrazole groups only.

## Facile and Selective Polynitrations at the 4-Pyrazolyl Dual Backbone: A Straightforward Access to a Series of High-Density Energetic Materials

The latter motif involves multiple set of bifurcate and weaker interactions (Fig. S1). The N3H group adopts H-bond to nitropyrazole moiety: it utilizes pyrazole N4<sup>ii</sup> and nitro O1<sup>ii</sup> [symmetry code (ii)  $y, -1+x, -z$ ] atoms as acceptors and the N3H...O1<sup>ii</sup> branch of this bifurcate bond is slightly stronger and more directional (Table S3).

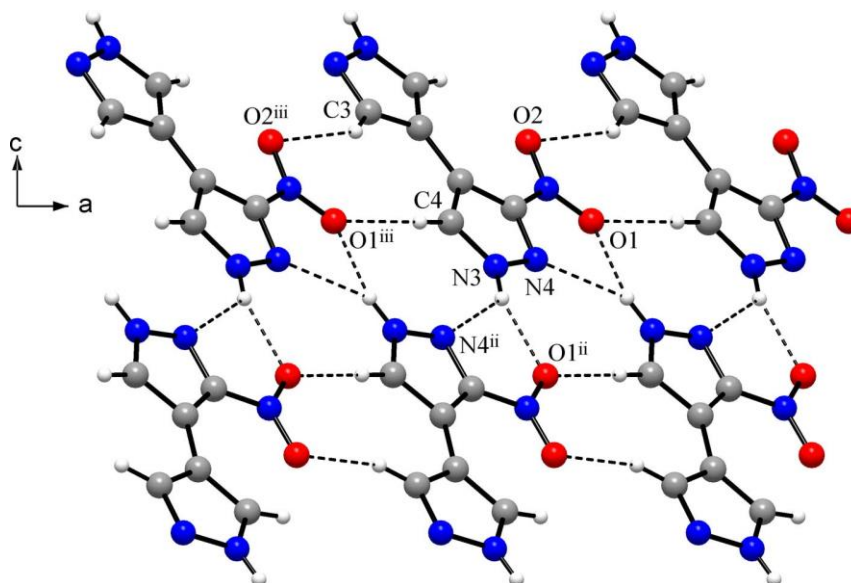


**Figure S1.** Hydrogen bonded motif of the structure of **2** involving nitropyrazole sides of the molecules. Note the bifurcation of the NH...N,O bonds and double CH...O bonding to nitro acceptor [Symmetry codes: (ii)  $y, -1+x, -z$ ; (iii)  $-1+x, -1+y, z$ ].

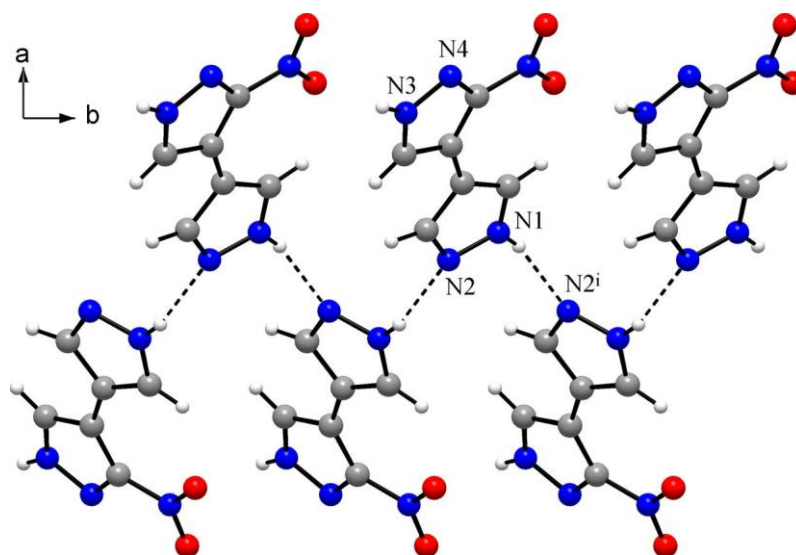


**Figure S2.** Hydrogen bonded motif of the structure of **2** involving pyrazole sides of the molecules, in the form of catemer [Symmetry code: (i)  $-1.5-x, 0.5+y, 0.25-z$ ].

## Facile and Selective Polynitrations at the 4-Pyrazolyl Dual Backbone: A Straightforward Access to a Series of High-Density Energetic Materials

Weaker CH $\cdots$ O bonds are found between the adjacent pyrazole cycles and nitro group [symmetry code (iii)  $-1+x, -1+y, z$ ]. These interactions connect the molecular into strips, which pack one on the top of another and are interconnected by H-bonds through unsubstituted pyrazole sites of the molecules. This pyrazole connectivity is sustained with relatively short and directional N1H $\cdots$ N2<sup>i</sup> bonds [N $\cdots$ N = 2.8665(17) Å;  $\angle$ NH $\cdots$ N = 152.1(11) $^\circ$ ; symmetry code (i)  $-1.5-x, 0.5+y, 0.25-z$ ] and it exists in the form of catemer (Fig. S2), very similar to the structure of 4,4'-bipyrazole itself.<sup>[S2]</sup> The entire H-bonded structure represents 3D framework of exceptional topology. When considering only the strongest interactions of conventional NH donors, every molecule is bonded with four closest neighbors, and thus the uninodal four-coordinated 3D framework with a point (Schläfli) symbol  $\{6^3.8^3\}$  is found [extended point symbol: 6.6.6.8(8).8(4).8(4)] (See Fig. S3). Alternatively, with a single pyrazole cycle as three-connected net node, two NH-hydrogen bonds and central covalent C-C bonds as the net links, the topology may be regarded as binodal 3,3-coordinated net with a point (Schläfli) symbol  $\{10^2.12\}\{10^3\}$ .

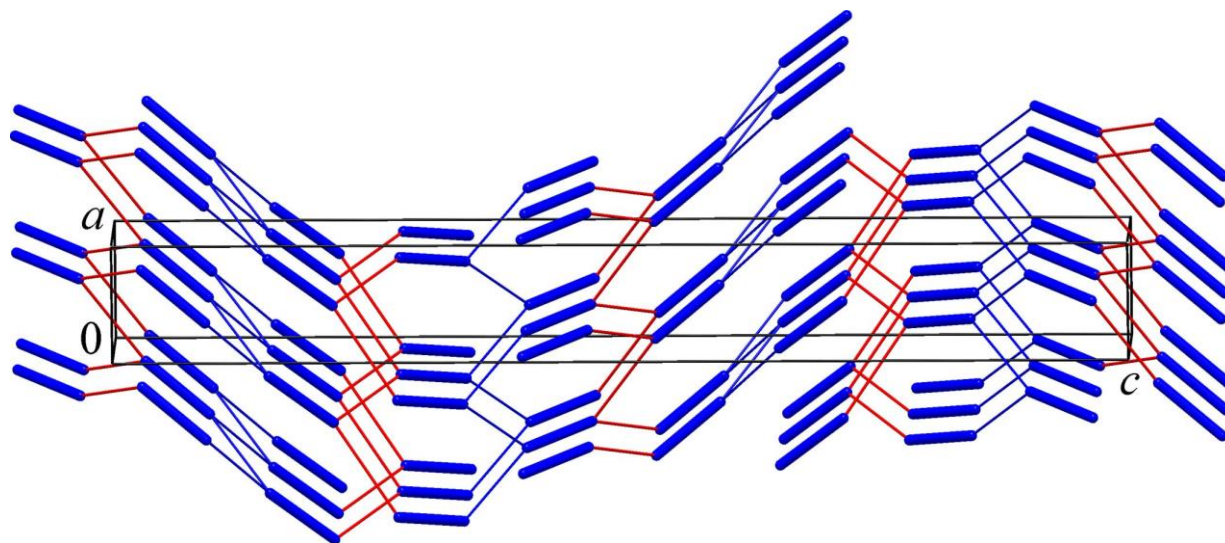


**Figure S3.** Supramolecular connectivity in the structure of **2**: Blue sticks represent molecules of the bipyrazole, thin blue lines are NH $\cdots$ N links of unsubstituted pyrazole sides whereas thin red lines are NH $\cdots$ N,O bonds of nitropyrazole sides. Note very long period of translation along  $c$  axis [47.463(3) Å].

**Table S3.** Hydrogen-bond geometry (Å,  $^\circ$ ) for the structure of 3-nitro-4,4'-bipyrazole (**2**).

Donor (D)	Hydrogen (H)	Acceptor (A) <sup>a)</sup>	D-H	H $\cdots$ A	D $\cdots$ A	$\angle$ DH $\cdots$ A
-----------	--------------	----------------------------	-----	--------------	--------------	------------------------



**Facile and Selective Polynitrations at the 4-Pyrazolyl Dual Backbone: A Straightforward Access to a Series of High-Density Energetic Materials**

N1	H1N	N2 <sup>i</sup>	0.87(2)	2.07(2)	2.8665(17)	152.1(11)
N3	H2N	N4 <sup>ii</sup>	0.89(2)	2.463(19)	3.1272(16)	131.8(15)
N3	H2N	O1 <sup>ii</sup>	0.89(2)	2.04(2)	2.8808(16)	157.6(16)
C1	H1	O2	0.92(2)	2.314(18)	2.8784(18)	119.3(13)
C3	H3	O1 <sup>iii</sup>	0.95(2)	2.76(2)	3.6786(18)	162.1(15)
C3	H3	O2 <sup>iii</sup>	0.95(2)	2.53(2)	3.3657(18)	146.7(15)
C4	H4	O1 <sup>iii</sup>	0.933(19)	2.42(2)	3.3478(17)	175.7(16)

<sup>a)</sup> Symmetry codes: (i)  $-1.5-x, 0.5+y, 0.25-z$ ; (ii)  $y, -1+x, -z$ ; (iii)  $-1+x, -1+y, z$ .

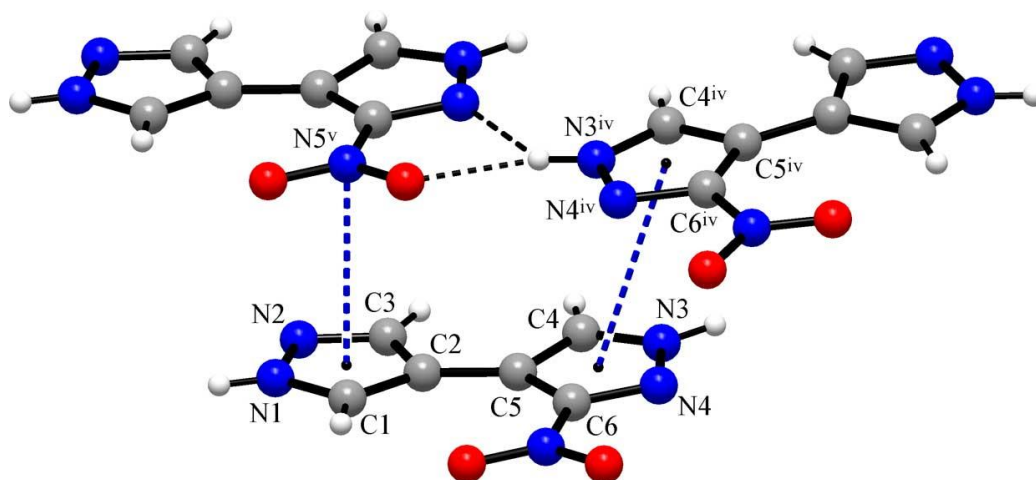


**Figure S4.** Weak stacking interactions in the structure of **2**: slipped  $\pi/\pi$  interaction of two nitropyrazole groups and  $\pi$ -hole/ $\pi$  contact involving nitro group [Symmetry codes: (iv)  $y, x, -z$ ; (v)  $-1+x, y, z$ ].

Structure of **2** is the only example for stacking interactions, within a full set of the examined nitro-4,4'-bipyrazoles. Very weak slipped  $\pi/\pi$  interactions is observed between the nitropyrazole rings (Fig. S4) whereas nitro group establishes contact with the pyrazole ring. The latter one may be attributes to a very weak  $\pi$ -hole/ $\pi$  interaction, with the nitro-N atom situated almost exactly above the ring centroid [ $N\cdots\pi = 3.226(2)$  Å; slippage angle is  $5.07^\circ$ ]. It is not surprising that such kind of interactions occurs for unsubstituted pyrazole ring, but it is totally eliminated for more electron deficient nitropyrazoles (**3-6**).

**Table S4.** Geometry parameters of stacking interactions in the structure of **2**.<sup>a)</sup>

Type	Group 1	Group 2	Shortest contact/ Å	IPD/ Å	CCD/ Å	SA/ °

$\pi/\pi$	(C4C5C6N3N4)	(C4C5C6N3N4) <sup>iv</sup>	3.254(2)	3.265(2)	3.562(2)	23.58
$\text{NO}_2/\pi$	(C1C2C3N1N2)	(N5O1O2) <sup>v</sup>	3.322(2)	3.213(2)	3.226(2)	5.07

<sup>a)</sup> See Fig. S4. IPD is the interplanar distance (distance from one plane to the neighboring centroid), CCD is the centre-to-centre distance (distance between ring centroids), SA is the slippage angle (angle subtended by the intercentroid vector to the plane normal). For  $\text{NO}_2/\pi$  stacking, IPD and CCD refer to distances between plane of Group 1 and N5<sup>v</sup>; and distance between centroid of Group 1 and N5<sup>v</sup>, respectively [Symmetry codes: (iv)  $y, x, -z$ ; (v)  $-1+x, y, z$ .]

#### 7.8.2.2. Crystal structure of 3,3'-dinitro-4,4'-bipyrazole (3)

The compound crystallizes in space group  $C2/c$  and the molecule resides on a two-fold axis passing through the centroid of the central C-C bond. Thus two pyrazole halves of the molecules are symmetry equivalent. This causes significant simplification of the supramolecular array, as may be compared with the previous structure. Loss of the coplanarity of two pyrazole rings, now subtending dihedral angle of  $46.48(4)^\circ$ , is also an important factor. First, this eliminates stacking interactions, which are favorable for packing of flat molecules. Second, the twisted structure mitigates against efficiency of double  $\text{CH}\cdots\text{O}$  bonding from two pyrazole rings to a nitro acceptor seen in the structure of **2**. The primary supramolecular pattern in **3** exists as 2D flat four-connected network parallel to a  $ab$  plane, which is sustained with a set of bifurcate  $\text{NH}\cdots\text{N}, \text{O}$  bonds (Fig. S5). Two branches of such bonds are nearly identical in the view of  $\text{D}\cdots\text{A}$  separations [ $\text{N}\cdots\text{N} = 3.0433(13)$  vs.  $\text{N}\cdots\text{O} = 2.9946(13)$  Å], although interaction with N-acceptor is more directional [ $\angle\text{NH}\cdots\text{N} = 160.9(16)^\circ$  vs.  $\angle\text{NH}\cdots\text{O} = 128.4(15)^\circ$ , Table S5]. This is accompanied with a set of very weak  $\text{CH}\cdots\text{O}$  bonds [ $\text{C}\cdots\text{O} = 3.5742(17)$  and  $3.6982(16)$  Å], which are also bifurcated and one of these branches is involved for connection of successive layers, separated at 3.92 Å (Fig. S6). It worths noting that within the single layer the orientation of the molecules is identical and therefore the layer is polar. However, polarities of separate layers compensate each other by anti-alignment.

Facile and Selective Polynitrations at the 4-Pyrazolyl Dual Backbone: A Straightforward Access to a Series of High-Density Energetic Materials

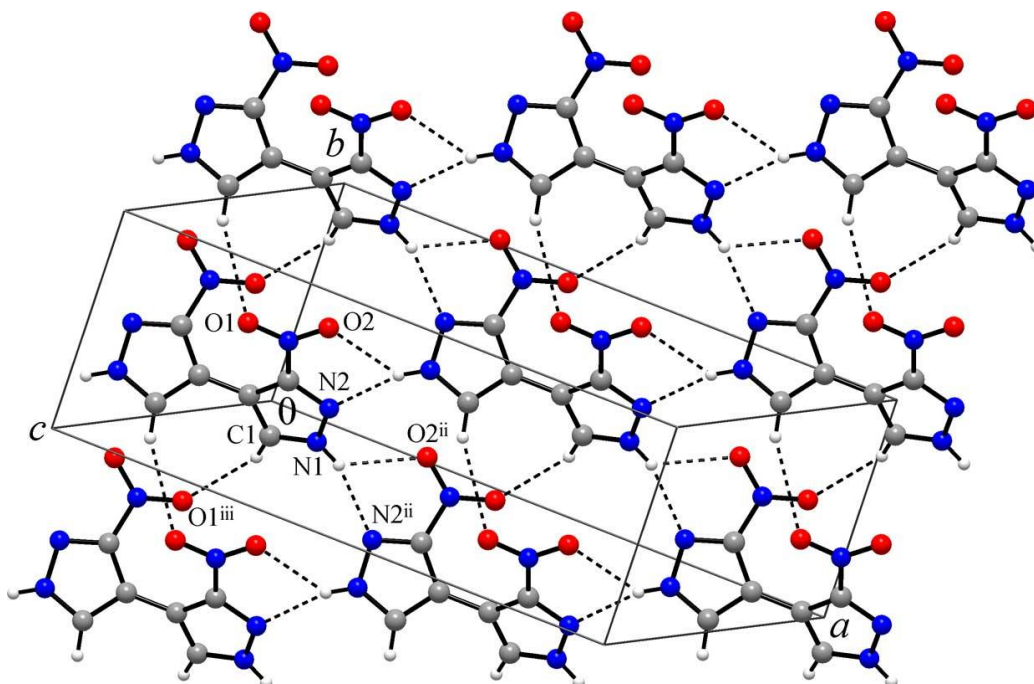


**Figure S5.** Fragment of the structure of **3** showing the flat hydrogen bonded network, which is parallel to a *ab* plane. [Symmetry codes: (ii) 0.5-*x*, -0.5+*y*, 0.5-*z*; (iii) -*x*, -1+*y*, 0.5-*z*].

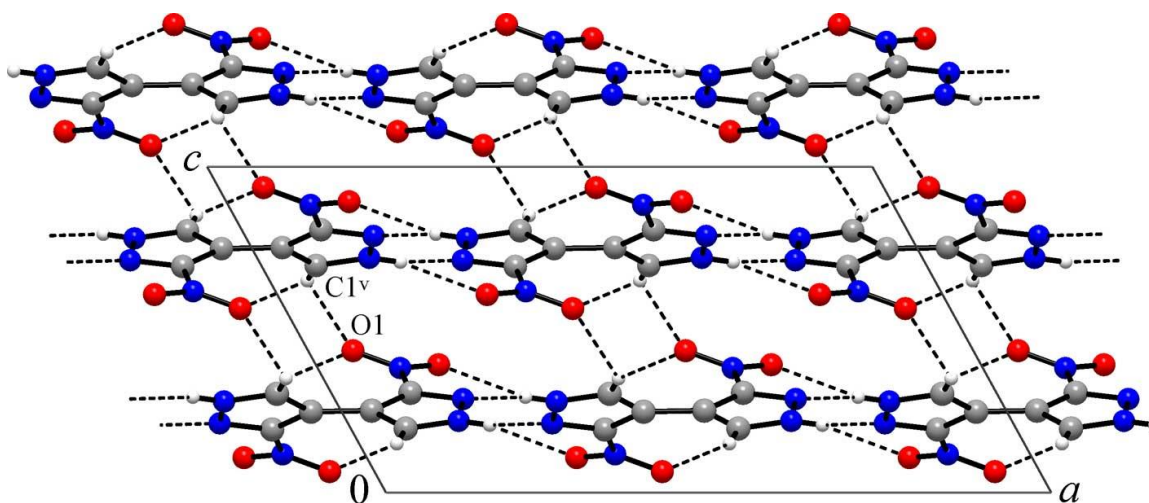


**Figure S6.** Projection on a *ac* plane: Packing of successive layers in the structure of **3**, with a set of very weak interlayer CH...O bonding [Symmetry code (v) *x*, -*y*, 0.5+*z*].

**Table S5.** Hydrogen-bond geometry (Å, °) for structure of 3,3'-dinitro-4,4'-bipyrazole **3**.

Donor (D)	Hydrogen (H)	Acceptor (A) <sup>a)</sup>	D-H	H...A	D...A	∠DH...A
N1	H1N	N2 <sup>ii</sup>	0.869(18)	2.208(18)	3.0433(13)	160.9(16)

**Facile and Selective Polynitrations at the 4-Pyrazolyl Dual Backbone: A Straightforward Access to a Series of High-Density Energetic Materials**

N1	H1N	O2 <sup>ii</sup>	0.869(18)	2.376(18)	2.9946(13)	128.4(15)
C1	H1	O1 <sup>iii</sup>	0.951(16)	2.803(16)	3.6982(16)	157.2(11)
C1	H1	O1 <sup>iv</sup>	0.951(16)	2.794(16)	3.5742(17)	139.9(11)

<sup>a)</sup> Symmetry codes: (ii) 0.5-x, -0.5+y, 0.5-z; (iii) -x, -1+y, 0.5-z; (iv) x, -y, -0.5+z.

### 7.8.2.3. Crystal structure of 3,5-dinitro-4,4'-bipyrazole (**4**)

3,5-Dinitrocompound presents a particular example, since basic pyrazole site and appreciably acidic 3,5-dinitropyrazole ( $pK_a = 3.14$  for 3,5-dinitropyrazole<sup>[S14]</sup>) site appear incompatible within the molecule and the latter exists rather in a peculiar pyrazolium/dinitropyrazolate zwitter-ionic form. The compound crystallizes in  $C2/c$  space group and the molecule lies on a 2-fold axis passing through the central C-C bond and centroids of pyrazolium and dinitropyrazolate N-N bonds. That the symmetry equivalence of two nitrogen sites for every of the rings is not an apparent effect of equal disorder of two protons, may be illustrated by the results of mean-square displacement amplitude analysis, which provides a sensitive parameter for anambiguous detection of subtle effects of the disorder.<sup>[S15]</sup> Absolute differences of ADPs along the directions of the bonds are calculated using *THMA11*<sup>[S16]</sup> and they essentially fit a limit of  $0.0010 \text{ \AA}^2$  suggested by Hirshfeld for rigid bonds (in particular, for N1-C1 and N2-C4  $|\Delta ADP|$  are 0.0012(7) and 0.0002(7)  $\text{\AA}^2$ , respectively).

The zwitter-ionic pyrazolium/dinitropyrazolate structure of the molecule has clear impact for the hydrogen bonding: instead of a set of weaker H-bond donors and acceptors in the structure of **3**, one can find now a combination of very potent functionalities in the form of highly acidic polarized pyrazolium-NH<sup>+</sup> and anionic pyrazolate-N<sup>-</sup> sites. Such difference is essential for more strong hydrogen bonding in the structure of **4**. First, bifurcation of the bonding between N and O acceptors disappears and actually only strong and directional bond to a more competitive N-site is established [ $\angle \text{NH}\cdots\text{N} = 165.4(19)^\circ$  vs.  $\angle \text{NH}\cdots\text{O} = 120.2(16)^\circ$ , Table S6]. Second, this NH $\cdots$ N bond is significantly stronger than the one in the structure of **3** (N $\cdots$ N separations are 2.8410(14) and 3.0433(13)  $\text{\AA}$ , respectively). Therefore, in spite of a somewhat greater molecular twist angle, packing of 3,5-isomer (**4**) is even slightly more dense than the packing of 3,3'-isomer (**3**), as is suggested by crystal densities (1.836 and 1.817  $\text{g cm}^{-3}$ ) and packing indices (76.6 and 76.5, respectively).

Facile and Selective Polynitrations at the 4-Pyrazolyl Dual Backbone: A Straightforward Access to a Series of High-Density Energetic Materials

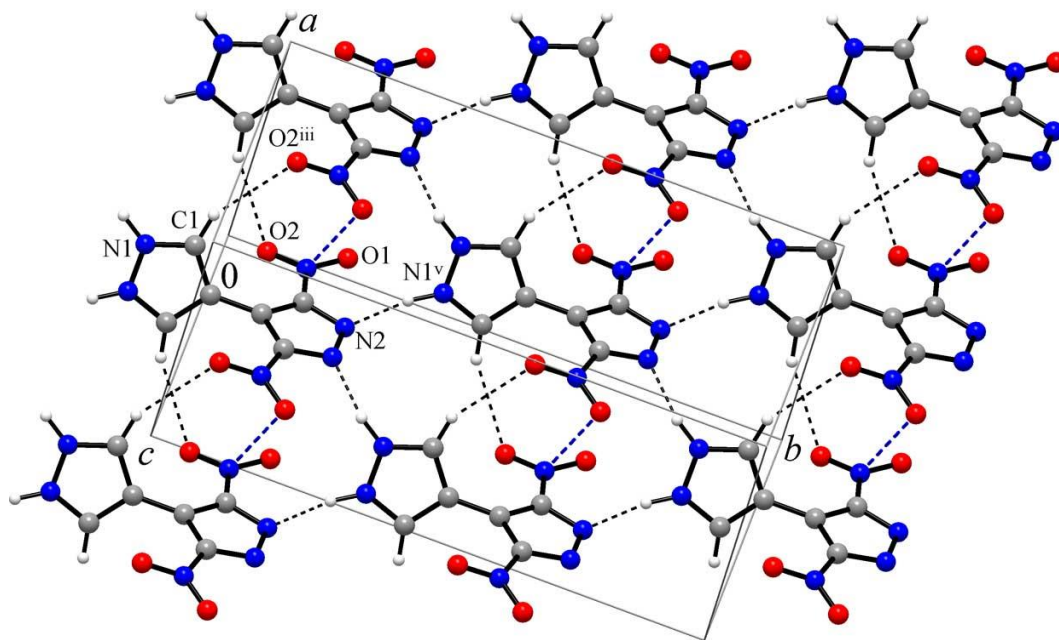


**Figure S7.** Fragment of hydrogen bonded layer in the structure of **4**, with dotted lines indicating H-bonds and intermolecular  $\pi$ -hole/lone pair interactions. [Symmetry codes: (iii)  $1-x, y, 0.5-z$ ; (v)  $0.5-x, 0.5+y, 0.5-z$ ].

Second important consequence of the zwitter-ionic pyrazolium/dinitropyrazolate structure of **4** is strict mutual orientation of the molecules (head-to-tail) imprinted into their supramolecular connectivity. The latter one exists in the form of flat four-connected network (similar to the network in the structure of **3**) and the orientation of all integrated molecular dipoles is concerted and additive (Fig. S7). Thus the polar hydrogen bonded layer is generated, although bulk polarity of the entire structure is eliminated by anti-alignment of the polarities from successive layers (Fig. S8). Nevertheless, the hydrogen bonding scheme in **4** could be viewed as important paradigm for the developing of polar crystals.

**Facile and Selective Polynitrations at the 4-Pyrazolyl Dual Backbone: A Straightforward Access to a Series of High-Density Energetic Materials**

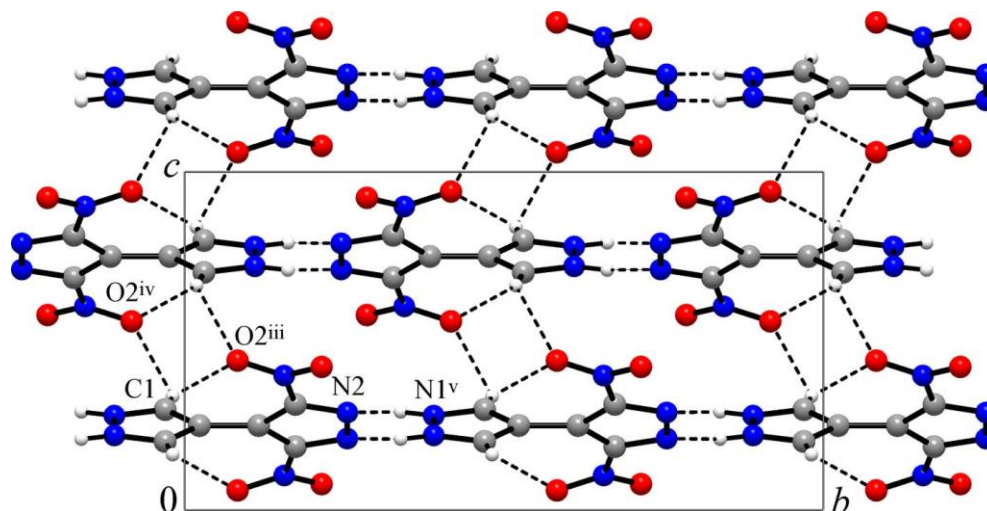


**Figure S8.** The interlayer interactions, bifurcate CH...O bonding, seen in the structure of **4**. Note that the polarity of the successive layers is opposite.

**Table S6.** Hydrogen-bond geometry (Å, °) for structure of 3,5-dinitro-4,4'-bipyrazole **4**.<sup>a)</sup>

Donor (D)	Hydrogen (H)	Acceptor (A) <sup>a)</sup>	D-H	H...A	D...A	∠DH...A
N1	H1N	N2 <sup>ii</sup>	0.97(2)	1.89(2)	2.8410(14)	165.4(19)
N1	H1N	O1 <sup>ii</sup>	0.97(2)	2.45(2)	3.0522(13)	120.2(16)
C1	H1	O2 <sup>iii</sup>	0.951(17)	2.652(17)	3.5292(16)	153.7(12)
C1	H1	O2 <sup>iv</sup>	0.951(17)	2.742(16)	3.5093(17)	138.3(12)

<sup>a)</sup> The bond N1H...N2<sup>ii</sup> is considered as strong and directional; the parameters for N1H...O1<sup>ii</sup> are given for comparison with bifurcate bonding in the structure of **3**. <sup>b)</sup> Symmetry codes: (ii) 0.5-x, -0.5+y, 0.5-z; (iii) 1-x, y, 0.5-z; (iv) x, -y, -0.5+z.

#### 7.8.2.4. Crystal structure of 3,3',5-trinitro-4,4'-bipyrazole (**5**)

Supramolecular structure of the compound is very similar to the above layered structures of **3** and **4**. Primary intermolecular linkage is provided by bifurcate NH...N,O hydrogen bonding (Table S7), which connects the molecules to four closest neighbors. It worths noting that the most acidic and polarized NH site of the dinitropyrazole moiety establishes the bond to the most basic of the N-sites (*i.e.* mononitropyrazole) (Fig. S9). For this bond, the effect of bifurcation is only very minor, and the branch to nitro-O acceptor is very weak (if present) as may be found from comparison of N1...N4<sup>i</sup> and N1... O5<sup>i</sup> separations (2.877(2), 3.107(2) Å, respectively) and N1H...N4<sup>i</sup> and N1H...O5<sup>i</sup> bond angles (157(2), 124(2)°, respectively) [symmetry code: (i) -1+x, y, z]. For the

## Facile and Selective Polynitrations at the 4-Pyrazolyl Dual Backbone: A Straightforward Access to a Series of High-Density Energetic Materials

second H-bond, nitropyrazole NH donor to dinitropyrazole-N,O acceptor, two branches are comparable, and the N...O5 separation is even shorter (Table S7).

In addition to these stronger hydrogen bonds, the layer comprises also weaker CH...O interactions [C4...O4<sup>iii</sup> = 3.353(2) Å; Symmetry code: (iii)  $x, 0.5-y, 0.5+z$ ], very similar to **4**. However, with the increased number of the NO<sub>2</sub> groups at the expense of number of the CH groups (**3** to **5**), the CH...O bond network thins out and, instead of the hydrogen bonds present in **3**, short  $\pi$ -hole/lone pair between the adjacent NO<sub>2</sub> groups are generated [N...O = 2.947(2) Å, See Fig. S9]. That the overall supramolecular structure actually remains intact under such a substitution, suggests comparable energetics and steric demands for these two kinds of interactions. Recently we have illustrated such inheritance of the motifs sustained by CH...O and  $\pi$ -hole/lone pair NO<sub>2</sub>/NO<sub>2</sub> bonding, for a series of non-covalent frameworks formed by 1,4-dinitrobutadienes.<sup>[S17]</sup> The layers in the structure of **5** pack in the *ac* plane and weak interlayer interactions are provided by a second branch of bifurcate CH...O bond [C4...O2<sup>iv</sup> = 3.260(3) Å;  $\angle$  C4H...O2<sup>iv</sup> = 140.4(15)°; Symmetry code: (iv)  $1-x, -y, 1-z$ ]. This pack visualizes clear scheme for evolution of supramolecular patterns in the structures of polynitro-4,4'-bipyrazoles, as depicted in Fig. S10. With the increased number of NO<sub>2</sub> groups and larger molecular twist angle (**2**, **3**  $\rightarrow$  **4**), the flat four-connected nets observed in **2** and **3** experience corrugation yet preserving either dimensionality or topology. Such feature as bent along the chain of the molecules (already accumulated in **5**) is a major step towards disintegration of favorable stack of successive layers. With further increase in a number of NO<sub>2</sub> groups, even larger molecular twist angle (**5**  $\rightarrow$  **6**) and loss of any CH...O bonding, the present array collapses into one-periodic four-connected net, which is described below for the structure of **6**.



Facile and Selective Polynitrations at the 4-Pyrazolyl Dual Backbone: A Straightforward Access to a Series of High-Density Energetic Materials

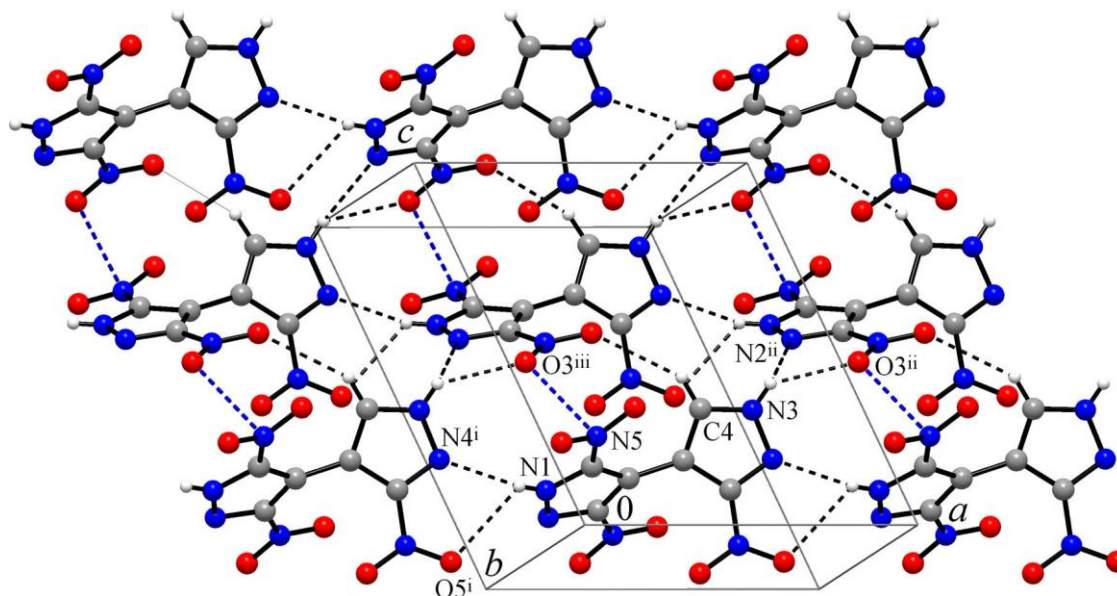


**Figure S9.** Fragment of hydrogen bonded layer in the structure of **5**, with dotted lines indicating H-bonds and intermolecular  $\pi$ -hole/lone pair interactions. [Symmetry codes: (i)  $-1+x, y, z$ ; (ii)  $1+x, 0.5-y, 0.5+z$ ; (iii)  $x, 0.5-y, 0.5+z$ ].

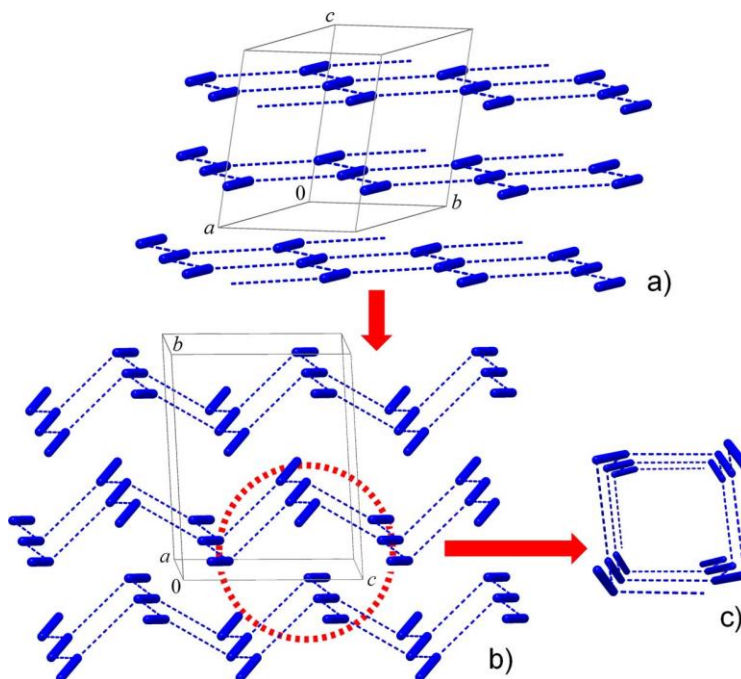


**Figure S10.** Evolution of supramolecular organization of polynitro-4,4'-bipyrazoles (blue sticks represent four-connected molecules and dotted lines refer to principal hydrogen bonding): a) Flat layers in the structures of **3** and **4**; b) Corrugated layers in the structure of **5**; c) One-periodic arrangement in the structure of **6**.



**Facile and Selective Polynitrations at the 4-Pyrazolyl Dual Backbone: A Straightforward Access to a Series of High-Density Energetic Materials**

**Table S7.** Hydrogen-bond geometry (Å, °) for structure of 3,3',5-trinitro-4,4'-bipyrazole **5**.

Donor (D)	Hydrogen (H)	Acceptor (A) <sup>a)</sup>	D-H	H...A	D...A	∠DH...A
N1	H1N	N4 <sup>i</sup>	0.78(2)	2.15(2)	2.877(2)	157(2)
N1	H1N	O5 <sup>i</sup>	0.78(2)	2.61(2)	3.107(2)	124(2)
N3	H2N	O3 <sup>ii</sup>	0.81(2)	2.33(2)	2.996(2)	138.9(19)
N3	H2N	N2 <sup>ii</sup>	0.81(2)	2.65(2)	3.202(2)	126.2(18)
C4	H4	O4 <sup>iii</sup>	0.93(2)	2.54(2)	3.353(2)	145.8(15)
C4	H4	O2 <sup>iv</sup>	0.93(2)	2.49(2)	3.260(3)	140.4(15)

<sup>a)</sup> Symmetry codes: (i) -1+x, y, z; (ii) 1+x, 0.5-y, 0.5+z; (iii) x, 0.5-y, 0.5+z; (iv) 1-x, -y, 1-z.

#### 7.8.2.5. Crystal structure of 3,5,3',5'-tetranitro-4,4'-bipyrazole (**6**)

The compound crystallizes in a tetragonal space group  $P4_2/n$  and it exhibits very original supramolecular structure, while providing further evolution of general trends observed for **2-5**. In particular, interactions with the nitro oxygen atoms appear to be most crucial for organization of hydrogen bonded framework, while bonding to pyrazole N-acceptor is present only as a less directional branch of bifurcate NH...O,N bond [ $\angle \text{N3H}\cdots\text{O3}^{\text{ii}} = 166.4(18)^\circ$  vs.  $\angle \text{N3H}\cdots\text{N2}^{\text{ii}} = 124.7(16)^\circ$ ; symmetry code: (ii) x, y, -1+z]. This indicates weak basicity of pyrazole-N atoms and their less steric accessibility.

As may be compared to **5**, with a larger twist angle imposed by the molecular frame and loss of interlayer CH...O linkage, the 2D array of H-bonded molecules collapses forming supramolecular tubes, *i.e.* one-periodic 2D structure. First, the strongest and very directional bonds N1H... O8<sup>i</sup> [ $\text{N}\cdots\text{O} = 2.8457(14) \text{ \AA}$ ;  $\angle \text{NH}\cdots\text{O} = 171.7(16)^\circ$ ; symmetry code: (i) y, 0.5-x, 0.5-z] assemble the molecules into tetramers, possessing shape of the **Figure eight (Fig. S11)**. Second, weaker bifurcate bonding of the second pyrazole NH-donor donor (**Table S8**) itself leads to a connection of the molecules into linear chains along *c* axis (within the chain the molecules are related by a simple translation). With this bifurcate hydrogen bonding, the tetramers shown in Fig. S11 aggregate forming supramolecular tubes down the *c* axis (See Fig. S12 and Fig. 3 of the main text).

Facile and Selective Polynitrations at the 4-Pyrazolyl Dual Backbone: A Straightforward Access to a Series of High-Density Energetic Materials

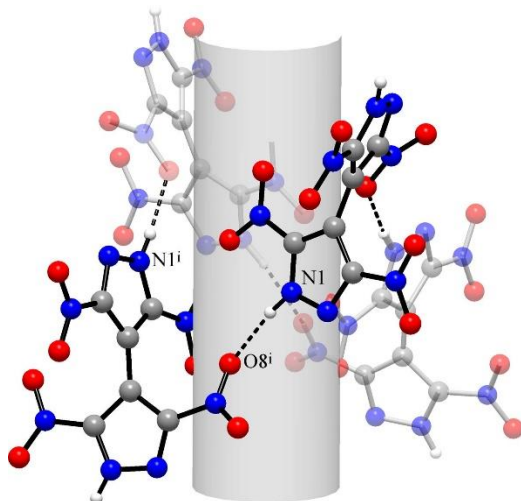


**Figure S11.** Structure of **6**: A finite arrangement of four molecules, in the form of **Figure eight**, which is maintained by a set of strongest hydrogen bonds  $\text{N1H}\cdots\text{O8}^{\text{i}}$  [Symmetry code: (i)  $y, 0.5-x, 0.5-z$ ].

With a total elimination of competitive  $\text{CH}\cdots\text{O}$  and stacking interactions seen in **2-5**, the role of nitro groups becomes crucial even beyond the hydrogen bonding: in total twelve short  $\pi$ -hole/lone pair  $\text{N}\cdots\text{O}$  contacts (with a cut-off limit of  $3.25\text{ \AA}$ ) of  $\text{NO}_2/\text{NO}_2$  and  $\text{NO}_2/\text{pyrazole}$  types contribute to the dense packing. The shortest nitro/nitro contacts in the structure of **6** [ $\text{N8}\cdots\text{O2}^{\text{iv}} = 2.9115(15)\text{ \AA}$ ; symmetry code (iv)  $0.5-y, x, -0.5-z$ ] (**Fig. S13**) approach the parameters of strongest  $\text{NO}_2/\text{NO}_2$  interactions observed in the structure of the energetic material heptanitrocubane ( $2.80\text{ \AA}$ ).<sup>[S18]</sup> These contacts constitute the most notable environment of the  $\text{N8O7O8}$  group, which supports interactions at both axial sides simultaneously (**Fig. S13, a**).

## Facile and Selective Polynitrations at the 4-Pyrazolyl Dual Backbone: A Straightforward Access to a Series of High-Density Energetic Materials

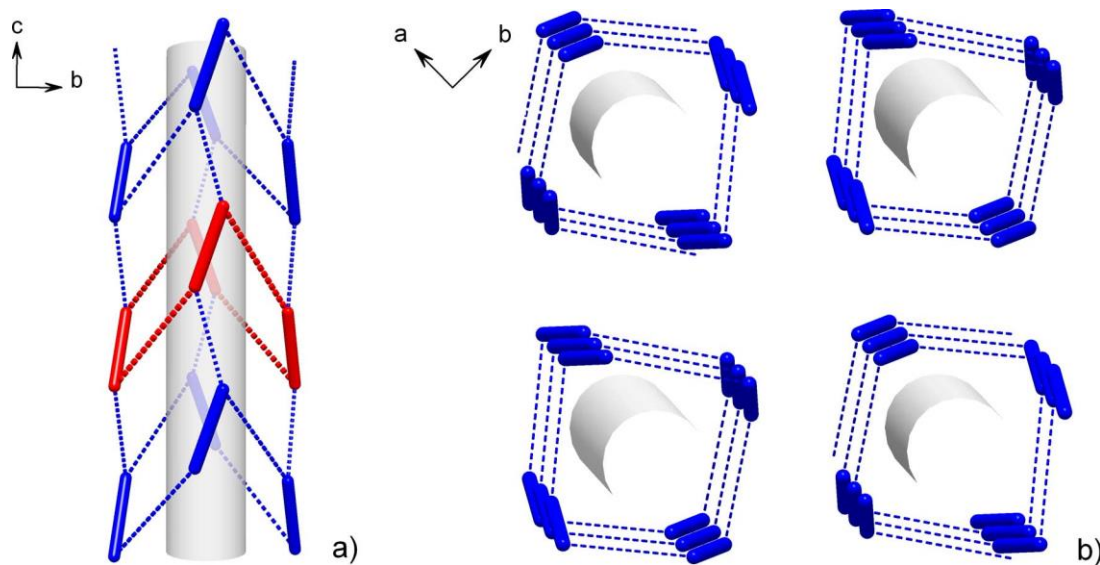


**Figure S12.** A schematic representation of the structure of **6** (the bipyrzole molecules are shown as sticks and their hydrogen bonding to four closest neighbors as dotted lines): a) Supramolecular tubes running down *c* axis. The tetramer presented in the previous **Figure** is marked in red. b) View down the *c* direction, showing packing of four neighboring tubes.

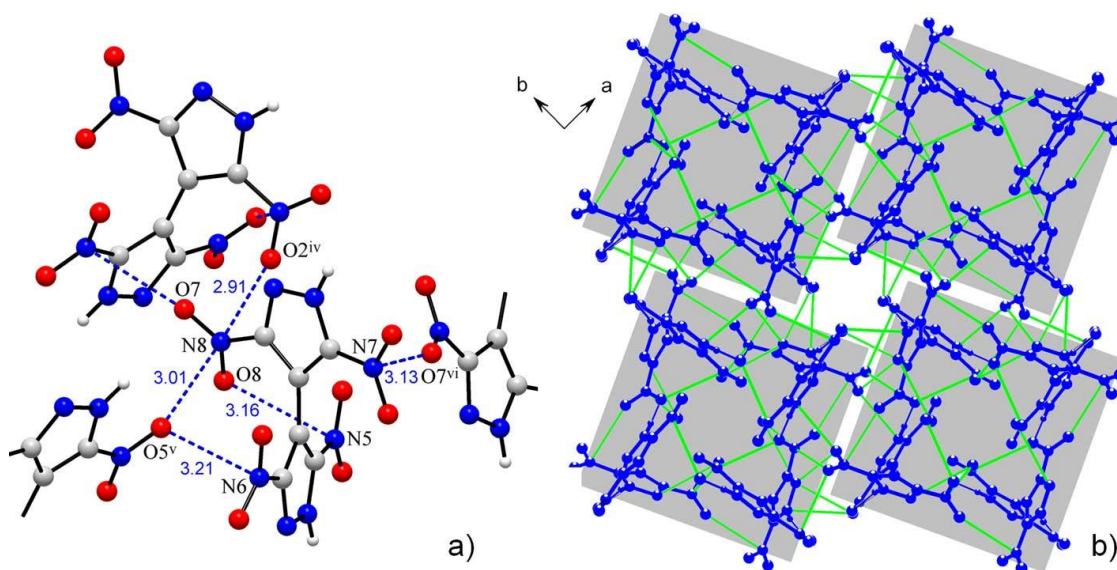


**Figure S13.** a) Short N...O (nitro/nitro) contacts in the structure of **6**, which are marked with dotted lines; b) Significance of  $\pi$ -hole/lone pair interactions for the packing of **6**: Grey squares distinguish supramolecular tubes and green lines indicate the arising short N...O contacts (cut-off limit is 3.25 Å), either of nitro/nitro or nitro/pyrazole types [Symmetry codes (iv)  $0.5-y, x, -0.5-z$ ; (v)  $0.5+y, -x, 0.5+z$ ; (vi)  $y, 0.5-x, -0.5-z$ ].

**Facile and Selective Polynitrations at the 4-Pyrazolyl Dual Backbone: A Straightforward Access to a Series of High-Density Energetic Materials**

**Table S8.** Hydrogen-bond geometry (Å, °) for structure of 3,5,3',5'-tetranitro-4,4'-bipyrazole **6**.

Donor (D)	Hydrogen (H)	Acceptor (A) <sup>a)</sup>	D-H	H...A	D...A	∠DH...A
N1	H1N	O8 <sup>i</sup>	0.904(18)	1.949(18)	2.8457(14)	171.7(16)
N3	H2N	O3 <sup>ii</sup>	0.87(2)	2.33(2)	3.1849(16)	166.4(18)
N3	H2N	N2 <sup>ii</sup>	0.87(2)	2.418(19)	3.0027(15)	124.7(16)

<sup>a)</sup> Symmetry codes: (i)  $y, 0.5-x, 0.5-z$ ; (ii)  $x, y, -1+z$ .

#### 7.8.2.6. Crystal structure of 3,3',5,5'-tetranitro-4,4'-bipyrazole hydrate **6·H<sub>2</sub>O**

Formation of this molecular adduct dominates isolation and purification of **6** from aqueous solutions and a variety of wet solvents. The hydrate possesses higher packing index [73.6%] and slightly higher density [1.857 g cm<sup>-3</sup>] than the anhydrous material [72.2% and 1.847 g cm<sup>-3</sup>], which is suggestive for stronger intermolecular interactions. Thus, the acidic dinitropyrazole moiety is a very strong donor, but only weak acceptor for conventional H-bonding and therefore one can rationalize benefit from the formation of NH...O bonds with appropriate guests rather than the weaker NH...O interactions with nitro-groups. This factor could be favorable for crystallization of molecular adducts incorporating **6**.

In fact, the role of water molecules is crucial for sustaining the entire supramolecular structure, as revealed by evolution of the hydrogen bonding patterns from **6** to **6·H<sub>2</sub>O**. The weak interactions involving pyrazole and nitro-O acceptors are eliminated at all. Instead, one strong and directional bond to O1w atom [N1...O1w<sup>i</sup> = 2.6470(16) Å; ∠ N1H...O1w<sup>i</sup> = 176.2(18)°; Symmetry code: (i) -1+x, y, z;] (Fig. S14) is established and, although the second NH group still secures bonding to the adjacent pyrazole acceptor, the bifurcation of this interaction (compare with the one present in **5**) disappears. As a result, relatively short and directional N3H...N2<sup>ii</sup> bonds are formed [Symmetry code: 0.5+x, 0.5-y, -0.5+z] (Table S9) and these bonds connect the bipyrazole molecules into linear chains (**Fig. S15**).

Facile and Selective Polynitrations at the 4-Pyrazolyl Dual Backbone: A Straightforward Access to a Series of High-Density Energetic Materials

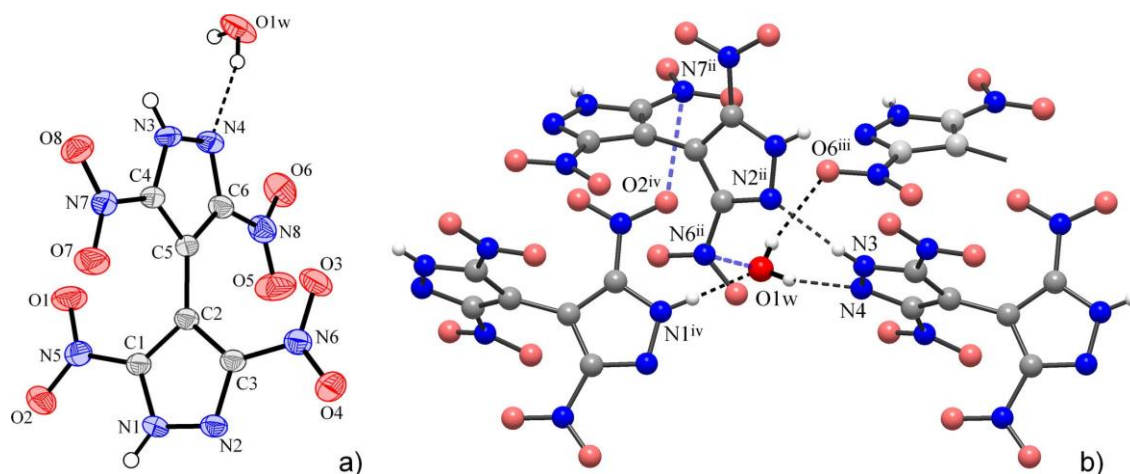


**Figure S14.** a) Molecular structure of **6·H<sub>2</sub>O** showing the atom labeling scheme and thermal ellipsoids drawn at 50% probability level; b) Structural role of water molecule, which establishes three directional H-bonds and one short  $\pi$ -hole/lone pair contact [ $\text{N}(\text{nitro})\cdots\text{OH}_2 = 3.058(2) \text{ \AA}$ ].

Such chains are the clearly distinguishable common motif for both the structures, **6** and **6·H<sub>2</sub>O**. The water molecules unite the chains into the slightly corrugated layers parallel to the *ac* plane, while providing “extended bridges” between the pyrazole-NH and pyrazole-N sites [ $\text{NH}\cdots\text{OH}\cdots\text{N}$ ]. The only remaining OH hydrogen bond donor is used for interlayer linkage, which involves the nitro-O acceptor [ $\text{O1w}\cdots\text{O6}^{\text{iii}} = 2.9300(18) \text{ \AA}$ ;  $\angle \text{O1wH}\cdots\text{O6}^{\text{iii}} = 146(2)^\circ$ ; Symmetry code: (iii)  $x, -y, -0.5+z$ ]. Thus the entire hydrogen bonded structure represents 3D framework of complex (and new) topology. When considering the bipyrazole (linked to two bipyrazoles and three water molecules) and water (linked to three bipyrazoles) molecules as the net nodes, the three- and five-coordinated binodal net with a point (Schläfli) symbol  $\{6^3\}\{6^7.8^3\}$  is found.

However, the role of water molecule is important even beyond the conventional hydrogen bonding. In the environment of multiple nitro groups, in addition to the above bonds, it adopts relatively short  $\pi$ -hole/lone pair contact with nitro-N acceptor [ $\text{N}(\text{nitro})\cdots\text{OH}_2 = 3.058(2) \text{ \AA}$ ], which completes nearly tetrahedral environment of O1w (N1<sup>iv</sup>, N4, O6<sup>iii</sup> and N6<sup>ii</sup>, see **Fig. S14b**). Therefore the aqua guest exactly follows the trend for generation of multiple  $\pi$ -hole/lone pair interactions, as already mentioned for structures of **5** and **6**. As may be compared with a latter example, significance of such interactions in **6·H<sub>2</sub>O** is slightly diminished in a favor of more competitive conventional hydrogen bonding. However, the pack still generates nine short  $\text{N}\cdots\text{O}$  contacts (with a cut-off limit of  $3.25 \text{ \AA}$ ) corresponding to the  $\text{NO}_2\cdots\text{NO}_2$ ,  $\text{NO}_2\cdots\text{pyrazole}$  and

**Facile and Selective Polynitrations at the 4-Pyrazolyl Dual Backbone: A Straightforward Access to a Series of High-Density Energetic Materials**

H<sub>2</sub>O...NO<sub>2</sub> types, with a shortest separations found for two interacting nitro groups [N7...O2<sup>v</sup> = 2.9714(18) Å; Symmetry code: (v) 0.5+x, 0.5-y, 0.5+z] (Fig. S14b).

**Table S9.** Hydrogen-bond geometry (Å, °) for structure of **6·H<sub>2</sub>O**.

Donor (D)	Hydrogen (H)	Acceptor (A) <sup>a)</sup>	D-H	H...A	D...A	∠DH...A
N1	H1N	O1W <sup>i</sup>	0.828(18)	1.821(19)	2.6470(16)	176.2(18)
N3	H2N	N2 <sup>ii</sup>	0.85(2)	2.083(19)	2.9058(16)	161.7(17)
O1W	H1W	N4	0.85(3)	2.22(3)	3.0479(16)	166(2)
O1W	H2W	O6 <sup>iii</sup>	0.82(3)	2.21(3)	2.9300(18)	146(2)

<sup>a)</sup> Symmetry codes: (i) -1+x, y, z; (ii) 0.5+x, 0.5-y, -0.5+z; (iii) x, -y, -0.5+z.

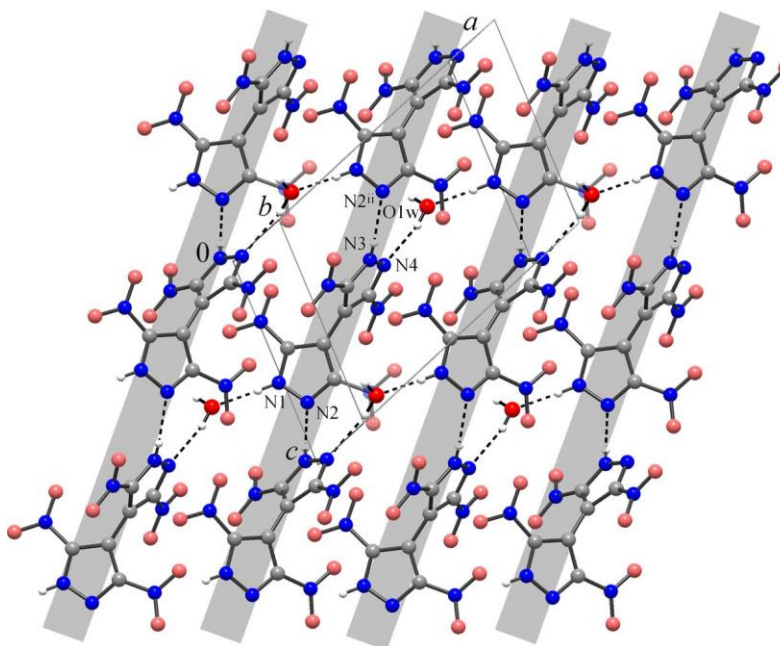


**Figure S15.** Fragment of the structure of **6·H<sub>2</sub>O**, in a projection nearly to *ac* plane: Hydrogen bonded layer comprising chains of NH...N bonded bipyrazole molecules (indicated with grey strips), which are interlinked with water molecules [NH...OH... N].



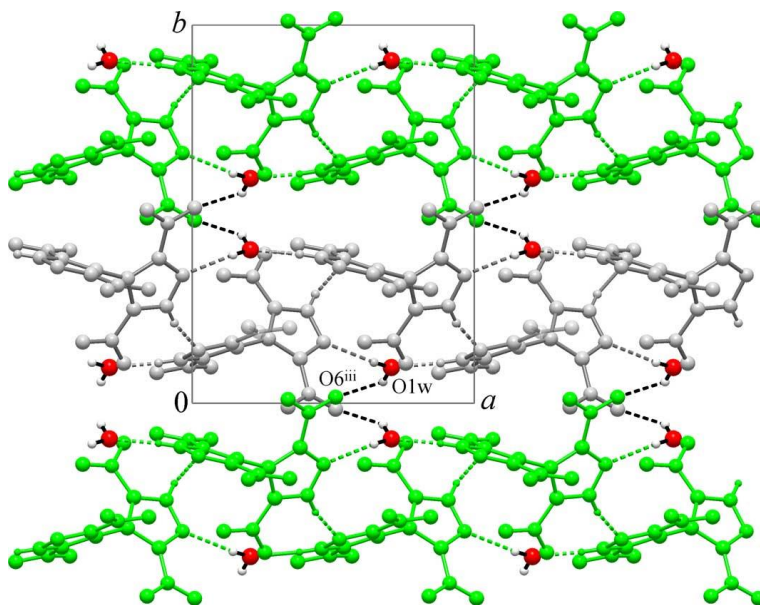


**Figure S16.** Projection of the structure of **6·H<sub>2</sub>O** on a *ab* plane, showing packing of three successive layers (marked in green, grey and green) and interlayer hydrogen bond interactions of water molecules to NO<sub>2</sub> acceptors [Symmetry code: (iii) *x*, -*y*, -0.5+*z*.]

### 7.8.3. Computations

All calculations were carried out using the Gaussian G09W (revision A.02) program package.<sup>[S19]</sup> The enthalpies (*H*), were calculated using the complete basis set (CBS) method of Petersson and coworkers. The CBS models use the known asymptotic convergence of pair natural orbital expressions to extrapolate from calculations using a finite basis set to the estimated complete basis set limit. CBS-4 begins with a HF/3-21G(d) structure optimization and the zero-point energy computation. Subsequently, applying a larger basis set a base energy is computed. A MP2/6-31+G calculation with a CBS extrapolation gives the perturbation-theory corrected energy (takes the electron correlation into account). A MP4(SDQ)/6-31+(d,p) calculation is used to correlate higher order contributions. In this study we applied the modified CBS-4M method (M referring to the use of minimal population localization) which is a re-parameterized version of the original CBS-4 method and also includes some additional empirical corrections.<sup>[S20]</sup> The gas-phase enthalpies ( $\Delta_f H^\circ_{(g, M, 298)}$ ) of the species were computed according to the atomization energy method (equation 1).<sup>[S21]</sup>

$$\Delta_f H^\circ_{(g, M, 298)} = H_{(g, M, 298)} - \sum H^\circ_{(g, Ai, 298)} + \sum \Delta_f H^\circ_{(g, Ai, 298)} \quad (1)$$

## Facile and Selective Polynitrations at the 4-Pyrazolyl Dual Backbone: A Straightforward Access to a Series of High-Density Energetic Materials

$\Delta_f H^\circ(g, A_i, 298)$  for the corresponding atoms ( $A_i$ ) were determined experimentally and are reported in the literature while  $H^\circ(g, A_i, 298)$  were calculated theoretically (**Table S10**).<sup>[S22]</sup>

**Table S10.** CBS-4M electronic enthalpies for atoms C, H, N and O and their literature values for atomic  $\Delta_f H^\circ_{298} / \text{kJ mol}^{-1}$ .

Atom	$-H^{298} / \text{a.u.}$	$\Delta_f H^\circ(g, A_i, 298) [\text{kcal mol}^{-1}]$
H	0.500991	52.103
C	37.786156	171.29
N	54.522462	112.97
O	74.991202	59.56

Standard molar enthalpies of formation were calculated using and the standard molar enthalpies of  $\Delta_f H^\circ(g, M, 298)$  sublimation (estimated using Trouton's rule, equation 2).<sup>[S23]</sup>

$$\Delta_f H^\circ_M = \Delta_f H^\circ(g, M, 298) - \Delta_{\text{sub}} H^\circ_M = \Delta_f H^\circ(g, M, 298K) - 188 \cdot T \left[ \frac{J}{\text{mol}} \right] \quad (2)$$

Where [K] is either the melting point or the decomposition temperature (if no melting occurs prior to decomposition). The calculation results are summarized in Tables S11.

**Table S11.** Calculation results.

Compound	$-H^{298}$ <sup>[a]</sup> a.u.	$\Delta_f H^\circ(g, M)$ kJ mol <sup>-1</sup> <sup>[b]</sup>	$\Delta_f H^\circ(s)$ kJ mol <sup>-1</sup> <sup>[c]</sup>	$\Delta_f U(s)$ kJ kg <sup>-1</sup> <sup>[d]</sup>
<b>6</b>	1267.704422	334.0	227.8	796.1
<b>5</b>	1063.413895	333.6	224.9	909.3
<b>4</b>	859.068778	476.5	371.7	1735.9
<b>3</b>	859.126194	325.7	203.5	985.4
<b>2</b>	654.836114	324.1	224.6	1337.0

<sup>[a]</sup> CBS-4M electronic enthalpy; <sup>[b]</sup> gas phase enthalpy of formation; <sup>[c]</sup> standard solid state enthalpy of formation; <sup>[d]</sup> solid state energy of formation.

### 7.8.4. Detonation Parameters

The Chapman-Jouguet (C-J) characteristics, (*i.e.* heat of detonation,  $\Delta E U^\bullet$ ; detonation temperature,  $TC-J$ ; detonation pressure,  $PC-J$ ; detonation velocity  $VC-J$ ) based on the calculated  $\Delta_f H^\circ_M$  values, and the theoretical maximum densities were computed using the EXPLO5 V6.03 thermochemical



## Facile and Selective Polynitrations at the 4-Pyrazolyl Dual Backbone: A Straightforward Access to a Series of High-Density Energetic Materials

computer code.<sup>[S24]</sup> Calculations for explosives assume ideal behaviour. The estimation of detonation parameters is based on the chemical equilibrium steady-state model of detonation. The Becker-Kistiakowsky-Wilson equation of state (BKW EOS) with the following sets of constants:  $\alpha = 0.5$ ,  $\beta = 0.38$ ,  $\kappa = 9.4$ , and  $\Theta = 4120$  for gaseous detonation products and the Murnaghan equation of state for condensed products (compressible solids and liquids) were applied. The calculation of the equilibrium composition of the detonation products uses modified White, Johnson and Dantzig's free energy minimization technique. The specific energies of explosives ( $f$ ) were calculated according to the ideal gas equation of state assuming isochoric conditions (equation 3).

$$f = p_e \cdot V = n \cdot R \cdot T_c \left[ \frac{JkJ}{molkg} \right] \quad (3)$$

Where  $p_e$  is the maximum pressure through the explosion,  $V$  is the volume of detonation gases ( $m^3 \cdot kg^{-1}$ ),  $n$  is the number of moles of gas formed by the explosion per kilogram of explosive (*Volume of Explosive Gases*),  $R$  is the ideal gas constant and  $T_c$  is the absolute temperature of the explosion.<sup>[S24,S25]</sup>

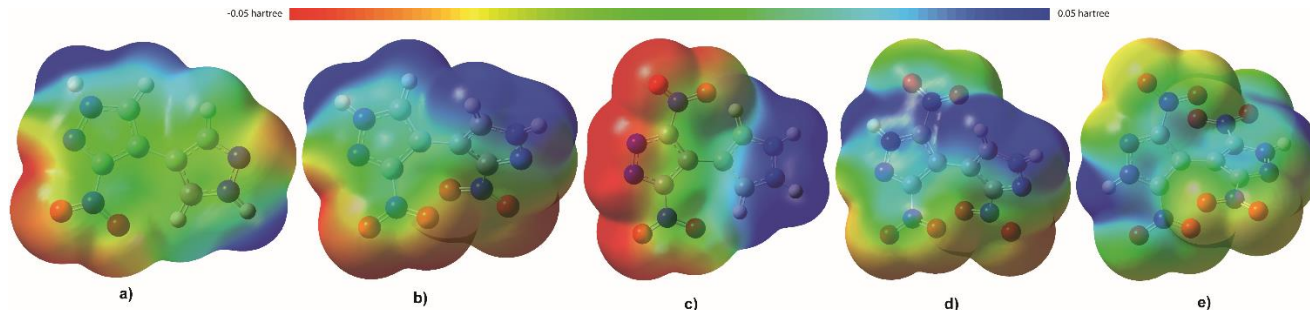


**Figure S17.** Depiction of the calculated [B3LYP/6-31G(d,p)] electrostatic potentials of **2–6** (a:**2**, b:**3**, c:**4**, d:**5**, e:**6**). The 3D isosurface of electron density is shown between  $-0.05$  hartree (electron-rich regions) and  $+0.05$  hartree (electron-poor regions).

### 7.8.5. Small-scale shock reactivity test (SSRT)

To evaluate the shock reactivity (explosiveness) of a small-scale shock reactivity test (SSRT) was performed. The SSRT measures the shock reactivity of potentially energetic materials, often below critical diameter, without requiring a transition to detonation.<sup>[26]</sup> The test setup combines the benefits from a lead block test and a gap test. The experimental setup for the small-scale shock

## Facile and Selective Polynitrations at the 4-Pyrazolyl Dual Backbone: A Straightforward Access to a Series of High-Density Energetic Materials

reactivity test has been prepared as previously reported in the literature.<sup>[27]</sup> The amount  $ms$  of the was calculated using the following formula:  $ms = V_s \cdot \rho \cdot 0.95$ , (where:  $V_s = 284 \text{ mm}^3$ ). Compounds **5** and **6** were pressed at a consolidation dead load of 3 t with a dwell time of 5 s into a perforated steel block. Neither attenuator (between detonator and sample) nor air gap (between sample and aluminum block) were applied. Initiation of the tested explosive was performed using a commercially available detonator (Orica-DYNADET C2-0ms).

### 7.8.6. Thermal stability

Decomposition temperatures were measured *via* differential thermal analysis (DTA) with an OZM Research DTA 552-Ex instrument at a heating rate of  $5 \text{ }^\circ\text{C min}^{-1}$  and in a range of room temperature to  $400 \text{ }^\circ\text{C}$ .

Facile and Selective Polynitrations at the 4-Pyrazolyl Dual Backbone: A Straightforward Access to a Series of High-Density Energetic Materials

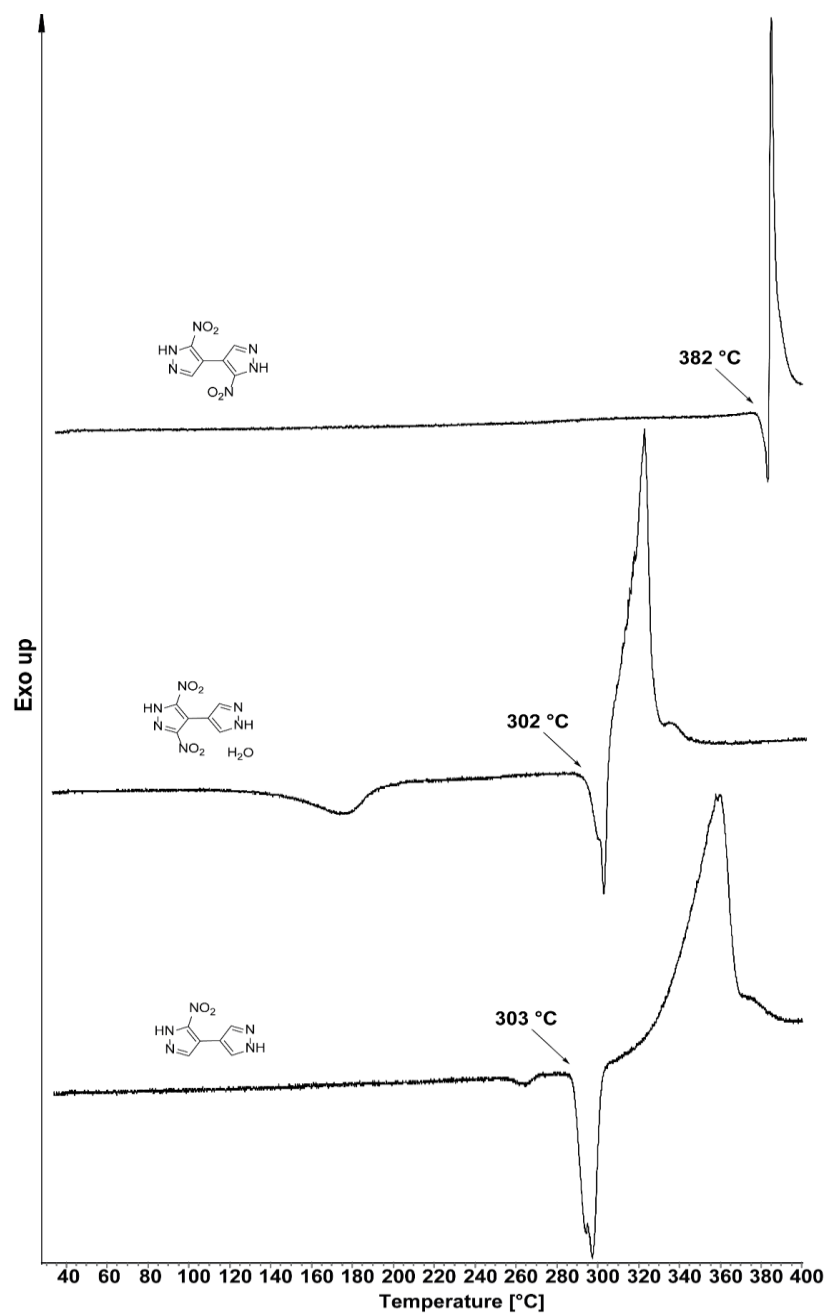


**Figure S18.** DTA plot for compounds 3-nitro-4,4'-bipyrazole (**2**), 3,3'-dinitro-4,4'-bipyrazole (**3**) and 3,5-dinitro-4,4'-bipyrazole monohydrate (**4**·H<sub>2</sub>O).

Facile and Selective Polynitrations at the 4-Pyrazolyl Dual Backbone: A Straightforward Access to a Series of High-Density Energetic Materials

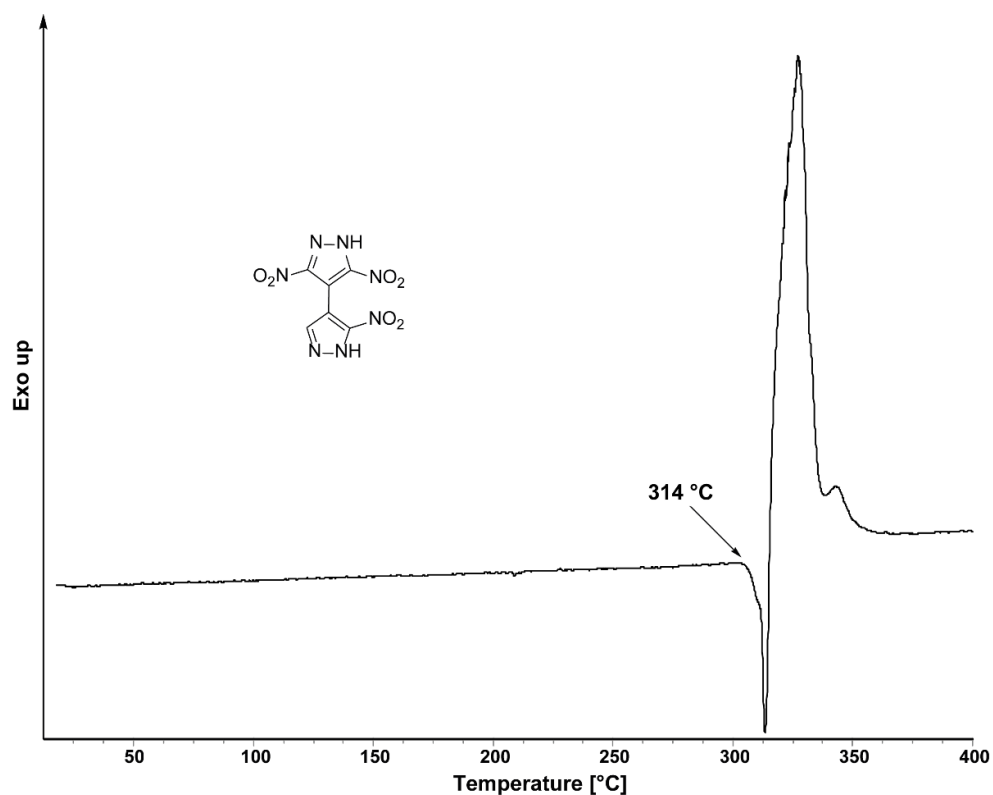


Figure S19. DTA plot for compound 5.

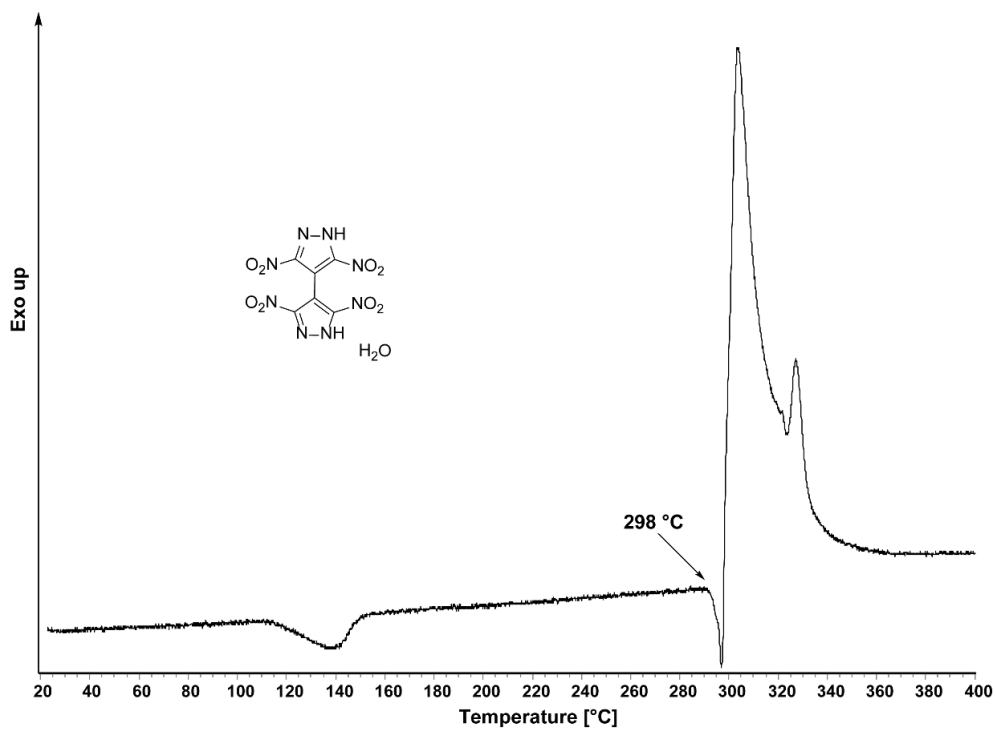


Figure S20. DTA plot for compound 6·H<sub>2</sub>O.

## Facile and Selective Polynitrations at the 4-Pyrazolyl Dual Backbone: A Straightforward Access to a Series of High-Density Energetic Materials

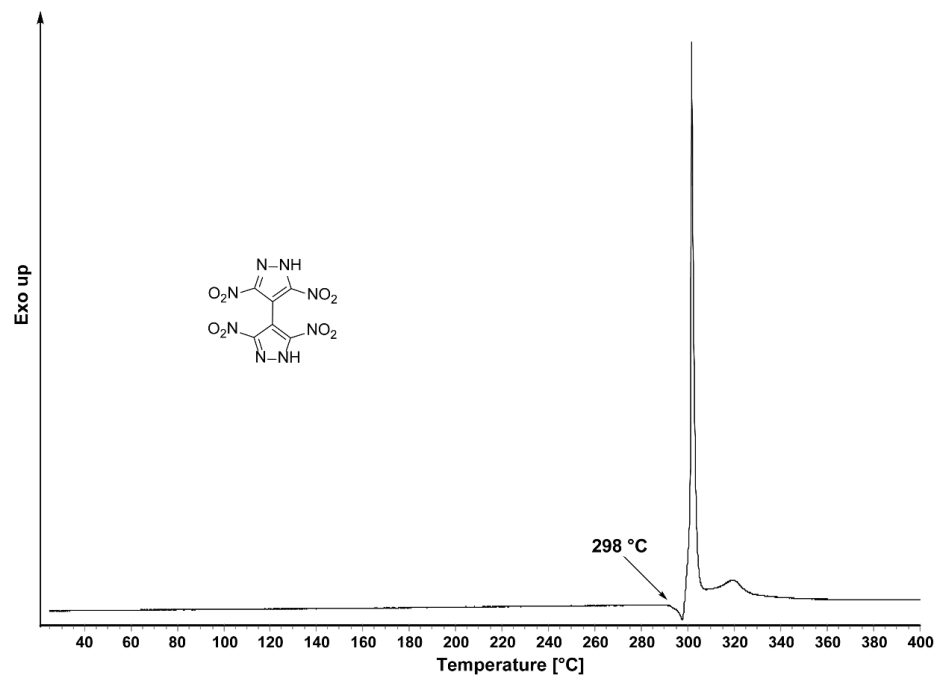


Figure S21. DTA plot for compound 6.

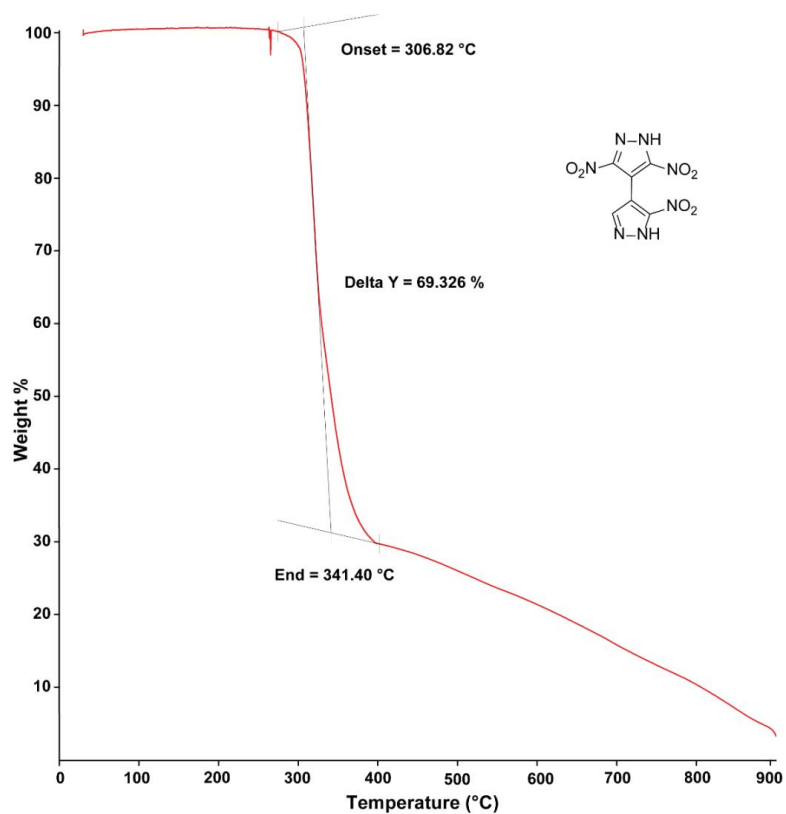
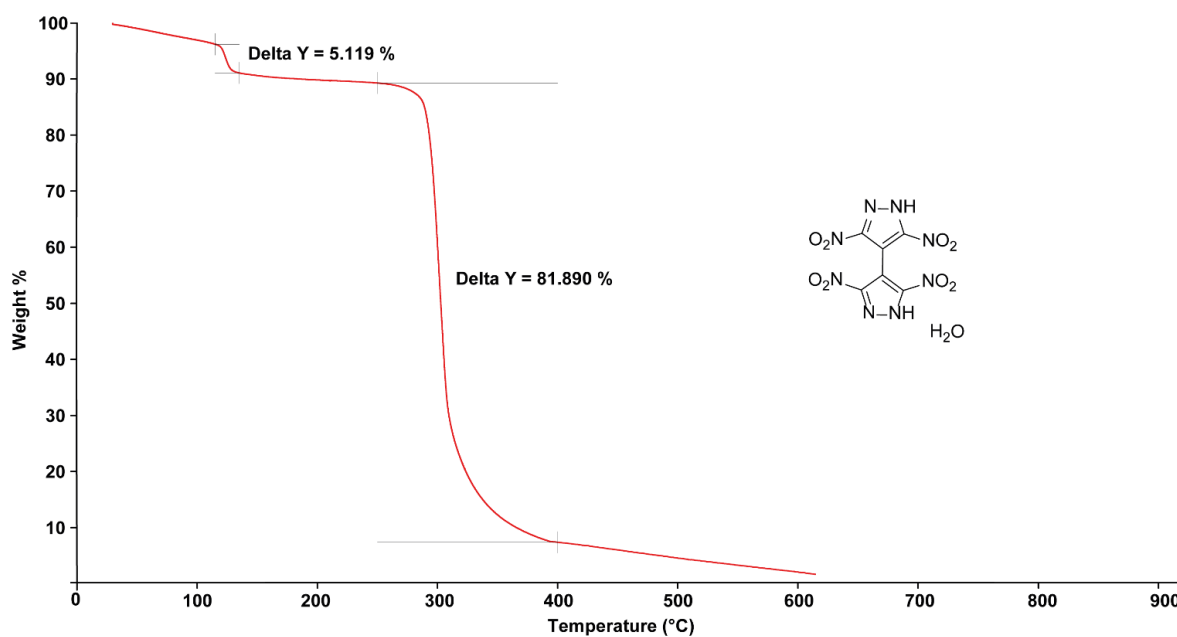
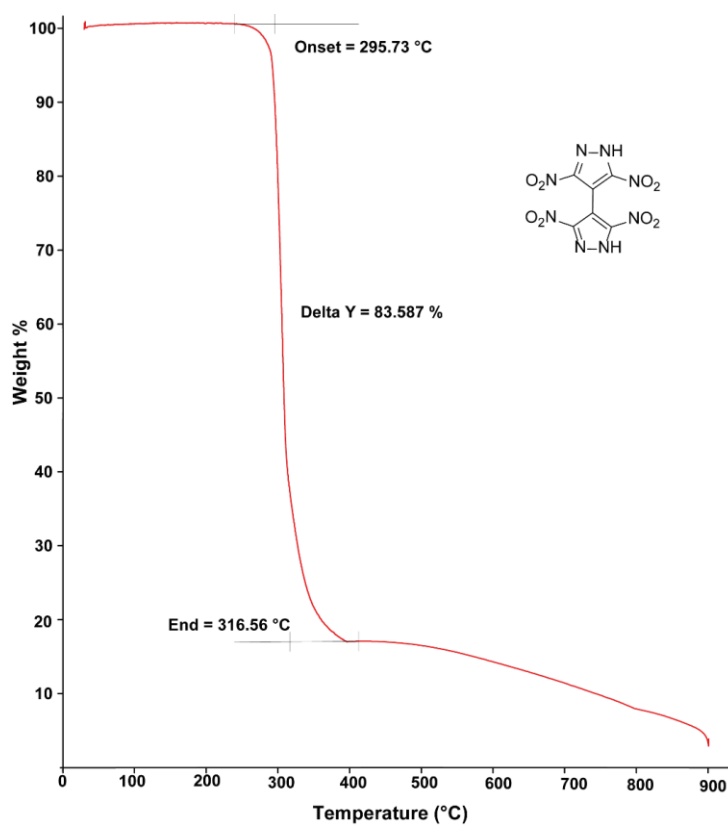


Figure S22. TGA plot for compound 5.

## Facile and Selective Polynitrations at the 4-Pyrazolyl Dual Backbone: A Straightforward Access to a Series of High-Density Energetic Materials



**Figure S23.** TGA plot for compound **6·H<sub>2</sub>O**.



**Figure S24.** TGA plot for compound **6**.

Facile and Selective Polynitrations at the 4-Pyrazolyl Dual Backbone: A Straightforward  
Access to a Series of High-Density Energetic Materials

7.8.7.  $^1\text{H}$  and  $^{13}\text{C}$  NMR spectra

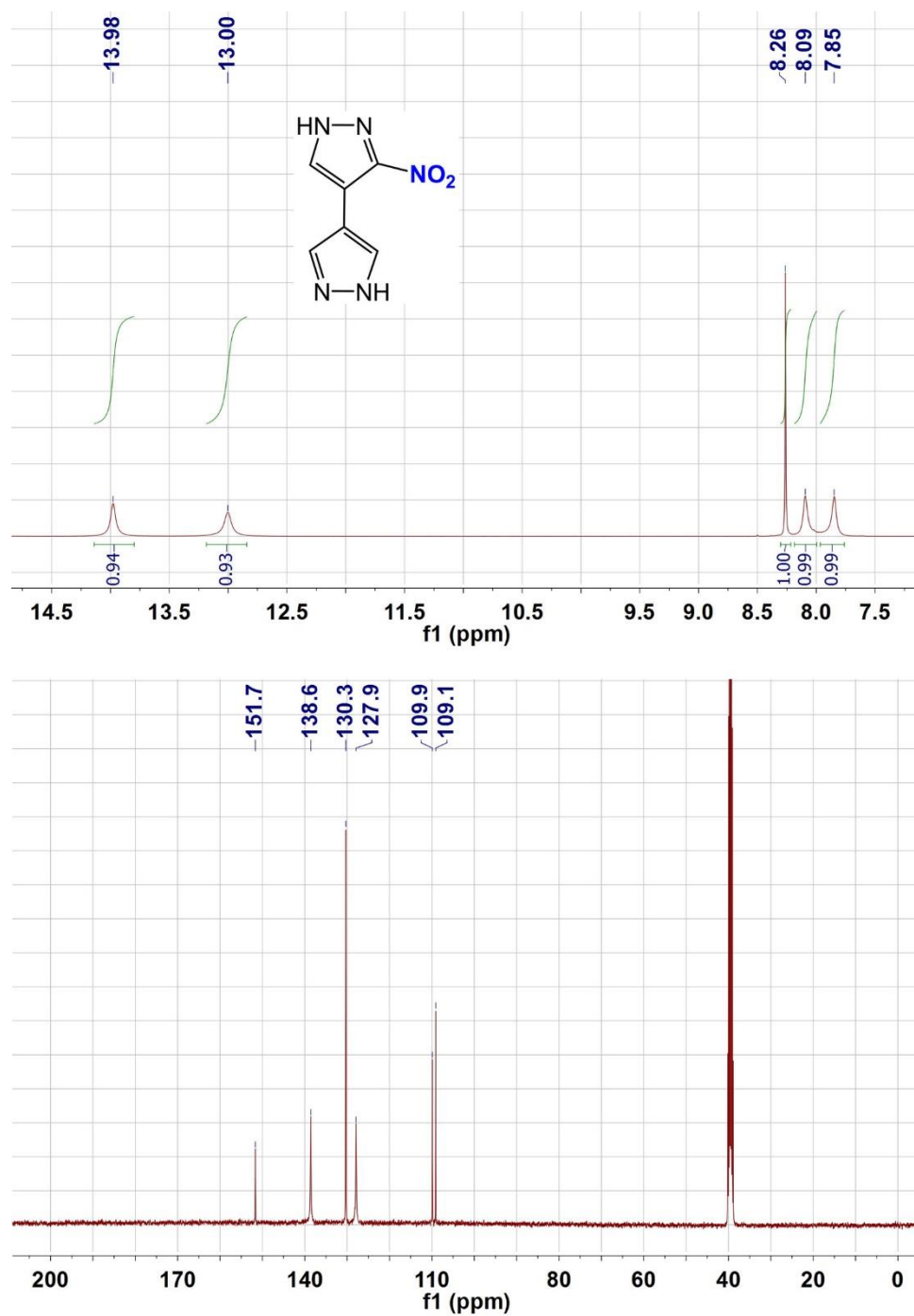


**Figure S25.**  $^1\text{H}$  and  $^{13}\text{C}$  NMR spectra for 3-nitro-4,4'-bipyrazole (2).

Facile and Selective Polynitrations at the 4-Pyrazolyl Dual Backbone: A Straightforward  
Access to a Series of High-Density Energetic Materials

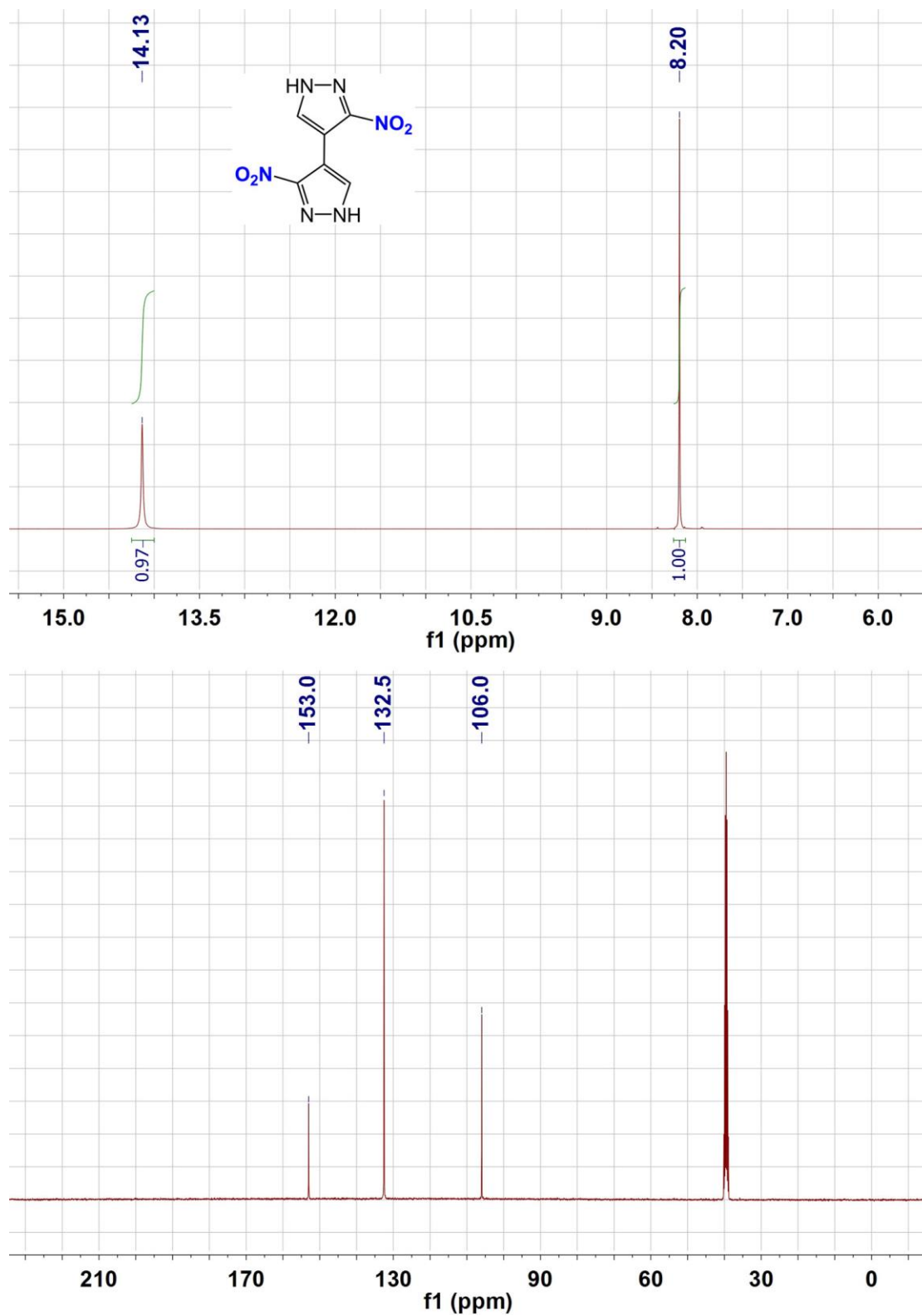


**Figure S26.** <sup>1</sup>H and <sup>13</sup>C NMR spectra for 3,3'-dinitro-4,4'-bipyrzole (3).



Facile and Selective Polynitrations at the 4-Pyrazolyl Dual Backbone: A Straightforward Access to a Series of High-Density Energetic Materials

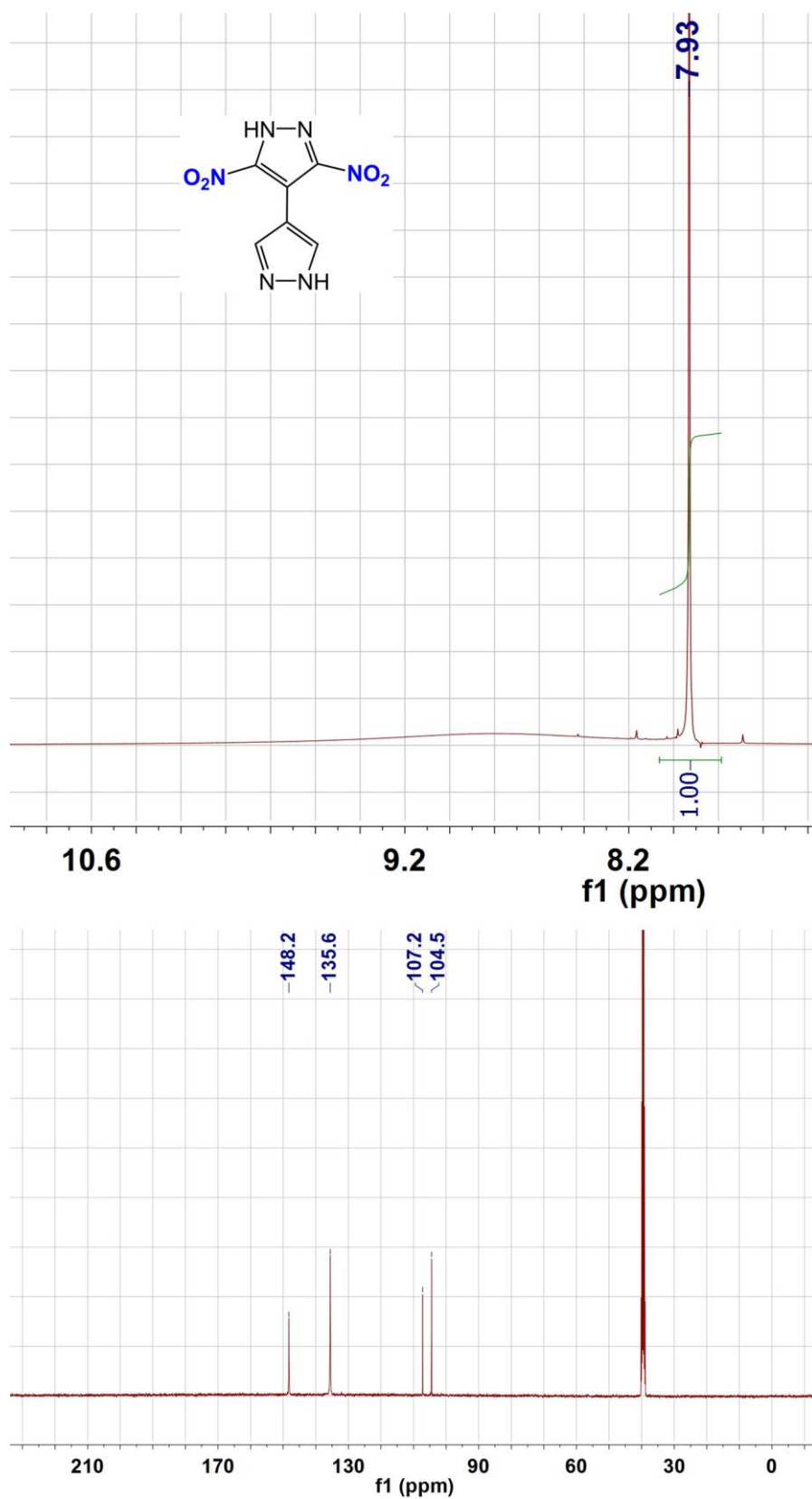


**Figure S27.**  $^1\text{H}$  and  $^{13}\text{C}$  NMR spectra for 3,5-dinitro-4,4'-bipyrazole (4).

Facile and Selective Polynitrations at the 4-Pyrazolyl Dual Backbone: A Straightforward  
Access to a Series of High-Density Energetic Materials

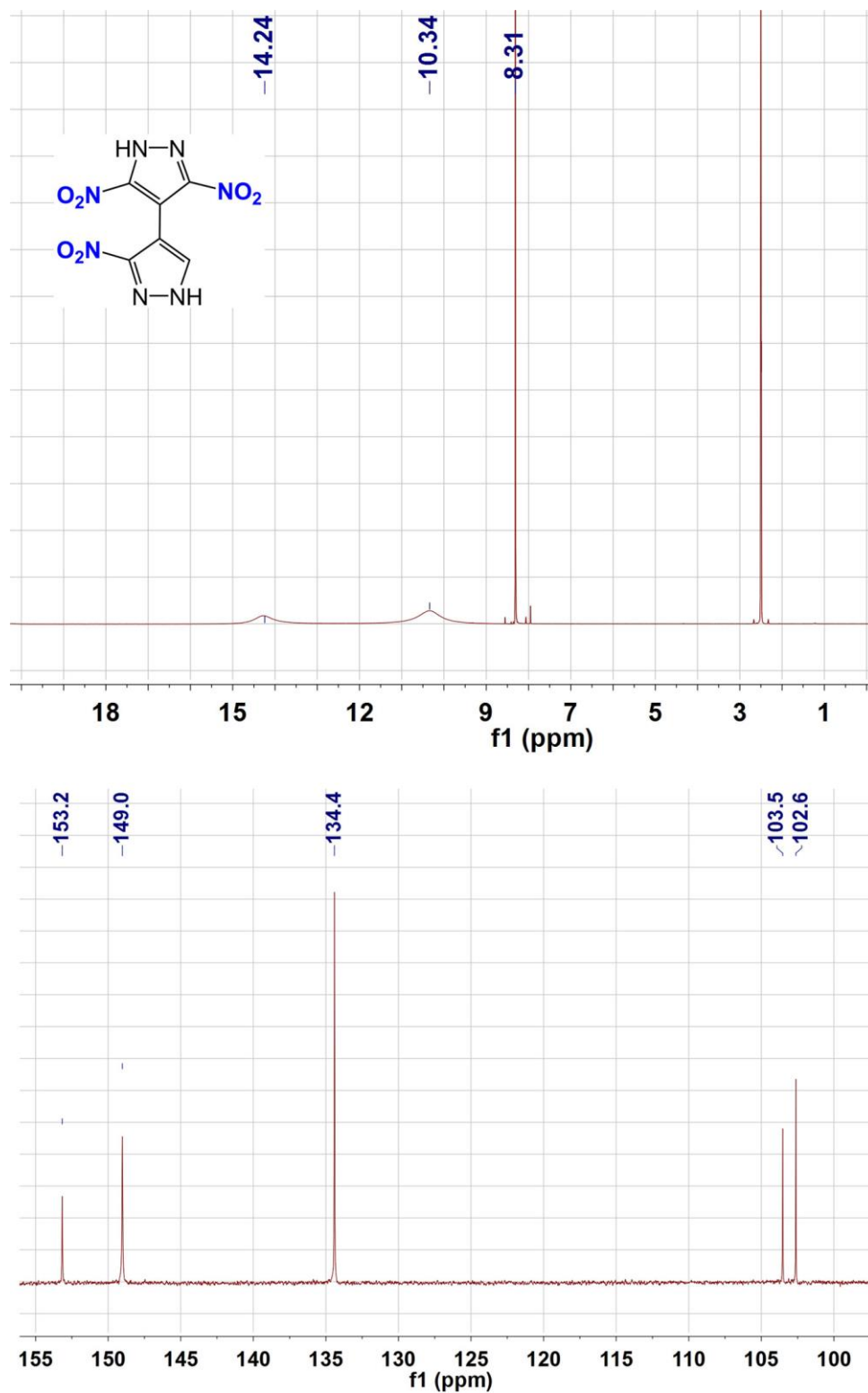


**Figure S28.**  $^1\text{H}$  and  $^{13}\text{C}$  NMR spectra for 3,3',5-trinitro-4,4'-bipyrazole (5).

Facile and Selective Polynitrations at the 4-Pyrazolyl Dual Backbone: A Straightforward  
Access to a Series of High-Density Energetic Materials

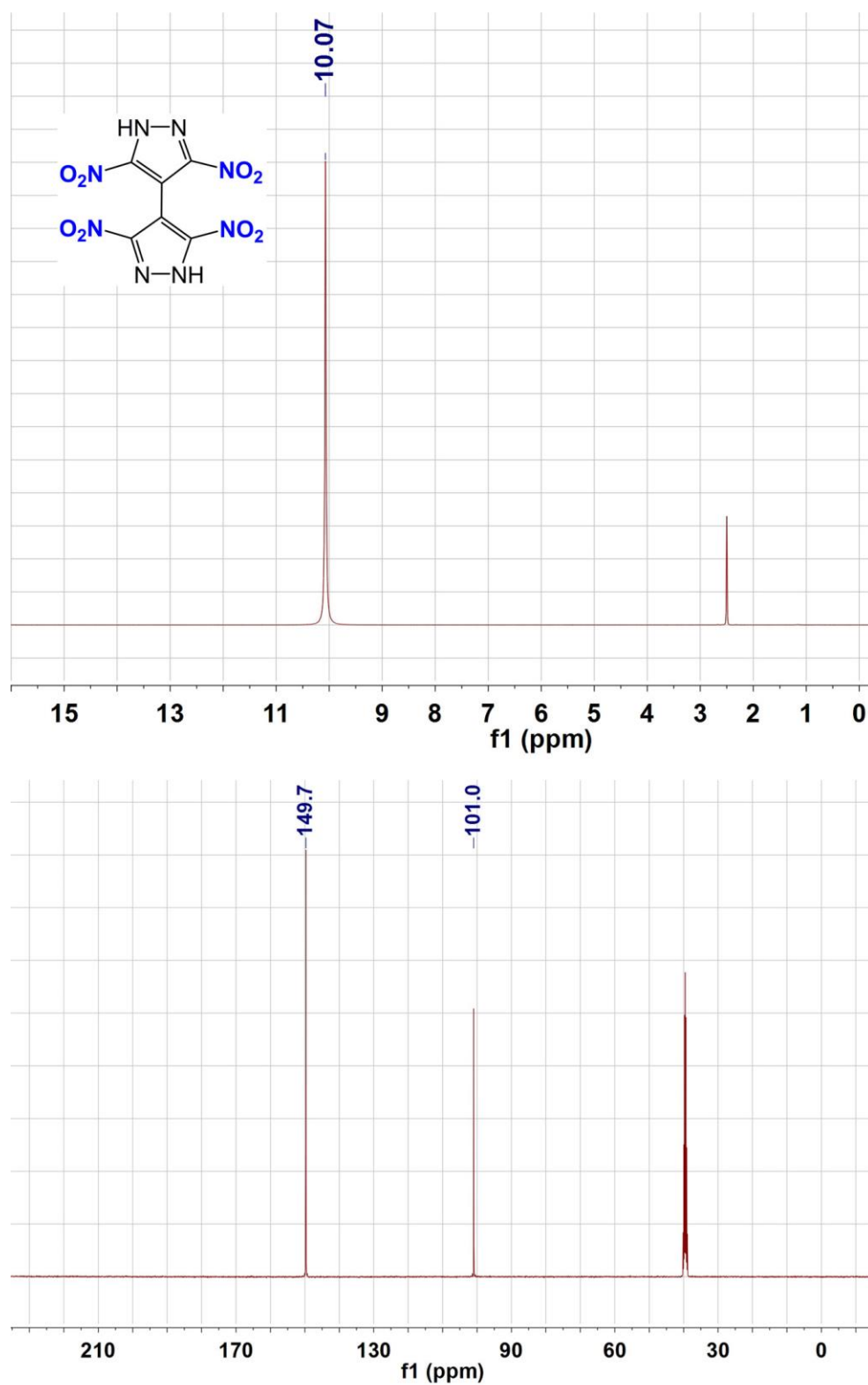


**Figure S29.** <sup>1</sup>H and <sup>13</sup>C NMR spectra for 3,3',5,5'-tetranitro-4,4'-bipyrazole (6).

Facile and Selective Polynitrations at the 4-Pyrazolyl Dual Backbone: A Straightforward  
Access to a Series of High-Density Energetic Materials

7.8.8.  $^{15}\text{N}$  NMR spectroscopy

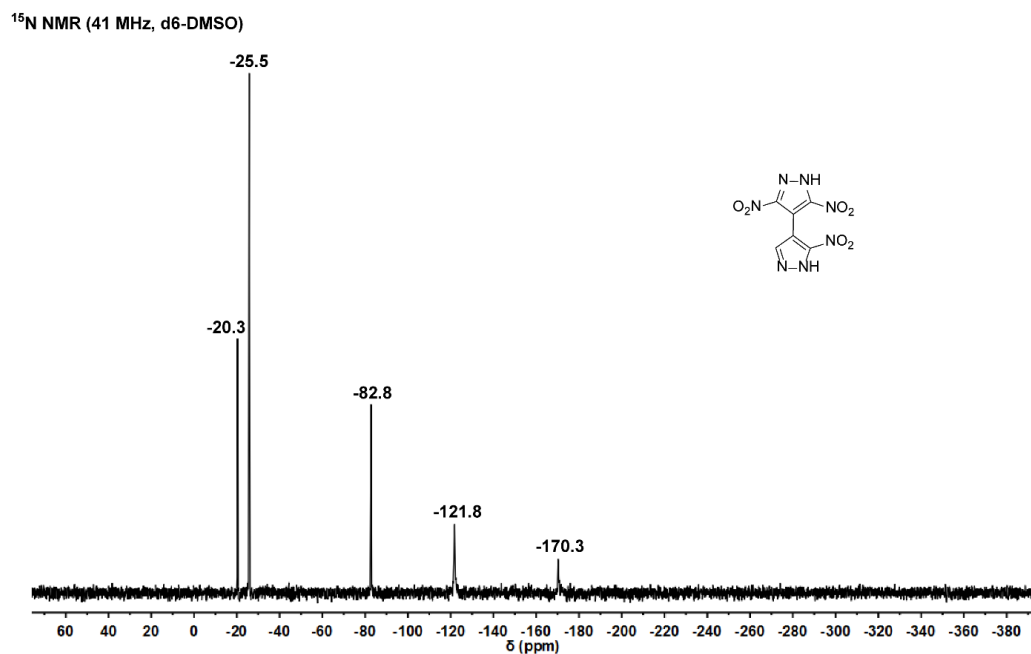


Figure S30.  $^{15}\text{N}$  NMR spectrum of 3,3',5-trinitro-4,4'-bipyrazole (5).

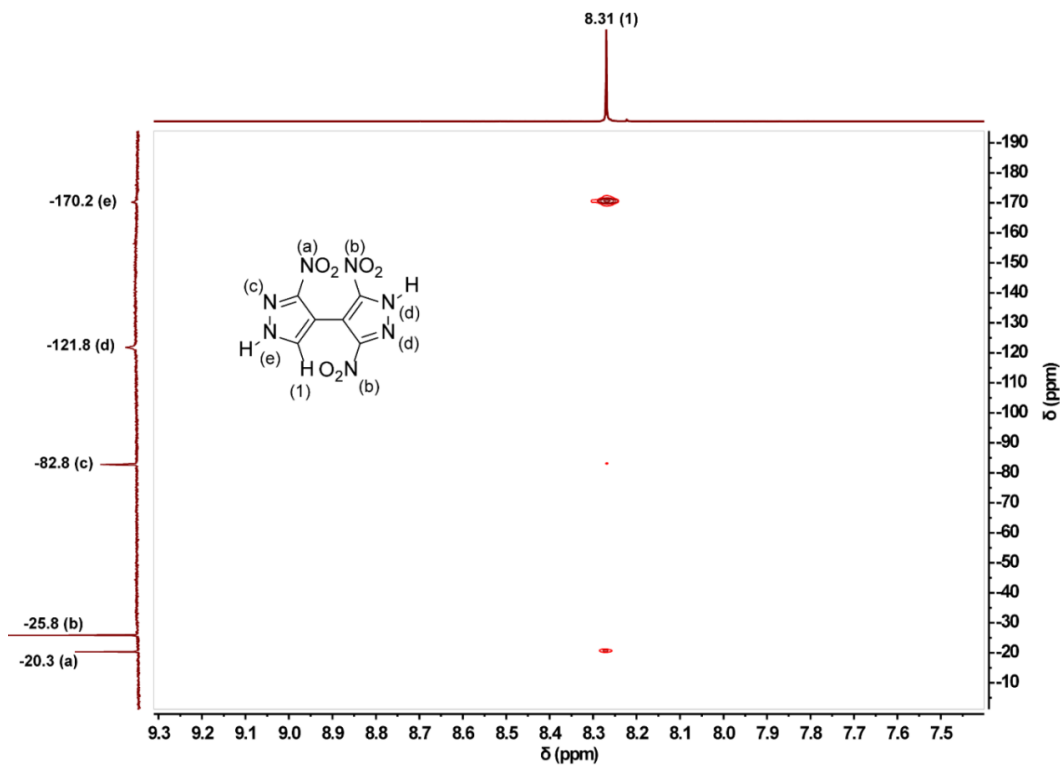
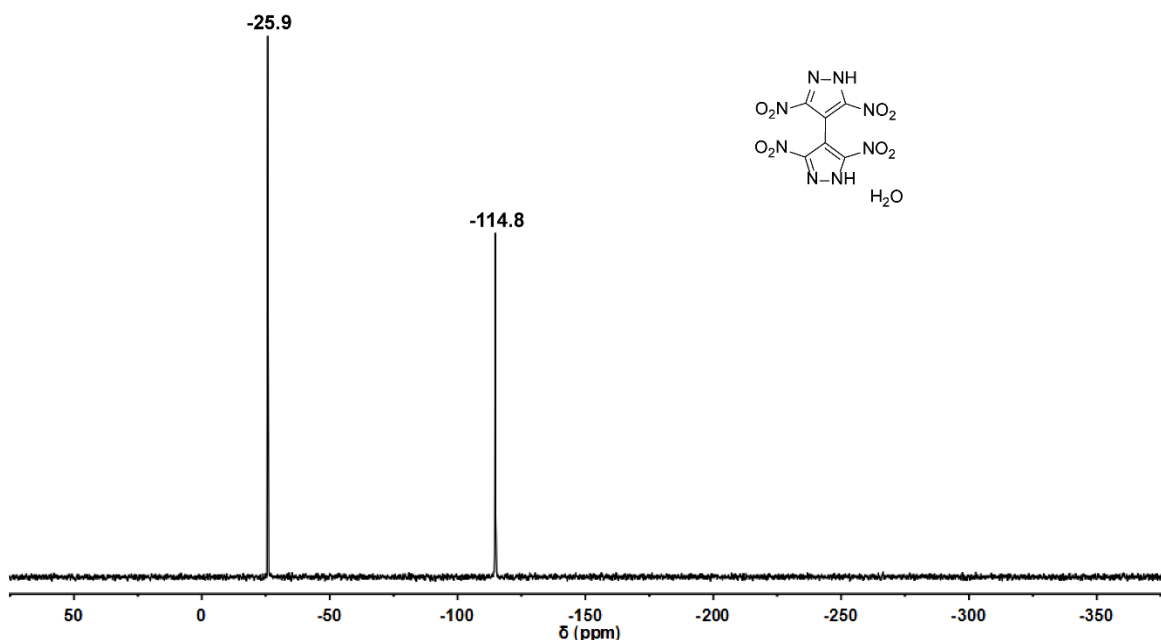


Figure S31.  $^1\text{H}$ ,  $^{15}\text{N}$  HMBC spectrum of 3,3',5-trinitro-4,4'-bipyrazole (5).

## Facile and Selective Polynitrations at the 4-Pyrazolyl Dual Backbone: A Straightforward Access to a Series of High-Density Energetic Materials

<sup>15</sup>N NMR (41 MHz, d6-DMSO)



**Figure S32.** <sup>15</sup>N NMR spectrum of 3,3',5,5'-tetranitro-4,4'-bipyrazole monohydrate (**6**·H<sub>2</sub>O).

### 7.8.9. References

- [S1] a) Reichel & Partner GmbH, <http://www.reichelt-partner.de>; b) Test methods according to the UN Recommendations on the Transport of Dangerous Goods, Manual of Test and Criteria, 4th edn., United Nations Publication, New York and Geneva, **2003**, ISBN 92–1-139087 7, Sales No. E.03.VIII.2; 13.4.2 Test 3 a (ii) BAM Fallhammer.
- [S2] I. Boldog, E.B. Rusanov, A.N. Chernega, J. Sieler, K.V. Domasevitch, *Angew. Chem. Int. Ed.* **2001**, *40*, 3435-3438.
- [S3] A.W. Johnson, *J. Chem. Soc.* **1946**, 1009-1014.
- [S4] I. Iwai, K. Tomita, *Chem. Pharm. Bull.* **1961**, *9*, 976-979.
- [S5] D. H. R. Barton, C.C. Dawes, G. Franceschi, M. Foglio, S.V. Ley, *J. Chem. Soc. Perkin Trans I* **1980**, 643.
- [S6] M.F. Fegley, N.M. Bortnick, C.H. McKeever, *J. Am. Chem. Soc.*, **1957**, *79*, 4140-4144.
- [S7] Z. Arnold, *Collect. Czech. Chem. Commun.* **1962**, *27*, 2993-2995.

**Facile and Selective Polynitrations at the 4-Pyrazolyl Dual Backbone: A Straightforward  
Access to a Series of High-Density Energetic Materials**

- [S8] Stoe & Cie. *IPDS software*. Stoe & Cie, **2000**, Darmstadt, Germany.
- [S9] a) G. M. Sheldrick, *Acta Crystallogr.* **2008**, *A64*, 112-122. b) G. M. Sheldrick, *Acta Crystallogr.* **2015**, *C71*, 3-8.
- [S10] K. Brandenburg, *Diamond 2.1e*, Crystal Impact GbR, Bonn, **1999**.
- [S11] a) V. A. Blatov, TOPOS, *IUCr CompComm Newsletter* **2006**, *7*, 4; b) V. A. Blatov, A. P. Shevchenko, V. N. Serezhkin, *J. Appl. Crystallogr.* **2000**, *33*, 1193.
- [S12] I. Boldog, J.-C. Daran, A.N. Chernega, E.B. Rusanov, H. Krautscheid, K.V. Domasevitch, *Cryst. Growth Des.* **2009**, *9*, 2895-2905.
- [S13] a) N. Mosca, R. Vismara, J. A. Fernandes, S. Casassa, K. V. Domasevitch, E. Bailón-García, F. J. Maldonado-Hódar, C. Pettinari, S. Galli, *Cryst. Growth Des.* **2017**, *17*, 3854-3867; b) I. Boldog, J. Sieler, A.N. Chernega, K.V. Domasevitch, *Inorg. Chim. Acta*, **2002**, *338*, 69-77.
- [S14] J. W. A. M. Janssen, C. C. Kruse, H. J. Koeners, C.L. Habraken, *J. Heterocycl. Chem.* **1973**, *10*, 1055-1058.
- [S15] J. D. Dunitz, V. Schomaker, K. N. Trueblood, *J. Phys. Chem.*, **1988**, *92*, 856.
- [S16] V. Schomaker, K. N. Trueblood, *Acta Crystallogr., Sect. B: Structural Science, Crystal Engineering and Materials*, **1998**, *54*, 507.
- [S17] A. Bauzá, A.V. Sharko, G.A. Senchyk, E.B. Rusanov, A. Frontera, K.V. Domasevitch, *CrystEngComm* **2017**, *19*, 1933-1937.
- [S18] M.-X. Zhang, P. E. Eaton, R. Gilardi, *Angew. Chem. Int. Ed.*, **2000**, *39*, 401.
- [S19] M. J. Frisch, G. W. Trucks, B. Schlegel, G. E. Scuseria, M. A. Robb, J. R. Cheeseman, G. Scalmani, V. Barone, B. Mennucci, G. A. Petersson, H. Nakatsuji, M. Caricato, X. Li, H.P. Hratchian, A. F. Izmaylov, J. Bloino, G. Zheng, J. L. Sonnenberg, M. Hada, M. Ehara, K. Toyota, R. Fukuda, J. Hasegawa, M. Ishida, T. Nakajima, Y. Honda, O. Kitao, H. Nakai, T. Vreven, J. A. Montgomery, Jr., J. E. Peralta, F. Ogliaro, M. Bearpark, J. J. Heyd, E. Brothers, K. N. Kudin, V. N. Staroverov, R. Kobayashi, J. Normand, K. Raghavachari, A. Rendell, J. C. Burant, S. S. Iyengar, J. Tomasi, M. Cossi, N. Rega, J. M. Millam, M. Klene, J. E. Knox, J. B. Cross, V. Bakken, C.

**Facile and Selective Polynitrations at the 4-Pyrazolyl Dual Backbone: A Straightforward  
Access to a Series of High-Density Energetic Materials**

Adamo, J. Jaramillo, R. Gomperts, R. E. Stratmann, O. Yazyev, A. J. Austin, R. Cammi, C. Pomelli, J. W. Ochterski, R. L. Martin, K. Morokuma, V. G. Zakrzewski, G. A. Voth, P. Salvador, J. J. Dannenberg, S. Dapprich, A. D. Daniels, O. Farkas, J.B. Foresman, J. V. Ortiz, J. Cioslowski, D. J. Fox, Gaussian 09 A.02, Gaussian, Inc., Wallingford, CT, USA, **2009**.

[S20] a) J. W. Ochterski, G. A. Petersson, and J. A. Montgomery Jr., *J. Chem. Phys.* **1996**, *104*, 2598-2619; b) J. A. Montgomery Jr., M. J. Frisch, J. W. Ochterski G. A. Petersson, *J. Chem. Phys.* **2000**, *112*, 6532-6542.

[S21] a) L. A. Curtiss, K. Raghavachari, P. C. Redfern, J. A. Pople, *J. Chem. Phys.* **1997**, *106*, 1063-1079; b) E. F. C. Byrd, B. M. Rice, *J. Phys. Chem. A* **2006**, *110*, 1005-1013; c) B. M. Rice, S. V. Pai, *Comb. Flame* **1999**, *118*, 445-458.

[S22] P. J. Linstrom, W. G. Mallard, *National Institute of Standards and Technology*, Gaithersburg MD, 20899.

[S23] a) F. Trouton, *Philos. Mag. (1876-1900)* **1884**, *18*, 54-57; b) M. S. Westwell, M. S. Searle, D. J. Wales, D. H. Williams, *J. Am. Chem. Soc.* **1995**, *117*, 5013-5015.

[S24] M. Sućeska, *EXPLO5 Version 6.03 User's Guide*, Zagreb, Croatia: OZM; **2015**.

[S25] a) R. Meyer, J. Köhler, A. Homburg, *Explosives*, 6th edn., Wiley, Weinheim, 2007, p. 291-292; b) T. M. Klapötke, *Chemistry of High-Energy Materials*, Walter de Gruyter, Berlin, **2015**;

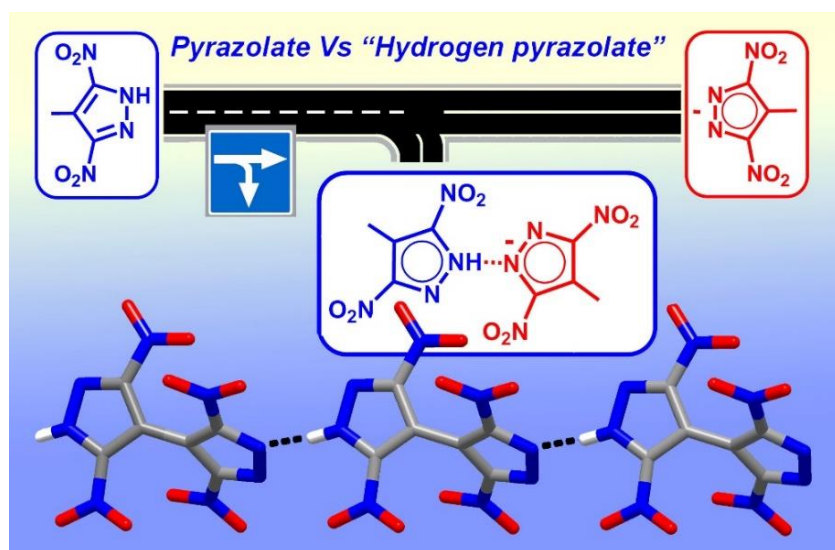
[S26] a) H. W. Sandusky, R. H. Granholm, D. G. Bohl, IHTR 2701, Naval Surface Warfare Center, Indian Head Division, MD, USA, August 12, **2005**; b) J. E. Felts, H. W. Sandusky, R. H. Granholm, *AIP Conf. Proc.* **2009**, *1195*, 233-236.

[S27] T. M. Klapötke, T. G. Witkowski, *ChemPlusChem* **2016**, *81*, 357-360.

## 8. On a Midway Between Energetic Molecular Crystals and High-Density Energetic Salts: Crystal Engineering with Hydrogen Bonded Chains of Polynitro Bipyrazoles

Ivan Gospodinov, Kostiantyn V. Domasevitch, Cornelia C. Unger, Thomas M. Klapötke and Jörg Stierstorfer

Submitted to *Cryst. Growth Des.*



**Abstract:** A new strategy for supramolecular synthesis of energetic salts is reported. It is still a challenge to address packing patterns and crystal morphologies of such materials due to lack of reliable supramolecular synthons, which are applicable to polynitro substituted species. 3,5-Dinitro-4,4'-bipyrazole (**1**), 3,3',5-trinitro-4,4'-bipyrazole (**2**) and 3,3',5,5'-tetranitro-4,4'-bipyrazole (**3**) are excellent functional models those provide higher degree of control over the structure by manipulating robust self-assembly molecular building blocks of lower dimensionality. A variety of  $\text{K}^+$ ,  $\text{Cs}^+$  and nitrogen-rich salts (*e.g.* ammonium, aminoguanidinium, hydrazinium, and hydroxylammonium) **4-18**, prepared by single deprotonation of NH-acidic **1-3**, are based upon polar anionic chains sustained with strong  $\text{NH}\cdots\text{N}$  bonding of conjugated acidic and basic pyrazole/pyrazolate sites. Gradual increase of NH-acidity (dinitropyrazolyl > nitropyrazolyl >> pyrazolyl) productively contributes to the strenght of  $\text{NH}\cdots\text{N}$  bonds and reliability of such supramolecular synthon. New synthesized energetic materials **9-17** were fully characterized by



## On a Midway Between Energetic Molecular Crystals and High-Density Energetic Salts: Crystal Engineering with Hydrogen Bonding Chains of Polynitro Bipyrazoles

NMR ( $^1\text{H}$ ,  $^{13}\text{C}$  and  $^{14}\text{N}$ ) spectroscopy, infrared spectroscopy, differential thermal analysis (DTA), elemental analysis and the heats of formation were calculated using the atomization method based on CBS-4M enthalpies. Several detonation parameters, such as detonation pressure, velocity and energy, were calculated by using the X-ray room temperature densities and the calculated standard molar enthalpies of formation. The sensitivities toward external stimuli were tested according to the BAM standards.

### 8.1. Introduction

Synthesis of energetic co-crystals<sup>[1]</sup> and high-density energetic salts<sup>[2,3]</sup> is a particular issue for the development of new materials, which meet current criteria for performance, thermal stability and insensitivity toward external stimuli.<sup>[4]</sup> This approach receives a growing attention for especially rich and versatile possibilities of the control over a range of properties those are relevant to the solid state. Rational combination of chemically different counterparts, for sustaining integrity of the crystal lattice, may be viewed as a major step towards materials with valuable energetic characteristics.<sup>[5]</sup> For example, ionic derivatives are suited for proper handling of unstable, liquid or deliquescent, acidic and corrosive species.<sup>[6]</sup> This may be relevant to many common types of nitro-functionalized molecules (e.g. polynitroazoles, nitroamines), since accumulation of explosophore nitro groups results in dramatic increase of the acidity.<sup>[7]</sup> Such components as hydroxylammonium cations productively contribute to energy release of the salts due to inherently high nitrogen and oxygen contents and high heat of formation. From the perspective of crystal structure, higher energies of ionic lattices, together with extensive hydrogen bonding typically mediating structures of nitrogen-rich salts, are beneficial for higher densities and thermal stabilities of energetic materials.<sup>[2]</sup> Subtle features of supramolecular interactions, packing patterns and morphologies of the structures are particularly prevalent.

## On a Midway Between Energetic Molecular Crystals and High-Density Energetic Salts: Crystal Engineering with Hydrogen Bonding Chains of Polynitro Bipyrzoles

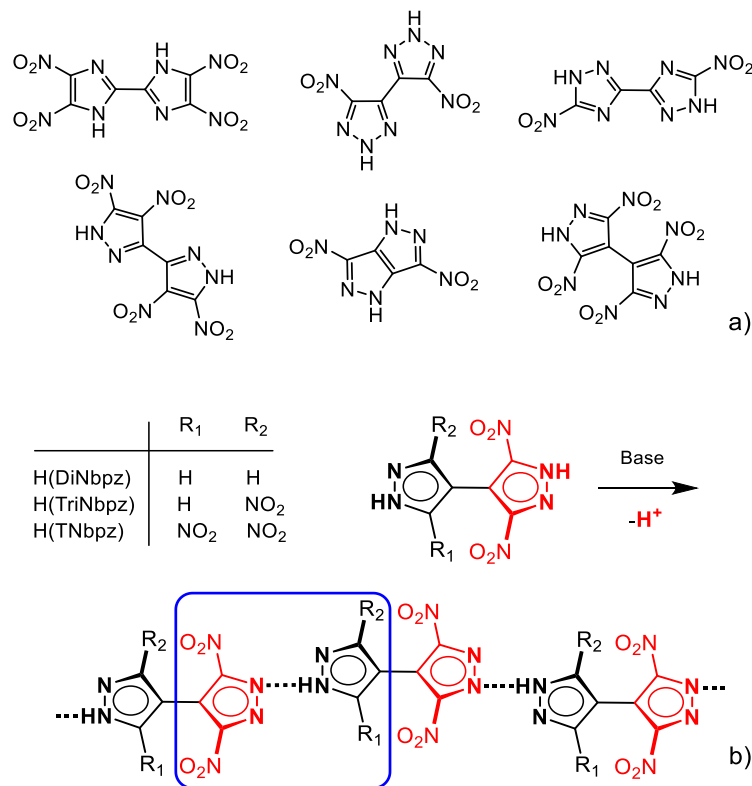


**Figure 1.** Selected literature known fully C-nitrated *bis*-heterocyclic compounds (a) and proposed approach toward generation of self-assembly molecular building block, with supramolecular synthon indicated in blue (b).

For example, recent findings provide insights into the sensitivity mechanism and allow some correlation of impact sensitivity and crystal packing, while suggesting ability of layered patterns to buffer against external mechanical stimuli.<sup>[8]</sup> This paradigm is applicable for high-performance insensitive materials, including  $\text{NH}_3\text{OH}^+$  salts.<sup>[9]</sup>

In this view, methodology of crystal engineering presents a promising avenue for developing of energetic materials.<sup>[10]</sup> Aakeröy et al. succeeded in generation of hydrogen bonded chains by combining ethylenedinitramine (EDNA) and common bitopic N-donor spacers.<sup>[11]</sup> However, supramolecular synthesis of energetic materials was hitherto complicated due to the inherently inappropriate molecular functionalities of many relevant species. Common explosophore  $\text{NO}_2$  groups are only weak acceptors of hydrogen bonds,<sup>[12]</sup> which are the primary forces (beyond the Coulomb attraction) for construction of nitrogen-rich salts. At the same time, availability of many closely separated acceptor N-atoms at the framework of polynitrogen azole, azine and acyclic species mitigates against efficient

## On a Midway Between Energetic Molecular Crystals and High-Density Energetic Salts: Crystal Engineering with Hydrogen Bonding Chains of Polynitro Bipyrazoles

control over hydrogen bonding, which is particularly the case of energetic salts with small multiple H-bond donor cations ( $\text{NH}_4^+$ ,  $\text{N}_2\text{H}_5^+$ ,  $\text{NH}_3\text{OH}^+$ , *etc.*).<sup>[2]</sup> Therefore, a suite of high-probability supramolecular interactions for crystal engineering of energetic materials is relatively scarce.<sup>[11]</sup>

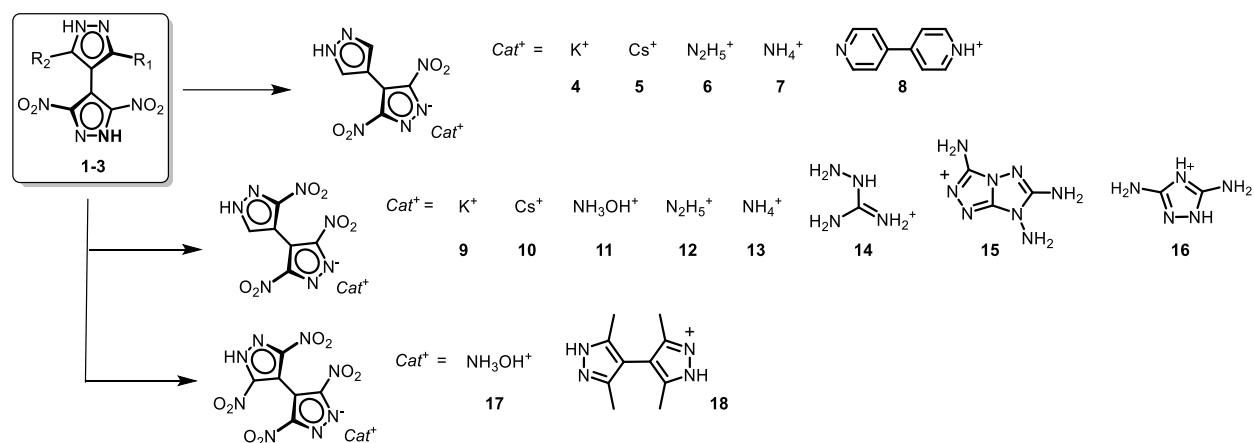
Taking into account numerous examples of strongest hydrogen bonds, typically sustained by conjugate acids and bases<sup>[12a]</sup> (ranging from simple inorganic systems of  $\text{HF}_2^-$  and hydrogen oxoanions<sup>[13]</sup> to organic hydrogen carboxylates, oximates,<sup>[14]</sup> *etc.*), one may anticipate a special self-assembly scenario. The elements of reliable supramolecular synthons are already present at the molecular frameworks for vast variety of energetic species combining several acidic sites, *e.g.* nitroderivatives of 2,2'-bisimidazole,<sup>[15]</sup> 3,3'-bipyrazole,<sup>[16]</sup> 4,4'-bipyrazole,<sup>[17]</sup> pyrazolo[4,3-*c*]pyrazole,<sup>[18]</sup> 3,3'-bi(1,2,4-triazole)<sup>[19]</sup> and *etc.* The conjugated acidic and basic functions, such as pyrazole-NH and pyrazolate-N sites in the case of bipyrazoles, arise with partial deprotonation of the molecule to form singly charged “hydrogen bipyrazolate” anions. This is a key pre-requisite for higher degree of control over the structure. Instead of the common case of charge diffuse dianions held by multiple (and often weak, less directional or bifurcated) hydrogen bonds, linear polar chains could actualize by head-to-tail self-assembly of single charged anions by strong hydrogen bonding (**Figure 1**). A suitable prototype may be found with a series of 5,5'-bitetrazole “mono salts” reported by Sundermeyer.<sup>[20]</sup> In addition to the evident benefit from strong primary  $\text{NH}\cdots\text{N}^-$  bonds, antiparallel pairing of polar elements of lower dimensionality could also contribute to the density of the crystal packing. As well, such pairing favors generation of stacks and layers rather than 3D frameworks and this feature may facilitate construction of layered energetic materials.

With this in mind we explored family of 4,4'-bipyrazole tectons. A full library of C-nitro 4,4'-bipyrazoles was recently accessible by straightforward and selective reaction sequences.<sup>[17]</sup> Evolution of their protolytic properties follows progressive nitro-substitution at the bipyrazole platforms and this results in different combinations of basic pyrazole, amphoteric nitropyrazole and acidic dinitropyrazole sites.

## 8.2. Results and Discussion

### 8.2.1. Synthesis

Either in the case of 3,5-dinitro- or 3,3',5-trinitro-4,4'-bipyrazoles, significant differentiation of two pyrazole sites in the view of acidity ( $pK_a = 14.63$  for the parent pyrazole; 9.81 for 3(5)-nitro and 3.14 for 3,5-dinitropyrazoles)<sup>[7]</sup> provides total selectivity in the formation of singly charged anions. When combined with relatively weak bases, these bipyrazoles act as monobasic acids only, retaining weakly acidic pyrazole (nitropyrazole) group neutral. Reactions of acidic 3,3',5,5'-tetranitro-4,4'-bipyrazole are less predictable due to easy formation of dianions. Nevertheless, two salts of the desired composition  $Cat^+(TNBbpz)$  were successfully prepared (**Scheme 1**).



**Scheme 1.** Synthesis of the energetic compounds based on 3,5-diinitro-4,4'-bipyrazole H(DiNBpz) **1**, 3,3',5-trinitro-4,4'-bipyrazole H(TriNBpz) **2** and 3,3',5,5'-tetranitro-4,4'-bipyrazole H(TNBpz) **3**.

### 8.2.2. Single crystal X-ray diffraction studies

The solid-state structures of compounds **4–18** were determined by XRD. Presence of anionic pyrazolate groups is best detected by nearly identical angles at the ring N-atoms [106.4-108.4°], which is contrary to the neutral pyrazole (nitropyrazole) groups [CN(H)N = 110.9-113.0°; CNN(H) = 103.2-104.7°] constituting second part of the singly charged anions. The dihedral angles between these two rings are similar for all compounds [ $\varphi = 34.09(4)$ -66.53(7)°] and therefore introduction of third and fourth nitro group makes no significant impact to the molecular conformation. In fact,

## On a Midway Between Energetic Molecular Crystals and High-Density Energetic Salts: Crystal Engineering with Hydrogen Bonding Chains of Polynitro Bipyrzoles

the intramolecular NO<sub>2</sub>/NO<sub>2</sub> interactions may be regarded as attractive,<sup>[21]</sup> as a special case of lone pair- $\pi$  hole bonding,<sup>[22]</sup> which in effect decreases the steric strain. Moreover, with formation of singly charged anions, the twist angles within molecular frameworks decrease [ $\varphi$  = 50.3; 58.6 and 71.4° for **1-3**, respectively]<sup>[17]</sup> and this may be favorable for sustaining more dense packing. The nitro groups are nearly coplanar with the atoms of carrier rings (**Table 1**).

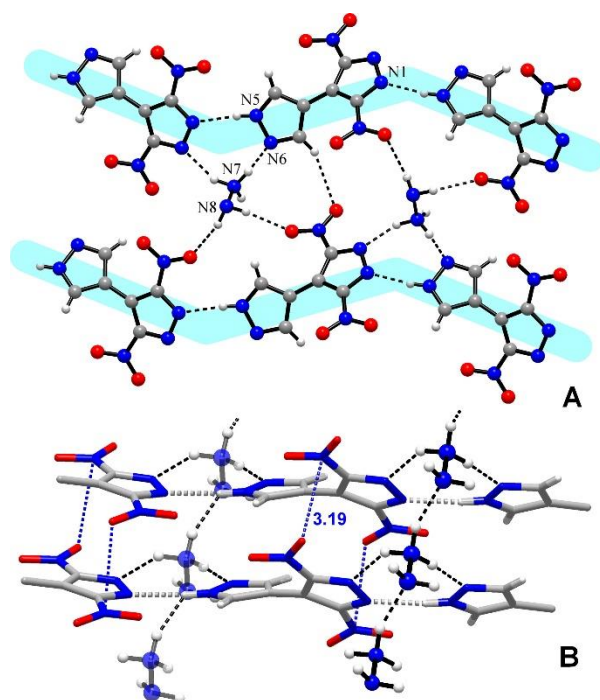


**Figure 2.** Polar hydrogen-bonded chains in the structure of **6** (indicated with blue strips) (A) and the side-view showing bonding of N<sub>2</sub>H<sub>5</sub><sup>+</sup> cations and stacking of dinitropyrazolate groups (B).

Even a more important consequence of deprotonation is stronger and more directional hydrogen bonding NH $\cdots$ N, which is superior to weaker and bifurcated H-bonds in the structures of parent molecular species **2** and **3** [N $\cdots$ N = 2.88 and 3.00 Å, respectively]. This bonding represents one of the strongest intermolecular interactions in the structures, being a basic supramolecular synthon for assembly of polar anionic chains. Reliability of this synthon coincides with strength of the bonds with different kinds of pyrazole-NH donors and therefore the optimal configuration of molecular functionalities may be easily derived.

**On a Midway Between Energetic Molecular Crystals and High-Density Energetic Salts:  
Crystal Engineering with Hydrogen Bonding Chains of Polynitro Bipyrazoles**

**Table 1.** Selected structural features of **4–18**.

	Packing index	Twist angles /° [a]		Principal pzH...pz bonding			N...O contacts (NO <sub>2</sub> /NO <sub>2</sub> ) / Å [b]
		Ring/Ring	Ring/NO <sub>2</sub>	H...N / Å	N...N / Å	∠NH...N /°	
<b>4-H<sub>2</sub>O</b>	82.1	39.65(6)	14.3(2)-15.2(2)	2.03(3)	2.898(2)	169(3)	3.224(3)
<b>5-H<sub>2</sub>O</b>	80.7	39.19(12)	6.8(2)-22.5(2)	1.92(3)	2.835(3)	171(3)	3.046(3)
<b>6</b>	74.8	41.90(6)	10.2(2)-12.3(2)	2.02(2)	2.877(2)	172(2)	3.183(2)
<b>7-H<sub>2</sub>O</b>	73.4	34.09(4)	5.8(2)-6.0(2)	None			3.2570(18)
<b>8</b>	71.7	49.82(6)	8.4(3)-13.8(3)	None			3.029(2)
<b>9-H<sub>2</sub>O</b>	84.2	49.59(8)	3.73(8)-19.6(3)	1.95(3)	2.809(2)	169(2)	–
<b>10-H<sub>2</sub>O</b>	80.9	56.90(9)	11.9(4)-20.7(3)	2.00(3)	2.814(3)	162(3)	3.024(3)
<b>11</b>	74.3	42.75(6)	5.2(3)-21.8(3)	1.94(2)	2.8474(18)	172.2(17)	3.1169(17)
<b>12</b>	75.7	44.89(8)	4.86(4)-21.8(3)	1.92(3)	2.810(2)	171(3)	3.195(2)
<b>13-H<sub>2</sub>O</b>	73.6	49.65(7)	4.5(2)-15.9(3)	1.89(3)	2.760(2)	166(2)	–
<b>14-MeOH</b>	71.5	62.57(4)	2.1(2)-16.7(2)	1.92(2)	2.8294(15)	168.4(16)	2.8976(14)
<b>15</b>	70.6	54.38(6)	4.3(3)-11.9(2)	1.89(4)	2.784(3)	169(3)	2.894(2)
<b>17</b>	74.1	66.53(7)	3.6(2)-6.7(2)	1.89(2)	2.7661(18)	158(2)	3.2429(18)
<b>18-H<sub>2</sub>O</b>	71.4	57.07(8)	3.2(3)-13.2(2)	1.82(3)	2.7618(19)	170(3)	3.198(2)

[a] Dihedral angles subtended by mean planes of two pyrazole rings (Ring/Ring) or plane of NO<sub>2</sub> group and mean plane of the carrier pyrazole ring (Ring/NO<sub>2</sub>) ; [b] Intermolecular nitro...nitro contacts with a cut-off limit of 3.30 Å.

The bonds of less polarized pyrazole-NH donors, as they occur for DiNBpz<sup>−</sup> series, are somewhat weaker [mean N...N = 2.870(3) Å]. It is not surprising that this system is more

**On a Midway Between Energetic Molecular Crystals and High-Density Energetic Salts:  
Crystal Engineering with Hydrogen Bonding Chains of Polynitro Bipyrazoles**

flexible and less appropriate for the needs of crystal design. With examples of polar anionic chains observed for **4-6**, failure of the above supramolecular synthon in ammonium (**7·H<sub>2</sub>O**) and bipyridinium (**8**) salts should be also noted. This is contrary to the compounds of (TriNbpz)<sup>−</sup> and (TNbpz)<sup>−</sup>. Increased acidity of pzH sites enhances hydrogen bonding with dinitropyrazolate sites. This is indicated by perceptible shortening of N...N separations [mean 2.808(3) Å] in chains subtended by (TriNbpz)<sup>−</sup> anions, but for (TNbpz)<sup>−</sup> this effect is even stronger [mean N...N = 2.764(2) Å] (**Table 1**). The latter approaches value for very strong NH...N bond between conjugated acid and base pair in morpholinium hydrogen 3,5-dinitroindazolate [2.727 Å].<sup>[23]</sup> As a result of more competitive pzH...pz<sup>−</sup> bonding, polar anionic chains become prevalent for the entire series, including very different alkali metal and H-bond donating cations. In the monopotassium salt of isomeric tetranitro-3,3'-bipyrazole reported by Shreeve,<sup>[16]</sup> double pzH...pz<sup>−</sup> bonds led to discrete dimers only. Structures of potassium (**4·H<sub>2</sub>O**) and hydrazinium (**6**) salts exhibit dense packing of the above chains of (DNBpz)<sup>−</sup>, with a set of slipped  $\pi/\pi$  stacking interactions between two kinds of identical rings and lone pair- $\pi$  hole interactions of NO<sub>2</sub> groups (**Table 1**). In addition to pzH...pz interactions, the primary hydrogen bonds in **6** concern three most polarized −NH<sub>3</sub><sup>+</sup> donors (with a distinct subtopology of N<sub>2</sub>H<sub>5</sub><sup>+</sup> cations, in the form of polar chains, **Fig. 2**) whereas weaker interactions of −NH<sub>2</sub> donors are restricted to less directional bonds with nitro groups. Chain of N<sub>2</sub>H<sub>5</sub><sup>+</sup> cations is a predictable motif for the systems lacking H-bond O-acceptors and it is well-known for energetic hydrazinium salts.<sup>[24,25]</sup>

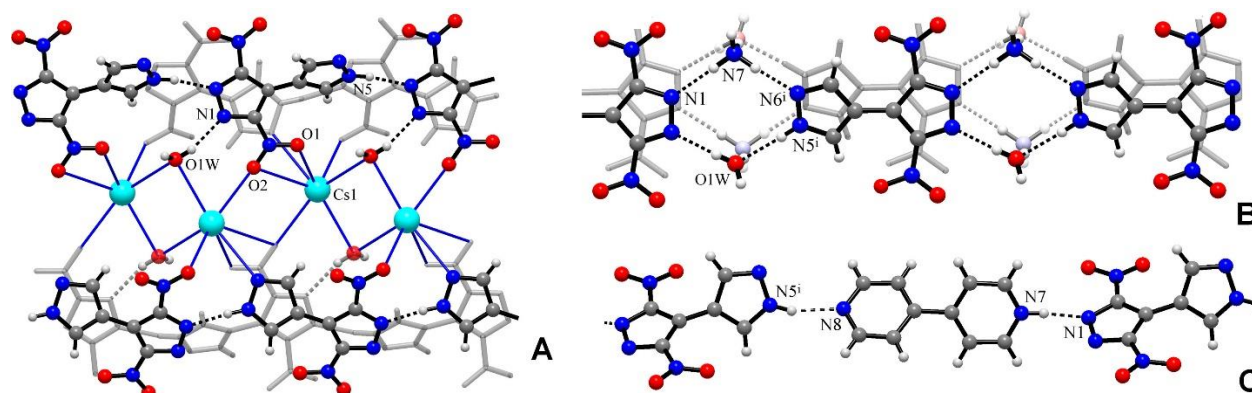


**Figure 3.** A) Fragment of the crystal structure of **5·H<sub>2</sub>O** showing hydrogen bonding of dinitropyrazolate group and Cs...N bonding of pyrazole group. Note the antialignment of polar

## On a Midway Between Energetic Molecular Crystals and High-Density Energetic Salts: Crystal Engineering with Hydrogen Bonding Chains of Polynitro Bipyrroles

anionic chains. Structures of **7**·H<sub>2</sub>O (B) and **8** (C): disintegration of the anionic chains in the favour of stronger hydrogen bonding.

Packing pattern in **4**·H<sub>2</sub>O is almost identical, with a set of K<sup>+</sup>···O(N) ion-dipole interactions (2.6608(17)-3.2959(18) Å) instead of the hydrogen bonds. Cesium analog **5**·H<sub>2</sub>O retains most features of morphology, but in total three more M<sup>+</sup>···O<sub>2</sub>N contacts are generated in addition to two M<sup>+</sup>···N, two M<sup>+</sup>···OH<sub>2</sub> and three M<sup>+</sup>···O<sub>2</sub>N bonds seen in **4**·H<sub>2</sub>O. One can conclude that ion-dipole interactions with K<sup>+</sup> or Cs<sup>+</sup> are less competitive with respect to the conventional hydrogen bonding. The metal cations coordinate pyrazole-N atoms only (as weaker acceptors of hydrogen bonds), while pyrazolate-N sites accept H-bonds with water molecules. This allows to rationalize disintegration of the (DiNBpz)<sup>-</sup> chains, in combination with stronger H-bond donors. In the structure of **8**, the chain embeds singly charged *Hbipy*<sup>+</sup> cations, as complementary H-bond donor and acceptor links between the anions (**Fig. 3**). Interaction of the type PyH<sup>+</sup>···pz<sup>-</sup> (N···N = 2.671(2) Å) is far stronger with respect to the other kinds of bonding. More complicated pattern in **7** is based upon supramolecular cubes, with a double set of pyrazolate and pyrazole rings, NH<sub>4</sub><sup>+</sup> cations and water molecules.

As stated above, increased acidity of pyrazole-NH group has striking impact on crystal chemistry of (TriNBpz)<sup>-</sup> series. With stronger pzH<sup>+</sup>···pz<sup>-</sup> bonding (**Table 1**), polar anionic chains invariably survive significant changes in the crystal environment and nature of supramolecular interactions. Such morphology is relevant for very similar frameworks in structures of **9-13** (**Fig. 4, 5**). When consider the H-bonded NH<sub>3</sub>OH<sup>+</sup> and N<sub>2</sub>H<sub>5</sub><sup>+</sup> cations as simple links between the chains, nearly uniform planar nets are found for isomorphous compounds **11** and **12**.



On a Midway Between Energetic Molecular Crystals and High-Density Energetic Salts:  
Crystal Engineering with Hydrogen Bonding Chains of Polynitro Bipyrazoles

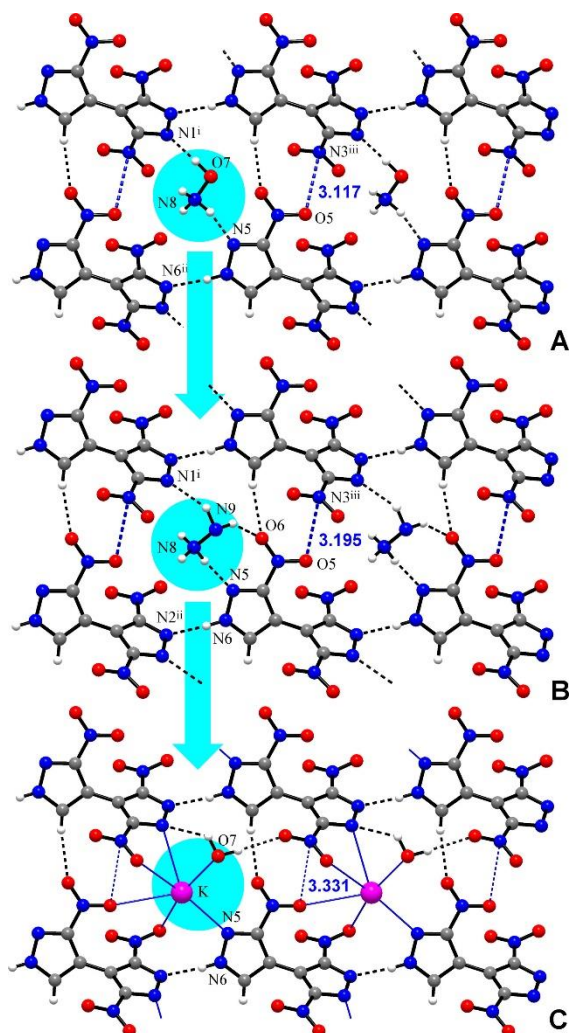


**Figure 4.** Inheritance of the supramolecular motifs for **11** (A), **12** (B) and **9·H<sub>2</sub>O** (C). Note the unexpected bonding mode of N<sub>2</sub>H<sub>5</sub><sup>+</sup> cations, which establish the –NH<sub>2</sub>⋯N bonds to the pyrazolate acceptors, but –NH<sub>3</sub><sup>+</sup>⋯N bond to the neutral pyrazole.

Bonding of NH<sub>3</sub>OH<sup>+</sup> follows the common trend: the strongest bond is established with OH donor<sup>[26]</sup> and most polarized pyrazolate-N acceptor (N⋯O = 2.7202(18) Å). Nevertheless, in the case of N<sub>2</sub>H<sub>5</sub><sup>+</sup> cations in **12**, much weaker and less directional bond with –NH<sub>2</sub> site is surprisingly formed [N⋯N = 3.082(3) Å; ∠NH⋯N = 139(3)°] instead of the anticipated –NH<sub>3</sub><sup>+</sup>⋯N<sup>–</sup> pattern, which is known for hydrazinium 3,5-dinitro pyrazolate.<sup>[25]</sup> This unusual mode is likely influenced by lone pair-π hole bonding of the cations and nitro groups [H<sub>2</sub>N⋯NO<sub>2</sub> = 3.106(2) Å in **12** vs. HO⋯NO<sub>2</sub> = 3.267(2) Å in **11**], which complements the primary bonds of N<sub>2</sub>H<sub>5</sub><sup>+</sup> and enables clear discrimination of the –NH<sub>2</sub> and –NH<sub>3</sub><sup>+</sup> sites. The CH⋯O and lone pair-π hole NO<sub>2</sub>/NO<sub>2</sub> interactions act in a synergy with strong hydrogen

## On a Midway Between Energetic Molecular Crystals and High-Density Energetic Salts: Crystal Engineering with Hydrogen Bonding Chains of Polynitro Bipyrazoles

bonds for sustaining the structure of the nets, while  $\text{XNH}_3\cdots\text{O}_2\text{N}$  bonds ( $\text{X} = \text{OH}, \text{NH}_2$ ) links the above nets into bilayers.

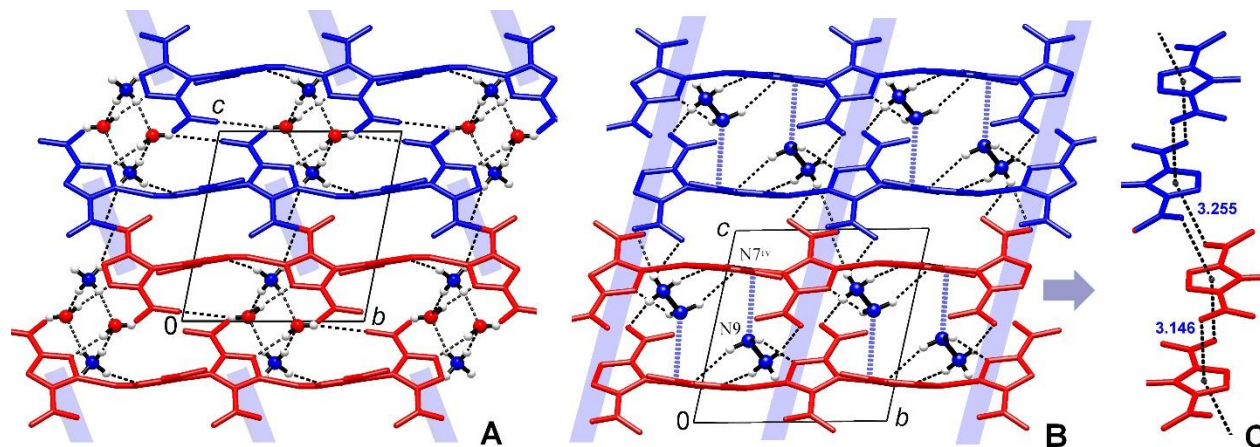


**Figure 5.** Delicate variations of the bilayer patterns in the structures of **13·H<sub>2</sub>O** (A) and **12** (B), with two successive bilayers marked in blue and red and stacks of dinitropyrazole groups indicated by light-blue strips. Lone pair- $\pi$  hole bonds of the type  $\text{H}_2\text{N}\cdots\text{NO}_2$  are shown as dotted blue bonds (B). Note that hosting of the large  $[(\text{NH}_4)_2(\text{H}_2\text{O})_2]$  ensemble is a result of mutual shift of two layers with loss of some stacking interactions. (C) Infinite stacking observed in the structure of **12**.

Three other salts,  $\text{Cat}^+(\text{TriNb pz})\cdot\text{H}_2\text{O}$  [ $\text{Cat}^+ = \text{K}^+$  **9**,  $\text{Cs}^+$  **10**, and  $\text{NH}_4^+$  **13**] reveal comparable bilayer pattern based upon interconnection of the polar anionic chains (**Fig. 5**). However, relatively distal ion-dipole interactions of  $\text{K}^+$  and  $\text{Cs}^+$  cations are largely destructive for the network of supramolecular interactions involving  $\text{NO}_2$  groups. In particular, distal  $\text{N}\cdots\text{O}$  contacts ( $>3.30$  Å) indicate loss of  $\text{NO}_2/\text{NO}_2$  interactions within the layers in **9** and **10**. In the case of **13·H<sub>2</sub>O**, strong hydrogen bonding of  $\text{NH}_4^+$  cations and water molecules is even more crucial. Unlike  $\text{NH}_4(\text{DiNb pz})\cdot\text{H}_2\text{O}$ , it does not affect disintegration of 1D polar chains. However, formation of centrosymmetric rhombs of two  $\text{NH}_4^+$  cations and two water molecules results in mutual shift of the layers, with loss of stacking interactions between dinitropyrazolate groups (**Fig. 5**). This kind of  $[(\text{NH}_4)_2(\text{H}_2\text{O})_2]^{2+}$  ensembles is well known for energetic ammonium salts.<sup>[27]</sup>

Structures of **14·MeOH** and **15** demonstrate new possibility for crystal engineering with polar chains of  $(\text{TriNb pz})^-$ . With 1,3-separated  $\text{NH}$ -donors of the cations, double  $\text{NH}\cdots\text{N}$  bonds are generated across stack of the anions (**Fig. 6**). Although both these  $\text{NH}\cdots\text{N}$  bonds are directional, the interaction of triazole  $\text{NH}$  and dinitropyrazolate acceptor in **15** is

**On a Midway Between Energetic Molecular Crystals and High-Density Energetic Salts:  
Crystal Engineering with Hydrogen Bonding Chains of Polynitro Bipyrazoles**

essentially stronger than bond of  $\text{NH}_2$  and pyrazole groups ( $\text{N}\cdots\text{N} = 2.810(2)$  and  $2.932(2)$  Å, respectively). Such combination of two different acceptors, to complement the  $\text{NH}/\text{NH}_2$  sites of the cation, is accessed with formation of antiparallel stack of the anions. The antialignment compensates polarities of the individual chains. Dense packing of the chains is indicated by a set of very short contacts between  $\text{NO}_2$  groups (**Table 1**), which are comparable with shortest reported contact of that type (2.80 Å) in the structure of the highly explosive heptanitrocubane.<sup>[28]</sup> However, the resulting dense layers of the anions are separated by ca. 11.3 Å, while intercalating strips of hydrogen bonded cations (**Fig. 6**). Such strips are actually fragments of 1D H-bonded connectivity seen in the structure of the parent free base,<sup>[29]</sup> and in this sense **15** is a hybrid collecting some features of both components.

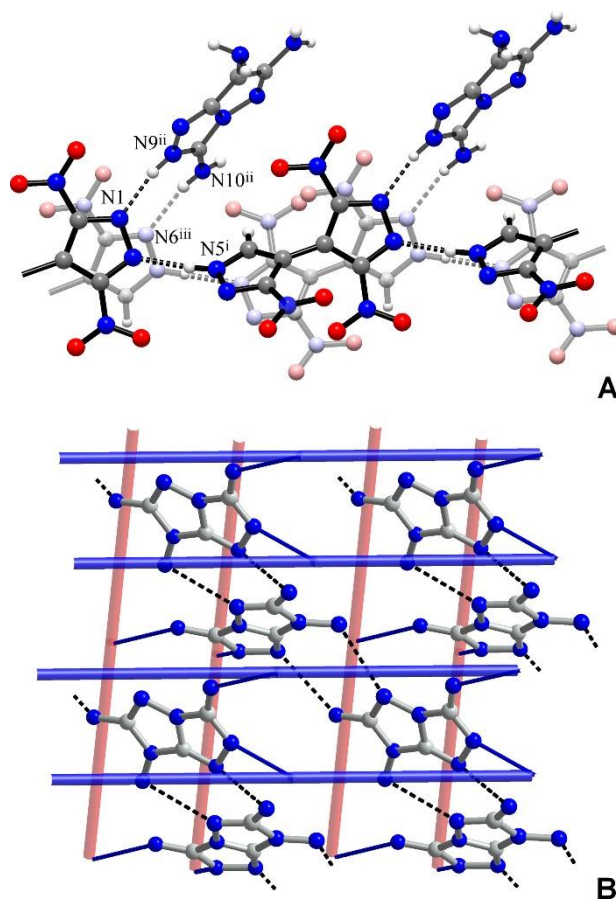


**Figure 6.** (A) Cross-linking of antiparallel anionic chains in the structure of **15**. (B) Two layers of anionic chains (indicated in blue and red), running in mutually orthogonal directions, are connected through 1D strips of hydrogen bonded cations.

**On a Midway Between Energetic Molecular Crystals and High-Density Energetic Salts:  
Crystal Engineering with Hydrogen Bonding Chains of Polynitro Bipyrzoles**

The polar chains of singly charged (TNbpz)<sup>−</sup> anions in **17** are cross-linked by NH<sub>3</sub>OH<sup>+</sup> cations into polar nets, which are topologically identical to the nets in trinitro analog **11** (**Fig. 7**). The bonding preferences of the ionic counterparts are unaltered since the strong OH⋯N bonds, to the same kind of dinitropyrazolate acceptor, are actually invariant [O⋯N = 2.6909(18) and 2.7202(17) Å, respectively]. This similarity, however, does not shed rather appreciable impact of fourth NO<sub>2</sub> group: the primary pzH⋯pz bonds are stronger (**Table 1**) and NH⋯N bonds of NH<sub>3</sub>OH<sup>+</sup> cations to weakly basic dinitropyrazole are much weaker (N⋯N = 3.081(2) and 2.8879(19) Å for **17** and **11**, respectively). With loss of CH⋯O bonding seen in **11**, the anionic layer collapses to give dense stack of chains. The cations are extruded to the interlayer space and produce own 1D subtopologies in the form of polar chains [N⋯O = 3.241(3) Å, see **Fig. 7**], running above and below the anionic layer. These chains unite NH<sub>3</sub>OH<sup>+</sup> from two successive layers and thus polarity of every next layer is identical.

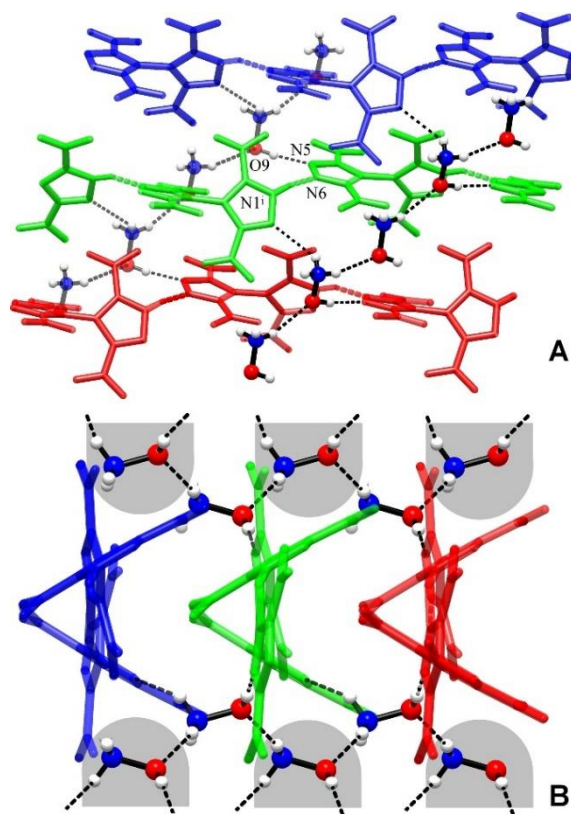


**Figure 7.** (A) Primary bonding in structure of **17**: Dense stack of polar anionic chains (individual chains are marked in red, green and blue) those are linked through polar chains of NH<sub>3</sub>OH<sup>+</sup> cations.



**On a Midway Between Energetic Molecular Crystals and High-Density Energetic Salts:  
Crystal Engineering with Hydrogen Bonding Chains of Polynitro Bipyrazoles**

(B) Side-view of the stack; grey background indicates  $\text{NH}_3\text{OH}^+$  moieties corresponding to the neighboring symmetry-related stacks.

Such extension of the structure in a second dimension, when combining anionic pyrazolate with cationic chains (*e.g.* chains of  $\text{N}_2\text{H}_5^+$  in **6** or  $\text{NH}_3\text{OH}^+$  in **17**) may be achieved even in a more predictable manner. A closer match of two kinds of chains, in the view of metrics and H-bond donor/acceptor functionality, is important. Therefore, the “mixed bipyrazole” structure of **18** is especially illustrative. Unlike formation of two-component  $(\text{Hbipy})^+/(\text{DiNBpz})^-$  chains in **8**, combination of acidic tetranitrobipyrazole and basic tetramethylbipyrazole yields two sorts of polar chains sustained by identical moieties only, namely singly charged  $(\text{TNBpz})^-$  anions or  $(\text{HMe}_4\text{Bpz})^+$  cations (**Fig. 8**). Such polar cationic chains are known for 4,4'-bipyrazole itself,<sup>[30]</sup> and different organic salts of tetramethylbipyrazole.<sup>[31]</sup> Hydrogen bonding of two kinds of conjugate acidic and basic sites (*i.e.* pyrazole/pyrazolate and pyrazole/pyrazolium) is equally strong and it is comparable in geometry [ $\text{N}\cdots\text{N} = 2.7618(19)$  and  $2.7776(19)$  Å, respectively]. The anionic and cationic chains are metrically equivalent (translation periods are 8.57 Å). This facilitates their connection into Lincoln-log bilayers, with third kind of strong  $\text{NH}\cdots\text{N}$  bonds [ $\text{N}\cdots\text{N} = 2.823(2)$  Å] established between the pyrazolium and pyrazolate sites (**Fig. 8**). Very weak acceptor properties of dinitropyrazole-N atom (*cf.* weakness of the corresponding  $\text{NH}\cdots\text{N}$  bonds in **17**) preclude further aggregation of the bilayers into the 3D framework.

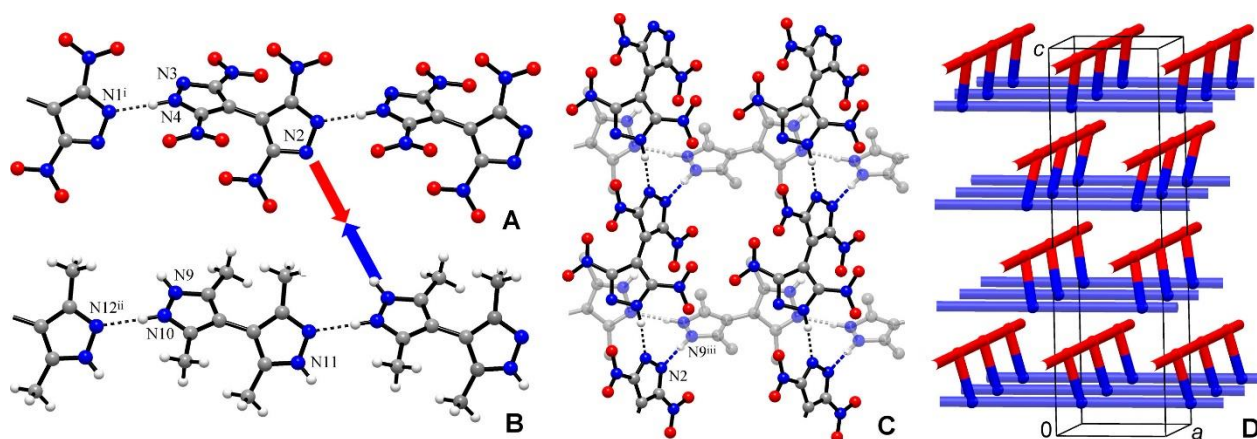


**Figure 8.** Two kinds of polar anionic pyrazolate (A) and cationic pyrazolium (B) chains in the structure of **18**· $\text{H}_2\text{O}$ . Their linkage (C), via the strongest H-bond donor and acceptor sites available

## On a Midway Between Energetic Molecular Crystals and High-Density Energetic Salts: Crystal Engineering with Hydrogen Bonding Chains of Polynitro Bipyrazoles

[N9-H and N2], with generation of Lincoln-log bilayeres (D). Anionic and cationic chains are presented in red and blue, respectively. Weaker pyrazole donor N11-H establishes bond to the water molecule [ $\text{N}\cdots\text{O} = 2.814(2) \text{ \AA}$ ].

### 8.2.3. Toxicity assessment

The aquatic toxicity of the nitrated bipyrazole **4** was determined using bioluminescent gram-negative *Vibrio fischeri* NRRL-B-11177 bacteria strains, which naturally are found in the seas. The measurements were carried out according to DIN/EN/ISO 11348 (without G1 level), starting with the preparation of a solution of the compounds with a specific concentration in 2% NaCl stock solution and adjustment of the pH value to 6–8, followed by a dilution series ranging from the concentrated solution to 1:16.<sup>[32]</sup> For the measurements a LUMI-Stox 300 spectrometer obtained by HACH LANGE GmbH was used, furthermore a cooling block from the same supplier was used to ensure a test-temperature of  $15 \text{ }^{\circ}\text{C} \pm 0.3 \text{ }^{\circ}\text{C}$ . The bioluminescence of untreated reactivated *Vibrio fischeri* bacteria was determined first, after addition of the possible toxicant the bioluminescence is determined again after 15 and 30 minutes exposure time. At the concentration level where the bioluminescence is decreased by 50%, the effective concentration ( $\text{EC}_{50}$ ) is obtained. According to the  $\text{EC}_{50}$  value at 30 minutes a classification as non-toxic ( $> 1.00 \text{ g/L}$ ); toxic ( $0.10\text{--}1.00 \text{ g L}^{-1}$ ) and very toxic ( $< 0.10 \text{ g L}^{-1}$ ) was made.<sup>[33]</sup> The potassium salt **9** of the TriNBPz anion, hence is considered as not toxic ( $\text{EC}_{50} (15 \text{ min}) = 2.86 \text{ g L}^{-1}$ ;  $\text{EC}_{50} (30 \text{ min}) = 1.42 \text{ g L}^{-1}$ ). Compared to the common used secondary explosive RDX salt **9** is less toxic according to *Vibrio fischeri* bacteria ( $\text{EC}_{50} (15 \text{ min}) = 0.33 \text{ g L}^{-1}$ ;  $\text{EC}_{50} (30 \text{ min}) = 0.24 \text{ g L}^{-1}$ ).<sup>[33,34]</sup>

### 8.2.4. Physical and detonation properties

Derivatives of tri- and tetranitrobipyrazoles, which possess appropriate oxygen balance, can be already classified as energetic materials and therefore we have examined their energetic behavior. All theoretically and experimentally determined detonation properties for the investigated compounds are reported in **Table 2**. The thermal behavior of the selected compounds was determined with OZM Research DTA 552-Ex instrument at a heating rate of  $5 \text{ }^{\circ}\text{C min}^{-1}$  (**Fig. 9**). From all synthesized derivatives with the TriNBPz<sup>−</sup> anion the

**On a Midway Between Energetic Molecular Crystals and High-Density Energetic Salts:  
Crystal Engineering with Hydrogen Bonding Chains of Polynitro Bipyrzoles**

potassium (**9**·H<sub>2</sub>O,  $T_{dec.} = 333$  °C), the ammonium (**13**·H<sub>2</sub>O,  $T_{dec.} = 286$  °C) salts show the highest thermal stability, while hydrazinium salt **12** decomposes at 218 °C. Thermal stability of **9**·H<sub>2</sub>O is higher than that of parent **2** ( $T_{dec.} = 314$  °C). Comparison of the hydroxylammonium derivatives **11** ( $T_{dec.} = 230$  °C) and **17** ( $T_{dec.} = 201$  °C) shows that the TriNBpz<sup>−</sup> anion based salt exhibits better thermal stability.

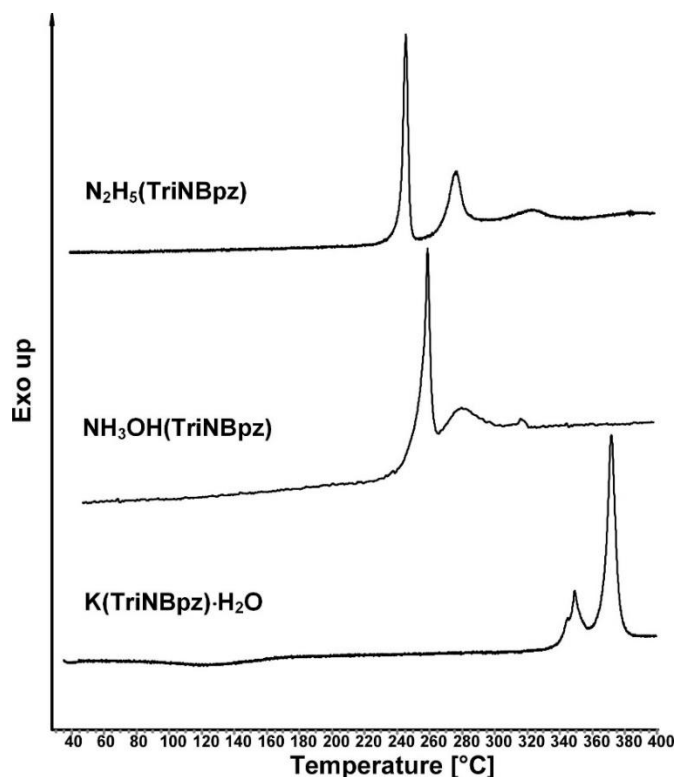


**Figure 9.** DTA Plots for potassium (**9**·H<sub>2</sub>O), hydroxylammonium (**11**) and hydrazinium (**12**) derivatives of (TriNBpz)<sup>−</sup>.

The lowest room temperature density for the TriNBpz<sup>−</sup> derivatives is 1.66 g cm<sup>−3</sup> for compound **15**. Relatively high density for salt **17** (1.81 g cm<sup>−3</sup>) approaches density of the parent H(TNBPz) (1.820 g cm<sup>−3</sup>). Experimentally determined sensitivities toward impact, friction and electrostatic discharge are also reported in Table 2. The determined sensitivities vary for impact from 2 to > 40 J, for friction from 216 to > 360 N and for electrostatic discharge from 0.10 J up to 1.50 J. The most impact sensitive material is the hydroxylammonium salt **17** with 2 J, which is below the value for H(TNBPz). The energetic materials **9** (7 J), **11** (10 J), **12** (15 J) and **15** (10 J) exhibit moderate impact sensitivity. In addition, the most synthesized derivatives exhibit low sensitivity toward friction. Only

**On a Midway Between Energetic Molecular Crystals and High-Density Energetic Salts:  
Crystal Engineering with Hydrogen Bonding Chains of Polynitro Bipyrazoles**

compound **17** show friction sensitivity with value of 216 N. Ammonium salt **13·H<sub>2</sub>O** is the most insensitive material, either toward impact (40 J), friction (> 360 N) or ESD (1.50 J) (**Table 2**). This case is particularly interesting since structures of **9·H<sub>2</sub>O**, **11**, **12** and **13·H<sub>2</sub>O** are very similar and therefore lower sensitivity of **13·H<sub>2</sub>O** may be, at least in part, associated with subtle features of the packing pattern. As stated above, evolution of **9·H<sub>2</sub>O**, **11** and **12** to **13·H<sub>2</sub>O** concerns mutual shift of hydrogen bonded layers and loss of stacking interactions between dinitropyrazolate groups (**Fig. 3**).



**On a Midway Between Energetic Molecular Crystals and High-Density Energetic Salts:  
Crystal Engineering with Hydrogen Bonding Chains of Polynitro Bipyrazoles**

**Table 2.** Physico-chemical properties of **9**, **11–13** and **15–16** compared to **2**, **3**<sup>[17]</sup> and HNS.<sup>[35]</sup>

	<b>9·H<sub>2</sub>O</b>	<b>11</b>	<b>12</b>	<b>13·H<sub>2</sub>O</b>	<b>15</b>	<b>17</b>	<b>2</b>	<b>3</b>	<b>HNS</b>
$IS^{[a]}$ [J]	7	10	15	40	10	2	20	4.5	5
$FS^{[b]}$ [N]	324	> 360	> 360	> 360	> 360	216	>360	192	240
$ESD^{[c]}$ [J]	0.10	0.50	0.55	1.50	0.20	0.25	0.50	0.30	0.80
$Q^{[d]}$ [%]	−38.8	−42.4	−50.5	−47.3	−62.4	−25.4	−44.6	−25.5	−67.6
$T_m^{[e]}$ [°C]	–	–	–	251	–	–	306	292	–
$T_{dec}^{[f]}$ [°C]	333	230	218	286	240	201	314	298	318
$\rho^{[g]}$ [g cm <sup>−3</sup> ]	1.84	1.76	1.75	1.68	1.66	1.81	1.855	1.820	1.74
$\Delta H^{o[h]}$ [kJ mol <sup>−1</sup> ]	−197.6	303.7	390.9	−50.4	740.7	295.7	224.9	227.8	78.2
EXPLO5 6.03 <sup>[36]</sup>									
$-_{\Delta E}U^{o[i]}$ [kJ kg <sup>−1</sup> ]	4258	5323	5082	4325	4341	5682	4821	5287	5142
$T_{C-J}^{[j]}$ [K]	3109	3720	3509	3119	3208	4041	3565	4054	3677
$p_{C-J}^{[k]}$ [kbar]	221	286	272	230	216	328	286	311	243
$D_{C-J}^{[l]}$ [m s <sup>−1</sup> ]	7384	8271	8223	7689	7563	8673	8256	8520	7612
$V_0^{[m]}$ [dm <sup>3</sup> kg <sup>−1</sup> ]	552	433	440	761	747	419	417	419	602

[a] Impact sensitivity (BAM drophammer, method 1 of 6); [b] friction sensitivity (BAM drophammer, method 1 of 6); [c] electrostatic discharge device (OZM research); [d] oxygen balance; [e] melting point (DTA,  $\beta = 5^\circ\text{C}\cdot\text{min}^{-1}$ ); [f] temperature of decomposition (DTA,  $\beta = 5^\circ\text{C}\cdot\text{min}^{-1}$ ); [g] density at 298 K; [h] standard molar enthalpy of formation; [i] detonation energy; [j] detonation temperature; [k] detonation pressure; [l] detonation velocity; [m] volume of detonation gases at standard temperature and pressure conditions.

For the most synthesized energetic materials positive standard molar enthalpies of formation were calculated, except for compounds **9·H<sub>2</sub>O** (−197.6 kJ mol<sup>−1</sup>) and **13·H<sub>2</sub>O** (−50.4 kJ mol<sup>−1</sup>). The highest calculated enthalpy of formation for a TriNBPz based derivative is 740.7 kJ mol<sup>−1</sup> (**15**). Using the room temperature densities (obtained from the

## On a Midway Between Energetic Molecular Crystals and High-Density Energetic Salts: Crystal Engineering with Hydrogen Bonding Chains of Polynitro Bipyrzoles

X-ray structures as described in the reference<sup>[37]</sup>) and the determined enthalpies of formation, several detonation properties were calculated by using the EXPLO5 code (6.03 Version).<sup>[36]</sup> The calculated values for the detonation energy ( $-_{\Delta E}U^{\circ}$ ) range from 4225 to 5682 kJ kg<sup>-1</sup> (for TNBPz<sup>-</sup> salt **17**). The latter salt is also the best performing compound regarding calculated detonation pressure ( $p_{C-J}$  = 328 kbar) and detonation velocity ( $D_{C-J}$  = 8673 m s<sup>-1</sup>), which are superior to the performance values of the parent H(TNBPz) (**Table 2**). From all characterized TriNBPz<sup>-</sup> based ionic derivatives compounds **11** ( $p_{C-J}$  = 286 kbar,  $D_{C-J}$  = 8271 m s<sup>-1</sup>) and **12** ( $p_{C-J}$  = 272 kbar,  $D_{C-J}$  = 8223 m s<sup>-1</sup>) exhibit the best performance values.

### 8.3. Conclusions

Our study extends strategies toward supramolecular synthesis of energetic materials, while establishing a useful link between molecular crystals and typical nitrogen-rich energetic salts. The reported ionic lattices still retain distinct organic/organic subtopologies related to the parent molecular compounds. Therefore, our approach supports engineering in a very rational way, by generation of low-dimensional self-assembly molecular building blocks and their subsequent extension to a variety of supramolecular motifs. It is worth noting that assembly of suitable building blocks, *e.g.* 1D polar chains in the present study, may be granted by inherent protolytic properties of common energetic molecules, without the needs for special functionalization. Currently we explore supramolecular synthesis and performance of layered energetic material based upon bipyrzole chains.

### 8.4. Experimental

#### 8.4.1. Crystallography

CCDC 1949728-1949741 contain the supplementary crystallographic data for this paper. These data can be obtained free of charge via [www.ccdc.cam.ac.uk/data\\_request/cif](http://www.ccdc.cam.ac.uk/data_request/cif), or by emailing [data\\_request@ccdc.cam.ac.uk](mailto:data_request@ccdc.cam.ac.uk), or by contacting The Cambridge Crystallographic Data Centre, 12, Union Road, Cambridge CB2 1EZ, UK; fax: +44 1223 336033.

## 8.5. Conflicts of interest

There are no conflicts to declare.

## 8.6. Acknowledgements

The financial support of this work by the Ludwig-Maximilian University of Munich (LMU), the Office of Naval Research (ONR) under grant no. ONR.N00014-16-1-2062 and the Strategic Environmental Research and Development Program (SERDP) under contact no. WP19-1287 are gratefully acknowledged. We thank Stefan Huber for his help with the sensitivity testing.

## 8.7. References

- [1] (a) S. R. Kennedy, C. R. Pulham, in *Co-crystals: Preparation, Characterization and Applications*, Monographs in Supramolecular Chemistry, The Royal Society of Chemistry, 2018, pp. 231-266; (b) J. Zhang and J. M. Shreeve, *CrystEngComm*, 2016, **18**, 6124-6133; (c) D. I. A. Millar, H. E. Maynard-Casely, D. R. Allan, A. S. Cumming, A. R. Lennie, A. J. Mackay, I. D. H. Oswald, C. C. Tang and C. R. Pulham, *CrystEngComm*, 2012, **14**, 3742-3749; (d) O. Bolton, L. R. Simke, P. F. Pagoria and A. J. Matzger, *Cryst. Growth Des.*, 2012, **12**, 4311-4314; (e) K. B. Landenberger and A. J. Matzger, *Cryst. Growth Des.*, 2010, **10**, 5341-5347.
- [2] H. Gao and J. M. Shreeve, *Chem. Rev.*, 2011, **111**, 7377-7436.
- [3] (a) C. Yang, C. Zhang, Z. Zheng, C. Jiang, J. Luo, Y. Du, B. Hu, C. Sun and K. O. Christe, *J. Am. Chem. Soc.* 2018, **140**, 16488-16494; (b) T. M. Klapötke, B. Krumm and C. C. Unger, *Inorg. Chem.* 2019, **58**, 2881-2887; (c) T. M. Klapötke, P. Mayer, C. M. Sabaté, J. M. Welch and N. Wiegand, *Inorg. Chem.*, 2008, **47**, 6014-6027; (d) T. M. Klapötke and C. M. Sabaté, *Chem. Mater.*, 2008, **20**, 1750-1763.
- [4] a) J. P. Agrawal, R. D. Hodgson, *Organic Chemistry of Explosives*, Wiley, New York, 2007. b) T. M. Klapötke, *Chemistry of High-Energy Materials*, 4th ed., De Gruyter, Berlin, 2017. c) M. H. Keshavarz, T. M. Klapötke, *Energetic Compounds: Methods for Prediction of Their Performance*, De Gruyter, Berlin, 2017. d) M. H. Keshavarz, T. M. Klapötke, *The Properties of Energetic Materials: Sensitivity, Physical and Thermodynamic Properties*, De Gruyter, Berlin, 2017.

**On a Midway Between Energetic Molecular Crystals and High-Density Energetic Salts:  
Crystal Engineering with Hydrogen Bonding Chains of Polynitro Bipyrazoles**

- [5] O. Bolton and A. J. Matzger, *Angew. Chem.*, 2011, **123**, 9122-9125.
- [6] C. B. Aakeröy, T. K. Wijethunga, J. Benton and J. Desper, *Chem. Commun.*, 2015, **51**, 2, 425-2428.
- [7] J. W. A. M. Janssen, C. C. Kruse, H. J. Koeners and C. L. Habraken, *J. Heterocycl. Chem.*, 1973, **10**, 1055-1058.
- [8] a) C. Zhang, X. Wang and H. Huang, *J. Am. Chem. Soc.*, 2008, **130**, 8359-8365. b) B. Tian, Y. Xiong, L. Chen and C. Zhang, *CrystEngComm*, 2018, **20**, 837-848.
- [9] J. Zhang, Q. Zhang, T. T. Vo, D. A. Parish and J. M. Shreeve, *J. Am. Chem. Soc.*, 2015, **137**, 1697-1704.
- [10] R. V. Kent, R. A. Wiscons, P. Sharon, D. Grinstein, A. A. Frimer and A. J. Matzger, *Cryst. Growth Des.*, 2018, **18**, 219-224.
- [11] C. B. Aakeröy, T. K. Wijethunga and J. Desper, *Chem. Eur. J.*, 2015, **21**, 11029-11037.
- [12] (a) T. Steiner, *Angew. Chem. Int. Ed.* 2002, **41**, 48-76; (b) J. M. A. Robinson, D. Philp, K. D. M. Harris and B. M. Kariuki, *New J. Chem.*, 2000, 24, 799-806; (c) W. F. Baitinger, P. von R. Schleyer, T. S. S. R. Murty and L. Robinson, *Tetrahedron*, 1964, **20**, 1635-1647.
- [13] A. F. Wells, *Structural Inorganic Chemistry*, 5<sup>th</sup> Ed., Clarendon Press, Oxford, 1986.
- [14] (a) K. V. Domasevitch, V. V. Ponomareva and E. B. Rusanov, *J. Chem. Soc. Dalton Trans.*, 1997, 1177-1180; (b) K. V. Domasevitch, V. V. Ponomareva, E. B. Rusanov, T. Gelbrich, J. Sieler and V. V. Skopenko, *Inorg. Chim. Acta*, 1998, **268**, 93-101.
- [15] (a) R. Lewczuk, *Propellants Explos. Pyrotech.*, 2018, **43**, 436-444; (b) L. Liu, Y. Zhang, S. Zhang and T. Fei, *J. Energ. Mater.*, 2015, **33**, 202-214.
- [16] Y. Tang, C. He, G. H. Imler, D. A. Parrish and J. M. Shreeve, *J. Mat. Chem. A*, 2018, **6**, 5136.
- [17] K. V. Domasevitch, I. Gospodinov, H. Krautscheid, T. M. Klapötke, J. Stiertorfer, *New J. Chem.*, 2019, **43**, 1305-1312.
- [18] Y. Li, Y. Shu, B. Wang, S. Zhang and L. Zhai, *RSC Adv.*, 2016, **6**, 84760-84768.
- [19] (a) A. A. Dippold, T. M. Klapötke and N. Winter, *Eur. J. Inorg. Chem.*, 2012, 3474-3484; (b) A. A. Dippold and T. M. Klapötke, *Chem. Eur. J.*, 2012, **18**, 16742-16753.
- [20] L. H. Finger, F. G. Schröder and J. Sundermeyer, *Z. Anorg. Allg. Chem.*, 2013, **639**, 1140-1153.

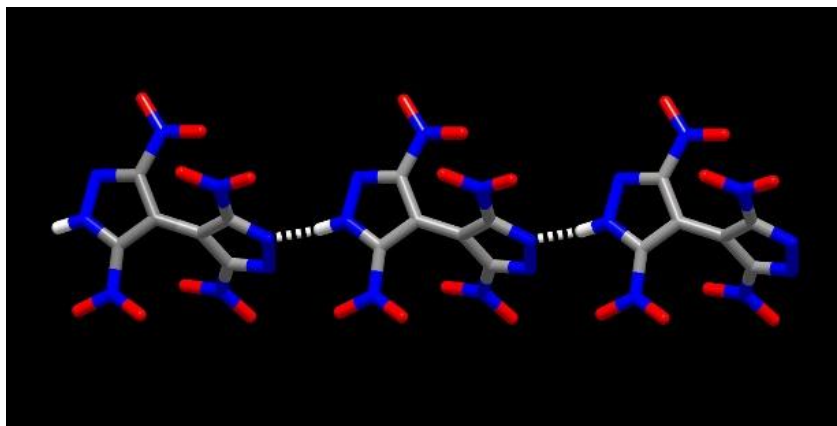
**On a Midway Between Energetic Molecular Crystals and High-Density Energetic Salts:  
Crystal Engineering with Hydrogen Bonding Chains of Polynitro Bipyrazoles**

- [21] A. Franconetti, A. Frontera and T. J. Mooibroek, *CrystEngComm*, 2019, **21**, DOI: 10.1039/C9CE01015G
- [22] (a) A. Bauzá, T. J. Mooibroek and A. Frontera, *Chem. Commun.*, 2015, **51**, 1491-1493; (b) A. Bauzá, A. V. Sharko, G. A. Senchyk, E. B. Rusanov, A. Frontera and K. V. Domasevitch, *CrystEngComm*, 2017, **19**, 1933-1937.
- [23] A. Gzella, U. Wrzeciono and T. Borowiak, *Acta Crystallogr., Sect.C: Cryst. Struct. Commun.*, 1989, **45**, 644.
- [24] (a) C. Yang, C. Zhang, Z. Zheng, C. Jiang, J. Luo, Y. Du, B. Hu, C. Sun and K. O. Christe, *J. Am. Chem. Soc.*, 2018, **140**, 16488; (b) N. Sasidharan, A. Sudheer Kumar and H.H. Hng, *Chem. Sci.*, 2018, **3**, 12544; (c) A. Hammerl, T. M. Klapotke, H. Noth, M. Warchhold, G. Holl, M. Kaiser and U. Ticmanis, *Inorg.Chem.*, 2001, **40**, 3570.
- [25] M. F. Bölter, A. Harter, T.M. Klapötke and J. Stierstorfer, *ChemPlusChem*, 2018, **83**, 804-811.
- [26] M. Lozinšek, *Acta Chim. Slov.*, 2015, **62**, 378–384.
- [27] (a) D. Fischer, T. M. Klapotke, M. Reymann and J. Stierstorfer, *Chem.-Eur. J.*, 2014, **20**, 6401; (b) T. M. Klapotke, C. M. Sabate and M. Rasp, *J. Mater. Chem.*, 2009, **19**, 2240.
- [28] M.-X. Zhang, P. E. Eaton and R. Gilardi, *Angew. Chem. Int. Ed.*, 2000, **39**, 401.
- [29] T. M. Klapötke, P.C. Schmid, S. Schnell and J. Stierstorfer, *Chem. Eur. J.*, 2015, **21**, 9219-9228.
- [30] K. V. Domasevitch and I. Boldog, *Acta Crystallogr., Sect. C: Cryst. Struct. Commun.*, 2005, **61**, o373-o376.
- [31] (a) U. P. Singh, N. Goel, G. Singh and P. Srivastava, *Supramol. Chem.*, 2012, **24**, 285; (b) U. P. Singh, K. Tomar, S. Kashyap and P. Verma, *J. Chem. Cryst.*, 2017, **47**, 69.
- [32] Wasserbeschaffenheit - Bestimmung der Hemmwirkung von Wasserproben auf die Lichtemission von *Vibrio Fischeri* (Leuchtbakterientest). In *Wasserbeschaffenheit - Bestimmung der Hemmwirkung von Wasserproben auf die Lichtemission von Vibrio Fischeri (Leuchtbakterientest)*, 2009; Vol. DIN EN ISO 11348-2.
- [33] C. J. Cao, M. S. Johnson, M. M. Hurley, T. M. Klapötke, *J. Propuls. Energet.* **2012**, **5**, 41–51.
- [34] D. Fischer, T. M. Klapötke, M. Reymann, J. Stierstorfer, *Chem. - Eur. J.* **2014**, **20**, 6401–6411.

## On a Midway Between Energetic Molecular Crystals and High-Density Energetic Salts: Crystal Engineering with Hydrogen Bonding Chains of Polynitro Bipyrroles

- [35] a) T. M. Klapötke and T. G. Witkowski, *ChemPlusChem*, 2016, **81**, 357. b) Klapötke, T. M. *Energetic Materials Encyclopedia*, de Gruyter, Berlin / Boston, **2018**.
- [36] M. Sućeska, *EXPLO5 Version 6.03 User's Guide*, Zagreb, Croatia: OZM; 2015.
- [37] J. S. Murray and P. Politzer, *J. Mol. Model.* 2014, **20**, 2223.

### 8.8. Supporting Information



#### 8.8.1. General Information

$^1\text{H}$ ,  $^{13}\text{C}$ ,  $^{14}\text{N}$  and  $^{15}\text{N}$  NMR spectra were recorded on JEOL 270 and BRUKER AMX 400 instruments. The samples were measured at room temperature in standard NMR tubes ( $\varnothing$  5 mm). Chemical shifts are reported as  $\delta$  values in ppm relative to the residual solvent peaks of  $d_6$ -DMSO ( $\delta$  H: 2.50,  $\delta$  C: 39.5). Solvent residual signals and chemical shifts for NMR solvents were referenced against tetramethylsilane (TMS,  $\delta$  = 0 ppm) and nitromethane. Unless stated otherwise, coupling constants were reported in hertz (Hz) and for the characterization of the observed signal multiplicities the following abbreviations were used: s (singlet), d (doublet), t (triplet), m (multiplet) and br (broad). Low resolution mass spectra were recorded on a JEOL JMS-700 MStation mass spectrometer (EI+/DEI+). Infrared spectra (IR) were recorded from  $4500\text{ cm}^{-1}$  to  $650\text{ cm}^{-1}$  on a PERKIN ELMER Spectrum BX-59343 instrument with SMITHS DETECTION DuraSamplIR II Diamond ATR sensor. The absorption bands are reported in wavenumbers ( $\text{cm}^{-1}$ ). Elemental analysis was carried out by the department's internal micro analytical laboratory on a Elementar Vario el by pyrolysis of the sample and subsequent analysis of the formed gases. Decomposition temperatures were measured via differential thermal analysis (DTA) with an OZM Research DTA 552-Ex instrument at a heating rate of  $5\text{ }^{\circ}\text{C min}^{-1}$  and in a range of room

## On a Midway Between Energetic Molecular Crystals and High-Density Energetic Salts: Crystal Engineering with Hydrogen Bonding Chains of Polynitro Bipyrazoles

temperature to 400 °C. All sensitivities toward impact (IS) and friction (FS) were determined according to BAM (German: Bundesanstalt für Materialforschung und -prüfung) standards using a BAM drop hammer and a BAM friction apparatus. All energetic compounds were tested for sensitivity towards electrical discharge using an Electric Spark Tester ESD 2010 EN.

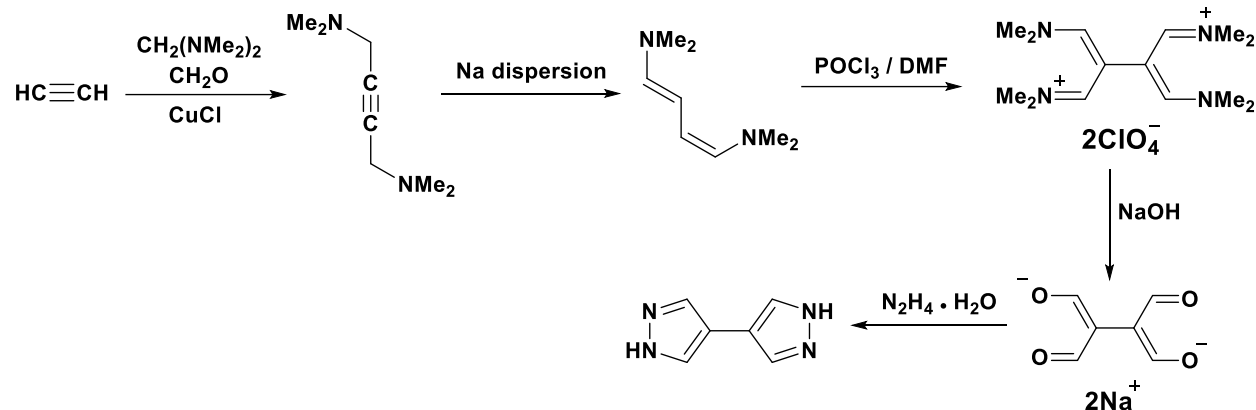
### 8.8.2. Synthesis

**CAUTION!** All investigated compounds are potentially explosive materials, although no hazards were observed during preparation and handling these compounds. Nevertheless, safety precautions (such as wearing leather coat, face shield, Kevlar sleeves, Kevlar gloves, earthed equipment and ear plugs) should be drawn.

#### 8.8.2.1. 4,4'-Bipyrazole and its nitroderivatives

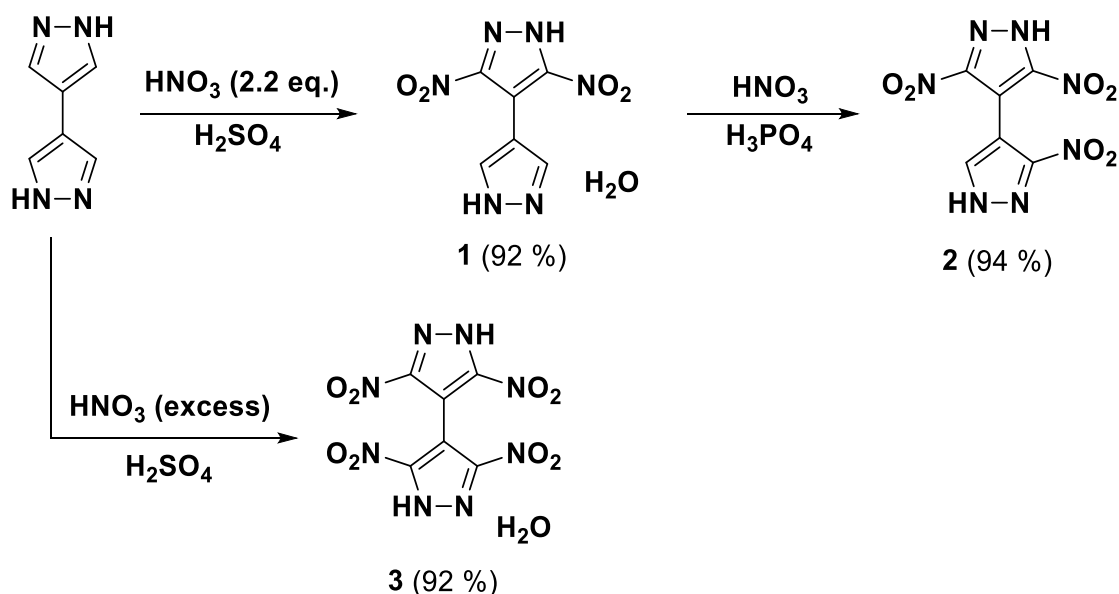
The synthesis of starting 4,4'-bipyrazole was performed by compilation of the literature known methods (**Scheme S1**).<sup>[S1-S6]</sup> 1,4-Bis(dimethylamino)-*cis-trans*-butadiene undergoes standard Vilsmeier-Haack-Arnold formylation to give symmetric *bis*-vinamidinium salt (isolated and purified as perchlorate salt).<sup>[S6]</sup> The latter was hydrolyzed to *bis*-dialdehyde and then converted into the desired 4,4'-bipyrazole. Key intermediate of the synthesis, 1,4-*bis*(dimethylamino)-2-butyne, may be prepared by a two-stage reaction sequence starting with inexpensive industrial product 2-butyne-1,4-diole. Its reactions with SOCl<sub>2</sub><sup>[S2]</sup> or POCl<sub>3</sub><sup>[S3]</sup> yield 1,4-dichloro-2-butyne, which undergoes amination by action of excess dimethylamine in benzene solution.<sup>[S4]</sup> This method was not sufficient for large scale preparations. Alternative synthesis of 1,4-*bis*(dimethylamino)-2-butyne was based upon direct aminomethylation of acetylene, as reported by Fegley *et al.*<sup>[S5]</sup> Main disadvantages of this attractive method concern handling of compressed acetylene gas as well as extra pressure applied during the reaction. In our work, we have found that extra pressure is not required for the synthesis and acetylene may be conveniently generated using industrial product calcium carbide. This allowed us to improve the preparation of 1,4-*bis*(dimethylamino)-2-butyne, making it accessible in a kilogram scale by very simple procedure denoted below.

**On a Midway Between Energetic Molecular Crystals and High-Density Energetic Salts:  
Crystal Engineering with Hydrogen Bonding Chains of Polynitro Bipyrazoles**



**Scheme S1.** Synthesis of 4,4'-bipyrazole.

Three nitrosubstituted 4,4'-bipyrazoles used in the present work were synthesized by nitration of 4,4'-bipyrazole in mixed acid, following previously published procedures (Scheme S2).<sup>[S7]</sup> Recently, we have found that all five possible C-nitro derivatives of 4,4'-bipyrazole may be



**Scheme S2.** Synthesis of 3,5-dinitro-4,4'-bipyrazole (**1**), 3,5,3'-trinitro-4,4'-bipyrazole (**2**) and 3,5,3',5'-tetranitro-4,4'-bipyrazole (**3**).

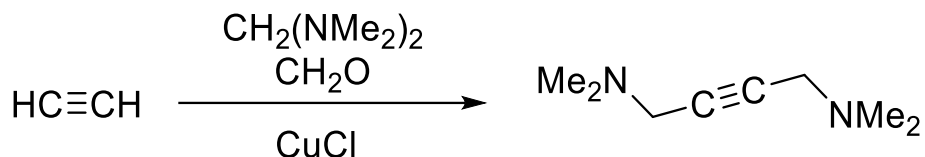
prepared selectively and in high yields.<sup>[S7]</sup> In particular, 3,5-dinitro-4,4'-bipyrazole (**1**) is a sole product of nitration in mixed acid (100°C) when 2.2 eq of  $\text{HNO}_3$  is used. With excess of  $\text{HNO}_3$  (8 eq.), 3,5,3',5'-tetranitro-4,4'-bipyrazole (**3**) was isolated in high yield under the same conditions.



**On a Midway Between Energetic Molecular Crystals and High-Density Energetic Salts:  
Crystal Engineering with Hydrogen Bonding Chains of Polynitro Bipyrazoles**

3,5,3'-Trinitro-4,4'-bipyrazole (**2**) was prepared also selectively, by nitration of **1** in the media of 80% H<sub>3</sub>PO<sub>4</sub>.

**8.8.2.2. Improved synthesis of 1,4-bis(dimethylamino)-2-butyne**



**Scheme S3.** Improved synthesis for 1,4-bis(dimethylamino)-2-butyne.

780 mL of 37% aqueous formaldehyde solution ( $d = 1.09 \text{ g cm}^{-3}$ ; 850 g) was added dropwise to stirred and water-cooled net 1200 mL bis(dimethylamino)methane (900 g) [**Note 1**]. Heat effect of the reaction is very small and therefore the addition was completed within 1 h. The mixture was stirred for 30 min and then it was divided into three portions by weights of 700, 600 and 450 g, which were transferred into three 1 L reaction flasks. To these three portions of the mixture, respectively, 15.0 g, 12.8 g and 9.6 g portions of copper(I) chloride [**Note 2**] were added at once with stirring. These three flasks were connected successively, in decreasing weight of the reaction mixture. For the first two flasks, the gas outlet, through the Dimroth reflux condenser, led to the gas inlet of the next flask. Medium to fast stream of acetylene gas (about 1.0 to 1.5 moles per hour) was passed through the well-stirred mixtures for 7 h [**Note 3**], with the occasional water-cooling to maintain temperature below 40° C. Nearly complete absorption of acetylene was observed when passed through the present battery of three flasks. After 7 h, the temperature of the reaction mixtures slowly decreased. At this moment, the reaction mixtures were heated to 40-45 ° C, and passing of acetylene gas was continued for additional 3 h. During course of the reaction, color of the mixtures changed from orange-red to crimson-red.

The reaction mixtures were left overnight at r.t. and then red copper catalyst was filtered and discarded. To the ice-cooled filtrate, solid NaOH was added in portions, as long as it dissolves (1.2 kg). The undissolved NaOH was filtered. The organic phase was separated and dried over NaOH pellets for 2 d at 5° C. After separation of NaOH, the resulting clear light-yellow colored liquid was distilled in vacuum. Any volatiles were removed at 200 mbar and bath temperature of 110-120° C. Then the bath temperature was decreased and the reaction product distilled at 73-74 °C/ 19 mbar or 86-87 ° C / 35 mbar. Yield: 1037 g (84 %).

On a Midway Between Energetic Molecular Crystals and High-Density Energetic Salts:  
Crystal Engineering with Hydrogen Bonding Chains of Polynitro Bipyrazoles

NMR  $^{13}\text{C}$  ( $\text{CDCl}_3$ ,  $\delta$ , ppm): 42.63, 42.96, 78.80.



**Figure S1.** Synthesis of 1,4-*bis*(dimethylamino)-2-butyne, showing two of three connected flasks, with red-colored reaction mixtures.

**Note 1.** *bis*(Dimethylamino)methane was prepared reacting 37% aqueous formaldehyde and 38% aqueous dimethylamine solution.<sup>[S8]</sup>

**Note 2.** Copper(I) chloride was freshly prepared as colorless crystalline powder. However, old green-colored sample of CuCl served equally well due to the fast reduction of Cu(II) ions in the reaction medium.

**Note 3.** Acetylene gas was generated by adding pieces of industrial calcium carbide to large volume of saturated NaCl solution, with external ice-water cooling. Sufficient purification of the gas was achieved by passing it through solution of CuCl<sub>2</sub>, FeCl<sub>3</sub> and HCl (5:1:1 v/v mixture of 30% aqueous solutions), then through conc. H<sub>2</sub>SO<sub>4</sub> and finally through short column with KOH pellets.

### 8.8.2.3. Salts of 3,5-dinitro-, 3,5,3'-trinitro- and 3,5,3',5'-tetranitro-4,4'-bipyrazoles

#### Potassium and caesium 4-(pyrazol-4-yl)-3,5-dinitropyrazolates monohydrates (4·H<sub>2</sub>O and 5·H<sub>2</sub>O)

3,5-Dinitro-4,4'-bipyrazole **1** (448 mg, 2.00 mmol) and K<sub>2</sub>CO<sub>3</sub> (139 mg, 1.00 mmol) were dissolved in 10 mL water with stirring and heating to 70–80 °C. Yellow solution was cooled to r.t. and thin needle-like light-yellow crystals of the product **4·H<sub>2</sub>O** were filtered and dried in air. Yield: 432 mg (77 %). Salt **5·H<sub>2</sub>O**, light-yellow needles, was prepared similarly in 83 % yield, reacting **1** (448 mg, 2.00 mmol) and Cs<sub>2</sub>CO<sub>3</sub> (326 mg, 1.00 mmol).

DTA (5 °C min<sup>-1</sup>): 120 (H<sub>2</sub>O), 269 (melt.), 299 °C (exo.); BAM: drop hammer: 30 J (100–500 μm); friction tester: > 360 N (100–500 μm); ESD: 0.75 J (100–500 μm). IR (ATR),  $\tilde{\nu}$  (cm<sup>-1</sup>) = 3545 (m), 3162 (br), 2949 (w), 1602 (m), 1530 (w), 1497 (w), 1468 (s), 1393 (s), 1331 (vs), 1291 (s), 1267 (s), 1222 (m), 1159 (m), 1034 (m), 1011 (m), 932 (s), 876 (m), 845 (s), 766 (m). <sup>1</sup>H NMR (*d*<sub>6</sub>-DMSO, 400 MHz, ppm)  $\delta$  = 12.84 (s, 1H), 7.87 (s, 1H), 7.57 (s, 1H). <sup>13</sup>C NMR (*d*<sub>6</sub>-DMSO, 101 MHz, ppm)  $\delta$  = 154.1, 140.1, 129.4, 108.4, 105.4. <sup>14</sup>N NMR (*d*<sub>6</sub>-DMSO, 29 MHz, ppm)  $\delta$  = -16. Elem. Anal. (C<sub>6</sub>H<sub>6</sub>KN<sub>6</sub>O<sub>5</sub>, 280.24 g mol<sup>-1</sup>) calcd.: C 25.71, H 1.80, N 29.99 %. Found: C 25.92, H 2.02, N 29.71 %.

DTA (5 °C min<sup>-1</sup>): 87 (H<sub>2</sub>O), 337 (melt.), 241 °C (exo.); BAM: drop hammer: 30 J (100–500 μm); friction tester: > 360 N (100–500 μm); ESD: 0.84 J (100–500 μm). IR (ATR),  $\tilde{\nu}$  (cm<sup>-1</sup>) = 3378 (br), 2779 (vw), 1681 (w), 1605 (m), 1504 (m), 1475 (s), 1391 (s), 1322 (vs), 1288 (s), 1265 (m), 1222 (m), 1143 (m), 1027 (m), 941 (s), 908 (s), 847 (s). <sup>1</sup>H NMR (*d*<sub>6</sub>-DMSO, 400 MHz, ppm)  $\delta$  = 12.84 (s, 1H), 7.87 (s, 1H), 7.57 (s, 1H). <sup>13</sup>C NMR (*d*<sub>6</sub>-DMSO, 101 MHz, ppm)  $\delta$  = 154.1, 140.1, 129.4, 108.4, 105.4. <sup>14</sup>N NMR (*d*<sub>6</sub>-DMSO, 29 MHz, ppm)  $\delta$  = -15. Elem. Anal. (C<sub>6</sub>H<sub>6</sub>CsN<sub>6</sub>O<sub>5</sub>, 374.05 g mol<sup>-1</sup>) calcd.: C 19.26, H 1.35, N 22.47 %. Found: C 19.37, H 1.25, N 22.60 %.

#### Hydrazinium 4-(pyrazol-4-yl)-3,5-dinitropyrazolate (**6**)

Hydrazine hydrate (100 μL, 2.06 mmol) was added to the suspension of **1** (448 mg, 2.00 mmol) in 10 mL water and the mixture was stirred and heated to 70–80 °C until total dissolution of the starting material was observed. After cooling to r.t., yellow crystals of the product (359 mg, 70 %) were collected and dried in air.

**On a Midway Between Energetic Molecular Crystals and High-Density Energetic Salts:  
Crystal Engineering with Hydrogen Bonding Chains of Polynitro Bipyrazoles**

DTA (5 °C min<sup>-1</sup>): 250 °C (exo.); BAM: drop hammer: 8 J (100–500 μm); friction tester: > 360 N (100–500 μm); ESD: 0.48 J (100–500 μm). IR (ATR),  $\tilde{\nu}$  (cm<sup>-1</sup>) = 3353 (m), 3298 (w), 3122 (vw), 2952 (vw), 1657 (vw), 1622 (w), 1601 (m), 1538 (w), 1477 (s), 1389 (s), 1322 (vs), 1295 (s), 1268 (s), 1224 (m), 1159 (m), 1093 (s), 1039 (m), 1008 (m), 967 (m), 939 (s), 879 (m), 843 (s), 806 (m). <sup>1</sup>H NMR (*d*<sub>6</sub>-DMSO, 400 MHz, ppm)  $\delta$  = 7.72 (s), 7.23 (br). <sup>13</sup>C NMR (*d*<sub>6</sub>-DMSO, 101 MHz, ppm)  $\delta$  = 154.1, 135.2 (br), 108.4, 105.4. <sup>14</sup>N NMR (*d*<sub>6</sub>-DMSO, 29 MHz, ppm)  $\delta$  = -16. Elem. Anal. (C<sub>6</sub>H<sub>8</sub>N<sub>8</sub>O<sub>4</sub>, 256.18 g mol<sup>-1</sup>) calcd.: C 28.13, H 3.15, N 43.75 %. Found: C 28.29, H 3.08, N 43.52%.

**Ammonium 4-(pyrazol-4-yl)-3,5-dinitropyrizolate monohydrate (7·H<sub>2</sub>O)**

3,5-Dinitro-4,4'-bipyrazole **1** (448 mg, 2.00 mmol) was dissolved at 70-80 °C in 10 mL water containing 1 mL of 25 % aqueous ammonia solution (excess). After cooling to r.t., yellow cotton-like crystalline deposit of **7·H<sub>2</sub>O** (342 mg, 66 %) was filtered and dried in air.

Anal. Calcd for C<sub>6</sub>H<sub>9</sub>N<sub>7</sub>O<sub>5</sub>: C 27.80, H 3.50, N 37.84 %. Found: C 28.01, H 3.47, N 37.71%.

**4-(Pyridine-4-yl)pyridinium 4-(pyrazol-4-yl)-3,5-dinitropyrizolate (8)**

3,5-Dinitro-4,4'-bipyrazole **1** (67 mg, 0.30 mmol) and 4,4'-bipyridine (55 mg, 0.35 mmol) were dissolved in 10 mL water. Yellow crystals of **8** (51 mg, 45 %) were obtained by slow evaporation of the solution to a half-volume.

Anal. Calcd for C<sub>16</sub>H<sub>12</sub>N<sub>8</sub>O<sub>4</sub>: C 50.52, H 3.18, N 29.47 %. Found: C 50.29, H 3.16, N 29.26 %.

**Potassium and caesium 4-(3-nitropyrazol-4-yl)-3,5-dinitropyrizolate monohydrates (9·H<sub>2</sub>O and 10·H<sub>2</sub>O)**

3,3',5-Trinitro-4,4'-bipyrazole (539 mg, 2.00 mmol) was solved in ethanol (20 mL) and potassium carbonate (139 mg, 1.0 mmol, 0.5 eq.) dissolved in water (5 mL) was added. The resulting solution was heated to 75 °C for 30 min. After cooling the solvent was removed in vacuo and the obtained solid was dried on air to yield compound **9·H<sub>2</sub>O** as yellow solid (613 mg, 1.89 mmol, 95 %). **10·H<sub>2</sub>O**, yellow prisms, was prepared similarly, reacting **2** (539 mg, 2.00 mmol) and Cs<sub>2</sub>CO<sub>3</sub> (326 mg, 1.00 mmol).

**On a Midway Between Energetic Molecular Crystals and High-Density Energetic Salts:  
Crystal Engineering with Hydrogen Bonding Chains of Polynitro Bipyrazoles**

**9·H<sub>2</sub>O:** DTA (5 °C min<sup>-1</sup>): 333 °C (exo.); BAM: drop hammer: 7 J (100–500 μm); friction tester: 324 N (100–500 μm); ESD: 0.10 J (100–500 μm). IR (ATR),  $\nu$  (cm<sup>-1</sup>) = 3662 (m), 3139 (w), 2799 (w), 1552 (w), 1532 (m), 2486 (s), 1377 (s), 1332 (vs), 1230 (s), 1098 (m), 1016 (m), 993 (m), 851 (s), 834 (s), 819 (s), 769 (m); <sup>1</sup>H NMR (*d*<sub>6</sub>-DMSO, 400 MHz, ppm)  $\delta$  = 14.00 (s), 8.11 (s), 7.00 (br). <sup>13</sup>C NMR (*d*<sub>6</sub>-DMSO, 101 MHz, ppm)  $\delta$  = 154.1, 153.5, 133.2, 106.8, 102.0. <sup>14</sup>N NMR (*d*<sub>6</sub>-DMSO, 29 MHz, ppm)  $\delta$  = -15. Elem. Anal. (C<sub>6</sub>H<sub>4</sub>KN<sub>7</sub>O<sub>7</sub>, 325.24 g mol<sup>-1</sup>) calcd.: C 22.16, H 1.24, N 30.15 %. Found: C 22.24, H 1.25, N 30.03 %.

**10·H<sub>2</sub>O:** Anal. Calcd for C<sub>6</sub>H<sub>4</sub>CsN<sub>7</sub>O<sub>7</sub>: C 17.20, H 0.96, N 23.40 %. Found: C 17.02, H 1.08, N 23.28 %.

**Hydroxylammonium 4-(3-nitropyrazol-4-yl)-3,5-dinitropyrzolate (11)**

A solution of **2** (404 mg, 1.50 mmol, 1.0 eq.) in 20 mL ethanol was heated to 75 °C and aqueous hydroxylamine solution (250 mg, 3.78 mmol) was added. Filtration and removing the solvent at room temperature results the product as yellow crystals (420 mg, 1.39 mmol, 93 %).

DTA (5 °C min<sup>-1</sup>): 230 °C (exo.); BAM: drop hammer: 10 J (100–500 μm); friction tester: >360 N (100–500 μm); ESD: 0.50 J (100–500 μm). IR (ATR),  $\nu$  (cm<sup>-1</sup>) = 3189 (w), 3118 (w), 3823 (m), 2688 (m), 1742 (vw), 1611 (w), 1521 (m), 1489 (s), 1420 (m), 1385 (s), 1338 (vs), 1306 (s), 1199 (m), 1107 (m), 1022 (w), 998 (s), 936 (w), 906 (w), 854 (s), 835 (s), 820 (s), 768 (m), 672 (w), 626 (m), 589 (w), 552 (w), 524 (vw). <sup>1</sup>H NMR (*d*<sub>6</sub>-DMSO, 400 MHz, ppm)  $\delta$  = 13.77 (br), 10.02 (br), 8.11 (s). <sup>13</sup>C NMR (*d*<sub>6</sub>-DMSO, 101 MHz, ppm)  $\delta$  = 154.0, 153.4, 133.2, 106.8, 102.0. <sup>14</sup>N NMR (*d*<sub>6</sub>-DMSO, 29 MHz, ppm)  $\delta$  = -17. Elem. Anal. (C<sub>6</sub>H<sub>6</sub>N<sub>8</sub>O<sub>7</sub>, 302.16 g mol<sup>-1</sup>) calcd.: C 23.85, H 2.00, N 37.08 %. Found: C 24.00, H 2.08, N 36.84 %.

**Hydrazinium 4-(3-nitropyrazol-4-yl)-3,5-dinitropyrzolate (12)**

3,3',5-Trinitro-4,4'-bipyrazole (404 mg, 1.50 mmol) was dissolved in 20 mL of ethanol. The solution was heated to 75 °C and hydrazine hydrate (160 mg, 3.20 mmol) was added. Filtration and removing the solvent at room temperature results the product as yellow crystals (426 mg, 1.41 mmol, 94 %).

DTA (5 °C min<sup>-1</sup>): 218 °C (exo.); BAM: drop hammer: 15 J (100–500 μm); friction tester: >360 N (100–500 μm); ESD: 0.55 J (100–500 μm). IR (ATR),  $\nu$  (cm<sup>-1</sup>) = 3349 (w), 3154 (m), 2799 (m),

**On a Midway Between Energetic Molecular Crystals and High-Density Energetic Salts:  
Crystal Engineering with Hydrogen Bonding Chains of Polynitro Bipyrazoles**

2685 (m), 2596 (m), 1597 (w), 1520 (m), 1487 (s), 1374 (s), 1329 (vs), 1301 (m), 1192 (m), 1089 (s), 1017 (m), 993 (m), 929 (m), 854 (s), 834 (s), 819 (s), 768 (m), 703 (m), 671 (m), 629 (m), 589 (m), 551 (w).  $^1\text{H}$  NMR ( $d_6$ -DMSO, 400 MHz, ppm)  $\delta$  = 8.07 (s), 4.54 (br).  $^{13}\text{C}$  NMR ( $d_6$ -DMSO, 101 MHz, ppm)  $\delta$  = 154.1, 153.5, 133.5, 106.8, 102.2, 99.6.  $^{14}\text{N}$  NMR ( $d_6$ -DMSO, 29 MHz, ppm)  $\delta$  = -15. Elem. Anal. ( $\text{C}_6\text{H}_7\text{N}_9\text{O}_6$ , 301.18 g mol $^{-1}$ ) calcd.: C 23.93, H 2.34, N 41.86 %. Found: C 24.13, H 2.56, N 41.49 %.

**Ammonium 4-(3-nitropyrazol-4-yl)-3,5-dinitropyrizolate monohydrate (13·H<sub>2</sub>O)**

To a solution of **2** (404 mg, 1.50 mmol) in ethanol (20 mL) heated to 75 °C, ammonium carbonate (144 mg, 1.50 mmol) was added. Filtration and removing the solvent at room temperature results the product as yellow crystals (432 mg, 1.42 mmol, 95 %).

DTA (5 °C min $^{-1}$ ): 251 °C (melt.), 286 °C (exo.); BAM: drop hammer: 40 J (100–500  $\mu\text{m}$ ); friction tester: >360 N (100–500  $\mu\text{m}$ ); ESD: 1.50 J (100–500  $\mu\text{m}$ ). IR (ATR),  $\nu$  (cm $^{-1}$ ) = 3631 (w), 3283 (m), 3136 (m), 3054 (m), 2832 (m), 1557 (m), 1520 (w), 1492 (m), 1454 (m), 1417 (s), 1381 (s), 1336 (vs), 1302 (s), 1223 (m), 1190 (m), 1102 (w), 1021 (m), 996 (m), 947 (vw), 849 (m), 832 (s), 817 (m), 769 (m), 702 (w), 673 (w), 626 (m), 592 (w), 548 (w), 526 (vw).  $^1\text{H}$  NMR ( $d_6$ -DMSO, 400 MHz, ppm)  $\delta$  = 13.96 (br), 8.11 (s), 7.11 (t).  $^{13}\text{C}$  NMR ( $d_6$ -DMSO, 101 MHz, ppm)  $\delta$  = 154.0, 153.5, 133.1, 106.8, 102.0.  $^{14}\text{N}$  NMR ( $d_6$ -DMSO, 29 MHz, ppm)  $\delta$  = -18, -359. Elem. Anal. ( $\text{C}_6\text{H}_8\text{N}_8\text{O}_7$ , 304.18 g mol $^{-1}$ ) calcd.: C 23.69, H 2.65, N 36.84 %. Found: C 23.77, H 2.67, N 36.39 %.

**Aminoguanidinium 4-(3-nitropyrazol-4-yl)-3,5-dinitropyrizolate monohydrate (14·H<sub>2</sub>O)**

3,3',5-Trinitro-4,4'-bipyrazole (403 mg, 1.50 mmol, 1.0 eq.) was dissolved in EtOH (15 mL) and water (6 mL). Aminoguanidinium carbonate (204 mg, 1.50 mmol, 1.0 eq.) was added and the mixtures was heated to reflux for 30 min. After cooling down to room temperature, the solvent was removed in vacuo to yield **14·H<sub>2</sub>O** (493 mg, 1.36 mmol, 67 %).

DTA (5 °C min $^{-1}$ ): 92 °C (-H<sub>2</sub>O), 209 °C (melt.), 220 °C (exo.); BAM: drop hammer: 35 J (100–500  $\mu\text{m}$ ); friction tester: > 360 N (100–500  $\mu\text{m}$ ); ESD: 0.48 (100–500  $\mu\text{m}$ ). IR (ATR),  $\nu$  (cm $^{-1}$ ) = 3588 (m), 3425 (w), 3354 (w), 3327 (w), 3147 (w), 1673 (s), 1626 (w), 1547 (s), 1482 (s), 1410 (w), 1381 (vs), 1336 (vs), 1317 (s), 1299 (m), 1169 (m), 994 (m), 848 (s), 835 (s), 817 (s), 490 (s).

**On a Midway Between Energetic Molecular Crystals and High-Density Energetic Salts:  
Crystal Engineering with Hydrogen Bonding Chains of Polynitro Bipyrazoles**

$^1\text{H}$  NMR ( $d_6$ -DMSO, 400 MHz, ppm)  $\delta$  = 14.00 (br, 1H), 8.55 (s, 1H), 8.11 (s, 1H), 7.23 (br, 2H), 6.71 (br, 2H), 4.68 (br, 2H).  $^{13}\text{C}$  NMR ( $d_6$ -DMSO, 101 MHz, ppm)  $\delta$  = 158.7, 154.1, 153.5, 133.1, 106.9, 102.0.  $^{14}\text{N}$  NMR ( $d_6$ -DMSO, 29 MHz, ppm)  $\delta$  = -16. Elem. Anal. ( $\text{C}_7\text{H}_{11}\text{N}_{11}\text{O}_7$ , 361.24 g mol $^{-1}$ ) calcd.: C 23.27, H 3.07, N 42.65 %. Found: C 23.55 H 3.20, N 43.13 %.

Crystals of **14-MeOH** were obtained by recrystallization of the above product from methanol. Anal. Calcd for  $\text{C}_8\text{H}_{13}\text{N}_{11}\text{O}_7$ : C 26.60, H 3.49, N 41.06 %. Found: C 26.35, H 3.47, N 40.89 %.

**3,6,7-Triamino-[1,2,4]triazolo[4,3-*b*][1,2,4]triazolium 4-(3-nitropirazol-4-yl)-3,5-dinitropirazolate (15)**

3,3',5-Trinitro-4,4'-bipyrazole (500 mg, 1.86 mmol) was dissolved in a mixture of EtOH (20 mL) and water (10 mL) and the solution was heated to 80 °C. 3,6,7-Triamino-[1,2,4]triazolo[4,3-*b*][1,2,4]triazole (154 mg, 1.86 mmol) was added in one portion and the mixture was stirred for 30 min at the same temperature. After cooling to ambient temperature the solvents were removed *in vacuo* to yield compound **15** as yellow powder (782 mg, 1.85 mmol, 99 %).

DTA (5 °C min $^{-1}$ ): 240 °C (exo.); BAM: drop hammer: 10 J (100–500  $\mu\text{m}$ ); friction tester: 360 N (100–500  $\mu\text{m}$ ); ESD: 0.20 J (100–500  $\mu\text{m}$ ). IR (ATR),  $\nu$  (cm $^{-1}$ ) = 3453 (w), 3340 (vw), 3089 (w), 2683 (vw), 1650 (s), 1570 (w), 1524 (m), 1486 (s), 1421 (w), 1387 (vs), 1339 (vs), 1305 (s), 1190 (w), 1001 (m), 853 (s), 833 (s), 711 (m).  $^1\text{H}$  NMR ( $d_6$ -DMSO, 400 MHz, ppm)  $\delta$  = 13.99 (s, 1H), 13.31 (br, 1H), 8.18 (s, 2H), 8.11 (s, 1H), 7.23 (s, 2H), 5.77 (s, 2H).  $^{13}\text{C}$  NMR ( $d_6$ -DMSO, 101 MHz, ppm)  $\delta$  = 160.2, 154.1, 153.4, 147.5, 141.2, 133.2, 106.9, 102.0.  $^{14}\text{N}$  NMR ( $d_6$ -DMSO, 29 MHz, ppm)  $\delta$  = -18. Elem. Anal. ( $\text{C}_9\text{H}_9\text{N}_{15}\text{O}_6$ , 423.27 g mol $^{-1}$ ) calcd.: C 25.54, H 2.14, N 49.64 %. Found: C 25.74, H 2.21, N 49.37 %.

**3,5-Diamino-1,2,4-triazolium 4-(3-nitropirazolyl)-3,5-dinitropirazolate (16)**

3,3',5-Trinitro-4,4'-bipyrazole (404 mg, 1.50 mmol, 1.0 eq.) was dissolved in a mixture of abs. EtOH (10 mL) and water (5 mL) and the solution was heated to 80 °C. 3,5-Diamino-1,2,4-triazole (150 mg, 1.50 mmol, 1.0 eq.) was added and the reaction mixture was stirred for 30 min. After cooling the solvent was removed *in vacuo* and compound **16** was obtained as yellow solid (520 mg, 1.41 mmol, 94 %).

**On a Midway Between Energetic Molecular Crystals and High-Density Energetic Salts:  
Crystal Engineering with Hydrogen Bonding Chains of Polynitro Bipyrazoles**

DTA (5 °C min<sup>-1</sup>): 237 °C (melt.), 273 °C (exo.); BAM: drop hammer: 15 J (100–500 µm); friction tester: 360 N (100–500 µm); ESD: 0.23 (100–500 µm). IR (ATR),  $\tilde{\nu}$  (cm<sup>-1</sup>) = 3454 (m), 3425 (m), 3359 (m), 3195 (br), 1678 (m), 1654 (s), 1546 (s), 1494 (m), 1477 (m), 1378 (vs), 1325 (vs), 1298 (s), 1179 (m), 1021 (m), 993 (s), 855 (s), 835 (s); <sup>1</sup>H NMR (*d*<sub>6</sub>-DMSO, 400 MHz, ppm)  $\delta$  = 14.00 (s), 8.12 (s), 7.00 (br). <sup>13</sup>C NMR (*d*<sub>6</sub>-DMSO, 101 MHz, ppm)  $\delta$  = 154.0, 153.4, 151.6, 133.2, 106.8, 102.0. <sup>14</sup>N NMR (*d*<sub>6</sub>-DMSO, 29 MHz, ppm)  $\delta$  = -19. Elem. Anal. (C<sub>8</sub>H<sub>8</sub>N<sub>12</sub>O<sub>6</sub>, 368.23 g mol<sup>-1</sup>) calcd.: C 26.09, H 2.19, N 45.65 %. Found: C 26.19, H 2.11, N 45.38 %.

**Hydroxylammonium 4-(3,5-dinitropyrazol-4-yl)-3,5-dinitropyrizolate (17)**

3,3',5,5'-Tetranitro-4,4'-bipyrazole monohydrate **3·H<sub>2</sub>O** (499 mg, 1.50 mmol) was dissolved in ethanol (12 mL). The solution was heated to 75 °C. Aqueous 50 % hydroxylamine solution (200 mg, 3.0 mmol) was added. Filtration and removing the solvent at room temperature gave compound **17** as yellow crystals (27, 520 mg, 1.50 mmol, 100 %).

DTA (5 °C min<sup>-1</sup>): 201 °C (exo.); BAM: drop hammer: 3 J (100–500 µm); friction tester: 216 N (100–500 µm); ESD: 0.25 J (100–500 µm). IR (ATR),  $\nu$  (cm<sup>-1</sup>) = 3213 (w), 3148 (w), 2874 (w), 2470 (w), 1916 (vw), 1739 (vw), 1603 (vw), 1552 (m), 1482, 1423 (m), 1388 (s), 1349 (vs), 1323 (s), 1309 (s), 1216 (m), 1179 (s), 1022 (m), 1003 (s), 846 (vs), 769 (m), 757 (m), 699 (m), 664 (w), 637 (w), 594 (w), 527 (w). <sup>1</sup>H NMR (*d*<sub>6</sub>-DMSO, 400 MHz, ppm)  $\delta$  = 10.16 (s, 3H). <sup>13</sup>C NMR (*d*<sub>6</sub>-DMSO, 101 MHz, ppm)  $\delta$  = 153.1, 103.6. <sup>14</sup>N NMR (*d*<sub>6</sub>-DMSO, 29 MHz, ppm)  $\delta$  = -16. Elem. Anal. (C<sub>6</sub>H<sub>5</sub>N<sub>9</sub>O<sub>9</sub>, 347.16 g mol<sup>-1</sup>) calcd.: C 20.76, H 1.45, N 36.31 %. Found: C 19.63, H 1.96, N 37.27 %.

**4-(3,5-Dimethylpyrazol-4-yl)-3,5-dimethylpyrazolium 4-(3,5-dinitropyrazol-4-yl)-3,5-dinitropyrizolate monohydrate (18·H<sub>2</sub>O)**

**3·H<sub>2</sub>O** (332 mg, 1.00 mmol) and 3,3',5,5'-tetramethyl-4,4'-bipyrazole semihydrate (199 mg, 1.00 mmol) were dissolved in 15 mL of boiling water. The solution was cooled and allowed to stand over 3-4 d. Yellow prisms of the product were filtered and dried (220 mg, 40 %).

Anal. Calcd for C<sub>16</sub>H<sub>18</sub>N<sub>12</sub>O<sub>9</sub>: C 36.78, H 3.47, N 32.18 %. Found: C 36.70, H 3.34, N 32.39 %.



### 8.8.3. Crystallography

Single-crystal X-ray diffraction data were collected with graphite-monochromated Mo K $\alpha$  radiation ( $\lambda = 0.71073$  Å) using a Stoe Image Plate Diffraction System ( $\varphi$  oscillation scans) for **4·H<sub>2</sub>O** to **8**, **10·H<sub>2</sub>O** and **18·H<sub>2</sub>O** (face-indexed numerical absorption correction using X-RED and X-SHAPE).<sup>[S9]</sup> Data for **9·H<sub>2</sub>O** and **11-17** were collected using Oxford Xcalibur3 diffractometer equipped with a CCD area detector. The structures were solved by direct methods and refined by full-matrix least-squares on  $F^2$  using the programs SHELXS-97 and SHELXL-2014/7 (Table S1).<sup>[S10]</sup> For the heavy-atom structures **5·H<sub>2</sub>O** and **10·H<sub>2</sub>O**, the hydrogen atoms were located and then refined as riding with C–H = 0.97 Å, N–H = 0.87 Å, O–H = 0.85 Å, and with  $U_{\text{iso}}(\text{H}) = 1.2U_{\text{eq}}(\text{C})$  or  $1.5U_{\text{eq}}(\text{N}, \text{O})$ . For other structures, all hydrogen atoms were located and freely refined with isotropic thermal parameters. A set of similarity restraints was applied to the N–H bond distances of the hydrazinium cation in **6**. In the case of **18·H<sub>2</sub>O**, the hydrogen atoms of methyl groups were refined as riding with C–H = 0.98 Å and with  $U_{\text{iso}}(\text{H}) = 1.5U_{\text{eq}}(\text{C})$ . Crystallographic data for the reported structures in this contribution have been deposited with the Cambridge Crystallographic Data Centre as supplementary publication numbers (CCDC 1949728-1949741 for **4-18·H<sub>2</sub>O**, respectively). These data can be obtained free of charge from the Cambridge Crystallographic Data Centre via [www.ccdc.cam.ac.uk/data\\_request/cif](http://www.ccdc.cam.ac.uk/data_request/cif).

**On a Midway Between Energetic Molecular Crystals and High-Density Energetic Salts: Crystal Engineering with Hydrogen Bonding Chains of Polynitro Bipyrzoles**

**Table S1.** Crystal data for K(DiNBpz)·H<sub>2</sub>O (**4·H<sub>2</sub>O**), Cs(DiNBpz)·H<sub>2</sub>O (**5·H<sub>2</sub>O**), N<sub>2</sub>H<sub>5</sub>(DiNBpz) (**6**), NH<sub>4</sub>(DiNBpz)·H<sub>2</sub>O (**7·H<sub>2</sub>O**) and (BipyH)(DiNBpz) (**8**).

	<b>4·H<sub>2</sub>O</b>	<b>5·H<sub>2</sub>O</b>	<b>6</b>	<b>7·H<sub>2</sub>O</b>	<b>8</b>
Formula	C <sub>6</sub> H <sub>5</sub> KN <sub>6</sub> O <sub>5</sub>	C <sub>6</sub> H <sub>5</sub> CsN <sub>6</sub> O <sub>5</sub>	C <sub>6</sub> H <sub>8</sub> N <sub>8</sub> O <sub>4</sub>	C <sub>6</sub> H <sub>9</sub> N <sub>7</sub> O <sub>5</sub>	C <sub>16</sub> H <sub>12</sub> N <sub>8</sub> O <sub>4</sub>
<i>M</i>	280.26	374.07	256.20	259.20	380.34
<i>T</i> / K	213	173	213	213	173
Diffractometer	IPDS <i>Stoe</i>	IPDS <i>Stoe</i>	IPDS <i>Stoe</i>	IPDS <i>Stoe</i>	IPDS-2T <i>Stoe</i>
Color and habit	yellow needle	yellow needle	yellow prism	yellow prism	yellow prism
Size / mm	0.15 × 0.12 × 0.12	0.20 × 0.17 × 0.14	0.25 × 0.24 × 0.19	0.24 × 0.24 × 0.19	0.27 × 0.25 × 0.20
Crystal system	Monoclinic	Monoclinic	Monoclinic	Monoclinic	Monoclinic
Space group, <i>Z</i>	<i>Pn</i> , 2	<i>P2<sub>1</sub>/n</i> , 4	<i>Pn</i> , 2	<i>I2/a</i> , 8	<i>P2<sub>1</sub>/c</i> , 4
<i>a</i> / Å	3.7606(3)	7.5056(9)	3.6839(3)	13.8084(11)	13.2099(4)
<i>b</i> / Å	8.5150(4)	18.4706(14)	8.3746(7)	10.5769(6)	7.5313(2)
<i>c</i> / Å	16.2611(12)	8.5938(11)	16.259(2)	14.3961(13)	17.3941(5)
$\alpha$ / °	90	90	90	90	90
$\beta$ / °	91.230(8)	112.168(9)	93.800(13)	96.286(10)	107.603(2)
$\gamma$ / °	90	90	90	90	90
<i>V</i> / Å <sup>3</sup>	520.58(6)	1103.3(2)	500.51(9)	2089.9(3)	1649.47(8)
$\mu$ (Mo-K $\alpha$ )/ mm <sup>-1</sup>	0.539	3.383	0.144	0.143	0.116
<i>D</i> <sub>calc</sub> / g cm <sup>-3</sup>	1.788	2.252	1.700	1.648	1.532
2 $\theta$ <sub>max</sub> / °	27.965	28.311	27.964	27.930	26.946
Measd/ Unique reflns	4507/ 2306	8278/ 2717	4270/ 2214	8875/ 2482	14466/ 3532
Completeness/ %	99.1	99.2	94.5	98.9	98.5
Reflns with <i>I</i> > 2 $\sigma$ ( <i>I</i> )	2052	2303	1804	1399	2581
<i>R</i> <sub>int</sub>	0.0249	0.0561	0.0207	0.0317	0.0532
Parameters refined	183	164	195	199	301
<i>R</i> 1, w <i>R</i> 2 ( <i>I</i> > 2 $\sigma$ ( <i>I</i> ))	0.0288, 0.0654	0.0268, 0.0618	0.0296, 0.0630	0.0323, 0.0711	0.0472, 0.1302
<i>R</i> 1, w <i>R</i> 2 (all data)	0.0328, 0.0663	0.0334, 0.0633	0.0363, 0.0638	0.0617, 0.0751	0.0662, 0.1430
Goof on <i>F</i> <sup>2</sup>	0.953	1.000	0.914	0.783	1.050
Max, min peak/ e Å <sup>-3</sup>	0.288, -0.202	1.144, -1.036	0.332, -0.175	0.302, -0.157	0.307, -0.286
CCDC number	1949728	1949729	1949730	1949731	1949732

**On a Midway Between Energetic Molecular Crystals and High-Density Energetic Salts: Crystal Engineering with Hydrogen Bonding Chains of Polynitro Bipyrzoles**

**Table S2.** Crystal data for K(TriNBpz)·H<sub>2</sub>O (**9·H<sub>2</sub>O**), Cs(TriNBpz)·H<sub>2</sub>O (**10·H<sub>2</sub>O**), NH<sub>3</sub>OH(TriNBpz) (**11**), N<sub>2</sub>H<sub>4</sub>(TriNBpz)(**12**), NH<sub>4</sub>(TriNBpz)·H<sub>2</sub>O (**13·H<sub>2</sub>O**)

	<b>9·H<sub>2</sub>O</b>	<b>10·H<sub>2</sub>O</b>	<b>11</b>	<b>12</b>	<b>13·H<sub>2</sub>O</b>
Formula	C <sub>6</sub> H <sub>4</sub> KN <sub>7</sub> O <sub>7</sub>	C <sub>6</sub> H <sub>4</sub> CsN <sub>7</sub> O <sub>7</sub>	C <sub>6</sub> H <sub>6</sub> N <sub>8</sub> O <sub>7</sub>	C <sub>6</sub> H <sub>7</sub> N <sub>9</sub> O <sub>6</sub>	C <sub>6</sub> H <sub>8</sub> N <sub>8</sub> O <sub>7</sub>
<i>M</i>	325.26	419.07	302.19	301.21	304.20
<i>T</i> / K	130	213	143	143	143
Diffractionmeter	Xcalibur Sapphire3	IPDS-2T <i>Stoe</i>	Xcalibur Sapphire3	Xcalibur Sapphire3	Xcalibur Sapphire3
Color and habit	yellow block	yellow prism	yellow block	yellow block	yellow prism
Size / mm	0.38 × 0.19 × 0.10	0.20 × 0.17 × 0.15	0.30 × 0.25 × 0.15	0.25 × 0.15 × 0.15	0.22 × 0.14 × 0.06
Crystal system	Triclinic	Triclinic	Triclinic	Triclinic	Triclinic
Space group, <i>Z</i>	<i>P</i> -1, 2	<i>P</i> -1, 2	<i>P</i> -1, 2	<i>P</i> -1, 2	<i>P</i> -1, 2
<i>a</i> / Å	7.6299(8)	7.5655(5)	7.6736(6)	7.6797(8)	7.7412(5)
<i>b</i> / Å	8.5549(10)	8.5672(6)	8.6244(6)	8.5684(5)	8.5278(6)
<i>c</i> / Å	8.9257(9)	10.1918(6)	8.6380(6)	8.7353(7)	9.0812(5)
$\alpha$ / °	100.138(9)	112.225(7)	77.845(6)	76.964(6)	78.785(5)
$\beta$ / °	90.416(8)	95.707(7)	87.993(6)	88.498(8)	85.558(5)
$\gamma$ / °	92.544(9)	90.708(8)	87.851(6)	88.023(7)	87.716(5)
<i>V</i> / Å <sup>3</sup>	572.88(11)	607.58(7)	558.24(7)	559.56(8)	586.10(7)
$\mu$ (Mo-K $\alpha$ )/ mm <sup>-1</sup>	0.519	3.100	0.164	0.159	0.156
<i>D</i> <sub>calc</sub> / g cm <sup>-3</sup>	1.886	2.291	1.798	1.788	1.724
2 $\theta$ <sub>max</sub> / °	25.997	27.944	26.496	26.497	26.493
Measd/ Unique reflns	4258/ 2241	6585/ 2870	4375/ 2305	4243/ 2309	4453/ 2423
Completeness/ %	99.5	98.6	99.6	99.5	99.6
Reflns with <i>I</i> > 2 $\sigma$ ( <i>I</i> )	1836	2488	1977	1790	1787
<i>R</i> <sub>int</sub>	0.0289	0.0214	0.0205	0.0311	0.0288
Parameters refined	206	190	214	218	222
<i>R</i> 1, w <i>R</i> 2 ( <i>I</i> > 2 $\sigma$ ( <i>I</i> ))	0.0369, 0.0866	0.0180, 0.0423	0.0341, 0.0808	0.0410, 0.0917	0.0398, 0.0801
<i>R</i> 1, w <i>R</i> 2 (all data)	0.0474, 0.0942	0.0220, 0.0428	0.0413, 0.0871	0.0582, 0.1013	0.0654, 0.0903
Goof on <i>F</i> <sup>2</sup>	1.060	0.937	1.060	1.025	1.011
Max, min peak/ e Å <sup>-3</sup>	0.302, -0.389	0.889, -0.344	0.279, -0.243	0.267, -0.237	0.243, -0.258
CCDC number	1949733	1949734	1949735	1949736	1949737

**On a Midway Between Energetic Molecular Crystals and High-Density Energetic Salts: Crystal Engineering with Hydrogen Bonding Chains of Polynitro Bipyrzoles**

**Table S3.** Crystal data for (AG)(TriNBpz)·MeOH (**14·MeOH**), (TATOT)(TriNBpz) (**15**), NH<sub>3</sub>OH(TNBpz) (**17**), and (Me<sub>4</sub>BpzH)(TNBpz)·H<sub>2</sub>O (**18·H<sub>2</sub>O**).

	<b>14·MeOH</b>	<b>15</b>	<b>17</b>	<b>18·H<sub>2</sub>O</b>
Formula	C <sub>8</sub> H <sub>13</sub> N <sub>11</sub> O <sub>7</sub>	C <sub>9</sub> H <sub>9</sub> N <sub>15</sub> O <sub>6</sub>	C <sub>6</sub> H <sub>5</sub> N <sub>9</sub> O <sub>9</sub>	C <sub>16</sub> H <sub>18</sub> N <sub>12</sub> O <sub>9</sub>
<i>M</i>	375.29	423.31	347.19	522.42
<i>T</i> / K	143	143	130	173
Diffractionmeter	Xcalibur Sapphire3	Xcalibur Sapphire3	Xcalibur Sapphire3	IPDS-2T <i>Stoe</i>
Color and habit	Colorless block	Colorless block	Colorless block	yellow prism
Size / mm	0.40 × 0.40 × 0.20	0.30 × 0.30 × 0.25	0.28 × 0.19 × 0.16	0.24 × 0.23 × 0.20
Crystal system	Monoclinic	Tetragonal	Monoclinic	Tetragonal
Space group, <i>Z</i>	<i>I</i> 2/ <i>a</i> , 8	<i>P</i> 4 <sub>3</sub> 2 <sub>1</sub> 2, 8	<i>Cc</i> , 4	<i>P</i> 4 <sub>3</sub> , 4
<i>a</i> / Å	16.3433(4)	8.5520(2)	11.2031(4)	8.5740(4)
<i>b</i> / Å	8.4692(2)	8.5520(2)	15.3611(5)	8.5740(4)
<i>c</i> / Å	22.3564(5)	45.1136(8)	7.6669(3)	29.928(2)
$\alpha$ / °	90	90	90	90
$\beta$ / °	90.825(2)	90	109.478(5)	90
$\gamma$ / °	90	90	90	90
<i>V</i> / Å <sup>3</sup>	3094.13(13)	3299.46(17)	1243.90(9)	2200.1(3)
$\mu$ (Mo-K $\alpha$ )/ mm <sup>-1</sup>	0.140	0.145	0.174	0.131
<i>D</i> <sub>calc</sub> / g cm <sup>-3</sup>	1.611	1.704	1.854	1.577
2 $\theta$ <sub>max</sub> / °	25.989	28.280	27.998	26.553
Measd/ Unique reflns	22435/ 3028	33075/ 4069	10304/ 3005	8144/ 3952
Completeness/ %	0.996	0.991	0.997	0.993
Reflns with <i>I</i> > 2 $\sigma$ ( <i>I</i> )	2742	3881	2822	3579
<i>R</i> <sub>int</sub>	0.0215	0.0490	0.0275	0.0341
Parameters refined	287	305	237	362
<i>R</i> 1, <i>wR</i> 2 ( <i>I</i> > 2 $\sigma$ ( <i>I</i> ))	0.0287, 0.0750	0.0389, 0.0861	0.0286, 0.0670	0.0287, 0.0644
<i>R</i> 1, <i>wR</i> 2 (all data)	0.0319, 0.0776	0.0410, 0.0871	0.0313, 0.0684	0.0330, 0.0656
Goof on <i>F</i> <sup>2</sup>	1.047	1.092	1.019	0.988
Max, min peak/ e Å <sup>-3</sup>	0.263, -0.187	0.229, -0.206	0.185, -0.206	0.137, -0.191
CCDC	1949738	1949739	1949740	1949741

8.8.3.1. ORTEP Drawings, atoms labeling schemes and geometry of hydrogen bonding

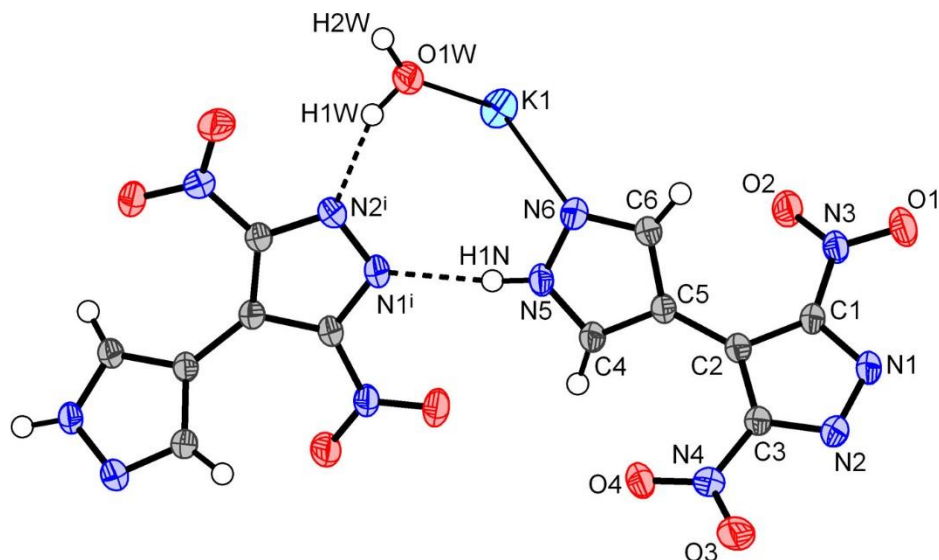


**Figure S2.** Molecular structure of **4·H<sub>2</sub>O**, showing the atom labeling scheme and thermal ellipsoids drawn at 50% probability level. Symmetry code: (i)  $-0.5+x, 1-y, 0.5+z$ .

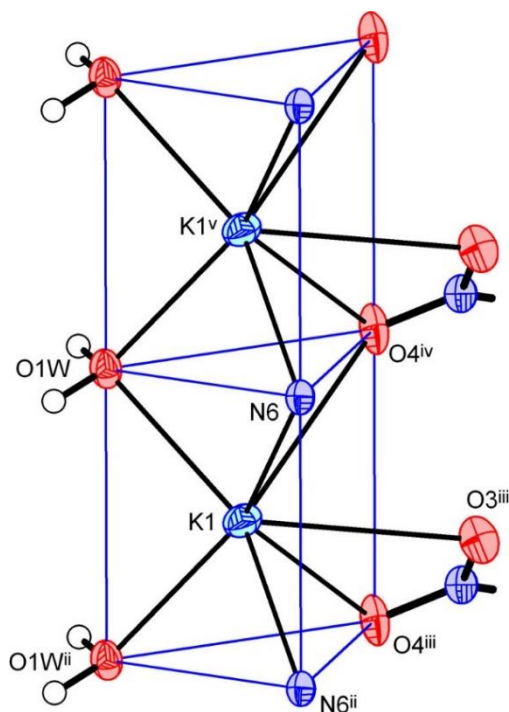


**Figure S3.** Coordination environment of the potassium ion, in the form of capped trigonal prism (CN = 7), in the structure of structure of **4·H<sub>2</sub>O**. Symmetry codes: (ii)  $-1+x, y, z$ ; (iii)  $-1+x, 1+y, z$ ; (iv)  $x, 1+y, z$ ; (v)  $1+x, y, z$ .

**On a Midway Between Energetic Molecular Crystals and High-Density Energetic Salts:  
Crystal Engineering with Hydrogen Bonding Chains of Polynitro Bipyrazoles**

**Table S4.** Hydrogen-bond geometry (Å, °) for structure of **K(DiNBPZ)·H<sub>2</sub>O (4·H<sub>2</sub>O)**.

Donor (D)	H-Atom	Acceptor (A)	D-H	H...A	D...A	∠DH...A
N5	H1N	N1 (-0.5+x, 1-y, 0.5+z)	0.88(4)	2.03(4)	2.898(3)	169(4)
N5	H1N	O1 (-0.5+x, 1-y, 0.5+z)	0.88(4)	2.57(4)	3.095(3)	119(3)
O1W	H1W	N2 (-0.5+x, 1-y, 0.5+z)	0.92(5)	1.94(5)	2.819(3)	160(4)
O1W	H2W	O2 (0.5+x, 2-y, 0.5+z)	0.83(4)	2.09(4)	2.926(3)	174(4)
C4	H4	O1 (-0.5+x, 1-y, 0.5+z)	0.89(4)	2.60(3)	3.148(4)	120(3)
C6	H6	O3 (x, 1+y, z)	0.91(3)	2.71(3)	3.498(4)	146(2)

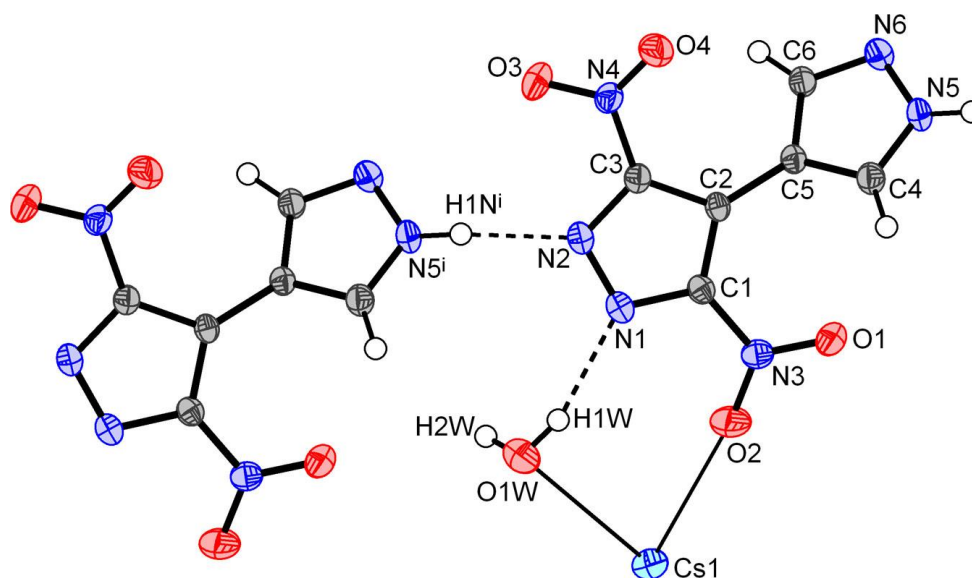


**Figure S4.** Molecular structure of **5·H<sub>2</sub>O**, showing the atom labeling scheme and thermal ellipsoids drawn at 50% probability level. Symmetry code: (i)  $x, y, 1+z$ .

**Table S5.** Hydrogen-bond geometry (Å, °) for structure of **Cs(DiNBPZ)·H<sub>2</sub>O (5·H<sub>2</sub>O)**.

Donor (D)	H-Atom	Acceptor (A)	D-H	H...A	D...A	∠DH...A
N5	H1N	N2 (x, y, -1+z)	0.88	1.97	2.836(3)	169
O1W	H1W	N1	0.85	2.12	2.943(3)	163
O1W	H2W	O1 (x, y, 1+z)	0.85	2.75	3.304(3)	124
C6	H6	O3 (-x, 1-y, 1-x)	0.95	2.78	3.298(3)	115

**On a Midway Between Energetic Molecular Crystals and High-Density Energetic Salts:  
Crystal Engineering with Hydrogen Bonding Chains of Polynitro Bipyrroles**

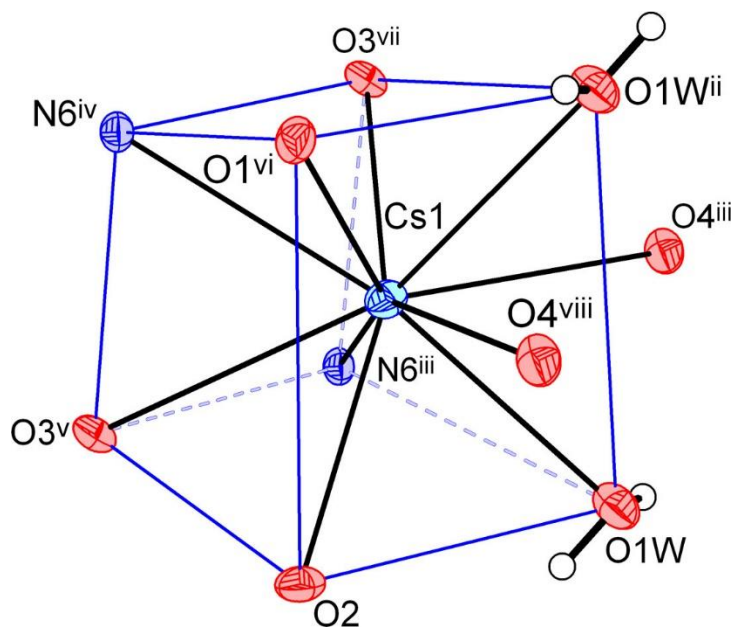


**Figure S5.** Coordination environment of the caesium ion, in the form of distorted bicapped cube (CN = 10), in the structure of structure of **5·H<sub>2</sub>O**. Symmetry codes: (ii)  $-x, -y, 2-z$ ; (iii)  $-0.5+x, 0.5-y, 0.5+z$ ; (iv)  $-0.5-x, -0.5+y, 0.5-z$ ; (v)  $-0.5+x, 0.5-y, -0.5+z$ ; (vi)  $-x, -y, 1-z$ ; (vii)  $-0.5-x, -0.5+y, 1.5-z$ ; (viii)  $0.5-x, -0.5+y, 1.5-z$ .

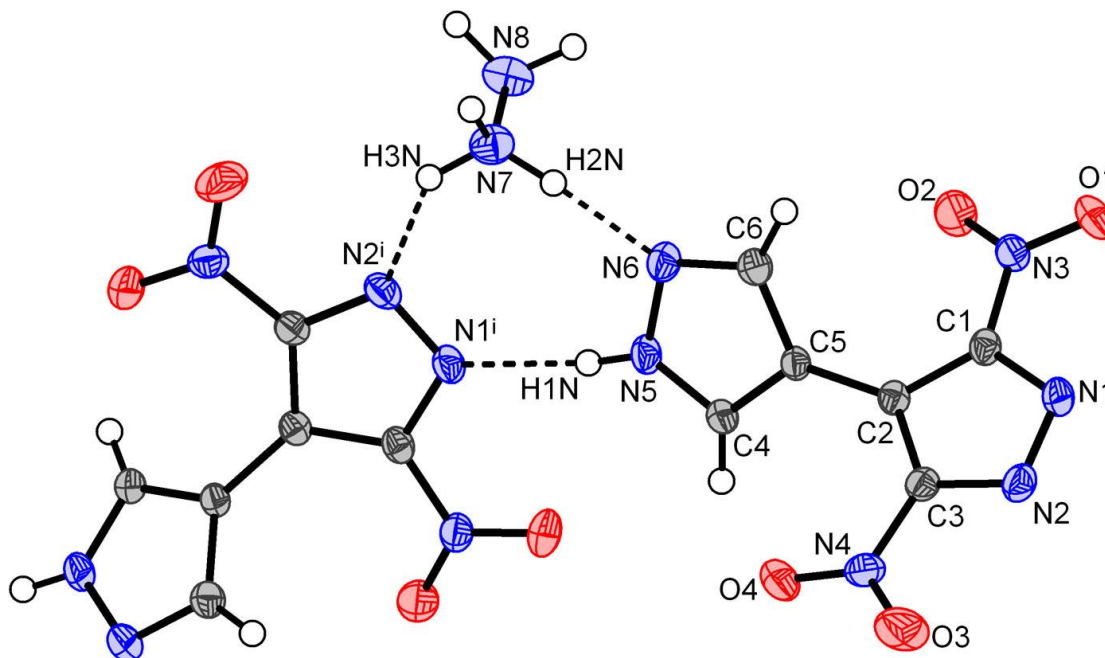


**Figure S6.** Molecular structure of **N<sub>2</sub>H<sub>5</sub>(DiNBPZ) (6)**, showing the atom labeling scheme and thermal ellipsoids drawn at 50% probability level. Symmetry code: (i)  $-0.5+x, -y, 0.5+z$ .

**On a Midway Between Energetic Molecular Crystals and High-Density Energetic Salts:  
Crystal Engineering with Hydrogen Bonding Chains of Polynitro Bipyrazoles**

**Table S6.** Hydrogen-bond geometry (Å, °) for structure of **N<sub>2</sub>H<sub>5</sub>(DiNBZPZ) (6)**.

Donor (D)	H-Atom	Acceptor (A)	D-H	H...A	D...A	∠DH...A
N5	H1N	N1 (-0.5+x, -y, 0.5+z)	0.86(3)	2.02(3)	2.878(3)	172(3)
N7	H2N	N6	0.975(17)	1.81(2)	2.781(3)	174(4)
N7	H3N	N2 (-0.5+x, -y, 0.5+z)	0.974(17)	2.06(3)	2.862(3)	139(3)
N7	H4N	N8 (1+x, y, z)	0.974(17)	1.96(2)	2.888(4)	158(3)
N8	H5N	O4 (x, 1+y, z)	0.970(17)	2.21(3)	3.080(3)	149(4)
N8	H6N	O1 (0.5+x, 1-y, 0.5+z)	0.974(18)	2.44(4)	3.239(3)	139(4)
N8	H6N	O2 (0.5+x, 1-y, 0.5+z)	0.974(18)	2.47(2)	3.384(3)	156(3)
C4	H4	O4 (-1+x, y, z)	0.90(3)	2.59(3)	3.367(4)	144(2)
C6	H6	O3 (x, 1+y, z)	0.95(3)	2.75(3)	3.628(4)	155(2)

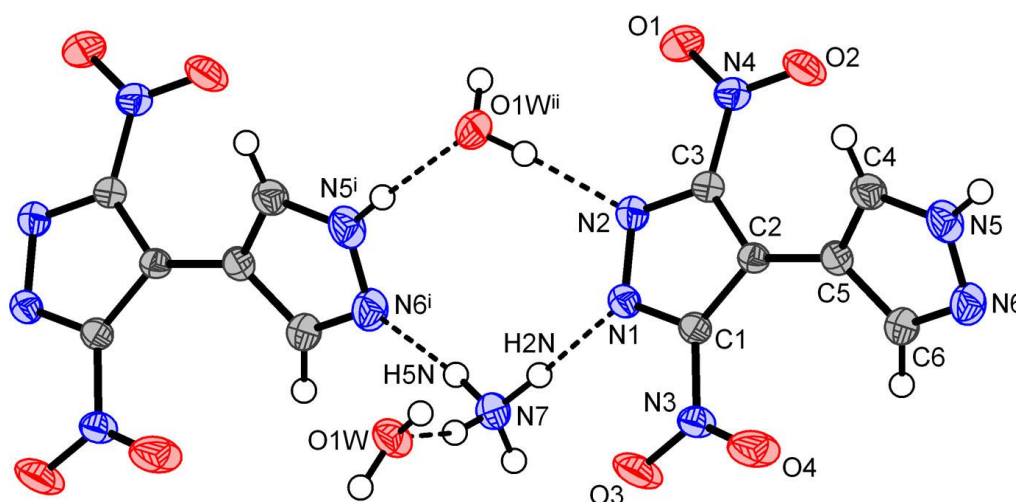


**Figure S7.** Molecular structure of **NH<sub>4</sub>(DiNBZPZ)·H<sub>2</sub>O (7·H<sub>2</sub>O)**, showing the atom labeling scheme and thermal ellipsoids drawn at 50% probability level. Symmetry code: (i)  $x, 1+y, z$ ; (ii)  $0.5-x, y, -z$ .

**Table S7.** Hydrogen-bond geometry (Å, °) for structure of **NH<sub>4</sub>(DiNBZPZ)·H<sub>2</sub>O (7·H<sub>2</sub>O)**.

Donor (D)	H-Atom	Acceptor (A)	D-H	H...A	D...A	∠DH...A
N5	H1N	O1W (-x+0.5, -1+y, -z)	0.856(17)	2.037(17)	2.8911(17)	176.2(17)
N7	H2N	N1	0.94(2)	1.96(2)	2.8973(18)	170.9(17)
N7	H3N	O1W	0.96(2)	1.99(2)	2.908(2)	159.9(16)



**On a Midway Between Energetic Molecular Crystals and High-Density Energetic Salts:  
Crystal Engineering with Hydrogen Bonding Chains of Polynitro Bipyrroles**

N7	H4N	O1W (-x+0.5, -y+1.5, -z+0.5)	0.89(2)	2.60(2)	3.3764(18)	146.1(16)
N7	H4N	O1 (x, -y+1.5, z+0.5)	0.89(2)	2.52(2)	3.1704(19)	130.8(16)
N7	H5N	N6 (x, 1+y, z)	0.99(2)	1.87(2)	2.8451(18)	170.3(17)
O1W	H1W	O2 (x+0.5, y+0.5, z+0.5)	0.93(2)	2.00(2)	2.9130(15)	166.4(16)
O1W	H2W	N2 (-x+0.5, y, -z)	0.84(2)	1.91(2)	2.7468(16)	171(2)
C4	H4	O4 (-x+0.5, y, -z)	0.913(15)	2.692(15)	3.294(2)	124.2(12)
C6	H6	O2 (x, -y+0.5, z+0.5)	0.980(14)	2.783(15)	3.6960(18)	155.3(12)

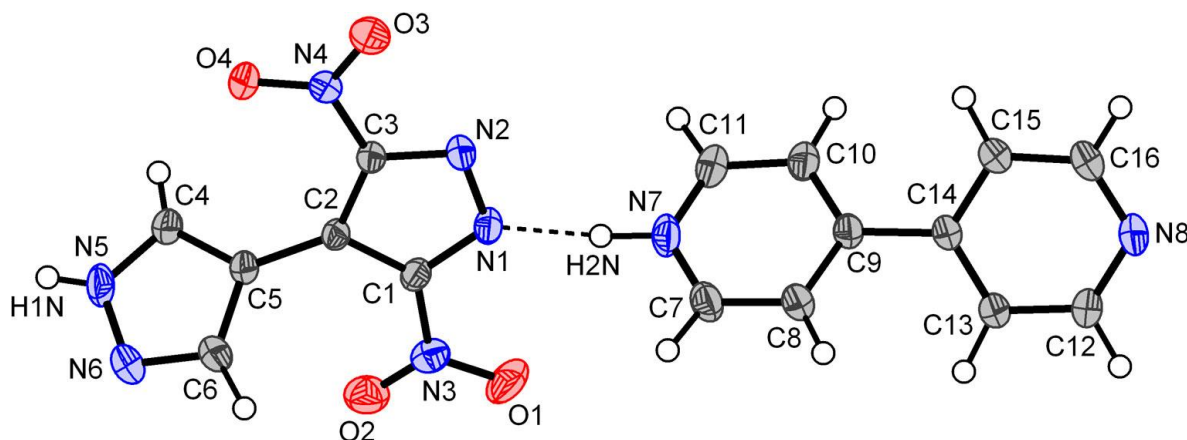


**Figure S8.** Molecular structure of **[BipyH](DiNBPZ) (8)**, showing the atom labeling scheme and thermal ellipsoids drawn at 40% probability level.

**Table S8.** Hydrogen-bond geometry (Å, °) for structure of **[BipyH](DiNBPZ) (8)**.

Donor (D)	H-Atom	Acceptor (A)	D-H	H...A	D...A	∠DH...A
N5	H1N	N8 (1+x, y, 1+z)	0.82(3)	2.10(3)	2.902(2)	167(2)
N7	H2N	N1	1.01(4)	1.70(4)	2.671(2)	162(3)
C7	H7	O4 (1-x, 1-y, 1-z)	1.01(3)	2.24(3)	3.205(2)	159(2)
C8	H8	O1 (1-x, y+0.5, -z+0.5)	1.01(3)	2.73(3)	3.501(3)	134(2)
C8	H8	O2 (1-x, y+0.5, -z+0.5)	1.01(3)	2.53(3)	3.544(3)	178(2)
C13	H13	N2 (x, -y+0.5, z-0.5)	1.05(3)	2.56(3)	3.600(2)	171(2)
C15	H15	N6 (-1+x, -y+0.5, z-0.5)	1.00(3)	2.74(3)	3.612(3)	145.7(19)
C16	H16	O2 (-1+x, -y+0.5, z-0.5)	0.97(3)	2.35(3)	3.253(3)	154(2)

**On a Midway Between Energetic Molecular Crystals and High-Density Energetic Salts:  
Crystal Engineering with Hydrogen Bonding Chains of Polynitro Bipyrazoles**

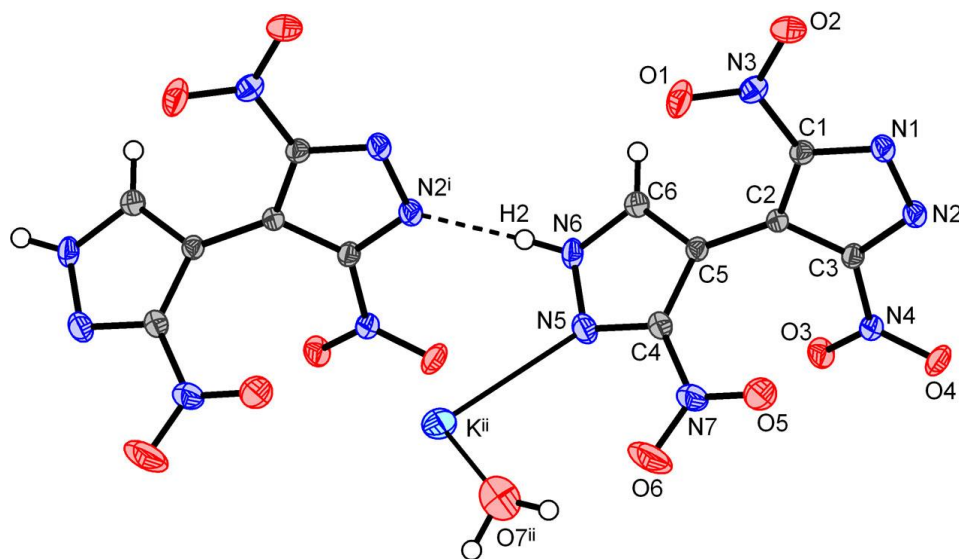


**Figure S9.** Molecular structure of **K(TriNBPZ)·H<sub>2</sub>O (9·H<sub>2</sub>O)**, showing the atom labeling scheme and thermal ellipsoids drawn at 50% probability level. Symmetry code: (i)  $x, 1+y, z$ ; (ii)  $1-x, 1-y, 1-z$ .

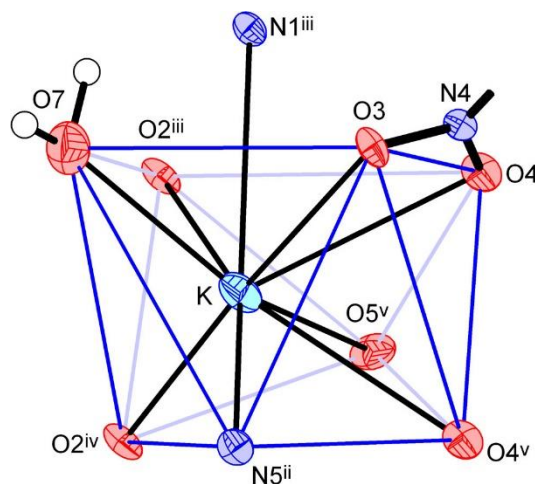


**Figure S10.** Coordination environment of the caesium ion, in the form of distorted capped tetragonal antiprism (CN = 9), in the structure of structure of **9·H<sub>2</sub>O**. Symmetry codes: (ii)  $1-x, 1-y, 1-z$ ; (iii)  $-x, -y, 1-z$ ; (iv)  $1+x, y, 1+z$ ; (v)  $1-x, -y, 1-z$ .

**Table S9.** Hydrogen-bond geometry (Å, °) for structure of **K(TriNBPZ)·H<sub>2</sub>O (9·H<sub>2</sub>O)**.

Donor (D)	H-Atom	Acceptor (A)	D-H	H...A	D...A	∠DH...A
N6	H2	N2 ( $x, 1+y, z$ )	0.87(3)	1.95(3)	2.809(2)	169(2)

**On a Midway Between Energetic Molecular Crystals and High-Density Energetic Salts:  
Crystal Engineering with Hydrogen Bonding Chains of Polynitro Bipyrazoles**

O7	H7B	O1 (-x, 1-y, 1-z)	0.93(5)	2.23(5)	3.152(3)	171(4)
C6	H1	O6 (-1+x, y, z)	0.90(2)	2.41(2)	3.286(3)	164.5(19)

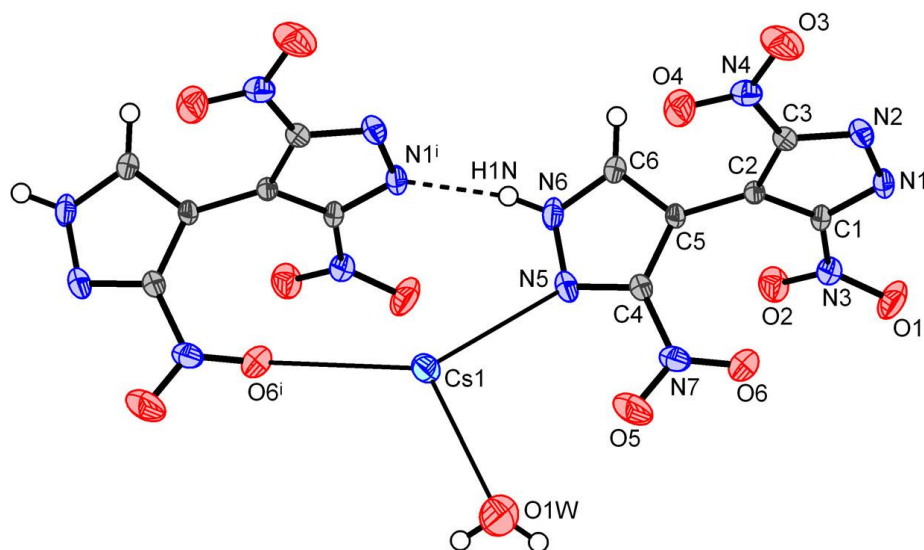


**Figure S11.** Molecular structure of **Cs(TriNBPZ)·H<sub>2</sub>O (10·H<sub>2</sub>O)**, showing the atom labeling scheme and thermal ellipsoids drawn at 50% probability level. Symmetry code: (i)  $x, 1+y, z$ .

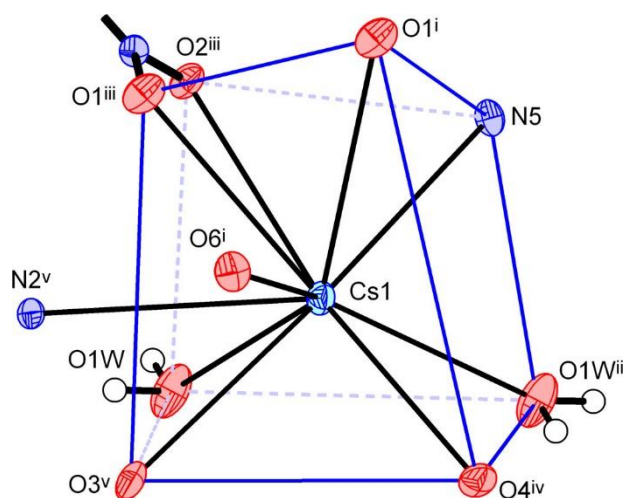


**Figure S12.** Coordination environment of the caesium ion, in the form of distorted bicapped cube (CN = 10), in the structure of structure of **10·H<sub>2</sub>O**. Symmetry codes: (i)  $x, 1+y, z$ ; (ii)  $1-x, 1-y, -z$ ; (iii)  $1-x, 1-y, 1-z$ ; (iv)  $-x, 1-y, -z$ ; (v)  $1+x, 1+y, z$ .

**Table S10.** Hydrogen-bond geometry (Å, °) for structure of **Cs(TriNBPZ)·H<sub>2</sub>O (10·H<sub>2</sub>O)**.

Donor (D)	H-Atom	Acceptor (A)	D-H	H...A	D...A	∠DH...A
-----------	--------	--------------	-----	-------	-------	---------

**On a Midway Between Energetic Molecular Crystals and High-Density Energetic Salts:  
Crystal Engineering with Hydrogen Bonding Chains of Polynitro Bipyrazoles**

N6	H1N	N1 ( <i>x</i> , 1+ <i>y</i> , <i>z</i> )	0.87	2.00	2.813(2)	155
N6	H1N	O2 ( <i>-x</i> , 1- <i>y</i> , 1- <i>z</i> )	0.87	2.83	3.332(2)	119
O1W	H1W	N2 (1+ <i>x</i> , 1+ <i>y</i> , <i>z</i> )	0.85	2.13	2.885(3)	148
O1W	H2W	O4 (1+ <i>x</i> , <i>y</i> , <i>z</i> )	0.85	2.49	3.201(3)	141
C6	H6	O2 ( <i>-x</i> , 1- <i>y</i> , 1- <i>z</i> )	0.94	2.71	3.273(3)	120
C6	H6	O5 (-1+ <i>x</i> , <i>y</i> , <i>z</i> )	0.94	2.55	3.417(3)	153

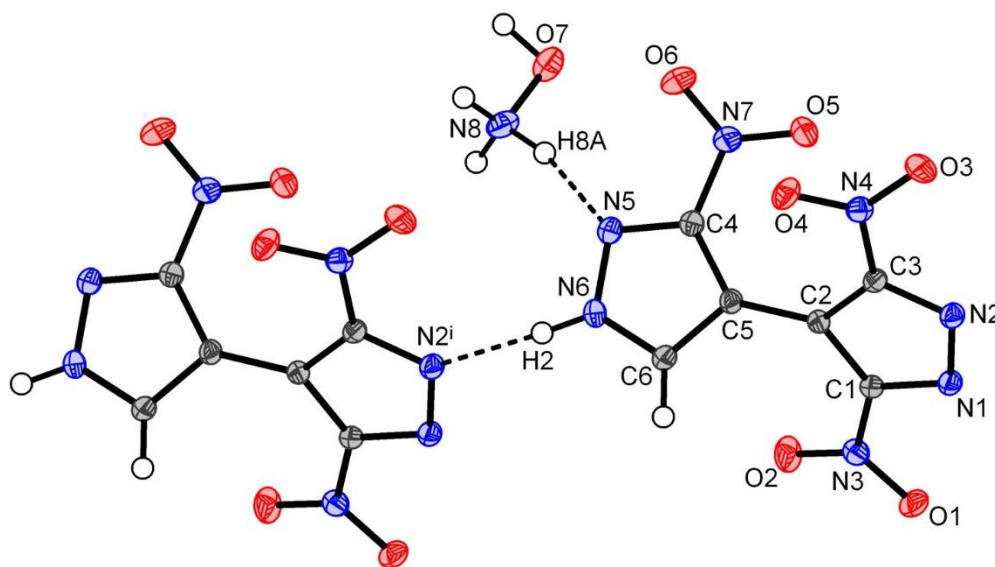


**Figure S13.** Molecular structure of (NH<sub>3</sub>OH)(TriNBPZ) (**11**), showing the atom labeling scheme and thermal ellipsoids drawn at 50% probability level. Symmetry code: (i) *x*, *y*, -1+*z*.

**Table S11.** Hydrogen-bond geometry (Å, °) for structure of (NH<sub>3</sub>OH)(TriNBPZ) (**11**).

Donor (D)	H-Atom	Acceptor (A)	D-H	H...A	D...A	∠DH...A
N6	H2	N2 ( <i>x</i> , <i>y</i> , -1+ <i>z</i> )	0.912(17)	1.942(17)	2.8474(18)	172.0(17)
O7	H7	N1 (1+ <i>x</i> , <i>y</i> , -1+ <i>z</i> )	0.96(2)	1.77(2)	2.7202(18)	170(2)
N8	H8A	N5	0.98(3)	1.92(2)	2.888(2)	167(2)
N8	H8B	O1 ( <i>-x</i> , - <i>y</i> , 1- <i>z</i> )	0.93(2)	2.01(3)	2.9255(19)	169(2)
N8	H8C	O3 (1- <i>x</i> , 1- <i>y</i> , 1- <i>z</i> )	0.913(19)	2.433(18)	3.3439(19)	175.6(15)
N8	H8C	O4 (1- <i>x</i> , 1- <i>y</i> , 1- <i>z</i> )	0.913(19)	2.310(19)	2.8998(19)	122.1(14)
C6	H1	O6 (-1+ <i>x</i> , <i>y</i> , <i>z</i> )	0.950(15)	2.361(15)	3.297(2)	168.4(14)

**On a Midway Between Energetic Molecular Crystals and High-Density Energetic Salts:  
Crystal Engineering with Hydrogen Bonding Chains of Polynitro Bipyrazoles**

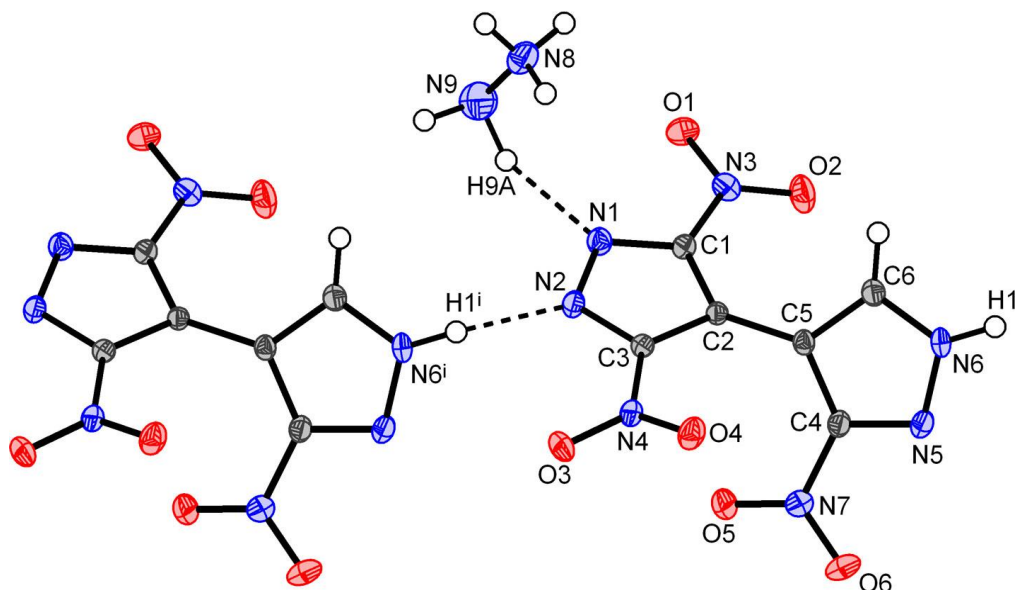


**Figure S14.** Molecular structure of **N<sub>2</sub>H<sub>4</sub>(TriNBPZ) (12)**, showing the atom labeling scheme and thermal ellipsoids drawn at 50% probability level. Symmetry code: (i)  $x, -1+y, z$ .

**Table S12.** Hydrogen-bond geometry (Å, °) for structure of **N<sub>2</sub>H<sub>4</sub>(TriNBPZ) (12)**.

Donor (D)	H-Atom	Acceptor (A)	D-H	H...A	D...A	∠DH...A
N6	H1	N2 ( $x, 1+y, z$ )	0.90(3)	1.92(3)	2.810(2)	171(3)
N8	H8A	O3 ( $1-x, 1-y, -z$ )	0.92(3)	2.42(3)	3.317(2)	163(2)
N8	H8A	O4 ( $1-x, 1-y, -z$ )	0.92(3)	2.33(3)	2.916(2)	121.4(19)
N8	H8A	N4 ( $1-x, 1-y, -z$ )	0.92(3)	2.69(3)	3.499(3)	148(2)
N8	H8B	N5 ( $1+x, -1+y, z$ )	0.94(3)	1.99(3)	2.920(3)	167(2)
N8	H8C	O1 ( $2-x, 1-y, 1-z$ )	0.93(3)	2.01(3)	2.914(2)	166(2)
N9	H9A	N1	1.05(4)	2.21(4)	3.082(3)	139(3)
N9	H9B	O6 ( $1+x, -1+y, z$ )	0.96(3)	2.34(4)	3.158(3)	143(3)
C6	H2	O4 ( $1-x, 2-y, -z$ )	0.96(2)	2.62(2)	3.234(2)	122.2(15)
C6	H2	O6 ( $1+x, y, z$ )	0.96(2)	2.38(2)	3.314(3)	164.6(16)

**On a Midway Between Energetic Molecular Crystals and High-Density Energetic Salts:  
Crystal Engineering with Hydrogen Bonding Chains of Polynitro Bipyrzoles**

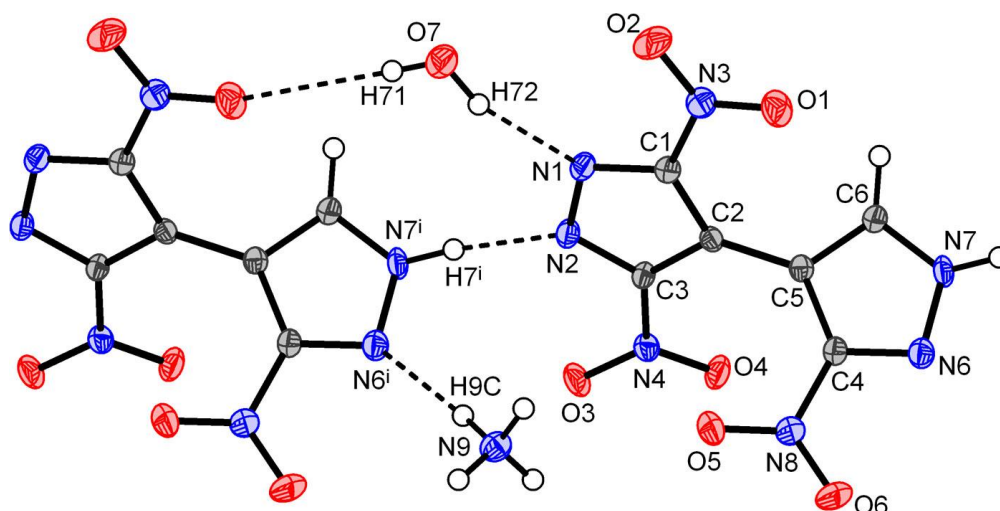


**Figure S15.** Molecular structure of  $\text{NH}_4(\text{TriNBPZ})\cdot\text{H}_2\text{O}$  ( $13\cdot\text{H}_2\text{O}$ ), showing the atom labeling scheme and thermal ellipsoids drawn at 50% probability level. Symmetry code: (i)  $x, -1+y, z$ .

**Table S13.** Hydrogen-bond geometry ( $\text{\AA}$ ,  $^\circ$ ) for structure of  $\text{NH}_4(\text{TriNBPZ})\cdot\text{H}_2\text{O}$  ( $13\cdot\text{H}_2\text{O}$ ).

Donor (D)	H-Atom	Acceptor (A)	D-H	H...A	D...A	$\angle\text{DH}\cdots\text{A}$
N7	H7	N2 ( $x, 1+y, z$ )	0.89(3)	1.89(3)	2.760(2)	166(2)
O7	H71	O1 ( $x, -1+y, z$ )	0.78(3)	2.60(3)	3.369(2)	171(3)
O7	H72	N1	0.91(3)	1.97(3)	2.843(2)	162(2)
N9	H9A	O3 ( $-x, 1-y, 1-z$ )	0.87(3)	2.30(3)	3.138(2)	161(2)
N9	H9B	O7 ( $1-x, 1-y, -z$ )	0.88(3)	2.00(3)	2.856(2)	163(2)
N9	H9C	N6 ( $x, -1+y, z$ )	0.98(3)	1.98(3)	2.931(3)	165(2)
N9	H9D	O7 ( $-1+x, y, z$ )	0.94(3)	1.99(3)	2.912(3)	169(2)
C6	H6	O6 ( $1+x, y, z$ )	0.987(19)	2.367(19)	3.348(2)	172.2(15)

**On a Midway Between Energetic Molecular Crystals and High-Density Energetic Salts:  
Crystal Engineering with Hydrogen Bonding Chains of Polynitro Bipyrazoles**

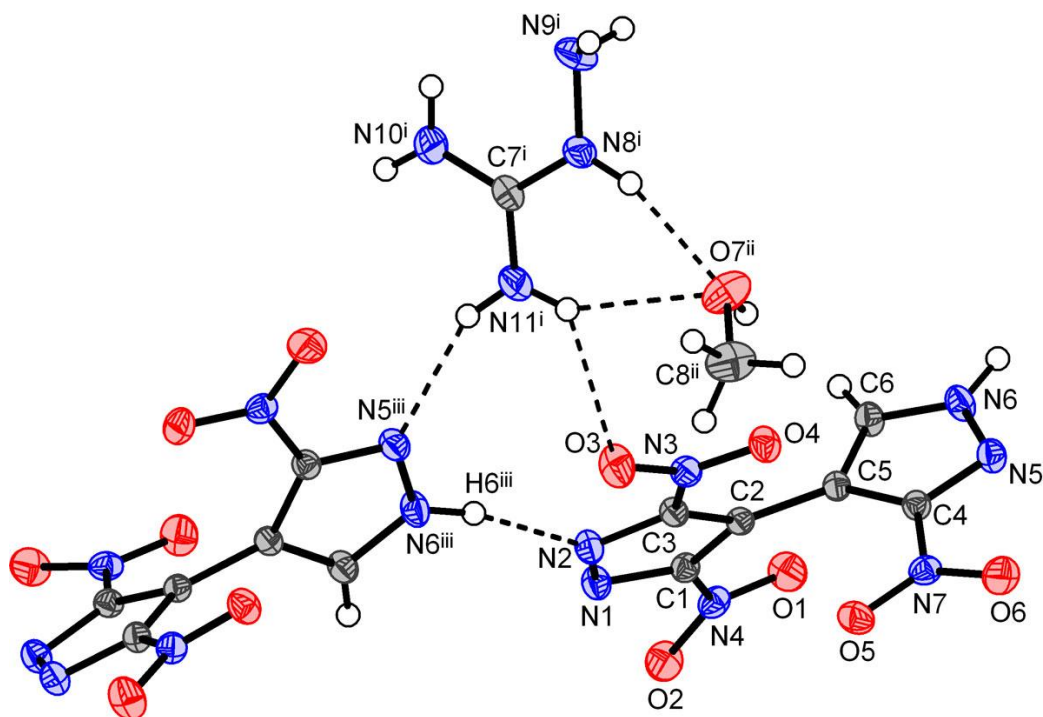


**Figure S16.** Molecular structure of (AG)(TriNBPZ)·MeOH (14·MeOH), showing the atom labeling scheme and thermal ellipsoids drawn at 50% probability level. Symmetry codes: (i) 0.5-*x*, 0.5-*y*, 0.5-*z*; (ii) *x*, 0.5-*y*, 0.5+*z*; (iii) 0.5+*x*, 1-*y*, *z*.

**Table S14.** Hydrogen-bond geometry (Å, °) for (AG)(TriNBPZ)·MeOH (14·MeOH).

Donor (D)	H-Atom	Acceptor (A)	D-H	H...A	D...A	∠DH...A
N6	H6	N2 ( <i>x</i> -0.5, 1- <i>y</i> , <i>z</i> )	0.919(19)	1.923(19)	2.8294(15)	168.4(16)
N8	H8	O7 (- <i>x</i> +0.5, <i>y</i> , - <i>z</i> )	0.852(17)	2.073(18)	2.8970(16)	162.4(15)
N9	H9A	O2 (- <i>x</i> +0.5, <i>y</i> , - <i>z</i> )	0.88(2)	2.27(2)	3.0740(15)	151.2(17)
N10	H10B	N1	0.863(19)	2.164(19)	3.0261(16)	176.6(16)
N11	H11A	N5 (- <i>x</i> , <i>y</i> -0.5, - <i>z</i> +0.5)	0.863(19)	2.191(19)	2.9959(16)	155.2(16)
N11	H11B	O3 (- <i>x</i> +0.5, - <i>y</i> +0.5, - <i>z</i> +0.5)	0.84(2)	2.469(19)	3.0490(16)	126.7(15)
N11	H11B	O7 (- <i>x</i> +0.5, <i>y</i> , - <i>z</i> )	0.84(2)	2.45(2)	3.1863(18)	146.6(16)
O7	H7	O1 (- <i>x</i> , 1- <i>y</i> , - <i>z</i> )	0.80(2)	2.52(2)	3.0746(14)	127.4(18)
O7	H7	O4 ( <i>x</i> , - <i>y</i> +0.5, <i>z</i> -0.5)	0.80(2)	2.34(2)	3.0528(14)	147.8(19)
C6	H5	O5 (- <i>x</i> , <i>y</i> -0.5, - <i>z</i> +0.5)	0.937(15)	2.473(15)	3.2640(15)	142.1(11)
C8	H8A	O2 ( <i>x</i> , -1+ <i>y</i> , <i>z</i> )	0.97(3)	2.65(3)	3.4036(19)	134(2)



**On a Midway Between Energetic Molecular Crystals and High-Density Energetic Salts:  
Crystal Engineering with Hydrogen Bonding Chains of Polynitro Bipyrazoles**

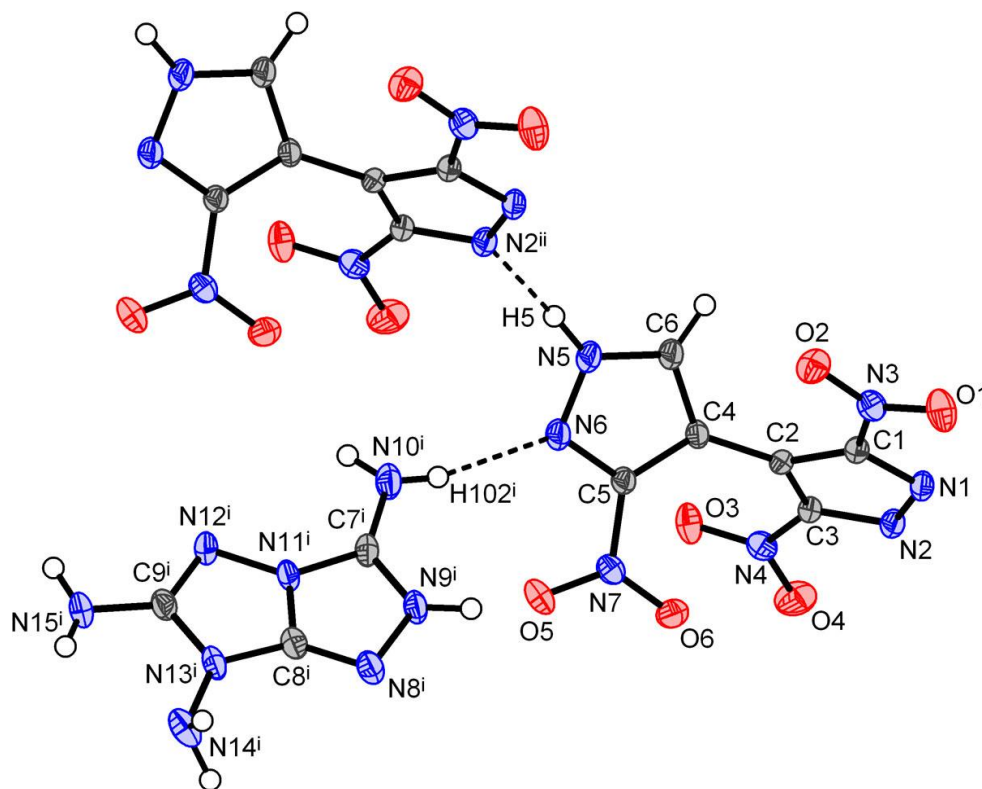


**Figure S17.** Molecular structure of (TATOT)(TriNBPZ) (**15**), showing the atom labeling scheme and thermal ellipsoids drawn at 50% probability level. Symmetry codes: (i)  $x, 1+y, z$ ; (ii)  $-1+x, y, z$ .

**Table S15.** Hydrogen-bond geometry (Å, °) for structure of (TATOT)(TriNBPZ) (**15**).

Donor (D)	H-Atom	Acceptor (A)	D-H	H...A	D...A	∠DH...A
N5	H5	N2 (-1+x, y, z)	0.90(4)	1.89(4)	2.784(3)	169(3)
N9	H9	O5 (x, -1+y, z)	0.90(3)	2.66(3)	3.123(3)	113(2)
N9	H9	N1 (-x+1.5,y-0.5, -z+1.75)	0.90(3)	1.93(3)	2.810(3)	165(3)
N10	H101	O4 (-1+x, -1+y, z)	0.85(5)	2.49(5)	2.935(3)	113(4)
N10	H102	N6 (x, -1+y, z)	0.83(4)	2.12(4)	2.932(3)	166(3)
N14	H141	N12 (y, 1+x, 2-z)	0.96(5)	2.41(4)	3.302(4)	153(3)
N14	H142	O4 (-1+x, y, z)	0.88(4)	2.55(4)	3.272(3)	141(3)
N15	H151	N8 (-1+y, x, 2-z)	0.90(4)	2.20(4)	3.090(4)	169(3)
N15	H152	O1 (-1.5+y, -x+1.5, z+0.25)	0.85(4)	2.63(4)	3.043(3)	111(3)
N15	H152	O3 (-1+y, x, 2-z)	0.85(4)	2.60(4)	3.342(3)	147(3)
N15	H152	N14	0.85(4)	2.44(3)	2.851(4)	110(3)



**On a Midway Between Energetic Molecular Crystals and High-Density Energetic Salts:  
Crystal Engineering with Hydrogen Bonding Chains of Polynitro Bipyrazoles**

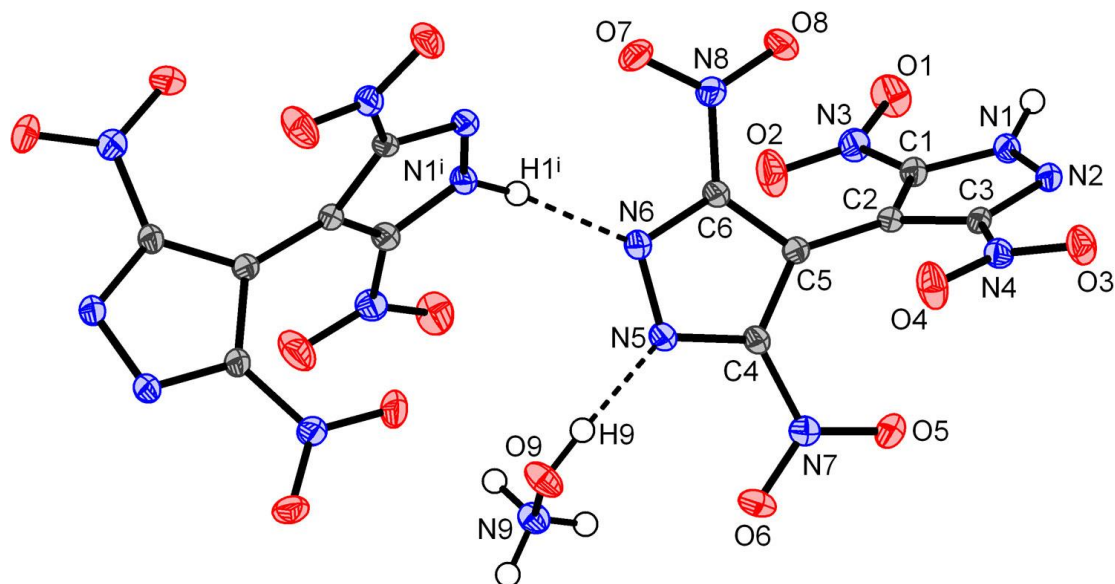


**Figure S18.** Molecular structure of **NH<sub>3</sub>OH(TNBPZ) (17)**, showing the atom labeling scheme and thermal ellipsoids drawn at 50% probability level. Symmetry code: (i) 0.5+x, 0.5-y, -0.5+z.

**Table S16.** Hydrogen-bond geometry (Å, °) for structure of **NH<sub>3</sub>OH(TNBPZ) (17)**.

Donor (D)	H-Atom	Acceptor (A)	D-H	H...A	D...A	∠DH...A
N1	H1	N6 (-0.5+x, -y+0.5, z+0.5)	0.92(4)	1.89(4)	2.766(3)	158(3)
O9	H9	N5	0.89(4)	1.80(5)	2.691(3)	175(4)
N9	H91	O1 (x+0.5, -y+0.5, -0.5+z)	0.90(6)	2.50(5)	3.190(3)	134(4)
N9	H91	O7 (x+0.5, -y+0.5, z+0.5)	0.90(6)	2.43(5)	3.106(3)	132(4)
N9	H91	N2 (1+x, y, z)	0.90(6)	2.48(5)	3.081(3)	125(4)
N9	H92	O6	0.85(4)	2.57(4)	3.168(3)	128(3)
N9	H92	O9 (x, -y, z+0.5)	0.85(4)	2.42(4)	3.241(3)	162(3)
N9	H93	O3 (1+x, y, z)	0.88(5)	2.47(5)	2.979(3)	118(4)
N9	H93	O7 (x+0.5, -0.5+y, z)	0.88(5)	2.19(5)	3.002(3)	153(4)

**On a Midway Between Energetic Molecular Crystals and High-Density Energetic Salts:  
Crystal Engineering with Hydrogen Bonding Chains of Polynitro Bipyrazoles**

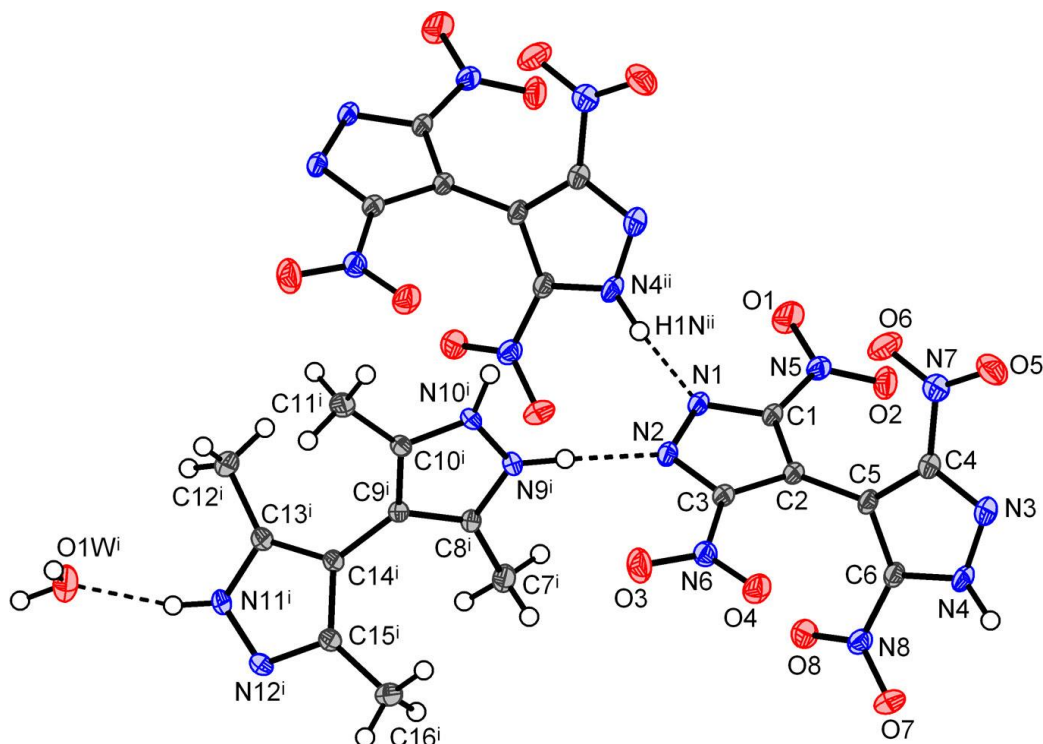


**Figure S19.** Molecular structure of **(Me<sub>4</sub>BpzH)(TNBPZ)·H<sub>2</sub>O (18·H<sub>2</sub>O)**, showing the atom labeling scheme and thermal ellipsoids drawn at 45% probability level. Symmetry code: (i) (i) 1+x, 1+y, z; (ii) x, 1+y, z.

**Table S17.** Hydrogen-bond geometry (Å, °) for **(Me<sub>4</sub>BpzH)(TNBPZ)·H<sub>2</sub>O (18·H<sub>2</sub>O)**.

Donor (D)	H-Atom	Acceptor (A)	D-H	H...A	D...A	∠DH...A
N4	H1N	N1 (x, -1+y, z)	0.93(4)	1.84(4)	2.763(3)	171(4)
N9	H2N	N2 (-1+x, -1+y, z)	0.96(4)	1.87(4)	2.823(3)	178(3)
N10	H3N	N12 (-1+x, y, z)	0.92(3)	1.86(3)	2.778(3)	173(3)
N11	H4N	O1W	0.88(4)	1.97(4)	2.814(3)	159(4)
O1W	H1W	N3 (1-y, x, -0.25+z)	0.94(4)	2.62(6)	3.297(3)	130(5)
O1W	H2W	O1 (2-y, x, -0.25+z)	0.94(4)	2.02(5)	2.880(3)	152(6)
C7	H7A	O7 (-1+x, y, z)	0.98	2.78	3.499(3)	130
C7	H7B	N3	0.98	2.58	3.488(3)	155
C7	H7C	O6 (x, -1+y, z)	0.98	2.55	3.346(3)	138
C11	H11A	O7 (-y, -1+x, -0.25+z)	0.98	2.70	3.665(3)	168
C11	H11B	O8 (1-y, -1+x, -0.25+z)	0.98	2.61	3.555(3)	162
C12	H12B	O5	0.98	2.81	3.425(4)	122

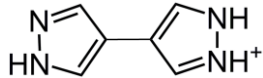
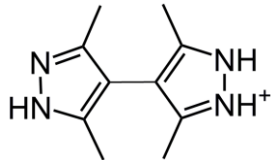
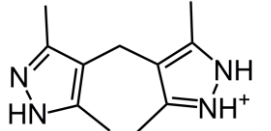
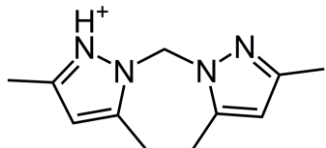
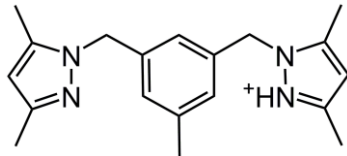
**On a Midway Between Energetic Molecular Crystals and High-Density Energetic Salts:  
Crystal Engineering with Hydrogen Bonding Chains of Polynitro Bipyrazoles**

C12	H12B	O3 (-1+x, y, z)	0.98	2.79	3.615(3)	142
C12	H12C	O2 (1-y, x, -0.25+z)	0.98	2.70	3.335(3)	123
C16	H16B	O2 (1-y, -1+x, -0.25+z)	0.98	2.42	3.358(3)	161

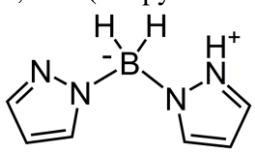
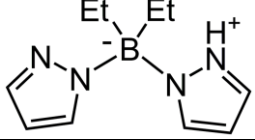
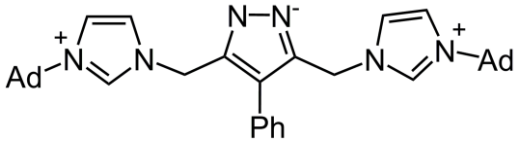
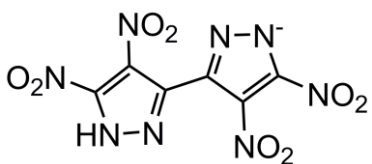
---

**On a Midway Between Energetic Molecular Crystals and High-Density Energetic Salts: Crystal Engineering with Hydrogen Bonding Chains of Polynitro Bipyrazoles**

**Table S18.** A survey of crystal structures exhibiting very strong hydrogen bonding between conjugate acid/base pyrazole pairs (pyrazolium cation to neutral pyrazole,  $\text{pzH}_2^+ \cdots \text{pzH}$  or neutral pyrazole to pyrazolate anion,  $\text{pzH} \cdots \text{pz}^-$ )

Type	Pyrazole	Compound	N...N/ Å	CSD Refcode	Ref.
<b><math>\text{pzH}_2^+ \cdots \text{pzH}</math></b>	Pyrazole	<b>I</b> [H( <b>I</b> ) <sup>+</sup> ][ <b>I</b> ] (Picrate) <sup>−</sup>	2.663	ENINIA	S1
	3,5-Dimethylpyrazole	<b>II</b> [H( <b>II</b> ) <sup>+</sup> ][ <b>II</b> ](2-Hydroxybenzoate) <sup>−</sup>	2.709	ODOHIZ	S2
		[H( <b>II</b> ) <sup>+</sup> ][ <b>II</b> ](CF <sub>3</sub> SO <sub>3</sub> ) <sup>−</sup>	2.634	WEHDET	S3
	3,4,5-Tribromopyrazole	<b>III</b> [H( <b>III</b> ) <sup>+</sup> ][ <b>III</b> ] Br <sup>−</sup>	2.609	XIRVAX	S4
	1H-Indazole	<b>IV</b> [H( <b>IV</b> ) <sup>+</sup> ][ <b>IV</b> ] (Ru( <b>IV</b> )(CO)Cl <sub>4</sub>	2.685	OKACEK	S5
	3-Methyl-4,5-dihydro-2H-naphtho(1,2-d)-pyrazole	<b>V</b> [H( <b>V</b> ) <sup>+</sup> ][ <b>V</b> ] Br <sup>−</sup>	2.714	GUFKOH	S6
		H( <b>VI</b> ) <sup>+</sup> [H( <b>VI</b> ) <sup>+</sup> ]Br <sup>−</sup> · H <sub>2</sub> O	2.712	YASTAO	S7
		[H( <b>VI</b> ) <sup>+</sup> ](ClO <sub>4</sub> ) <sup>−</sup> · H <sub>2</sub> O	2.742	YASTES	S7
		H( <b>VII</b> ) <sup>+</sup> [H( <b>VII</b> ) <sup>+</sup> ](2,5-dicarboxyterephthalate)	2.691	ZEBDIW	S8
		[H( <b>VII</b> ) <sup>+</sup> ] (Picrate) <sup>−</sup> · MeCN	2.705	ZEBDIW01	S9
			2.785	SASLAB	S10
		H( <b>VIII</b> ) <sup>+</sup> [H( <b>VIII</b> ) <sup>+</sup> ] (I <sub>3</sub> ) <sup>−</sup>	2.664	KUBHEW	S11
		[H( <b>VIII</b> ) <sup>+</sup> ][ <b>VIII</b> ]	2.698	NOLVIV	S12
		(HO <sub>2</sub> CCH <sub>2</sub> PO <sub>3</sub> H) <sup>−</sup> · MeOH			
		[H( <b>VIII</b> ) <sup>+</sup> ] (HO <sub>2</sub> CCH <sub>2</sub> PO <sub>3</sub> H) <sup>−</sup>	2.764	NOLVUH	S12
		H( <b>IX</b> ) <sup>+</sup> [H( <b>IX</b> ) <sup>+</sup> ] <sub>2</sub> (UCl <sub>6</sub> ) <sup>2−</sup>	2.734	IJUYIX	S13
		H( <b>X</b> ) <sup>+</sup> [H( <b>X</b> ) <sup>+</sup> ] <sub>2</sub> (FeCl <sub>4</sub> ) <sup>2−</sup>	2.668	CINTAX	S14

**On a Midway Between Energetic Molecular Crystals and High-Density Energetic Salts: Crystal Engineering with Hydrogen Bonding Chains of Polynitro Bipyrzoles**

Type	Pyrazole	Compound	N...N/ Å	CSD Refcode	Ref.
	1,2-Bis(1H-pyrazol-1-yl)benzene	<b>XI</b>	2.712	SUNTUR	S15
		<b>XII</b>	2.719	SOKNEL	S16
		<b>XIII</b>	2.773	WEQPEN	S17
<b>pzH...pz</b>		<b>XIV</b> <sup>+</sup>	2.635	VUPGUJ	S18
	3,5-Dinitroindazole	<b>XV</b>	2.727	VUXTAJ	S19
		<b>XVI</b> <sup>+</sup>	2.815		S20

### 8.8.4. Computations

Quantum chemical calculations were carried out using the Gaussian G09 program package.<sup>[S31]</sup> The enthalpies (H) and free energies (G) were calculated using the complete basis set (CBS) method of Petersson and co-workers in order to obtain very accurate energies. The CBS models use the known asymptotic convergence of pair natural orbital expressions to extrapolate from calculations using a finite basis set to the estimated CBS limit. CBS-4 begins with an HF/3-21G(d) geometry optimization; the zero point energy is computed at the same level. It then uses a large basis set SCF calculation as a base energy, and an MP2/6-31+G calculation with a CBS extrapolation to correct the energy through second order. An MP4(SDQ)/6-31+ (d,p) calculation is used to approximate higher order contributions. In this study, we applied the modified CBS.

Heats of formation of ionic compounds were calculated using the atomization method (equation 1) using room temperature CBS-4M enthalpies summarized in **Table S19**.<sup>[S32,S33]</sup>

$$\Delta_f H^\circ_{(g, M, 298)} = H_{(Molecule, 298)} - \sum H^\circ_{(Atoms, 298)} + \sum \Delta_f H^\circ_{(Atoms, 298)} \quad (1)$$

**Table S19.** CBS-4M electronic enthalpies for atoms C, H, N and O and their literature values for atomic  $\Delta_f H^\circ_{298}$  / kJ mol<sup>-1</sup>

	$-H^{298}$ / a.u.	NIST <sup>[S34]</sup>
H	0.500991	218.2
C	37.786156	717.2
N	54.522462	473.1
O	74.991202	249.5

In the case of the ionic compounds, the lattice energy ( $U_L$ ) and lattice enthalpy ( $\Delta H_L$ ) were calculated from the corresponding X-ray molecular volumes according to the equations provided by *Jenkins* and *Glasser*.<sup>[S35]</sup> With the calculated lattice enthalpy the gas-phase enthalpy of formation was converted into the solid state (standard conditions) enthalpy of formation. These molar standard enthalpies of formation ( $\Delta H_m$ ) were used to calculate the molar solid state energies of formation ( $\Delta U_m$ ) according to equation 2.

$$\Delta U_m = \Delta H_m - \Delta nRT \quad (2)$$

( $\Delta n$  being the change of moles of gaseous components)

The calculation results are summarized in **Tables S20** and **S21**.

**On a Midway Between Energetic Molecular Crystals and High-Density Energetic Salts:  
Crystal Engineering with Hydrogen Bonding Chains of Polynitro Bipyrazoles**

**Table S20.** CBS-4M results and calculated gas-phase enthalpies.

Ion	M [g mol <sup>-1</sup> ] [a]	-H <sup>298</sup> [b] / a.u.	$\Delta_f H^\circ(\text{g,M})$ / kJ mol <sup>-1</sup> [c]
<b>TriNBPz<sup>-</sup></b>	268.13	1062.92568	82.0
<b>HTNBPz<sup>-</sup></b>	313.12	1267.22419	61.5
<b>K<sup>+</sup></b>	39.1	599.03597	487.4
<b>NH<sub>4</sub><sup>+</sup></b>	18.1	56.796608	635.3
<b>N<sub>2</sub>H<sub>5</sub><sup>+</sup></b>	66.1	112.030523	773.4
<b>NH<sub>3</sub>OH<sup>+</sup></b>	34.04	131.863249	686.4
<b>TATOT<sup>+</sup></b>	155.14	555.474133	1080.0

[a] Molecular weight; [b] CBS-4M electronic enthalpy; [c] gas phase enthalpy of formation;

**Table S21.** Calculation results.

Compound	$\Delta_f H^\circ(\text{g,M})$ / kJ mol <sup>-1</sup> [a]	$V_M$ / nm <sup>3</sup> [b]	$\Delta U_L$ kJ mol <sup>-1</sup> [c]	$\Delta H_L$ kJ mol <sup>-1</sup> [d]	$\Delta_f H^\circ(\text{s})$ kJ mol <sup>-1</sup> [e]	$\Delta_f U(\text{s})$ kJ kg <sup>-1</sup> [f]
<b>9·H<sub>2</sub>O</b>	–	0.293545	521.5	525.2	–197.6	–538.9
<b>11</b>	771.4	0.286040	459.9	464.8	303.7	1091.1
<b>12</b>	858.4	0.286720	459.6	464.5	390.9	1388.6
<b>13·H<sub>2</sub>O</b>	–	0.300320	518.5	525.9	–50.4	–72.0
<b>15</b>	1166.0	0.422661	416.4	421.4	740.7	1837.9
<b>17</b>	751.4	0.318688	447.3	452.2	295.7	934.0

[a] gas phase enthalpy of formation; [b] molecular volumes taken from X-ray structures and corrected to room temperature; [c] lattice energy (calculated using Jenkins and Glasser equations); [d] lattice enthalpy (calculated using Jenkins and Glasser equations); [e] standard solid state enthalpy of formation; [f] solid state energy of formation.

## 8.8.5. References

- [S1] Boldog, I.; Rusanov, E. B.; Chernega, A. N; Sieler, J.; Domasevitch, K. V. *Angew. Chem. Int. Ed.* **2001**, *40*, 3435-3438.
- [S2] Johnson, A.W. *J. Chem. Soc.* **1946**, 1009-1014.

**On a Midway Between Energetic Molecular Crystals and High-Density Energetic Salts:  
Crystal Engineering with Hydrogen Bonding Chains of Polynitro Bipyrazoles**

- [S3] Iwai, I.; Tomita, K.; *Chem. Pharm. Bull.* **1961**, 9, 976-979.
- [S4] Barton, D. H. R.; Dawes, C. C.; Franceschi, G.; Foglio, M.; Ley, S. V. *J. Chem. Soc. Perkin Trans 1* **1980**, 643.
- [S5] Fegley, M. F.; Bortnick, N. M.; McKeever, C. H. *J. Am. Chem. Soc.*, **1957**, 79, 4140-4144.
- [S6] Arnold, Z. *Collect. Czech. Chem. Commun.* **1962**, 27, 2993-2995.
- [S7] Domasevitch, K. V.; Gospodinov, I.; Krautscheid, H.; Klapötke, T. M.; Stiertorfer, J. *New J. Chem.*, **2019**, 43, 1305–1312.
- [S8] Lednicer, D.; Hauser, C. R. N,N-dimethylaminomethylferrocene methiodide. *Org. Synth.*, **1973**, Coll. Vol. 5, 434.
- [S9] Stoe & Cie. *X-SHAPE*. Revision 1.06. Stoe & Cie GmbH, Darmstadt, Germany, **1999**; Stoe & Cie. *X-RED*. Version 1.22. Stoe & Cie GmbH, Darmstadt, Germany, **2001**.
- [S10] (a) Sheldrick, G. M. *Acta Crystallogr., Sect. A: Found. Crystallogr.*, **2008**, 64, 112. (b) Sheldrick, G. M. *Acta Crystallogr., Sect. C: Cryst. Struct. Commun.*, **2015**, 71, 3.
- [S11] Su, P.; Song, X.; Sun, R.; Xu, X. *Acta Crystallogr., Sect. E: Cryst. Commun.* **2016**, 72, 861.
- [S12] Lopez, C.; Claramunt, R. M.; Garcia, M. A.; Pinilla, E.; Torres, M. R.; Alkorta, I.; Elguero, J. *Cryst. Growth Des.* **2007**, 7, 1176.
- [S13] Zubarev, D. Yu.; Filimonova, N. B.; Timokhina, E. N.; Bozhenko, K. V.; Moiseeva, N. I.; Nefedov, S. E.; Dolin, S. P.; Gekhman, A. E.; Moiseev, I. I. *Dokl. Akad. Nauk SSSR (Russ.) (Proc. Nat. Acad. Sci. USSR)* **2005**, 404, 650.
- [S14] Pejic, M.; Popp, S.; Bolte, M.; Wagner, M.; Lerner, H.-W. *Z. Naturforsch., B: Chem. Sci.* **2014**, 69, 83.
- [S15] Kuhn, P.-S.; Meier, S.M.; Jovanovic, K.K.; Sandler, I.; Freitag, L.; Novitchi, G.; Gonzalez, L.; Radulovic, S.; Arion, V. B. *Eur. J. Inorg. Chem.* **2016**, 1566.



**On a Midway Between Energetic Molecular Crystals and High-Density Energetic Salts:  
Crystal Engineering with Hydrogen Bonding Chains of Polynitro Bipyrazoles**

- [S16] Bertolasi, V.; Gilli, P.; Ferretti, V.; Gilli, G.; Fernandez-Castano, C. *Acta Crystallogr., Sect. B: Struct.Sci.* **1999**, *55*, 985.
- [S17] Domasevitch, K.V.; Boldog, I. () *Acta Crystallogr., Sect. C: Cryst. Struct. Commun.*, **2005**, *61*, o373.
- [S18] Singh, U. P.; Tomar, K.; Kashyap, S.; Verma, P. *J. Chem. Cryst.* **2017**, *47*, 69.
- [S19] Hunger, J. *CSD Communication (Private Communication)*, **2017**.
- [S20] Singh, U. P.; Goel, N.; Singh, G.; Srivastava, P. *Supramol. Chem.* **2012**, *24*, 285.
- [S21] Goswami, A.; Samanta, P. N.; Das, K K; Mondal, R. *CSD Communication (Private Communication)*, **2015**.
- [S22] Singh, U. P.; Narang, S. *CrystEngComm* **2014**, *16*, 7777.
- [S23] Carretas, J. M.; Cui, J.; Cruz, A.; Santos, I. C.; Maralo, J. *Zh. Strukt. Khim. (Russ.) (J. Struct. Chem.)* **2015**, *56*, 189.
- [S24] Hernandez, L.; Quevedo-Acosta, Y.; Vazquez, K.; Gomez-Trevino, A.; Zarate-Ramos, J. J.; Macias, M. A.; Hurtado, J. J. *Vector-Borne and Zoonotic Diseases* **2018**, *18*, 548.
- [S25] Ivashchuk, O.; Sorokin, V. I. *Tetrahedron* **2009**, *65*, 4652.
- [S26] Jung, O.-S.; Jeong, J. H.; Sohn, Y. S. *Organometallics* **1991**, *10*, 2217.
- [S27] Dabrowski, M.; Lulinski, S.; Madura, I.; Serwatowski, J.; Zachara, J. *J. Organomet. Chem.* **2000**, *597*, 190.
- [S28] Georgiou, M.; Wockel, S.; Konstanzer, V.; Dechert, S.; John, M.; Meyer, F. Z. *Naturforsch., B: Chem. Sci.* **2009**, *64*, 1542.
- [S29] Gzella, A.; Wrzeciono, U.; Borowiak, T. *Acta Crystallogr. Sect. C: Cryst. Struct. Commun.* **1989**, *45*, 644.
- [S30] Tang, Y.; He, C.; Imler, G. H.; Parrish D. A.; Shreeve, J. M. *J. Mat. Chem. A*, **2018**, *6*, 5136.

**On a Midway Between Energetic Molecular Crystals and High-Density Energetic Salts:  
Crystal Engineering with Hydrogen Bonding Chains of Polynitro Bipyrzoles**

- [S31] Frisch, M. J.; Trucks, G. W.; Schlegel, H. B.; Scuseria, G. E.; Robb, M. A.; Cheeseman, J. R.; Scalmani, G.; Barone, V.; Mennucci, B.; Petersson, G. A.; Nakatsuji, H.; Caricato, M.; Li, X.; Hratchian, H. P.; Izmaylov, A. F.; Bloino, J.; Zheng, G.; Sonnenberg, J. L.; Hada, M.; Ehara, M.; Toyota, K.; Fukuda, R.; Hasegawa, J.; Ishida, M.; Nakajima, T.; Honda, Y.; Kitao, O.; Nakai, H.; Vreven, T.; Montgomery, Jr., J. A.; Peralta, J. E.; Ogliaro, F.; Bearpark, M.; Heyd, J. J.; Brothers, E.; Kudin, K. N.; Staroverov, V. N.; Kobayashi, R.; Normand, J.; Raghavachari, K.; Rendell, A.; Burant, J. C.; Iyengar, S. S.; Tomasi, J.; Cossi, M.; Rega, N.; Millam, J. M.; Klene, M.; Knox, J. E.; Cross, J. B.; Bakken, V.; Adamo, C.; Jaramillo, J.; Gomperts, R.; Stratmann, R. E.; Yazyev, O.; Austin, A. J.; Cammi, R.; Pomelli, C.; Ochterski, J. W.; Martin, R. L.; Morokuma, K.; Zakrzewski, V. G.; Voth, G. A.; Salvador, P.; Dannenberg, J. J.; Dapprich, S.; Daniels, A. D.; Farkas, O.; Foresman, J. B.; Ortiz, J. V.; Cioslowski, J.; Fox, D. J. *Gaussian 09 A.02*, Gaussian, Inc., Wallingford, CT, USA, **2009**.
- [S32] (a) Ochterski, J. W.; Petersson, G. A.; Montgomery Jr., J. A.; *J. Chem. Phys.* **1996**, *104*, 2598–2619; (b) Montgomery Jr., J. A.; Frisch, M. J.; Ochterski, J. W.; Petersson, G. A. *J. Chem. Phys.* **2000**, *112*, 6532–6542.
- [S33] (a) Curtiss, L. A.; Raghavachari, K.; Redfern, P. C.; Pople, J. A. *J. Chem. Phys.* **1997**, *106*, 1063–1079; (b) Byrd, E. F. C.; Rice, B. M. *J. Phys. Chem. A* **2006**, *110*, 1005–1013; (c) Rice, B. M.; Pai, S. V.; Hare, J. *Comb. Flame* **1999**, *118*, 445–458.
- [S34] Lindstrom, P. J.; Mallard, W. G. (Eds), NIST Standard Reference Database Number 69, <http://webbook.nist.gov/chemistry/> (accessed September **2019**).
- [S35] (a) Jenkins, H. D. B.; Roobottom, H. K.; Passmore, J. *Inorg. Chem.* **1999**, *38*, 3609–3620. (b) Jenkins, H. D. B.; Tudela, D.; Glasser, L. *Inorg. Chem.* **2002**, *41*, 2364–2367.

## 9. Energetic Derivatives of 3,3',5,5'-Tetranitro-4,4'- bipyrazole (TNBPz): Synthesis, Characterization and Properties

Ivan Gospodinov, Kostiantyn V. Domasevitch, Cornelia C. Unger, Thomas M. Klapötke and Jörg Stierstorfer

To Be Submitted to *New J. Chem.*

**Abstract:** 3,3',5,5'-tetranitro-4,4'-bipyrazole monohydrate (TNBPz, **1**·H<sub>2</sub>O) is an excellent precursor for the synthesis of new energetic materials (**2**–**12**). Several nitrogen-rich salts (*e.g.* guanidinium, aminoguanidinium, hydrazinium, ammonium and hydroxylammonium) were prepared from **1**·H<sub>2</sub>O by neutralization reactions. In addition, the *N*-methylation and *N*-amination of compound TNBPz was investigated and is reported. All new synthesized energetic materials were fully characterized by NMR (<sup>1</sup>H, <sup>13</sup>Ca, <sup>14</sup>N, and <sup>15</sup>N) spectroscopy, infrared spectroscopy, differential thermal analysis (DTA) and elemental analysis. Compounds **2**, **4**–**8** and **10** were characterized with single crystal X-ray diffraction. The heats of formation for compounds **2**, **4**–**6**, **8**, **11** and **12** were calculated using the atomization method based on CBS-4M enthalpies. Several detonation parameters, such as detonation pressure, velocity and energy, were calculated by using the X-ray densities and the calculated standard molar enthalpies of formation. The sensitivities of all energetic materials toward external stimuli were tested according to the BAM standards. In addition, the toxicity toward vibrio fischeri bacteria of few energetic salts (**3** and **4**) is reported.

### 9.1. Introduction

The research on new energetic materials has increased in the last decades due to arising safety regulations.<sup>[1]</sup> The key in the development of new energetic materials is to design high energy density materials with good detonation parameters and low sensitivity.<sup>[2]</sup> Currently used high explosives (*e.g.* TNT and RDX) show high toxicity which makes the research on new energetic materials based on nitrogen-rich heterocycles very attractive. The functionalization of azoles with different explosphore groups (*e.g.* –NO<sub>2</sub>, –ONO<sub>2</sub>, –NHNO<sub>2</sub>, –C(NO<sub>2</sub>)<sub>3</sub>) is a good approach for the synthesis of new high energy dense

## Energetic Derivatives of 3,3',5,5'-Tetranitro-4,4'-bipyrazole (TNBPz): Synthesis, Characterization and Properties

materials.<sup>[3]</sup> There are few strategies that can be used by the design of new energetic materials in order to combine performance with sensitivity; formation of nitrogen-rich salts, introduction of alternating NO<sub>2</sub>/NH<sub>2</sub> groups in the molecule and the introduction of a conjugation.<sup>[4,5]</sup>

The chemistry of C-nitrated nitrogen-rich heterocyclic rings has been extensively investigated in the last decade.<sup>[6]</sup> **Figure 1** shows few examples of polynitrated nitrogen-rich heterocycles which exhibit very interesting properties, such as high detonation velocities and pressure, but show also good stability toward external stimuli. The formation of nitrogen-rich salts with polynitrated pyrazole derivatives leads mostly to the formation of energetic materials with high densities and good thermal stability as a result of their high lattice energy.<sup>[7,8]</sup> Using nitrogen-rich cations for the formation of energetic salts leads to a stabilization of the structure, due to high positive heat of formation of the cation and the potential intra- and intermolecular hydrogen bond formation.<sup>[9,10]</sup>

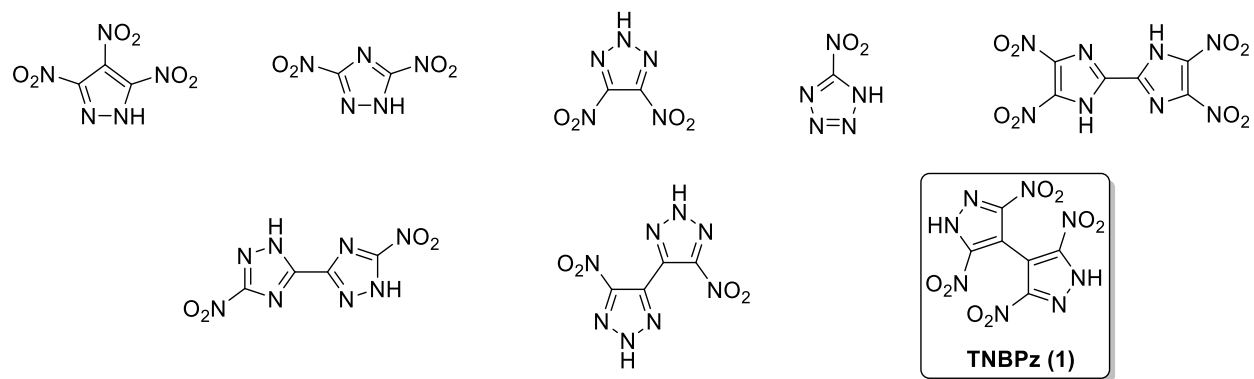


**Figure 1.** Literature known fully C-nitrated heterocyclic compounds and the investigated nitro pyrazole **1·H<sub>2</sub>O** during this work.

However, the functionalization of 3,3',5,5'-tetranitro-4,4'-bipyrazole monohydrate (TNBPz, **1·H<sub>2</sub>O**) has not been reported and their energetic derivatives are not known. The extensive synthesis of compound **1·H<sub>2</sub>O** have been recently reported and it exhibits excellent properties to be starting material for new energetic materials.<sup>[11]</sup> In our study the formation of energetic salts with **1·H<sub>2</sub>O** and the *N*-methylation and *N*-amination of **1·H<sub>2</sub>O** was investigated. Many energetic materials were reported **2–12** and fully characterized. All new synthesized energetic materials were experimentally and theoretically investigated.

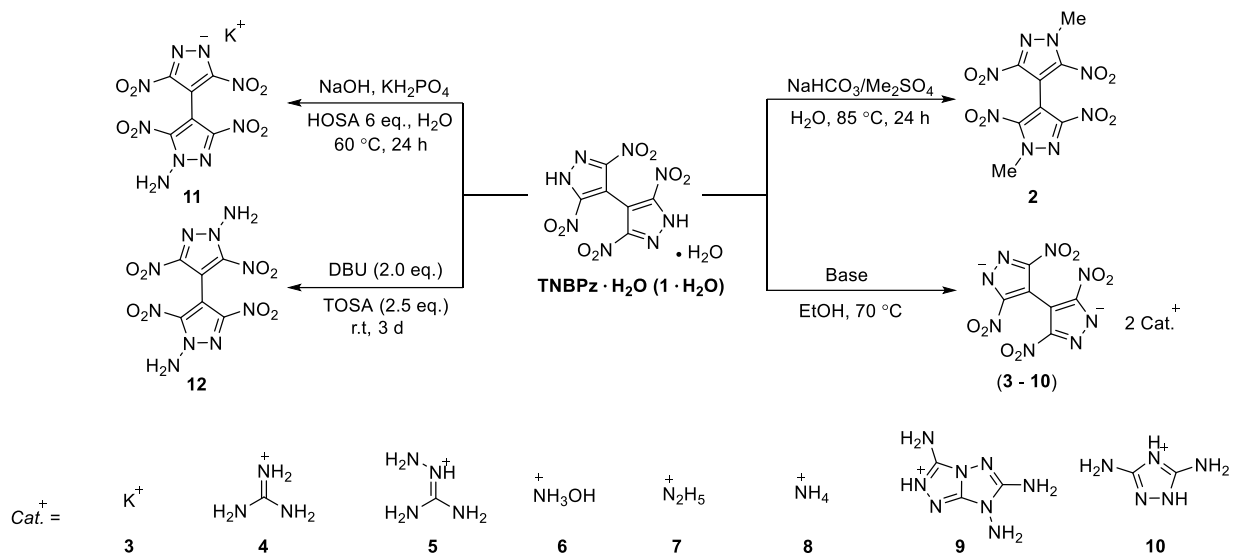
## 9.2. Results and discussion

### 9.2.1. Synthesis

The starting material 3,3',5,5'-tetranitro-4,4'-bipyrazole monohydrate (TNBPz, **1·H<sub>2</sub>O**) was obtained by nitration of the 4,4'-bipyrazole scaffold. The synthesis of **1·H<sub>2</sub>O** has been reported previously in the literature.<sup>[11]</sup> Numerous new energetic compounds (**2–12**) were obtained by reacting TNBPz (**1·H<sub>2</sub>O**) with several nitrogen-rich bases or further *N*-functionalizing TNBPz (**Scheme 1**). The resulting salts were isolated in good yields and are stable at room temperature.

The *N*-functionalization of TNBPz (**1·H<sub>2</sub>O**) *e.g.* *N*-methylation and *N*-amination was extensively investigated. The synthesis of 1,1'-dimethyl-3,3',5,5'-tetranitro-4,4'-bipyrazole ((Me)<sub>2</sub>TNBPz, **2**) has been previously reported in the literature, however we present a new and simpler procedure.<sup>[12]</sup> Hence, compound **2** was obtained by simple *N*-methylation of **1·H<sub>2</sub>O** with excess of dimethyl sulfate in the presence of a weak base. In addition, the *N*-amination of compound **1·H<sub>2</sub>O** was investigated and the effect of the amination reagent was extensively investigated. For this type of reactions, the well-known amination reagents hydroxylamine-*O*-sulfonic acid (HOSA) and *O*-*p*-toluenesulfonylhydroxylamine (TOSA) were selected. The reaction of compound **1·H<sub>2</sub>O** with HOSA in the presence of a buffer solution (NaOH/KH<sub>2</sub>PO<sub>4</sub>) did not yield the expected 1,1'-diamino-3,3',5,5'-tetranitro-4,4'-bipyrazole ((NH<sub>2</sub>)<sub>2</sub>TNBPz, **12**) but resulted in the formation of the potassium salt of 4-(1-amino-3,5-dinitropyrazolyl)-3',5'-dinitropyrazolate (**11**). Further study of this reaction did not provide the desired compounds **12**. Hence, TNBPz was reacted furtherly with TOSA in an CH<sub>3</sub>CN/DCM solution with the presence of a weak organic base 1,8-diazabicyclo[5.4.0]undec-7-en (DBU). This resulted in 1,1'-diamino-3,3',5,5'-tetranitro-4,4'-bipyrazole ((NH<sub>2</sub>)<sub>2</sub>TNBPz, **12**). All reactions are shown in **Scheme 1**.

## Energetic Derivatives of 3,3',5,5'-Tetranitro-4,4'-bipyrazole (TNBPz): Synthesis, Characterization and Properties



**Scheme 1.** Synthesis of the energetic compounds **2–12** based on 3,3',5,5'-tetranitro-4,4'-bipyrazole monohydrate (**1·H<sub>2</sub>O**).

### 9.2.2. Single crystal X-ray diffraction studies

During this work the crystal structures of **2**, **4–8** and **10** were determined by low-temperature X-ray diffraction. Selected data and parameters from the low-temperature X-ray data collection and refinements are given in the Supporting Information (**Tables S1** and **S2**). Compounds **2**, **4–6**, **8** and **10** crystallize anhydrously whereas compound **7** crystallizes as a hemihydrate.

Compound **2** crystallizes monoclinic space group *Cc* with 4 formulas per unit cell. The lattice parameters are  $a = 8.9141(5) \text{ \AA}$ ,  $b = 22.3417(15) \text{ \AA}$ ,  $c = 7.8114(4) \text{ \AA}$  and  $\beta = 124.432(2)^\circ$ , giving a cell volume of  $1283.13(13) \text{ \AA}^3$  with calculated density of  $1.771 \text{ g cm}^{-3}$ . The asymmetric unit includes one unit of **2**. It itself consists out of two planar pyrazole-rings ( $|\theta_{\text{out of plane}}| \leq 1.1^\circ$ ) with averaged dihedral angle of  $73.2^\circ$  between both. This twist is higher compared to that found in solventfree TNBPz ( $71.44(5)^\circ$ ), but lower in comparison to TNBPz·H<sub>2</sub>O (**1·H<sub>2</sub>O**) ( $78.99(6)^\circ$ ).<sup>[11]</sup> The bond lengths and angles found in the pyrazole-rings are similar to those of the ionic derivatives of the TNBPz<sup>−1</sup> anion (e.g. compound **6**), but are generally more distinct in each ring due to the abolished indistinguishability of the nitrogen through the methyl-groups. The lengths of the nitrogen-nitrogen bonds are  $1.330 \text{ \AA}$  and  $1.340 \text{ \AA}$ . In comparison the carbon-nitrogen bonds closer to the methyl-group are longer with each having a length of  $1.355 \text{ \AA}$ , while the other carbon-

## Energetic Derivatives of 3,3',5,5'-Tetranitro-4,4'-bipyrazole (TNBPz): Synthesis, Characterization and Properties

nitrogen bonds are shorter (1.325 Å, 1.329 Å). In return the carbon-carbon bonds closer to the methyl-group with lengths of 1.382 Å and 1.384 Å are shorter compared to the other carbon-carbon bonds with lengths of 1.399 Å and 1.403 Å. The angles at the ring-nitrogen are not similar anymore, with methylated nitrogen are widened (110.58°, 111.72°) and the angles at the other nitrogen are compressed (104.56°, 104.91°) compared to those found in **6**. The bond angles at the nitro-carbon more distant to the methyl-group are very similar to those of compound **6** (113.9°, 114.1°), while the nitro-carbon closer to the methyl-group are slightly compressed (109.4°, 109.6°). The carbon-carbon bond between the rings and the carbon-nitrogen bonds of the nitro-groups have aromatic character with a length of 1.465 Å and 1.438–1.447 Å, respectively. Compared to the nitro-groups the carbon-nitrogen bonds of the methyl-groups possess higher length of 1.469 Å and 1.472 Å, showing that they are in contrast not a part of the aromatic system. The nitrogen of the nitro-groups and carbon of the methyl-groups lie in the plane of its pyrazol ring ( $|\theta_{out\ of\ plane}| \leq 3.8^\circ$ ).

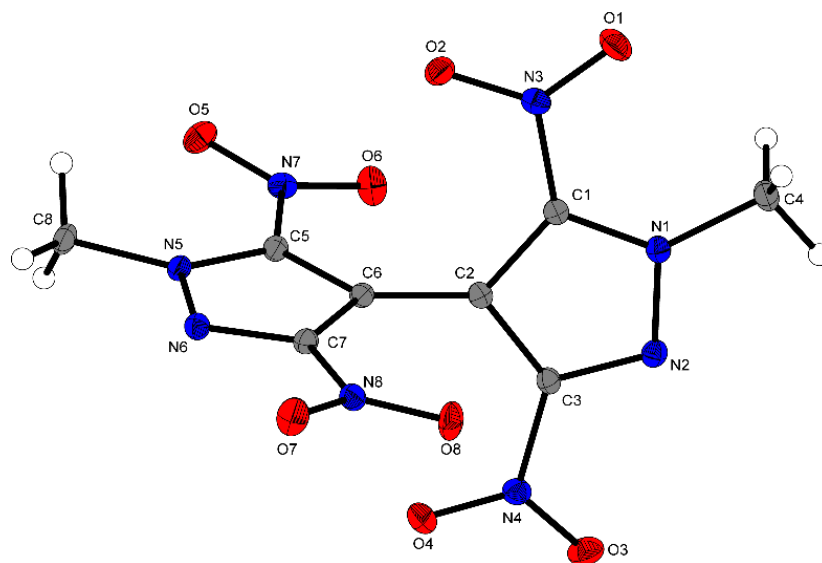


**Figure 2.** Molecular unit of 1,1'-dimethyl-3,3',5,5'-tetranitro-4,4'-bipyrazole (**2**) in the crystalline state. Ellipsoids correspond to 50% probability levels. Hydrogen radii are arbitrary. Selected bond lengths (Å) and angles [deg.]: N1–N2 1.329(3), N1–C1 1.356(4), N1–C4 1.466(4), C1–C2 1.382(3), C2–C6 1.465(4), C6–C7 1.399(3), O1–N3 1.231(3), N3–C1 1.438(3), N2–N1–C1 110.7(2), N2–N1–C4 118.1(2), C1–N1–C4 131.2(2), N2–C3–N4 118.6(2), O1–N3–C1 118.2(3), C1–C2–C6 129.2(2), C2–C6–C7 129.2(3), C1–N1–N2–C3 –0.8(3), C4–N1–N2–C3 178.2(2), C4–N1–C1–N3 1.6(4), N2–N1–C1–C2 1.1(3), C1–C2–C6–C7 –104.2(3), C1–C2–C6–C5 74.4(4), O1–N3–C1–N1 –13.7(4).

### Energetic Derivatives of 3,3',5,5'-Tetranitro-4,4'-bipyrazole (TNBPz): Synthesis, Characterization and Properties

The crystal structure of bis(guanidinium) 3,3',5,5'-tetranitro-4,4'-bipyrazolate (**4**) is shown in **Figure 3** with bond lengths and angles. Compound **3** crystallizes in the monoclinic space group  $P2_1/c$  with four molecules in the unit cell. The volume of the unit cell is  $1721.9(4) \text{ \AA}^3$  with lattice constants  $a = 10.7792(15)$ ,  $b = 17.441(12)$ ,  $c = 9.6177(15) \text{ \AA}$  and  $\beta = 107.766(15)^\circ$ . The calculated density at 298 K is  $1.63 \text{ g/cm}^3$ . The molecule of **4** can be divided in two components: the biyprazolate anion and the guanidinium cations. The bond lengths between the carbon and the nitrogen atoms in the guanidinium cation exhibit similar values of  $1.32 \text{ \AA}$  and  $1.34 \text{ \AA}$ . The average bond angle between the carbon atom and the nitrogen atoms in the cation is around  $120^\circ$ . Both pyrazole rings and their nitro groups have a similar arrangement. The planes which are defined through each ring are twisted by  $63.4(3)^\circ$  ( $C3-C2-C5-C6$ ) to each other. The N–O bonds of the nitro groups show the standard length for nitro groups of  $1.24 \text{ \AA}$ .<sup>[13]</sup> The bond lengths between N3–C1 of  $1.433(3) \text{ \AA}$ , N4–C3 of  $1.431(3) \text{ \AA}$ , N7–C4 of  $1.432(3) \text{ \AA}$  and N8–C6 of  $1.434(3) \text{ \AA}$  are close to the standard value for C–N single bonds of  $1.47 \text{ \AA}$ .<sup>[13]</sup> The bonds between N1–N2 ( $1.346(3) \text{ \AA}$ ), N1–C1 ( $1.347(3) \text{ \AA}$ ) and N2–C3 ( $1.349(3) \text{ \AA}$ ) all have similar lengths. The bonds between C1–C2 and C2–C3 have lengths of  $1.393(3) \text{ \AA}$  and  $1.391(3) \text{ \AA}$ . So, they all have the standard length for aromatic systems of these elements. The bond lengths and angles differ slightly from the ones of the anhydrous pyrazole.<sup>[14]</sup> The distance between C2 and C5, the atoms which connect both rings, is with  $1.467(3) \text{ \AA}$  between the standard length for C=C double bonds and C–C single bonds. A comparable C–C bond length between two nitrogen-rich aromatic rings can be observed in TKX-50 with  $1.444(3) \text{ \AA}$ .<sup>[15]</sup> The angles in the ring ( $106.96(18)^\circ$  ( $N2-N1-C1$ ),  $113.36(19)^\circ$  ( $N1-C1-C2$ )) coincide with the different bond lengths ( $1.346(3) \text{ \AA}$  ( $N1-N2$ ),  $1.391(3) \text{ \AA}$  ( $C2-C3$ )). This means the rings are slightly deformed. The angles in the nitro groups and between the nitro groups and the ring differ just very slightly among the four nitro groups ( $O3-N4-O4$   $123.0(2)^\circ$ ,  $O3-N4-C3$   $119.70(19)^\circ$ ,  $O5-N7-O6$   $122.82(19)^\circ$ ,  $O5-N7-C4$   $118.86(18)^\circ$ ,  $O1-N3-O2$   $123.1(2)^\circ$ ,  $O1-N3-C1$   $118.59(19)^\circ$ ,  $O7-N8-O8$   $123.03(19)^\circ$ ,  $O7-N8-C6$   $118.58(18)^\circ$ ). The torsion angles show that both pyrazole rings are twisted to each other.



## Energetic Derivatives of 3,3',5,5'-Tetranitro-4,4'-bipyrazole (TNBPz): Synthesis, Characterization and Properties

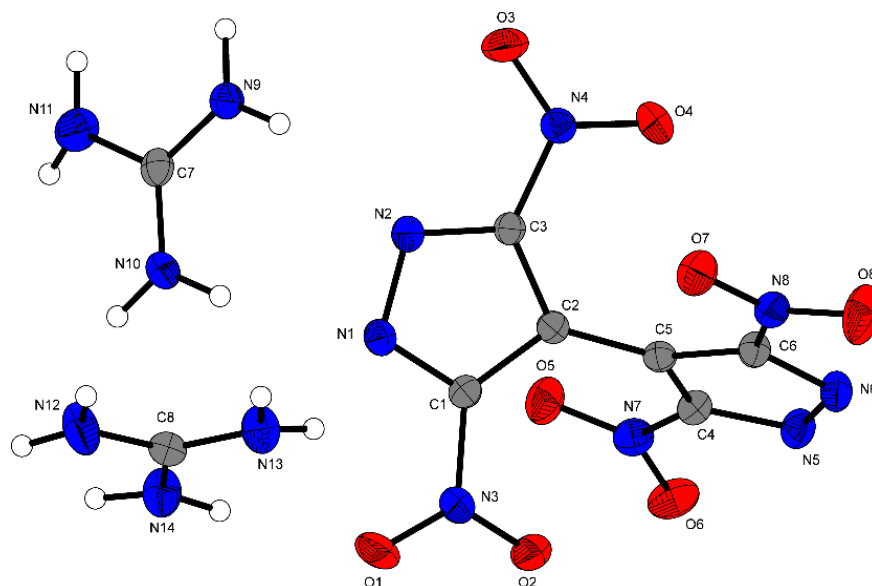


**Figure 3.** Molecular unit of bis(guanidinium) 3,3',5,5'-tetranitro-4,4'-bipyrazolate (**4**) in the crystalline state. Ellipsoids correspond to 50% probability levels. Hydrogen radii are arbitrary. Selected bond lengths (Å) and angles [deg.]: O1–N3 1.229(3), N1–N2 1.346(3), N1–C1 1.347(3), C1–C2 1.393(3), C2–C5 1.467(3), N2–C3 1.349(3), N3–C1 1.433(3), N9–C7 1.320(3), N10–C7 1.316(4), N2–N1–C1 106.96(18), N1–C1–N3 118.7(2), O1–N3–C1 118.3(2), C1–C2–C5 129.60(19), N10–C7–N11 119.6(2), C1–N1–N2–C3 –0.8(2), N2–N1–C1–N3 –179.87(17), N2–N1–C1–C2 1.4(2), O1–N3–C1–C2 170.0(2), C1–C2–C5–C6 –115.4(3), C3–C2–C5–C4 –122.1(3), C3–C2–C5–C6 63.4(3).

Compound **5** (**Figure 4**) crystallizes in the orthorhombic space group  $Pccn$  with a cell volume of 1802.61(6) Å<sup>3</sup> and four formula units per cell. The cell constants are  $a = 10.2845(2)$  Å,  $b = 18.8916(4)$  Å and  $c = 9.2779(2)$  Å. The calculated density at 298 K is 1.66 g/cm<sup>3</sup>. The different cation has no influence on the structure of the bipyrazolate, compared to compound **4**. The rings are twisted by 56.04° (C1–C2–C2'–C3') against each other. The bonds between N1–N2 (1.3398(13) Å), N1–C1 (1.3475(13) Å), N2–C3 (1.3441(14) Å), C1–C2 (1.3934(15) Å) and C2–C3 (1.3964(14) Å) have aromatic character.<sup>[13]</sup> The bonds between N1'–N2', N1'–C1', N2'–C3', C1'–C2' and C2'–C3' have the same length. The bond between C2 and C2' is with 1.4623(14) Å between the standard length for C–C double bonds and C–C single bonds.<sup>[13]</sup> The rings are slightly deformed and the oxygens are slightly displaced out of the plane. The bonds between C4 and the surrounding nitrogens N5, N7 and N8 have the typical length for aromatic

## Energetic Derivatives of 3,3',5,5'-Tetranitro-4,4'-bipyrazole (TNBPz): Synthesis, Characterization and Properties

bonds. The N5–N6 bond is with a length of 1.4062(16) Å between a single and an aromatic bond.<sup>[13]</sup> The bond angles between N5–C4–N8, N7–C4–N8, N5–C4–N7 and N6–N5–C4 defer slightly from 120°.

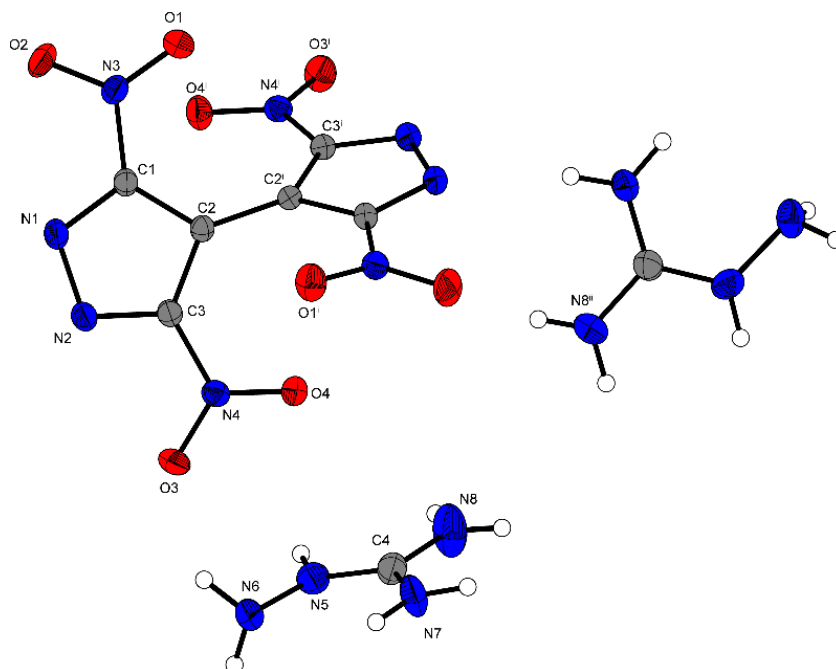


**Figure 4.** Molecular unit of bis(aminoguanidinium) 3,3',5,5'-tetranitro-4,4'-bipyrazolate (**5**) in the crystalline state. Ellipsoids correspond to 50% probability levels. Hydrogen radii are arbitrary. Selected bond lengths (Å) and angles [deg.]: N1–N2 1.3398(13), N1–C1 1.3475(13), C1–C2 1.3934(15), C2–C2' 1.4623(14), N8–C4 1.3280(18), N2–N1–C1 106.98(9), N1–N2–C3 106.87(9), C1–C2–C3 99.11(8), C1–C2–C2' 130.42(9), N7–C4–N8 119.66(13), C1–N1–N2–C3 0.34(11), C1–C2–C2'–C1' 130.13(13), C61–N5–C4–N8 –176.91(13).

**Compound 6** crystallizes orthorhombic space group  $Pca2_1$  with 16 formulas per unit cell. The lattice parameters are  $a = 17.1257(5)$  Å,  $b = 9.8507(3)$  Å and  $c = 33.8680(11)$  Å, giving a cell volume of 5713.5(3) Å<sup>3</sup>. The calculated density is 1.768 g cm<sup>-3</sup>, which is slightly lower than the density of anhydrous TNBPz (1.820 g cm<sup>-3</sup>) and TNBPz·H<sub>2</sub>O (**1·H<sub>2</sub>O**) (1.830 g cm<sup>-3</sup>).<sup>[11]</sup>

The asymmetric unit includes four units of **6**. The anions consist each out of two planar pyrazole-rings ( $|\theta_{out\ of\ plane}| \leq 2.2^\circ$ ) with averaged dihedral angle of 70.8° between both. This twist is lower compared to that found in anhydrous TNBPz (71.44(5)°) and TNBPz·H<sub>2</sub>O (**1·H<sub>2</sub>O**) (78.99(6)°).<sup>[11]</sup>

The carbon-carbon bond in the pyrazole-rings have a medium length of 1.388 Å. The carbon-

## Energetic Derivatives of 3,3',5,5'-Tetranitro-4,4'-bipyrazole (TNBPz): Synthesis, Characterization and Properties

nitrogen and nitrogen-nitrogen bond lengths are very similar with 1.342 Å and 1.345 Å on average, respectively. The medium bond length between the ring-connecting carbon is 1.465 Å, which is sustainably smaller than a typical carbon-carbon single bond, displaying its aromatic character. Similarly, the carbon-nitrogen bond to the nitro-groups have a reduced length of 1.430 Å on average, also showing their affiliation to the aromatic system. The medium bond angle located at one nitrogen of the pyrazole-rings is 106.9°, nearly matching the angle of an equilateral pentagon (108°). In comparison the bond angles at the nitro-carbons are widened (averaged 113.3°), while bond angles located at the ring-connecting carbon are compressed (averaged 99.8°). All nitrogen of the nitro-groups nearly lies in the plane of its pyrazole-ring ( $|\theta_{out\ of\ plane}| \leq 6.9^\circ$ ), while the oxygen shows different amount of rotation against this plane ( $0.2^\circ \leq |\theta_{out\ of\ plane}| \leq 30.7^\circ$ ) (**Figure 5**).

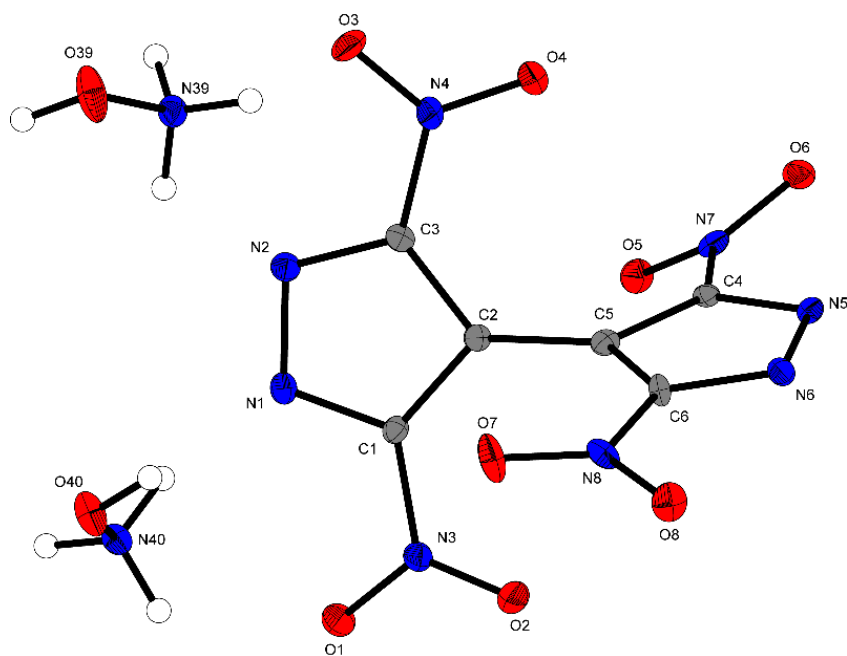


**Figure 5.** Molecular unit of bis(hydroxylammonium) 3,3',5,5'-tetranitro-4,4'-bipyrazolate (**6**) in the crystalline state. Ellipsoids correspond to 50% probability levels. Hydrogen radii are arbitrary. Selected bond lengths (Å) and angles [deg.]: N1–N2 1.348(7), N1–C1 1.341(7), C1–C2 1.395(7), C2–C5 1.461(7), N3–C1 1.424(7), N4–C3 1.430(7), O39–N39 1.408(7), O3–N4 1.243(6), N2–N1–C1 107.4(5), N3–C1–C2 128.2(5), C1–C2–C5 131.2(5), C3–C2–C5 129.2(5), C3–C2–C5 129.2(5), C1–N1–N2–C3 1.2(6), N2–N1–C1–N3 179.9(5), N2–N1–C1–N3 179.9(5), N1–N2–C3–N4 178.8(4), C1–C2–C5–C4 117.6(8), C1–C2–C5–C6 –66.3(9).

### 9.2.3. $^{15}\text{N}$ NMR spectroscopy

All synthesized compounds were characterized via multinuclear  $^1\text{H}$ ,  $^{13}\text{C}$  and  $^{14}\text{N}$  NMR spectroscopy, elemental analysis, vibrational spectroscopy (IR), mass spectrometry. In addition, the  $^{15}\text{N}$  NMR spectra of potassium 4-(1-amino-3,5-dinitropyrzoly)-3',5'-dinitropyrzolate (**11**) and 1,1'-diamino-3,3',5,5'-tetranitro-4,4'-bipyrazole (**12**) were recorded and the spectrum is shown in **Figure 6**. Compound **11** exhibits nine resonances in the  $^{15}\text{N}$  NMR spectrum. All eight resonances for the nitro groups and the pyrazole nitrogen atoms are observed in the range between  $-16.1$  and  $165.2$  ppm. The amino group is observed at  $-284.4$  ppm as a triplet with a coupling constant of  $^1J_{\text{NH}} = 73.6$  Hz.  $^{15}\text{N}$  NMR spectrum of **12** exhibits five resonances; both nitro groups show resonances at  $-26.1$  (N1) and  $-32.4$  (N2) ppm, both N atoms of the pyrazole ring-system are observed at  $-81.4$  (N3) and  $-163.0$  (N4) ppm, whereas the amino groups are visible at  $-283.3$  (N5) ppm. The  $\text{NH}_2$  groups are observed as a singlet resonance in the  $^1\text{H}$  coupled  $^{15}\text{N}$  spectrum and not as the expected triplet resonance. Possible reason for this result is the potential  $^1\text{H}/^2\text{D}$  exchange of  $(\text{NH}_2)_2\text{TNBPz}$  (**12**) with the  $d_6$ -DMSO solvent, in which the sample was measured.

## Energetic Derivatives of 3,3',5,5'-Tetranitro-4,4'-bipyrazole (TNBPz): Synthesis, Characterization and Properties

$^{15}\text{N}$  NMR (41 MHz,  $d_6$ -DMSO)

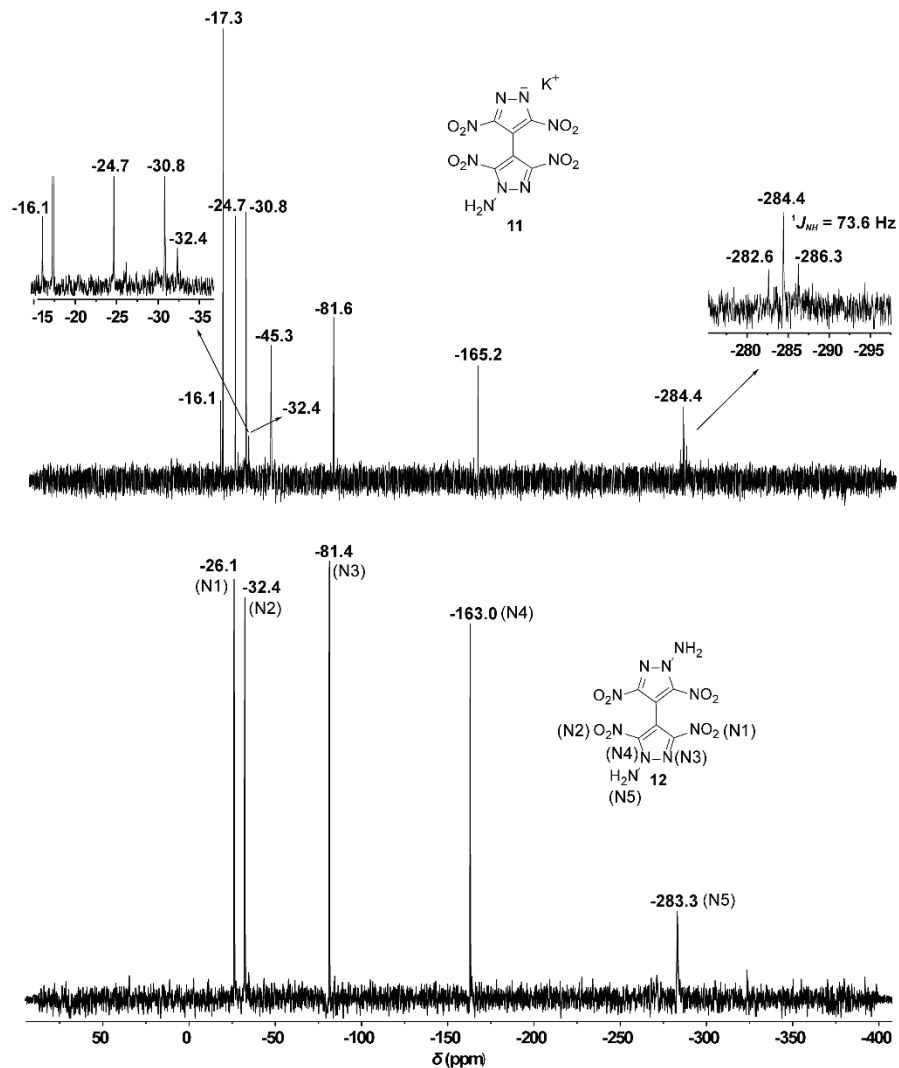


**Figure 6.**  $^{15}\text{N}$  NMR spectra of potassium 4-(1-amino-3,5-dinitropyrazolyl)-3',5'-dinitropyrazolate (**11**) and 1,1'-diamino-3,3',5,5'-tetranitro-4,4'-bipyrazole (**12**) in  $d_6$ -DMSO.

### 9.2.4. Toxicity assessment

To get a first impression how toxic the nitrated bipyrazole salts **11** and **12** act towards the aquatic environment, they were exposed to *Vibrio fischeri* bacteria strains. These bioluminescent bacteria strains are naturally found in the seas, therefore the measurements with different concentrations of the desired compounds are carried out in a stock solution of 2% NaCl at  $15\text{ }^{\circ}\text{C} \pm 0.3\text{ }^{\circ}\text{C}$ .<sup>[16]</sup> The bioluminescence of the bacteria was measured after 15 and 30 minutes exposure time with the

## Energetic Derivatives of 3,3',5,5'-Tetranitro-4,4'-bipyrazole (TNBPz): Synthesis, Characterization and Properties

compounds again and leads to the EC<sub>50</sub> (effective concentration, where the bioluminescence is decreased to 50%). At first, they were classified as non-toxic (> 1.00 g/L); toxic (0.10–1.00 g L<sup>-1</sup>) and very toxic (< 0.10 g L<sup>-1</sup>).<sup>[17]</sup> For the guanidinium salt **4**, EC<sub>50</sub> values of 2.09 g L<sup>-1</sup> (15 min) and 1.49 g L<sup>-1</sup> (30 min) were measured, the potassium salt **3** of the same TNBPz anion led to values of 1.66 g L<sup>-1</sup> and 1.27 g L<sup>-1</sup>. Therefore, this anion is considered as not-toxic. This is in quite good agreement with the potassium salt of the TriNBPz anion (EC<sub>50</sub> (15 min) = 2.86 g L<sup>-1</sup>; EC<sub>50</sub> (30 min) = 1.42 g L<sup>-1</sup>).<sup>[18]</sup> Eventually, compared to the corresponding monomer, the potassium salt of the 3,4-dinitro-5-pyrazole, this is an interesting finding, because it has an EC<sub>50</sub> value of 1.21 g/L and 0.95 g/L, respectively and is considered as toxic.<sup>[19]</sup> The values for the potassium salts of the corresponding N-oxides are suggesting that they are even more toxic.<sup>[20]</sup> The common used secondary explosive RDX is more toxic towards the bacteria strain compared to the herein presented compounds (EC<sub>50</sub> (15 min) = 0.33 g L<sup>-1</sup>; EC<sub>50</sub> (30 min) = 0.24 g L<sup>-1</sup>).<sup>[17,21]</sup>

**Table 1.** Toxicity assessment results for compounds **3** and **4**.

Compound	EC <sub>50</sub> [g L <sup>-1</sup> ] (15 min)	EC <sub>50</sub> [g L <sup>-1</sup> ] (30 min)	Toxicity level <sup>[a]</sup>
<b>3</b>	>>1.64	>>1.64	+
<b>4</b>	2.06	1.49	+

[a] Toxicity level (incubation 30 min): very toxic (–) < 0.10 g L<sup>-1</sup>; toxic (o) 0.10–1.00 g L<sup>-1</sup>; less toxic (+) > 1.00 g L<sup>-1</sup>.

### 9.2.5. Physical and detonation properties

Since all synthesized compounds (**2**–**12**) in this work are energetic materials their properties were investigated. In addition, all theoretically and experimentally determined detonation properties for compounds **2**, **4**–**6**, **8**, **11**, and **12** are reported in **Table 2**. The thermal behavior of all compounds was determined with OZM Research DTA 552-Ex instrument at a heating rate of 5 °C min<sup>-1</sup>. In the case of all TNBPz based energetic materials compounds **2** (*T*<sub>dec.</sub> = 270 °C), **4** (*T*<sub>dec.</sub> = 300 °C), **8** (*T*<sub>dec.</sub> = 276 °C) and **11** (*T*<sub>dec.</sub> = 280 °C) show the highest thermal stability, whereas **2** and **4** decompose prior melting at 186 °C and 251 °C, respectively. Comparison of the hydroxylammonium salts (NH<sub>3</sub>OH)HTriNBPz (**6** *T*<sub>dec.</sub> = 230 °C), (NH<sub>3</sub>OH)HTNBPz (**15** *T*<sub>dec.</sub> = 201 °C) and (NH<sub>3</sub>OH)<sub>2</sub>TNBPz (**16** *T*<sub>dec.</sub> = 194 °C) to each other shows that the TNBPz<sup>–</sup> anion based salt exhibits better thermal stability than the related hydroxylammonium salts.<sup>[18]</sup>

## Energetic Derivatives of 3,3',5,5'-Tetranitro-4,4'-bipyrazole (TNBPz): Synthesis, Characterization and Properties

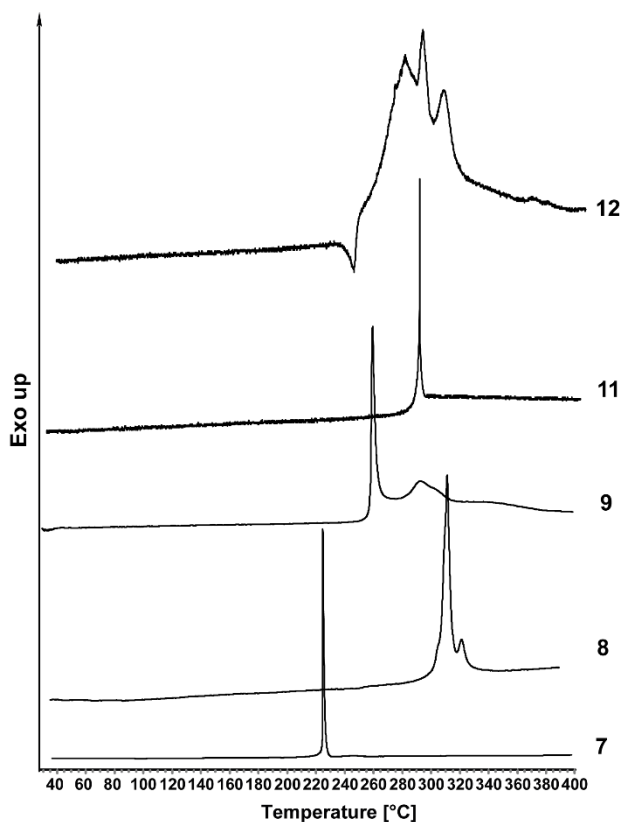


**Figure 7.** DTA plots for selected compounds.

The plotted DTAs of compounds **7–9**, **11** and **22** are presented in **Figure 7**. The ionic compounds **7** (215 °C), **8** (276 °C), **9** (250 °C) and **11** (280 °C) show sharp decomposition signals in the DTA plots, whereas the organic compound (NH<sub>2</sub>)<sub>2</sub>TNBPz (**12**) decomposes at 244 °C prior melting (234 °C).

The lowest room temperature densities for the TNBPz based ionic derivatives are 1.66 g cm<sup>-3</sup> for compound **5** and 1.63 g cm<sup>-3</sup> for compound **4**. The highest reported density for the TNBPz based energetic derivatives is of the potassium salt **11** with 2.00 g cm<sup>-3</sup>, followed by 1.75 g cm<sup>-3</sup> for compound **12**.

**Table2.** Physico-chemical properties of **2**, **4–6**, **8**, **11**, and **12**.

Compound	<b>2</b>	<b>4</b>	<b>5</b>	<b>6</b>	<b>8</b>	<b>11</b>	<b>12</b>
<i>IS</i> <sup>[a]</sup> [J]	10	40	10	5	10	10	15
<i>FS</i> <sup>[b]</sup> [N]	350	> 360	> 360	324	360	48	324
<i>ESD</i> <sup>[c]</sup> [J]	0.041	1.50	1.25	0.20	0.50	0.025	0.013
<i>Ω</i> <sup>[d]</sup> [%]	-51.4	-51.8	-51.9	-25.3	-36.8	-23.9	-27.9

## Energetic Derivatives of 3,3',5,5'-Tetranitro-4,4'-bipyrazole (TNBPz): Synthesis, Characterization and Properties

$T_m^{[e]}$ [°C]	186	251	179	–	–	–	234
$T_{dec}^{[f]}$ [°C]	270	300	210	194	276	280	244
$\rho^{[g]}$ [g cm <sup>-3</sup> ]	1.72	1.63	1.66	1.72	1.69	2.00	1.75*
$\Delta H_f^{[h]}$ [kJ mol <sup>-1</sup> ]	200.9	88.8	308.5	236.7	108.7	139.3	464.5
<b>EXPLO5 6.03</b>							
$-\Delta_E U^{[i]}$ [kJ kg <sup>-1</sup> ]	4795	3903	4224	5657	4759	5172	5540
$T_{C-J}^{[j]}$ [K]	4041	2909	3009	3934	3421	3633	4114
$p_{C-J}^{[k]}$ [kbar]	242	208	231	302	258	318	305
$D_{C-J}^{[l]}$ [m s <sup>-1</sup> ]	7711	7484	7866	8456	8003	8517	8469
$V^{[m]}$ [dm <sup>3</sup> kg <sup>-1</sup> ]	693	474	467	770	452	560	738

[a] Impact sensitivity (BAM drophammer, method 1 of 6); [b] friction sensitivity (BAM drophammer, method 1 of 6); [c] electrostatic discharge device (OZM research); [d] oxygen balance; [e] melting point (DTA,  $\beta = 5^\circ\text{C}\cdot\text{min}^{-1}$ ); [f] temperature of decomposition (DTA,  $\beta = 5^\circ\text{C}\cdot\text{min}^{-1}$ ); [g] density at 298 K; [h] standard molar enthalpy of formation; [i] detonation energy; [j] detonation temperature; [k] detonation pressure; [l] detonation velocity; [m] volume of detonation gases at standard temperature and pressure conditions. \*pycnometric density measurement.

Experimentally determined sensitivities toward impact, friction and electrostatic discharge are also reported in **Table 2**. The determined sensitivities vary for impact from 5 to 40 J, for friction from 48 to > 360 N and for electrostatic discharge from 0.013 J up to 1.50 J. The most impact sensitive material is the hydroxylammonium salt **6** with 5 J. The most impact insensitive compound with 40 J is the guanidinium salt **4**. The energetic materials **2** (10 J), **5** (10 J), **8** (10 J), **11** (10 J) and **12** (15 J) exhibit moderate impact sensitivity values. In addition, the most synthesized ionic and neutral polynitrated bipyrazole derivatives exhibit low sensitivity toward friction. Only compound **12** shows high friction sensitivity with value of **48** N. In contrast to this results, the most sensitive compound to ESD is **12** with 0.013 J, followed by the potassium salt **11** with 0.025 J.

For the most synthesized energetic materials positive standard molar enthalpies of formation were calculated. The highest calculated enthalpy of formation for a TNBPz based derivative is 464.5 kJ mol<sup>-1</sup> (**12**). The lowest positive enthalpy of formation was observed for the guanidinium salt **4** (88.8 kJ mol<sup>-1</sup>). Using the room temperature densities<sup>[22]</sup> and the determined enthalpies of formation, several detonation properties were calculated for compounds **2**, **4–6**, **8**, **11**, and **12** by using the EXPLO5 code (6.03 Version).<sup>[23]</sup> The calculated values for the detonation energy ( $-\Delta_E U^\circ$ ) range from 3900 to 5700 kJ kg<sup>-1</sup>. The highest values were calculated for compounds **5** (5657 kJ kg<sup>-1</sup>), **11** (5172 kJ kg<sup>-1</sup>) and **22** (5540 kJ kg<sup>-1</sup>), whereas the lowest were determined for the guanidinium salt **4** with 3903 kJ kg<sup>-1</sup>. In addition, the best performing



## Energetic Derivatives of 3,3',5,5'-Tetranitro-4,4'-bipyrazole (TNBPz): Synthesis, Characterization and Properties

compounds regarding calculated detonation pressure ( $p_{C-J}$ ) and detonation velocity ( $D_{C-J}$ ) are the ionic compounds **6** ( $p_{C-J}$  = 328 kbar,  $D_{C-J}$  = 8673 m s<sup>-1</sup>), **11** ( $p_{C-J}$  = 318 kbar,  $D_{C-J}$  = 8517 m s<sup>-1</sup>) and the *N*-aminated compound **12** ( $p_{C-J}$  = 305 kbar,  $D_{C-J}$  = 8469 m s<sup>-1</sup>).

Additionally, the explosive performance (explosiveness) of 1,1'-diamino-3,3',5,5'-tetranitro-4,4'-bipyrazole ((NH<sub>2</sub>)<sub>2</sub>TNBPz, **12**) was investigated in the small scale by the small-scale shock reactivity test (SSRT). For this purpose, a specific amount of the sample was put in a calendric whole in a steel block on the top of an aluminum block. Compound **12** was pressed at a consolidation dead load of 3 t with a dwell time of 5 s into a perforated steel block. The sample was initiated by a commercially available detonator (Orica-DYNADET C2-0ms). The set-up for this test is shown in **Figure 8** and has been previously reported in the literature.<sup>[24]</sup>

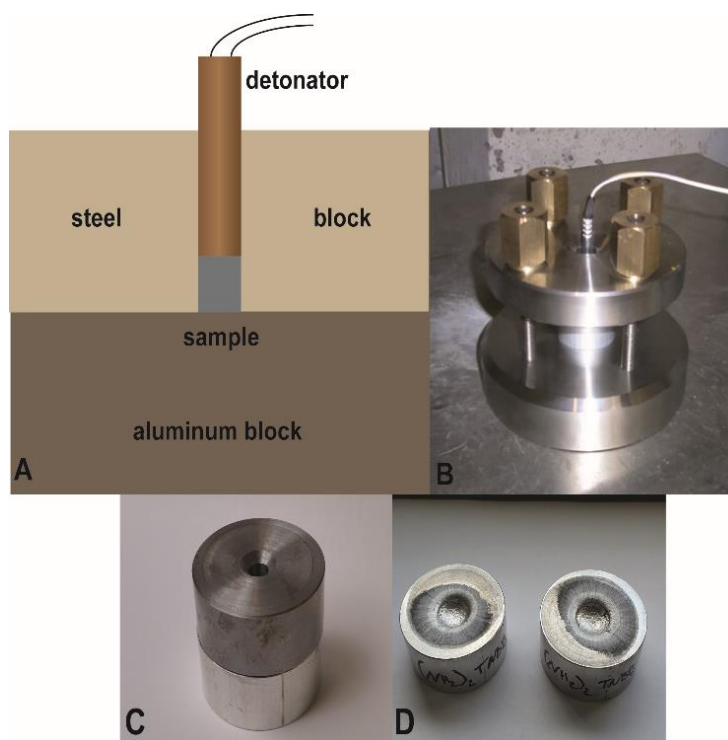


**Figure 8.** SSRT results: A) schematical illustration; B) photograph of the setup; C) aluminum block and steel block filled with compound **12**; D) dented aluminum block after initiation of the explosive with a commercial detonator.

The obtained results after the initiation of compound **12** are shown in **Figure 8** (D). The dent size was filled with a fine powdered SiO<sub>2</sub> sand and the resulting weight of SiO<sub>2</sub> was reported. The results for **12** are shown together with the corresponding value for HNS, PYX

## Energetic Derivatives of 3,3',5,5'-Tetranitro-4,4'-bipyrazole (TNBPz): Synthesis, Characterization and Properties

and TKX-55 in **Table 3**. The obtained value for (NH<sub>2</sub>)<sub>2</sub>TNBPz (**12**, 786 mg) compared to HNS (672 mg), PYX (637 mg) and TKX-55 (641 mg) shows that the explosive performance of double aminated **12** higher is than the heat resisting explosives HNS, PYX and TKX-55.

**Table 3.** The SSRT for **12** compared to HNS, PYX and TKX-55.<sup>[24]</sup>

	HNS	PYX	TKX-55	<b>12</b>
$m_E$ [mg] <sup>[a]</sup>	469	474	496	472
$m$ [mg] <sup>[b]</sup>	672	637	641	786

[a] Mass of the explosive:  $m_E = V_s \rho$  0.95; [b] Mass of SiO<sub>2</sub>.

### 9.3. Conclusions

During this work the energetic functionalization of TNBPz (**1·H<sub>2</sub>O**) was achieved. We report the neutralization reactions of TNBPz with different nitrogen-rich bases, which yielded many different ionic based energetic materials. In addition, the *N*-methylation and *N*-amination of **1·H<sub>2</sub>O** is reported. All new synthesized compounds were obtained from good to excellent yields. The *N*-methylation of TNBPz (**1·H<sub>2</sub>O**) was achieved with dimethyl sulfate at elevated temperatures. The mono *N*-amination of TNBPz (**1·H<sub>2</sub>O**) was obtained by reacting **1·H<sub>2</sub>O** with hydroxylamine-*O*-sulfonic acid (HOSA) in a NaOH/KH<sub>2</sub>PO<sub>4</sub> buffer solution at 60 °C. Whereas, the double *N*-amination of TNBPz was obtained by reacting **1·H<sub>2</sub>O** with *O*-*p*-toluenesulfonylhydroxylamine (TOSA). All synthesized compounds were extensively investigated and the physico-chemical properties of the following compounds **2**, **4–6**, **8**, **11** and **12** are reported. From all synthesized energetic compounds, the ionic derivatives **6** ( $p_{C-J}$  = 302 kbar,  $D_{C-J}$  = 8456 m s<sup>-1</sup>), **11** ( $p_{C-J}$  = 318 kbar,  $D_{C-J}$  = 8517 m s<sup>-1</sup>) and the *N*-aminated **12** ( $p_{C-J}$  = 305 kbar,  $D_{C-J}$  = 8469 m s<sup>-1</sup>) show the best performance. The hydroxylammonium salt **6** (IS = 5 J) exhibits the highest impact sensitivity, whereas the potassium salt **11** (FS = 48 N) is the most friction sensitive compound. Finally, the toxicity of compounds **3** and **4** toward aquatic bacteria (*Vibrio fischeri*) was investigated and the obtained results show that the ionic derivatives based on TNBPz are not toxic.

## 9.4. Experimental Part

### 9.4.1. General Information

$^1\text{H}$ ,  $^{13}\text{C}$ ,  $^{14}\text{N}$  and  $^{15}\text{N}$  NMR spectra were recorded on JEOL 270 and BRUKER AMX 400 instruments. The samples were measured at room temperature in standard NMR tubes ( $\varnothing$  5 mm). Chemical shifts are reported as  $\delta$  values in ppm relative to the residual solvent peaks of  $d_6$ -DMSO ( $\delta$  H: 2.50,  $\delta$  C: 39.5). Solvent residual signals and chemical shifts for NMR solvents were referenced against tetramethylsilane (TMS,  $\delta$  = 0 ppm) and nitromethane. Unless stated otherwise, coupling constants were reported in hertz (Hz) and for the characterization of the observed signal multiplicities the following abbreviations were used: s (singlet), d (doublet), t (triplet), q (quartet), quint (quintet), sept (septet), m (multiplet) and br (broad). Low resolution mass spectra were recorded on a JEOL JMS-700 MStation mass spectrometer (EI+/DEI+). Infrared spectra (IR) were recorded from  $4500\text{ cm}^{-1}$  to  $650\text{ cm}^{-1}$  on a PERKIN ELMER Spectrum BX-59343 instrument with SMITHS DETECTION DuraSamplIR II Diamond ATR sensor. The absorption bands are reported in wavenumbers ( $\text{cm}^{-1}$ ). Elemental analysis was carried out by the department's internal micro analytical laboratory on a Elementar Vario el by pyrolysis of the sample and subsequent analysis of the formed gases. Decomposition temperatures were measured via differential thermal analysis (DTA) with an OZM Research DTA 552-Ex instrument at a heating rate of  $5\text{ }^\circ\text{C min}^{-1}$  and in a range of room temperature to  $400\text{ }^\circ\text{C}$ . All sensitivities toward impact (IS) and friction (FS) were determined according to BAM (German: Bundesanstalt für Materialforschung und -prüfung) standards using a BAM drop hammer and a BAM friction apparatus.<sup>[25]</sup> All energetic compounds were tested for sensitivity towards electrical discharge using an Electric Spark Tester ESD 2010 EN.

### 9.4.2. Synthesis

#### 1,1'-Dimethyl-3,3',5,5'-tetranitro-4,4'-bipyrazole (2)

3,3',5,5'-Tetranitro-4,4'-bipyrazole monohydrate (500 mg, 1.51 mmol) was dissolved in water (10 mL) and  $\text{NaHCO}_3$  (260 mg, 3.1 mmol) was added. The yellow solution was then heated to  $65\text{ }^\circ\text{C}$  and dimethyl sulfate (0.60 mL, 6.0 mmol) was added dropwise. The reaction

## Energetic Derivatives of 3,3',5,5'-Tetranitro-4,4'-bipyrazole (TNBPz): Synthesis, Characterization and Properties

mixture was stirred for 12 h at 85 °C. The white precipitate was filtered, washed with small amount of ice-water and dried on air to yield **2** (450 mg, 1.32 mmol, 88 %) as a white solid.

DTA (5 °C min<sup>-1</sup>): 186 (melt.), 270 °C (exo.); DTA (5 °C min<sup>-1</sup>): 186 °C (melt.), 270 °C (exo.); BAM: drop hammer: 10 J (100–500 μm); friction tester: 360 N (100–500 μm); ESD: 41 μJ (100–500 μm). IR (ATR),  $\tilde{\nu}$  (cm<sup>-1</sup>) = 1566 (s), 1553 (w), 1504 (vs), 1428 (s), 1328 (vs), 1292 (s), 1011 (m), 890 (m), 876 (m), 767 (m), 767 (m), 694 (m). <sup>1</sup>H NMR (*d*<sub>6</sub>-DMSO, 400 MHz, ppm)  $\delta$  = 4.40 (s, 6H). <sup>13</sup>C NMR (*d*<sub>6</sub>-DMSO, 101 MHz, ppm)  $\delta$  = 149.4, 144.0, 101.8. <sup>14</sup>N NMR (*d*<sub>6</sub>-DMSO, 29 MHz, ppm)  $\delta$  = -32. Elem. Anal. (C<sub>6</sub>H<sub>6</sub>N<sub>8</sub>O<sub>8</sub>, 342.18 g mol<sup>-1</sup>) calcd.: C 28.08, H 1.77, N 32.75 %. Found: C 27.97, H 1.61, N 32.52 %.

### Dipotassium 3,3',5,5'-tetranitro-4,4'-bipyrazolate monohydrated (3·H<sub>2</sub>O)

3,3',5,5'-Tetranitro-4,4'-bipyrazole monohydrate (665 mg, 2.0 mmol, 2.0 eq.) was dissolved in a mixture of EtOH (10 mL) and water (5 mL) and to the solution was added potassium carbonate (277 mg, 2.00 mmol, 2.0 eq.). The mixture was heated to reflux for 30 min and after cooling down to room temperature the solvent was removed *in vacuo* to yield compound **3·H<sub>2</sub>O** as yellow solid (716 mg, 1.75 mmol, 97 %).

BAM: drop hammer: 1.5 J (100–500 μm); friction tester: 120 N (100–500 μm); ESD: 0.16 J (100–500 μm). IR (ATR),  $\tilde{\nu}$  (cm<sup>-1</sup>) = 3454 (m), 3425 (m), 3359 (m), 3195 (br), 1678 (m), 1654 (s), 1546 (s), 1494 (m), 1477 (m), 1378 (vs), 1325 (vs), 1298 (s), 1179 (m), 1021 (m), 993 (s), 855 (s), 835 (s); <sup>1</sup>H NMR (*d*<sub>6</sub>-DMSO, 400 MHz, ppm)  $\delta$  = 3.33 (s, H<sub>2</sub>O). <sup>13</sup>C NMR (*d*<sub>6</sub>-DMSO, 101 MHz, ppm)  $\delta$  = 153.9, 104.4. <sup>14</sup>N NMR (*d*<sub>6</sub>-DMSO, 29 MHz, ppm)  $\delta$  = -14.

Compound **3·H<sub>2</sub>O** was dried *in vacuo* for 6 hours to yield the anhydrous dipotassium 3,3',5,5'-tetranitro-4,4'-bipyrazolate (**3**).

Elem. Anal. (C<sub>6</sub>K<sub>2</sub>N<sub>8</sub>O<sub>8</sub>, 390.31 g mol<sup>-1</sup>) calcd.: C 18.46, H 0.00, N 28.71 %. Found: C 18.15, H 0.00 N 27.82 %.

### Bis(guanidinium) 3,3',5,5'-tetranitro-4,4'-bipyrazolate (4)

3,3',5,5'-Tetranitro-4,4'-bipyrazole monohydrate (166 mg, 0.5 mmol, 1.0 eq.) was dissolved in ethanol (10 mL) and the solution was heated to 75 °C. Guanidine carbonate (91 mg, 0.5 mmol, 1.0 eq.) was added. Filtration and removing the solvent at room temperature yielded the product as yellow crystals (23, 216 mg, 0.50 mmol, 100 %).

**Energetic Derivatives of 3,3',5,5'-Tetranitro-4,4'-bipyrazole (TNBPz): Synthesis,  
Characterization and Properties**

DTA (5 °C min<sup>-1</sup>): 251 (melt.), 300 °C (exo.); BAM: drop hammer: 40 J (100–500 μm); friction tester: >360 N (100–500 μm); ESD: 1.50 J (100–500 μm). IR (ATR),  $\tilde{\nu}$  (cm<sup>-1</sup>) = 3430 (s), 3375 (m), 3154 (m), 2797 (w), 1634 (s), 1574 (w), 1528 (m), 1474 (s), 1402 (m), 1377 (m), 1336 (vs), 1310 (s), 1300 (vs), 1166 (w), 1001 (m), 846 (s), 772 (vw), 713 (w), 692 (w), 614 (vw), 549 (vw), 524 (vw). Raman (1064 nm, 200 mW, 25 °C):  $\tilde{\nu}$  (cm<sup>-1</sup>) = 1631 (13), 1505 (11), 1478 (5), 1385 (72), 1360 (45), 1321 (26), 1282 (13), 1216 (7), 1169 (100), 1009 (17), 830 (35), 816 (3), 776 (2), 761 (5), 671 (4), 526 (6), 381 (3), 307 (5), 277 (9), 121 (35). <sup>1</sup>H NMR (*d*<sub>6</sub>-DMSO, 400 MHz, ppm)  $\delta$  = 6.93 (s, 12H). <sup>13</sup>C NMR (*d*<sub>6</sub>-DMSO, 101 MHz, ppm)  $\delta$  = 157.9, 153.8, 104.3. <sup>14</sup>N NMR (*d*<sub>6</sub>-DMSO, 29 MHz, ppm)  $\delta$  = -17. Elem. Anal. (C<sub>8</sub>H<sub>12</sub>N<sub>14</sub>O<sub>8</sub>, 432.27 g mol<sup>-1</sup>) calcd.: C 22.23, H 2.80, N 45.36 %. Found: C 22.51, H 2.84, N 45.31 %.

**Bis(aminoguanidinium) 3,3',5,5'-tetranitro-4,4'-bipyrazolate (5)**

3,3',5,5'-Tetranitro-4,4'-bipyrazole monohydrate (332 mg, 1.00 mmol, 1.0 eq.) was solved in ethanol (20 mL) and water (10 mL). The solution was heated to 75 °C. Aminoguanidine bicarbonate (273 mg, 2.0 mmol, 2.0 eq.) was added. Filtration and removing the solvent at room temperature results the product as yellow crystals (**5**, 463 mg, 1.00 mmol, 100 %).

DTA (5 °C min<sup>-1</sup>): 179 (melt.), 210 °C (exo.); BAM: drop hammer: 10 J (100–500 μm); friction tester: >360 N (100–500 μm); ESD: 1.25 J (100–500 μm). IR (ATR),  $\tilde{\nu}$  (cm<sup>-1</sup>) = 3476 (w), 3430 (m), 3354 (m), 3319 (m), 3167 (w), 2827 (w), 1670 (s), 1532 (m), 1478 (s), 1405 (w), 1379 (m), 1338 (vs), 1309 (s), 1217 (w), 1160 (w), 1078 (vw), 998 (m), 844 (s), 759 (vw), 708 (w), 633 (w), 517 (vw). Raman (1064 nm, 200 mW, 25 °C):  $\tilde{\nu}$  (cm<sup>-1</sup>) = 1627 (17), 1506 (11), 1481 (8), 1407 (29), 1388 (100), 1362 (49), 1318 (26), 1312 (23), 1280 (15), 1215 (11), 1178 (80), 1162 (60), 1023 (5), 1000 (6), 971 (7), 832 (48), 814 (4), 761 (7), 667 (4), 633 (3), 501 (5), 307 (4), 293 (6), 279 (9), 194 (8), 155 (13). <sup>1</sup>H NMR (*d*<sub>6</sub>-DMSO, 400 MHz, ppm)  $\delta$  = 8.58 (s, 2H), 7.27 (s, 4H), 6.76 (s, 4H), 4.69 (s, 4H). <sup>13</sup>C NMR (*d*<sub>6</sub>-DMSO, 101 MHz, ppm)  $\delta$  = 159.2, 154.3, 104.7. <sup>14</sup>N NMR (*d*<sub>6</sub>-DMSO, 29 MHz, ppm)  $\delta$  = -19. Elem. Anal. (C<sub>8</sub>H<sub>14</sub>N<sub>16</sub>O<sub>8</sub>, 462.30 g mol<sup>-1</sup>) calcd.: C 20.78, H 3.05, N 48.48 %. Found: C 21.04, H 3.07, N 48.25 %.

**Energetic Derivatives of 3,3',5,5'-Tetranitro-4,4'-bipyrazole (TNBPz): Synthesis,  
Characterization and Properties**

**Bis(hydroxylammonium) 3,3',5,5'-tetranitro-4,4'-bipyrazolate (6)**

3,3',5,5'-Tetranitro-4,4'-bipyrazole monohydrate (500 mg, 1.50 mmol, 1.00 eq.) was dissolved in Et<sub>2</sub>O (20 mL) and EtOH (5 mL). Aqueous NH<sub>2</sub>OH (241 mg, 50-wt%, 6.00 mmol, 4.00 eq.) was added dropwise and the resulting reaction mixture was stirred for 1 h at room temperature. Removal of the solvents *in vacuo* afforded compound **6** as a yellow solid (570 mg, 1.50 mmol, 100%).

DTA (5 °C min<sup>-1</sup>): 194 °C (exo.); BAM: drop hammer: 5 J (100–500 μm); friction tester: 324 N (100–500 μm); ESD: 200 mJ (100–500 μm). IR (ATR),  $\tilde{\nu}$  (cm<sup>-1</sup>) = 3138 (br), 2605 (br), 1538 (m), 1481 (s), 1393 (s), 1341 (vs), 1311 (vs), 1191 (m), 1028 (m), 1004 (s), 850 (vs), 769 (w), 692 (w). <sup>1</sup>H NMR (*d*<sub>6</sub>-DMSO, 400 MHz, ppm)  $\delta$  = 10.13 (s, 6H), 9.96 (s, 2H). <sup>13</sup>C NMR (*d*<sub>6</sub>-DMSO, 101 MHz, ppm)  $\delta$  = 153.6, 104.1. <sup>14</sup>N NMR (*d*<sub>6</sub>-DMSO, 29 MHz, ppm)  $\delta$  = -14. Elem. Anal. (C<sub>6</sub>H<sub>8</sub>N<sub>10</sub>O<sub>10</sub>, 380.19 g mol<sup>-1</sup>) calcd.: C 18.95, H 2.12, N 36.84 %. Found: C 19.40, H 2.00, N 36.34 %.

**Bis(hydrazinium) 3,3',5,5'-tetranitro-4,4'-bipyrazolate (7)**

3,3',5,5'-Tetranitro-4,4'-bipyrazole monohydrate (499 mg, 1.5 mmol, 1.0 eq.) was solved in ethanol (12 mL). The solution was heated to 75 °C. Hydrazine hydrate (150 mg, 3.0 mmol, 2.0 eq.) was added. Filtration and removing the solvent at room temperature results the product as yellow crystals (**7**, 567 mg, 1.50 mmol, 100 %).

BAM: drop hammer: 4 J (100–500 μm); friction tester: 216 N (100–500 μm); ESD: 0.25 J (100–500 μm). IR (ATR),  $\tilde{\nu}$  (cm<sup>-1</sup>) = 3339 (vw), 3205 (w), 2592 (m), 1610 (w), 1530 (m), 1474 (s), 1374 (m), 1340 (vs), 1315 (vs), 1303 (s), 1284 (s), 1180 (m), 1089 (m), 1002 (m), 947 (m), 845 (vs), 772 (w), 760 (w), 713 (w), 689 (w), 630 (w), 591 (w), 521 (w). Raman (1064 nm, 200 mW, 25 °C):  $\tilde{\nu}$  (cm<sup>-1</sup>) = 1625 (32), 1514 (7), 1478 (5), 1395 (100), 1364 (68), 1327 (28), 1320 (27), 1286 (17), 1217 (10), 1192 (94), 1182 (90), 1025 (6), 1003 (5), 951 (3), 833 (57), 814 (2), 775 (3), 761 (12), 668 (5), 596 (2), 526 (2), 375 (4), 309 (8), 282 (9), 175 (9), 113 (4). <sup>1</sup>H NMR (*d*<sub>6</sub>-DMSO, 400 MHz, ppm)  $\delta$  = 6.33 (s, 10H). <sup>13</sup>C NMR (*d*<sub>6</sub>-DMSO, 101 MHz, ppm)  $\delta$  = 153.0, 103.6. <sup>14</sup>N NMR (*d*<sub>6</sub>-DMSO, 29 MHz, ppm)  $\delta$  = -17. Elem. Anal. (C<sub>6</sub>H<sub>10</sub>N<sub>12</sub>O<sub>8</sub>, 378.22 g mol<sup>-1</sup>) calcd.: C 19.05, H 2.67, N 44.44 %. Found: C 19.31, H 2.98, N 42.06 %.

**Energetic Derivatives of 3,3',5,5'-Tetranitro-4,4'-bipyrazole (TNBPz): Synthesis,  
Characterization and Properties**

**Bis(ammonium) 3,3',5,5'-tetranitro-4,4'-bipyrazolate (8)**

3,3',5,5'-Tetranitro-4,4'-bipyrazole monohydrate (332 mg, 1.00 mmol, 1.0 eq.) was solved in ethanol (10 mL). The solution was heated to 75 °C. Ammonium carbonate (96 mg, 1.0 mmol, 2.0 eq.) was added. Filtration and removing the solvent at room temperature gave the product as yellow crystals (25, 368 mg, 1.00 mmol, 100 %).

DTA (5 °C min<sup>-1</sup>): 276 °C (exo.); BAM: drop hammer: 10 J (100–500 μm); friction tester: >360 N (100–500 μm); ESD: 0.50 J (100–500 μm). IR (ATR),  $\tilde{\nu}$  (cm<sup>-1</sup>) = 3635 (vw), 3482 (vw), 3246 (w), 2897 (w), 2775 (w), 1824 (vw), 1645 (vw), 1540 (m), 1483 (s), 1422 (s), 1401 (s), 1341 (vs), 1310 (s), 1182 (m), 1080 (vw), 1046 (vw), 1026 (w), 1003 (s), 841 (s), 772 (w), 758 (w), 696 (m), 591 (m), 513 (w). Raman (1064 nm, 200 mW, 25 °C):  $\tilde{\nu}$  (cm<sup>-1</sup>) = 1644 (12), 1526 (10), 1397 (100), 1318 (20), 1288 (8), 1216 (9), 1186 (75), 1025 (4), 1003 (5), 829 (38), 760 (7), 669 (3), 592 (4), 527 (4), 374 (4), 278 (12). <sup>1</sup>H NMR (*d*<sub>6</sub>-DMSO, 400 MHz, ppm)  $\delta$  = 5.65 (s, 8H). <sup>13</sup>C NMR (*d*<sub>6</sub>-DMSO, 101 MHz, ppm)  $\delta$  = 151.7, 102.4. <sup>14</sup>N NMR (*d*<sub>6</sub>-DMSO, 29 MHz, ppm)  $\delta$  = -17, -357. Elem. Anal. (C<sub>6</sub>H<sub>8</sub>N<sub>10</sub>O<sub>8</sub>, 348.19 g mol<sup>-1</sup>) calcd.: C 20.70, H 2.32, N 40.23 %. Found: C 20.59, H 2.46, N 39.33 %.

**Bis(3,6,7-triamino-[1,2,4]triazolo[4,3-*b*][1,2,4]triazolium) 3,3',5,5'-tetranitro-4,4'-bipyrazolate (9)**

3,3',5,5'-Tetranitro-4,4'-bipyrazole monohydrate (450 mg, 1.36 mmol, 1.0 eq.) was dissolved in a mixture of abs. EtOH (20 mL) and water (10 mL). The solution was heated to 80 °C and 3,6,7-triamino-[1,2,4]triazolo[4,3-*b*][1,2,4]triazole (TATOT, 419 mg, 2.72 mmol, 2.0 eq.) was added. The reaction mixture was stirred at the same temperature for 30 min and then cooled to room temperature. The solvent was removed in vacuo to yield compound **9** as a yellow powder (812 mg, 1.31 mmol, 96 %).

BAM: drop hammer: > 40 J (100–500 μm); friction tester: 360 N (100–500 μm); ESD: 63 mJ (100–500 μm). IR (ATR),  $\tilde{\nu}$  (cm<sup>-1</sup>) = 3462 (m), 3349 (m), 3228 (vw), 3117 (w), 1673 (s), 1642 (s), 1594 (vw), 1571 (vw), 1547 (m), 1496 (m), 1418 (vw), 1387 (m), 1328 (vs), 1303 (vs), 1178 (m), 1120 (vw), 1080 (vw), 1026 (s), 1002 (m), 921 (m), 839 (vs), 770 (vw), 707 (m), 593 (m). <sup>1</sup>H NMR (*d*<sub>6</sub>-DMSO, 400 MHz, ppm)  $\delta$  = 13.36 (s, 2H), 8.18 (s, 4H), 7.23 (s, 4H), 5.77 (s, 4H). <sup>13</sup>C NMR (*d*<sub>6</sub>-DMSO, 101 MHz, ppm)  $\delta$  = 160.2, 153.8,

**Energetic Derivatives of 3,3',5,5'-Tetranitro-4,4'-bipyrazole (TNBPz): Synthesis,  
Characterization and Properties**

147.4, 141.2, 104.3.  $^{14}\text{N}$  NMR ( $d_6$ -DMSO, 29 MHz, ppm)  $\delta = -17$ . Elem. Anal. ( $\text{C}_{12}\text{H}_{14}\text{N}_{24}\text{O}_8$ , 622.40 g mol $^{-1}$ ) calcd.: C 23.16, H 2.27, N 54.01 %. Found: C 23.43, H 2.08, N 53.78 %.

**Bis(3,5-diamino-1,2,4-triazolium) 3,3',5,5'-tetranitro-4,4'-bipyrazolate (10)**

3,3',5,5'-Tetranitro-4,4'-bipyrazole monohydrate (416 mg, 1.25 mmol, 1.0 eq.) was dissolved in a mixture of abs. EtOH (10 mL) and water (5 mL) and the solution was heated to 80 °C. 3,5-Diamino-1,2,4-triazole (248 mg, 2.50 mmol, 2.0 eq.) was added and the reaction mixture was stirred for 30 min. After cooling the solvent was removed in vacuo and compound **10** was obtained as yellow solid (631 mg, 1.23 mmol, 99 %).

DTA (5 °C min $^{-1}$ ): 252 °C (melt.), 289 °C (exo.); BAM: drop hammer: > 40 J (100–500  $\mu\text{m}$ ); friction tester: > 360 N (100–500  $\mu\text{m}$ ); ESD: 0.61 (100–500  $\mu\text{m}$ ). IR (ATR),  $\tilde{\nu}$  (cm $^{-1}$ ) = 3456 (m), 3359 (m), 1682 (w), 1659 (s), 1610 (vw), 1596 (vw), 1538 (m), 1489 (m), 1412 (w), 1390 (m), 1338 (vs), 1300 (s), 1180 (w), 1019 (m), 1002 (m), 845 (s);  $^1\text{H}$  NMR ( $d_6$ -DMSO, 400 MHz, ppm)  $\delta = 7.37$  (br, 4H).  $^{13}\text{C}$  NMR ( $d_6$ -DMSO, 101 MHz, ppm)  $\delta = 153.7$ , 151.7, 104.2.  $^{14}\text{N}$  NMR ( $d_6$ -DMSO, 29 MHz, ppm)  $\delta = -17$ . Elem. Anal. ( $\text{C}_{10}\text{H}_{12}\text{N}_{18}\text{O}_8$ , 512.32 g mol $^{-1}$ ) calcd.: C 23.44, H 2.36, N 49.21 %. Found: C 23.29, H 2.25, N 48.20 %.

**Potassium 4-(1-amino-3,5-dinitropyrazolyl)-3',5'-dinitropyrazolate (11)**

Sodium hydroxide (1.02 g, 25.0 mmol) and potassium dihydrogen phosphate (3.77 g, 28.0 mmol) were dissolved in water (15 mL) and TNBPz • H $_2\text{O}$  (500 mg, 1.50 mmol) was added. The reaction mixture was heated to 60 °C and hydroxylamine-*O*-sulfonic acid (1.70 g, 15.0 mmol, 10.0 eq.) was added slowly. The suspension was stirred overnight at 60 °C. The formed precipitate was filtered, washed with small amount of water and dried on air to yield compound **11** (377 mg, 69 %) as a yellow powder.

DTA (5 °C min $^{-1}$ ): 280 °C (exo.); BAM: drop hammer: 10 J (100–500  $\mu\text{m}$ ); friction tester: 48 N (100–500  $\mu\text{m}$ ); ESD: 25  $\mu\text{J}$  (100–500  $\mu\text{m}$ ). IR (ATR),  $\tilde{\nu}$  (cm $^{-1}$ ) = 3347 (w), 3043 (br), 1534 (s), 1481 (s), 1399 (s), 1368 (s), 1325 (vs), 1310 (vs), 1007 (m), 847 (vs), 756 (m), 741 (m).  $^1\text{H}$  NMR ( $d_6$ -DMSO, 400 MHz, ppm)  $\delta = 7.86$  (s, 2H).  $^{13}\text{C}$  NMR ( $d_6$ -DMSO, 101 MHz, ppm)  $\delta = 153.9$ , 153.7, 145.3, 139.7, 106.1, 97.9.  $^{14}\text{N}$  NMR ( $d_6$ -DMSO, 29 MHz, ppm)  $\delta = -33$ .  $^{15}\text{N}$  NMR ( $d_6$ -DMSO, 41 MHz, ppm)  $\delta = -16.1$ ,  $-17.3$ ,  $-24.7$ ,  $-30.8$ ,  $-32.4$ ,



## Energetic Derivatives of 3,3',5,5'-Tetranitro-4,4'-bipyrazole (TNBPz): Synthesis, Characterization and Properties

−45.3, −81.6, −165.2, −284.4 ( $^1J_{NH} = 73.6$  Hz) Elem. Anal. ( $C_6H_2KN_9O_8$ , 367.24 g mol<sup>−1</sup>) calcd.: C 19.62, H 0.55, N 34.33 %. Found: C 19.72, H 0.74, N 33.95 %.

### 1,1'-Diamino-3,3',5,5'-tetranitro-4,4'-bipyrazole (12)

3,3',5,5'-Tetranitro-4,4'-bipyrazole monohydrate (2.00 g, 6.00 mmol, 1.0 eq.) was dissolved in acetonitrile (100 mL) and 1,8-diazabicyclo[5.4.0]undec-7-en (DBU, 1.85 mL, 12.3 mmol, 2.05 eq.) was added. The resulting solution was stirred for 1 h at room temperature and a freshly prepared solution of *O*-*p*-toluenesulfonylhydroxylamine (TOSA, 2.8 eq.) in DCM was added in one portion. The resulting reaction mixture was stirred for 2 d at room temperature and the solvent was removed *in vacuo*. The resulting crude product was recrystallized from EtOH/H<sub>2</sub>O to result in compound **12** (1.80 g, 87 %) as a pale yellow solid.

DTA (5 °C min<sup>−1</sup>): 234 °C (melt.), 244 °C (exo.); BAM: drop hammer: 15 J (100–500 μm); friction tester: 324 N (100–500 μm); ESD: 13 μJ (100–500 μm). IR (ATR),  $\tilde{\nu}$  (cm<sup>−1</sup>) = 3338 (m), 3273 (m), 1551 (s), 1490 (s), 1430 (m), 1380 (m), 1324 (vs), 1132 (m), 1104 (w), 1012 (m), 932 (w), 869 (s), 731 (m). <sup>1</sup>H NMR (*d*<sub>6</sub>-DMSO, 400 MHz, ppm)  $\delta$  = 8.03 (s, 4H). <sup>13</sup>C NMR (*d*<sub>6</sub>-DMSO, 101 MHz, ppm)  $\delta$  = 145.5, 140.1, 100.5. <sup>14</sup>N NMR (*d*<sub>6</sub>-DMSO, 29 MHz, ppm)  $\delta$  = −32. <sup>15</sup>N NMR (*d*<sub>6</sub>-DMSO, 41 MHz, ppm)  $\delta$  = −26.1 (N1), −32.4 (N2), −81.4 (N3), −163.0 (N4), −283.3 (N5). Elem. Anal. ( $C_8H_4N_{10}O_8$ , 344.16 g mol<sup>−1</sup>) calcd.: C 20.94, H 1.17, N 40.70 %. Found: C 21.21, H 1.25, N 40.50 %. *m/z* (DEI<sup>+</sup>): 344.03 [M]<sup>+</sup>, 210.02, 103.00, 77.00;

## 9.5. Conflicts of interest

There are no conflicts to declare.

## 9.6. Acknowledgements

The financial support of this work by the Ludwig-Maximilian University of Munich (LMU), the Office of Naval Research (ONR) under grant no. ONR.N00014-16-1-2062 and the Strategic Environmental Research and Development Program (SERDP) under contact no.

WP19-1287 are gratefully acknowledged. We thank Stefan Huber for his help with the sensitivity testing.

## 9.7. References

- [1] a) J. P. Agrawal, R. D. Hodgson, *Organic Chemistry of Explosives*, Wiley, New York, 2007. b) T. M. Klapötke, *Chemistry of High-Energy Materials*, 4th ed., De Gruyter, Berlin, 2017. c) M. H. Keshavarz, T. M. Klapötke, *Energetic Compounds: Methods for Prediction of Their Performance*, De Gruyter, Berlin, 2017. d) M. H. Keshavarz, T. M. Klapötke, *The Properties of Energetic Materials: Sensitivity, Physical and Thermodynamic Properties*, De Gruyter, Berlin, 2017.
- [2] a) G. Gao, J. M. Shreeve, *Chem. Rev.*, 2011, **111**, 7377–7436. b) Y. Tang, J. Zhang, L. A. Mitchell, D. A. Parrish, J. M. Shreeve, *J. Am. Chem. Soc.*, 2015, **137**, 15984–15987.
- [3] a) D. Fischer, J. L. Gottfried, T. M. Klapötke, K. Karaghiosoff, J. Stierstorfer, T. G. Witkowski, *Angew. Chem. Int. Ed.*, 2016, **55**, 16132–16135. b) Z. Xu, G. Cheng, H. Yang, J. Zhang, J. M. Shreeve, *Chem. Eur. J.*, 2018, **24**, 1–11. c) Y. Zhang, C. Zhou, B. Wang, Y. Zhou, K. Xu, S. Jia, F. Zhao, *Propellants Explos. Pyrotech.*, 2014, **39**, 809–814. d) I. Gospodinov, T. Hermann, T. M. Klapötke, J. Stierstorfer, *Propellants Explos. Pyrotech.*, 2018, **43**, 355–363.
- [4] a) J. P. Agrawal, *Prog. Energy Combust. Sci.*, 1998, **24**, 1–30. b) I. Gospodinov, T. M. Klapötke, J. Stierstorfer, *Eur. J. Org. Chem.*, 2018, 1004–1010.
- [5] T. M. Klapötke, *Energetic Materials Encyclopedia*, De Gruyter, Berlin/Boston, 2018.
- [6] a) D. E. Chavez, *Topics in Heterocyclic Chemistry*, Springer, Berlin, Heidelberg, 2017, 1–27. b) P. F. Pagoria, G. S. Lee, A. R. Mitchell, R. D. Schmidt, *Thermochimica Acta*, 2002, **384**, 187–204. c) T. M. Klapötke, R. D. Chapman, *Struct. Bond.*, 2016, **172**, 49–64.
- [7] T. M. Klapötke, P. C. Schmid, S. Schnell, J. Stierstorfer, *J. Mat. Chem. A*, 2015, **3**, 2658–2668.
- [8] Y. tang, C. He, G. H. Imler, D. A. Parrish, J. M. Shreeve, *J. Mater. Chem., A* 2018, **6**, 5136–5142.
- [9] D. E. Chavez, M. A. Hiskey, R. D. Gilardi, *Angew. Chem.*, 2000, **112**, 1861–1863.
- [10] T. M. Klapötke, P. Mayer, C. M. Sabaté, J. M. Welch, N. Weigand, *Inorg. Chem.*, 2008, **47**, 6014–6027.

**Energetic Derivatives of 3,3',5,5'-Tetranitro-4,4'-bipyrazole (TNBPz): Synthesis,  
Characterization and Properties**

- [11] K. V. Domasevitch, I. Gospodinov, H. Krautscheid, T. M. Klapötke, J. Stierstorfer, *New J. Chem.*, 2019, **43**, 1305–1312.
- [12] M. D. Coburn, *J. Heterocycl. Chem.* **1971**, 8, 153–154.
- [13] T. L. Cottrell, *The Strengths of Chemical Bonds*, Butterworths Scientific Publications, London, **1958**.
- [14] H. Ehrlich, *Acta Crystallogr.* **1960**, 13, 946–952.
- [15] N. Fischer, D. Fischer, T. M. Klapötke, D. G. Piercey, J. Stierstorfer, *J. Mater. Chem.* **2012**, 22, 20418–20422.
- [16] Wasserbeschaffenheit - Bestimmung der Hemmwirkung von Wasserproben auf die Lichtemission von *Vibrio Fischeri* (Leuchtbakterientest). In *Wasserbeschaffenheit - Bestimmung der Hemmwirkung von Wasserproben auf die Lichtemission von Vibrio Fischeri (Leuchtbakterientest)*, **2009**; Vol. DIN EN ISO 11348-2.
- [17] C. J. Cao, M. S. Johnson, M. M. Hurley, T. M. Klapötke, T. M., *J. Propuls. Energet.* **2012**, 5, 41–51.
- [18] I. Gospodinov, K. V. Domasevitch, C. C. Unger, T. M. Klapötke, J. Stierstorfer, On a midway between energetic molecular crystals and high-density energetic salts: Crystal engineering with hydrogen bonded chains of polynitro bipyrazoles, Submitted to *Cryst. Growth Des.* **2019**.
- [19] M. F. Bölter, A. Harter, T. M. Klapötke, J. Stierstorfer, *ChemPlusChem* **2018**, 83, 804–811.
- [20] M. F. Bölter, T. M. Klapötke, T. Kustermann, T. Lenz, J. Stierstorfer, *Eur. J. Inorg. Chem.* **2018**, 2018, 4125–4132.
- [21] D. Fischer, T. M. Klapötke, M. Reymann, J. Stierstorfer, *Chem. - Eur. J.* **2014**, 20, 6401–6411.
- [22] J. S. Murray, P. Politzer, *J. Mol. Model* **2014**, 20, 2223–2227.
- [23] M. Sućeska, *EXPLO5 Version 6.03 User's Guide*, Zagreb, Croatia: OZM; **2015**.
- [24] T. M. Klapötke, T. G. Witkowski, *ChemPlusChem* **2016**, 81, 357–360.
- [25] a) Reichel & Partner GmbH, <http://www.reichelt-partner.de>; b) Test methods according to the UN Recommendations on the Transport of Dangerous Goods, Manual of Test and Criteria, 4th edn., United Nations Publication, New York and Geneva, **2003**, ISBN 92–1-139087 7, Sales No. E.03.VIII.2; 13.4.2 Test 3 a (ii) BAM Fallhammer.

## 9.8. Supporting Information

### 9.8.1. Synthesis and general considerations

3,3',5,5'-Tetranitro-4,4'-bipyrazole monohydrate (TNBPz, **1·H<sub>2</sub>O**) was prepared as previously reported in the literature.<sup>[S1]</sup>

### 9.8.2. X-ray diffraction

The low-temperature single-crystal X-ray diffraction measurements were performed on an Oxford XCalibur3 diffractometer equipped with a Spellman generator (voltage 50 kV, current 40 mA) and a KappaCCD detector operating with MoK $\alpha$  radiation ( $\lambda = 0.7107 \text{ \AA}$ ). Data collection was performed using the CRYSLIS CCD software.<sup>[S2]</sup> The data reduction was carried out using the CRYSLIS RED software.<sup>[S3]</sup> The solution of the structure was performed by direct methods (SIR97)<sup>[S4]</sup> and refined by full-matrix least-squares on F<sup>2</sup> (SHELXL)<sup>[S5]</sup> implemented in the WINGX software package<sup>[S6]</sup> and finally checked with the PLATON software.<sup>[S7]</sup> All DIAMOND2 plots are shown with thermal ellipsoids at the 50% probability level and hydrogen atoms are shown as small spheres of arbitrary radius.

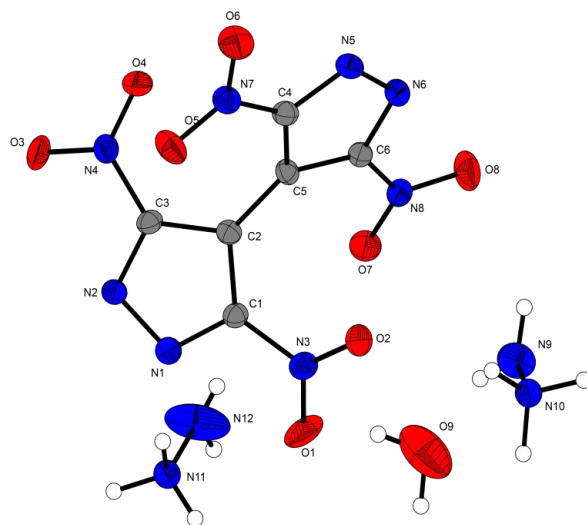


**Figure S1.** Representation of the molecular unit of **7·0.5H<sub>2</sub>O**.

# Energetic Derivatives of 3,3',5,5'-Tetranitro-4,4'-bipyrazole (TNBPz): Synthesis, Characterization and Properties

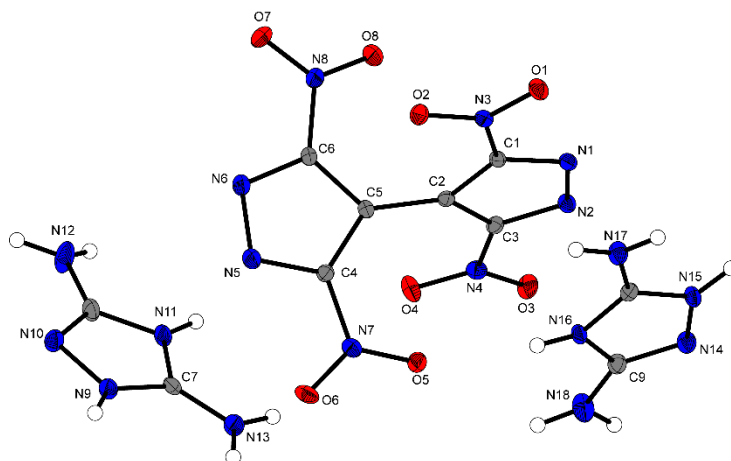


**Figure S2.** Representation of the molecular unit of **10**.

**Table S1.** Crystallographic details of compounds **2**, **4** and **5**.

Compound	<b>2</b>	<b>4</b>	<b>5</b>
Formula	C <sub>8</sub> H <sub>6</sub> N <sub>8</sub> O <sub>8</sub>	C <sub>8</sub> H <sub>12</sub> N <sub>14</sub> O <sub>8</sub>	C <sub>6</sub> H <sub>14</sub> N <sub>16</sub> O <sub>8</sub>
Form. Mass [g/mol]	342.18	432.32	462.35
Crystal system	monoclinic	monoclinic	orthorhombic
Space Group	<i>Cc</i> (No. 9)	<i>P21/c</i> (No. 14)	<i>Pcnn</i> (No. 56)
Color / Habit	Colorless platelet	yellow plate	yellow block
Size [mm]	0.02 × 0.06 × 0.09	0.09 × 0.29 × 0.55	0.16 × 0.41 × 0.48
<i>a</i> [Å]	8.91415)	10.7792(15)	10.2845(2)
<i>b</i> [Å]	22.2317(15)	17.441(2)	18.8916(4)
<i>c</i> [Å]	7.8114(4)	9.6177(15)	9.2779(2)
$\alpha$ [°]	90	90	90
$\beta$ [°]	124.432(2)	107.766(15)	90
$\gamma$ [°]	90	90	90
<i>V</i> [Å <sup>3</sup> ]	1283.13(13)	1721.9(4)	1802.61(6)
<i>Z</i>	4	4	4
$\rho_{\text{calc.}}$ [g cm <sup>-3</sup> ]	1.771	1.668	1.704
$\mu$ [mm <sup>-1</sup> ]	0.160	0.147	0.150
<i>F</i> (000)	696	888	952
$\lambda_{\text{MoK}\alpha}$ [Å]	0.71073	0.71073	0.71073
<i>T</i> [K]	111	143	130
$\theta$ min-max [°]	2.917, 28.321	4.3, 26.0	4.3, 27.0
Dataset <i>h</i> ; <i>k</i> ; <i>l</i>	−11:11; −29:29; −10:10	−13:13; −21:814; −11:11	−13:13; −24:24; −11:11
Reflect. coll.	6935	13507	26392
Independ. refl.	3126	3367	1958
<i>R</i> <sub>int</sub>	0.0265	0.063	0.030
Reflection obs.	3014	2279	1779

**Energetic Derivatives of 3,3',5,5'-Tetranitro-4,4'-bipyrazole (TNBPz): Synthesis,  
Characterization and Properties**

No. parameters	241	319	173
$R_1$ (obs)	0.0303	0.0438	0.0305
$wR_2$ (all data)	0.0772	0.1022	0.0834
$S$	1.08	1.04	1.06
Resd. Dens. [ $e \text{ \AA}^{-3}$ ]	0.195/−0.215	−0.23, 0.25	−0.26, 0.29
Device type	Oxford Xcalibur3 CCD	Oxford Xcalibur3 CCD	Oxford Xcalibur3 CCD
Solution	SIR-92	SIR-92	SIR-92
Refinement	SHELXL-97	SHELXL-97	SHELXL-97
Absorpt. corr.	multi-scan	multi-scan	multi-scan
CCDC	—	—	—

**Table S2.** Crystallographic details of compounds **6**, **7·0.5H<sub>2</sub>O** and **10**.

Compound	<b>6</b>	<b>7·0.5H<sub>2</sub>O</b>	<b>10</b>
Formula	C <sub>6</sub> H <sub>8</sub> N <sub>10</sub> O <sub>10</sub>	C <sub>12</sub> H <sub>38</sub> N <sub>24</sub> O <sub>17</sub>	C <sub>10</sub> H <sub>12</sub> N <sub>18</sub> O <sub>8</sub>
Form. Mass [g/mol]	380.19	774.54	512.38
Crystal system	orthorhombic	triclinic	monoclinic
Space Group	$Pca2_1$ (No. 29)	$P-1$	$P2_1/n$ (No. 14)
Color / Habit	colorless block	colorless block	colorless block
Size [mm]	0.15 × 0.15 × 0.20	0.07 × 0.12 × 0.18	0.10 × 0.15 × 0.25
$a$ [Å]	17.1257(5)	9.0304(15)	6.0153(3)
$b$ [Å]	9.8507(3)	9.9677(15)	15.5729(8)
$c$ [Å]	33.8680(11)	10.3061(13)	21.203(1)
$\alpha$ [°]	90	102.719(12)	90
$\beta$ [°]	90	106.417(13)	93.851(4)
$\gamma$ [°]	90	115.425(15)	90
$V$ [Å <sup>3</sup> ]	5713.5(3)	738.6(3)	1981.72(17)
$Z$	16	1	4
$\rho_{\text{calc.}}$ [g cm <sup>−3</sup> ]	1.768	1.741	1.717
$\mu$ [mm <sup>−1</sup> ]	0.167	0.159	0.148
$F(000)$	3104	398	1048
$\lambda_{\text{MoK}\alpha}$ [Å]	0.71073	0.71073	0.71073
$T$ [K]	127	143	143
$\vartheta$ min-max [°]	4.1, 26.0	4.1, 27.0	4.2, 26.0
Dataset h; k; l	−9:21; −12:12; 40:42	−11:10; −12:12; −13:13	−7:7; −19:18; −26:26
Reflect. coll.	30449	6076	16624
Independ. refl.	11501	3208	3896
$R_{\text{int}}$	0.072	0.050	0.076
Reflection obs.	8228	2035	2626

## Energetic Derivatives of 3,3',5,5'-Tetranitro-4,4'-bipyrazole (TNBPz): Synthesis, Characterization and Properties

No. parameters	954	292	373
$R_1$ (obs)	0.0513	0.0552	0.0478
$wR_2$ (all data)	0.0820	0.1196	0.1208
$S$	0.99	1.01	1.03
Resd. Dens. [ $e \text{ \AA}^{-3}$ ]	−0.31, 0.54	−0.43, 0.29	−0.27, 0.67
Device type	Oxford Xcalibur3 CCD	Oxford Xcalibur3 CCD	Oxford Xcalibur3 CCD
Solution	SIR-92	SIR-92	SIR-92
Refinement	SHELXL-97	SHELXL-97	SHELXL-97
Absorpt. corr.	multi-scan	multi-scan	multi-scan
CCDC	—	—	—

### 9.8.3. Computations

Quantum chemical calculations were carried out using the Gaussian G09 program package.<sup>[S8]</sup> The enthalpies (H) and free energies (G) were calculated using the complete basis set (CBS) method of Petersson and co-workers in order to obtain very accurate energies. The CBS models use the known asymptotic convergence of pair natural orbital expressions to extrapolate from calculations using a finite basis set to the estimated CBS limit. CBS-4 begins with an HF/3-21G(d) geometry optimization; the zero point energy is computed at the same level. It then uses a large basis set SCF calculation as a base energy, and an MP2/6-31+G calculation with a CBS extrapolation to correct the energy through second order. An MP4(SDQ)/6-31+ (d,p) calculation is used to approximate higher order contributions. In this study, we applied the modified CBS.

Heats of formation of ionic compounds were calculated using the atomization method (equation 1) using room temperature CBS-4M enthalpies summarized in **Table S3**.<sup>[S9,S10]</sup>

$$\Delta_f H^\circ_{(g, M, 298)} = H_{(Molecule, 298)} - \sum H^\circ_{(Atoms, 298)} + \sum \Delta_f H^\circ_{(Atoms, 298)} \quad (1)$$

**Table S3.** CBS-4M electronic enthalpies for atoms C, H, N and O and their literature values for atomic  $\Delta_f H^\circ_{298} / \text{kJ mol}^{-1}$

	$-H^{298} / \text{a.u.}$	NIST <sup>[S11]</sup>
H	0.500991	218.2
C	37.786156	717.2
N	54.522462	473.1
O	74.991202	249.5

In the case of the ionic compounds, the lattice energy ( $U_L$ ) and lattice enthalpy ( $\Delta H_L$ ) were calculated from the corresponding X-ray molecular volumes according to the equations provided

## Energetic Derivatives of 3,3',5,5'-Tetranitro-4,4'-bipyrazole (TNBPz): Synthesis, Characterization and Properties

by *Jenkins and Glasser*.<sup>[S12]</sup> With the calculated lattice enthalpy the gas-phase enthalpy of formation was converted into the solid state (standard conditions) enthalpy of formation. These molar standard enthalpies of formation ( $\Delta H_m$ ) were used to calculate the molar solid state energies of formation ( $\Delta U_m$ ) according to equation 2.

$$\Delta U_m = \Delta H_m - \Delta nRT \quad (2)$$

( $\Delta n$  being the change of moles of gaseous components)

The calculation results are summarized in **Tables S4** and **S5**.

**Table S4.** CBS-4M results and calculated gas-phase enthalpies.

Ion	M [g mol <sup>-1</sup> ] <sup>[a]</sup>	-H <sup>298</sup> <sup>[b]</sup> / a.u.	$\Delta_f H^\circ(g,M)$ / kJ mol <sup>-1</sup> <sup>[c]</sup>
<b>TNBPz<sup>2-</sup></b>	312.12	1266.63391	78.0
<b>(NH<sub>2</sub>)TNBPz<sup>-</sup></b>	328.14	1322.46768	177.3
<b>K<sup>+</sup></b>	39.1	599.03597	487.4
<b>G<sup>+</sup></b>	60.1	205.453192	571.2
<b>AG<sup>+</sup></b>	75.1	260.701802	671.6
<b>NH<sub>3</sub>OH<sup>+</sup></b>	34.04	131.863249	686.4
<b>NH<sub>4</sub><sup>+</sup></b>	18.1	56.796608	635.3

<sup>[a]</sup> Molecular weight; <sup>[b]</sup> CBS-4M electronic enthalpy; <sup>[c]</sup> gas phase enthalpy of formation;

**Table S5.** Calculation results.

Compound	$\Delta_f H^\circ(g,M)$ / kJ mol <sup>-1</sup> <sup>[a]</sup>	V <sub>M</sub> / nm <sup>3</sup> <sup>[b]</sup>	$\Delta U_L$ kJ mol <sup>-1</sup> <sup>[c]</sup>	$\Delta H_L$ kJ mol <sup>-1</sup> <sup>[d]</sup>	$\Delta_f H^\circ(s)$ kJ mol <sup>-1</sup> <sup>[e]</sup>	$\Delta_f U(s)$ kJ kg <sup>-1</sup> <sup>[f]</sup>
<b>2</b>	287.0	0.3207825	—	—	200.9	666.7
<b>4</b>	1224.5	0.4419661	1124.1	1131.5	88.8	303.0
<b>5</b>	1423.9	0.4627750	1103.4	1110.9	308.5	769.2
<b>6</b>	1450.8	0.3668638	1206.6	1214.1	236.7	713.9
<b>8</b>	1348.6	0.3471325	1232.4	1239.8	108.7	404.8
<b>11</b>	665.0	0.2887	525.9	525.7	139.3	443.5
<b>12</b>	660.1	—	—	—	464.5	1429.0

<sup>[a]</sup> gas phase enthalpy of formation; <sup>[b]</sup> molecular volumes taken from X-ray structures and corrected to room temperature; <sup>[c]</sup> lattice energy (calculated using Jenkins and Glasser equations); <sup>[d]</sup> lattice enthalpy (calculated using Jenkins and Glasser equations); <sup>[e]</sup> standard solid state enthalpy of formation; <sup>[f]</sup> solid state energy of formation.



#### 9.8.4. References

- [S1] K. V. Domasevitch, I. Gospodinov, H. Krautscheid, T. M. Klapötke, J. Stierstorfer, *New J. Chem.* **2019**, *43*, 1305–1312.
- [S2] CrysAlisPro, *Oxford Diffraction Ltd. version 171.33.41*, **2009**.
- [S3] CrysAlis RED, *Version 1.171.35.11 (release 16-05-2011 CrysAlis 171.Net)*, Oxford Diffraction Ltd., Abingdon, Oxford (U.K.), **2011**.
- [S4] A. Altomare, M. C. Burla, M. Camalli, G. L. Cascarano, C. Giacovazzo, A. Guagliardi, A. G. Moliterni, G. Polidori and R. Spagna, SIR97: A New Tool for Crystal Structure Determination and Refinement, *J. Appl. Crystallogr.*, **1999**, *32*, 115–119.
- [S5] G. M. Sheldrick, A Short History of SHELX, *Acta Crystallogr., Sect. A: Found. Crystallogr.*, **2008**, *64*, 112–122.
- [S6] L. J. Farrugia, WinGX Suite for Small-Molecule Single-Crystal Crystallography, *J. Appl. Crystallogr.*, **1999**, *32*, 837–838.
- [S7] A. L. Spek, *PLATON*, **1999**, A Multipurpose Crystallographic Tool, Utrecht University, The Diffraction Ltd.
- [S8] M. J. Frisch, G. W. Trucks, H. B. Schlegel, G. E. Scuseria, M. A. Robb, J. R. Cheeseman, G. Scalmani, V. Barone, B. Mennucci, G. A. Petersson, H. Nakatsuji, M. Caricato, X. Li, H.P. Hratchian, A. F. Izmaylov, J. Bloino, G. Zheng, J. L. Sonnenberg, M. Hada, M. Ehara, K. Toyota, R. Fukuda, J. Hasegawa, M. Ishida, T. Nakajima, Y. Honda, O. Kitao, H. Nakai, T. Vreven, J. A. Montgomery, Jr., J. E. Peralta, F. Ogliaro, M. Bearpark, J. J. Heyd, E. Brothers, K. N. Kudin, V. N. Staroverov, R. Kobayashi, J. Normand, K. Raghavachari, A. Rendell, J. C. Burant, S. S. Iyengar, J. Tomasi, M. Cossi, N. Rega, J. M. Millam, M. Klene, J. E. Knox, J. B. Cross, V. Bakken, C. Adamo, J. Jaramillo, R. Gomperts, R. E. Stratmann, O. Yazyev, A. J. Austin, R. Cammi, C. Pomelli, J. W. Ochterski, R. L. Martin, K. Morokuma, V. G. Zakrzewski, G. A. Voth, P. Salvador, J. J. Dannenberg, S. Dapprich, A. D. Daniels, O. Farkas, J.B. Foresman, J. V. Ortiz, J. Cioslowski, D. J. Fox, Gaussian 09 A.02, Gaussian, Inc., Wallingford, CT, USA, **2009**.
- [S9] (a) J. W. Ochterski, G. A. Petersson, and J. A. Montgomery Jr., A complete basis set model chemistry. V. Extensions of six or more heavy atoms, *J. Chem. Phys.* **1996**, *104*, 2598–2619;  
(b) J. A. Montgomery Jr., M. J. Frisch, J. W. Ochterski G. A. Petersson, A complete basis set

**Energetic Derivatives of 3,3',5,5'-Tetranitro-4,4'-bipyrazole (TNBPz): Synthesis,  
Characterization and Properties**

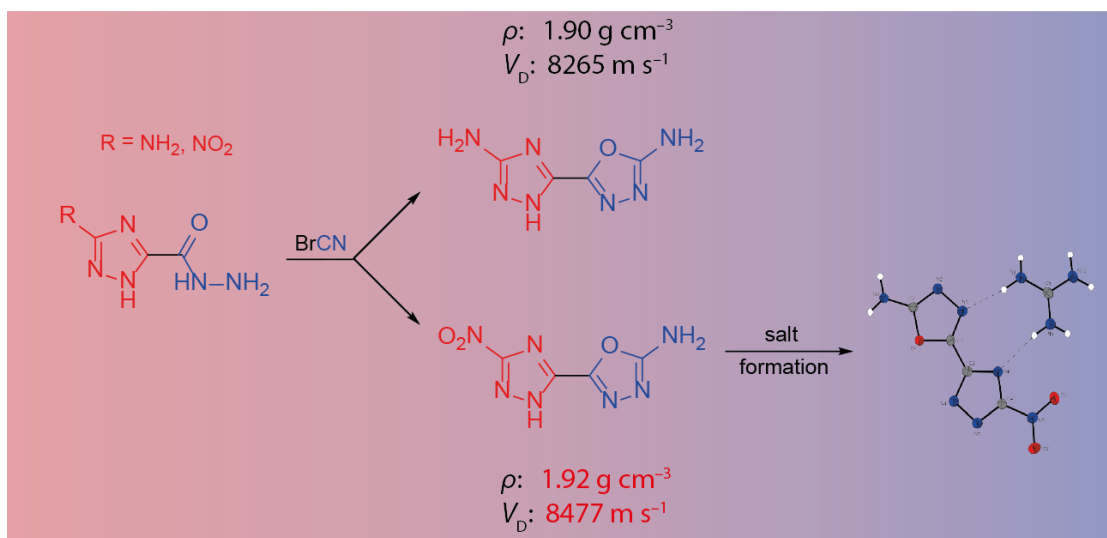
model chemistry. VII. Use of the minimum population localization method, *J. Chem. Phys.* **2000**, *112*, 6532–6542.

- [S10] (a) L. A. Curtiss, K. Raghavachari, P. C. Redfern, J. A. Pople, Assessment of Gaussian-2 and density functional theories for the computation of enthalpies of formation, *J. Chem. Phys.* **1997**, *106*, 1063–1079; (b) E. F. C. Byrd, B. M. Rice, Improved Prediction of Heats of Formation of Energetic Materials Using Quantum Mechanical Calculations, *J. Phys. Chem. A* **2006**, *110*, 1005–1013; (c) B. M. Rice, S. V. Pai, J. Hare, Predicting heats of formation of energetic materials using quantum mechanical calculations, *Comb. Flame* **1999**, *118*, 445–458.
- [S11] P. J. Lindstrom, W. G. Mallard (Editors), NIST Standard Reference Database Number 69, <http://webbook.nist.gov/chemistry/> (accessed November **2017**).
- [S12] (a) H. D. B. Jenkins, H. K. Roobottom, J. Passmore, L. Glasser, Relationships among Ionic Lattice Energies, Molecular (Formula Unit) Volumes, and Thermochemical Radii, *Inorg. Chem.* **1999**, *38*, 3609–3620. (b) H. D. B. Jenkins, D. Tudela, L. Glasser, Lattice Potential Energy Estimation for Ionic Salts from Density Measurements, *Inorg. Chem.* **2002**, *41*, 2364–2367.

## 10. Combination of Different Azoles – 1,2,4-Triazolyl-1,3,4-Oxadiazoles as Precursor for Energetic Materials

Marc F. Bölter, Ivan Gospodinov, Thomas M. Klapötke and Jörg Stierstorfer

Unpublished Results



**Abstract:** Two new bisheterocyclic compounds 2-amino-5-(5-amino-1H-1,2,4-triazol-3-yl)-1,3,4-oxadiazole (**5**) and 2-amino-5-(5-nitro-1H-1,2,4-triazol-3-yl)-1,3,4-oxadiazole (**6**) were synthesized and compared to each other. Further, four energetic salts of compound **6** were synthesized in order to improve the energetic performance and sensitivity values. The obtained compounds were characterized using IR, NMR (<sup>1</sup>H, <sup>13</sup>C, <sup>14</sup>N), mass, elemental analysis and thermal analysis (DSC). Crystal structures could be obtained of five compounds (**3**, **7–10**) by low temperature single crystal X-ray diffraction. Impact, friction and ESD values were determined according to *Bundesamt für Materialforschung* (BAM) standard methods. Both bisheterocyclic compounds and obtained salts are not sensitive toward external stimuli and show a thermal stability up to 296 °C. The energetic performance of the energetic salts was calculated using recalculated X-ray densities, heats of formation and the EXPLO5 code. Their detonation velocity and pressure lie in the range of 6965–7672 m s<sup>-1</sup> and 179–206 kbar. Both bisheterocycles (**5** and **6**) are suitable as precursors for new energetic materials indicating a high thermal stability.

## 10.1. Introduction

The research on new powerful explosives is an ongoing field of study due to their application in military and civilian areas.<sup>[1]</sup> Depending on their usage, high energetic dense materials (HEDMs) have to fulfil different requirements such as a safe handling, high detonation properties or high thermal stability.<sup>[2]</sup> The main goal is to substitute the current mostly used secondary explosive RDX and TNT due to its high toxicity to the environment and humans.<sup>[3]</sup> Modern research for alternatives to RDX and TNT focus on nitrogen-rich azoles, which show good sensitivity values, possess high positive heats of formation and mainly generate environmentally friendly dinitrogen gas during decomposition.<sup>[4]</sup> The heats of formation increase with the number of nitrogen atoms within the ring from imidazoles to tetrazoles (**Figure 1**).<sup>[5]</sup> 1,2,4-Triazoles are suitable heterocycles as building blocks for energetic materials due to the high nitrogen content, positive heat of formation and good thermal stability.<sup>[6]</sup> The introduction of oxygen to an azole leads to oxadiazoles, which combine a good oxygen balance, high energetic performance and likewise high thermal stability.<sup>[2c,7]</sup>

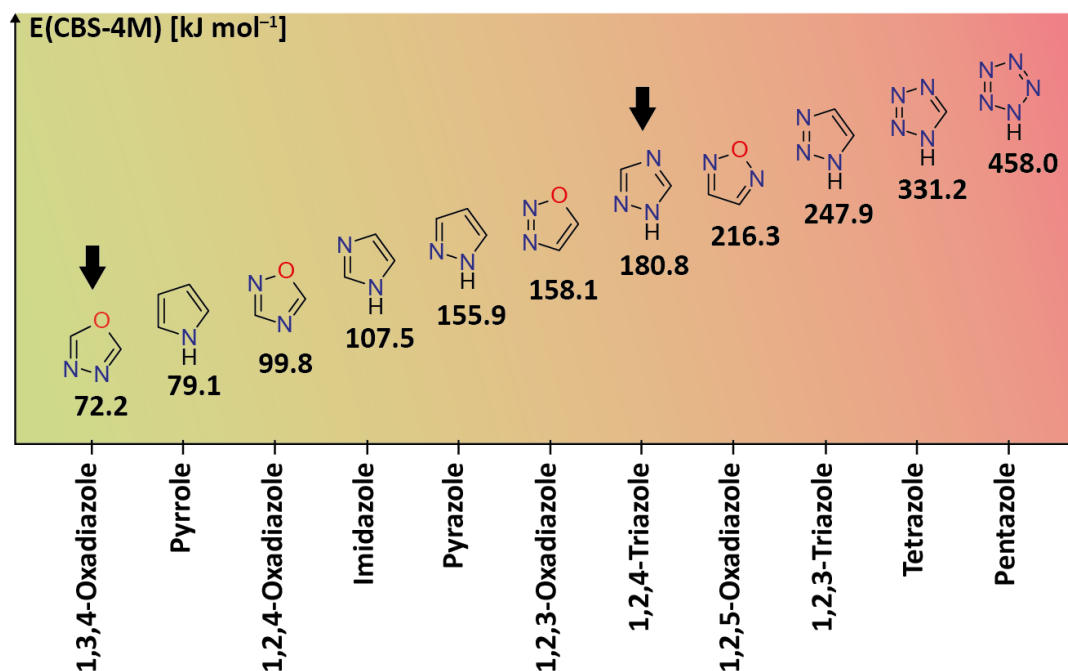


**Figure 1.** Overview of the heat of formation in kJ mol<sup>-1</sup> of selected azoles.

## Combination of Different Azoles – 1,2,4-Triazolyl-1,3,4-Oxadiazoles as Precursor for Energetic Materials

A huge number of C–C bonded bisheterocyclic nitrogen-rich compounds combining triazoles, tetrazoles, pyrazoles and oxadiazoles have been synthesized in the past showing promising physicochemical and energetic properties (**Figure 2**).<sup>[6b, 7b, 8]</sup>

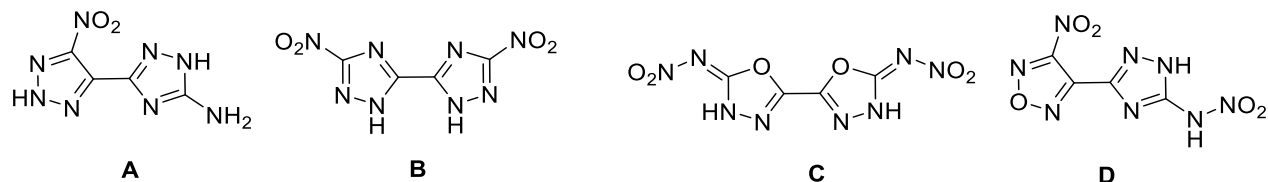


**Figure 2.** Different energetic materials based on bisheterocyclic compounds: A) 4-nitro-5-(5-amino-1,2,4-triazol-3-yl)-2H-1,2,3-triazole<sup>[6a]</sup>, B) 3,3'-dinitro-5,5'-bis(1H-1,2,4-triazole)<sup>[6b]</sup>, C) 2,2'-dinitramino-5,5'-bi(1-oxa-3,4-diazole)<sup>[7b]</sup>, D) 3-nitro-4-(5-nitramino-1,2,4-triazol-3-yl)furazane<sup>[8a]</sup>.

Bisheterocyclic compounds consisting of a 1,2,4-triazole and a 1,3,4-oxadiazole have not been reported in the literature yet. This contribution reports on the synthesis and intensive characterization of 3-amino-5-(5-amino-1H-1,2,4-triazol-3-yl)-1,3,4-oxadiazole (**5**) and 3-amino-5-(5-nitro-1H-1,2,4-triazol-3-yl)-(3-amino-1,3,4-oxadiazole) (**6**). In addition, four energetic salts with the derivative **6** were obtained. Both compounds **5** and **6** can be used as suitable precursors for the synthesis of energetic materials.

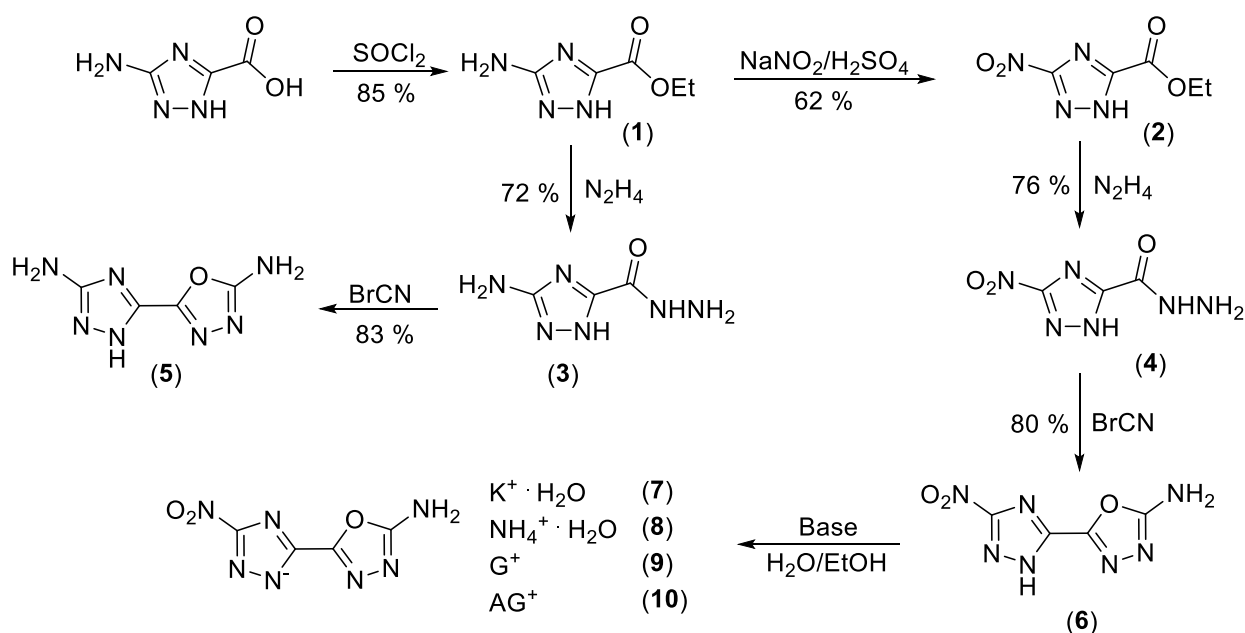
## 10.2. Results and Discussion

### 10.2.1. Synthesis

5-Amino-1H-1,2,4-triazole-3-carboxylic acid was used as the starting material for the synthesis of the heterocyclic compounds **5** and **6** (**Scheme 1**). The concept for the synthesis of 2-amino-5-(5-amino-1H-1,2,4-triazol-3-yl)-1,3,4-oxadiazole (**5**) was to obtain the triazole carboxylate, convert this compound into the triazole carbohydrazine (**3**) and perform a ring closure to yield the triazole-oxadiazole product. The first step was performed according to the known literature by reacting the starting material with thionyl chloride in abs. EtOH which led to the formation of the carboxylic acid ester (**1**).<sup>[9]</sup> The reaction of compound **1** with hydrazine hydrate in MeOH was carried out

## Combination of Different Azoles – 1,2,4-Triazolyl-1,3,4-Oxadiazoles as Precursor for Energetic Materials

similar to the work of Metelkina *et al.* leading to the formation of the triazole carbohydrazone derivative (3).<sup>[10]</sup> 2-Amino-5-(5-amino-1*H*-1,2,4-triazol-3-yl)-1,3,4-oxadiazole (5) was obtained by reacting 3 with the base KOH followed by the ring closure with BrCN.<sup>[11,12]</sup> 2-Amino-5-(5-nitro-1*H*-1,2,4-triazol-3-yl)-1,3,4-oxadiazole (6) was obtained similar to the synthesis of 5. For this purpose, compound 1 was nitrated with NaNO<sub>2</sub> and H<sub>2</sub>SO<sub>4</sub> according to the modified literature method to yield the nitro derivative 2.<sup>[13,14]</sup> Subsequent reaction first with hydrazine hydrate leads to the formation of compound 4 which can be further converted to the desired product 6 with BrCN and KOH.



**Scheme 1.** Synthesis of 2-amino-5-(5-amino-1*H*-1,2,4-triazol-3-yl)-1,3,4-oxadiazole (5) and 2-amino-5-(5-nitro-1*H*-1,2,4-triazol-3-yl)-1,3,4-oxadiazole (6) and energetic salts (7–10).

Different methods for improving the energetic character of azoles are known such as salt formation, *N*-oxidation, *N* or *C* functionalization, methylene or ethylene bridging, methylation or azo bridging.<sup>[2a,8b,16]</sup> The bisheterocyclic compounds (5 and 6) are suitable to serve as precursors for improving their energetic characteristics by synthesizing nitrogen-rich salts, *N*-oxidation or *N*-functionalization. For this purpose, compound 6 was reacted with the four different bases potassium carbonate, ammonia, guanidinium carbonate and aminoguanidinium carbonate.

### 10.2.2. NMR and Vibrational Spectroscopy

All compounds (**1–10**) were characterized by  $^1\text{H}$ ,  $^{13}\text{C}$  NMR spectroscopy, elemental analysis and IR spectroscopy. In the  $^1\text{H}$  NMR spectra, four signals were observed for compound **1** (12.60, 6.20, 4.22 and 1.26 ppm) and two for compound **2** (4.43 and 1.35 ppm). The carbohydrazide derivative **3** shows four signals (12.48–3.66 ppm) in the  $^1\text{H}$  spectrum whereas compound **4** only two signals at 9.35 and 4.11 ppm. The desired heterocycle **5** exhibit three signals (12.61, 7.21 and 6.27 ppm) in the  $^1\text{H}$  spectrum, whereas compound **6** shows only one resonance at 7.70 ppm. Both ester compounds **1** and **2** exhibit five resonances in the  $^{13}\text{C}$  NMR spectrum in the range of 162.2–13.9 ppm and the carbohydrazides **3** and **4** show only three resonances. The heterocyclic compounds **5** and **6** show four resonances in the  $^{13}\text{C}$  NMR spectra. For the energetic salts **7** and **8** were observed only four resonances in the  $^{13}\text{C}$  NMR spectrum whereas for the compounds **9** and **10** exhibit five signals.

IR spectra of compounds **1–10** were measured and all observed frequencies are reported in the Supporting Information. The deformation vibration of the amino groups for the guanidinium and aminoguanidinium salts **9** and **10** were observed at 1655 and 1652  $\text{cm}^{-1}$ , respectively. In addition, the asymmetric and symmetric vibration of the amino groups of compound **10** were observed at 3380 and 3328  $\text{cm}^{-1}$ .<sup>[15]</sup>

### 10.2.3. X-Ray crystallography

Suitable crystals of compounds **3** and **7–10** were obtained by recrystallization. The structures are shown in **Figures 3–5** and the structure of **3** and **8** can be found in the Supporting Information. Further information regarding the crystal-structure determinations have been deposited with the Cambridge Crystallographic Data Centre as supplementary publication Nos. 1869975 (**3**), 1869977 (**7**), 1869976 (**8**), 1869978 (**9**) and 1869979 (**10**).

## Combination of Different Azoles – 1,2,4-Triazolyl-1,3,4-Oxadiazoles as Precursor for Energetic Materials

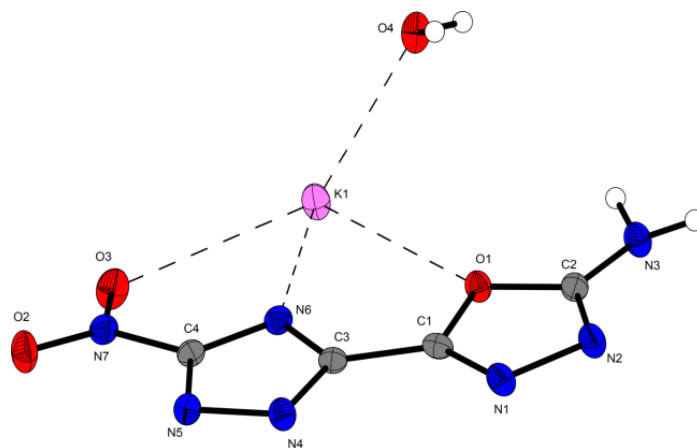


**Figure 3.** Molecular unit of compound **7** in the crystalline state. Ellipsoids correspond to 50% probability levels. Hydrogen radii are arbitrary. Selected bond lengths (Å) and angles [deg]: O1–C2 1.362(2), O1–C1 1.376(2), O1–K1 3.3846(13), N6–K1 2.7756(15), K1–O4 2.7078(15), N2–C2 1.305(2), N1–N2 1.414(2), N1–C1 1.286(2), N4–N5 1.364(2), O3–N7 1.2280(19), O2–N7 1.232(2), N6–C4 1.334(2), C1–C3 1.454(3), C1–N1–N2 106.09(14), C2–N2–N1 106.10(14), N2–C2–O1 112.46(15), C4–N6–C3 98.80(14), C2–O1–C1 102.32(13), O3–N7–O2 123.55(16), C1–N1–N2–C2 –0.1(2), C3–N4–N5–C4 –0.01(18), N2–N1–C1–C3 –179.28(18), N2–N1–C1–O1 0.1(2), C2–O1–C1–C3 179.44(15), N1–N2–C2–N3 –176.45(18), C1–O1–C2–N3 176.87(16), C4–N6–C3–N4 0.48(19), C4–N6–C3–C1 –179.62(16), O3–N7–C4–N5 –171.11(16).

The crystal structure of potassium 5-(2-amino-1,3,4-oxadiazolyl)-(3-nitrotriazolate) monohydrate **7** is shown in **Figure 3** with bond length and angles. Compound **7** crystallizes as colorless rods in the monoclinic space group  $P 2_1/n$  with four molecules in the unit cell. The volume of the unit cell is 898.68(5) Å<sup>3</sup> and lattice constants are  $a = 6.6407(2)$  Å,  $b = 11.2308(4)$  Å,  $c = 12.3709(3)$  Å and  $\beta = 103.0810(10)^\circ$ . The density is 1.872 g cm<sup>-3</sup> measured at a temperature of 100(2) K. The potassium salt of 5-(5-nitro-4*H*-1,2,4-triazol-3-yl)-2-amino-1,3,4-oxadiazole crystallize with one molecule water. Looking on the torsion angles, it is visible that the triazole-oxadiazole scaffold is planar. Furthermore, the oxygen atom of the oxadiazole, nitrogen N6 of the triazole and one oxygen atom of the nitro group are aligned at the potassium cation, what leads to a torsion of the nitro group against the plane. The oxygen atom of the crystal water is coordinating the cation, too. The distances to the potassium atom vary from 2.7078(15) Å (K1–O4) up to 3.3846(13) Å. The bond lengths and angles in the triazole correspond to the known values, while the bond angle of the nitro group O3–N7–O2 123.55(16) ° is a bit reduced compared to the expected value of about 125 °.<sup>[18,20]</sup>



## Combination of Different Azoles – 1,2,4-Triazolyl-1,3,4-Oxadiazoles as Precursor for Energetic Materials

The bond between the triazole and the oxadiazole has a length of 1.454(3) Å. Further to enhance the stability of the molecule small deformation of the oxadiazole scaffold are observable. This can be seen for example at elongation of N1–N2 (1.414(2) Å) or the reduction of N1–C1 (1.286(2) Å). The bond angles also differ a bit from the known values for 1,3,4-oxadiazoles, also the bond angle of the crystal water molecule is enlarged up to 108(3) °.<sup>[21,22]</sup>

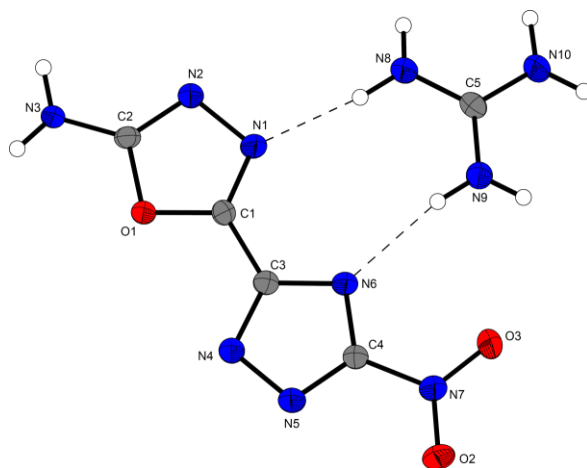


**Figure 4.** X-ray structure of compound **9**. Ellipsoids are drawn at the 50% probability level. Selected distances [Å]: C1–C3 1.448 (2), C4–N7 1.444 (2), C2–N3 1.329 (2). Selected bond angles [°]: O2–N7–C4 117.95 (15), N10–C5–N 9 120.12 (18), N3–C2–O1 118.65 (16). Selected torsion angles [°]: O1–C1–C3 N4 –0.8 (3), N6–C4–N7 O3 1.7 (3).

Compound **9** crystallizes in the monoclinic space group  $C2/c$  with a cell volume of 1991.0(3) Å<sup>3</sup> and eight formula units per cell. The cell constants are  $a = 20.3525(18)$  Å,  $b = 5.4863(4)$  Å and  $c = 18.5795(14)$  Å, while the density is 1.709 g cm<sup>-3</sup>. The distance between the two heterocycles of the molecule is C1–C3 1.448(2) Å. It is in the range of single and double bond like in all the other heterocycle atoms.<sup>[23]</sup> One guanidinium cation is bound by two hydrogen bonds to the N1-atom and the N6-atom of the anion. The angle N10–C5–N9 is at 120.12(18) ° which means the guanidine is planar and the positive charge is split over the whole cation. The torsion angles O1–C1–C3–N4 with 0.8(3)° and N6–C4–N7–O3 with 1.7(3) ° are close to zero, why the anion is almost planar.

## Combination of Different Azoles – 1,2,4-Triazolyl-1,3,4-Oxadiazoles as Precursor for Energetic Materials

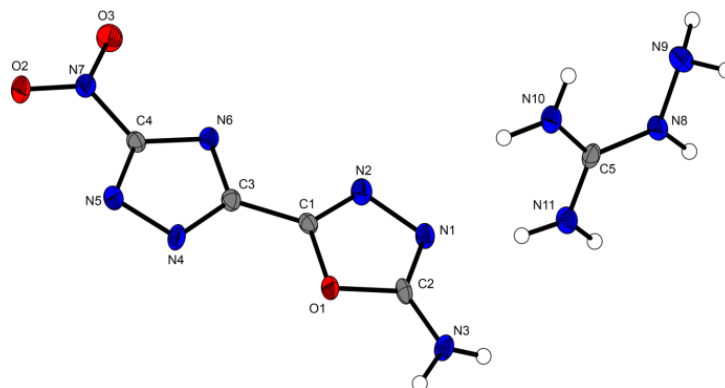


**Figure 5.** Crystal structure of aminoguanidinium 5-(5-amino-1,3,4-oxadiazol-2-yl)-3-nitro-1,2,4-triazolate (**10**). Ellipsoids of non-hydrogen atoms are drawn at the 50 % probability level. Selected distances [Å]: C4–N7 1.346(4), C2–N3 1.303(4), N7–C4 1.442(4), C2–N3 1.335(5). Selected bond angles [°]: C3–C1–O1 120.4(3), O1–C2–N3 118.0(3), C4–N6–C3 98.5(2), C1–O1–C2 101.6(2). Selected torsion angles [°]: N4–C3–C1–N2 176.5(3), O2–N7–C4–N5 –176.2(3), N3–C2–N1–N2 –179.0(3), N6–C3–C1–N2 –1.0(5).

Compound **10** crystallizes in the monoclinic space group  $P2_1/n$  with a cell volume of 1061.8 (2) Å<sup>3</sup> and four formula units per cell. The cell constants are  $a = 13.4494$  (17) Å,  $b = 5.2321$  (6) Å and  $c = 15.302$  (2) Å, while the density is 1.697 g cm<sup>-3</sup>. The distance between the two heterocycles of the molecule is C1–C3 1.454 (5) Å. It is in the range of single and double bond like in all the other heterocycle atoms.<sup>[23]</sup> One aminoguanidinium cation is bound by two hydrogen bonds to the N1-atom and the N2-atom of the anion. The angle N10 C5 N11 is at 120.5 (3) ° which means the aminoguanidine is planar and the positive charge is split over the whole cation. Also the torsion angle N11–C5–N8–N9 with -178.7(3) ° reinforces the assumption of a planar cation. The torsion angles O1–C1–C3–N4 with 0.3(5) ° and N6–C4–N7–O3 with 4.4(5) ° are close to zero which means that the anion is almost planar.

### 10.2.4. Thermal Analysis, Sensitivities and Physicochemical properties

Since compounds **7–10** can be classified as energetic materials their energetic behaviour was extensively investigated. All theoretical and experimentally determined values for the energetic salts of compound **6** are reported in **Table 1**. The thermal behaviour was investigated with a LINSEIS DSC PT10 instrument at a heating rate of 5 °C min<sup>-1</sup>. The decomposition point of the energetic salts is in the range of 240 to 300 °C, whereas the lowest decomposition (onset) was

## Combination of Different Azoles – 1,2,4-Triazolyl-1,3,4-Oxadiazoles as Precursor for Energetic Materials

observed for the aminoguanidinium salt (**10**, 246 °C) and the highest for the guanidinium salt (**9**, 296 °C). The sensitivities of all four compounds (**7–10**) were measured according the BAM standards.<sup>[24]</sup> The energetic salts show no sensitivity toward external stimuli with sensitivity values for friction of < 360 N and impact < 40 J, for each compound, and can be classified as insensitive. The reported detonation parameters were calculated using the EXPLO5\_V6.03 computer code.<sup>[25]</sup> The EXPLO5 detonation parameters of the energetic salts **7–10** were calculated by using the room-temperature density values obtained from the X-ray structures as described in reference.<sup>[26]</sup> The potassium (**7**) and ammonium (**8**) salts were obtained as monohydrates with recalculated room temperature densities of 1.84 and 1.61 g cm<sup>-3</sup>, respectively. The highest detonation pressure was calculated for the aminoguanidinium salt **10** ( $V_D = 7672 \text{ m s}^{-1}$ ) and the lowest for the potassium monohydrate salt **7** ( $V_D = 6965 \text{ m s}^{-1}$ ).

**Table 1.** Physicochemical properties and detonation parameters of **5–10** compared to RDX.

	<b>5</b>	<b>6</b>	<b>7 · H<sub>2</sub>O</b>	<b>8 · H<sub>2</sub>O</b>	<b>9</b>	<b>10</b>	<b>RDX<sup>[1d]</sup></b>
<i>IS</i> [J] <sup>a</sup>	40	40	40	40	40	40	7.5
<i>FS</i> [N] <sup>b</sup>	360	360	360	360	360	360	120
<i>ESD</i> [J] <sup>c</sup>	1.5	1.5	1.5	1.5	1.5	1.5	0.2
<i>N</i> [%] <sup>d</sup>	58.7	49.7	41.7	52.3	54.7	56.8	37.8
<i>Ω</i> [%] <sup>e</sup>	−90.9	−52.8	−41.1	−55.1	−68.7	−67.8	−21.6
<i>T<sub>dec.</sub></i> [°C] <sup>f</sup>	309 (melt.)	245	254	276	296	246	205
<i>ρ</i> [g cm <sup>-3</sup> ] (298K) <sup>g</sup>	1.90	1.92 <sup>o</sup>	1.84	1.61	1.66	1.64	1.81
<i>Δ<sub>f</sub>H<sup>o</sup></i> [kJ mol <sup>-1</sup> ] <sup>h</sup>	140.3	224.2	−277.1	−123.6	133.4	241.0	70.3
<i>Δ<sub>f</sub>U<sup>o</sup></i> [kJ kg <sup>-1</sup> ] <sup>i</sup>	935.6	1219.2	−1020.7	−425.5	622.2	993.7	417.0
<b>EXPLO5 V6.03:</b>							
<i>−Δ<sub>E</sub>U<sup>o</sup></i> [kJ kg <sup>-1</sup> ] <sup>j</sup>	1996	3933	3099	3153	2982	3281	5845
<i>T<sub>E</sub></i> [K] <sup>k</sup>	1737	2936	2446	2440	2334	2462	3810
<i>p<sub>CJ</sub></i> [kbar] <sup>l</sup>	238	285	179	190	197	206	345
<i>V<sub>D</sub></i> [m s <sup>-1</sup> ] <sup>m</sup>	8265	8477	6965	7337	7500	7672	8861
<i>V<sub>0</sub></i> [L kg <sup>-1</sup> ] <sup>n</sup>	429	413	438	485	473	478	785

<sup>a</sup> impact sensitivity (BAM drophammer, 1 of 6); <sup>b</sup> friction sensitivity (BAM friction tester, 1 of 6); <sup>c</sup> electrostatic discharge device (OZM); <sup>d</sup> nitrogen content; <sup>e</sup> oxygen balance; <sup>f</sup> decomposition temperature from DTA ( $\beta = 5^\circ\text{C}$ ); <sup>g</sup> recalculated from low temperature X-ray densities ( $\rho_{298\text{K}} = \rho_T / (1 + \alpha_V(298 - T_0))$ ;  $\alpha_V = 1.5 \cdot 10^{-4} \text{ K}^{-1}$ ); <sup>h</sup> calculated (CBS-4M) heat of formation; <sup>i</sup> calculated energy of formation; <sup>j</sup> energy of explosion; <sup>k</sup> explosion temperature; <sup>l</sup> detonation pressure; <sup>m</sup> detonation velocity; <sup>n</sup> assuming only gaseous products; <sup>o</sup> measured pycnometrically at room temperature.

### 10.3. Conclusions

In conclusion, we reported on the synthesis of two new energetic derivatives based on the heterocycles 1,2,4-1*H*-triazole and 1,3,4-oxadiazole. 2-Amino-5-(5-amino-1*H*-1,2,4-triazol-3-yl)-1,3,4-oxadiazole (**5**) can be synthesized in a three-step procedure and 2-amino-5-(5-nitro-1*H*-1,2,4-triazol-3-yl)-1,3,4-oxadiazole (**6**) in a four-step procedure by using 5-amino-1*H*-1,2,4-triazole-3-carboxylic acid as the starting material. The ring closing toward the 1,3,4-oxadiazole was carried out using cyanogen bromide and the corresponding triazole-carbohydrazides. Compounds **5** and **6** show high thermal stabilities, high densities ( $\rho = 1.90$  and  $1.92 \text{ g cm}^{-3}$ ) and acceptable detonation performances ( $V_D = 8265$  and  $8477 \text{ m s}^{-1}$ ). Both heterocycles are not sensitive toward impact friction or ESD. Compound **6** was further functionalized by reacting it with four bases to yield the potassium (**7**), ammonium (**8**), guanidinium (**9**) and aminoguanidinium (**10**) salt. The synthesized ionic derivatives of compound **6** are insensitive toward external stimuli with sensitivity values for impact of 40 J and for friction with 360 N, each. The thermal stability of all four compounds ranges from 246 °C for the aminoguanidinium salt (**10**) to 296 °C for the guanidinium salt (**9**). 2-Amino-5-(5-amino-1*H*-1,2,4-triazol-3-yl)-1,3,4-oxadiazole (**5**) and 2-amino-5-(5-nitro-1*H*-1,2,4-triazol-3-yl)-1,3,4-oxadiazole (**6**) can be used as precursors for the synthesis of new energetic materials.

### 10.4. References

- [1] a) H. Gao, J. M. Shreeve, *Chem. Rev.* **2011**, *111*, 7377–7436; b) D. M. Badgujar, M. B. Talawar, S. N. Asthana, P. P. Mahulikar, *J. Hazard. Mater.* **2008**, *151*, 289–305; c) Y. Tang, C. He, G. H. Imler, D. A. Parrish, J. M. Shreeve, *J. Mater. Chem. A* **2018**, *6*, 5136–5142; d) T. M. Klapötke, *Chemistry of High-Energy Materials*, 4th ed., De Gruyter, Berlin, **2017**.
- [2] a) D. Fischer, J. L. Gottfried, T. M. Klapötke, K. Karaghiosoff, J. Stierstorfer, T. G. Witkowski, *Angew. Chem. Int. Ed.* **2016**, *55*, 16132–16135; b) D. Kumar, G. H. Imler, D. A. Parrish, J. M. Shreeve, *New J. Chem.* **2017**, *41*, 4040–4047; c) T. M. Klapötke, T. G. Witkowski, *ChemPlusChem* **2016**, *81*, 357–360.
- [3] a) J. K. Stanley, G. R. Lotufo, J. M. Biedenbach, P. Chappell, K. A. Gust, *Environ. Toxicol. Chem.* **2015**, *34*, 873–879; b) G. A. Parker, G. Reddy, M. A. Major, *International Journal of Toxicology* **2006**, *25*, 373–378; c) H. Abadin, C. Smith, *Toxicological Profile For RDX*,

## Combination of Different Azoles – 1,2,4-Triazolyl-1,3,4-Oxadiazoles as Precursor for Energetic Materials

- U.S. Department of Health and Human Services, Public Health Service, Agency for Toxic Substances and Disease Registry, **2012**, available online at <https://www.atsdr.cdc.gov/toxprofiles/tp78.pdf>; d) Y. Weifei, L. Longyu, C. Feilan, H. Mingzhong, T. Dongmei, F. Guijuan, H. Shilong, L. Huanchang, *Int. J. Ecotoxicol Ecobiol.* **2016**, *1*, 88–93.
- [4] a) D. Kumar, G. H. Imler, D. A. Parrish, J. M. Shreeve, *Chem. Eur. J.* **2017**, *23*, 7876–7881; b) P. Yin, L. A. Mitchell, D. A. Parrish, J. M. Shreeve, *Chem. Asian J.* **2017**, *12*, 378–384; c) T. M. Klapötke, P. C. Schmid, S. Schnell, J. Stierstorfer, *J. Mater. Chem. A* **2015**, *3*, 2658–2668; d) Y. Tang, C. He, L. A. Mitchell, D. A. Parrish, J. M. Shreeve, *J. Mater. Chem. A* **2016**, *4*, 3879–3885; e) Y. Liu, J. Zhang, K. Wang, J. Li, Q. Zhang, J. M. Shreeve, *Angew. Chem. Int. Ed.* **2016**, *55*, 11548–11551; f) M. B. Talawar, R. Sivabalan, T. Mukundan, H. Muthurajan, A. K. Sikder, B. R. Gandhe, A. S. Rao, *J. Hazard. Mater.* **2009**, *161*, 589–607; g) O. S. Bushuyev, P. Brown, A. Maiti, R. H. Gee, G. R. Peterson, B. L. Weeks, L. J. Hope-Weeks, *J. Am. Chem. Soc.* **2012**, *134*, 1422–1425.
- [5] Z. Yu, E. R. Bernstein, *J. Phys. Chem. A* **2013**, *117*, 10889–10902.
- [6] a) Z. Xu, G. Cheng, S. Zhu, Q. Lin, H. Yang, *J. Mater. Chem. A* **2018**, *6*, 2239–2248; b) A. A. Dippold, T. M. Klapötke, *Chem. Eur. J.* **2012**, *18*, 16742–16753.
- [7] a) Y. Tang, H. Gao, L. A. Mitchell, D. A. Parrish, J. M. Shreeve, *Angew. Chem. Int. Ed.* **2016**, *55*, 3200–3203; b) T. S. Hermann, K. Karaghiosoff, T. M. Klapötke, J. Stierstorfer, *Chem. Eur. J.* **2017**, *23*, 12087–12091.
- [8] a) Z. Xu, G. Cheng, H. Yang, J. Zhang, J. n. M. Shreeve, *Chem. Eur. J.* **2018**, *24*, 10488–10497; b) N. Fischer, D. Fischer, T. M. Klapötke, D. G. Piercey, J. Stierstorfer, *J. Mater. Chem.* **2012**, *22*, 20418–20422; c) D. Fischer, T. M. Klapötke, J. Stierstorfer, *Angew. Chem. Int. Ed.* **2014**, *53*, 8172–8175; d) T. M. Klapötke, M. Leroux, P. C. Schmid, J. Stierstorfer, *Chem. Asian J.* **2016**, *11*, 844–851; e) K. Hafner, T. M. Klapötke, P. C. Schmid, J. Stierstorfer, *Eur. J. Inorg. Chem.* **2015**, *2015*, 2794–2803; f) A. A. Dippold, T. M. Klapötke, *Chem. Asian J.* **2013**, *8*, 1463–1471.
- [9] A. A. Dippold, T. M. Klapötke, *Chem. Asian J.* **2013**, *8*, 1463–1471.

**Combination of Different Azoles – 1,2,4-Triazolyl-1,3,4-Oxadiazoles as Precursor for  
Energetic Materials**

- [10] E. L. Metelkina, T. A. Novikova, S. N. Berdonosova, D. Y. Berdonosov, *Russ. J. Org. Chem.* **2005**, *41*, 440–443.
- [11] H. Gehlen, K. H. Uteg, *Arch. Pharm.* **1968**, *301*, 911–922.
- [12] S. Sanchit, P. S.N., *Int. J. Res. Ayurveda Pharm.* **2011**.
- [13] L. I. Bagal, M. S. Pevzner, A. N. Frolov, N. I. Sheludyakova, *Chem. Heterocycl. Compd.* **1970**, *6*, 240–244.
- [14] A. A. Dippold, D. Izsák, T. M. Klapötke, *Chem. Eur. J.* **2013**, *19*, 12042–12051.
- [15] M. Hesse, H. Meier, B. Zeeh, *Spektroskopische Methoden in der organischen Chemie*, 7. überarbeitete Auflage ed., Georg Thieme Verlag, Stuttgart, New York, **2005**.
- [16] F. H. Allen, O. Kennard, D. G. Watson, L. Brammer, A. G. Orpen, R. Taylor, *J. Chem. Soc., Perkin Trans. 2* **1987**, 1–19.
- [17] E. Wiberg, N. Wiberg, *Lehrbuch der anorganischen Chemie*, 102. Auflage ed., De Gruyter, Berlin, New York, **2007**.
- [18] L. Pauling, *The Nature of the Chemical Bond and the Structure of Molecules and Crystals: An Introduction to Modern Structural Chemistry*, Cornell University Press, New York, **1960**.
- [19] J. Zhang, T. Zhang, K. Yu, *Struc. Chem.* **2006**, *17*, 249–254.
- [20] A. D. Vasiliev, A. M. Astachov, R. S. Stepanov, S. D. Kirik, *Acta Cryst., Sect. C* **1999**, *55*, 830–832.
- [21] R. D. Brown, B. A. W. Collier, J. E. Kent, *Theor. Chim. acta* **1968**, *10*, 435–446.
- [22] A. R. Hoy, P. R. Bunker, *J. Mol. Spectrosc.* **1979**, *74*, 1–8.
- [23] S. Sanchit, S. N. Pandeya, *Int. J. Res. Ayurveda Pharm.* **2011**, *2*, 459–468.
- [24] a) Reichel & Partner GmbH, <http://www.reichelt-partner.de>; b) Test methods according to the UN Recommendations on the Transport of Dangerous Goods, Manual of Test and

## Combination of Different Azoles – 1,2,4-Triazolyl-1,3,4-Oxadiazoles as Precursor for Energetic Materials

Criteria, 4th edn., United Nations Publication, New York and Geneva, **2003**, ISBN 92–1-139087 7, Sales No. E.03.VIII.2; 13.4.2 Test 3 a (ii) BAM Fallhammer.

[25] M. Sućeska, *EXPLO5 Version 6.03 User's Guide*, Zagreb, Croatia: OZM; **2015**.

[26] J. S. Murray, P. Politzer, *J. Mol. Model* **2014**, 20, 2223–2227.

## 10.5. Supplementary Information

### 10.5.1. X-ray Diffraction

Single crystals were picked and measured on an Oxford Xcalibur3 diffractometer with a Spellman generator (voltage 50 kV, current 40 mA) and a CCD area detector for data collection using Mo- $K\alpha$  radiation ( $\lambda = 0.71073 \text{ \AA}$ ). The crystal structures of compound **5** was determined on a Bruker D8 Venture TXS diffractometer equipped with a multilayer monochromator, a Photon 2 detector, and a rotating-anode generator (Mo $K\alpha$  radiation). The data collection was carried out using CRYSLISPRO software<sup>[S1]</sup> and the reduction were performed. The structures were solved using direct methods (SIR-92,<sup>[S2]</sup> SIR-97<sup>[S3]</sup> or SHELXS-97<sup>[S4]</sup>) and refined by full-matrix least-squares on *F*<sup>2</sup> (SHELXL<sup>[S4]</sup>): The final check was done with the PLATON software<sup>[S5]</sup> integrated in the WinGX software suite. The non-hydrogen atoms were refined anisotropically and the hydrogen atoms were located and freely refined. The absorptions were corrected by a SCALE3 ABSPACK multiscan method.<sup>[S6]</sup> The DIAMOND2 plots are shown with thermal ellipsoids at the 50% probability level and hydrogen atoms are shown as small spheres of arbitrary radii. The SADABS program embedded in the Bruker APEX3 software has been used for multi-scan absorption corrections in all structures.<sup>[S7]</sup>

**Table S1.** Crystallographic data and refinement parameters of compound **3**, **7**, **8**, **9** and **10**.

	<b>3</b>	<b>7</b>	<b>8</b>	<b>9</b>	<b>10</b>
Formula	C <sub>3</sub> H <sub>6</sub> N <sub>6</sub> O	C <sub>4</sub> H <sub>4</sub> N <sub>7</sub> O <sub>4</sub> K	C <sub>7</sub> H <sub>4</sub> N <sub>8</sub> O <sub>8</sub>	C <sub>5</sub> H <sub>8</sub> N <sub>10</sub> O <sub>3</sub>	C <sub>5</sub> H <sub>9</sub> N <sub>14</sub> O <sub>3</sub>
FW [g mol <sup>-1</sup> ]	142.14	253.24	232.18	256.21	271.23
Crystal system	Monoclinic	Monoclinic	Monoclinic	Monoclinic	Monoclinic
Space Group	<i>P</i> -21/ <i>n</i>	<i>P</i> 2 <sub>1</sub> / <i>c</i>	<i>P</i> 2 <sub>1</sub> / <i>n</i>	<i>C</i> 2/ <i>c</i>	<i>P</i> 2 <sub>1</sub> / <i>n</i>
Color / Habit	Colorless	Orange	Orange	Yellow	Colorless
Size [mm]	0.09 × 0.10 × 0.59	0.06 × 0.14 × 0.34	0.01 × 0.05 × 0.3	0.10 × 0.25 × 0.5	0.01 × 0.03 × 0.05

**Combination of Different Azoles – 1,2,4-Triazolyl-1,3,4-Oxadiazoles as Precursor for Energetic Materials**

a [Å]	5.1775(5)	6.6407(2)	6.690(5)	20.3525(18)	13.4494(17)
b [Å]	8.5646(7)	11.2308(4)	11.426(5)	5.4863(4)	5.2321(6)
c [Å]	13.1752(12)	12.3709(3)	12.614(5)	18.5795(14)	15.302(2)
$\alpha$ [°]	90	90	90	90	90
$\beta$ [°]	97.917(11)	103.081(1)	104.623(5)	106.316(9)	99.583(5)
$\gamma$ [°]	90	90	90	90	90
$V$ [Å <sup>3</sup> ]	578.66(9)	898.69(5)	933.0(9)	1991.0(3)	1061.8(2)
$Z$	4	4	4	8	4
$\rho_{\text{calc.}}$ [g cm <sup>-3</sup> ]	1.632	1.872	1.653	1.709	1.697
$\mu$ [mm <sup>-1</sup> ]	0.130	0.608	0.145	0.143	0.142
$F(000)$	296	512	480	1056	560
$\lambda_{\text{MoK}\alpha}$ [Å]	0.71073	0.71073	0.71073	0.71073	0.71073
T [K]	173	100	123	130	100
$\vartheta$ min-max [°]	4.5, 26.2	3.1, 26.0	4.3, 26.5	4.2, 26.5	2.7, 25.4
Dataset h; k; l	-6:6;-10:10; -16:16	-8:8;-13:13; -15:15	-8:8;-14:13; -15:15	-25:25;-6:6; -23:16	-16:15;-6:5; -18:18
Reflect. coll.	4314	10517	7208	7599	6058
Independ. refl.	1171	1757	1925	2051	1946
$R_{\text{int}}$	0.032	0.040	0.057	0.042	0.049
Reflection obs.	943	1487	1398	1622	1566
No. parameters	115	161	177	195	208
$R_1$ (obs)	0.0394	0.0279	0.0531	0.0391	0.0613
$wR_2$ (all data)	0.1091	0.0682	0.1445	0.1020	0.1580
$S$	1.04	1.06	1.05	1.05	1.09
Resd. Dens.[e Å <sup>-3</sup> ]	-0.19, 0.30	-0.25, 0.23	-0.29, 0.44	-0.22, 0.27	-0.26, 0.47
Device type	Oxford Xcalibur3	Bruker D8 Venture TXS	Oxford Xcalibur3	Oxford Xcalibur3	Bruker D8 Venture TXS
Solution	SIR-92	SIR-92	SIR-92	SIR-92	SIR-92
Refinement	SHELXL-2013	SHELXL-2013	SHELXL-2013	SHELXL-2013	SHELXL-2013
Absorpt. corr.	multi-scan	multi-scan	multi-scan	multi-scan	multi-scan
CCDC	1869975	1869977	1869976	1869978	1869979



### 10.5.2. Heat of formation calculations

All quantum chemical calculations were carried out using the Gaussian G09 program package.<sup>S8</sup> The enthalpies (H) and free energies (G) were calculated using the complete basis set (CBS) method of Petersson and coworkers in order to obtain very accurate energies. The CBS models are using the known asymptotic convergence of pair natural orbital expressions to extrapolate from calculations using a finite basis set to the estimated CBS limit. CBS-4 starts with an HF/3-21G(d) geometry optimization; the zero-point energy is computed at the same level. It then uses a large basis set SCF calculation as a base energy, and an MP2/6-31+G calculation with a CBS extrapolation to correct the energy through second order. A MP4(SDQ)/6-31+ (d,p) calculation is used to approximate higher order contributions. In this study, we applied the modified CBS-4M. Heats of formation of the synthesized ionic compounds were calculated using the atomization method (equation E1) using room temperature CBS-4M enthalpies, which are summarized in Table S3.<sup>[S9,S10]</sup>

$$\Delta_f H^\circ_{(g, M, 298)} = H_{(Molecule, 298)} - \sum H^\circ_{(Atoms, 298)} + \sum \Delta_f H^\circ_{(Atoms, 298)} \quad (E1)$$

**Table S2.** CBS-4M enthalpies for atoms C, H, N and O and their literature values for atomic  $\Delta_f H^\circ_{298} / \text{kJ mol}^{-1}$

	$-H^{298}$ [a.u.]	NIST <sup>S11</sup>
H	0.500991	218.2
C	37.786156	717.2
N	54.522462	473.1
O	74.991202	249.5

For neutral compounds the sublimation enthalpy, which is needed to convert the gas phase enthalpy of formation to the solid state one, was calculated by the *Trouton* rule.<sup>S12</sup> For ionic compounds, the lattice energy ( $U_L$ ) and lattice enthalpy ( $\Delta H_L$ ) were calculated from the corresponding X-ray molecular volumes according to the equations provided by *Jenkins* and *Glasser*.<sup>S13</sup> With the calculated lattice enthalpy the gas-phase enthalpy of formation was converted into the solid state (standard conditions) enthalpy of formation. These molar standard enthalpies of formation ( $\Delta H_m$ ) were used to calculate the molar solid state energies of formation ( $\Delta U_m$ ) according to equation E2.

$$\Delta U_m = \Delta H_m - \Delta n RT \quad (E2)$$

( $\Delta n$  being the change of moles of gaseous components)

## Combination of Different Azoles – 1,2,4-Triazolyl-1,3,4-Oxadiazoles as Precursor for Energetic Materials

The calculation results are summarized in Table S3.

**Table S3.** Heat of formation calculation results.

	$-H^{298}$ [a] [a.u. ]	$\Delta_f H^\circ(\text{g,M})$ [kJ mol <sup>-1</sup> ] [b]	$V_M$ [Å <sup>3</sup> ] [c]	$\Delta U_L, \Delta H_L$ ; [d] [kJ mol <sup>-1</sup> ]	$\Delta_f H^\circ(\text{s})$ [e] [kJ mol <sup>-1</sup> ]	$\Delta n$ [f]	$\Delta_f U(\text{s})$ [g] [kJ kg <sup>-1</sup> ]
<b>5</b>		59.6			140.3	6.5	935.6
<b>6</b>		275.6			224.2	6.5	1219.2
<b>6 anion</b>	761.565028	41.7					
<b>K+</b>	599.035967	487.4					
<b>NH4+</b>	56.796608	635.8					
<b>G+</b>	205.453192	571.9					
<b>AG+</b>	260.701802	671.6					
<b>7 hydrate</b>			898.69	599.1, 562.9	-277.1	-7.5	-1020.7
<b>8 hydrate</b>			933.00	553.6, 557.3	-123.6	-10	-425.5
<b>9</b>		613.6	1991.0	476.8, 480.2	133.4	10.5	822.2
<b>10</b>		713.3	1061.8	468.8, 472.3	241.0	11.5	993.7

[a] CBS-4M electronic enthalpy; [b] gas phase enthalpy of formation; [c] molecular volumes taken from X-ray structures and corrected to room temperature; [d] lattice energy and enthalpy (calculated using Jenkins and Glasser equations); [e] standard solid state enthalpy of formation; [f]  $\Delta n$  being the change of moles of gaseous components when formed; [g] solid state energy of formation.

### 10.5.3. Experimental Part

#### 10.5.3.1. General Procedures

Differential Scanning Calorimetry (DSC) was recorded on a LINSEIS DSC PT10 with about 1 mg substance in a perforated aluminum vessel with a heating rate of 5 K·min<sup>-1</sup> and a nitrogen flow of 5 dm<sup>3</sup>·h<sup>-1</sup>. The NMR spectra were carried out using a 400 MHz instruments JEOL Eclipse 270, JEOL EX 400 or a JEOL Eclipse 400 (<sup>1</sup>H 399.8 MHz, <sup>13</sup>C 100.5 MHz, <sup>14</sup>N 28.9 MHz, and <sup>15</sup>N 40.6 MHz). Chemical shifts are given in parts per million (ppm) relative to tetramethylsilane (<sup>1</sup>H, <sup>13</sup>C) and nitromethane (<sup>14</sup>N, <sup>15</sup>N).

Infrared spectra were measured with a Perkin-Elmer Spectrum BX-FTIR spectrometer equipped with a Smiths DuraSamplIR II ATR device. Transmittance values are qualitatively described as “very strong” (vs), “strong” (s), “medium” (m), and “weak” (w). Raman spectra were recorded using a Bruker MultiRAM FT-Raman instrument fitted with a liquid-nitrogen cooled germanium detector and a Nd:YAG laser ( $\lambda = 1064$  nm). The intensities are quoted as percentages of the most intense peak and are given in parentheses. DTA spectra were carried out using a OZM DTA 551-EX with a heating rate of 5 K·min<sup>-1</sup>. Low-resolution mass spectra were recorded with a JEOL

## Combination of Different Azoles – 1,2,4-Triazolyl-1,3,4-Oxadiazoles as Precursor for Energetic Materials

MStation JMS 700 (DEI+ / FAB+/-). Elemental analysis (C/H/N) was carried out using a Vario Micro from the Elementar Company. Impact sensitivity tests were performed according to STANAG 4489<sup>[S14]</sup> modified instruction<sup>[S15]</sup> using a Bundesanstalt für Materialforschung (BAM) drophammer.<sup>[S16]</sup> Friction sensitivity tests were carried out according to STANAG 4487<sup>[S17]</sup> modified instruction<sup>[S18]</sup> using a BAM friction tester. The grading of the tested compounds results from the “UN Recommendations on the Transport of Dangerous Goods”.<sup>[S19]</sup> ESD values were carried out using the Electric Spark Tester ESD 2010 EN.<sup>[S20]</sup>

### Ethyl 5-amino-1*H*-1,2,4-triazole-3-carboxylate (1)<sup>[S21]</sup>

5-amino-1*H*-1,2,4-triazole-3-carboxylic acid (20.0 g, 137 mmol, 1.00 eq.) was suspended in ethanol (300 mL) and cooled down to 0 °C. Then thionyl chloride (26.2 g, 220 mmol, 1.60 eq.) was added dropwise at 0 °C and the mixture was stirred for 1 h at this temperature. Subsequently the solution was stirred for 3 d at 75 °C. The solvent was evaporated under reduced pressure and then saturated sodium acetate solution (180 mL) was added. The resulting solid was filtered and washed with water (50 mL) to yield compound **1** as a white powder (20.7 g, 133 mmol, 85 %).

<sup>1</sup>H-NMR (400 MHz, DMSO-*d*<sub>6</sub>): δ(ppm) = 12.60 (s, 1H, NH), 6.20 (s, 2H, NH<sub>2</sub>), 4.21 (q, 2H, <sup>3</sup>*J* = 7.1 Hz, CH<sub>2</sub>), 1.26 (t, 3H, <sup>3</sup>*J* = 7.1 Hz, CH<sub>3</sub>); <sup>13</sup>C NMR (101 MHz, DMSO-*d*<sub>6</sub>): δ(ppm) = 160.4 (C=O), 157.4 (C<sub>(triazole)</sub>), 151.9 (C<sub>(triazole)</sub>), 60.3 (CH<sub>2</sub>), 14.1 (CH<sub>3</sub>); IR (ATR, rel. int.): ν (cm<sup>-1</sup>) = 3447 (m), 3029 (w), 3000 (w), 2971 (w), 2918 (w), 1723 (s), 1635 (s), 1579 (w), 1507 (m), 1464 (m), 1443 (m), 1389 (m), 1356 (m), 1228 (s), 1155 (w), 1120 (s), 1051 (m), 1028 (s), 876 (w), 855 (m), 793 (m), 756 (m), 718 (s), 659 (m), 630 (m), 544 (w), 528 (w), 515 (w), DSC (5 °C min<sup>-1</sup>): *T*<sub>melt.</sub> = 239 °C.

### Ethyl 5-nitro-1*H*-1,2,4-triazole-3-carboxylate (2)

Compound (1) (5.00 g, 32.0 mmol, 1.00 eq.) was dissolved in water (40 mL) and sodium nitrate (21.1 g, 320 mmol, 10.0 eq.) was added. Sulfuric acid (20 %, 34.0 mL) was added dropwise over 4 h. Afterwards the mixture was stirred 2 h at 50 °C. The mixture was cooled down to room temperature and sulfuric acid (50 %, 50 mL) was added. The product was extracted with ethyl acetate (3 x 100 mL), the organic layer was separated and saturated NaHCO<sub>3</sub> solution (100 mL) was added. The organic layer was separated and the hydrous layer was extracted with ethyl acetate (2 x 70 mL). The combined organic layers were dried over anhydrous MgSO<sub>4</sub> and the solvent was

## Combination of Different Azoles – 1,2,4-Triazolyl-1,3,4-Oxadiazoles as Precursor for Energetic Materials

evaporated under reduced pressure to yield compound **2** as a yellow solid (23.70g, 19.8 mmol, 62 %).

$^1\text{H-NMR}$  (400 MHz,  $\text{DMSO-}d_6$ ):  $\delta(\text{ppm}) = 4.43$  (q, 2H,  $^3J = 7.1$  Hz,  $\text{CH}_2$ ), 1.35 (t, 3H,  $^3J = 7.1$  Hz,  $\text{CH}_3$ );  $^{13}\text{C NMR}$  (101 MHz,  $\text{DMSO-}d_6$ ):  $\delta(\text{ppm}) = 162.2$  ( $\text{C=O}$ ), 156.1 ( $\text{C}_{(\text{triazole})}$ ), 147.6 ( $\text{C}_{(\text{triazole})}$ ), 62.7 ( $\text{CH}_2$ ), 13.9 ( $\text{CH}_3$ );  $^{14}\text{N NMR}$  (29 MHz,  $\text{DMSO-}d_6$ ):  $\delta(\text{ppm}) = -26$ ; IR (ATR, rel. int.):  $\nu$  ( $\text{cm}^{-1}$ ) = 3564 (w), 3433 (w), 1920 (m), 1722 (s), 1552 (s), 1485 (m), 1462 (m), 1424 (m), 1382 (m), 1319 (s), 1244 (s), 1185 (m), 1091 (m), 1038 (m), 1016 (s), 842 (m), 801 (m), 759 (m), 652 (s), 601 (s), 550 (s); Mass spectrometry:  $m/z$  ( $\text{FAB}^+$ ) = 185.1 [ $\text{M}^+$ ];

### 5-Amino-1H-1,2,4-triazole-3-carbohydrazide (**3**)

Compound (**1**) (12.0 g, 76.8 mmol, 1.00 eq.) was dissolved in methanol (80 mL), hydrazine-monohydrate (11.4 g, 230 mmol, 3.00 eq.) was added slowly. The mixture was stirred for 24 h at 75 °C and cooled down to room temperature. Hydrochloric acid (37 %, 20.0 mL) was added, the solid was filtered and the residue was washed with water (3 x 30 mL), ethyl acetate (2 x 30 mL) and diethylether (2 x 30 mL) to yield compound **3** as a white solid (9.60 g, 55.8 mmol, 72 %).

$^1\text{H-NMR}$  (400 MHz,  $\text{DMSO-}d_6$ ):  $\delta(\text{ppm}) = 12.48$  (s, 1H,  $\text{NH}_{(\text{triazole})}$ ), 9.30 (m, 1H,  $\text{NH-NH}_2$ ), 6.07 (s, 2H,  $\text{NH}_{2(\text{triazole})}$ ), 3.66 (br s, 2H,  $\text{NH}_2\text{-NH}$ );  $^{13}\text{C NMR}$  (101 MHz,  $\text{DMSO-}d_6$ ):  $\delta(\text{ppm}) = 159.4$  ( $\text{C=O}$ ), 157.6 ( $\text{C}_{(\text{triazole})}$ ), 153.2 ( $\text{C}_{(\text{triazole})}$ );  $^{14}\text{N NMR}$  (29 MHz,  $\text{DMSO-}d_6$ ):  $\delta(\text{ppm}) = -26$ ; IR (ATR, rel. int.):  $\nu$  ( $\text{cm}^{-1}$ ) = 3412 (w), 3311 (m), 3196 (w), 2938 (w), 2893 (w), 2571 (w), 2453 (w), 2265 (w), 2204 (w), 2166 (w), 2063 (w), 2051 (w), 2023 (w), 2004 (w), 1982 (w), 1955 (w), 1941 (w), 1921 (w), 1720 (w), 1681 (s), 1648 (s), 1621 (s), 1584 (s), 1533 (m), 1499 (s), 1388 (m), 1355 (m), 1294 (m), 1253 (s), 1132 (s), 1094 (m), 1047 (s), 1011 (m), 969 (m), 862 (s), 822 (s), 757 (m), 723 (s), 661 (m), 631 (m), 569 (s), 532 (s); Mass spectrometry:  $m/z$  ( $\text{DEI}^+$ ) = 142.1 [ $\text{M}^+$ ], DSC (5 °C  $\text{min}^{-1}$ ):  $T_{\text{melt.}} = 175$  °C.

### 5-Nitro-1H-1,2,4-triazole-3-carbohydrazide (**4**)

Compound (**2**) (4.20 g, 24.4 mmol, 1.00 eq.) was dissolved in methanol (50 mL), hydrazine-monohydrate (3.80 mL, 73.2 mmol, 3.00 eq.) was added slowly. The mixture was stirred for 24 h at 75 °C and cooled down to room temperature. Hydrochloric acid (37 %, 12.0 mL) was added, the solid was filtered and the residue was washed with water (3 x 20 mL), ethyl acetate (2 x 20 mL) and diethylether (2 x 20 mL) to yield compound **4** as a brownish solid (3.20 g, 18.6 mmol, 76 %).

## Combination of Different Azoles – 1,2,4-Triazolyl-1,3,4-Oxadiazoles as Precursor for Energetic Materials

<sup>1</sup>H-NMR (400 MHz, DMSO-*d*<sub>6</sub>): δ(ppm) = 9.35 (s, 1H, NH-NH<sub>2</sub>), 4.11 (br s, 2H, NH-NH<sub>2</sub>); <sup>13</sup>C NMR (101 MHz, DMSO-*d*<sub>6</sub>): δ(ppm) = 165.2 (C=O), 160.3 (C<sub>(triazole)</sub>), 156.5 (C<sub>(triazole)</sub>); IR (ATR, rel. int.): ν (cm<sup>-1</sup>) = 3336 (w), 3312 (w), 3209 (w), 3119 (w), 2995 (w), 2861 (w), 2741 (w), 2637 (w), 1669 (m), 1623 (m), 1600 (m), 1540 (m), 1513 (m), 1468 (s), 1383 (s), 1332 (m), 1301 (m), 1280 (m), 1128 (m), 1102 (s), 1056 (m), 1033 (w), 986 (m), 967 (s), 892 (w), 871 (w), 838 (m), 803 (w), 785 (w), 770 (w), 720 (w), 640 (s), 585 (w), 520 (w), 502 (w); DSC (5 °C min<sup>-1</sup>): T<sub>melt.</sub> = 275 °C, T<sub>dec.</sub> = 295 °C.

### 2-Amino-5-(5-amino-1H-1,2,4-triazol-3-yl)-1,3,4-oxadiazole (5)

Compound (3) (3.00 g, 21.1 mmol, 1.00 eq.) was suspended in water (20 mL) and KOH (1.18 g, 21.1 mmol, 1.00 eq.) was added. The solution was cooled to 0 °C and cyanogen bromide (3.38 g, 31.7 mmol, 1.50 eq) was added slowly. The solution was stirred at 0 °C for 2 h and was further stirred at room temperature for 72 h. The formed residue was filtered under reduced pressure to yield compound **5** as a yellow solid (2.93 g, 17.5 mmol, 83 %).

<sup>1</sup>H-NMR (400 MHz, DMSO-*d*<sub>6</sub>): δ(ppm) = 12.48 (s, 1H, NH), 7.42 (s, 2H, NH<sub>2</sub>(oxadiazole)), 6.25 (s, 2H, NH<sub>2</sub>(triazole)); <sup>13</sup>C NMR (101 MHz, DMSO-*d*<sub>6</sub>): δ(ppm) = 163.5 (C-NH<sub>2</sub>(oxadiazole)), 159.3 (C-NH<sub>2</sub>(triazole)), 157.8 (C<sub>(oxadiazole)</sub>), 153.1 (C<sub>(triazole)</sub>); IR (ATR, rel. int.): ν (cm<sup>-1</sup>) = 3310 (m), 3153 (m), 2198 (w), 2166 (w), 2140 (w), 2050 (w), 2004 (w), 1979 (w), 1731 (w), 1635 (s), 1589 (s), 1518 (s), 1491 (m), 1394 (s), 1362 (s), 1288 (m), 1235 (m), 1192 (m), 1094 (m), 1043 (m), 1011 (m), 956 (w), 898 (w), 813 (m), 732 (s), 695 (s); Mass spectrometry: m/z (DEI+) = 167.1 [M<sup>+</sup>], DSC (5 °C min<sup>-1</sup>): T<sub>melt.</sub> = 309 °C

### 2-Amino-5-(5-nitro-1H-1,2,4-triazol-3-yl)-1,3,4-oxadiazole (6)

Compound (4) (4.11 g, 24.2 mmol, 1.00 eq.) was suspended in water (50 mL) and KOH (1.55 g, 26.6 mmol, 1.10 eq.) was added. The solution was cooled to 0 °C and cyanogen bromide (3.57 g, 33.9 mmol, 1.40 eq.) was added slowly. The solution was stirred at 0 °C for 2 h and was further stirred at room temperature for 72 h. The formed residue was filtered to yield compound **6** as a yellow solid (3.08 g, 19.3 mmol, 80 %).

<sup>1</sup>H-NMR (400 MHz, DMSO-*d*<sub>6</sub>): δ(ppm) = 7.70 (s, 2H, NH<sub>2</sub>); <sup>13</sup>C NMR (101 MHz, DMSO-*d*<sub>6</sub>): δ(ppm) = 164.5 (C-NO<sub>2</sub>), 162.9 (C-NH<sub>2</sub>), 148.8 (C<sub>(oxadiazole)</sub>), 144.5 (C<sub>(triazole)</sub>); <sup>14</sup>N NMR (29 MHz, DMSO-*d*<sub>6</sub>): δ(ppm) = -25; IR (ATR, rel. int.): ν (cm<sup>-1</sup>) = 3593 (w), 3496 (w), 3440 (w), 3365 (m),

## Combination of Different Azoles – 1,2,4-Triazolyl-1,3,4-Oxadiazoles as Precursor for Energetic Materials

3248 (w), 3129 (w), 2464 (w), 2209 (w), 2182 (w), 2051 (w), 2027 (w), 2004 (w), 1980 (w), 1693 (s), 1632 (m), 1584 (m), 1547 (s), 1477 (m), 1445 (m), 1413 (m), 1379 (m), 1346 (w), 1308 (s), 1196 (w), 1179 (w), 1100 (m), 1063 (m), 1032 (m), 1009 (m), 957 (m), 933 (w), 842 (s), 770 (w), 745 (w), 728 (w), 668 (w), 646 (m), 598 (w); Mass spectrometry:  $m/z$  (FAB<sup>+</sup>) = 196.0 [M<sup>+</sup>], DSC (5 °C min<sup>-1</sup>):  $T_{dec.}$  = 245 °C.

### 10.5.3.2. General procedure for the synthesis of salts

To a water/methanol 1:1 solution (7 mL/7 mL) of 6 (300 mg, 1.52 mmol) the corresponding base (K<sub>2</sub>CO<sub>3</sub>: 210 mg, 1.52 mmol; ammonia solution: 0.5 mL, 25 %, 1.52 mmol; guanidine carbonate: 136 mg, 1.52 mmol; aminoguanidine bicarbonate: 207 mg, 1.52 mmol;) was added and heated until everything was dissolved. The solutions were filtered and left for crystallization.

#### Potassium 3-(5-amino-1,3,4-oxadiazol-2-yl)-5-nitro-1,2,4-triazolate hydrate (7)

Yield: (334 mg, 1.32 mmol, 87 %) as a dark red solid.

<sup>1</sup>H-NMR (400 MHz, DMSO-*d*<sub>6</sub>):  $\delta$ (ppm) = 7.13 (s, 2H, NH<sub>2</sub>); <sup>13</sup>C NMR (101 MHz, DMSO-*d*<sub>6</sub>):  $\delta$ (ppm) = 165.9 (C-NO<sub>2</sub>), 163.4 (C-NH<sub>2</sub>), 153.3 (C<sub>(oxadiazole)</sub>), 150.4 (C<sub>(triazole)</sub>); <sup>14</sup>N NMR (29 MHz, DMSO-*d*<sub>6</sub>):  $\delta$ (ppm) = -27; IR (ATR, rel. int.):  $\nu$  (cm<sup>-1</sup>) = 3288 (w), 3127 (w), 1647 (m), 1614 (m), 1589 (m), 1560 (w), 1521 (m), 1455 (m), 1393 (m), 1325 (m), 1301 (m), 1250 (m), 1197 (m), 1172 (m), 1098 (m), 1046 (m), 1017 (m), 960 (m), 844 (m), 799 (m), 732 (s), 683 (s), 657 (s), 642 (s), 590 (s), 525 (m); Elemental analysis: calc. (%) for C<sub>4</sub>H<sub>4</sub>N<sub>7</sub>O<sub>4</sub> (M = 253.22 g mol<sup>-1</sup>): C 18.97, N 38.72, H 1.59; found: C 23.13, N 52.68, H 3.37; DSC (5 °C min<sup>-1</sup>):  $T_{dec.}$  = 254 °C; Sensitivities: ESD: 1.5 J, Friction: 360 N, Impact: 40 J.

#### Ammonium 3-(5-amino-1,3,4-oxadiazol-2-yl)-5-nitro-1,2,4-triazolate hydrate (8)

Yield: (220 mg, 1.03 mmol, 68 %) as a dark red solid.

<sup>1</sup>H-NMR (400 MHz, DMSO-*d*<sub>6</sub>):  $\delta$ (ppm) = 7.13 (s, 2H, NH<sub>2</sub>); <sup>13</sup>C NMR (101 MHz, DMSO-*d*<sub>6</sub>):  $\delta$ (ppm) = 165.8 (C-NO<sub>2</sub>), 163.4 (C-NH<sub>2</sub>), 153.3 (C<sub>(oxadiazole)</sub>), 150.4 (C<sub>(triazole)</sub>); IR (ATR, rel. int.):  $\nu$  (cm<sup>-1</sup>) = 3142 (w), 1652 (s), 1583 (w), 1528 (m), 1461 (m), 1425 (m), 1397 (s), 1327 (w), 1304 (m), 1107 (w), 1051 (w), 1016 (w), 843 (m), 734 (w), 655 (m); Elemental analysis: calc. (%) for

## Combination of Different Azoles – 1,2,4-Triazolyl-1,3,4-Oxadiazoles as Precursor for Energetic Materials

$\text{C}_4\text{H}_8\text{N}_8\text{O}_4$  ( $M = 232.18 \text{ g mol}^{-1}$ ): C 20.69, N 48.27, H 3.47; found: C 20.51, N 47.21, H 3.19; DSC ( $5^\circ\text{C m}^{-1}$ ):  $T_{\text{dec.}} = 276^\circ\text{C}$ ; Sensitivities: ESD: 1.5 J, Friction: 360 N, Impact: 40 J.

### Guanidinium 3-(5-amino-1,3,4-oxadiazol-2-yl)-5-nitro-1,2,4-triazolate (9)

Yield: (210 mg, 0.82 mmol, 54 %) as a brown solid.

$^1\text{H-NMR}$  (400 MHz,  $\text{DMSO-}d_6$ ):  $\delta(\text{ppm}) = 7.31$  (s, 2H,  $\text{NH}_{2(\text{oxodiazole})}$ ), 6.92 (s, 6H, 3 x  $\text{NH}_{2(\text{guanidine})}$ );  $^{13}\text{C NMR}$  (101 MHz,  $\text{DMSO-}d_6$ ):  $\delta(\text{ppm}) = 164.9$  (C- $\text{NO}_2$ ), 162.7 (C- $\text{NH}_2$ ), 157.8 ( $\text{C}_{(\text{guanidine})}$ ), 151.9 ( $\text{C}_{(\text{oxodiazole})}$ ), 148.6 ( $\text{C}_{(\text{triazole})}$ ); IR (ATR, rel. int.):  $\nu$  ( $\text{cm}^{-1}$ ) = 3565 (w), 3442 (m), 3130 (m), 2167 (w), 2003 (w), 1981 (w), 1655 (s), 1579 (m), 1517 (m), 1490 (m), 1436 (m), 1378 (s), 1317 (s), 1300 (s), 1201 (m), 1135 (w), 1092 (m), 1054 (m), 1036 (m), 1011 (m), 973 (w), 839 (s), 752 (m), 684 (m), 645 (s), 534 (s), 513 (s), Elemental analysis: calc. (%) for  $\text{C}_5\text{H}_8\text{N}_{10}\text{O}_3$  ( $M = 256.18 \text{ g mol}^{-1}$ ): C 22.44, N 54.68, H 3.15; found: C 23.13, N 52.68, H 3.37; DSC ( $5^\circ\text{C min}^{-1}$ ):  $T_{\text{dec.}} = 296^\circ\text{C}$ ; Sensitivities: ESD: 1.5 J, Friction: 360 N, Impact: 40 J.

### Aminoguanidinium 3-(5-amino-1,3,4-oxadiazol-2-yl)-5-nitro-1,2,4-triazolate (10)

Yield: (310 mg, 1.13 mmol, 74 %) as a brown solid.

$^1\text{H-NMR}$  (400 MHz,  $\text{DMSO-}d_6$ ):  $\delta(\text{ppm}) = 8.57$  (s, 1H, NH), 7.25 (m, 2H,  $\text{NH}_{2(\text{aminoguanidine})}$ ), 7.13 (s, 2H,  $\text{NH}_{2(\text{oxodiazole})}$ ), 6.76 (m, 2H,  $\text{NH}_{2(\text{aminoguanidine})}$ ), 4.68 (s, 2H,  $\text{NH}_{2(\text{aminoguanidine})}$ );  $^{13}\text{C NMR}$  (101 MHz,  $\text{DMSO-}d_6$ ):  $\delta(\text{ppm}) = 165.8$  (C- $\text{NO}_2$ ), 163.3 (C- $\text{NH}_2$ ), 158.7 ( $\text{C}_{(\text{aminoguanidine})}$ ), 153.3 ( $\text{C}_{(\text{oxodiazole})}$ ), 150.4 ( $\text{C}_{(\text{triazole})}$ ); IR (ATR, rel. int.):  $\nu$  ( $\text{cm}^{-1}$ ) = 3461 (m), 3380 (m), 3329 (m), 3303 (m), 3200 (s), 3152 (m), 3089 (s), 3076 (m), 1652 (s), 1602 (m), 1573 (m), 1551 (m), 1493 (m), 1439 (m), 1395 (m), 1325 (m), 1304 (m), 1199 (m), 1099 (m), 1057 (m), 1037 (m), 1021 (m), 974 (m), 952 (m), 839 (s), 686 (m), 648 (m), 613 (m), 592 (w), 544 (m), 522 (s); Elemental analysis: calc. (%) for  $\text{C}_5\text{H}_9\text{N}_{11}\text{O}_3$  ( $M = 271.23 \text{ g mol}^{-1}$ ): C 22.14, N 56.81, H 3.34; found: C 22.30, N 55.81, H 3.32; DSC ( $5^\circ\text{C min}^{-1}$ ):  $T_{\text{dec.}} = 246^\circ\text{C}$ ; Sensitivities: ESD: 1.5 J, Friction: 360 N, Impact: 40 J.

#### 10.5.4. Crystal Structures

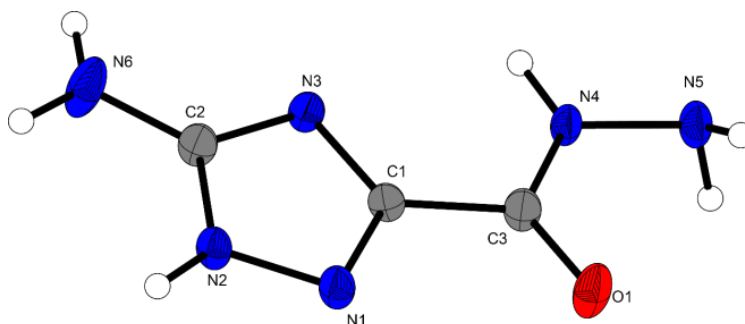


Figure S1. Crystal structure of 3.

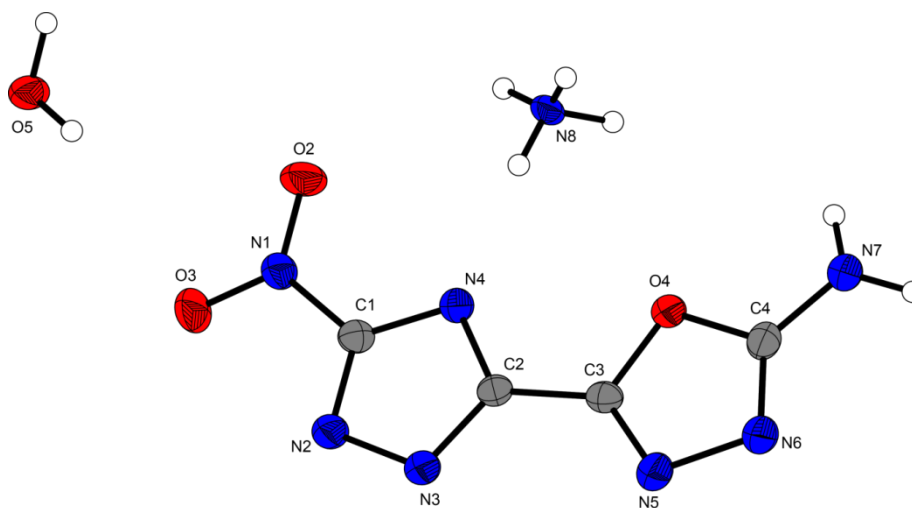


Figure S2. Crystal Structure of 8 as monohydrate.



### 10.5.5. References

- [S1] *CrysAlisPro*, Oxford Diffraction Ltd., version 171.33.41, **2009**.
- [S2] *SIR-92, A program for crystal structure solution*: A. Altomare, G. Cascarano, C. Giacovazzo, A. Guagliardi, *J. Appl. Crystallogr.* **1993**, 26, 343.
- [S3] a) A. Altomare, G. Cascarano, C. Giacovazzo, A. Guagliardi, A. G. G. Moliterni, M. C. Burla, G. Polidori, M. Camalli, R. Spagna, *SIR97*, **1997**; b) A. Altomare, M. C. Burla, M. Camalli, G. L. Cascarano, C. Giacovazzo, A. Guagliardi, A. G. G. Moliterni, G. Polidori, R. Spagna, *J. Appl. Crystallogr.* **1999**, 32, 115–119.
- [S4] a) G. M. Sheldrick, *SHELX-97*, University of Göttingen, Göttingen, Germany, **1997**; b) G. M. Sheldrick, *Acta Crystallogr., Sect. A* **2008**, 64, 112–122.
- [S5] A. L. Spek, *PLATON, A Multipurpose Crystallographic Tool*, Utrecht University, The Netherlands, **1999**.
- [S6] *SCALE3 ABSPACK – An Oxford Diffraction program* (1.0.4, gui: 1.0.3), Oxford Diffraction Ltd., **2005**.
- [S7] *APEX3*. Bruker AXS Inc., Madison, Wisconsin, USA.
- [S8] M. J. Frisch, G. W. Trucks, H. B. Schlegel, G. E. Scuseria, M. A. Robb, J. R. Cheeseman, G. Scalmani, V. Barone, B. Mennucci, G. A. Petersson, H. Nakatsuji, M. Caricato, X. Li, H.P. Hratchian, A. F. Izmaylov, J. Bloino, G. Zheng, J. L. Sonnenberg, M. Hada, M. Ehara, K. Toyota, R. Fukuda, J. Hasegawa, M. Ishida, T. Nakajima, Y. Honda, O. Kitao, H. Nakai, T. Vreven, J. A. Montgomery, Jr., J. E. Peralta, F. Ogliaro, M. Bearpark, J. J. Heyd, E. Brothers, K. N. Kudin, V. N. Staroverov, R. Kobayashi, J. Normand, K. Raghavachari, A. Rendell, J. C. Burant, S. S. Iyengar, J. Tomasi, M. Cossi, N. Rega, J. M. Millam, M. Klene, J. E. Knox, J. B. Cross, V. Bakken, C. Adamo, J. Jaramillo, R. Gomperts, R. E. Stratmann, O. Yazyev, A. J. Austin, R. Cammi, C. Pomelli, J. W. Ochterski, R. L. Martin, K. Morokuma, V. G. Zakrzewski, G. A. Voth, P. Salvador, J. J. Dannenberg, S. Dapprich, A. D. Daniels, O. Farkas, J.B. Foresman, J. V. Ortiz, J. Cioslowski, D. J. Fox, Gaussian 09 A.02, Gaussian, Inc., Wallingford, CT, USA, **2009**.

## Combination of Different Azoles – 1,2,4-Triazolyl-1,3,4-Oxadiazoles as Precursor for Energetic Materials

- [S9] a) J. W. Ochterski, G. A. Petersson, and J. A. Montgomery Jr., *J. Chem. Phys.* **1996**, *104*, 2598–2619; b) J. A. Montgomery Jr., M. J. Frisch, J. W. Ochterski G. A. Petersson, *J. Chem. Phys.* **2000**, *112*, 6532–6542.
- [S10] a) L. A. Curtiss, K. Raghavachari, P. C. Redfern, J. A. Pople, *J. Chem. Phys.* **1997**, *106*, 1063–1079; b) E. F. C. Byrd, B. M. Rice, *J. Phys. Chem. A* **2006**, *110*, 1005–1013; c) B. M. Rice, S. V. Pai, J. Hare, *Comb. Flame* **1999**, *118*, 445–458.
- [S11] P. J. Lindstrom, W. G. Mallard (Editors), NIST Standard Reference Database Number 69, <http://webbook.nist.gov/chemistry/> (accessed June **2011**).
- [S12] M. S. Westwell, M. S. Searle, D. J. Wales, D. H. Williams, *J. Am. Chem. Soc.* **1995**, *117*, 5013–5015; b) F. Trouton, *Philos. Mag.* **1884**, *18*, 54–57.
- [S13] a) H. D. B. Jenkins, H. K. Roobottom, J. Passmore, L. Glasser, *Inorg. Chem.* **1999**, *38*, 3609–3620; b) H. D. B. Jenkins, D. Tudela, L. Glasser, *Inorg. Chem.* **2002**, *41*, 2364–2367.
- [S14] NATO standardization agreement (STANAG) on explosives, *impact sensitivity tests*, no. 4489, 1st ed., Sept. 17, **1999**.
- [S15] WIWEB-Standardarbeitsanweisung 4-5.1.02, Ermittlung der Explosionsgefährlichkeit, hier der Schlagempfindlichkeit mit dem Fallhammer, Nov. 8, **2002**.
- [S16] <http://www.bam.de>
- [S17] NATO standardization agreement (STANAG) on explosive, *friction sensitivity tests*, no. 4487, 1st ed., Aug. 22, **2002**.
- [S18] WIWEB-Standardarbeitsanweisung 4-5.1.03, Ermittlung der Explosionsgefährlichkeit oder der Reibeempfindlichkeit mit dem Reibeapparat, Nov. 8, **2002**.
- [S19] Impact: insensitive > 40 J, less sensitive  $\geq 35$  J, sensitive  $\geq 4$  J, very sensitive  $\leq 3$  J; Friction: insensitive > 360 N, less sensitive = 360 N, sensitive < 360 N and > 80 N, very sensitive  $\leq 80$  N, extremely sensitive  $\leq 10$  N, According to: *Recommendations on the Transport of Dangerous Goods, Manual of Tests and Criteria*, 4th edition, United Nations, New York-Geneva, **1999**.

**Combination of Different Azoles – 1,2,4-Triazolyl-1,3,4-Oxadiazoles as Precursor for Energetic Materials**

[S20] <http://www.ozm.cz>

[S21] A. A. Dippold, T. M. Klapötke, *Chem. Asian J.* **2013**, 8, 1463–1471.

## 11. Toward the Synthesis of 3,5-Diamino-4,6-dinitropyridazine

Ivan Gospodinov, Thomas M. Klapötke and Jörg Stierstorfer

Unpublished Results

### 11.1. Introduction

Pyridazines, together with pyrimidines and pyrazines, belong to an important class of heterocyclic compounds known as diazines. These are present in many natural products and can be found in variety of medicinal agents. The diazines can be derived from benzene by replacing two of the ring carbon atoms with nitrogen. There are three possible diazine isomers respectively to the position of the nitrogen atoms to each other in the ring system, giving rise to pyridazine, pyrimidine and pyrazine (**Figure 1**).<sup>[1]</sup>

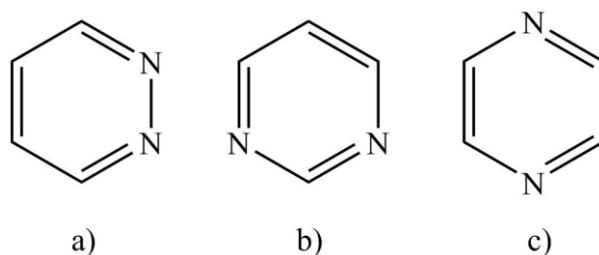


**Figure 1.** Diazine isomers: a) pyridazine, b) pyrimidine and c) pyrazine.

Diazine derivatives are interesting not only for their pharmaceutical properties, but also for their possible application in the field of energetic materials. The positive heat of formation of *N*-heterocycles and the formation of *N*-oxides which leads to higher density of the material, make nitrogen-rich heterocyclic compounds one of the most important structural motifs for the design of new high-energy dense materials.<sup>[2]</sup> There are already some examples for energetic pyrimidines and pyrazines reported by Millar *et al.*<sup>[3,4]</sup>

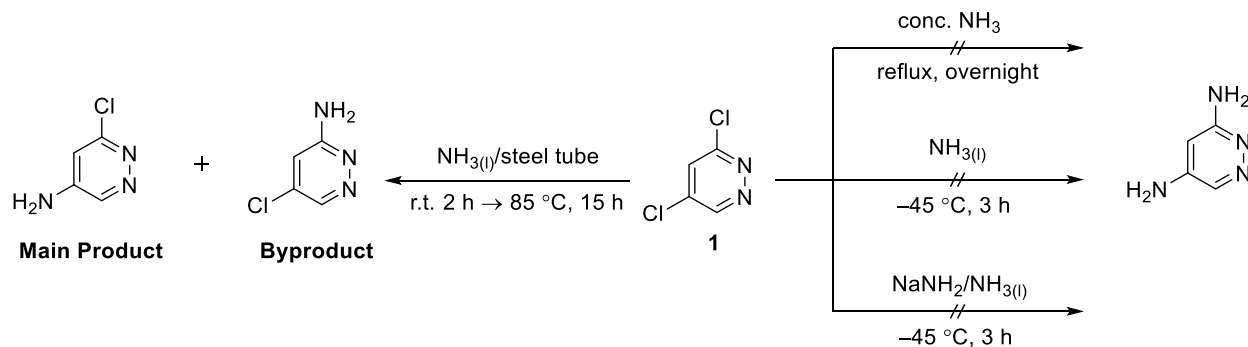
Even though there are examples for energetic pyrimidines and pyrazines, like pyridine they are electron deficient systems and even more resistant than pyridine toward electrophilic aromatic substitution.<sup>[5]</sup> For efficient electrophilic nitration on diazine derivatives an electron donating group has to be introduced to activate the *N*-heterocyclic backbone.<sup>[6]</sup> In this work, the chemistry of the

pyridazine backbone will be investigated. Specifically, a synthetic approach toward 3,5-diamino-4,6-dinitropyridazine and 4,6-diamino-3,5-dinitropyridazine-1-oxide will be investigated.

## 11.2. Results and Discussion

### 11.2.1. Synthesis

To achieve this goal 3,5-dichloropyridazine was used as starting materials. The idea of this synthesis is to increase the electron density in the pyridazine backbone by synthesizing 3,5-diaminopyridazine. Which will be followed by direct nitration of to yield the desired 3,5-diamino-4,6-dinitropyridazine. Direct displacement of the chlorine atoms in compound **1** with conc. ammonia or liquid ammonia was investigated, however with no success. In both cases the starting material was obtained or a decomposition was observed. Further amination with sodium amide in liquid ammonia was also investigated, however compound **1** decomposed during the reaction. Finally, 3,5-dichloropyridazine (**1**) was reacted with liquid ammonia at 85 °C in a steel tube for 15 h, which resulted in a mixture of 3-amino-5-chloropyridazine (byproduct) and 5-amino-3-chloropyridazine (main product). All reactions are shown in **Scheme 1**.

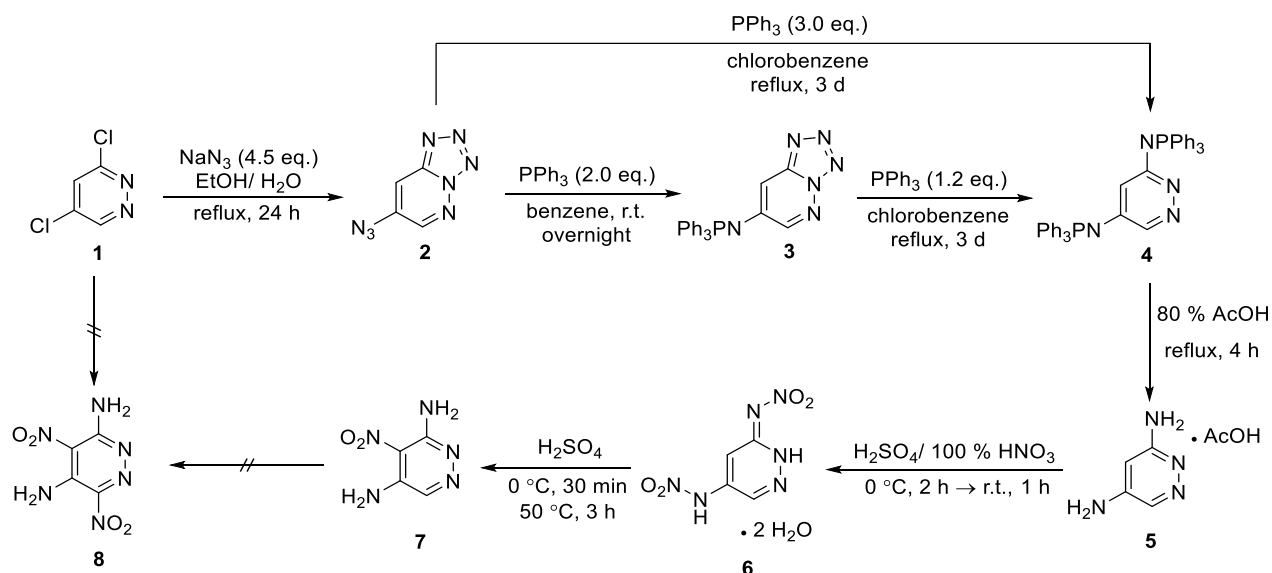


**Scheme 1.** Failed direct amination reactions of compound **1**.

Since direct amination of compound **1** was not possible, a different more complex synthetic route was investigated. First both chlorine atoms will be displaced with azido groups and then by using the Staudinger reaction both iminophosphorane groups will be hydrolysed to the desired amino groups. Similar procedure has been reported in the literature for a related compound.<sup>[7]</sup> The displacement of both chlorine atoms in compound **1** was successfully achieved with an inorganic azide such as sodium azide. Refluxing 3,5-dichloropyridazine (**1**) in  $\text{H}_2\text{O}/\text{EtOH}$  with  $\text{NaN}_3$  (4.5 eq.) gave the desired product. Compound 7-azidotetrazolo[1,5-*b*]pyridazine (**2**) was obtained in a

## Toward the Synthesis of 3,5-Diamino-4,6-dinitropyridazine

moderate yield (49 %). The reduction of an azide group to an amino group can be performed catalytically by using hydrogen or using inorganic reducing agents.<sup>[8]</sup> However heterocyclic compounds having an azide group adjacent to annular nitrogen atom show the so-called azido-tetrazole tautomerism.<sup>[9]</sup> A possible method for the conversion of the “masked” azide (tetrazole ring) to amino group is to use the Staudinger reduction.<sup>[10,11]</sup> For this purpose, the organic azides are reacted with tertiary phosphines, like triphenylphosphine, to give iminophosphoranes as intermediates, which can be hydrolyzed with aqueous acids to the desired amines and triphenylphosphine oxide. This type of reaction has been already used in the literature to convert 8-azidotetrazolo[1,5-*b*]pyridazine into 3,6-diaminopyridazine as acetate.<sup>[7]</sup>



**Scheme 2.** Toward the synthesis of 3,5-diamino-4,6-dinitropyridazine (8).

All performed Staudinger reactions with 7-azidotetrazolo[1,5-*b*]pyridazine (2) are shown in **Scheme 2**. The reaction of both azide groups can be performed in one step by refluxing compound 2 in chlorobenzene with an excess of triphenylphosphine (PPh<sub>3</sub>). This method gives, however, 3,5-bis(triphenylphosphoranylideneamino)pyridazine (4) in a low yield. Then again reacting compound 2 with PPh<sub>3</sub> (2.0 eq.) in benzene at room temperature gives 5-(triphenylphosphoranylideneamino)tetrazolo[1,5-*b*]pyridazine (3) in an excellent yield (95 %). For the reduction of the “masked” azide, compound 3 had to be refluxed in chlorobenzene for at least 24 h with PPh<sub>3</sub> (1.15–1.30 eq.). After removing the solvent and trituration with *c*-hexane 3,5-bis(triphenylphosphoranylideneamino)pyridazine (4) was obtained as a gray solid. <sup>1</sup>H and <sup>31</sup>P NMR spectroscopy showed that compound 4 was received with some impurities. 3,5-

Bis(triphenylphosphoranylideneamino)pyridazine (**4**) was hydrolyzed by using 80 % acetic acid as described in the literature for the 3,6-pyridazine isomer.<sup>[7]</sup> For this purpose, compound **4** was added to 80 % HOAc and refluxed for 2.5–4 h. After cooling down, H<sub>2</sub>O was given to the reaction to form triphenylphosphine oxide. The suspension was extracted with EtOAc to remove POPh<sub>3</sub> and the water phase was evaporated to dryness to give a dark brown oily liquid. Trituration with small amount of Et<sub>2</sub>O gave compound **5** as acetate salt.

Further nitration of compound **5** did not result in the desired 3,5-diamino-4,6-dinitropyridazine, but instead 5-nitramino-3-nitriminopyridazine dihydrate (**6·2H<sub>2</sub>O**) was obtained in a good yield (79 %). Even with two amino groups the pyridazine system in compound **5** is deactivated toward an electrophilic nitration and instead the amino groups are nitrated. However, compound **6·2H<sub>2</sub>O** can be heated in conc. H<sub>2</sub>SO<sub>4</sub>, which results in the cleavage of both nitramino and nitrimino groups and results in 3,5-diamino-4-nitropyridazine (**7**). The nitration of similar compound 3,5-diaminopyridazine hydrochloride has been previously reported in the literature. However, the reported product is 5-amino-3-nitraminopyridazine mononitrate, which can be converted to 3,5-diamino-4-nitropyridazine (**7**).<sup>[12]</sup> In this case we report that the obtained intermediate is not 5-amino-3-nitraminopyridazine mononitrate but 5-nitramino-3-nitriminopyridazine dihydrate (**6·2H<sub>2</sub>O**).

### 11.2.2. NMR Spectroscopy

Compound **2** was characterized by using various spectroscopic methods such as <sup>1</sup>H, <sup>13</sup>C, <sup>15</sup>N NMR, elemental analysis, infrared and mass spectrometry. <sup>1</sup>H NMR spectrum of **2** exhibits two signals at 8.84 ppm (d) and 8.60 ppm (d) with a coupling constant (<sup>4</sup>*J*) of 2.60 Hz for the aromatic pyridazine hydrogen protons. A <sup>13</sup>C NMR spectrum was also measured in *d*<sub>6</sub>-DMSO and shows four signals for the pyridazine carbon atoms at 143.8, 143.7, 139.3 and 110.6 ppm. <sup>15</sup>N NMR spectrum of compound **2** was also recorded and is shown in **Figure 2**. The assignment of the signals is based on comparison with the literature values for 8-azido-tetrazolo[1,5-*b*]pyridazine and on the analysis of the observed <sup>15</sup>N-<sup>1</sup>H coupling constants.<sup>[13]</sup> <sup>15</sup>N NMR spectrum of compound **2** taken in *d*<sub>6</sub>-DMSO solution shows only eight signals which are in typical range for both azide and tetrazole forms, excluding the presence of an tetrazole-azide equilibrium and indicating only the presence of 7-azidotetrazolo[1,5-*b*]pyridazine.<sup>[14-16]</sup> As shown in **Figure 2** all three signals at −140.7 (N<sub>γ</sub>), −143.8 (N<sub>β</sub>) and −283.6 (N<sub>α</sub>) ppm can be assigned to the nitrogen atoms of the azide group. The

pyridazine nitrogen atoms are observed at  $-70.0$  ppm (d) with  $^2J$  coupling constant of  $14.30$  Hz ( $N^1$ ) and at  $-106.6$  ppm (dd) with two different  $^3J$  coupling constants of  $9.60$  Hz and  $2.73$  Hz ( $N^2$ ). The remaining three proton resonances at  $15.0$  ( $N^4$ ),  $-28.0$  ( $N^3$ ) and  $-68.9$  ( $N^5$ ) ppm are assigned to the tetrazole ring nitrogen atoms.

**$^{15}\text{N}$  NMR (41 MHz,  $d_6$ -DMSO)**

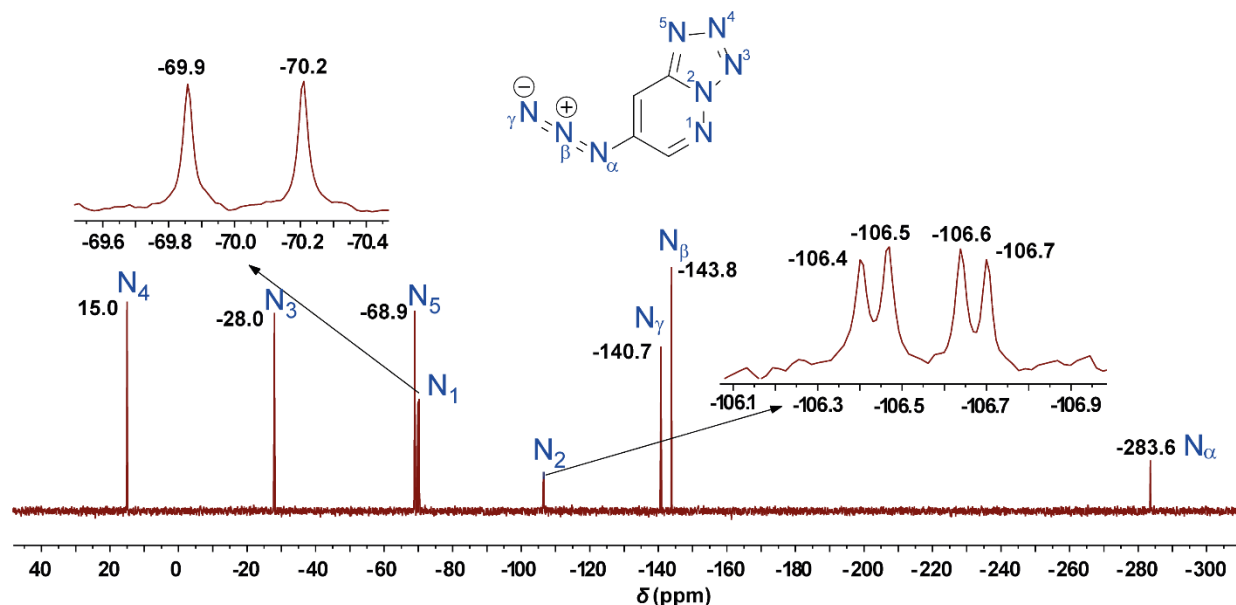


**Figure 2.**  $^{15}\text{N}$  NMR spectrum of 7-azidotetrazolo[1,5-*b*]pyridazine (2) in  $d_6$ -DMSO.

In addition to the  $^{15}\text{N}$  NMR spectrum of 7-azidotetrazolo[1,5-*b*]pyridazine (2), the  $^{15}\text{N}\{^1\text{H}\}$  spectrum was also recorded in  $d_6$ -DMSO. The comparison of both spectra is shown in **Figure 3**, in which the coupled  $^{15}\text{N}$  spectrum is stacked over the  $^1\text{H}$  decoupled  $^{15}\text{N}$  spectrum of compound 2. The only difference in both NMR spectra is the change of the multiplicity for the two pyridazine nitrogen protons from doublet for  $N^1$  to singlet and from dd (doublet of doublet) for  $N^2$  to singlet due to the  $^1\text{H}$  decoupling.



$^{15}\text{N}$  NMR (41 MHz,  $d_6$ -DMSO)

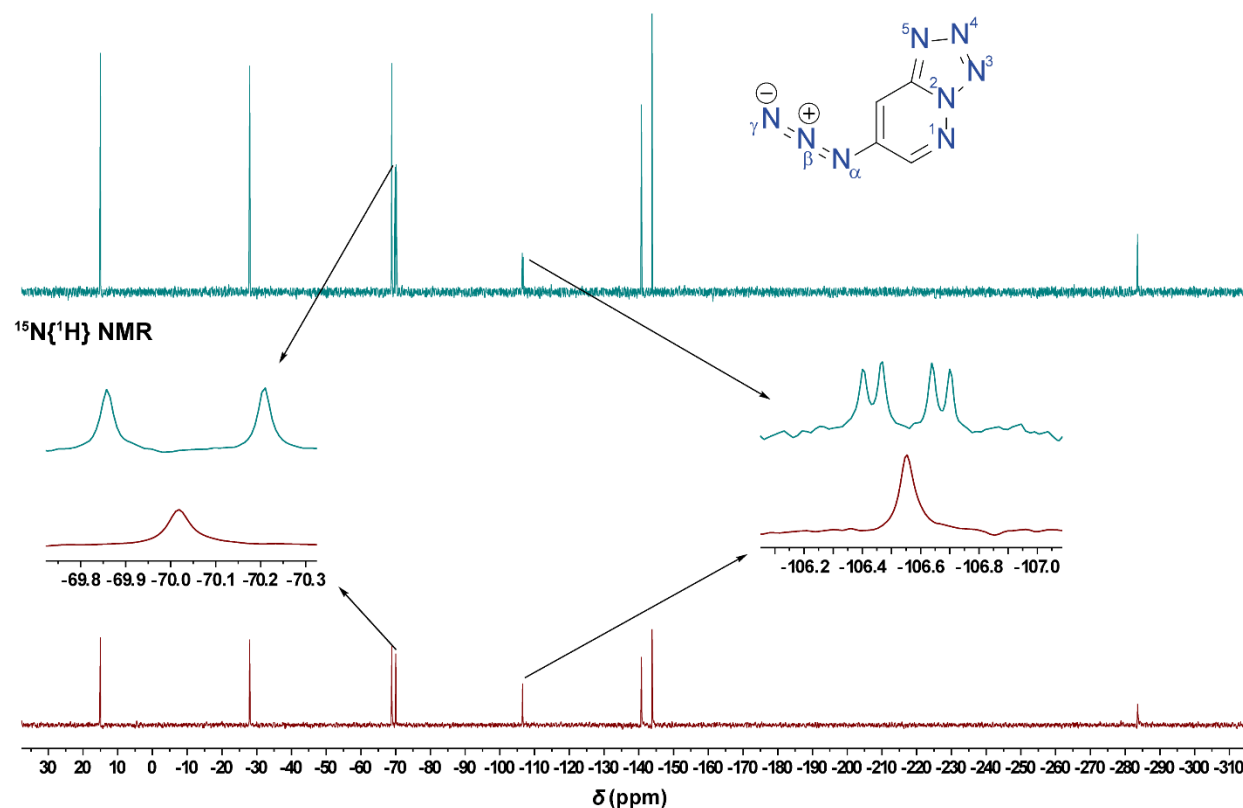


**Figure 3.** Stacked  $^{15}\text{N}$  and  $^{15}\text{N}\{^1\text{H}\}$  NMR spectra of compound **2** in  $d_6$ -DMSO.

5-(Triphenylphosphoranylidenamino)tetrazolo[1,5-*b*]pyridazine (**3**) has been characterized by  $^1\text{H}$ ,  $^{13}\text{C}$ ,  $^{31}\text{P}$  NMR, infrared spectroscopy and elemental analysis.  $^{31}\text{P}$  NMR spectrum of **3** shows only one signal at 13.1 ppm.  $^1\text{H}$  NMR spectrum of compound **3** exhibits five signals, two for the aromatic pyridazine hydrogen protons at 8.55 ppm and 6.47 ppm and three multiplet signals at 7.90–7.82 ppm, 7.76–7.70 ppm and 7.67–7.60 ppm. The two pyridazine protons and all four pyridazine carbon protons experience an additional splitting associated with scalar spin–spin interactions  $J$  ( $^{31}\text{P}$ ,  $^1\text{H}$  and  $^{31}\text{P}$ ,  $^{13}\text{C}$ ).<sup>[13]</sup> This can be explained with the introduction of the iminophosphoranes group ( $\text{NPPH}_3$ ) into the molecule.

### 11.2.3. Crystal Structures

For further support of all maintained NMR measurements, single crystals of compound **2** were grown for X-ray determination from abs. ethanol. The crystal structure of 7-azido-tetrazolo[1,5-*b*]pyridazine (**2**) is shown in **Figure 4**, with bond lengths and angles. Compound **2** crystalizes as

colorless plates in the monoclinic space group  $P2_1/n$  with four molecules in the unit cell. The volume of the unit cell is  $652.93(8) \text{ \AA}^3$  with lattice constants  $a = 10.8080(8)$ ,  $b = 5.5640(3)$ ,  $c = 11.2689(7) \text{ \AA}$  and  $\beta = 105.527(7)^\circ$ . The molecule of **2** can be divided in three components: the pyridazine scaffold, the tetrazole ring (“masked azide”) and the azide group. All three fragments are coplanar to each other. The formation of the bicyclic moiety tetrazolo[1,5-*b*]pyridazine leads to small deformation of the pyridazine ring expressed with the elongation of the N2–C4 ( $1.3562(16) \text{ \AA}$ ), N1–N2 ( $1.3483(18) \text{ \AA}$ ) and C3–C4 ( $1.408(2) \text{ \AA}$ ) bond lengths. This adjustment of the pyridazine scaffold can be observed also with the augmentation of the N1–N2–C4 bond angle ( $127.95(12)^\circ$ ) and reduction of the N2–N1–C1 ( $112.84(12)^\circ$ ) and N2–C4–C3 ( $118.46(13)^\circ$ ) angles, allowing the bicyclic structure to be stable. The smallest bond length in the tetrazole ring is between the nitrogen atoms N3 and N4 with  $1.3055(18) \text{ \AA}$  and the largest between N4 and N5 with  $1.3587(16) \text{ \AA}$ . The N–N and N–C bond lengths in the tetrazole ring are in the range with the known values for bicyclic tetrazole derivatives and vary between the corresponding values for single and double bond lengths for heterocyclic aromatic compounds containing  $sp^2$  hybridized carbon and nitrogen atoms.<sup>[17,18]</sup> The bond angles and lengths for the azide group correlate with the known values for covalent organic azides.<sup>[19]</sup> The bond length between C2 and N6 is  $1.4143(19) \text{ \AA}$  and compared to a C–N single bond ( $1.47 \text{ \AA}$ ) is shorter than expected. The bond angle N7–N6–C2 is  $113.99(12)^\circ$  and the angle between the atoms N6, N7 and N8 is  $173.55(16)^\circ$  which deviates from the expected  $180^\circ$ . Further deviations from the expected values are observed for the bond lengths between N6–N7 and N7–N8. The measured value for the N6–N7 bond length is  $1.2566(16) \text{ \AA}$  and it is shorter compared to the expected value for an N–N single bond. Vice versa the N7–N8 bond ( $1.1245(17) \text{ \AA}$ ) is longer than expected for N≡N bond with  $1.10 \text{ \AA}$ .<sup>[20]</sup> Possible reason for the deviation in the values for bond lengths and angles in the azide group can be the hyperconjugation between the C2–N6 single bond and the  $\pi^*$  N7–N8 double bond.<sup>[21,22]</sup>

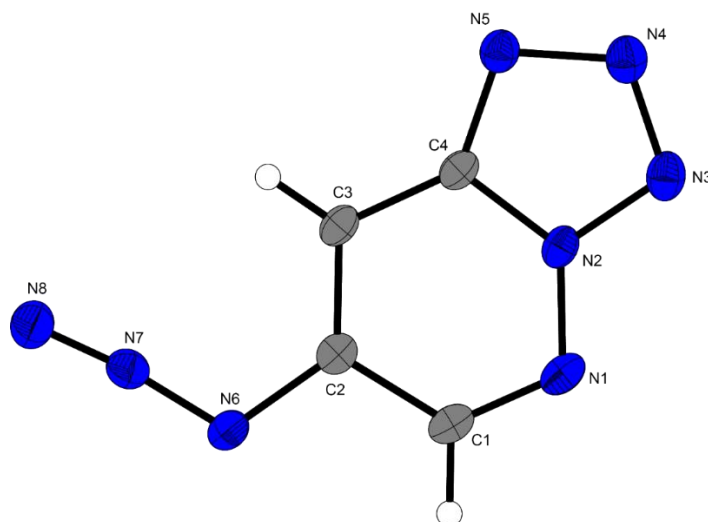


**Figure 4.** Molecular unit of 7-azidotetrazolo[1,5-*b*]pyridazine (**2**) in the crystalline state. Ellipsoids correspond to 50% probability levels. Hydrogen radii are arbitrary. Selected bond lengths (Å) and angles [deg.]: N1–N2 1.3483(18), N1–C1 1.303(2), N2–N3 1.3536(18), N2–C4 1.3562(16), N3–N4 1.3055(18), N4–N5 1.3587(16), N5–C4 1.332(2), N6–N7 1.2566(16), N6–C2 1.4143(19), N7–N8 1.1245(17), C1–C2 1.431(2), C2–C3 1.359(2), C3–C4 1.408(2), N2–N1–C1 112.84(12), N1–N2–N3 122.60(11), N1–N2–C4 127.95(12), N3–N2–C4 109.45(12), N2–N3–N4 104.90(11), N3–N4–N5 112.41(12), N4–N5–C4 105.44(11), N7–N6–C2 113.99(12), N6–N7–N8 173.55(16), N1–C1–C2 124.80(15), N6–C2–C1 113.84(13), N6–C2–C3 125.90(12), C1–C2–C3 120.26(14), C2–C3–C4 115.68(13), N2–C4–N5 107.80(12), N2–C4–C3 118.46(13), N5–C4–C3 133.74(12), C1–N1–N2–N3 178.52(13), C4–N2–N3–N4 –0.13(14), N1–N2–C4–N5 179.95(11), N1–N2–C4–C3 –0.2(2), N3–N2–C4–C3 –179.61(12).

In addition, single crystals of compound **3** were obtained from THF for an X-ray measurement. The crystal structure of 5-(triphenylphosphoranylidenamino)tetrazolo[1,5-*b*]pyridazine (**3**) is shown in **Figure 5**, with bond lengths and angles. Compound **3** crystallizes as colorless blocks in the triclinic space group *P*–1. The volume of the unit cell is 944.99(16) Å<sup>3</sup> and contains two molecules of **3**. The lattice constants of the unit cell are *a* = 8.9584(10), *b* = 9.6241(6), *c* = 13.3220(11) Å and  $\alpha$  = 68.892(7)°,  $\beta$  = 70.518(8)° and  $\gamma$  = 64.476(8)°. 5-(Triphenylphosphoranylidenamino)tetrazolo[1,5-*b*]pyridazine (**3**) can be divided in three fragments: the pyridazine scaffold, the tetrazole ring and the iminophosphorane group (NPPh<sub>3</sub>). Similar to the starting material the formation of the bicyclic moiety tetrazolo[1,5-*b*]pyridazine leads to deformation of the pyridazine ring. This adjustment can be observed with the elongation of the N3–

C4 (1.357(2) Å), C1–C2 (1.452(3) Å) and C3–C4 (1.401(3) Å) bond lengths. Further changes are observed with the deviation of the N2–N3–C4 (127.39(17) °), N3–N2–C1 (112.78(16) °) and N2–C1–C2 (127.04(18) °) bond angles from the ideal case of 120 °. The longest N–N bond in the tetrazole ring is between N4–N5 (1.362(2) Å) and the shortest is between N5–N6 (1.299(2) Å). All N–C, P–N and P–C bond lengths in NPPh<sub>3</sub> are in the range for reported values of iminophosphorane derivatives.<sup>[23]</sup> N1–C2 bond length lies between the literature reported values for N–C single and double bonds<sup>[24]</sup> with 1.367(3) Å. The angle of 124.11(13) ° between the three P1, N1 and C2 atoms indicates a *sp*<sup>2</sup> hybrid character of the N1 atom. The P1–N1 bond length of 1.5990(17) Å corresponds to the reported values for P=N bond lengths (1.57 Å) in iminophosphorane derivatives.<sup>[25]</sup> Angles N1–P1–C5 (112.93(10) °), N1–P1–C11 (114.10(9) °), N1–P1–C17 (106.33(8) °), C5–P1–C11 (109.72(9) °) and C5–P1–C17 (106.03(9) °) indicate a small deviation from the tetrahedral coordination of the P1 atom. All three phenyl groups exhibit the literature known pyramidal arrangement on the P1 atom.

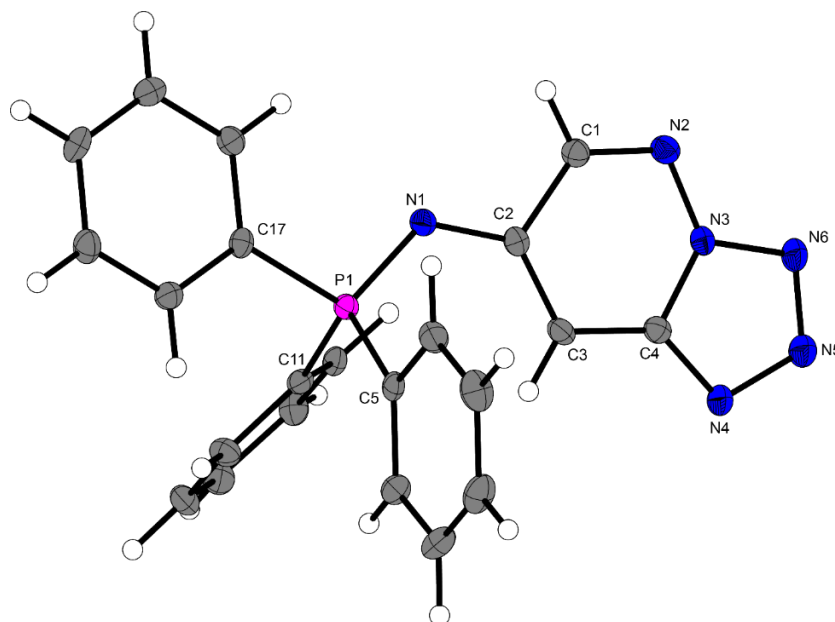


**Figure 5.** Molecular unit of compound **3** in the crystalline state. Ellipsoids correspond to 50% probability levels. Hydrogen radii are arbitrary. Selected bond lengths (Å) and angles [deg.]: P1–N1 1.5990(17), P1–C5 1.804(2), P1–C11 1.805(2), P1–C17 1.796(2), N1–C2 1.367(3), N2–N3 1.347(2), N2–C1 1.303(3), N3–N6 1.360(2), N3–C4 1.357(2), N4–N5 1.362(2), N4–C4 1.334(2), N5–N6 1.299(2), C1–C2 1.452(3), C2–C3 1.382(3), C3–C4 1.401(3), N1–P1–C5 112.93(10), N1–P1–C11 114.10(9), N1–P1–C17 106.33(8), C5–P1–C11 109.72(9), C5–P1–C17 106.03(9),

C11–P1–C17 107.19(9), P1–N1–C2 124.11(13), N2–N3–C4 127.39(17), N6–N3–C4 109.71(15), N3–N6–N5 104.67(15), N2–C1–C2 127.04(18), C2–C3–C4 117.88(17), C5–P1–N1–C2 57.58(19), C11–P1–N1–C2 –68.6(2), C17–P1–N1–C2 173.45(17), P1–N1–C2–C1 –175.96(15), P1–N1–C2–C3 5.4(3) N2–N3–C4–C3 –0.1(3), N4–N5–N6–N3 0.3(2), N2–C1–C2–C3 1.6(3).

Single crystals were obtained from *c*-hexane for an X-ray measurement. 3,5-Bis-(triphenylphosphoranylideneamino)pyridazine (**4**) crystallizes with one molecule *c*-hexane in the monoclinic space group *C2/c*. The unit cell contains eight molecules of compound **4** and has lattice constants  $a = 48.676(2)$ ,  $b = 8.7758(4)$ ,  $c = 16.1653(10)$  Å,  $\beta = 91.291(4)^\circ$  and a cell volume of 6903.6(6) Å<sup>3</sup>. The crystal structure of compound **4** is shown in **Figure 6** together with bond lengths and angles. Both P1–N2 (1.583(3) Å) and P2–N1 (1.584(3) Å) correspond to the expected value for P=N bond length (1.57 Å) in iminophosphoranes.<sup>[25]</sup> Both P1–N2–C19 with 124.9(2)° and P2–N1–C22 with 122.5(2)° indicate for  $sp^2$  hybrid character of the N1 and N2 atoms. Both P1 and P2 atoms are tetrahedral coordinated with small deviations from the ideal case.

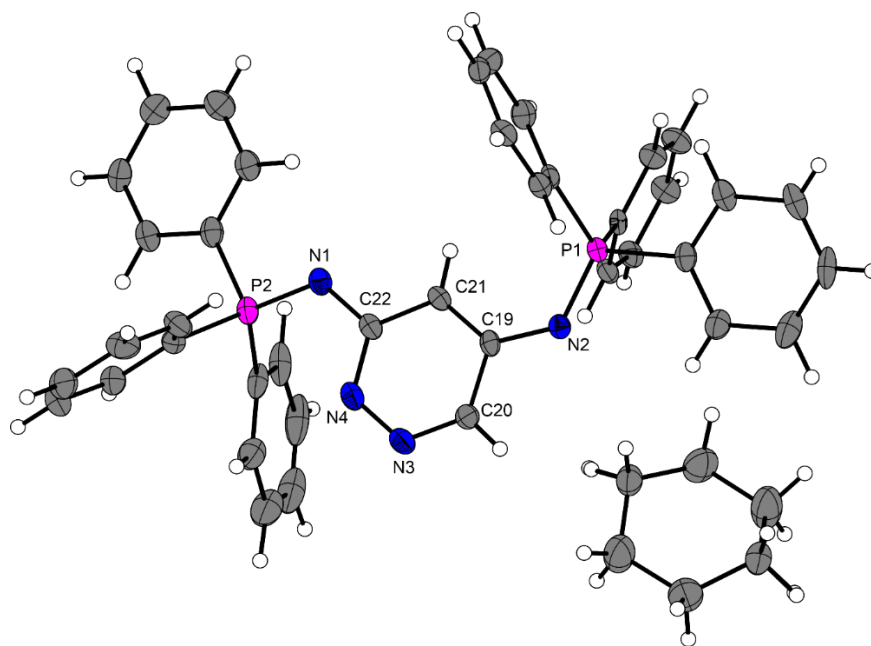


**Figure 6.** Molecular unit of compound **4** in the crystalline state. Ellipsoids correspond to 50 % probability levels. Hydrogen radii are arbitrary. Selected bond lengths (Å) and angles [deg]: P1–N2 1.583(3), P1–C1 1.802(3), N2–C19 1.382(4), N3–N4 1.350(4), N1–C22 1.377(4), P2–N1 1.584(3), N2–P1–C1 106.59(14), N2–P1–C7 116.10(14), P1–N2–C19 124.9(2), N2–C19–C21 128.6(3), N3–N4–C22 119.0(3), P2–N1–C22 122.5(2), P1–N2–C19–C20 176.6(2), C20–N3–N4–C22 1.1(4), P2–N1–C22–C21 169.6(2).

Compound **6·2H<sub>2</sub>O** (**Figure 7**) crystallizes in the monoclinic space group *C* 2/*c* with a cell volume of 1832.75(16) Å<sup>3</sup> and eight formula units per unit cell. The cell constants are *a* = 13.3872(6) Å, *b* = 9.1939(5) Å and *c* = 14.9838(8) Å with  $\beta$  = 96.393(5)°. The calculated density at 298 K is 1.67 g/cm<sup>3</sup>. The bond lengths in the pyridazine ring, the nitramino and the nitrimino group are all between the standard values for single and double bonds for these elements. This shows, that the species has an aromatic system across the entire molecule.<sup>[26]</sup> The bond lengths between N3–C1 (1.361(2) Å) and N5–C3 (1.379(2) Å) differ slightly. The bond between C2 and C3 has a length of 1.364(2) Å. This is close to the standard value for C–C double bonds.<sup>[26]</sup> The ring is slightly deformed (124.66(14)° (N1–N2–C1), 118.67(14)° (C1–C2–C3)) but in one plane (−0.5(2)° (N1–N2–C1–C29), −0.4(2)° (C2–C3–C4–N1)). The nitrimino group is in this plane too (179.50(13)° (N4–N3–C1–C2)), but the nitramino group slightly defers (176.53(14)° (N6–N5–C3–C4)). Both have very similar bond angles. The contact distance between oxygen and hydrogen is with approximately 2.0 Å far from the standard value for single bonds. Hydrogen bridge bonds occur between O1 and H3 (1.94(2) Å), O5 and H3 (2.08(2) Å), O2 and H4 (2.586(18) Å), O3 and H2 (2.24(2) Å) and O6 and H1 (1.93(2) Å).

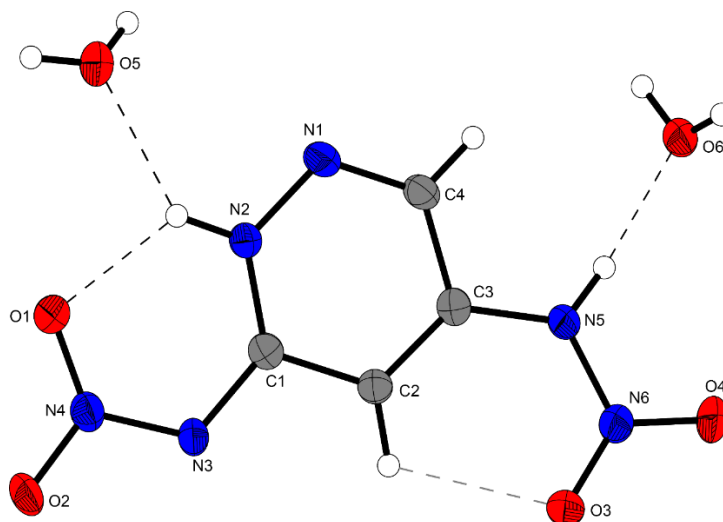


**Figure 7.** Molecular unit of compound **6·2H<sub>2</sub>O** in the crystalline state. Ellipsoids correspond to 50% probability levels. Hydrogen radii are arbitrary. Selected bond lengths (Å) and angles [deg.]: O1–N4 1.2386(18), N3–C1 1.361(2), O2–N4 1.2433(18), N3–N4 1.3494(19), O3–N6 1.2225(17), N5–N6 1.3689(19), O4–N6 1.2193(18), N5–C3 1.379(2), C1–C2 1.416(2), C2–C3 1.364(2), N1–C4 1.294(2), C3–C4 1.421(2), N1–N2 1.3510(19), N2–C1 1.342(2), N2–N1–C4 117.03(14), N2–C1–N3 127.72(14), N1–N2–C1 124.66(14), N4–N3–C1 118.68(13), N2–C1–C2 118.05(14),

C1–C2–C3 118.67(14), C2–C3–C4 117.65(14), O1–N4–N3 123.39(13), N6–N5–C3 125.33(13), N5–C3–C2 128.42(15), N1–C4–C3 123.93(15), O3–N6–N5 118.95(13), C4–N1–N2–C1 1.1(2), N2–N1–C4–C3 –0.6(2), N1–N2–C1–N3 178.21(15), N1–N2–C1–C2 –0.5(2), C1–N3–N4–O1 0.4(2), C1–N3–N4–O2 –178.52(14), N4–N3–C1–C2 179.50(13), C3–N5–N6–O3 –8.2(2), C3–N5–N6–O4 173.25(14), N6–N5–C3–C4 176.53(14), N3–C1–C2–C3 –179.46(14), N5–C3–C4–N1 179.50(15), C2–C3–C4–N1 –0.4(2), O1·H3 1.94(2), O5·H3 2.08(2), O2·H4 2.586(18), O3·H2 2.24(2), O6·H1 1.93(2).

Compound **7** (**Figure 8**) crystallizes in the monoclinic space group  $P 2_1/c$  with a cell volume of 1193.31(14) Å<sup>3</sup> and eight formula units per cell. The cell constants are  $a = 6.9987(5)$  Å,  $b = 11.7416(8)$  Å and  $c = 15.0305(10)$  Å with  $\beta = 104.955(4)^\circ$ . The calculated density at 298 K is 1.67 g/cm<sup>3</sup>. The bond lengths between O1–N4 (1.239(3) Å), O2–N4 (1.240(3) Å), N1–N2 (1.328(4) Å), N1–C4 (1.316(4) Å), N2–C1 (1.352(4) Å), N3–C1 (1.328(4) Å), C1–C2 (1.432(4) Å), N5–C3 (1.331(4) Å), C2–C3 (1.404(4) Å) and C3–C4 (1.430(4) Å) are in the typical range for aromatic systems. The bond between C2–N4, which has a length of 1.433(3) Å, is just slightly shorter than a single bond.<sup>[26]</sup> The angles between N2–N1–C4 (121.5(2) Å) and C2–C3–C4 (114.5(2) Å) show, that the pyridazine ring is slightly deformed. The torsion angles N1–N2–C1–C2 of –0.3(5)° and C2–C3–C4–N1 of –1.8(5)° show, that the pyridazine ring is almost in one plane.

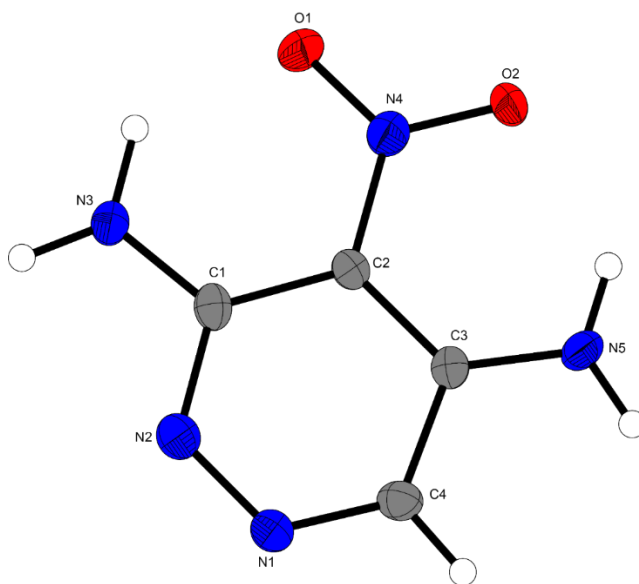


**Figure 8.** Molecular unit of compound **7** in the crystalline state. Ellipsoids correspond to 50% probability levels. Hydrogen radii are arbitrary. Selected bond lengths (Å) and angles [deg.]:

O1–N4 1.239(3), O2–N4 1.240(3), N1–N2 1.328(4), N1–C4 1.316(4), N2–C1 1.352(4), N3–C1 1.328(4), N4–C2 1.433(3), C1–C2 1.432(4), N5–C3 1.331(4), C2–C3 1.404(4), C3–C4 1.430(4), N2–N1–C4 121.5(2), C2–C3–C4 114.5(2), N1–C4–C3 123.9(3), C4–N1–N2–C1 1.5(5), N2–N1–C4–C3 –0.4(5), N1–N2–C1–N3 179.3(3), N1–N2–C1–C2 –0.3(5), C2–C3–C4–N1 –1.8(5).

#### 11.2.4. Physico-chemical Properties

During the course of this work three different energetic pyridazine derivatives were synthesized: 7-azido-tetrazolo[1,5-*b*]pyridazine (**2**), 5-nitramino-3-nitriminopyridazine dihydrate (**6**·2H<sub>2</sub>O) and 3,5-diamino-4-nitropyridazine (**7**). The experimentally and theoretically energetic properties of **2** and **7** were extensively investigated and all values are reported in Table 1. In addition, the DTA plots for both compounds are shown in **Figures 9** and **10**. 7-Azidotetrazolo[1,5-*b*]pyridazine (**2**) sharp decomposition peak at  $T_{onset} = 143$  °C, prior to melting and 134 °C. The low decomposition temperature of compound **2** can be attributed to the present azido groups in the pyridazine molecule. The dehydrate **6** loses both water molecules at 73 °C and decomposes sharply at 118 °C. 3,5-Diamino-4-nitropyridazine (**7**) shows sharp decomposition at 260 °C.



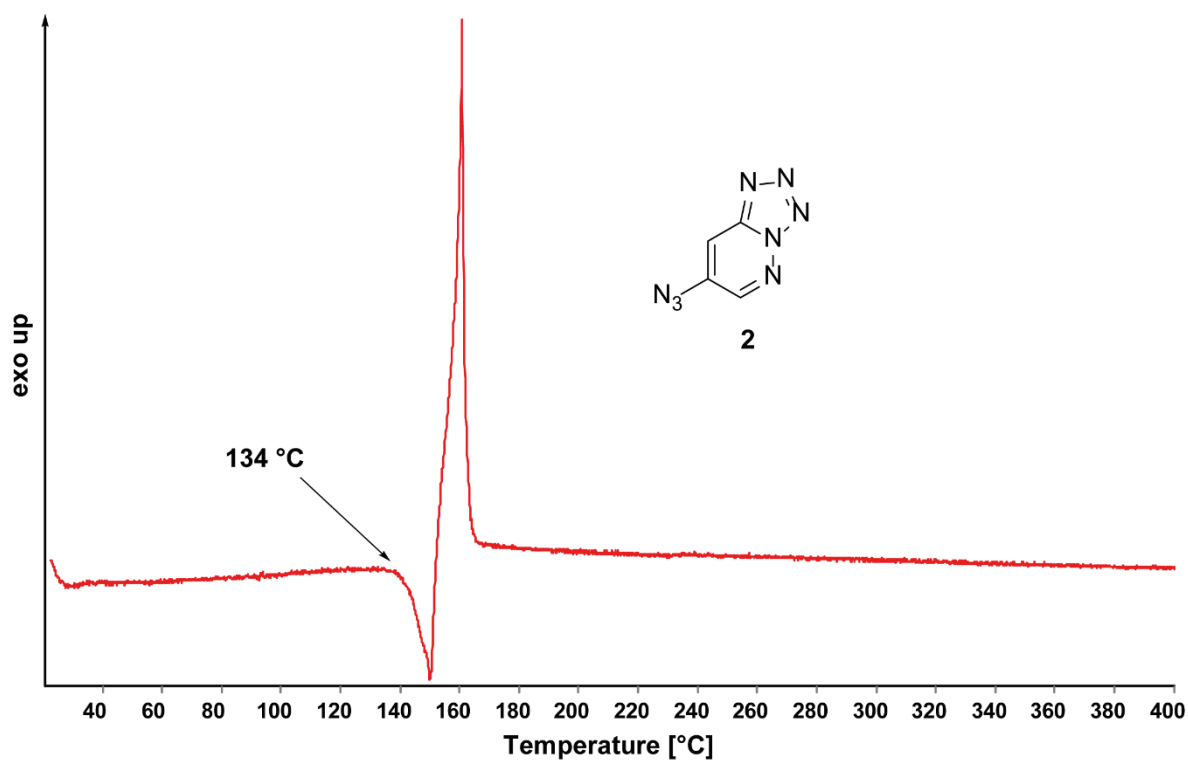


Figure 9. DTA plot for 7-azidotetrazolo[1,5-*b*]pyridazine (2).

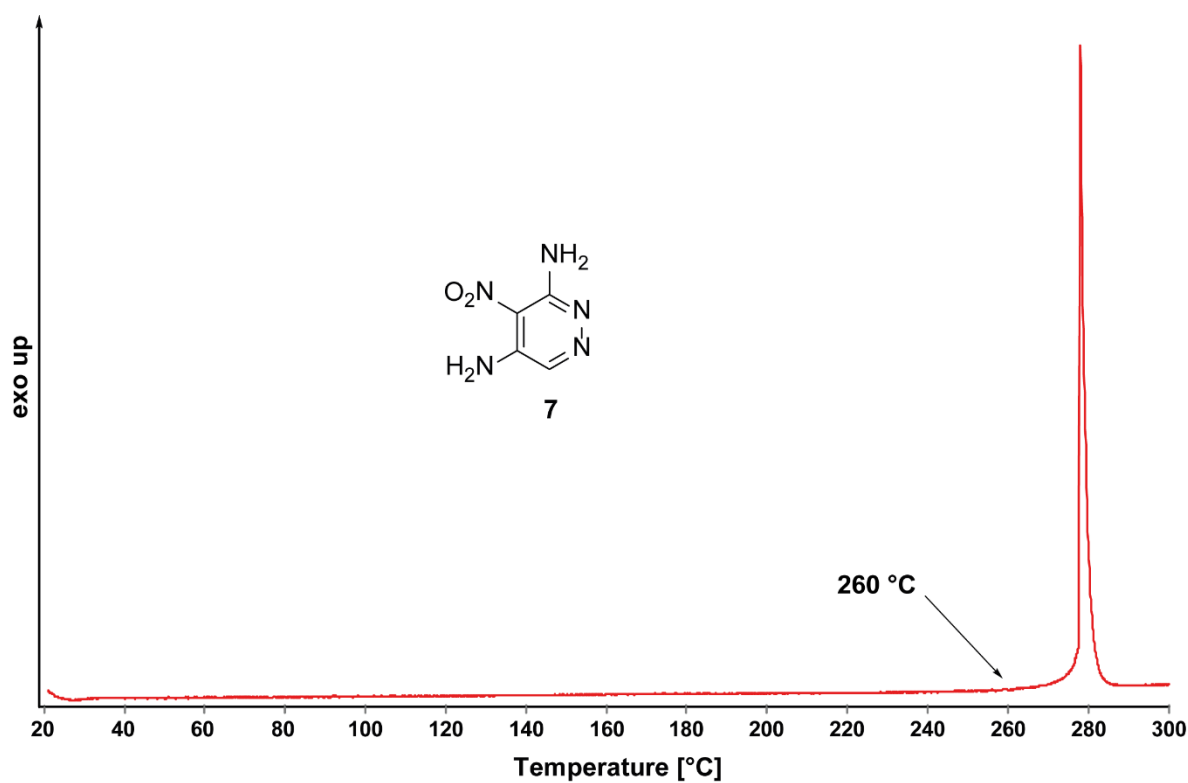


Figure 10. DTA plot for 3,5-diamino-4-nitropyridazine (7).

The extrapolated room temperature densities of compounds **2** and **7** are 1.61 and 1.67 g·cm<sup>-3</sup>, respectively. The experimentally determined sensitivity values toward impact, friction and electrostatic discharge for both compounds are reported in **Table 1**. Compound **2** is highly sensitive toward external stimuli with IS = 1.5 J, FS = 6 N and ESD = 0.022 J, whereas compound **7** is insensitive material with values of IS = 40 J, FS = > 360 N and ESD = 1.00 J. The high sensitivity of **2** is attributed again to the azido groups which are highly sensitive toward mechanical stimuli. Whereas the stability of compound **7** can be explained with the intra- and intermolecular hydrogen bonding throughout the structure. For both compounds were calculated positive standard molar enthalpies of formation (**2**, 817.1 kJ·mol<sup>-1</sup>) and (**7**, 112.4 kJ·mol<sup>-1</sup>). Using the room temperature densities several detonation properties were calculated for compounds **2** and **7** by using the EXPLO5 code (6.03 Version). The calculated values for the detonation energies of **2** and **7** are 4569 and 3253 kJ·kg<sup>-1</sup>, respectively. The detonation pressure and velocity values are  $p_{C-J}$  = 184 kbar,  $D_{C-J}$  = 7290 m·s<sup>-1</sup> for **2** and  $p_{C-J}$  = 185 kbar,  $D_{C-J}$  = 7222 m·s<sup>-1</sup> for **7**.

**Table 1.** Physico-chemical properties of compounds **2** and **7**.

	<b>2</b>	<b>7</b>
Formula	C <sub>4</sub> H <sub>2</sub> N <sub>8</sub>	C <sub>4</sub> H <sub>5</sub> N <sub>5</sub> O <sub>2</sub>
IS <sup>[a]</sup> [J]	1.5	40
FS <sup>[b]</sup> [N]	6	> 360
ESD <sup>[c]</sup> [J]	0.022	1.00
Ω <sup>[d]</sup> [%]	-88.8	-88.8
T <sub>m</sub> <sup>[e]</sup> [°C]	134	—
T <sub>dec</sub> <sup>[f]</sup> [°C]	143	260
ρ <sup>[g]</sup> [g·cm <sup>-3</sup> ]	1.61	1.67
Δ <sub>f</sub> H <sup>[h]</sup> [kJ·kg <sup>-1</sup> ]	5040.1	724.61
Δ <sub>f</sub> H <sup>[h]</sup> [kJ·mol <sup>-1</sup> ]	817.1	112.4
<b>EXPLO5 6.03</b>		
-Δ <sub>E</sub> U <sup>[i]</sup> [kJ·kg <sup>-1</sup> ]	4569	3253
T <sub>C-J</sub> <sup>[j]</sup> [K]	3377	2426
p <sub>C-J</sub> <sup>[k]</sup> [kbar]	184	185
D <sub>C-J</sub> <sup>[l]</sup> [m·s <sup>-1</sup> ]	7290	7222
V <sup>[m]</sup> [L <sup>3</sup> ·kg <sup>-1</sup> ]	676	742

[a] Impact sensitivity (BAM drophammer, method 1 of 6); [b] friction sensitivity (BAM drophammer, method 1 of 6); [c] electrostatic discharge device (OZM research); [d] oxygen balance with respect to CO<sub>2</sub>; [e] melting point (DTA, β = 5°C·min<sup>-1</sup>); [f] temperature of

---

decomposition (DTA,  $\beta = 5^{\circ}\text{C}\cdot\text{min}^{-1}$ ); [g] density at 298 K; [h] standard molar enthalpy of formation; [i] detonation energy; [j] detonation temperature; [k] detonation pressure; [l] detonation velocity; [m] volume of detonation gases at standard temperature and pressure conditions. \*experimentally determined values for LLM-105 (grain size 100–500  $\mu\text{m}$ ).

---

### 11.3. Conclusions

During this work we report a possible approach toward the synthesis of 3,5-diamino-4,6-dinitropyridazine. For this purpose, 3,5-dichloropyridazine (**1**) was reacted to 7-azidotetrazolo[1,5-*b*]pyridazine (**2**) and the Staudinger reaction was used to convert **2** into 3,5-diaminopyridazine acetate (**5**). Nitration reactions with **5** resulted only in 5-nitramino-3-nitriminopyridazine dihydrate (**6**·2H<sub>2</sub>O) in a good yield, which was then subsequently converted into 3,5-diamino-4-nitropyridazine (**7**). Further nitration attempts with compounds **5** and **7** were not successful and either only decomposition products or the starting material were obtained. Another synthetic approach has to be investigated in order to obtain the desired material 3,5-diamino-4,6-dinitropyridazine. In addition, during this work two energetic materials were synthesized and completely characterized. The intermediate azido compound **2** is a highly energetic material with sensitivity values of IS = 1.5 J, FS = 6 N and ESD = 0.022 J and can be classified as a primary explosive. Whereas compound **7** shows excellent thermal stability ( $T_{\text{onset}} = 260^{\circ}\text{C}$ ) and is also insensitive toward external stimuli (IS = 40 J, FS = > 360 N and ESD = 1.00 J).

### 11.4. Experimental Part

#### 11.4.1. General Information

All reagents and solvents were used as received. The synthesis of 3,5-dichloropyridazine (**1**) was performed by the previously published method.<sup>[27]</sup> Decomposition temperatures were measured *via* differential thermal analysis (DTA) with an OZM Research DTA 552-Ex instrument at a heating rate of  $5^{\circ}\text{C min}^{-1}$ . The NMR spectra were recorded with a 400 MHz instrument (<sup>1</sup>H 399.8 MHz, <sup>13</sup>C 100.5 MHz, <sup>14</sup>N 28.9 MHz, and <sup>15</sup>N 40.6 MHz) at ambient temperature. Chemical shifts are quoted in parts per million with respect to TMS (<sup>1</sup>H, <sup>13</sup>C) and nitromethane (<sup>14</sup>N, <sup>15</sup>N). Infrared spectra (IR) were recorded from 4500  $\text{cm}^{-1}$  to 650  $\text{cm}^{-1}$  on a Perkin Elmer Spectrum BX-59343 instrument with *Smiths Detection*

*DuraSamplIR II Diamond ATR* sensor. The absorption bands are reported in wavenumbers ( $\text{cm}^{-1}$ ). The sensitivities toward friction and impact of compounds **2**, **6·2H<sub>2</sub>O** and **7** were determined according the BAM standards and the detonation parameters were calculated using the EXPLO5-V6.03 computer code.<sup>[28]</sup> All detonation parameters for the polynitro derivatives **2–6** were calculated by using the room-temperature densities obtained from the X-ray structures as described in the reference.<sup>[29]</sup> Compounds **2**, **6·2H<sub>2</sub>O** and **7** were tested for sensitivity towards electrical discharge using an Electric Spark Tester ESD 2010 EN.

### 11.4.2. Synthesis

**CAUTION!** All investigated compounds are potentially explosive materials, although no hazards were observed during preparation and handling these compounds. Nevertheless, safety precautions such as (wearing leather coat, face shield, Kevlar sleeves, Kevlar gloves, earthed equipment and ear plugs) should be drawn.

#### 7-Azidotetrazolo[1,5-*b*]pyridazine (**2**)

3,5-Dichloropyridazine (**1**, 8.07 g, 54.2 mmol, 1.0 eq.) was dissolved in ethanol (70 mL) and  $\text{NaN}_3$  (15.84 g, 243.8 mmol, 4.5 eq.) dissolved in  $\text{H}_2\text{O}$  (50 mL) was added at room temperature. The reaction mixture was refluxed for 24 h. The resulting solution was cooled down and crystalline material precipitated. The precipitate was filtrated, washed with ice water and dried on air overnight to give compound **2** (4.27 g, 26.3 mmol, 49%).

DTA ( $5\text{ }^\circ\text{C min}^{-1}$ ): 134 (melt.),  $143\text{ }^\circ\text{C}$  (exo.); BAM: drop hammer: 1.5 J (100–500  $\mu\text{m}$ ); friction tester: 6 N (100–500  $\mu\text{m}$ ); ESD: 0.022 J (100–500  $\mu\text{m}$ ). **IR (ATR)**,  $\tilde{\nu}$  ( $\text{cm}^{-1}$ ) = 3037 (m), 2346 (vw), 2225 (vw), 2133 (vs), 1613 (m), 1530 (w), 1507 (vw), 1396 (s), 1380 (s), 1357 (s), 1315 (vw), 1293 (vw), 1272 (s), 1261 (s), 1236 (vs), 1110 (m), 1087 (m), 991 (m), 938 (w), 894 (s), 849 (m), 769 (m), 701 (vw), 676 (m). **<sup>1</sup>H NMR** ( $d_6$ -DMSO, 400 MHz, ppm)  $\delta$  = 8.85 (d,  $^4J$  = 2.6 Hz, 1H), 8.61 (d,  $^4J$  = 2.6 Hz, 1H). **<sup>13</sup>C NMR** ( $d_6$ -DMSO, 101 MHz, ppm)  $\delta$  = 143.8, 143.7, 139.3, 110.6. **<sup>15</sup>N NMR** ( $d_6$ -DMSO, 41 MHz, ppm)  $\delta$  = 15.0, –28.0, –68.9, –70.0 (d,  $^2J$  = 14.30 Hz), –106.6 (dd,  $^3J$  = 9.60 Hz,  $^3J$  = 2.73 Hz), –140.7, –143.8, –283.6. **<sup>15</sup>N{<sup>1</sup>H} NMR** ( $d_6$ -DMSO, 41 MHz, ppm)  $\delta$  = 15.0, –28.0, –68.9, –70.0, –106.6, –140.7, –143.8, –283.6. **Elem. Anal.** ( $\text{C}_4\text{H}_2\text{N}_8$ , 162.12  $\text{g}\cdot\text{mol}^{-1}$ ) calcd.: C 29.64, H 1.24, N 69.12%. Found: C 29.87, H 1.52, N 69.13%. ***m/z*** ( $\text{DEI}^+$ ): 162 (77)  $[\text{M}]^+$ .

**5-(Triphenylphosphoranylidenamino)tetrazolo[1,5-*b*]pyridazine (3)**

Azidotetrazolo[1,5-*b*]pyridazine (**2**, 4.27 g, 26.3 mmol, 1.0 eq.) was suspended in benzene (130 mL) and triphenylphosphine (13.8 g, 52.6 mmol, 2.0 eq.) was added. The reaction mixture was stirred overnight. After filtration and washing with cold ethanol the product was obtained as a light beige powder (**3**, 10.30 g, 25.97 mmol, 99%).

**IR (ATR)**,  $\tilde{\nu}$  (cm<sup>-1</sup>) = 3064 (vw), 1598 (s), 1512 (m), 1495 (s), 1478 (m), 1437 (m), 1407 (vs), 1332 (vw), 1302 (w), 1284 (s), 1249 (vw), 1228 (vs), 1178 (vw), 1159 (vw), 1109 (s), 1081 (m), 1027 (vw), 1009 (m), 998 (m), 937 (s), 925 (w), 863 (vw), 820 (s), 763 (w), 752 (w), 739 (m), 720 (vs), 693 (vs). **<sup>1</sup>H NMR** (*d*<sub>6</sub>-DMSO, 400 MHz, ppm)  $\delta$  = 8.54 (dd, <sup>4</sup>*J* = 2.6, <sup>5</sup>*J* = 1.0 Hz, 1H), 7.85 (ddd, <sup>2</sup>*J* = 12.4, <sup>3</sup>*J* = 8.3, <sup>4</sup>*J* = 1.4 Hz, 6H), 7.76 – 7.70 (m, 3H), 7.67 – 7.59 (m, 6H), 6.47 (dd, <sup>4</sup>*J* = 2.6, <sup>5</sup>*J* = 0.6 Hz, 1H). **<sup>13</sup>C NMR** (*d*<sub>6</sub>-DMSO, 101 MHz, ppm)  $\delta$  = 152.0, 151.7, 150.0, 145.12, 133.6, 133.6, 132.9, 132.8, 130.0, 129.9, 127.6, 126.6, 100.6, 100.4. **<sup>31</sup>P NMR** (*d*<sub>6</sub>-DMSO, 162 MHz, ppm)  $\delta$  = 13.6. **Elem. Anal.** (C<sub>22</sub>H<sub>17</sub>N<sub>6</sub>P, 396.39 g·mol<sup>-1</sup>) calcd.: C 66.66, H 4.32, N 21.20%. Found: C 66.70, H 4.38, N 21.18%. ***m/z*** (DEI<sup>+</sup>): 396 (27) [M]<sup>+</sup>.

**3,5-Bis(triphenylphosphoranylideneamino)pyridazine (4)**

(Triphenylphosphoranylidenamino)tetrazolo[1,5-*b*]pyridazine (**3**, 10.30 g, 25.97 mmol, 1.0 eq.) was suspended in chlorobenzene (290 mL) and triphenylphosphine (8.17 g, 31.2 mmol, 1.2 eq.) was added. The reaction mixture was refluxed for 3 d. The solvent was removed under reduced pressure and the crude product was resuspended in *c*-hexane. Filtration and washing with *c*-hexane gave compound **4** as a brown solid (16.37 g, 25.95 mmol, 100%).

**IR (ATR)**,  $\tilde{\nu}$  (cm<sup>-1</sup>) = 3056 (vw), 2923 (m), 2848 (m), 1599 (vw), 1576 (m), 1560 (s), 1497 (vw), 1482 (w), 1449 (vw), 1436 (m), 1409 (w), 1370 (s), 1352 (m), 1253 (vs), 1230 (w), 1184 (w), 1106 (s), 1027 (w), 997 (w), 938 (vw), 866 (s), 821 (vw), 739 (m), 716 (vs), 690 (vs). **<sup>1</sup>H NMR** (*d*<sub>6</sub>-DMSO, 400 MHz, ppm)  $\delta$  = 8.54 (dd, <sup>4</sup>*J* = 2.7, <sup>5</sup>*J* = 0.9 Hz, 1H), 7.77 – 7.55 (m, 30H), 6.47 (dd, <sup>4</sup>*J* = 2.6, <sup>5</sup>*J* = 0.6 Hz, 1H), 5.93 (s, 1H). **<sup>13</sup>C NMR** (*d*<sub>6</sub>-DMSO, 101 MHz, ppm)  $\delta$  = 151.45, 151.2, 149.5, 144.7, 134.5 – 125.0 (m), 100.1, 99.9, 26.3. **<sup>31</sup>P NMR** (*d*<sub>6</sub>-DMSO, 162 MHz, ppm)  $\delta$  25.5, 12.4, 11.2, 7.1, -6.77.

**3,5-Diaminopyridazine acetate (5)**

3,5-Bis(triphenylphosphoranylideneamino)pyridazine (**4**, 13.80 g, 21.88 mmol, 1.0 eq.) was dissolved in acetic acid (80%, 250 mL) and refluxed for 4.5 h. The resulting solution was poured on water (750 mL) and washed with ethyl acetate (3 × 300 mL). The water layer was evaporated to dryness *in vacuo* and the product was triturated with Et<sub>2</sub>O. Filtration and washing with diethyl ether yielded the product as brown solid (**5**, 2.90 g, 17.0 mmol, 78%).

**IR (ATR)**,  $\tilde{\nu}$  (cm<sup>-1</sup>) = 3360 (w), 3183 (m), 3057 (m), 1917 (vw), 1679 (m), 1651 (s), 1620 (s), 1534 (s), 1451 (s), 1426 (s), 1399 (vs), 1336 (m), 1271 (m), 1165 (w), 1045 (w), 1013 (m), 983 (s), 918 (w), 887 (w), 838 (s), 766 (m), 729 (vw), 652 (s), 581 (w), 557 (vw), 531 (s). **<sup>1</sup>H NMR** (D<sub>2</sub>O, 400 MHz, ppm)  $\delta$  = 7.87 (d, <sup>4</sup>*J* = 2.4 Hz, 1H), 6.12 (d, <sup>4</sup>*J* = 2.4 Hz, 1H), 1.93 (s, 3H). **<sup>13</sup>C NMR** (D<sub>2</sub>O, 101 MHz, ppm)  $\delta$  = 181.3, 154.2, 150.5, 136.2, 92.0, 23.2. **Elem. Anal.** (C<sub>6</sub>H<sub>10</sub>N<sub>4</sub>O<sub>2</sub>, 170.17 g·mol<sup>-1</sup>) calcd.: C 42.35, H 5.92, N 32.92%. Found: C 42.16, H 5.62, N 32.78%. ***m/z*** (FAB<sup>+</sup>): 221 [2M+H]<sup>+</sup>, 111 (cation); ***m/z*** (FAB<sup>-</sup>): 59 (anion); ***m/z*** (DEI<sup>+</sup>): 111 (6) [M+H]<sup>+</sup>, 110 (100) [M]<sup>+</sup>.

**5-Nitramino-3-nitriminopyridazine dihydrate (6·2H<sub>2</sub>O)**

3,5-Diaminopyridazine acetate (**5**, 1.50 g, 8.81 mmol, 1.0 eq.) was dissolved in conc. H<sub>2</sub>SO<sub>4</sub> (4.9 mL) at 0 °C and 100% HNO<sub>3</sub> (1.35 mL, 31.5 mmol, 3.6 eq.) was added dropwise over the period of 1 h. The reaction mixture was stirred for 2 h at 0 °C, then for 1.5 h at room temperature and subsequently poured on ice. The resulting suspension was filtered, the formed precipitate was washed with a small amount of ice water and dried on air to yield **6·2H<sub>2</sub>O** as beige solid (1.63 g, 6.92 mmol, 79%).

DTA (5 °C min<sup>-1</sup>): 73 °C (endo, H<sub>2</sub>O.), 118 °C (exo.); BAM: drop hammer: 12.5 J (100–500 μm); friction tester: >360 N (100–500 μm); ESD: 0.55 J (100–500 μm). **IR (ATR)**,  $\tilde{\nu}$  (cm<sup>-1</sup>) = 3095 (m), 2821 (m), 1629 (s), 1569 (s), 1515 (vw), 1451 (vs), 1381 (m), 1332 (m), 1296 (s), 1279 (s), 1229 (w), 1173 (vs), 1114 (s), 1055 (m), 997 (m), 957 (m), 896 (m), 860 (m), 779 (m), 750 (m), 711 (m), 693 (m), 641 (w). **<sup>1</sup>H NMR** (*d*<sub>6</sub>-DMSO, 400 MHz, ppm)  $\delta$  = 8.38 (d, <sup>4</sup>*J* = 2.5 Hz, 1H), 8.22 (d, <sup>4</sup>*J* = 2.5 Hz, 1H), 5.19 (br, 6H). **<sup>13</sup>C NMR** (*d*<sub>6</sub>-DMSO, 101 MHz, ppm)  $\delta$  = 157.9, 145.3, 137.5, 107.0. **<sup>14</sup>N NMR** (*d*<sub>6</sub>-DMSO, 29 MHz, ppm)  $\delta$  = -15, -27. **Elem. Anal.** (C<sub>4</sub>H<sub>8</sub>N<sub>6</sub>O<sub>6</sub>, 236.14 g·mol<sup>-1</sup>) calcd.: C 20.35, H 3.41, N 35.59%. Found: C 20.74, H 3.61, N 35.56%. ***m/z*** (DEI<sup>+</sup>): 200 (5) [M]<sup>+</sup>.

### 3,5-Diamino-4-nitropyridazine (7)

5-Nitramino-3-nitriminopyridazine dihydrate (**6** · 2H<sub>2</sub>O, 1.63 g, 6.92 mmol, 1.0 eq.) was added to conc. H<sub>2</sub>SO<sub>4</sub> (8.5 mL) at 0 °C. The solution was stirred for 30 min at 0 °C, 45 min at r.t. and 3 h at 50 °C. The resulting solution was poured on ice and neutralised with NaHCO<sub>3</sub>. Filtration of the suspension and washing with ice water yielded the product as yellow solid (**7**, 871 mg, 5.62 mmol, 81%).

DTA (5 °C min<sup>-1</sup>): 260 °C (exo.); BAM: drop hammer: 40 J (100–500 µm); friction tester: >360 N (100–500 µm); ESD: 1.00 J (100–500 µm). **IR (ATR)**,  $\tilde{\nu}$  (cm<sup>-1</sup>) = 3449 (m), 3316 (m), 3062 (m), 2993 (m), 1610 (s), 1581 (s), 1521 (m), 1504 (m), 1470 (m), 1267 (s), 1138 (m), 1095 (m), 1013 (m), 778 (m), 578 (m), 553 (m). **<sup>1</sup>H NMR** (*d*<sub>6</sub>-DMSO, 400 MHz, ppm)  $\delta$  = 8.33 (s, 2H), 8.20 (s, 1H), 7.55 (s, 2H). **<sup>13</sup>C NMR** (*d*<sub>6</sub>-DMSO, 101 MHz, ppm)  $\delta$  = 152.4, 142.1, 136.4, 114.8. **<sup>14</sup>N NMR** (*d*<sub>6</sub>-DMSO, 29 MHz, ppm)  $\delta$  = -12. **Elem. Anal.** (C<sub>4</sub>H<sub>5</sub>N<sub>5</sub>O<sub>2</sub>, 155.12 g·mol<sup>-1</sup>) calcd.: C 30.97, H 3.25, N 45.15%. Found: C 30.76, H 3.78, N 43.27%. ***m/z*** (DEI<sup>+</sup>): 155 (100) [M]<sup>+</sup>, 156 (6) [M+H]<sup>+</sup>, 157 (1) [M+2H]<sup>+</sup>.

## 11.5. References

- [1] Raj K. Bansal, *Heterocyclic Chemistry*, 3rd Ed., New Age International, New Delhi, **1999**.
- [2] P. Yin, C. He, J. M. Shreeve, *Chem. Eur. J.* **2016**, 22, 1–7.
- [3] R. P. Claridge, J. Hamid, R. W. Millar and S. P. Philbin, *Propell. Explos. Pyrotech.*, **2004**, 29, 81.
- [4] R. G. Coombes, R. W. Millar and S. P. Philbin, *Propell. Explos. Pyrotech.* **2000**, 25, 302.
- [5] J. A. Joule, K. Mills, *Heterocyclic Chemistry*, 5th Ed., Wiley, UK, **2010**.
- [6] J. P. Agrawal, R. D. Hodgson, *Organic Chemistry of Explosives*, Wiley, UK, **2007**.
- [7] A. Deeb, H. Sterk, T. Kappe, *Liebigs Ann. Chem.* **1991**, 1225–1227.
- [8] T. Kappe, A. Pfaffenschlager, W. Stadlbauer, *Synthesis* **1989**, 666.
- [9] M. Tišler, *Synthesis* **1973**, 123.
- [10] H. Staudinger, J. Meyer, *Helv. Chim. Acta* **1919**, 2, 635.

- [11] Y. G. Gololobov, I. N. Zhmurova, L. F. Kasukhin, *Tetrahedron* **1981**, 37, 437.
- [12] W. D. Guither, D. G. Clark, R. N. Castle, *J. Heterocycl. Chem.* **1965**, 2, 67–71.
- [13] P. Cmoch, *Magn. Reson. Chem.* **2002**, 40, 507–516.
- [14] P. Cmoch, L. Stefaniak, G. A. Webb, *Magn. Reson. Chem.* **1997**, 35, 237.
- [15] P. Cmoch, H. Korczak, L. Stefaniak, G. A. Webb, *J. Phys. Org. Chem.* **1999**, 12, 470.
- [16] P. Cmoch, J. W. Weinch, L. Stefaniak, G. A. Webb, *J. Mol. Struct.* **1999**, 510, 165.
- [17] M. Burke-Laing, M. Laing, *Acta Crystallogr.* **1976**, B32, 3216.
- [18] N–N values und N=N values from: International Tables for X-ray crystallography; Kluwer Academic Publisher: Dordrecht, The Netherlands, **1992**, Vol. C.
- [19] B. Lyhs, G. Jahnsen, D. Bläser, C. Wölper, S. Schulz, *Chem. Eur. J.* **2011**, 17, 11394–11398.
- [20] A. F. Holleman, E. Wiberg, N. Wiberg, *Lehrbuch der Anorganischen Chemie*, 102. Auflage, de Gruyter, **2007**.
- [21] R. Alsfasser, C. Janiak, T. M. Klapötke, H.-J. Meye, *Moderne Anorganische Chemie*, 3. Auflage, de Gruyter, Berlin, **2007**.
- [22] a) R. Haiges, A. Vij, J. A. Boatz, S. Schneider, T. Schroer, M. Gerken, K. O. Christe, *Chem. Eur. J.* **2004**, 10, 508–517. b) R. Haiges, J. A. Boatz, R. Bau, S. Schneider, T. Schroer, M. Yousufuddin, K. O. Christe, *Angew. Chem. Int. Ed.* **2005**, 44, 1860–1865. c) R. Haiges, J. A. Boatz, A. Vij, V. Vij, M. Gerken, S. Schneider, T. Schroer, M. Yousufuddin, K. O. Christe, *Angew. Chem. Int. Ed.* **2004**, 43, 6676–6680.
- [23] V. J. Kaiser, H. Hartung, R. Richter, *Z. Anorg. Allg. Chem.* **1980**, 469, 188.
- [24] The Kynoch Press, *International Tables for X-Ray Crystallography* **1962**, Vol. 111, Birmingham.
- [25] D. E. C. Corbidge, *The Structural Chemistry of Phosphorus*, Elsevier, Amsterdam, **1974**.
- [26] T. L. Cottrell, *The Strengths of Chemical Bonds*, Butterworths Scientific Publications, London, **1958**.
- [27] I. Gospodinov, T. M. Klapötke, J. Stierstoerfer, *Eur. J. Org. Chem.* **2018**, 1004–1010.



- [28] M. Sućeska, *EXPLO5 Version 6.03 User's Guide*, Zagreb, Croatia: OZM; 2015.
- [29] J. S. Murray and P. Politzer, *J. Mol. Model.*, 2014, **20**, 2223.

## 12. Appendix

### 1. List of Abbreviations

°C	degree Celsius
$\delta$	chemical shift in ppm
ADN	ammonium dinitramide
AG	aminoguanidium
ANPyO	4,6-diamino-3,5-dinitropyridine-1-oxide
AP	ammonium perchlorate
AN	ammonium nitrate
BC	Before Christ
BNCP	tetramin-cis-bis(5-nitrotetrazolato-N <sup>2</sup> )cobalt(III) perchlorate
br	broad
brine	saturated solution of sodium chloride
CA	cadmium azide
<i>c</i> -hexane	cyclohexane
Cl-20	6,8,10,12-hexanitro-2,4,6,8,10,12-hexaazaisowurtzitane
DCM	dichloromethane
DDNP	2-diazo-4,6-dinitrophenol
DDT	deflagration-to-detonation transition
DMF	dimethylformamide
EI	electron ionisation
EM	energetic material
eq.	equivalent
EtOAc	ethyl acetate

## Appendix

<i>et al.</i>	<i>et alii</i> (and others)
FAB	fast atom bombardment
g	gram
h	hour
HEDM	high-energy density material
HMX	1,3,5,7-tetranitro-1,3,5,7-tetrazocine
HNAB	hexanitroazobenzene
HNS	1,2-bis(2,4,6-trinitrophenyl)ethylen
Hz	Hertz
<i>in vacuo</i>	under pressure
IR	infrared
LA	lead azide
LLM-105	2,6-diamino-3,5-dinitropyrazine-1-oxide
LLX-112	3,6-diamino-1,2,4,5-tetrazine-1,4-dioxide
MF	mercury fulminate
mL	millilitre
mm	millimetre
NC	nitrocellulose
NG	nitroglycerine
NMR	nuclear magnetic resonance
NONA	2,2',2'',4,4',4'',6,6',6''-nonanitroterphenyl
ONC	1,2,3,4,5,6,7,8-octanitro-pentacyclo-[4.2.0.0 <sup>2,5</sup> .0 <sup>3,8</sup> .0 <sup>4,7</sup> ]octan
PAC	pentammin(1,5-cyclopentamethylentetrazolato-N <sup>3</sup> )cobalt(III) perchlorate
PETN	pentaerythritetranitrat

## Appendix

PP	potassium perchlorate
ppm	parts per million
<i>p</i> TsOH	<i>p</i> -toluenesulfonic acid
PYX	2,6-bis(picrylamino)-3,5-dinitropyridine
RDX	1,3,5-trinitro-1,3,5-triazine
STP	standard temperature and pressure
r.t.	room temperature
TACOT	tetranitro dibenzo-1,2a,4,4a-tetraazapentalene
TATB	1,3,5-triamino-2,4,6-trinitrobenzene
TATNB	1,3,5-triazido-2,4,6-trinitrobenzol
Tetryl	<i>N</i> -methyl- <i>N</i> -2,4,6-tetranitroanilin
TNAZ	1,3,3'-trinitroazetidine
TNT	2,4,6-trinitrotoluene
vw	very weak (IR)
w	weak (IR)

## 2. Curriculum Vitae

### Ivan Georgiev Gospodinov | Curriculum Vitae

#### Persönliches

---

Name	<b>Ivan Georgiev Gospodinov</b>
Nationalität	Bulgarisch

#### Fachliche Kompetenzen

---

Forschung:	Synthese und Charakterisierung organischer und anorganischer Verbindungen; retrosynthetische Analyse und Funktionalisierung von neuen heterozyklischen Systemen; Auswertung der energetischen Leistung von Sprengstoffen mit dem Small Scale Shock Reactivity Test (SSRT).
Analytik:	NMR Spektroskopie ( $^1\text{H}$ , $^{13}\text{C}$ , $^{14}\text{N}$ , $^{15}\text{N}$ , $^{31}\text{P}$ , $^{77}\text{Se}$ ); Massenspektrometrie; Schwingungsspektroskopie (IR und RAMAN); Klassifizierung der Sensitivitäten energetischen Verbindungen nach BAM (Bundesanstalt für Materialforschung und -prüfung) Vorschrift; thermische Analyse (DSC, DTA, TGA).
Sicherheit:	Erfahrung im sicheren Umgang mit energetischen, gefährlichen und toxischen Verbindungen.

#### Beruflicher Werdegang

---

04/2016 bis 12/2019	<b>Fakultät für Chemie und Pharmazie, Ludwig-Maximilians-Universität München, Deutschland</b> <i>Wissenschaftlicher Mitarbeiter und Lehrbeauftragter</i> Strategisch und zielgeführte Forschung und Synthese im Labor; enge Zusammenarbeit mit Studierenden der unteren Semester innerhalb von Bachelor- und Masterarbeiten.
03/2017 bis heute 04/2011 bis 03/2016	<b>FOM Hochschule für Ökonomie und Management GmbH, Hochschule für Berufstätige, München, Deutschland</b> <i>Werkstudent im Aufgabenbereich Veranstaltungsmanagement</i> Betreuung von Studenten und Dozenten; Administration der Bibliothek am Standort; Planung und Ausführung von Sonderveranstaltungen

## Appendix

(Bachelor- und Masterverabschiedungsfeier, Semestereröffnungsfeier);  
Diverse Bürotätigkeiten und Rechercheaufgaben; Teilnahme an  
Messeveranstaltungen.

### Akademischer & Schulischer Werdegang

---

- 04/2016 bis 10/2019: **Fakultät für Chemie und Pharmazie, Ludwig-Maximilians-Universität München, Deutschland**  
Promotion in anorganischer Chemie; Dissertation: „*Synthesis and Characterization of New and Advanced Energetic Materials Based on Azoles and Diazines*”  
Prof. Dr. Thomas M. Klapötke, Ludwig-Maximilians-Universität München
- 04/2014 bis 03/2016: **Fakultät für Chemie und Pharmazie, Ludwig-Maximilians-Universität München, Deutschland**  
Master of Science (120 ECTS) in Chemie (1.39); Masterarbeit: „*Pyridazine Derivatives as Potentially High-Energy Dense Materials*“ (1.0)
- 09/2010 bis 03/2014 **Fakultät für Chemie und Pharmazie, Ludwig-Maximilians-Universität München, Deutschland**  
Bachelor of Science (180 ECTS) in Chemie und Biochemie (2.4);  
Bachelorarbeit: „*Synthese stickstoffreicher Heterozyklen als mögliche Liganden energiereicher Übergangsmetallkomplexe*“ (1.0)
- 09/2005 bis 07/2010 **Fremdsprachengymnasium „Geo Milev“, Dobritsch, Bulgarien**  
Allgemeine Hochschulreife (1.13)

### Fort- & Weiterbildungen

---

- 10/2018 bis 12/2018 **Ludwig-Maximilians-Universität München, Deutschland**  
„*Betriebswirtschaftliche Grundlagen*“  
Dr. Christian Jörg, Dr. Ralph Stöckle
- 11/2018 **Ludwig-Maximilians-Universität München, Workshop des GraduateCenter<sup>LMU</sup>, Deutschland**  
„*Teams und Gruppen leiten*“
- 10/2018 **Ludwig-Maximilians-Universität München, Workshop des GraduateCenter<sup>LMU</sup>, Deutschland**  
„*Promotion – und dann? (Natur- und Wirtschaftswissenschaften)*“

### Fähigkeiten & Kenntnisse

---

Sprachen:	Bulgarisch (Muttersprache) Deutsch (verhandlungssicher) Englisch (verhandlungssicher)
PC Kenntnisse:	MS Office (Word, Excel, Power Point, Outlook); Adobe Illustrator.

### Publikationen

---

- 1) **I. Gospodinov**, K. V. Domasevitch, C. C. Unger, T. M. Klapötke, J. Stierstorfer, *Cryst. Growth Des.*, submitted.
- 2) **I. Gospodinov**, T. M. Klapötke, J. Singer, J. Stierstorfer, *Z. Anorg. Allg. Chem.* **2019**, 645, 1–9.
- 3) K. V. Domasevitch, **I. Gospodinov**, H. Krautscheid, T. M. Klapötke, J. Stierstorfer, *New. J. Chem.* **2019**, 43, 1305 – 1312.
- 4) J. Glück, **I. Gospodinov**, T. M. Klapötke, J. Stierstorfer, *Z. Anorg. Allg. Chem.* **2019**, 645, 370–376.
- 5) **I. Gospodinov**, T. Hermann, T. M. Klapötke, J. Stierstorfer, *Propellants, Explos., Pyrotech.* **2018**, 43, 355–365.
- 6) **I. Gospodinov**, T. M. Klapötke, J. Stierstorfer, *Eur. J. Org. Chem.* **2018**, 1004–1010.
- 7) J. Evers, **I. Gospodinov**, M. Joas, T. M. Klapötke, J. Stierstorfer, *Inorg. Chem.* **2014**, 53, 11749–11756.

### Präsentationen

---

- 1) **I. Gospodinov**, K. V. Domasevitch, T. M. Klapötke, J. Stierstorfer, *4,4'-Bipyrazole as a building block for new energetic materials*, New Trends in Research of Energetic Materials (NTREM), Pardubice, Czech Republic, **2019**.
- 2) **I. Gospodinov**, T. M. Klapötke, J. Stierstorfer, *Pyridazine Scaffold as a New Building Block for the Design of Energetic Materials*, International Annual Conference of the Fraunhofer ICT: Energetic Materials, Synthesis, Processing, Performance, 49<sup>th</sup>, Karlsruhe, Deutschland, 26–28 June, **2018**.
- 3) **I. Gospodinov**, T. M. Klapötke, J. Stierstorfer, *Synthesis and Characterization of New Insensitive Explosives Based on 1,2-Diazines*, International Annual Conference of the Fraunhofer

## Appendix

ICT: Energetic Materials, Synthesis, Processing, Performance, 49<sup>th</sup>, Karlsruhe, Deutschland, 26–28 June, **2018**.

4) **I. Gospodinov**, T. M. Klapötke, J. Stierstorfer, *Pyridazine Scaffold as a New Building Block for the Design of Energetic Materials*, Gordon Research Conference on Energetic Materials: Exploiting Advances in Additively-Manufactured, Nano- and Non-Crystalline Materials, Synthetic Methods, Modeling and Simulation, and In Situ Diagnostics for Energetic Materials, Newry, Maine, USA, 3–8 June, **2018**.

5) **I. Gospodinov**, T. M. Klapötke, J. Stierstorfer, *3,5-Diamino-4,6-dinitropyridazine-1-oxide: New Insensitive High Explosive Based on the Pyridazine Scaffold*, Gordon Research Conference on Energetic Materials: Exploiting Advances in Additively-Manufactured, Nano- and Non-Crystalline Materials, Synthetic Methods, Modeling and Simulation, and In Situ Diagnostics for Energetic Materials, Newry, Maine, USA, 3–8 June, **2018**.

6) **I. Gospodinov**, T. M. Klapötke, J. Stierstorfer, *Pyridazine Scaffold as a New Building Block for the Design of Energetic Materials*, Gordon Research Seminar on Energetic Materials: Advances and Modeling, Experimental Developments and Synthesis of Energetic Materials, Newry, Maine, USA, 2–3 June, **2018**.

7) **I. Gospodinov**, T. M. Klapötke, J. Stierstorfer, *Nitrogen-rich salts of 3,4-bis(4-nitramino-1,2,5-oxadiazol-3-yl)-1,2,5-furoxan (BNAFF)*, New Trends in Research of Energetic Materials (NTREM), Pardubice, Czech Republic, **2017**.